Deliverable 8.3: SFC Training materials.

Work Package 8

This project has received funding from the European Union's Horizon 2020 research and innovation programme under grant agreement N°847593.

Document information

Project Acronym	**EURAD**
Project Title	**European Joint Programme on Radioactive Waste Management**
Project Type	**European Joint Programme (EJP)**
EC grant agreement No.	**847593**
Project starting / end date	**1st June 2019 – 30 May 2024**
Work Package No.	8
Work Package Title	**Spent Fuel Characterization and Evolution Until Disposal**
Work Package Acronym	**SFC**
Deliverable No.	**8.3**
Deliverable Title	**SFC Training materials**
Lead Beneficiary	**CIEMAT**
Contractual Delivery Date	**Month 48**
Actual Delivery Date	**Month 60**
Type	Report
Dissemination level	**PU**
Authors	**Llorente Herranz, Cristina (CIEMAT), López del Pra, Claudia (CIEMAT), Schillebeeckx Peter (JRC).**

To be cited as:

Llorente Herranz C., López del Pra C. Peter Schillebeeckx (2023): SFC Training materials. Final version as of 15.11.2023 of deliverable D8.3 of the HORIZON 2020 project EURAD. EC Grant agreement no: 847593.

Acknowledgement

This document is a deliverable of the European Joint Programme on Radioactive Waste Management (EURAD). EURAD has received funding from the European Union's Horizon 2020 research and innovation programme under grant agreement No 847593.

The SFC Training materials document consists of two volumes. This document corresponds to the first volume.

Status of deliverable		
	By	Date
Delivered (Lead Beneficiary)	CIEMAT	03/05/2024.
Verified (WP Leader)	SKB	03/05/2024.
Reviewed (Reviewers)	Niels Belmans and Paul Carbol	15/05/2024.
Approved (PMO)	Paul Carbol	16/05/2024.
Submitted to EC (Coordinator)	ANDRA	17/05/2024.

Executive Summary

This report collects the main training materials (documents used in all kind of training actions, such as courses, for new members or grant holders training, etc.) produced by WP8 team in tasks 2-4.

Forty documents are grouped into six different categories, depending on the type of event for which the material was developed:

EURAD annual event	6 documents
External training course	6 documents
Internal meeting	2 documents
Participation to a Conference	6 documents
Participation to a Workshop	9 documents
Participation to an Event other than a Conference or a Workshop	6 documents

Each section lists the documents embedded its pdf version.

These training materials contain the state-of-the-art of nuclear fuel modelling, characterisation and evolution of nuclear fuel until disposal.

If any parts of this training material is used, it is free, but must be acknowledged to EURAD

Table of content

Glossary

ARIANE	Actinide Research In A Nuclear Element
ATF	Accident Tolerant Fuels
BDBA	Beyond Design Base Accident
BU	Burnup
BUC	Burnup Credit
BWR	Boiling Water Reactor
CIRFT	Cyclic Integrated Reversible-bending Fatigue Tester
CRAM	Chebyshev Rational Approximation Method
DA	Destructive Analysis
DBA	Basis Accidents
DBTT	Ductile-to-Brittle Transition Temperature
DDEP	Decay Data Evaluation Project
DHC	Delayed Hydride Cracking
DBRC	Doppler-Broadening Rejection Correction
EGADSNF	Expert Group on Assay Data of Spent Nuclear Fuel

EGBCC	Expert Group on Burnup Credit Criticality
ENDF	Evaluated Nuclear Data Files
EOL	End Of Life
ESARDA	European Safeguards Research and Development Association
FA	Fuel Assembly
FCCI	Fuel/Cladding Chemical Interaction
FDC	Final Disposal Canister
FEA/FEM	Finite Element Analysis/Finite Element Modelling
FIP	Fuel Integrity Project
FP	Fission Product
IAEA	International Atomic Energy Agency
ICP-SF-MS	Inductively Coupled Plasma – Sector Field – Mass Spectrometer
ICPS	Inductively Coupled Plasma Spectrometer
IE	Initial Enrichment
INL	Idaho National Laboratory

JRC	Joint Research Center
LWR	Light Water Reactor
MCNP	Monte Carlo N-Particle Transport Code
NDA	Non-Destructive Analysis
NEA	Nuclear Energy Agency
NPP	Nuclear Power Plants
ORNL	Oak Ridge National Laboratory
PGET	Passive Gamma Emission Tomography
PCI	Pellet-Cladding Interaction
PCMI	Pellet-Cladding Mechanical Interaction
PIE	Post-Irradiation Examination
PNNL	Pacific Northwest National Laboratory
PWR	Pressurised Water Reactor
RCT	Ring Compression Test
RHCF	Radial Hydride Continuity Factor
SCC	Stress Corrosion Cracking

SCIP	Studsvik Cladding Integrity Project
SNF	Spent Nuclear Fuel
SPAR	Spent fuel Performance Assessment and Research
TIMS	Thermal Ionisation Mass Spectrometer
TSC	Transport Storage Cask
UFDC	Used Fuel Disposition Campaign

EURAD Spent Fuel characterisation and evolution until disposal (SFC) training materials.

1. EURAD annual event

- Thermal power produced by spent nuclear fuel; P. Schillebeeckx, JRC Geel; EURAD Annual event 2021; 16 - 18/03/2021
- Neutrons as a signature for the characterisation of spent nuclear fuel; P. Schillebeeckx, JRC Geel; EURAD Annual event 2021; 16 - 18/03/2021
- Validation and uncertainty analysis of SNF characterization based on SCALE code system; A. Shama, NAGRA; EURAD Annual event 2021; 16 - 18/03/2021
- Fuel dry storage modelling with INL's BISON code at VTT; A. Arkoma, VTT; WP8 SFC Annual Meeting 2023; 11/1/2023
- Statistical approach for evaluating the safety of spent fuel during transport accidents; C. Aguado, F. Feria, L.E. Herranz, CIEMAT; WP8 SFC Annual Meeting 2023; 11/1/2023
- Mechanical behaviour of pre- hydrided cladding; Miguel Cristóbal-Beneyto, Jesus Ruiz-Hervias, Daniel Pérez-Gallego; WP8 SFC Annual Meeting 2023; 11/01/2023

1.1 Thermal power produced by spent nuclear fuel; P. Schillebeeckx, JRC Geel; EURAD Annual event 2021; 16 - 18/03/2021

THERMAL POWER OF SPENT NUCLEAR FUEL

17 March 2021 • Peter Schillebeeckx (EC – JRC)
WP8: Spent Fuel Characterisation

This project has received funding from the European Union's Horizon 2020 research and innovation programme 2014-2018 under grant agreement N°847593

WP8: SPENT FUEL CHARACTERISATION

How accurate can we determine the thermal power of spent nuclear fuel for transport, intermediate storage and final disposal?

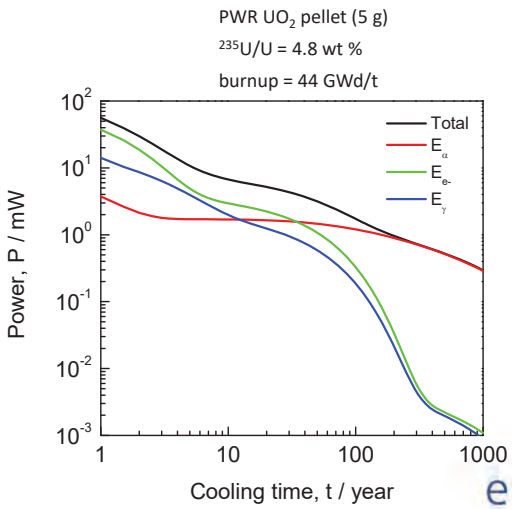

THERMAL POWER PRODUCED BY SNF

- 1 a ≤ t ≤ 10 a
  - ^{144}Ce / ^{144}Pr
  - ^{106}Ru / ^{106}Rh
  - ^{134}Cs
  - ^{90}Sr / ^{90}Y
  - ^{137}Cs / ^{137m}Ba
- 10 a ≤ t ≤ 100 a
  - ^{90}Sr / ^{90}Y
  - ^{137}Cs / ^{137m}Ba
  - ^{238}Pu
  - ^{241}Am
  - ^{244}Cm
- 100 a ≤ t
  - ^{241}Am
  - ^{238}Pu
  - $^{239,241}Pu$

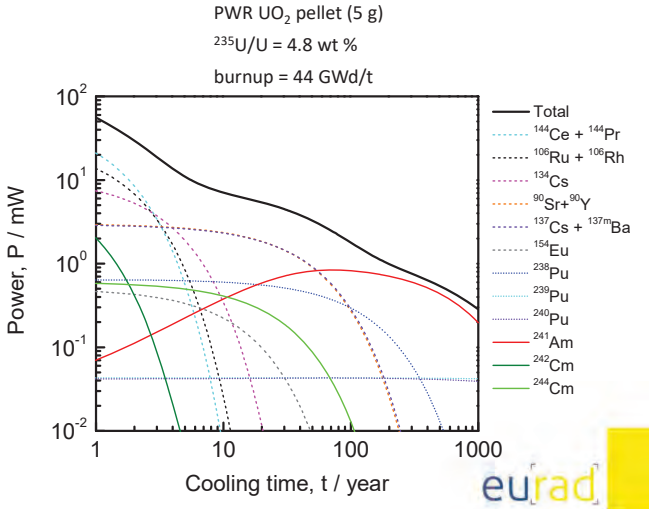

THERMAL POWER PRODUCED BY SNF

- 1 a ≤ t ≤ 10 a
  - **^{144}Ce / ^{144}Pr**
  - **^{106}Ru / ^{106}Rh**
  - **^{134}Cs**
  - ^{90}Sr / ^{90}Y
  - ^{137}Cs / ^{137m}Ba
- 10 a ≤ t ≤ 100 a
  - ^{90}Sr / ^{90}Y
  - ^{137}Cs / ^{137m}Ba
  - ^{238}Pu
  - ^{241}Am
  - ^{244}Cm
- 100 a ≤ t
  - ^{241}Am
  - ^{238}Pu
  - $^{239,241}Pu$

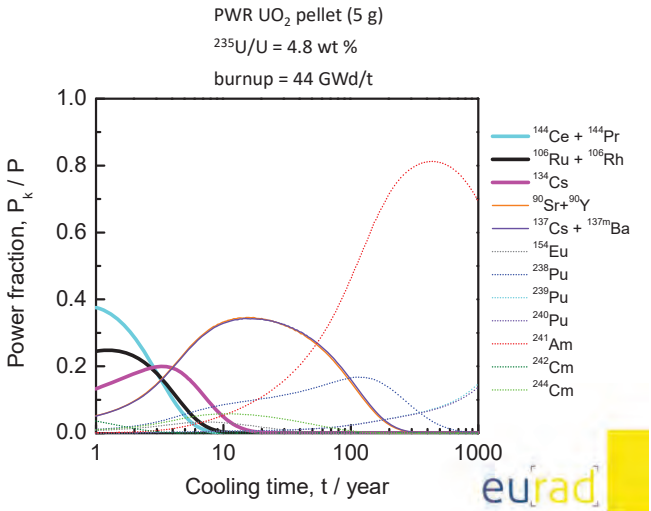

THERMAL POWER PRODUCED BY SNF

- 1 a ≤ t ≤ 10 a
  - ^{144}Ce / ^{144}Pr
  - ^{106}Ru / ^{106}Rh
  - ^{134}Cs
  - ^{90}Sr / ^{90}Y
  - ^{137}Cs / ^{137m}Ba
- 10 a ≤ t ≤ 100 a
  - **^{90}Sr / ^{90}Y**
  - **^{137}Cs / ^{137m}Ba**
  - ^{238}Pu
  - ^{241}Am
  - ^{244}Cm
- 100 a ≤ t
  - ^{241}Am
  - ^{238}Pu
  - $^{239,241}Pu$

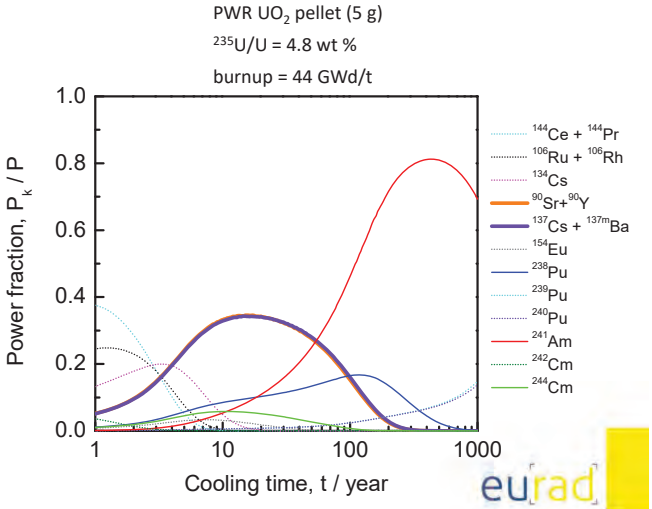

THERMAL POWER PRODUCED BY SNF

- 1 a ≤ t ≤ 10 a
  - ^{144}Ce / ^{144}Pr
  - ^{106}Ru / ^{106}Rh
  - ^{134}Cs
  - ^{90}Sr / ^{90}Y
  - ^{137}Cs / ^{137m}Ba
- 10 a ≤ t ≤ 100 a
  - ^{90}Sr / ^{90}Y
  - ^{137}Cs / ^{137m}Ba
  - ^{238}Pu
  - ^{241}Am
  - ^{244}Cm
- 100 a ≤ t
  - **^{241}Am**
  - ^{238}Pu
  - $^{239,241}Pu$

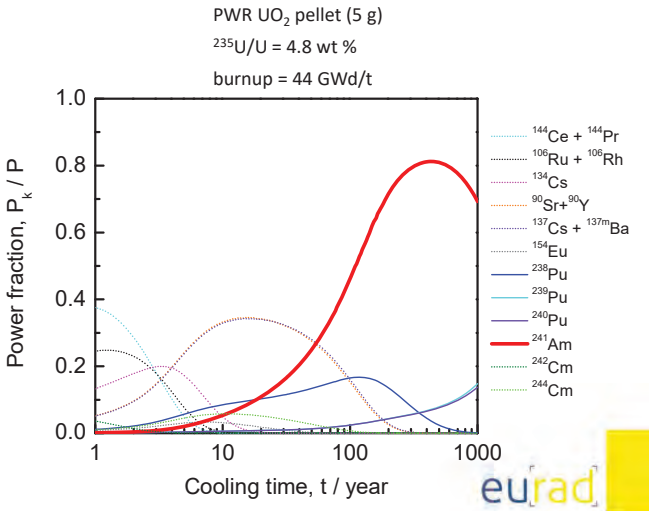

THERMAL POWER PRODUCED BY SNF

$$P(t) = \sum_k p_k N_k(t)$$

t: cooling time or time after end of irradiation

$P(t_2 > t_1)$ cannot be extrapolated from $P(t_1)$

$N_k(t)$: nuclide inventory at time t

- $N_k(t_0)$: nuclide inventory at time t_0 with $t > t_0$
- Nuclide inventory at **$t > t_0$**

$$\frac{dN_k}{dt} = \sum_i \lambda_i N_i - \lambda_k N_k$$

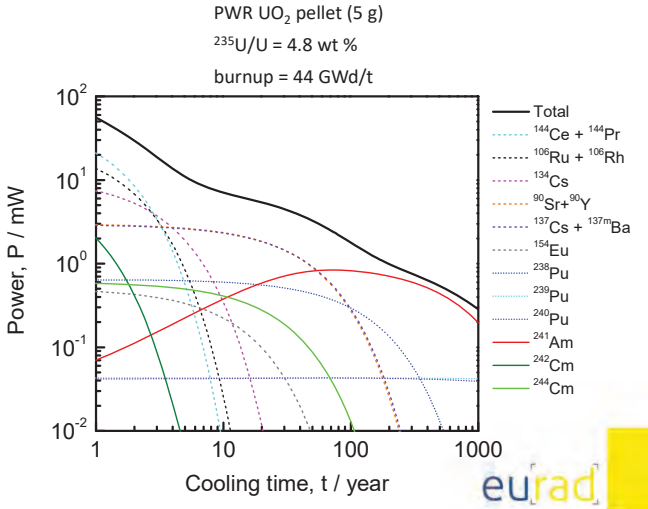

17/03/2021 EURAD Annual Event 2021

THEORETICAL CALCULATIONS OF NUCLIDE INVENTORY

Burnup code: coupled neutron transport – nuclide depletion/creation calculations

Neutron transport

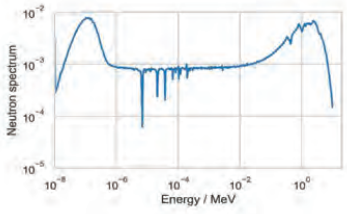

Bateman equation

$$\frac{dN_k}{dt} = Y N_f \sigma_f \varphi + \sum_i \lambda_i N_i + \sum_j \sigma_j N_j \varphi - (\lambda_k + \sigma_{k,a}\varphi) N_k$$

Update nuclide vector

17/03/2021 EURAD Annual Event 2021

BURNUP CALCULATIONS

Nuclear data
- Cross sections: (n,γ), (n,f), …
- Fission Yields
- Decay data
  - Half-lives
  - Emission probabilities
  - Recoverable energy

SNF input data
- Fuel properties
  - design
  - material data (IE)
- Operational history
  - burn-up (BU)
  - cooling time (CT)
  - …

Burnup code

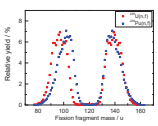

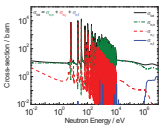

Nuclide inventory
Source terms
- Power (P, u_p)
- Neutron emission
- …

BURNUP CALCULATIONS

Nuclear data
- Cross sections: (n,γ), (n,f), …
- Fission Yields
- Decay data
  - Half-lives
  - Emission probabilities
  - Recoverable energy

SNF input data
- Fuel properties
  - design
  - material data (IE)
- Operational history
  - burn-up (BU)
  - cooling time (CT)
  - …

Burnup code

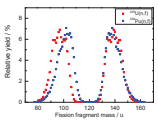

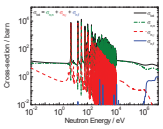

Nuclide inventory
Source terms
- **Power (P, u_p)**
- Neutron emission
- …

Ilas et al., Nucl. Eng. Des. 319 (2017) 176
u_p/P = 1.3%, is this realistic?

Data set	Data set	Uncertainty (1σ) (%)
Modeling data	Fuel design	0.20
	Operating data	0.85
	Total	0.87
Nuclear data	Cross sections	0.88
	Fission yields	0.26
	Total	0.92
Overall effect	Total	1.27

PRODUCTION OF ^{137}Cs

$$\frac{dN_k}{dt} = Y\, N_f\, \sigma_f\, \varphi + \sum_i \lambda_i N_i + \sum_j \sigma_j N_j\, \varphi - (\lambda_k + \sigma_{k,a}\varphi) N_k$$

$$n + {}^{235}_{92}U \rightarrow {}^{97}_{40}Zr + {}^{13}_{52}Te + 2n$$

$${}^{137}_{52}Te \rightarrow {}^{13}_{53}I + e^- + \bar{\nu}_e$$

$${}^{137}_{53}I \rightarrow {}^{137}_{54}Xe + e^- + \bar{\nu}_e$$

$${}^{137}_{54}Xe \rightarrow {}^{13}_{55}Cs + e^- + \bar{\nu}_e$$

^{137}Cs production: only by (n,f) followed by β^- (decay of short lived precursors)

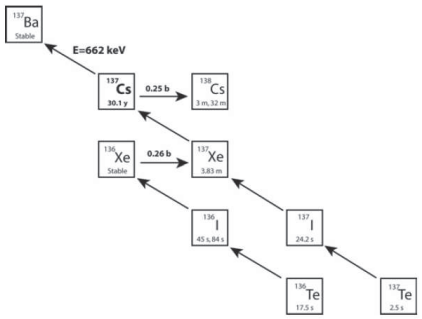

PRODUCTION OF ^{137}Cs

$$\frac{dN_k}{dt} = Y\, N_f\, \sigma_f\, \varphi + \sum_i \lambda_i N_i + \sum_j \sigma_j N_j\, \varphi - (\lambda_k + \sigma_{k,a}\varphi) N_k$$

$$N_k(t') \approx \frac{Y_c\, \sigma_f\, N_f\, \varphi}{\lambda_k + \sigma_{k,\gamma}\, \varphi} \left[1 - e^{-(\lambda_k + \sigma_{k,\gamma}\varphi)t'}\right]$$

$$(\lambda_k + \sigma_{k,\gamma}\, \varphi) << 1$$

$$N_k(t') \approx Y_c\, \sigma_f\, N_f\, \varphi\, t'$$

t' : irradiation time

Y_c : cumulative fission yield (nuclear data)
σ_f : fission cross section (nuclear data)
N_f : number of fissile nuclei, i.e. ^{235}U (fuel properties)
$\varphi t'$: total neutron fluence (operation history)

^{137}Cs production: only by (n,f) followed by β^- (decay of short lived precursors)

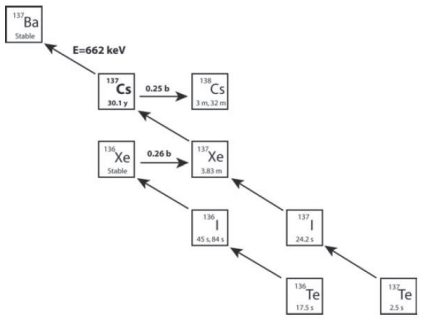

PRODUCTION OF ^{137}Cs DURING REACTOR OPERATION

$$\frac{dN_k}{dt} = Y\,N_f\,\sigma_f\,\varphi + \sum_i \lambda_i N_i + \sum_j \sigma_j N_j\,\varphi - (\lambda_k + \sigma_{k,a}\varphi)N_k$$

$$N_k(t') \approx \frac{Y_c\,\sigma_f\,N_f\,\varphi}{\lambda_k + \sigma_{k,\gamma}\,\varphi}\left[1 - e^{-(\lambda_k+\sigma_{k,\gamma}\varphi)t'}\right]$$

$$(\lambda_k + \sigma_{k,\gamma}\,\varphi) << 1$$

$$N_k(t') \approx Y_c\,\sigma_f\,N_f\,\varphi\,t'$$

$(\sigma_f\,N_f\,\varphi\,t')$: total number of fissions

$(\sigma_f\,N_f\,\varphi\,t')$ x E_f : time integrated reactor power

E_f = recoverable energy per fission

$$N_k(t_0) \propto Y_c\,BU$$

$\Rightarrow N_k(t_0) \propto BU$

^{137}Cs production: only by (n,f) followed by β^- (decay of short lived precursors)

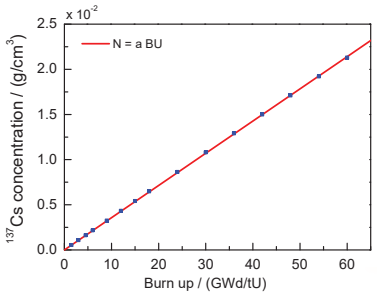

17/03/2021 EURAD Annual Event 2021 13

PRODUCTION OF THERMAL POWER BY ^{137}Cs

Thermal power by ^{137}Cs at t (cooling time):

$$P_k(t) = p_k\,N_k(t_0)\,e^{-\lambda_k\,(t-t_0)}$$ t_0 : end of irradiation

- Production: ^{137}Cs inventory at end of irradiation

  $N_k(t_0) \propto Y_c\,BU$

  - Y_c : cumulative fission yield for ^{137}Cs
  - BU : burnup

- Decay : (λ_k , E_{dk}) $p_k = E_{dk}\,\lambda_k$
  - λ_k : decay constant
  - E_{dk} : recoverable energy

Production

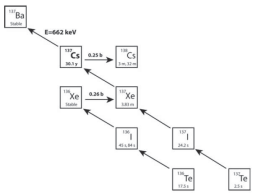

Decay

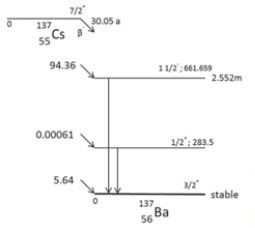

17/03/2021 EURAD Annual Event 2021 14

PRODUCTION OF THERMAL POWER BY ^{137}Cs

Thermal power by ^{137}Cs at t (cooling time):

$P_k(t) = p_k\, N_k(t_0)\; e^{-\lambda_k (t-t_0)}$ t_0 : end of irradiation

- Production: ^{137}Cs inventory at end of irradiation

  $N_k(t_0) \propto Y_c\, BU$

  – Y_c : cumulative fission yield for ^{137}Cs
  – BU : burnup

- Decay : (λ_k , E_{dk}) $p_k = E_{dk}\, \lambda_k$

  – λ_k : decay constant
  – E_{dk} : recoverable energy

Production

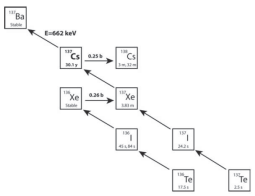

Decay

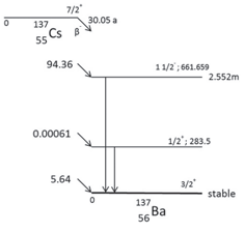

CONTRIBUTION TO THERMAL POWER FROM ^{137}Cs AND ^{90}Sr

$P_k(t) = p_k\, N_k(t_0)\; e^{-\lambda_k (t-t_0)}$ $N_k(t_0) \propto Y_c\, BU$ $p_k = E_{dk}\, \lambda_k$

$$\Rightarrow \frac{u_{P_k}}{P_k} = = \sqrt{\left(\frac{u_{BU}}{BU}\right)^2 + \left(\frac{u_{Y_c}}{Y_c}\right)^2 + \left(\frac{u_{E_{dk}}}{E_{dk}}\right)^2}$$

- Operational history: BU

- Nuclear data : (Y_c, E_{dk}) $p_k = E_{dk}\, \lambda_k$

  – λ_k : decay constant
  – E_{dk} : recoverable energy

Note: contribution of ^{137}Cs and ^{90}Sr are simple cases, in addition, with rather well determined nuclear data
e.g. ^{134}Cs production $\propto$ BU^b with b ~ 2 $\Rightarrow \frac{u_{N_k}}{N_k} = 2\frac{u_{BU}}{BU}$

NUCLEAR DATA (Y_c,E_d): ^{137}Cs

$T_{1/2}$ = 30.05 (8) a

	^{137}Cs					
Library	E_d / keV	Ratio	100 x Y_c	Ratio	(Y_c x E_d) / keV	Ratio
DDEP/IAEA	811.8 (18)	1	6.221 (69)	1	50.5 (6)	1
JEF-2.2	812.0 (69)	1.000 (8)	6.244 (54)	1.004 (9)	50.7 (6)	1.004 (12)
JEFF-3.1.1	**810.1 (23)**	**0.998 (3)**	**6.221 (69)**	**1.000 (11)**	**50.4 (6)**	**0.998 (11)**
JEFF-3.3	**801.8 (23)**	**0.988 (3)**	**6.090 (63)**	**0.979 (10)**	**48.8 (5)**	**0.967 (10)**
ENDF/B-VI.8	813.4 (41)	1.002 (5)	6.188 (31)	0.995 (5)	50.3 (4)	0.997 (7)
ENDF/B-VII.0	805.7 (16)	0.992 (2)	6.188 (31)	0.995 (5)	49.9 (3)	0.987 (5)
ENDF/B-VIII.0	**805.8 (18)**	**0.993 (2)**	**6.188 (31)**	**0.995 (5)**	**49.9 (3)**	**0.987 (5)**

NUCLEAR DATA (Y_c,E_d): ^{90}Sr

$T_{1/2}$ = 28.80 (7) a

	^{90}Sr					
Library	E_d / keV	Ratio	100 x Y_c	Ratio	(Y_c x E_d) / keV	Ratio
DDEP/IAEA	1129.4 (14)	1	5.730 (130)	1	64.7 (15)	1
JEF-2.2	1129.6 (7)	1.000 (1)	**5.847 (188)**	**1.020 (33)**	**66.0 (21)**	**1.021 (33)**
JEFF-3.1.1	1107.8 (13)	0.981 (1)	5.729 (132)	1.000 (23)	63.5 (15)	0.981 (23)
JEFF-3.3	1127.3 (13)	0.998 (1)	**5.676 (131)**	**0.991 (23)**	**64.0 (15)**	**0.989 (23)**
ENDF/B-VI.8	1129.9 (12)	1.000 (1)	5.782 (58)	1.009 (10)	65.3 (7)	1.010 (10)
ENDF/B-VII.0	1129.4 (13)	1.000 (1)	5.782 (58)	1.009 (10)	65.3 (7)	1.009 (10)
ENDF/B-VIII.0	1128.8 (11)	0.999 (1)	**5.782 (58)**	**1.009 (10)**	**65.3 (7)**	**1.009 (10)**
Ramthun (Exp. 1976)	**1147.0 (90)**					

NUCLEAR DATA (Y_c,E_d): ^{90}Sr and ^{137}Cs

Library	^{90}Sr		^{137}Cs	
	(E_d x Y_c) / keV	Ratio	(Y_c x E_d) / keV	Ratio
DDEP/IAEA	64.7 (15)	1	50.5 (6)	1
JEF-2.2	**66.0 (21)**	**1.021 (33)**	**50.7 (7)**	**1.004 (12)**
JEFF-3.1.1	63.5 (15)	0.981 (23)	50.4 (6)	0.998 (11)
JEFF-3.3	**64.0 (15)**	**0.989 (23)**	**48.8 (5)**	**0.967 (10)**
ENDF/B-VI.8	65.3 (7)	1.010 (10)	50.3 (4)	0.997 (7)
ENDF/B-VII.0	65.3 (7)	1.009 (10)	49.9 (3)	0.987 (5)
ENDF/B-VIII.0	**65.3 (7)**	**1.009 (10)**	**49.9 (3)**	**0.987 (5)**

CONCLUSIONS

- Prediction of thermal power of SNF strongly depends on
  - Nuclear data
  - Operational history
- u_P/P = 1.3 % : not realistic

⇒ WP8: Spent fuel characterisation until final disposal

"Define best practice procedures to determine thermal power with realistic confidence limits"

1.2 Neutrons as a signature for the characterisation of spent nuclear fuel; P. Schillebeeckx, JRC Geel; EURAD Annual event 2021; 16 - 18/03/2021

Neutrons as a signature for the characterisation of spent nuclear fuel

18 March 2021 • Peter Schillebeeckx (EC – JRC)
WP8: Spent Fuel Characterisation

This project has received funding from the European Union's Horizon 2020 research and innovation programme 2014-2018 under grant agreement N°847593

SPENT NUCLEAR FUEL (SNF): INTERMEDIATE STORAGE OR FINAL DISPOSAL

A **safe**, **secure**, **ecological** and **economical** transport, storage and final disposal requires that **SNF** is **characterised** for the main source terms of interest:

- Decay Heat
- Neutron emission
- γ-ray emission
- Reactivity
  (fissioning nuclides + nuclides with high neutron absorption cross sections for BUC)
- Fissile material (Nuclear Safeguards)
- Specific long-lived radionuclides for long term safety
  (e.g. ^{14}C, ^{79}Se, ^{94}Nb, ^{99}Tc, ^{129}I, ^{226}Ra)



⇒ Requires a **nuclide inventory** that can only be determined by **theoretical calculations**

THEORETICAL CALCULATIONS OF NUCLIDE INVENTORY

Burnup code: coupled neutron transport – nuclide depletion/creation calculations

Neutron transport

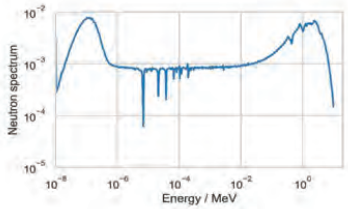

Bateman equation

$$\frac{dN_k}{dt} = Y N_f \sigma_f \varphi + \sum_i \lambda_i N_i + \sum_j \sigma_j N_j \varphi - (\lambda_k + \sigma_{k,a}\varphi) N_k$$

Update nuclide vector

18/03/2021 EURAD Annual Event 2021 3

BURNUP CALCULATIONS

Verify by NDA experiments:
- Gamma-ray
- **Neutron**

Nuclear data
- Cross sections: (n,γ), (n,f), …
- Fission Yields
- Decay data
  - Half-lives
  - Emission probabilities
  - Recoverable energy

Burnup code

SNF input data
- Fuel properties
  - design
  - material data (IE)
- Operational history
  - burn-up (BU)
  - irradiation cycles
  - cooling time (CT)
  - …

Source terms
- Power
- Neutron emission
- …

18/03/2021 EURAD Annual Event 2021 4

NEUTRON EMISSION OF SNF

PWR UO_2 pellet (5 g)

$^{235}U/U$ = 4.8 wt %

burnup = 44 GWd/t

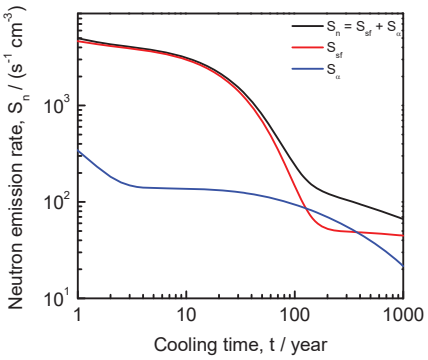

$$S_n(t) = \sum_k (s_{sf,k} + s_{\alpha n,k})\, N_k(t)$$

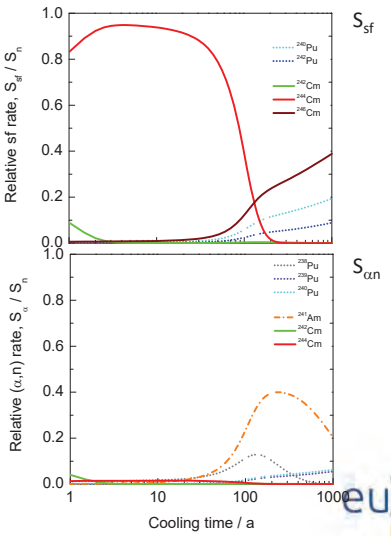

NEUTRON EMISSION OF SNF

- **Neutron emission** rate: main contribution due to **^{244}Cm(sf)**
- **^{244}Cm inventory** depends on **operational history**

⇒ **Neutron measurement** provides information about **operational history**

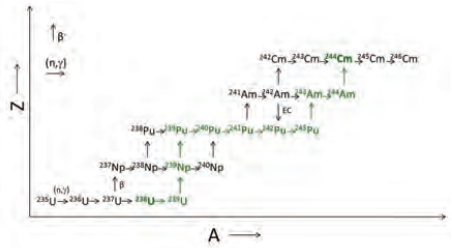

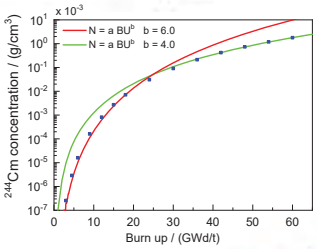

VERIFICATION OF SNF INPUT DATA BY NEUTRON MEASUREMENTS

Neutron based NDA **measurements** of **SNF assemblies**

Nuclear safeguards: DOE (NGSI), IAEA, EURATOM

- Total neutron emission rate (Fork) : routine inspections
- Passive Neutron Albedo Reactivity (**PNAR**) : Finland
- Differential Die Away Self-Interrogation (**DDSI**) : Sweden

PNAR and **DDSI: also** sensitive to **neutron multiplication**

PNAR: Tupasela et al., NIMA 986 (2021) 164707

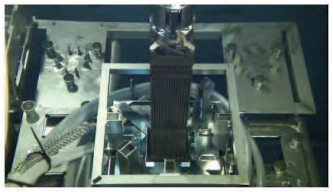

DDSI: Trahan et al., NIMA 955 (2020) 1643329

18/03/2021 EURAD Annual Event 2021 7

BURNUP CALCULATIONS

Nuclear data
- Cross sections: (n,γ), (n,f), …
- Fission Yields
- Decay data
  - Half-lives
  - Emission probabilities
  - Recoverable energy

Burnup code

SNF input data
- Fuel properties
  - design
  - material data (IE)
- Operational history
  - burn-up (BU)
  - cooling time (CT)
  - …

Validate by experiment

Source terms
- Power
- **Neutron emission**
- …

18/03/2021 EURAD Annual Event 2021 8

ABSOLUTE MEASUREMENT OF NEUTRON EMISSION RATE OF A SNF SAMPLE

- Procedure to **transfer SNF** segment **sample** from hot cell **to neutron detection system**
  - Based on a multi-layer barrier encapsulation making use of special features of hot cell facilities at SCK•CEN (LHMA)

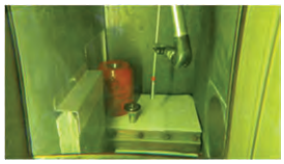
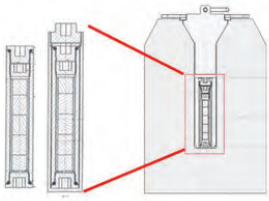

- **Absolute** determination of **neutron emission rate** by NDA in **standard controlled area conditions** using **conventional well-counter** for nuclear safeguards applications

SELECTION AND CHARACTERISATION OF SNF SEGMENT SAMPLE

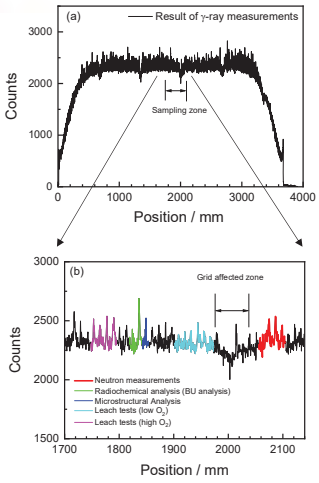

- Irradiation history of the SNF
  - Segment (~50 mm) from rod of a PWR Assembly
  - PWR (15 x 15): 188 UO_2 rod (4.5 wt% $^{235}U/U$) and 16 $(U,Gd)O_2$ rods
  - Irradiated at Tihange 1 (BE)
  - Rod used for other international project (First-Nuclides, REGAL, WETFUEL & AGAF, SF-ALE)
- SNF segment sample characteristics

  Part of a set of 4 samples (**REGAL project**)
  - **Radiochemical analysis (BU)**
  - Microstructural analysis
  - Leach tests (low O_2)
  - Leach tests (high O_2)

EURAD – SFC (NDA): neutron measurements

SELECTION AND CHARACTERISATION OF SNF SEGMENT SAMPLE

- SNF segment sample: nuclide inventory and BU

BU indicator	Nuclide inventory mg/g	Burnup GWd/t
^{137}Cs	1.288 (30)	52.6 (10)
^{143}Nd + ^{144}Nd	3.029 (32)	53.0 (6)
^{143}Nd + ^{144}Nd	1.962 (21)	53.1 (6)
^{148}Nd	0.534 (12)	53.3 (12)
^{150}Nd	0.257 (11)	52.2 (23)
Average		**52.8 (4)**

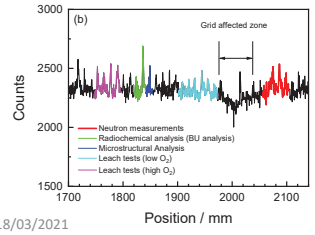

- SNF segment sample: characteristics

Parameter	Value
Length	52.01 (4) mm
Segment weight	42.616 (1) g
Cladding weight	6.71 (4) g
Net fuel weight	35.91 (4) g

18/03/2021 EURAD Annual Event 2021 11

RESULTS AND COMPARISON WITH THEORETICAL CALCULATIONS

- Neutron emission rate determined by absolute neutron measurements

  S_{sf} = 682 (10) $s^{-1}g^{-1}$ $S_{\alpha n}$ = 25 (10) $s^{-1}g^{-1}$

- Comparison with theoretical calculations

Code	Library	(α,n) Method	(α,n) Library	S_{sf} / ($g^{-1}s^{-1}$)	S_α / ($g^{-1}s^{-1}$)	Calculation/Experiment S_{sf}	Calculation/Experiment $S_{\alpha n}$
SCALE	ENDF/B-VII.1	Y(α,n)		665	11.8	0.974	0.48
SERPENT(1)	ENDF/B-VII.1	Y(α,n)		662	14.2	0.971	0.58
SERPENT(2)	**ENDF/B-VII.1**	Y(α,n)		694	14.2	**1.017**	0.58
	ENDF/B-VIII.0	Y(α,n)		692	14.1	**1.013**	0.57
	JEFF-3.1.2	Y(α,n)		629	13.2	0.922	0.56
	JEFF-3.3	Y(α,n)		658	13.8	0.964	0.56
	JEFF-4T0	Y(α,n)		695	13.7	**1.018**	0.56
ALEPH28	ENDF/B-VIII.0	σ(α,n)	TENDL2015	660	26.5	0.968	1.08
		σ(α,n)	JENDL_AN/500		22.4		0.91
	JEFF-3.3	σ(α,n)	TENDL2015	641	28.1	0.940	1.14
		σ(α,n)	JENDL_AN/500		23.9		0.97

18/03/2021 EURAD Annual Event 2021 12

RESULTS AND COMPARISON WITH THEORETICAL CALCULATIONS

- Neutron emission rate determined by absolute neutron measurements

  S_{sf} = 682 (10) $s^{-1}g^{-1}$ $S_{\alpha n}$ = 25 (10) $s^{-1}g^{-1}$

- Comparison with theoretical calculations

Code	Library	(α,n)		S_{sf} / ($g^{-1}s^{-1}$)	S_{α} / ($g^{-1}s^{-1}$)	Calculation/Experiment	
		Method	Library			S_{sf}	$S_{\alpha n}$
SCALE	ENDF/B-VII.1	Y(α,n)		665	11.8	0.974	0.48
SERPENT(1)	ENDF/B-VII.1	Y(α,n)		**662**	14.2	**0.971**	0.58
SERPENT(2)	ENDF/B-VII.1	Y(α,n)		**694**	14.2	**1.017**	0.58
	ENDF/B-VIII.0	Y(α,n)		692	14.1	1.013	0.57
	JEFF-3.1.2	Y(α,n)		629	13.2	0.922	0.56
	JEFF-3.3	Y(α,n)		658	13.8	0.964	0.56
	JEFF-4T0	Y(α,n)		695	13.7	1.018	0.56
ALEPH28	ENDF/B-VIII.0	σ(α,n)	TENDL2015	660	26.5	0.968	1.08
		σ(α,n)	JENDL_AN/500		22.4		0.91
	JEFF-3.3	σ(α,n)	TENDL2015	641	28.1	0.940	1.14
		σ(α,n)	JENDL_AN/500		23.9		0.97

RESULTS AND COMPARISON WITH THEORETICAL CALCULATIONS

- Neutron emission rate determined by absolute neutron measurements

  S_{sf} = 682 (10) $s^{-1}g^{-1}$ $S_{\alpha n}$ = 25 (10) $s^{-1}g^{-1}$

- Comparison with theoretical calculations

Code	Library	(α,n)		S_{sf} / ($g^{-1}s^{-1}$)	S_{α} / ($g^{-1}s^{-1}$)	Calculation/Experiment	
		Method	Library			S_{sf}	$S_{\alpha n}$
SCALE	ENDF/B-VII.1	**Y(α,n)**		665	11.8	0.974	**0.48**
SERPENT(1)	ENDF/B-VII.1	**Y(α,n)**		662	14.2	0.971	**0.58**
SERPENT(2)	ENDF/B-VII.1	**Y(α,n)**		694	14.2	1.017	**0.58**
	ENDF/B-VIII.0	**Y(α,n)**		692	14.1	1.013	**0.57**
	JEFF-3.1.2	**Y(α,n)**		629	13.2	0.922	**0.56**
	JEFF-3.3	**Y(α,n)**		658	13.8	0.964	**0.56**
	JEFF-4T0	**Y(α,n)**		695	13.7	1.018	**0.56**
ALEPH28	ENDF/B-VIII.0	**σ(α,n)**	TENDL2015	660	26.5	0.968	**1.08**
		σ(α,n)	JENDL_AN/500		22.4		**0.91**
	JEFF-3.3	**σ(α,n)**	TENDL2015	641	28.1	0.940	**1.14**
		σ(α,n)	JENDL_AN/500		23.9		**0.97**

SUMMARY AND OUTLOOK

- Absolute **neutron emission rate measurements** of SNF sample with **uncertainty < 2%** in **standard controlled area conditions**
  - **Calculated S_{sf}** with latest libraries (ENDF/B-VIII.0, JEFF-4T0): **within experimental uncertainty**
  - **Differences** in S_{sf} only due to methodology can be **about 5 %**
  - Calculated $S_{\alpha n}$: best agreement by including **α- transport**

- Development of **optimised neutron counter** and **transfer container**
  Increased detection efficiency and reduced γ-ray sensitivity
  - **Reduce uncertainty of** both S_{sf} and $S_{\alpha n}$
  - **Broader application range**:
    MOX, short cooling times, low burnup, end of rod, …

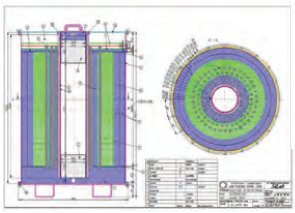

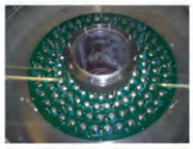

18/03/2021 EURAD Annual Event 2021 15

THANK YOU FOR YOUR ATTENTION

- JRC Geel (BE) and Ispra (IT)
  G. Alaerts, J. Paepen, P. Schillebeeckx, R. Wynants, G. Žerovnik* (JRC Geel)
  B. Pedersen, G. Varasano (JRC Ispra)
- SCK CEN (BE)
  K. Govers**, N. Messaoudi, Y. Parthoens, P. Romojaro, A. Stankovskiy, M. Verwerft

*JSI (SI)
**FANC (BE)

18/03/2021 EURAD Annual Event 2021 16

1.3 Validation and uncertainty analysis of SNF characterization based on SCALE code system; A. Shama, NAGRA; EURAD Annual event 2021; 16 - 18/03/2021

Validation and Uncertainty Analyses of SNF Characterization based on SCALE Code System

EURAD WP8/Subtask 2.1

A. Shama (EPFL / Switzerland), 17.03.2021

1

Nagra's activities in WP8/Subtask 2.1

- Subtask 2.1: Theoretical study of SNF source terms
- Subtask leader: PSI
- Contributors: CIEMAT, JSI, NAGRA, PSI, SCK.CEN, VTT, KIT, JRC-Geel, ENRESA
- **Nagra's activities:**

  (1) Selection of SNF benchmarks (decay heat / nuclide inventory)

  (2) Modelling of SNF benchmarks

  Comparison with existing measurements:
  - Calculations using simplified assumptions and modelling
  - Calculations using advanced method

  (3) Uncertainty propagation

  Estimate uncertainties of different origins:
  - Nuclear Data (ND)
  - SNF design and irradiation

  (4) Identification of parameters contributing to uncertainties

2

1. Selection of SNF benchmarks

SNF Decay Heat calorimetric measurements	1. Clab PWR 0E2
	2. Clab BWR 6432

SNF Nuclide Inventory PIE samples	1. Takahama SF95-5
	2. KKB BM1
	3. Gundremmingen-7
	4:11. ENRESA 1:8

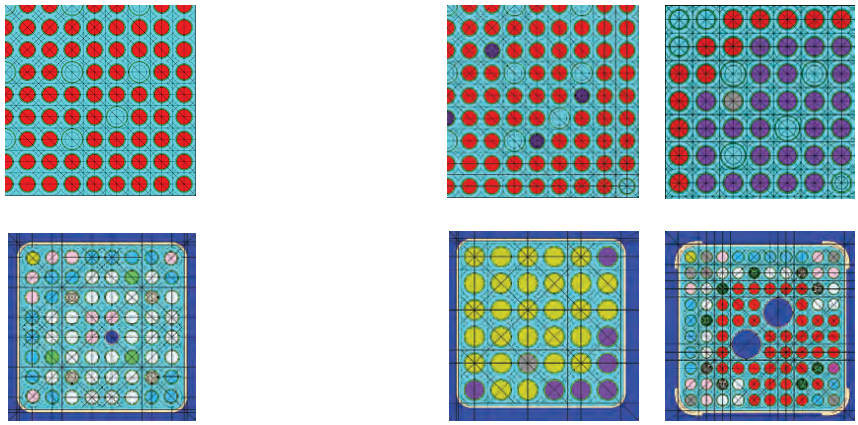

3

nagra.

2. Modelling of SNF benchmarks

Comparison with existing measurements:

- Calculations using simplified assumptions/modelling
  - ORIGEN, prepared one-group XS libraries
- Calculations using advanced method
  - Polaris, 2D lattice code with multi-group XS libraries

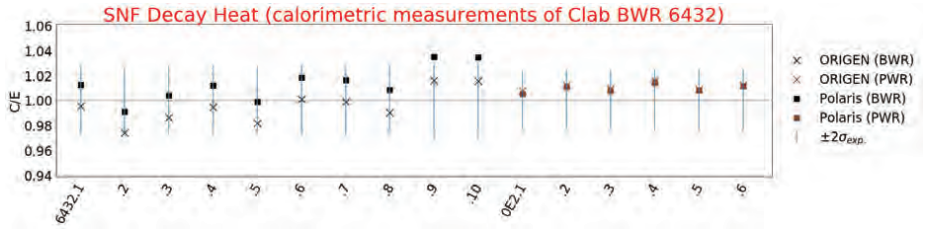

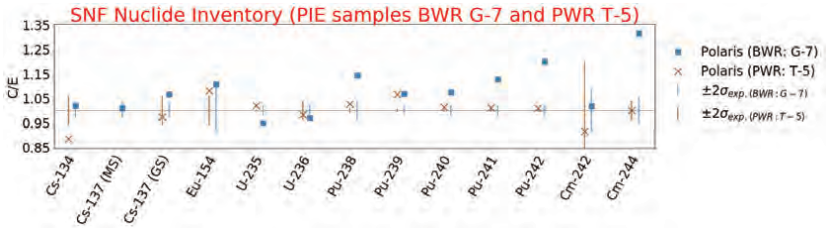

4

nagra.

3. Uncertainty Propagation

Estimate uncertainties of different origins:

- Nuclear Data (ND)
  - Cross-sections, Fission-yield, Decay Data: SCALE data based on ENDF/B-VII.1
- SNF design and irradiation
  - Material, geometrical, operational (whenever provided by operators and fuel vendors)
  - NEA/NSC "Evaluation Guide for the Evaluated Spent Nuclear Fuel Assay Database (SFCOMPO)"

Parameter	1 σ
Clad thickness	16.7 µm
Clad diameter	67/100 µm (PWR/BWR)
Pellet density	0.67%
Pellet diameter	6.7 µm
U-235 wt.%	0.0167%
SFA powers	1.67%
Water temp. (PWR)	2 K
Water density (PWR)	0.005 g/cm^3
Void fraction (BWR)	6%
Fuel temp.	50 K
Boron (PWR)	10 ppm

Based on [NEA/NSC, 2015]

5

nagra.

3. Uncertainty Propagation

Estimate uncertainties of different origins:

- Nuclear Data (ND)
- SNF design and irradiation

Decay Heat of Clab BWR 6432

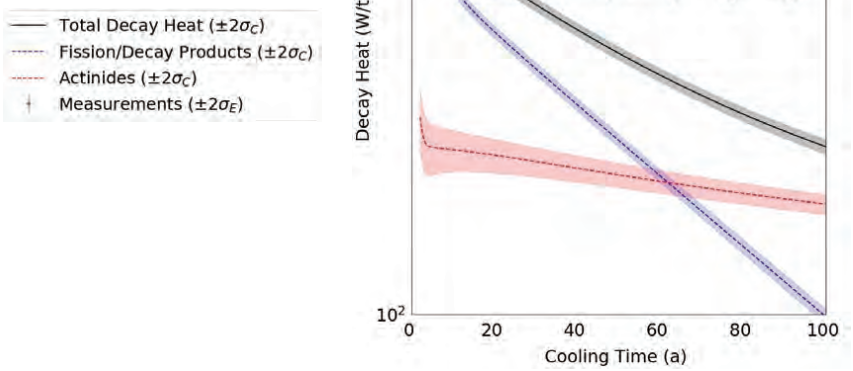

6

nagra.

3. Uncertainty Propagation

Estimate uncertainties of different origins:

- Nuclear Data (ND)
- SNF design and irradiation

Nuclide conc. in Gundremmingen (BWR) B23 – E3 sample

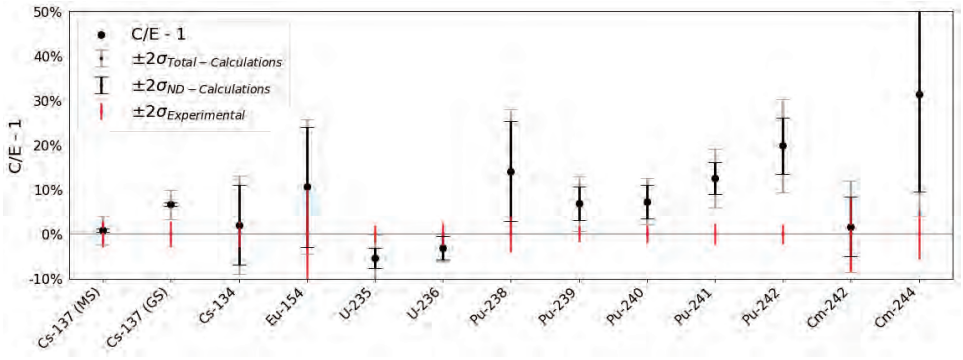

7

nagra.

4. Identification of relevant parameters contributing to uncertainties

Nuclear Data:

by analyzing fractional variances

XS: Cross-sections
FY: Fission yield
DY: Decay
ND: Nuclear Data
DO: Design and Operation

$\sigma^2_{Total} = \sigma^2_{ND} + \sigma^2_{DO}$ $\sigma^2_{ND} = \sigma^2_{XS} + \sigma^2_{FY} + \sigma^2_{DY}$

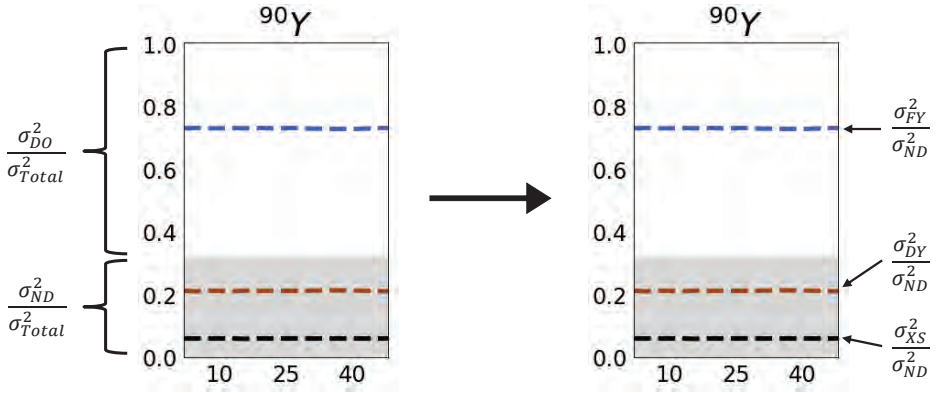

8

nagra.

4. Identification of relevant parameters contributing to uncertainties

Nuclear Data:

by analyzing fractional variances

$\sigma^2_{Total} = \sigma^2_{ND} + \sigma^2_{DO}$ $\sigma^2_{ND} = \sigma^2_{XS} + \sigma^2_{FY} + \sigma^2_{DY}$

XS: Cross-sections
FY: Fission yield
DY: Decay
ND: Nuclear Data
DO: Design and Operation

Decay Heat of Clab BWR 6432

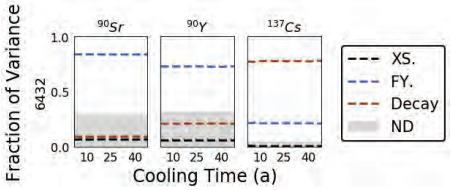

Nuclide conc. in Gundremmingen B23 – E3 sample

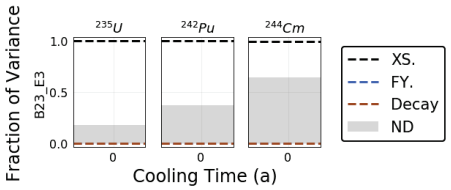

9

nagra.

4. Identification of parameters contributing to uncertainties

Model Parameters:

Correlation Analysis
Decay Heat of Clab PWR 0E2 and BWR 6432

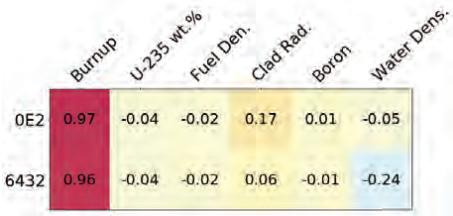

Correlation Analysis
Nuclide conc. in Gundremmingen B23 – E3 sample

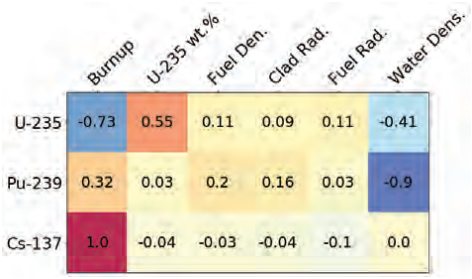

10

nagra.

Publications

(1) Related to SNF decay heats

- **Accepted** in Nuclear Engineering and Technology
  "Uncertainty Analyses of Spent Nuclear Fuel Decay Heat Calculations using SCALE Modules"
- **Submitted** to Annals of Nuclear Energy
  "Validation of Spent Nuclear Fuel Decay Heat Calculations Using Polaris, TRITON/ORIGEN-ARP and CASMO5"

(2) Related to SNF nuclide concentration

- **Planned**

11 nagra.

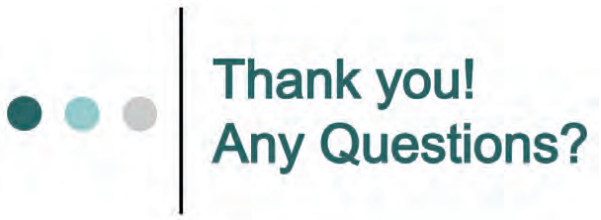

12 nagra.

Appendix

(1) Area of Applicability (AOA)

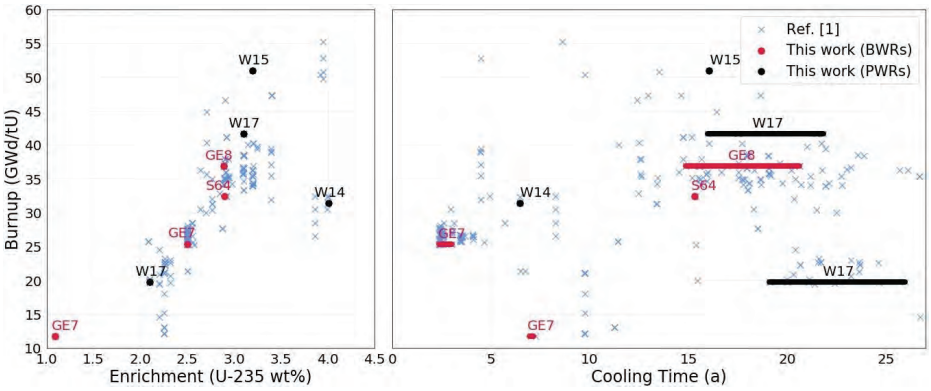

Burnups, enrichments, and cooling times of the selected SFAs

nagra.

Appendix

(2) Uncertainties of the Measurements

Table 1. Uncertainties (2σ) in the decay heat measurements at the Clab facility based on [15].

SFA	Power (W)	Uncertainty (W)	Uncertainty (%)
BWR	50	4.2	8.4
	350	6.2	1.8
PWR	250	9.2	3.7
	900	18.8	2.1

Table 2. Uncertainties (2σ) in the decay heat measurements at the GE-Morris facility based on [5]. The values correspond to both PWRs and BWRs.

SFA	Power (W)	Uncertainty (W)	Uncertainty (%)
GE	200	16	8
	700	28	4

nagra.

Appendix

(3) Hypothesis Testing on Calc. and Meas.

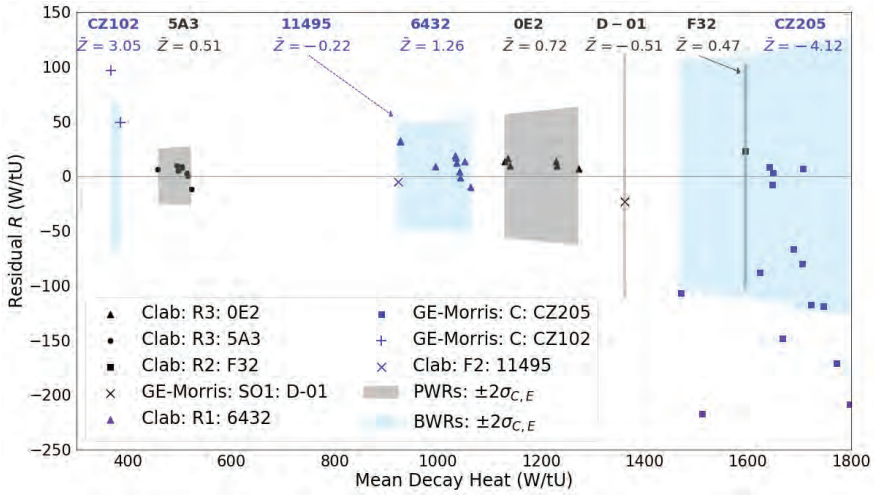

Mean-difference plot of calculations and measurements along with shaded total uncertainty band. Combined z-scores are shown for each SFA (top).

15

nagra.

Appendix

(4) Uncertainties Components

	Burnup (GWd/tU)	Cooling time (a)	Decay heat (W/tU)	Meas.	Calc.	Total
				(2σ) %		
PWRs	51.0	16.1	1595	2.3	5.6	6.1
BWRs	36.9	16.6	1015	2.8	4.6	5.4

	Burnup (GWd/tU)	Cooling time (a)	Decay heat (W/tU)	Calc.	ND	DO
				(2σ) %		
PWRs	51.0	16.1	1595	5.6	3.1	4.7
BWRs	36.9	16.6	1015	4.6	1.8	4.2

16

nagra.

Appendix

(5) Validation (Clab)

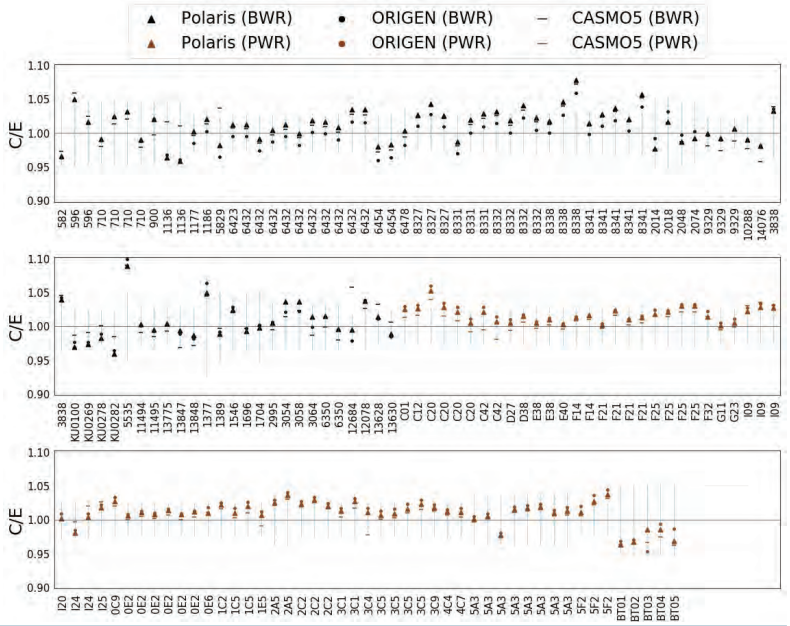

17

nagra.

Appendix

(5) Validation (GE and HEDL)

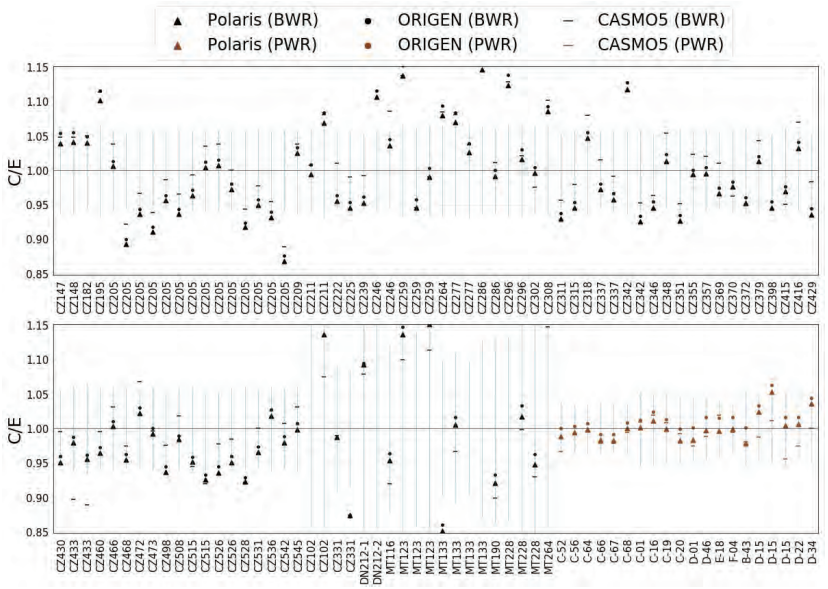

18

nagra.

1.4 Fuel dry storage modelling with INL's BISON code at VTT; A. Arkoma, VTT; WP8 SFC Annual Meeting 2023; 11/1/2023

THERMO-MECHANICAL PROPERTIES OF THE SNF CLADDING: CREEP MODELLING WITH THE BISON CODE

1 November 2023 • Asko Arkoma (VTT)

This project has received funding from the European Union's Horizon 2020 research and innovation programme under grant agreement N°847593.

Outline

- Background for the investigation
- Applied simulation tool
- Modifications to the code
- Simulation cases
- Results of the verification simulation
- Creep results of the CIP0-1 mother rod
- Summary and conclusions

Background for the study

- Creep rupture is one of the postulated cladding failure mechanism during dry storage, another being embrittlement caused by hydrides
- In this work, CIEMAT's dry storage creep law (Feria and Herranz, 2011; Feria et al., 2015) was implemented into fuel performance code BISON
  - Previously, the model has been implemented (Arkoma et al., 2018) into VTT's version of the ENIGMA code
  - No dry storage creep model was available in BISON

Simulation tool: BISON fuel performance code

- Developed by Idaho National Laboratories (INL) since 2009 (Newman et al., 2009)
- BISON is built within the INL's MOOSE (Multi-physics Object-Oriented Simulation Environment) framework (Gaston et al., 2009)
  - MOOSE is a general solver that uses finite element method (FEM) to solve partial differential equations
- BISON solves the fully coupled thermo-mechanics and species diffusion in 1D-, 2D-(axisymmetric) and 3D-geometries
- Fuel models describe temperature and burnup dependent thermal properties, swelling, densification, thermal and irradiation creep, relocation, fracture, and fission gas production and release
- In order to model cladding mechanical behaviour, plasticity, irradiation growth, and thermal and irradiation creep models are included
- Models are also able to simulate gap heat transfer, mechanical contact, and the evolution of free volume pressure
- The calculation mesh can be generated with an external tool, or a simple mesh created through the input file

Modifications to the code

- The implemented dry storage creep law by CIEMAT (Feria and Herranz, 2011; Feria et al., 2015):

$$\dot{\varepsilon}_\theta = \frac{a\sigma_\theta^b \, e^{-c/T} \, e^{-d/\phi t}}{\sqrt{t_{dry\_storage}}}$$

- a, b, c and d are fitted constants
- $t_{dry\_storage}$ is the time spent in dry storage, ϕt is the fast neutron fluence
- The law is based on experimental database of stress-relieved annealed Zircaloy-4 cladding alloy
- The default creep model in BISON by Limbäck and Hoppe is used before entering the dry storage period (INL, 2023)
- The cladding oxidation model in BISON is modified to stop outer surface oxidation during wet and dry storage
  - Without this modification, the default EPRI/KWU/C-E oxidation model in BISON continues to produce significant oxidation during dry storage

31 October - 2 November 2023 WP8 SFC Annual Meeting 2023 5

Simulation cases

Verification case

- To verify the implementation, the creep model was first tested with a spent fuel example input delivered with BISON
- In this simple case, constant linear heat rate of 25 kW/m and axially flat power profile is used throughout the irradiation
- Rod segment consisted of ten pellets, and the calculation mesh was generated with an external meshing tool (the mesh file was also provided with the code delivery)
- Three radial and 40 axial meshes in the cladding
- Average burnup of 58 GWd/tU

Application to a full rod irradiated in a commercial reactor (CABRI CIP0-1 mother rod)

- Next, the law was applied to the mother rod of a reactivity-initiated accident (RIA) test made in CABRI test reactor, the CIP0-1 test: 17x17 PWR rod with Zirlo cladding, mother rod average burnup 68 GWd/tU
- 2D axisymmetric mesh with smeared solid fuel pellets (i.e., no dishes and chamfers) was generated within the BISON input file
- For the sake of simplicity, wet storage period was not modelled except that there is a period of one week with 50 °C in between the irradiation and dry storage
- The number of pellet and cladding elements in axial direction was 200 and in radial direction 12 and 4, respectively
- Cladding thermal boundary conditions during steady-state calculated by the built-in coolant channel model of BISON
  - Flat axial temperature profile was imposed during dry storage, the evolution given by Penalva et al., 2021

31 October - 2 November 2023 WP8 SFC Annual Meeting 2023 6

Verification of the creep model

- The results show high creep at the beginning of dry storage, and after a few years, the creep rate slows down
  - The results are qualitatively reasonable
  - The behaviour is consistent with the earlier results with the CIEMAT correlation calculated with FRAPCON-xt (Feria et al., 2015)

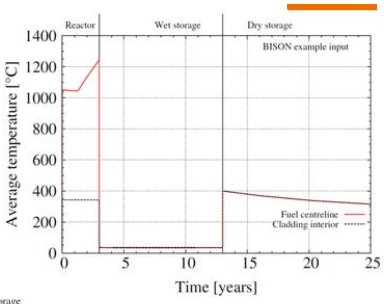

Applied temperature history

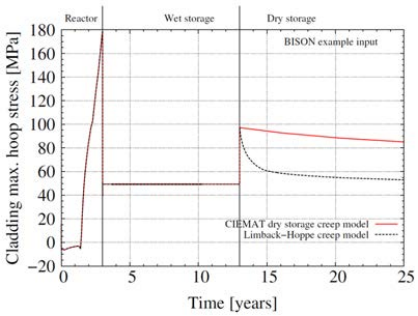

Axially maximum cladding hoop stress calculated with the CIEMAT model and compared with the default Limbäck-Hoppe creep model

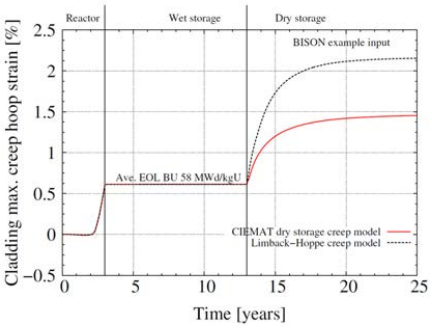

Axially maximum cladding creep hoop strain calculated with the CIEMAT model and compared with the default Limbäck-Hoppe creep model

Simulated state of CIP0-1 mother rod prior to dry storage

- Calculated FGR is 8.2% and measured is 7.4% (NEA, 2022)
- Calculated end-of-life plenum volume is 10.5 cm³ at 20 °C; measured free volume 12.26 cm³
- Measured plenum pressure 5.85 MPa at 0 °C

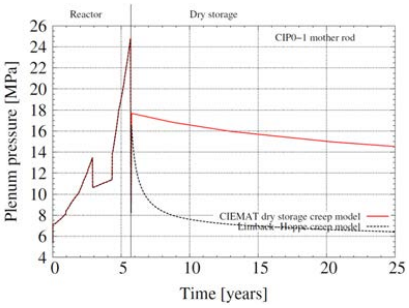

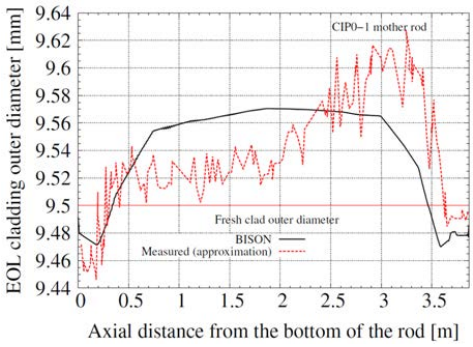

Cladding outer surface diameter axial profile after irradiation at 20 °C. Comparison is made to paper by Georgenthum et al. (2017), where the measurement result is published. In the figure, one of the curves from the paper is digitalized (approximation)

Creep results of the CIP0-1 mother rod (1/2)

- Creep is highest at both ends of the rod
  - Calculated hoop stress axial distribution is quite uniform, but the fast neutron fluence distribution is non-uniform
  - Fast fluence (thus, burnup) is lower at the end parts of the rod, and according to the CIEMAT creep correlation that results in higher creep
  - The maximum creep strain after 19.2 years of dry storage in is 3.0% (at the ends of the rods) and 0.9% in the axial middle part of the rod

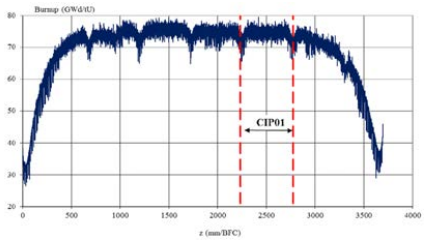

Axial burnup profile in CIP0-1 mother rod (NEA, 2022)

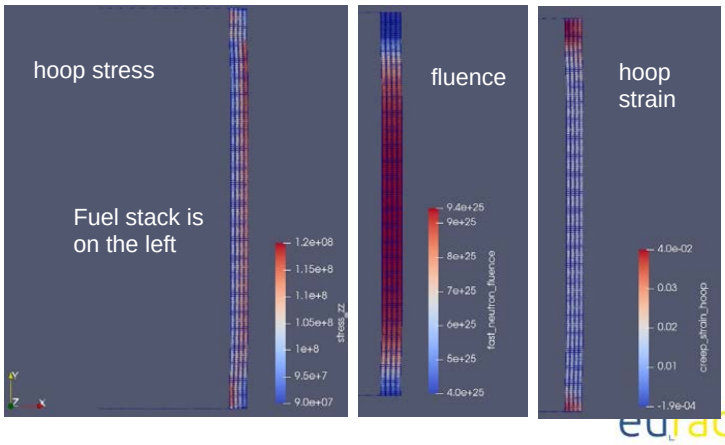

Creep results of the CIP0-1 mother rod (2/2)

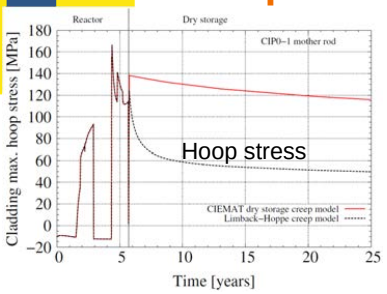

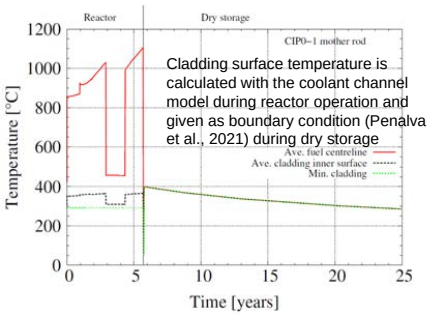

Cladding surface temperature is calculated with the coolant channel model during reactor operation and given as boundary condition (Penalva et al., 2021) during dry storage

- The Limbäck-Hoppe steady-state creep model for Zirlo applies a factor of 0.8 to decrease the creep given by the creep law of Zry-4. However, during dry storage, this model is bypassed and replaced by the CIEMAT model in which this reduction was not applied
  - If the 0.8 multiplication factor is applied, the innerwall axial midplane hoop creep strain at the end of dry storage simulation is reduced from 0.9% to 0.7%

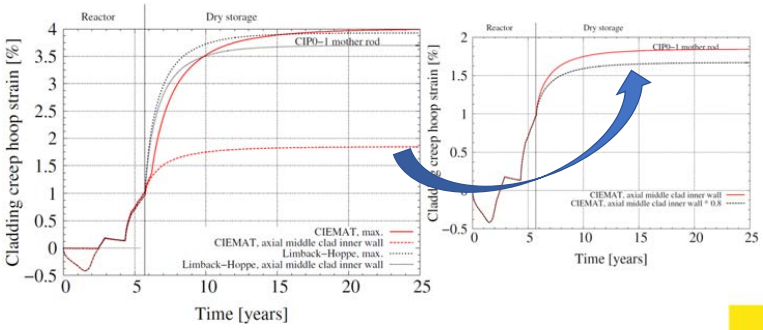

Creep hoop strain

Summary and conclusions

- CIEMAT's dry storage creep law was implemented into INL's fuel performance code BISON
- The creep law was tested with a spent fuel example input delivered with BISON, and the results were found to be qualitatively reasonable
- Then the law was applied to the mother rod of a RIA test rodlet tested in CABRI sodium loop, the CIP0-1 test
- In addition to creep, cladding hydrogen radial distribution in the beginning of dry storage was modelled in CIP0-1 mother rod with BISON by making use of the existing models in BISON (results are given in VTT Research Report)
- Compared to FRAPCON-xt results of the CIP0-1 mother rod, creep calculated with BISON is considerable higher
  - According to analysis by CIEMAT, the differences can be explained by the differences in calculated rod internal pressure and fast neutron fluence prior to dry storage, and different calculated stress evolution during the dry storage
- In the CIP0-1 mother rod, dry storage creep was found to be mostly reasonable (i.e., less than 1%) but in the top and bottom parts of the rod, the creep was considerable higher
  - In these parts, the fast neutron fluence (burnup) was lower, and that results in higher creep according to the CIEMAT creep correlation

References

- Arkoma, A., Huhtanen, R., Leppänen, J., Peltola, J., Pättikangas, T., 2018. Calculation chain for the analysis of spent nuclear fuel in long-term interim dry storage. Annals of Nuclear Energy, Vol. 119, pp. 129–138
- Feria, F., Herranz, L.E., Penalva, J., 2015. On the way to enabling FRAPCON-3 to model spent fuel under dry storage conditions: the thermal evolution. Annals of Nuclear Energy 85, 995–1002.
- Feria, F., Herranz, L.E., 2011. Creep assessment of Zry-4 cladded high burnup fuel under dry storage. Prog. Nucl. Energy 53, 395–400.
- Gaston, D., Newman, C., Hansen, G., Lebrun-Grandié, D., 2009. MOOSE: A parallel computational framework for coupled systems of nonlinear equations. Nuclear Engineering and Design, Vol. 239, pp.1768–1778.
- Georgenthum, V., Folsom, C., Moal, A., Marchand, O., Williamson, R., Ban, H., Wachs, D., 2017. SCANAIR-BISON BENCHMARK ON CIP0-1 RIA TEST. Water Reactor Fuel Performance Meeting 2017, September 10-14, Korea
- INL, 2023. Complete BISON input syntax and reference manual. https://mooseframework.inl.gov/bison/syntax/index.html (accessed 2 Aug. 2023)
- NEA, 2022. Reactivity Initiated Accident Benchmark Phase III Report. NEA/CSNI/R(2020)10
- Newman, C., Hansen, G., Gaston, D., 2009. Three dimensional coupled simulation of thermomechanics, heat, and oxygen diffusion in UO2 nuclear fuel rods. Journal of Nuclear Materials, Vol. 392, pp. 6–15.
- Penalva, J., Feria, F., Herranz, L.E., 2021. Modeling maximum fuel temperature in dry storage: From the CFD analysis to the engineering approach. Nuclear Engineering and Design, Volume 383, 111435.

1.5 Statistical approach for evaluating the safety of spent fuel during transport accidents; C. Aguado, F. Feria, L.E. Herranz, CIEMAT; WP8 SFC Annual Meeting 2023; 11/1/2023

Subtask 4.1 - CIEMAT

Statistical approach for evaluating the safety of spent fuel during transport accidents

C. Aguado, F. Feria, L.E. Herranz (CIEMAT)

EURAD WP8 SFC – Spent Fuel Characterization and evolution until disposal

SFC Annual meeting, November 01-02, 2023

This project has received funding from the European Union's Horizon 2020 research and innovation programme under grant agreement N°847593.

OUTLINE

- ❑ INTRODUCTION
- ❑ METHODOLOGY
- ❑ APPLICATION
- ❑ FINAL REMARKS

INTRODUCTION

3D codes based full mechanical evaluation of SNF under handling/transport accidents require high computational cost…

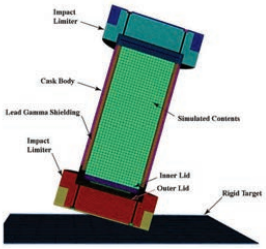

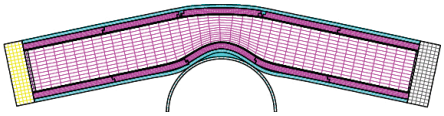

… and further clad characterization after irradiation & storage is needed

Hydrides embrittlement

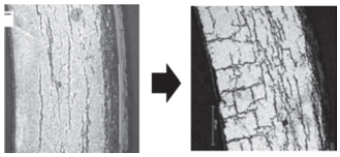

Irradiation damage annealing

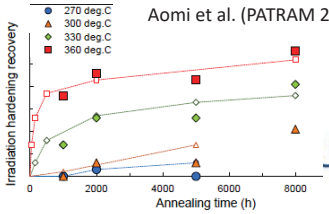

INTRODUCTION

Main goal

Development of a methodology for the assessment of SNF performance under handling/transport accident from statistical cladding characterization based on 1D T-M tools

Main achievements

- Derivation and verification of proof of concept from information available
- Assessment of factors affecting cladding mechanics:
  - Radial hydrides embrittlement
  - Irradiation damage annealing

METHODOLOGY

APPROACH

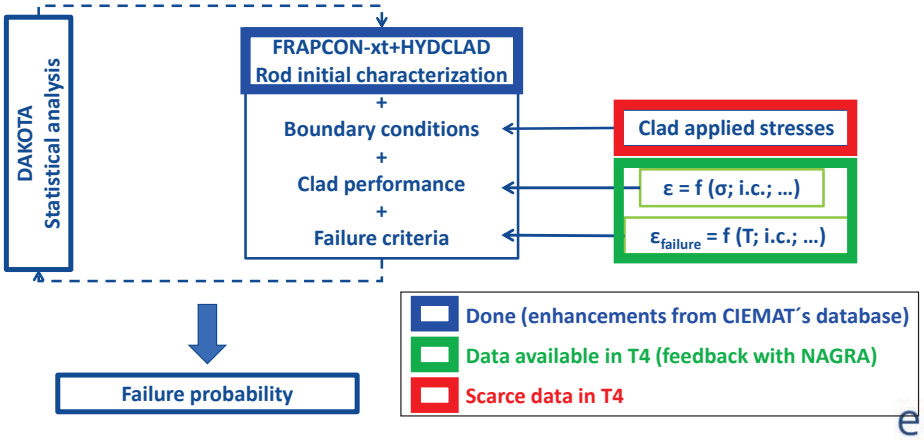

31 Oct - 2 Nov 2023 WP8 SFC Annual Meeting 2023

METHODOLOGY

APPROACH

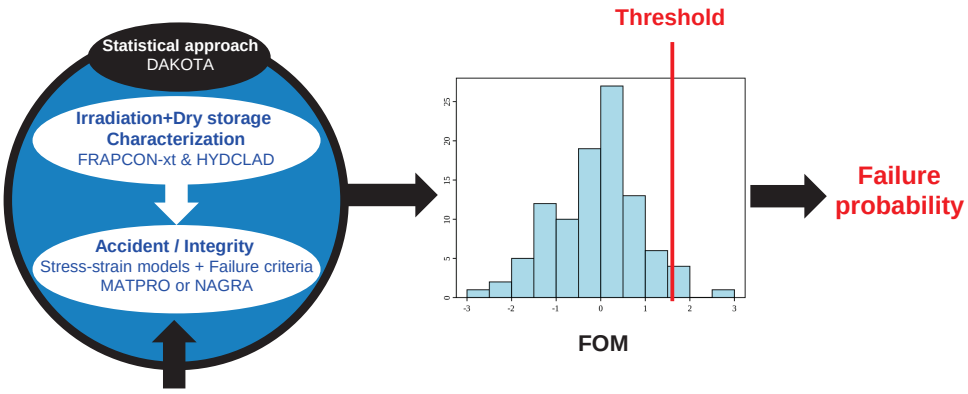

31 Oct - 2 Nov 2023 WP8 SFC Annual Meeting 2023

METHODOLOGY

TOOLS (UPDATE IN T3.1)

CIEMAT´s FRAPCON extension to dry storage

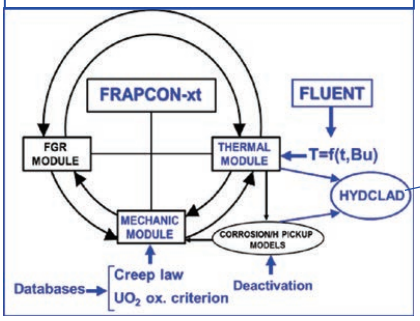

FRAPCON-xt*
(↑Bu → FGR)

CIEMAT´s in-clad H model

Precipitation modelling update
(more phenomenological)

METHODOLOGY

CRITERIA

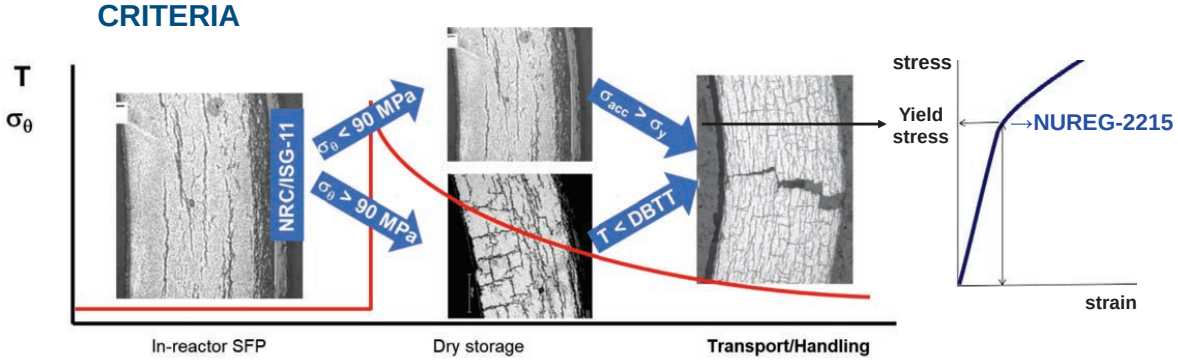

METHODOLOGY

CRITERIA

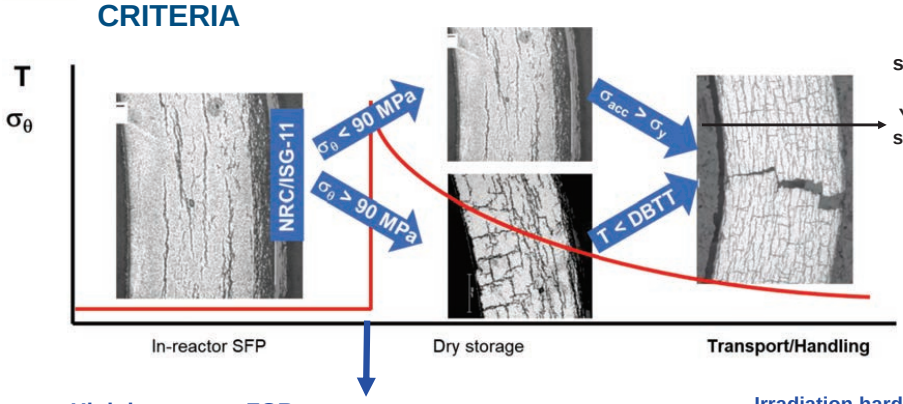

High burnup→ ↑FGR → ↑σ_θ
↓
FRAPCON-xt*

Irradiation hardening→ ↑σ_y
Annealing in dry storage→ ↓σ_y
FRAPCON-xt*

METHODOLOGY

CRITERIA

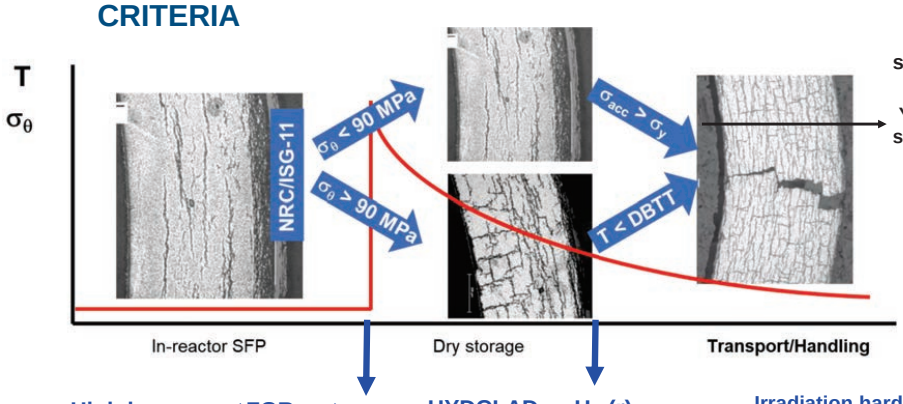

High burnup→ ↑FGR → ↑σ_θ
↓
FRAPCON-xt*

HYDCLAD → H_R (r)
(alternative if σ_θ<90 MPa)
Criterion: $H_R > H_{R\ lim}$

Irradiation hardening→ ↑σ_y
Annealing in dry storage→ ↓σ_y
FRAPCON-xt*

METHODOLOGY

CRITERIA

Conservative → Strain limits (ε_{lim})

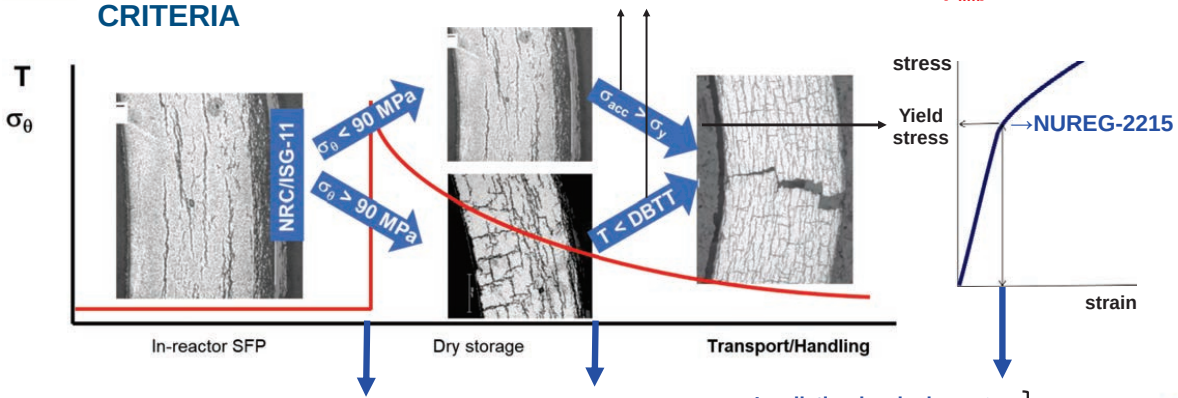

High burnup→ ↑FGR → ↑σ_θ → FRAPCON-xt*

HYDCLAD → H_R (r) (alternative if σ_θ<90 MPa)

Criterion: $H_R > H_{R\ lim}$

Irradiation hardening→ ↑σ_y
Annealing in dry storage→ ↓σ_y
FRAPCON-xt*

METHODOLOGY

CRITERIA

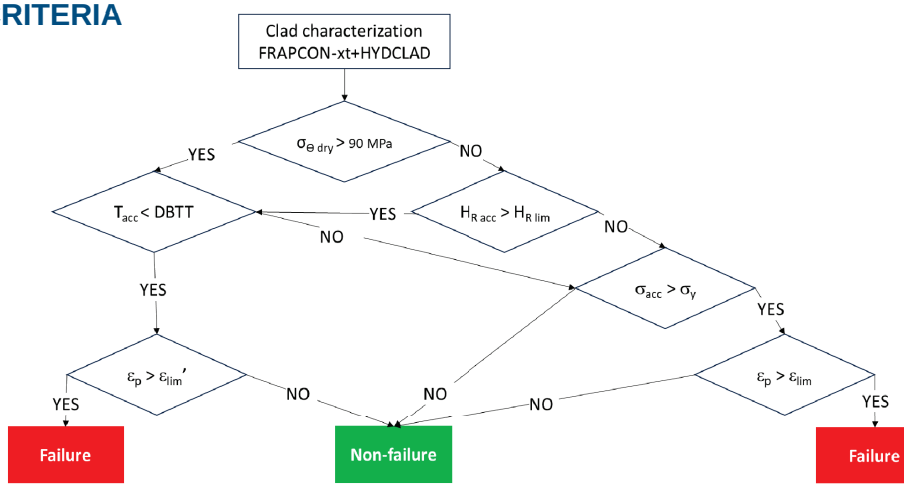

METHODOLOGY

CRITERIA

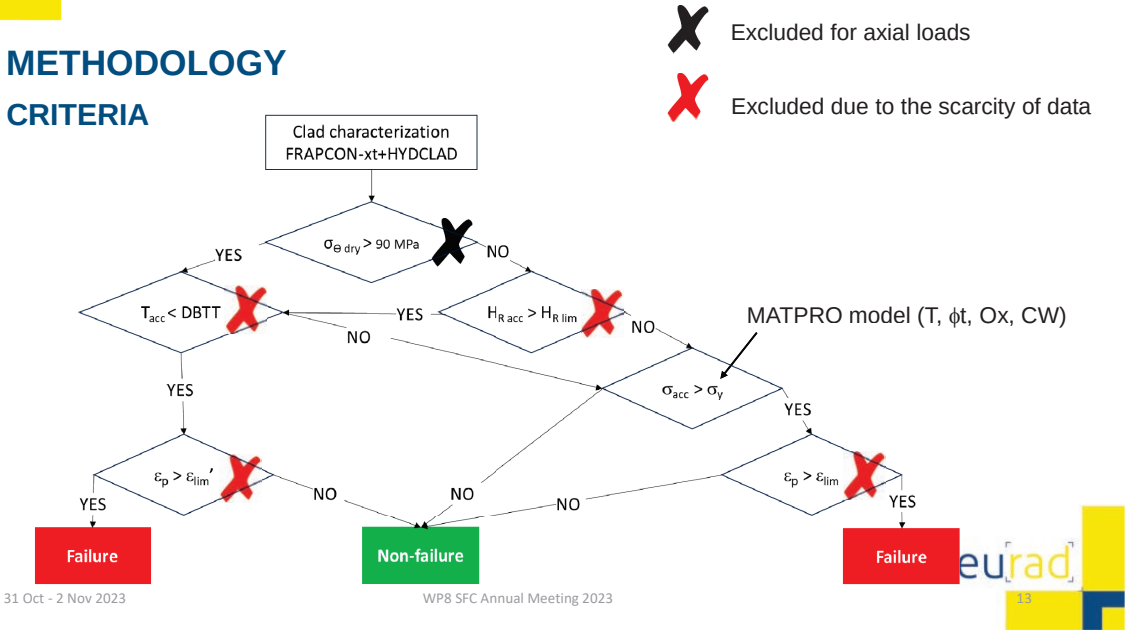

METHODOLOGY

CRITERIA

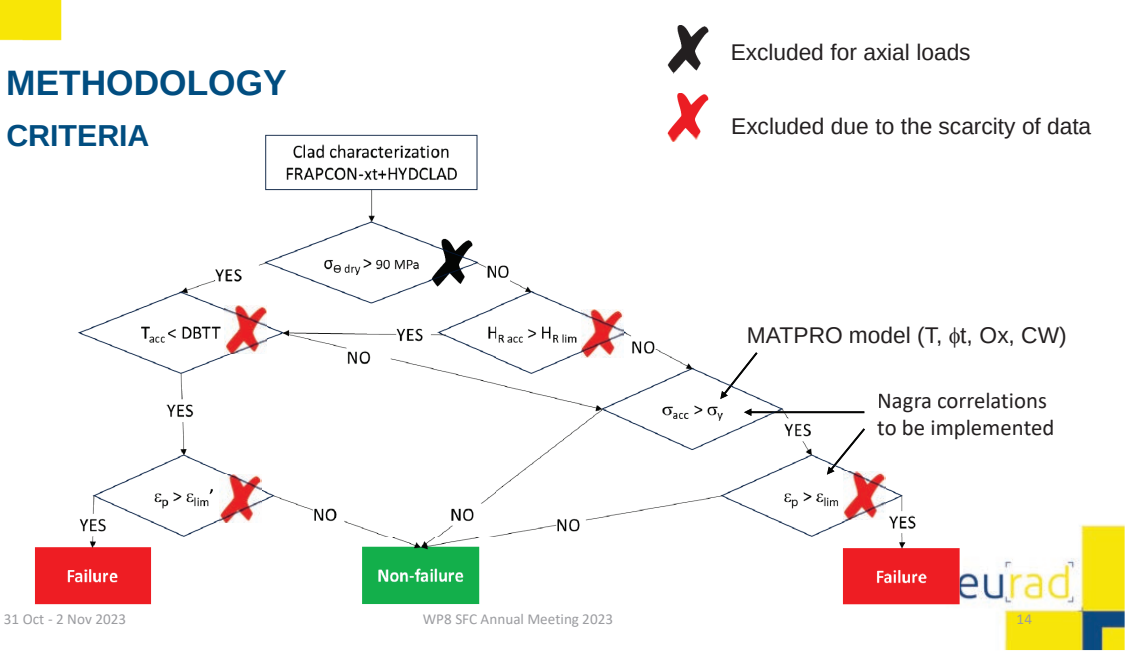

METHODOLOGY

STATITICAL ANALYSIS - MONTECARLO BASED

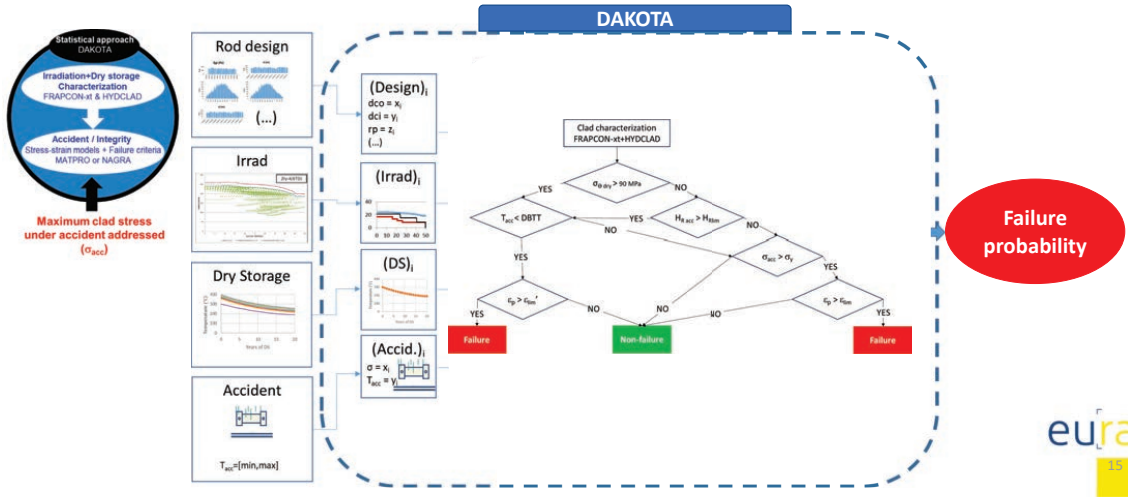

APPLICATION

SCENARIO

PWR 17x17 **Irradiation** **Dry storage - Metallic cask** **Handling accident**

Variability: Rod design + Power history + Clad temperature (DS&Accident) + Clad maximum stress (σ_{acc})

↑ Open literature

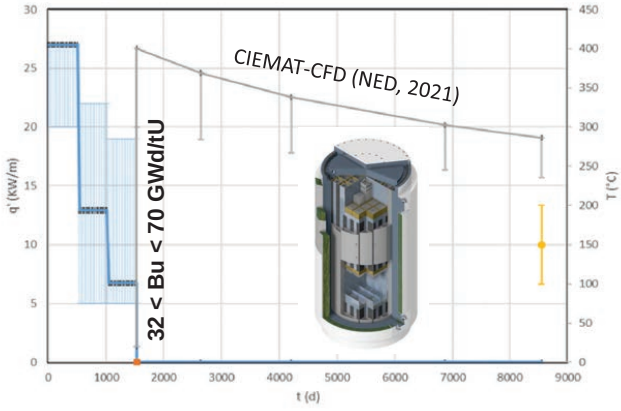

↓ 405 MPa (IDOM, sT 4.1, 2021)

Maximum stress in cladding during a 75 g side drop accident (17x17 fuel assembly)

APPLICATION
BASE CASE

$\sigma_{\Theta\ dry} > 90$ MPa

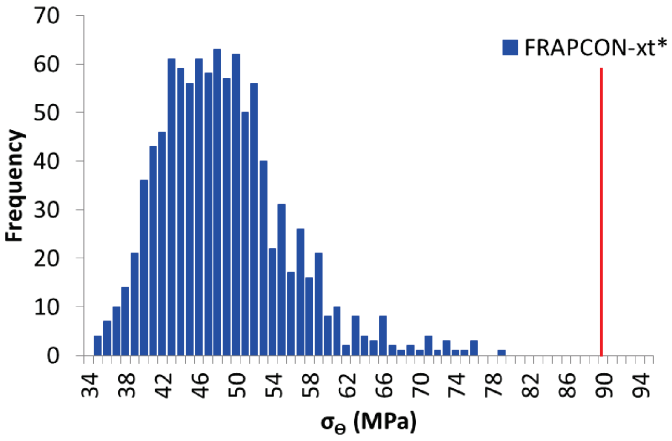

No radial hydrides embrittlement

APPLICATION
BASE CASE

$\sigma_{\Theta\ dry} > 90$ MPa

No

$\sigma_{acc} > \sigma_y$

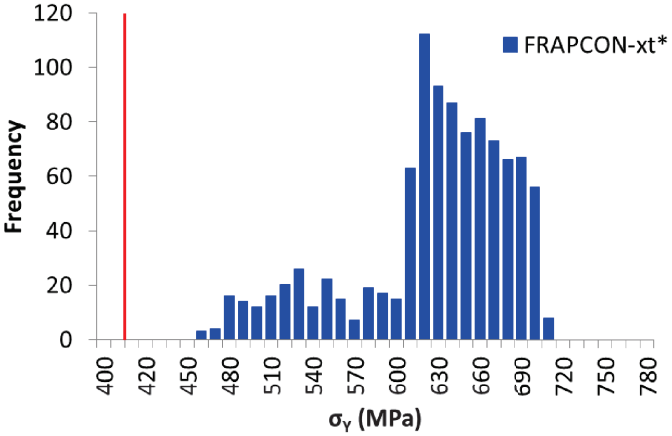

Failure probability = 0%

APPLICATION
SCOPING CALCULATIONS

- **Stress at drying for radial hydrides embrittlement –** FRAPCON-xt vs FRAPCON-xt*
- **Yield stress at accident –** Full annealing vs no annealing

APPLICATION
STRESS AT DRYING

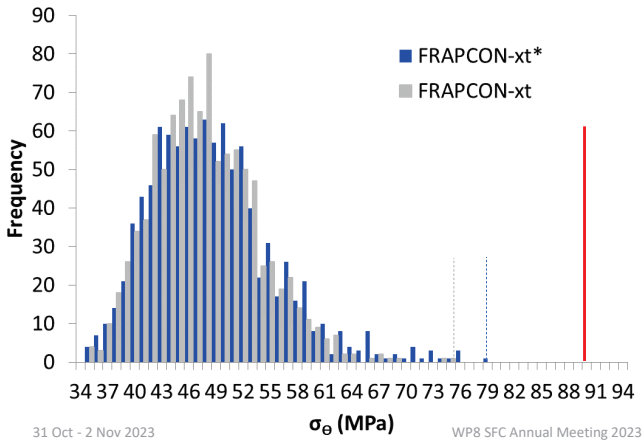

No significant impact of the FGR modeling improvement up to 70 GWd/tU

APPLICATION

YIELD STRESS AT ACCIDENT

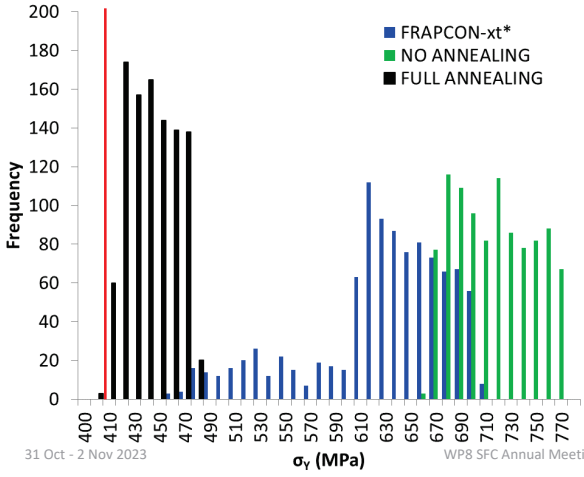

Significant impact of the IDA model

APPLICATION

YIELD STRESS AT ACCIDENT - ANNEALING DATA FROM LITERATURE

FRAPCON-xt (MATPRO):
- 220 – 700 °C
- $3.6 \cdot 10^{23} – 4.4 \cdot 10^{25}$ n/m^2

New data (Aomi et al., 2023):
- 270 – 360 °C
- $11.9 – 13.2 \cdot 10^{25}$ n/m^2

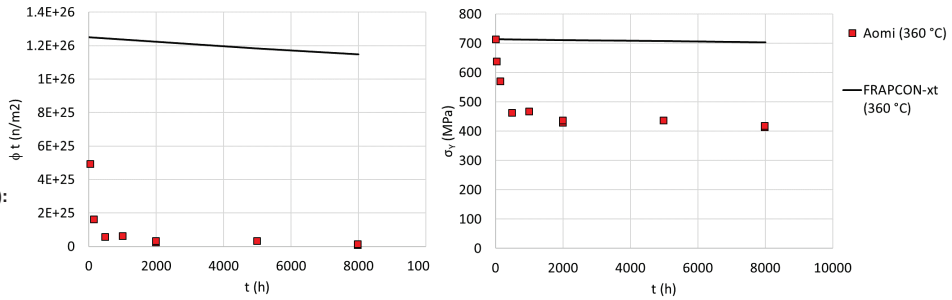

Significant differences between MATPRO and new data

FINAL REMARKS

- **CIEMAT has developed a methodology to evaluate SNF under handling/transport accidents, based on statistical cladding characterization.**
- **The proof of concept derived has been verified. It allows analyzing the impact of aspects of interest for the cladding characterization.**
- **Main conclusions:**
  - **Safety margin of hoop stress at drying for radial hydrides embrittlement (up to 70 GWd/tU).**
  - **Potential impact of irradiation damage annealing.**
- **Further work:**
  - **Continuation of irradiation damage annealing analysis.**
  - **NAGRA's data implementation.**

THANK YOU FOR YOUR ATTENTION!!

1.6 Mechanical behaviour of pre- hydrided cladding; Miguel Cristóbal-Beneyto, Jesus Ruiz-Hervias, Daniel Pérez-Gallego; WP8 SFC Annual Meeting 2023; 11/01/2023

Mechanical behaviour of pre-hydrided cladding

Miguel Cristóbal-Beneyto, Jesus Ruiz-Hervias, Daniel Pérez-Gallego

Department of Materials Science
Universidad Politécnica de Madrid (UPM), Spain
miguel.cristobal@upm.es

INDEX

INTRODUCTION

- Cladding is the first engineering barrier: let us take advantage of it.
- In-reactor cladding degradation: irradiation, corrosion, creep, H pickup
- Effect on cladding safety? (particularly in case of accident)
- Structural integrity cladding/rod: irradiated samples (scarce & expensive)
- Non-irradiated material: alternative to develop testing protocols applicable to irradiated material, increasing test outcome

INTRODUCTION

Cask drop accident: rod failure modes

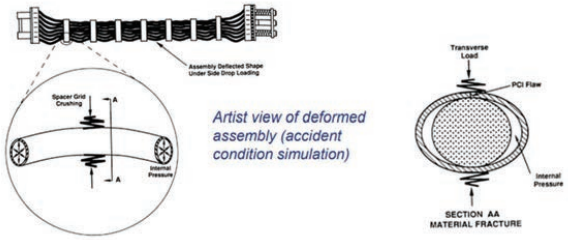

Pinch loading: ring compression test

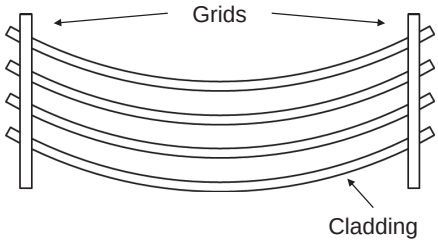

Rod bending: 3 point bending test

INTRODUCTION

- **Objective**
  - **Study the mechanical behavior of un-irradiated pre-hydrided cladding in accident conditions**
    - Perform RCT test and TPB in pre-hydrided samples
      - Effect of hydride morphology
      - Effect of surrogate fuel pellet
      - Effect of temperature

Ring compression test

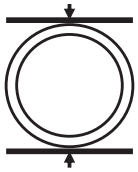

3 point bending test

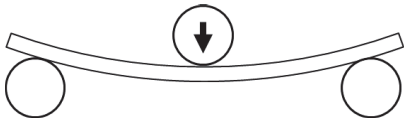

EXPERIMENTAL

- **Hydrogen charge**
  - ZIRLO[1] cladding samples
  - Charge through the outer surface of cladding
  - Cathodic charge: 3h, 0.1 M KOH, 0.25 A/cm^2
  - Precipitation treatment:
    - 7h at 450 °C
    - Cooling at 60 °C/h

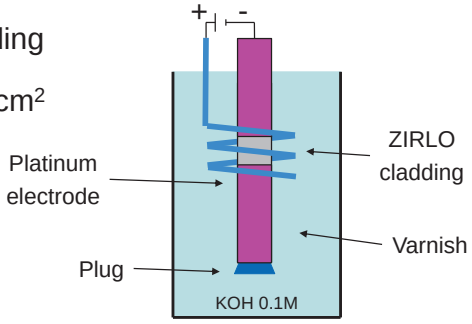

1 ZIRLO® is a registered trademark of Westinghouse Electric Company, LLC, its affiliates and/or its subsidiaries in the United States of America and may be registered in other countries throughout the world. All rights reserved. Unauthorized use is strictly prohibited.

EXPERIMENTAL

- **Hydride Reorientation treatment (RHT)**
  - Using internal pressure (argon gas)
  - Independent temperature and pressure control
  - T = 400 °C
  - P = 19 MPa → σ_θ = 140 MPa

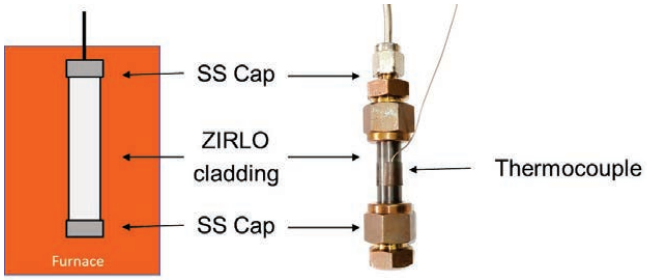

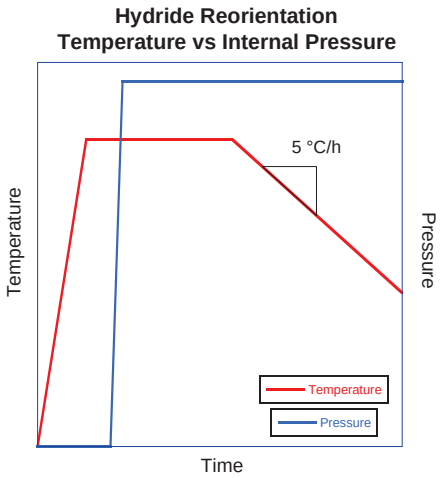

EXPERIMENTAL

- **Ring compression test**
  - Sample is compressed between two parallel plates

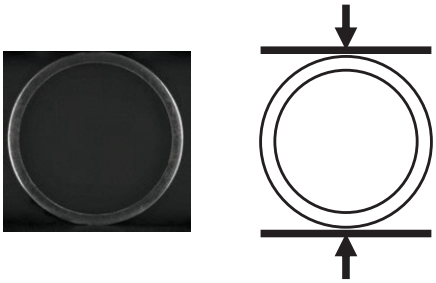

RCT setup

- **Three point bending**
  - Sample is placed over two supports, and load is applied in the middle point
  - Similar to JRC-KA

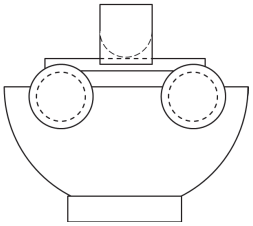

TPB device schematic

EXPERIMENTAL

- **Test conditions:**

	Filling	Hydrides	Temperature
RCT	Hollow	Circumferential	20, 135 and 300 °C
		Radial	20, 135 and 300 °C
	Inserts	Circumferential	20°C
		Radial	20°C

TPB	Hollow	As Received	20, 135 and 300 °C
		Circumferential	20, 135 and 300 °C
	Inserts	As Received	20, 135 and 300 °C
		Circumferential	20, 135 and 300 °C

RESULTS

Hydride Reorientation treatment: 140 MPa hoop stress

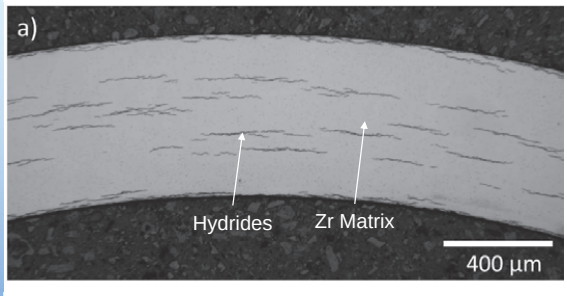

Before RHT (≈ 75 wppm Hydrogen)

Microstructure of samples: (a) before and (b) after reorientation treatment

After RHT

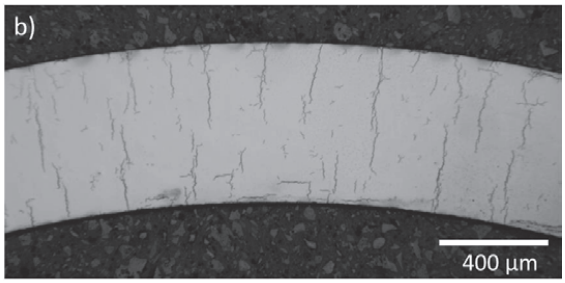

RESULTS

Ring compression tests (RCT): hollow samples

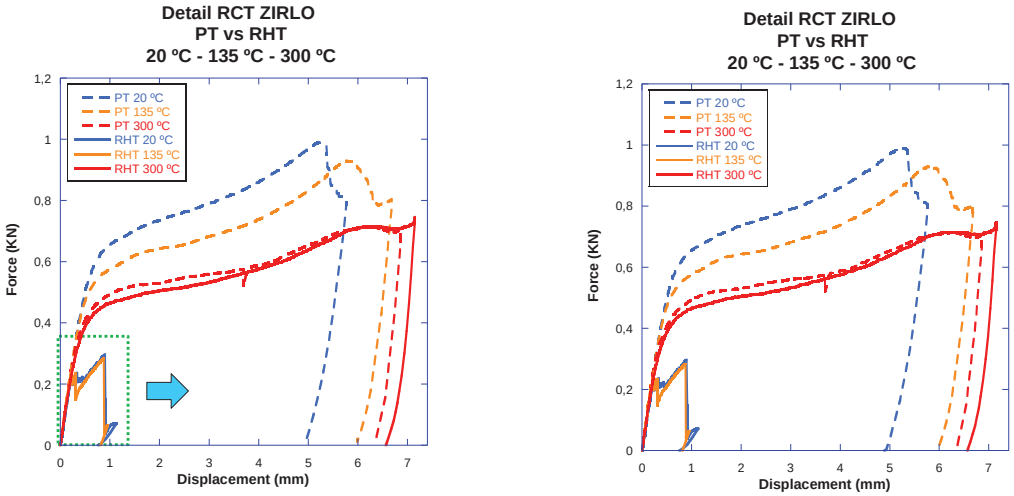

RESULTS

Ring compression tests (RCT): surrogate pellet

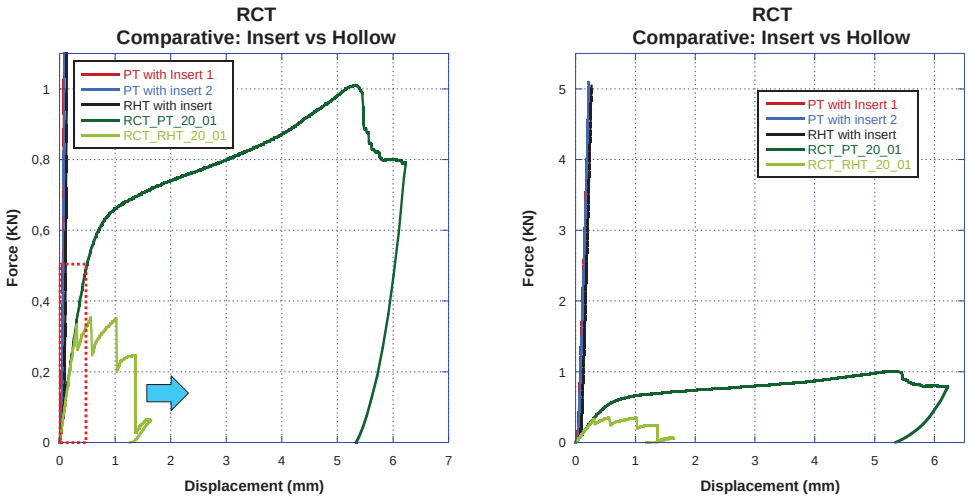

RESULTS

Ring compression tests (RCT)

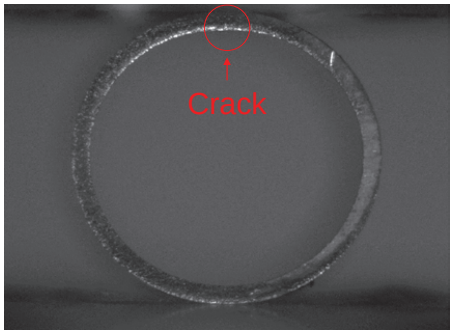

Image of hollow sample with radial hydrides during RCT at failure

Max. Load: 0,33 KN
Displacement: 0,32 mm

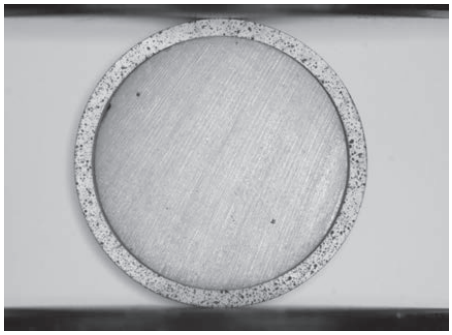

Image of sample with insert and circumferential hydrides during RCT at same load

Load: 0,33 KN
Displacement: 0,1 mm

RESULTS

Three point bending tests

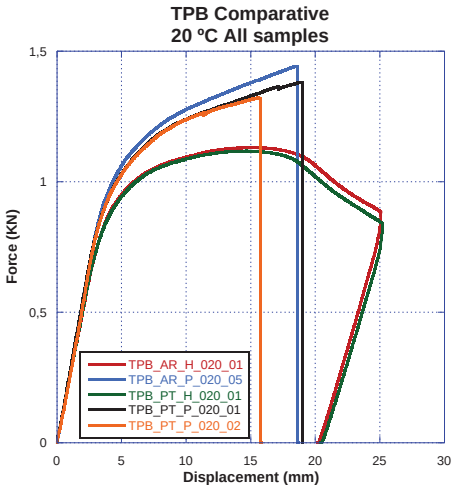

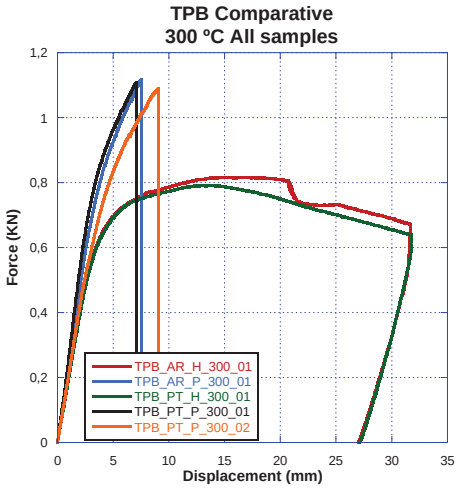

RESULTS

Three point bending tests

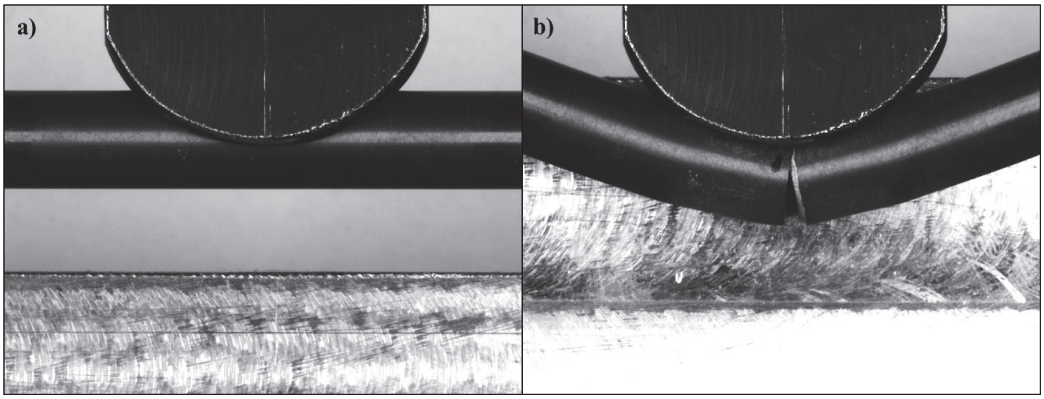

Images taking during the TPB test of a sample with ceramic inserts at 20 °C at a) beginning of the test, and b) after max load

CONCLUSIONS

- **ZIRLO ® samples were charged with ≈ 100 wppm hydrogen**
- **Hydrogen reorientation treatment (hoop stress=140 MPa)**
  - **Almost full reorientation**
  - **Long radial hydrides: almost 100 % cladding thickness in some cases**
- **RCT tests**
  - **Hollow samples: brittle failure with radial hydrides (RT and 135ºC)**
  - **Samples with inserts: no failure with radial hydrides**
- **TPB tests**
  - **Cladding behavior dominated by inserts**
  - **Failure mode: cladding cracking in the boundary between pellets**
  - **Increasing temperature decreases displacement at failure**

2. External training course

- Characterization of spent nuclear fuel for intermediate storage and final disposal; P. Schillebeeckx, JRC Geel; ANNETTE school "Final stage of the nuclear lifecycle" KIT, Karlsruhe; 2 - 6/12/2019
- Characterization of spent nuclear fuel by theoretical calculations; P. Schillebeeckx, JRC Geel; Online available (JRC127309);
- Neutron resonance experiments; P. Schillebeeckx, JRC Geel; Summer school on neutron detectors and related applications, Riva del Garda; 30/06 - 04/07/2022
- Spent Nuclear Fuel Characterisation, P. Schillebeeckx, JRC Geel, Training for DG-ENER EURATOM; 28/06/2023
- SNF characterisation by NDA; P. Schillebeeckx, JRC Geel; School on "Nuclear data for depletion calculations; 11/09 - 15/09/2023
- Observables of interest (in spent fuel); G. Žerovnik, JSI-; School on "Nuclear data for depletion calculations"11/09 - 15/09/2023

2.1 Characterization of spent nuclear fuel for intermediate storage and final disposal; P. Schillebeeckx, JRC Geel; ANNETTE school "Final stage of the nuclear lifecycle" KIT, Karlsruhe; 2 - 6/12/2019

Characterisation of spent nuclear fuel for intermediate storage and final disposal

ANNETTE
"Final stage of the nuclear lifecycle"

2 – 6 December 2019, Karlsruhe

European Commission

Contents

- Introduction
- Source terms
  - Neutron
  - Gamma-ray
  - Heat
- Theoretical estimation of source terms
  - Principles
  - Nuclear data
  - Fuel properties and irradiation history
- Application: CLAB (SE)

European Commission

Spent Nuclear Fuel (SNF) intermediate storage or final disposal

A **safe**, **secure**, **ecological** and **economic** transport**,** storage and final disposal requires that **SNF** is **characterised** for the main source terms of interest:

- Decay heat : H
- Neutron emission : S_n
- γ-ray emission : S_γ
- Reactivity : R
  i.e. FP, actinides (Burn Up Credit)
- Fissile material (Nuclear Safeguards)
  i.e. ^{235}U, ^{239}Pu
- Specific nuclides (Long term safety)
  e.g. ^{14}C, ^{36}Cl, ^{79}Se, ^{94}Nb, ^{99}Tc, ^{129}I, ^{226}Ra, ^{237}Np

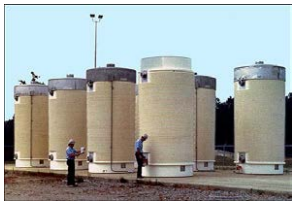

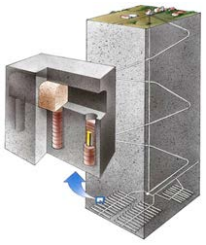

European Commission

Nuclear spent fuel: nuclide inventory

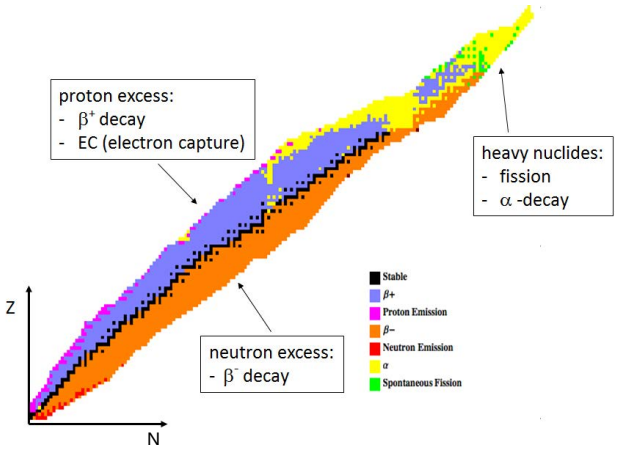

- Fission products
  e.g. ^{99}Tc, ^{137}Cs, ^{154}Eu, …

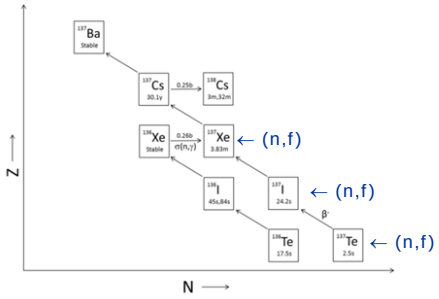

- Actinides / minor actinides
  e. g. ^{239}Pu, ^{241}Am, ^{244}Cm, …

$$n + {}^{238}_{92}U \xrightarrow{(n,\gamma)} {}^{239}_{92}U \xrightarrow[23.5\ min]{\beta^-} {}^{239}_{93}Np \xrightarrow[2.36\ d]{\beta^-} {}^{239}_{94}Pu$$

European Commission

β^- decay: ^{137}Cs (neutron rich)

- $T_{1/2}$ = 30.05 (8) a
- Q_{β^-} = 1175.73 (17) keV

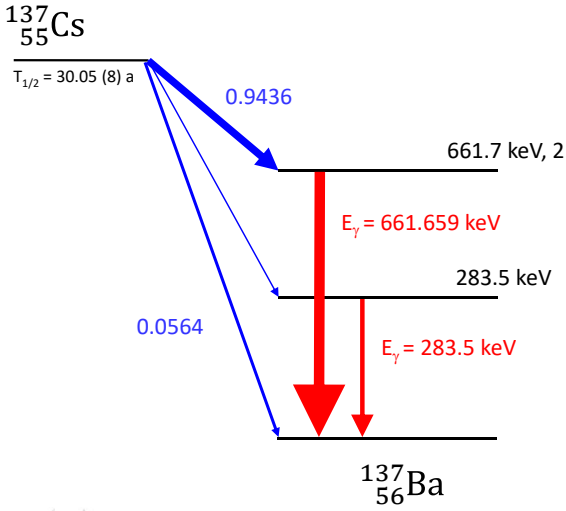

$$^{137}_{55}Cs \rightarrow {}^{137}_{56}Ba^{*} + e^{-} + \bar{\nu}_e$$

$$\downarrow$$

$$^{137}_{56}Ba + E_\gamma$$

Gamma-ray emission probability: β

E_γ	β
661.7 keV	**0.8436 (20)**
283.5 keV	5.8 (8) x 10^{-6}

http://www.nucleide.org/DDEP_WG/Nuclides/Cs-137_tables.pdf

α decay: ^{241}Am

- $T_{1/2}$ = 432.6 (6) a
- Q_α = 5637.82 (12) keV

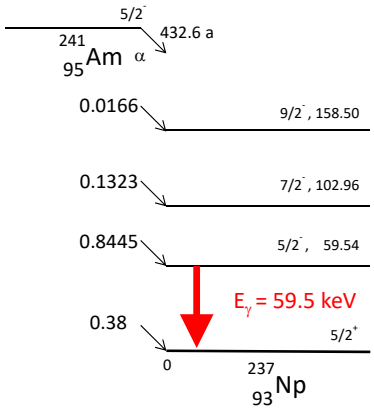

Emission of α-particles

P. Kandlakunta and L. Cao, Rad. Prot. Dos. 151 (2012) 586

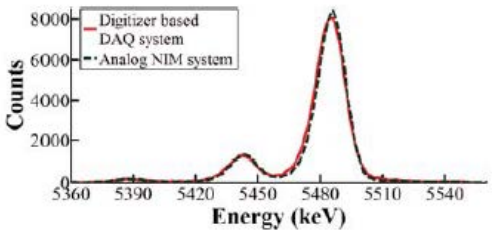

E_α / keV	$P(E_\alpha)$
5388.3	0.0166 (3)
5442.9	0.1323 (10)
5485.6	**0.8445 (10)**

http://www.nucleide.org/DDEP_WG/Nuclides/Am-241_tables.pdf

Spontaneous fission

Fission: nucleus splits up into fission products (FP)

e.g. ^{238,240,242}Pu(sf), ^{242,244,246}Cm(sf), ^{252}Cf(sf)

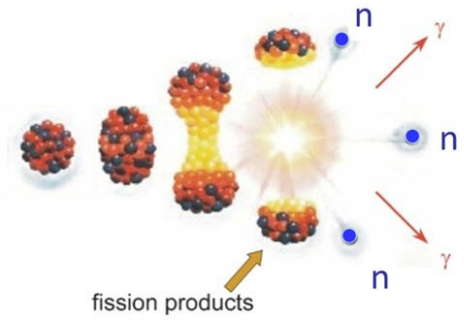

- FP : acceleration due to Coulomb repulsion
- FP : strongly excited, emission of
  - Prompt fission neutrons
  - Prompt fission γ-rays
- Prompt fission neutrons important for NDA
  (see K. Abbas)

Prompt fission neutron energy distribution

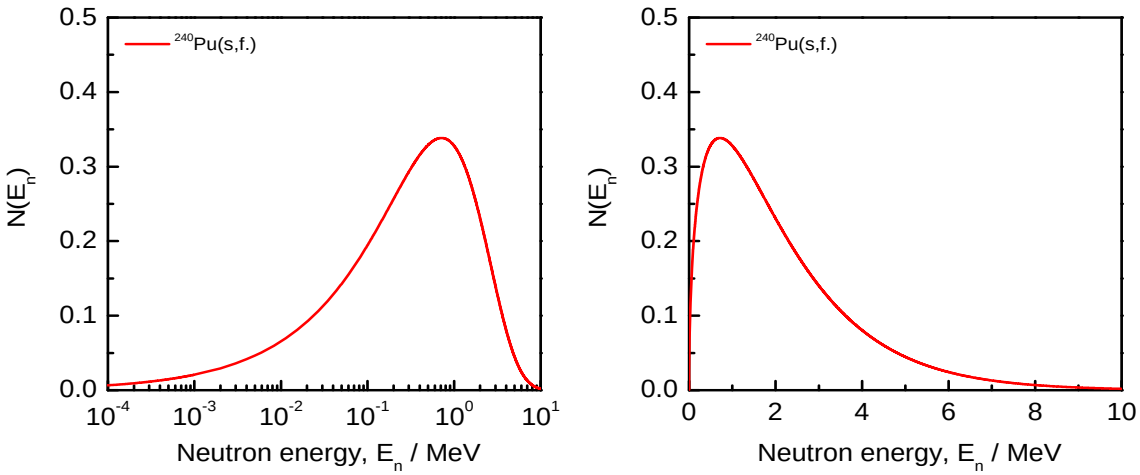

$< E_n > \approx 2$ MeV

Prompt fission neutron multiplicity

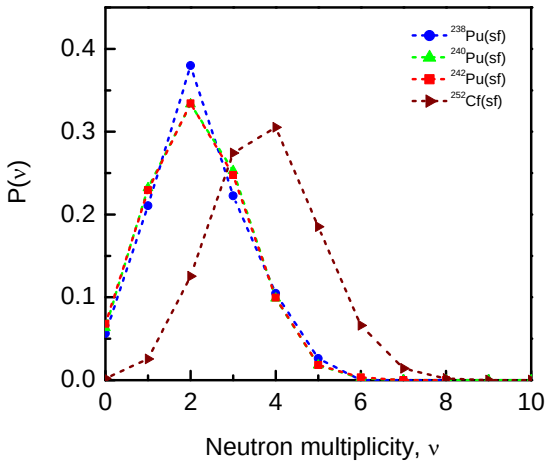

Emission of prompt fission neutrons:
- statistical process
- on average ν > 1

Nuclide	$\nu_{s(1)}$	$\nu_{s(2)}$	$\nu_{s(3)}$
^{238}Pu	2.210	1.978	0.933
^{240}Pu	2.154	1.895	0.868
^{242}Pu	2.145	1.882	0.867
^{252}Cf	3.756	5.978	5.287

$$\nu_{s(j)} = \sum_{\nu=j}^{\infty} \binom{\nu}{j} P_{s\nu}$$

Spontaneous fission: neutron emission

Nuclide	$T_{1/2}$ / a	Main decay mode	(sf) branch x 100	<ν>	$S_{n,sf}$ ($s^{-1}g^{-1}$)
^{238}U	4.468 10^{9}	α	5.45 10^{-5}	1.990	1.35 10^{-2}
^{238}Pu	**87.74**	**α**	**1.85 10^{-7}**	**2.21**	**2592**
^{239}Pu	24110	α	3.1 10^{-10}	2.219	2.18 10^{-2}
^{240}Pu	**6561**	**α**	**5.7 10^{-6}**	**2.154**	**1023**
^{241}Pu	14.29	β^-	5.74 10^{-13}	2.27	4.5 10^{-2}
^{242}Pu	**373500**	**α**	**5.49 10^{-4}**	**2.145**	**1725**
^{241}Am	432.6	α	4.30 10^{-10}	2.46	1.3
^{242}Cm	**0.446**	α	6.36 10^{-4}	2.54	**2.10 10^{7}**
^{244}Cm	**18.1**	α	1.37 10^{-4}	2.72	**1.08 10^{7}**
^{252}Cf	**2.645**	**α**	**3.10**	**3.757**	**2.31 10^{12}**

Neutron production by (α,n)

Additional neutron source, $S_{n,\alpha}$

SNF: α - decay of actinides followed by (α,n) reaction in light elements

- (α,n) reactions
  - $^{18}O(\alpha,n)^{21}Ne$
  - $^{17}O(\alpha,n)^{20}Ne$
  - $^{19}F(\alpha,n)^{22}Na$
- Neutron energy (emission)
  - O(α,n) : $<E_n> \sim 2$ MeV
  - F(α,n) : $<E_n> \sim 1$ MeV
- $P(\nu) \equiv 1$
  used to separate prompt fission neutrons from (α,n) neutrons in neutron correlation counting (NDA)

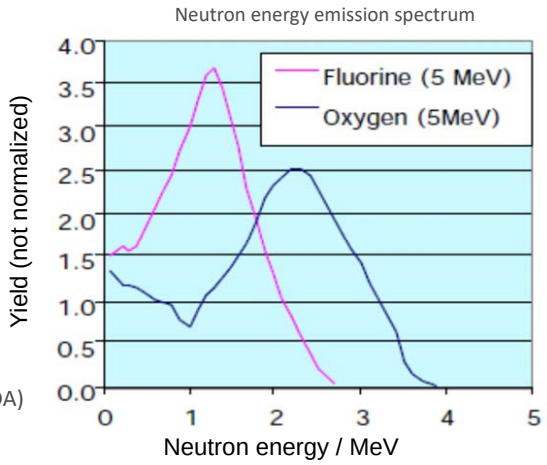

European Commission

ANNETTE, 2 - 6 December 2019, Karlsruhe

Neutron emission by SNF

$$S_n(t) = \sum_k S_{n,k}(t)$$

- $S_{n,k}(t)$: contribution of radionuclide k
- $S_{n,k}(t) = (s_{sf,k} + s_{\alpha n,k})\, N_k(t)$
  - $N_k(t)$: number of nuclei of nuclide k at time t
  - $s_{sf,k}$: specific neutron emission rate of nuclide k due to sf
  - $s_{\alpha,k}$: specific neutron emission rate of nuclide k due to (α,n) reactions

PWR UO_2 pellet (5 g)
$^{235}U/U = 4.8$ %
burnup = 44 GWd/tU

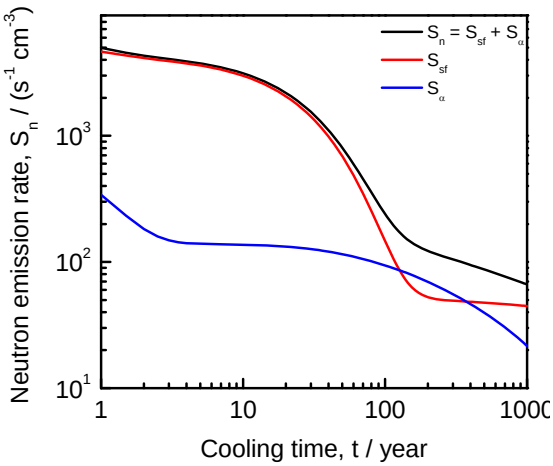

European Commission

ANNETTE, 2 - 6 December 2019, Karlsruhe

Neutron emission by SNF

$$S_n(t) = \sum_k (s_{sf,k} + s_{\alpha n,k})\, Nk(t)$$

PWR UO_2 pellet (5 g)
$^{235}U/U$ = 4.8 %
burnup = 44 GWd/tU

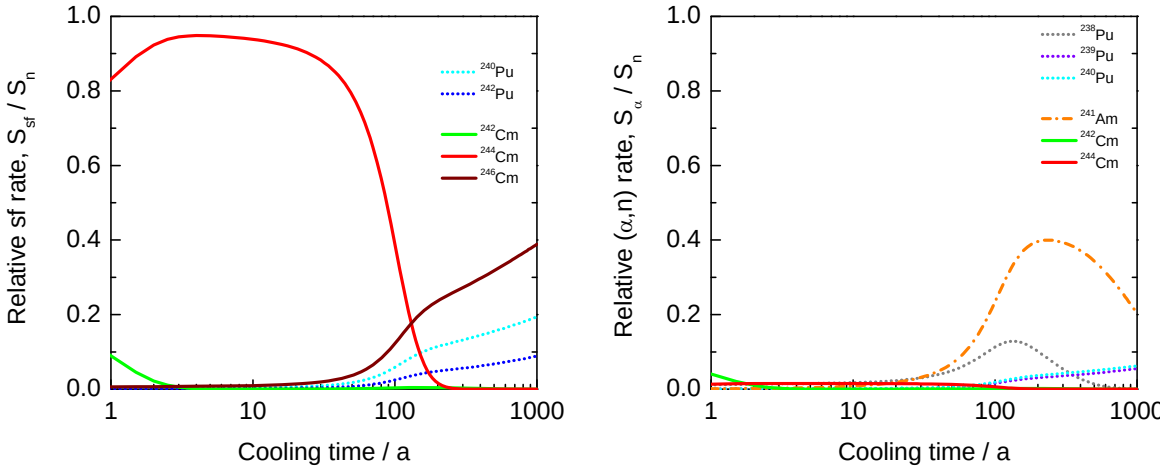

European Commission

Gamma-ray emission by SNF

$$S_\gamma(t) = \sum_k S_{\gamma,k}(E_\gamma, t)$$

PWR UO_2 pellet (5 g)
$^{235}U/U$ = 4.8 %
burnup = 44 GWd/tU

^{95}Nb	35.0 d
^{95}Zr	64.0 d
^{144}Ce/^{144}Pr	284.9 d
^{106}Ru/^{106}Rh	1.02 a
^{134}Cs	2.06 a
^{154}Eu	8.8 a
^{137}Cs/^{137m}Ba	30.0 a

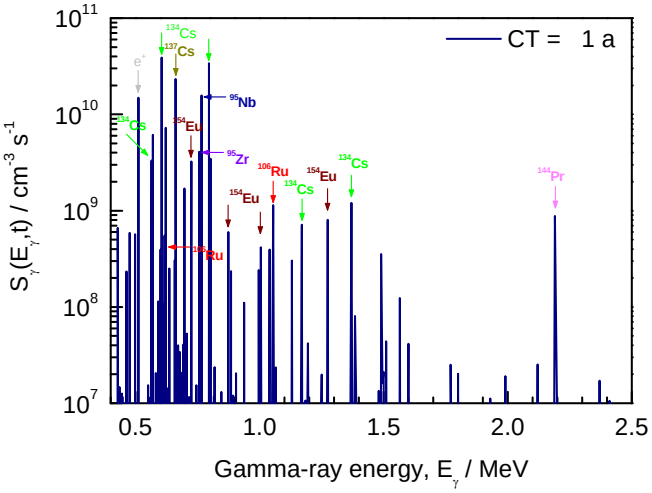

European Commission

Gamma-ray emission by SNF

$$S_\gamma(t) = \sum_k S_{\gamma,k}(E_\gamma, t)$$

^{95}Nb	35.0 d
^{95}Zr	64.0 d
^{144}Ce/^{144}Pr	284.9 d
^{106}Ru/^{106}Rh	**1.02 a**
^{134}Cs	**2.06 a**
^{154}Eu	**8.8 a**
^{137}Cs/^{137m}Ba	**30.0 a**

PWR UO_2 pellet (5 g)
^{235}U/U = 4.8 %
burnup = 44 GWd/tU

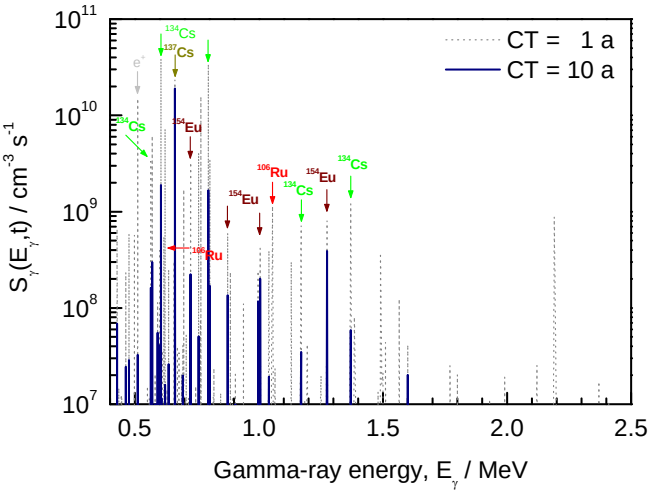

European Commission

Gamma-ray emission by SNF

$$S_\gamma(t) = \sum_k S_{\gamma,k}(E_\gamma, t)$$

^{95}Nb	35.0 d
^{95}Zr	64.0 d
^{144}Ce/^{144}Pr	284.9 d
^{106}Ru/^{106}Rh	1.02 a
^{134}Cs	2.06 a
^{154}Eu	**8.8 a**
^{137}Cs/^{137m}Ba	**30.0 a**

PWR UO_2 pellet (5 g)
^{235}U/U = 4.8 %
burnup = 44 GWd/tU

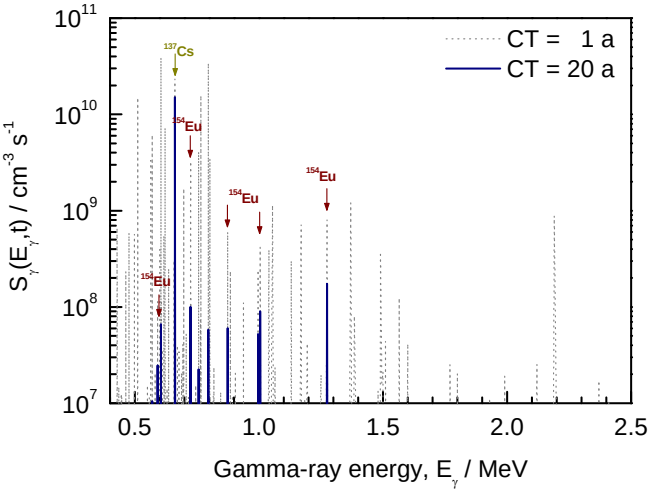

European Commission

ANNETTE, 2 - 6 December 2019, Karlsruhe

Gamma-ray emission by SNF

$$S_\gamma(t) = \sum_k S_{\gamma,k}(E_\gamma, t)$$

^{95}Nb	35.0 d
^{95}Zr	64.0 d
^{144}Ce/^{144}Pr	284.9 d
^{106}Ru/^{106}Rh	1.02 a
^{134}Cs	2.06 a
^{154}Eu	**8.8 a**
^{137}Cs/^{137m}Ba	**30.0 a**

PWR UO_2 pellet (5 g)
^{235}U/U = 4.8 %
burnup = 44 GWd/tU

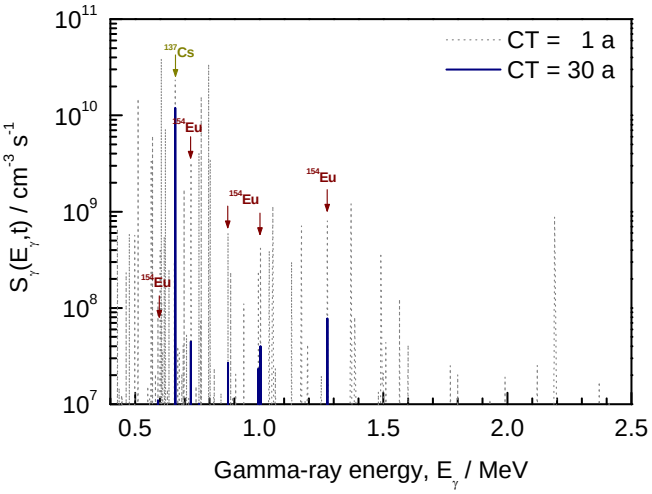

Gamma-ray emission by SNF: recoverable thermal power

$$P_\gamma(t) = \sum_k \lambda_k N_k(t) \int E_\gamma S_{\gamma,k}(E_\gamma, t) dE_\gamma$$

Recoverable energy

^{95}Nb	35.0 d
^{95}Zr	64.0 d
^{144}Ce/^{144}Pr	284.9 d
^{106}Ru/^{106}Rh	1.02 a
^{134}Cs	2.06 a
^{154}Eu	8.8 a
^{137}Cs/^{137m}Ba	30.0 a
^{241}Am	432.6 a

PWR UO_2 pellet (5 g)
^{235}U/U = 4.8 %
burnup = 44 GWd/tU

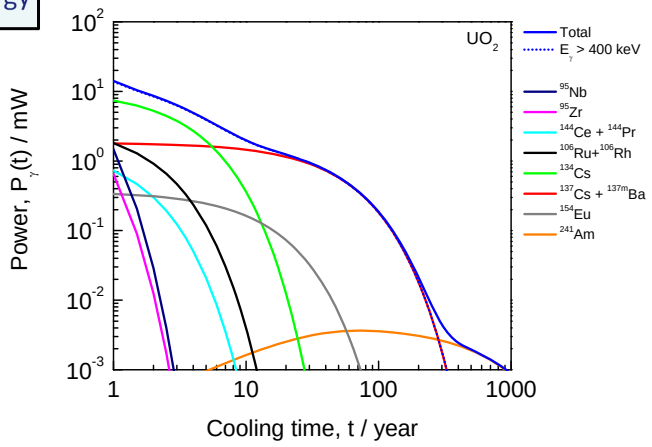

Thermal power produced by SNF (recoverable)

$$P(t) = \sum_k P_k(t)$$

- $P_k(t)$: contribution of radionuclide k
- $P_k(t) = p_k N_k(t)$
  - $N_k(t)$: number of nuclei of nuclide k at time t
  - p_k : specific decay heat rate of nuclide k

PWR UO_2 pellet (5 g)
$^{235}U/U$ = 4.8 %
burnup = 44 GWd/tU

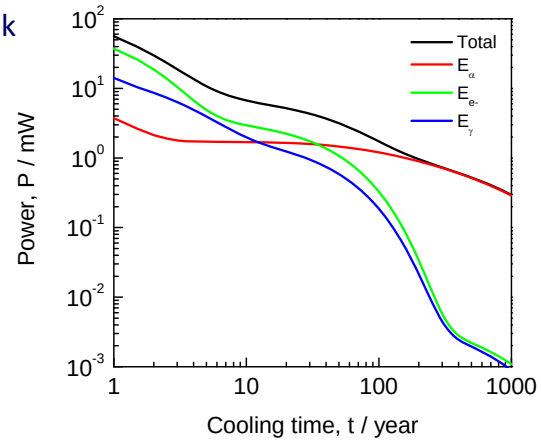

Thermal power produced by SNF

- 1 a ≤ t ≤ 10 a
  - ^{144}Ce / ^{144}Pr
  - ^{106}Ru / ^{106}Rh
  - ^{134}Cs
  - ^{90}Sr / ^{90}Y
  - ^{137}Cs / ^{137m}Ba
- 10 a ≤ t ≤ 100 a
  - ^{90}Sr / ^{90}Y
  - ^{137}Cs / ^{137m}Ba
  - ^{238}Pu
  - ^{241}Am
  - ^{244}Cm
- 100 a ≤ t
  - ^{241}Am
  - ^{238}Pu
  - $^{239,241}Pu$

PWR UO_2 pellet (5 g)
$^{235}U/U$ = 4.8 %
burnup = 44 GWd/tU

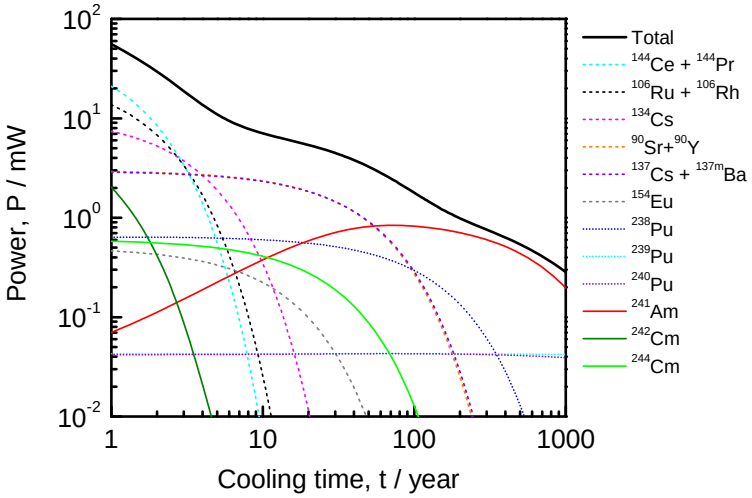

Thermal power produced by SNF

- 1 a ≤ t ≤ 10 a
  - **^{144}Ce / ^{144}Pr**
  - **^{106}Ru / ^{106}Rh**
  - **^{134}Cs**
  - ^{90}Sr / ^{90}Y
  - ^{137}Cs / ^{137m}Ba
- 10 a ≤ t ≤ 100 a
  - ^{90}Sr / ^{90}Y
  - ^{137}Cs / ^{137m}Ba
  - ^{238}Pu
  - ^{241}Am
  - ^{244}Cm
- 100 a ≤ t
  - ^{241}Am
  - ^{238}Pu
  - ^{239,241}Pu

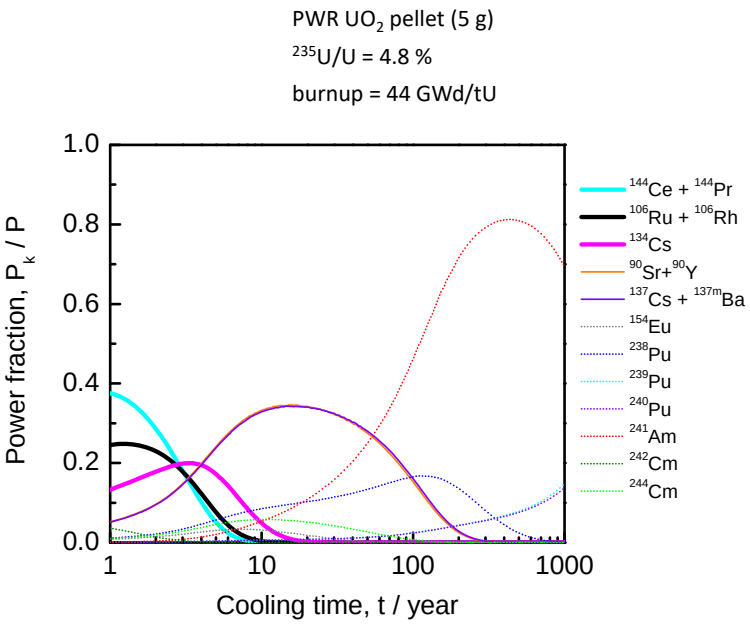

ANNETTE, 2 - 6 December 2019, Karlsruhe

Thermal power produced by SNF

- 1 a ≤ t ≤ 10 a
  - ^{144}Ce / ^{144}Pr
  - ^{106}Ru / ^{106}Rh
  - ^{134}Cs
  - ^{90}Sr / ^{90}Y
  - ^{137}Cs / ^{137m}Ba
- 10 a ≤ t ≤ 100 a
  - **^{90}Sr / ^{90}Y**
  - **^{137}Cs / ^{137m}Ba**
  - ^{238}Pu
  - ^{241}Am
  - ^{244}Cm
- 100 a ≤ t
  - ^{241}Am
  - ^{238}Pu
  - ^{239,241}Pu

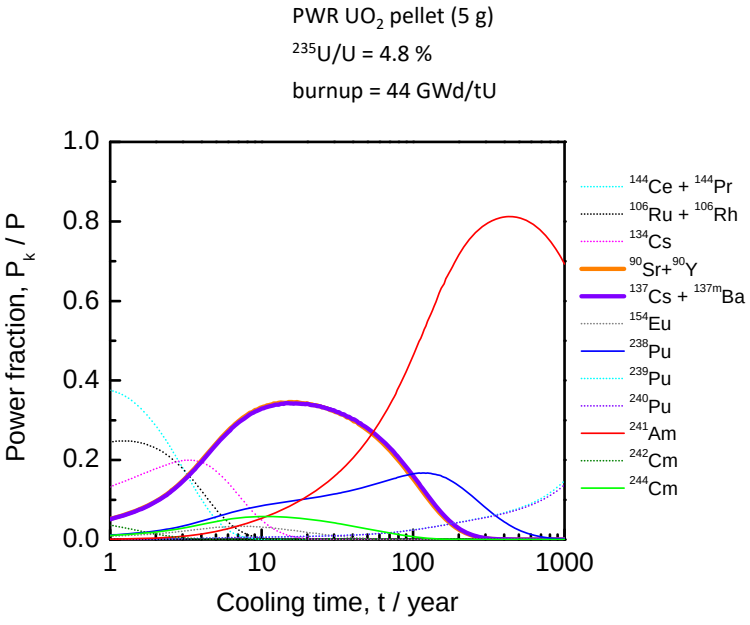

ANNETTE, 2 - 6 December 2019, Karlsruhe

Thermal power produced by SNF

- 1 a ≤ t ≤ 10 a
  - ^{144}Ce / ^{144}Pr
  - ^{106}Ru / ^{106}Rh
  - ^{134}Cs
  - ^{90}Sr / ^{90}Y
  - ^{137}Cs / ^{137m}Ba
- 10 a ≤ t ≤ 100 a
  - ^{90}Sr / ^{90}Y
  - ^{137}Cs / ^{137m}Ba
  - ^{238}Pu
  - ^{241}Am
  - ^{244}Cm
- 100 a ≤ t
  - **^{241}Am**
  - ^{238}Pu
  - $^{239,241}Pu$

PWR UO_2 pellet (5 g)
$^{235}U/U$ = 4.8 %
burnup = 44 GWd/tU

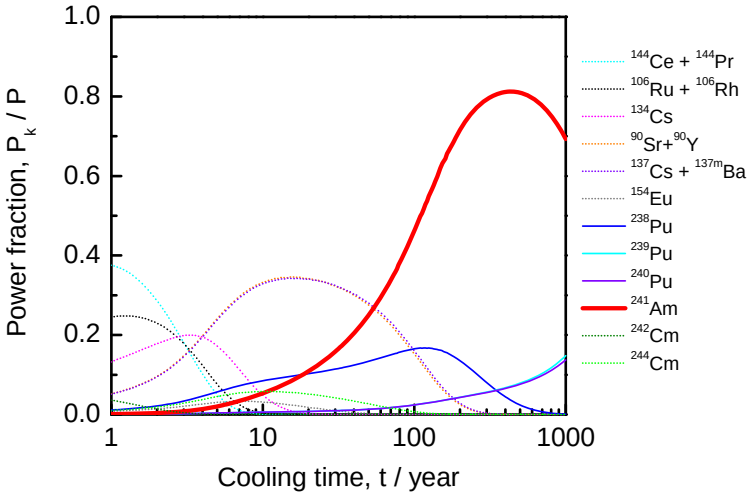

Thermal power produced by SNF

$$P(t) = \sum_k p_k N_k(t)$$

$P(t_2 > t_1)$ cannot be extrapolated from $P(t_1)$

$N_k(t)$: number of nuclei at time t

- **$N_k(t_0)$** : number of nuclei at time t_0 with $t > t_0$
- Nuclide vector at **$t > t_0$**

$$\frac{dN_k}{dt} = \sum_i \lambda_i N_i - \lambda_k N_k$$

PWR UO_2 pellet (5 g)
$^{235}U/U$ = 4.8 %
burnup = 44 GWd/tU

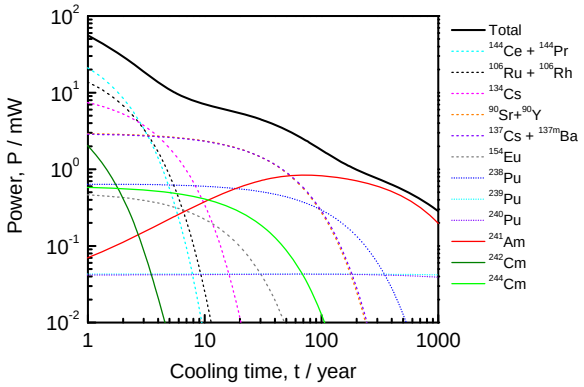

Characterisation of SNF

Main **source terms** of SNF are

- Decay heat : H
- Neutron emission : S_n
- γ-ray emission : S_γ
- Reactivity : ^{235}U, ^{239}Pu, Fission Products (BUC)
- Fissile material : ^{235}U, ^{239}Pu
- Long-term safety : e.g. ^{14}C, ^{36}Cl, ^{79}Se, ^{94}Nb, ^{99}Tc, ^{129}I, ^{226}Ra, ^{237}Np

- a **complex contribution** of **different nuclides**
- **prediction** at cooling time t **requires nuclide vector** $N_k(t)$, k = 1, …,n
- **difficult** to be **measured** directly, in particular during **industrial operation** (e.g. decay heat, reactivity)

⇒ Determined/estimated by **theoretical calculations** using a burnup code
Neutron transport + depletion/creation code

Burn-up calculations

Coupled neutron transport – nuclide depletion/creation calculation

Neutron transport

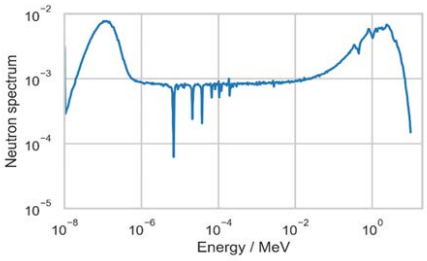

Bateman equation

$$\frac{dN_k}{dt} = Y\, N_f\, \sigma_f\, \varphi + \sum_i \lambda_i N_i + \sum_j \sigma_j N_j\, \varphi - (\lambda_k + \sigma_{k,a}\varphi) N_k$$

Update nuclide vector

ALEPH-2 (SCK•CEN)

Coupled neutron transport – fuel depletion calculation

Neutron transport

MCNP®

- Simple 1D to complex 3D
- Multi-particle physics
- Detailed energy-angle treatment
- Parallelization and PC based cluster computing

Bateman equation

RADAU-5
Runge-kutta solver

$$\frac{dN_k}{dt} = Y N_f \sigma_f \varphi + \sum_i \lambda_i N_i + \sum_j \sigma_j N_j \varphi - (\lambda_k + \sigma_{k,a}\varphi) N_k$$

Production of ^{137}Cs

$$\frac{dN_k}{dt} = Y N_f \sigma_f \varphi + \sum_i \lambda_i N_i + \sum_j \sigma_j N_j \varphi - (\lambda_k + \sigma_{k,a}\varphi) N_k$$

^{137}Cs production: only by (n,f) followed by β^- (decay of short lived precursors)

$$n + {}^{235}_{92}U \xrightarrow{(n,f)} {}^{97}_{40}Zr + {}^{137}_{52}Te + \nu_p$$

$${}^{137}_{52}Te \rightarrow {}^{137}_{53}I + e^- + \bar{\nu}_e$$

$${}^{137}_{53}I \rightarrow {}^{137}_{54}Xe + e^- + \bar{\nu}_e$$

$${}^{137}_{54}Xe \rightarrow {}^{137}_{55}Cs + e^- + \bar{\nu}_e$$

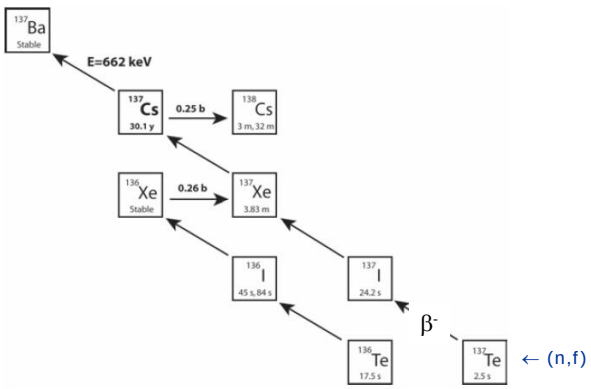

Production of ^{137}Cs

$$\frac{dN_k}{dt} = Y\, N_f\, \sigma_f\, \varphi + \sum_i \lambda_i N_i + \sum_j \sigma_j N_j\, \varphi - (\lambda_k + \sigma_{k,a}\varphi) N_k$$

^{137}Cs production: only by (n,f) followed by β^- (decay of short lived precursors)

$$N_k(t) \approx \frac{Y_c\, \sigma_f\, N_f\, \varphi}{\lambda_k + \sigma_{k,\gamma}\, \varphi}\left[1 - e^{-(\lambda_k + \sigma_{k,\gamma}\varphi)t}\right]$$

$$(\lambda_k + \sigma_{k,\gamma}\, \varphi) << 1$$

$$N_k(t) \approx Y_c\, \sigma_f\, N_f\, \varphi\, t$$

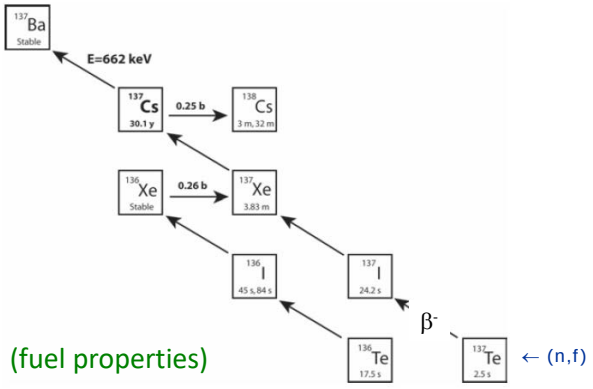

Y_c : cumulative fission yield
σ_f : fission cross section
N_f : number of fissile nuclei, i.e. ^{235}U (fuel properties)
φt : total neutron fluence (operation history)

Estimation of SNF nuclide inventory by theoretical calculations

- Burn up code: Neutron transport + nuclear fuel depletion
- Input data:
  - **Nuclear Data (ND)**
    - Cross sections (neutron interactions)
    - Fission yields
    - Neutron emission probabilities
    - Decay data
  - **Fuel History (FH)**
    - Fuel fabrication data (design, composition) e.g. Initial enrichment (IE)
    - Reactor operation and irradiation conditions e.g. Burnup (BU)
    - Cooling time (CT)

BurnUp (BU):
time integrated power per mass of initial fuel (MWd/kg)

$\propto$ *total number of fission x energy per fission event*

European Commission
ANNETTE, 2 - 6 December 2019, Karlsruhe

Estimation of SNF nuclide vector and source terms by theory

- Nuclide vector $N(t_0)$ **at time t_0** after irradiation : burn-up code
  - **Nuclear Data (ND)**
    - Cross sections
    - Fission yields
    - Neutron emission probabilities
    - Decay data
  - **Fuel History (FH)**
    - Fuel fabrication data (design, composition) e.g. Initial enrichment (IE)
    - Reactor operation and irradiation conditions e.g. Burnup (BU)
    - Cooling time (CT)
- Nuclide vector **at $t > t_0$**

$$\frac{dN_k}{dt} = \sum_i \lambda_i N_i - \lambda_k N_k$$

- Source terms **at $t > t_0$**

$$\text{e.g. } P(t) = \sum_k p_k N_k(t)$$

Depends on **well-known decay data**
(except for reactivity relying on BUC)

European Commission

^{137}Cs : gamma-ray emission + decay heat

- Production : σ(n,f) + Fission yields
  - ^{235}U(n,f) : 1.0 %
  - Fission yields : 1.5 %
- Gamma-ray emission :
  - $T_{1/2}$: 30.18 (15) a
  - $P(E_\gamma = 661.66\text{keV})$: 0.851 (2)
- Decay heat: specific decay heat rate, $p_k = E_{dk}\,\lambda_k$
  - $T_{1/2}$: 30.18 (15) a
  - Q_{β^-} : 1175.63 (17) keV
  - Recoverable energy
    - Average electron + recoil energy : 247.9 (12) keV
    - $\langle E_\gamma \rangle$: 565.4 (13) keV

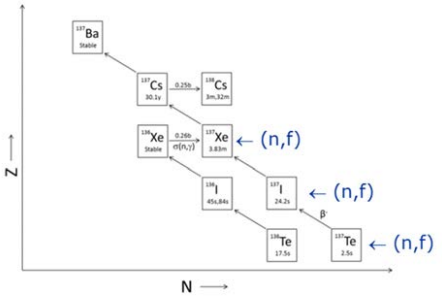

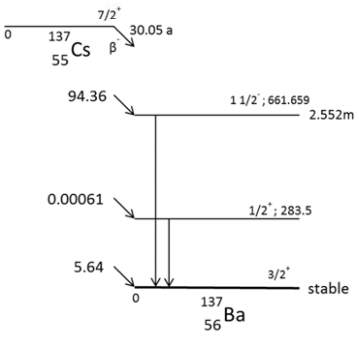

European Commission

Decay heat: ^{90}Sr and ^{137}Cs

- Production : σ(n,f) + fission yields
  - ^{235}U(n,f) : 1.0 %
  - Fission yields

Library	Cumulative yield x 100	
	^{90}Sr	^{137}Cs
IAEA	**5.730 (130)**	**6.221 (69)**
JEF-2.2	5.847 (188)	6.244 (54)
JEFF-3.1.1	5.729 (132)	6.221 (69)
JENDL-4.0	5.772 (59)	6.175 (34)
ENDF/B-V	5.913 (42)	6.220 (31)
ENDF/B-VI.8	5.782 (58)	6.188 (31)
ENDF/B-VII.1	5.782 (58)	6.188 (31)

- Specific decay heat rate (recoverable)

	^{90}Sr + ^{90}Y		^{137}Cs+ ^{137m}Ba		
	<E_e>/keV	E_γ /keV	<E_e>/keV	<E_γ>/keV	<E_e+ E_γ>/keV
Exp. (Ramthun)	1147 (9)				
Theory (Collé)	1130				
Decay data	1129.4 (14)	~ 0.0	247.9 (12)	565.4 (13)	813.3 (18)
JEFF-3.1.1	1107	0.0	245	567	812
JENDL/FPD-2011	1130	0.0	248	563	811
ENDF/B-VII.1	1129	0.0	240	566	806

	Rel. Uncertainties	
	^{90}Sr	^{137}Cs
– Cross section :	1.0 %	1.0 %
– Fission yield :	2.3 %	1.5 %
– Specific heat :	0.8 %	0.2 %
	2.6 %	1.8%

Production ^{244}Cm

$$n + {}^{238}_{92}U \xrightarrow{(n,\gamma)} {}^{239}_{92}U \xrightarrow{\beta^-} {}^{239}_{93}Np + e^- + \bar{\nu}_e$$

$${}^{239}_{93}Np \rightarrow {}^{239}_{94}Pu + e^- + \bar{\nu}_e$$

$$n + {}^{239}_{94}Pu \xrightarrow{(n,\gamma)} {}^{240}_{94}Pu$$

$$n + {}^{240}_{94}Pu \xrightarrow{(n,\gamma)} {}^{241}_{94}Pu$$

$$n + {}^{241}_{94}Pu \xrightarrow{(n,\gamma)} {}^{242}_{94}Pu$$

$$n + {}^{242}_{94}Pu \xrightarrow{(n,\gamma)} {}^{243}_{94}Pu \xrightarrow{\beta^-} {}^{243}_{95}Am + e^- + \bar{\nu}_e$$

$$n + {}^{243}_{95}Am \xrightarrow{(n,\gamma)} {}^{244}_{95}Am \xrightarrow{\beta^-} {}^{244}_{96}Cm + e^- + \bar{\nu}_e$$

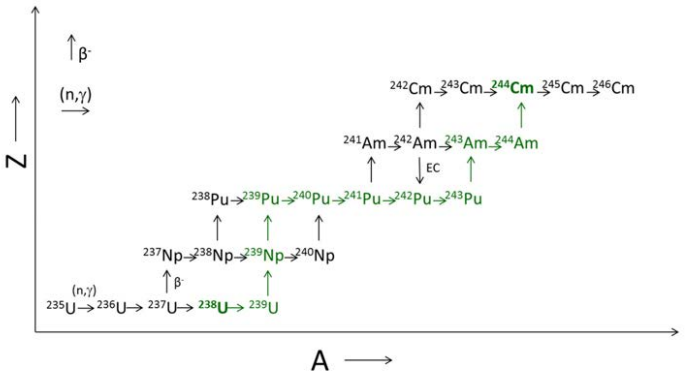

European Commission
ANNETTE, 2 - 6 December 2019, Karlsruhe

$^{242, 244}$Cm : production in MOX

Borella et al. MC 2017, Jeju, Korea

- MOX
  - PWR: 17 x 17
  - Single pin model

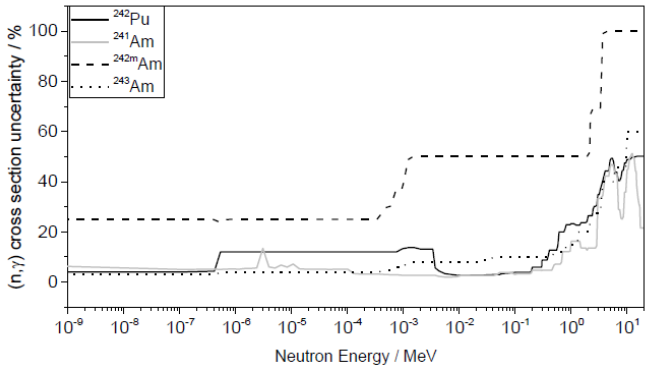

- Production : σ(n,γ)
  - ^{242}Cm : 2.5 % ^{241}Am(n,γ), ^{242m}Am(n,γ)
  - ^{244}Cm : 10 % ^{242}Pu(n,γ), ^{243}Am(n,γ)

Fuel design and irradiation history: initial enrichment and burnup

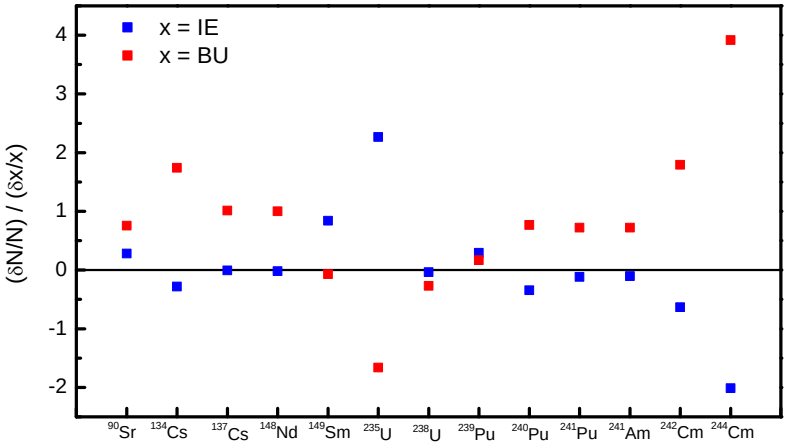

PWR UO_2 pellet (5 g)
^{235}U/U = 4.8 %
burnup = 44 GWd/tU

Production of ^{137}Cs

$$\frac{dN_k}{dt} = Y\, N_f\, \sigma_f\, \varphi + \sum_i \lambda_i N_i + \sum_j \sigma_j N_j\, \varphi - (\lambda_k + \sigma_{k,a}\varphi) N_k$$

$N_k(t) \approx a\ BU$

^{137}Cs production: only by (n,f) followed by β^- (decay of short lived precursors)

$$N_k(t) \approx \frac{Y_c\, N_f\, \sigma_f\, \varphi}{\lambda_k + \sigma_{k,\gamma}\, \varphi}\left[1 - e^{-(\lambda_k + \sigma_{k,\gamma}\varphi)t}\right]$$

$$(\lambda_k + \sigma_{k,\gamma}\, \varphi) << 1$$

$$N_k(t) \approx Y_c\ \sigma_f\, N_f\, \varphi\, t$$

$(\sigma_f\, N_f\, \varphi\, t)$: total number of fissions

$(\sigma_f\, N_f\, \varphi\, t)$ x E_f : time integrated power

$\Rightarrow N_k(t) \propto BU$

E_f : recoverable energy per fission

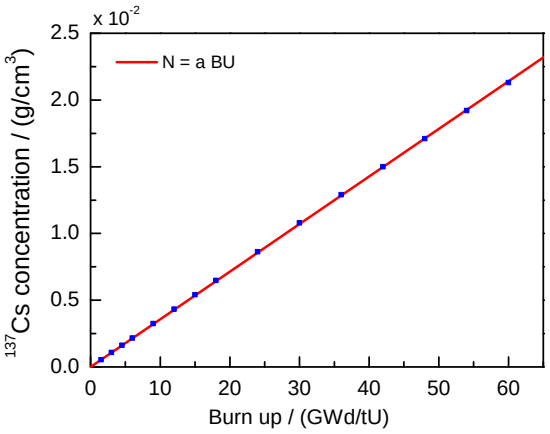

^{137}Cs used as burn-up indicator

$$N_k(t) \approx Y_c\, N_f\, \sigma_f\, \varphi\, t$$

- N ∝ BU
  (long half-life, small σ_γ)
- Fixed BU: not sensitive to IE
- Cumulative fission yields (x 100)

	^{235}U(n,f)	^{239}Pu(n,f)
^{106}Ru	0.41 (1)	4.19 (9)
^{137}Cs	**6.22 (7)**	**6.59 (8)**

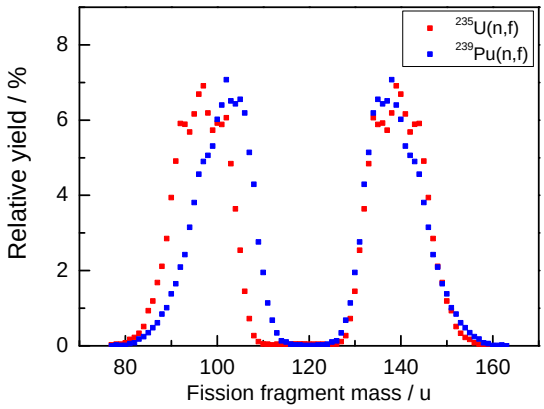

Production of ^{134}Cs

$$\frac{dN_k}{dt} = Y\,N_f\,\sigma_f\,\varphi + \sum_i \lambda_i N_i + \sum_j \sigma_j N_j\,\varphi - (\lambda_k + \sigma_{k,a}\varphi)N_k$$

$N = aBU^b$

$b = 2$ for $BU < 30$ GWd/tU

^{134}Cs production:

(n,f) followed by β^- and (n,γ)

$$n + {}^{235}_{92}U \xrightarrow{(n,f)} {}^{100}_{40}Zr + {}^{133}_{52}Te + \nu_p$$

$${}^{133}_{52}Te \xrightarrow[12.4\ min]{\beta^-} {}^{133}_{53}I + e^- + \bar{\nu}_e$$

$${}^{133}_{53}I \xrightarrow[20.8\ h]{\beta^-} {}^{133}_{54}Xe + e^- + \bar{\nu}_e$$

$${}^{133}_{54}Xe \xrightarrow[5.24\ d]{\beta^-} {}^{133}_{55}Cs + e^- + \bar{\nu}_e$$

$$n + {}^{133}_{55}Cs \xrightarrow{(n,\gamma)} {}^{134}_{55}Cs$$

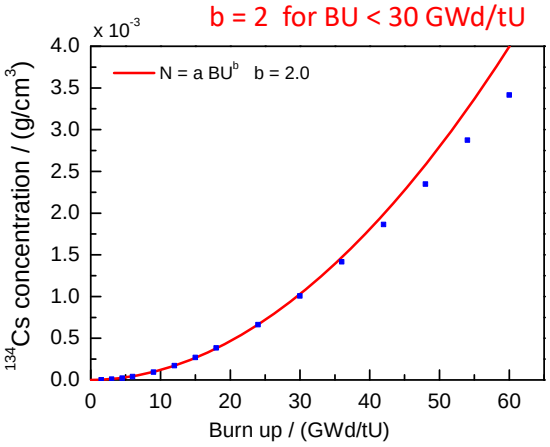

Production of ^{154}Eu

$$\frac{dN_k}{dt} = Y\,N_f\,\sigma_f\,\varphi + \sum_i \lambda_i N_i + \sum_j \sigma_j N_j\,\varphi - (\lambda_k + \sigma_{k,a}\varphi)N_k$$

$N = aBU^b$

$b = 2$ for $BU < 35$ GWd/tU

^{154}Eu production: complex

(n,f), β^- and (n,γ) from 5 mass chains

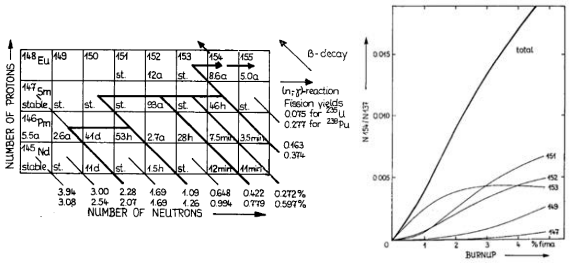

R. Berndt, Kernenergie 31 (1988) 59

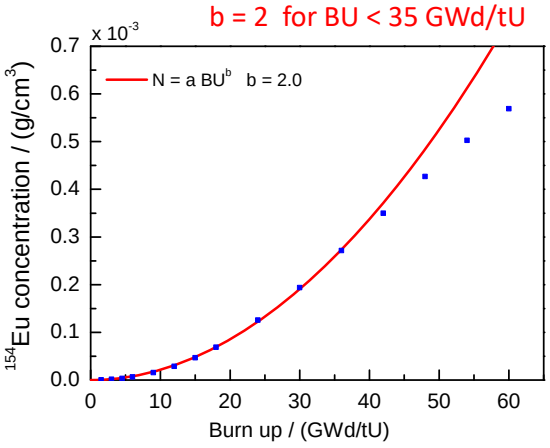

Production of ^{244}Cm

$$\frac{dN_k}{dt} = Y\,N_f\,\sigma_f\,\varphi + \sum_i \lambda_i N_i + \sum_j \sigma_j N_j\,\varphi - (\lambda_k + \sigma_{k,a}\varphi)N_k$$

$$n + {}^{238}_{92}U \xrightarrow{(n,\gamma)} {}^{239}_{92}U \xrightarrow[23.5\ min]{\beta^-} {}^{239}_{93}Np + e^- + \bar{\nu}_e$$

$${}^{239}_{93}Np \xrightarrow[2.4\ d]{\beta^-} {}^{239}_{94}Pu + e^- + \bar{\nu}_e$$

$$n + {}^{239}_{94}Pu \xrightarrow{(n,\gamma)} {}^{240}_{94}Pu$$

$$n + {}^{240}_{94}Pu \xrightarrow{(n,\gamma)} {}^{241}_{94}Pu$$

$$n + {}^{241}_{94}Pu \xrightarrow{(n,\gamma)} {}^{242}_{94}Pu$$

$$n + {}^{242}_{94}Pu \xrightarrow{(n,\gamma)} {}^{243}_{94}Pu \xrightarrow[5.0\ h]{\beta^-} {}^{243}_{95}Am + e^- + \bar{\nu}_e$$

$$n + {}^{243}_{95}Am \xrightarrow{(n,\gamma)} {}^{244}_{95}Am \xrightarrow[10.1\ h]{\beta^-} {}^{244}_{96}Cm + e^- + \bar{\nu}_e$$

N = aBU^b
b = 6 for BU < 20 GWd/tU

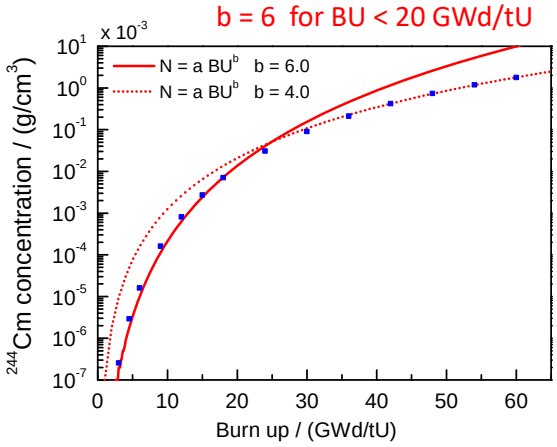

European Commission

Experimental characterisation

- Code validation
  - Radiochemical analysis of pin segments (KIT, JRC Karlsruhe)
    (chemistry + mass spectrometry and α and γ–spectrometry)
  - Calorimetric measurements of fuel assemblies (CLAB)

- Verification of input parameters (fuel design and irradiation history) by NDA (see S. Vaccaro)
  - Gamma-ray spectroscopic measurements
  - Neutron counting
  - Advanced systems developed at LANL (simulations) and tested at CLAB

EURAD/SFC:
develop NDA methods to characterise fuel assemblies under industrial operation conditions

European Commission

ANNETTE, 2 - 6 December 2019, Karlsruhe

EURAD: relies on experiments at CLAB (intermediate storage SE)

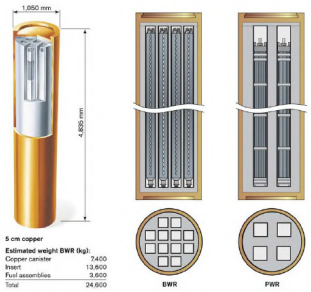

Installed systems

- Calorimeter
- Gamma-ray spectroscopic scanner

Testing

- Differential Die-Away Self-Interrogation (DDSI)
- Differential Die-Away (DDA)

European Commission

Calorimeter at CLAB

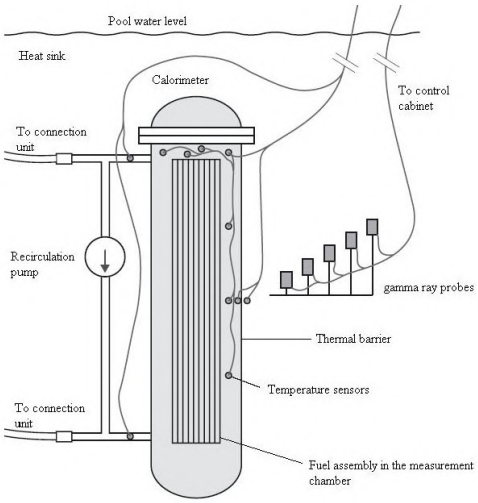

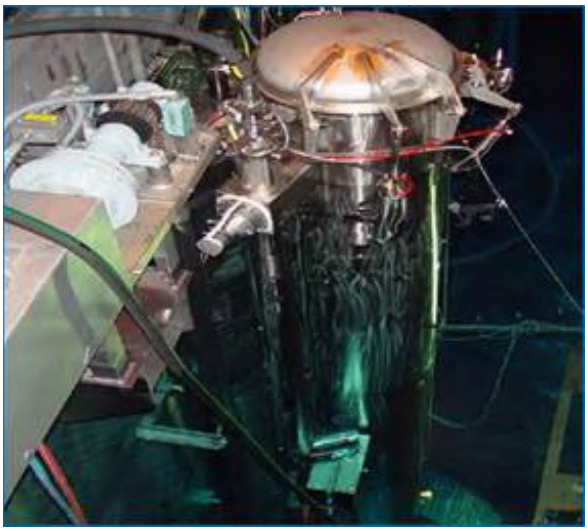

European Commission

Calorimeter at CLAB: principle

Calibration with an electrical heater

- Determine $\Delta T = T_{cal} - T_{pool}$ vs time
- Determine $d\Delta T/dt$ for $\Delta T = 0$
- Fit to data: $P = a_0 + a_1\, d\Delta T/dt$

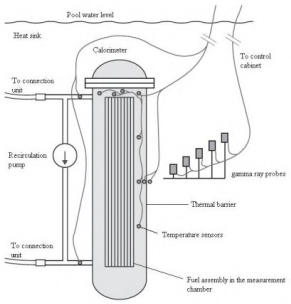

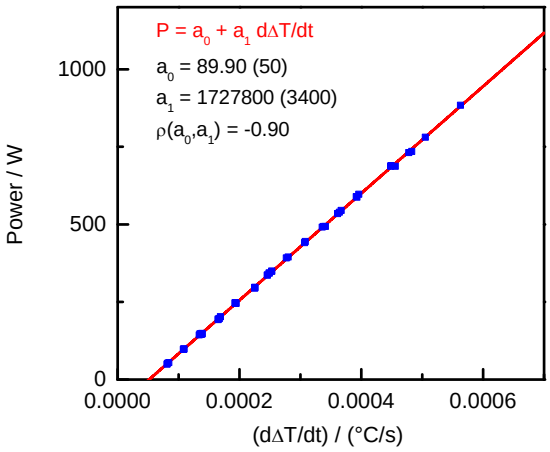

Calorimeter at CLAB: principle

Calibration with an electrical heater

- Determine $\Delta T = T_{cal} - T_{pool}$ vs time
- Determine $d\Delta T/dt$ for $\Delta T = 0$
- Fit to data: $P = a_0 + a_1\, d\Delta T/dt$

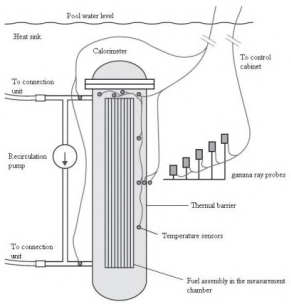

Spent nuclear fuel assembly

- Determine $\Delta T = T_{cal} - T_{pool}$ vs time
- Determine $d\Delta T/dt$ when $\Delta T = 0$
- $Q = a_0 + a_1\, \mathbf{K}\, d\Delta T/dt$
- $\mathbf{P} = Q + \mathbf{P_e}$
  - **K** : correction factor due to thermal capacity difference between electrical heater and fuel assembly
  - $\mathbf{P_e}$: heat loss due to γ-rays escaping from the calorimeter

European Commission
ANNETTE, 2 - 6 December 2019, Karlsruhe

Gamma-ray spectroscopic scanning system at CLAB

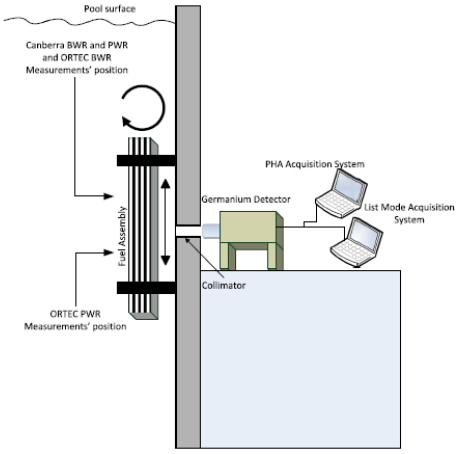

Vaccaro et al. NIMA 830 (2016) 325

^{134}Cs, ^{137}Cs, ^{154}Eu

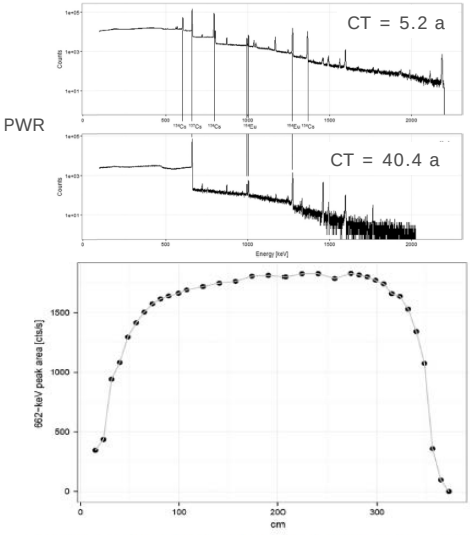

Fig. 8. Count rate for the 662-keV 137Cs net peak area as a function of axial location along BWR9. These data were measured with the ORTEC GMX detector and Canberra Lynx MCA from the 45° corner. The axial location is specified as downward along the uranium containing portion of the fuel (The indicated absolute positions are accurate to ± 10 cm, the error bars are much smaller than the data points).

Fuel assemblies: DDSI and DDA (LANL development, NGSI)

- Differential Die Away Self-Interrogation (DDSI, passive) *A.C. Trahan, LA-UR_16_20026*

LANL, Kaplan et al., NIMA 764 (2014) 347 - 351

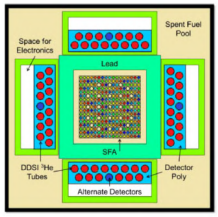

- Differential Die Away (DDA, active) *V. Henzl, LANL-UR-123025*

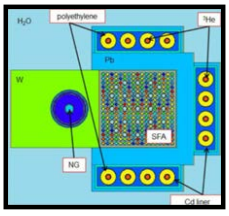

Thank you for the attention

- EURAD project (SNF characterisation)
  - PhD position at Uppsala University
    https://www.uu.se/en/about-uu/join-us/details/?positionId=300024
  - NUGENIA
    http://nugenia.org/call-for-mobility-grants-open/
- JRC Geel and Karlsruhe: open access
  - https://ec.europa.eu/jrc/en/research-facility/open-access

European Commission

ANNETTE, 2 - 6 December 2019, Karlsruhe

2.2 Characterization of spent nuclear fuel by theoretical calculations; P. Schillebeeckx, JRC Geel; Online available (JRC127309).

CHARACTERISATION OF SPENT NUCLEAR FUEL BY THEORETICAL CALCULATIONS

PWR UO_2 SNF

P. Schillebeeckx, L. Fiorito, P. Romojaro, G. Žerovnik • WP 8 Task 2

This project has received funding from the European Union's Horizon 2020 research and innovation programme 2014-2018 under grant agreement N°847593

Training material

1

KEY WORDS

- Actinides
- Alpha-decay
- Bateman equation
- Beta-decay
- Burnup
- Cooling time
- Decay heat
- Depletion codes
- Final disposal
- Fission product
- Gamma-ray emission
- Initial enrichment
- Light water reactor
- Irradiation history
- Neutron transport
- Pressurised water reactor
- Spent nuclear fuel
- Spontaneous fission
- Thermal power

Training material

2

CONTENTS

LEARNING OUTCOMES

After the completion of this training lesson, the participants should be able to

- identify the observables or source terms that are important for the transport, handling, intermediate storage and final disposal of spent nuclear fuel
- identify key nuclides determining the observables
- breakdown the complexity to theoretically estimate the observables
- identify the different components involved in the theoretical calculations of the observables
- understand the importance of nuclear data and operational history for an accurate theoretical estimation of the observables
- realise the need of more accurate data to improve the theoretical calculations

INTRODUCTION

A **safe**, **secure**, **ecological** and **economic** transport**,** storage and final disposal requires that **Spent Nuclear Fuel (SNF)** is **characterised** for the main observables or source terms of interest:

- Decay heat
- Neutron emission
- γ-ray emission
- Reactivity (Burn Up Credit (BUC), i.e. Fission Product (FP), actinides)
- Fissile material (Nuclear Safeguards, i.e. ^{235}U, ^{239}Pu)
- Specific nuclides (Long term safety)
  i.e. ^{14}C, ^{36}Cl, ^{79}Se, ^{94}Nb, ^{99}Tc, ^{129}I, ^{226}Ra, ^{237}Np

⇒ requires knowledge of a **complex nuclide inventory**



Training material

5

SPENT NUCLEAR FUEL: NUCLIDE INVENTORY

- Fission products (FP): neutron induced fission (n,f)

  e.g. ^{99}Tc, **^{137}Cs**, ^{154}Eu, …

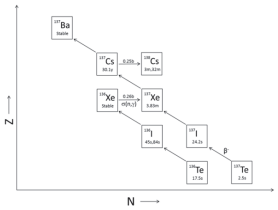

- Actinides: major and minor actinides

  e. g. ^{235}U, ^{238}U, **^{239}Pu**, ^{241}Am, ^{244}Cm, …

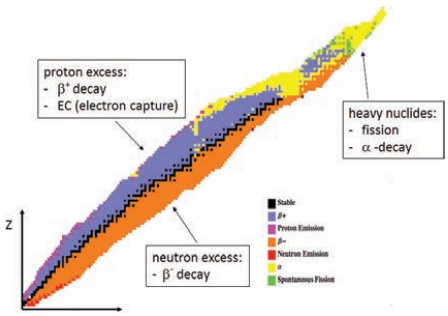

$$n + {}^{238}_{92}\mathbf{U} \xrightarrow{(n,\gamma)} {}^{239}_{92}\mathrm{U} \xrightarrow[23.5\ \mathrm{min}]{\beta^-} {}^{239}_{93}\mathrm{Np} \xrightarrow[2.36\ \mathrm{d}]{\beta^-} {}^{239}_{94}\mathbf{Pu}$$

Training material

6

β^- - DECAY BY NEUTRON RICH NUCLIDES

Isobaric transition in which a neutron
is transformed into a proton
and an electron + anti-neutrino are emitted

$$^{A}_{Z}X \rightarrow ^{A}_{Z+1}Y^{*} + e^{-} + \bar{\nu}_e$$

$$\downarrow$$

$$^{A}_{Z+1}Y + E_\gamma$$

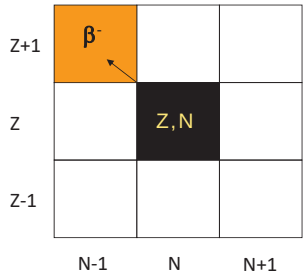

Training material

β^- - DECAY BY NEUTRON RICH NUCLIDES: e.g. ^{137}Cs

- $T_{1/2}$ = 30.05 (8) a
- Q_{β^-} = 1175.73 (17) keV

$$^{137}_{55}Cs \rightarrow ^{137}_{56}Ba^{*} + e^{-} + \bar{\nu}_e$$

$$\downarrow$$

$$^{137}_{56}Ba + E_\gamma$$

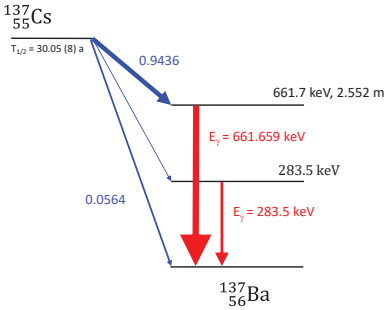

Gamma-ray emission probability: P_γ

E_γ	P_γ
661.7 keV	**0.8499 (20)**
283.5 keV	5.8 (8) x 10^{-6}

http://www.nucleide.org/DDEP_WG/Nuclides/Cs-137_tables.pdf

Training material

α - DECAY

Radioactive decay in which a nucleus **emits** an **α-particle** (^{4}He nucleus) and transforms into a nucleus with 4 less nucleons (2n, 2p)

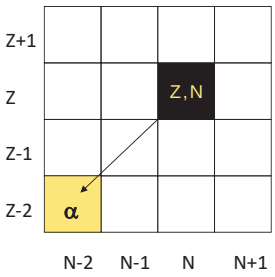

$$^{A}_{Z}X \rightarrow ^{A-4}_{Z-2}Y^{*} + \alpha$$

$$^{A-4}_{Z-2}Y + E_{\gamma}$$

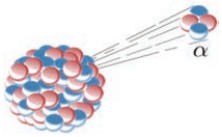

in heavy nuclei

Training material

α - DECAY BY ACTINIDES: e.g. ^{241}Am

- $T_{1/2}$ = 432.6 (6) a
- Q_{α} = 5637.82 (12) keV

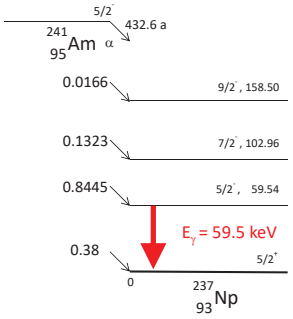

$$^{241}_{95}\mathrm{Am} \rightarrow ^{237}_{93}\mathrm{Np}^{*} + \alpha$$

$$^{237}_{93}\mathrm{Np} + E_{\gamma}$$

α -particle emission probability:

E_{α}	$P(E_{\alpha})$
5388.3 keV	0.0166 (3)
5442.9 keV	0.1323 (10)
5485.6 keV	**0.8445 (10)**

http://www.nucleide.org/DDEP_WG/Nuclides/Am-241_tables.pdf

Training material

SPONTANEOUS FISSION

Fission: nucleus splits up into fission products (FP)

e.g. ^{238,240,242}Pu(sf), ^{242,244,246}Cm(sf), ^{252}Cf(sf)

- FP : acceleration due to Coulomb repulsion
- FP : strongly excited, emission of
  - Prompt fission neutrons (PFN)
  - Prompt fission γ-rays (PFG)
- Prompt fission neutrons important for Non-Destructive Analysis (NDA)

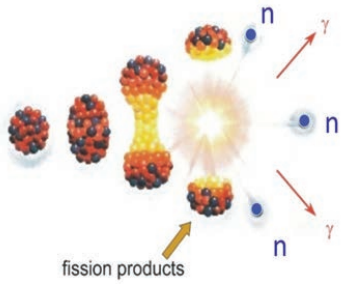

Training material

11

PROMPT FISSION NEUTRONS: MULTIPLICITY

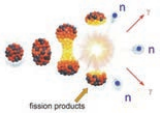

Emission of prompt fission neutrons:

- statistical process
- on average ν > 1

Nuclide	$\nu_{s(1)}$	$\nu_{s(2)}$	$\nu_{s(3)}$
^{238}Pu	2.210	1.978	0.933
^{240}Pu	2.154	1.895	0.868
^{242}Pu	2.145	1.882	0.867
^{252}Cf	3.756	5.978	5.287

$$\nu_{s(j)} = \sum_{\nu=j}^{\infty} \binom{\nu}{j} P_{s\nu}$$

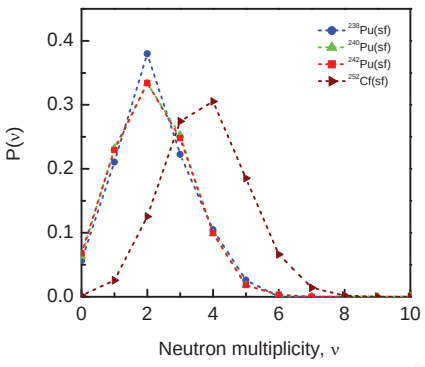

Training material

12

PROMPT FISSION NEUTRONS: DATA

Nuclide	$T_{1/2}$	(sf) branching	<ν>	S_{sf} / (s^{-1} g^{-1})
^{238}Pu	8 .774 (3) x 10^{1} a	1.85 (5) x 10^{-9}	1.980 (30)	2.59 (11) x 10^{3}
^{240}Pu	6.561 (7) x 10^{3} a	5.70 (20) x 10^{-8}	2.154 (5)	1.031 (36) x 10^{3}
^{242}Pu	3.73 (3) x 10^{5} a	5.49 (9) x 10^{-6}	2.149 (8)	1.728 (32) x 10^{3}
^{242}Cm	162.86 (8) d	6.36 (14) x 10^{-8}	2.540 (20)	1.980 (46) x 10^{7}
^{244}Cm	1.811 (3) x 10^{1} a	1.36 (1) x 10^{-6}	2.710 (10)	1.107 (10) x 10^{7}
^{246}Cm	4.72 (3) x 10^{3} a	2.61 (4) x 10^{-6}	2.930 (30)	8.70 (13) x 10^{6}

Decay data from Nichols et al., INDC-2453, , INDC(NDS) – 0534, August 2008
<ν> from Santi and Miller, NucL; Sci. Eng. 160 (2017) 190

Training material

13

PROMPT FISSION NEUTRONS: ENERGY DISTRIBUTION

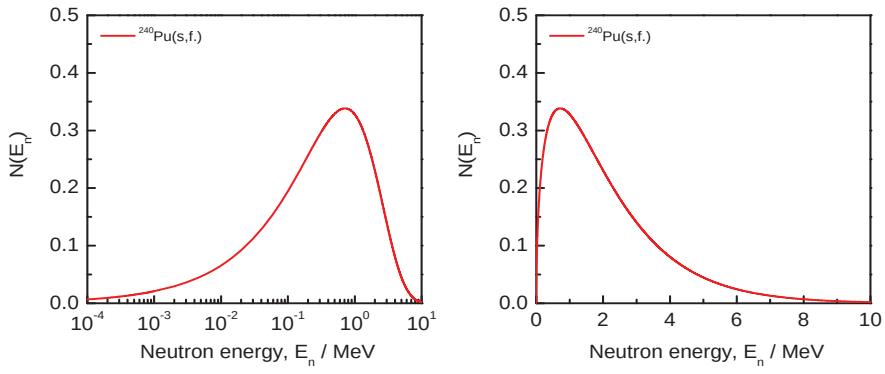

$< E_n > \approx 2$ MeV

Training material

14

NEUTRON PRODUCTION BY (α,n) REACTIONS

- (α,n) reaction with light nuclides
  - $^{18}O(\alpha,n)^{21}Ne$
  - $^{17}O(\alpha,n)^{20}Ne$
  - $^{19}F(\alpha,n)^{22}Na$
- Neutron energy (emission)
  - O(α,n) : $<E_n> \sim 2$ MeV
  - F(α,n) : $<E_n> \sim 1$ MeV
- P(ν) = 1
  used to separate prompt fission neutrons from (α,n) neutrons in neutron correlation counting (NDA)

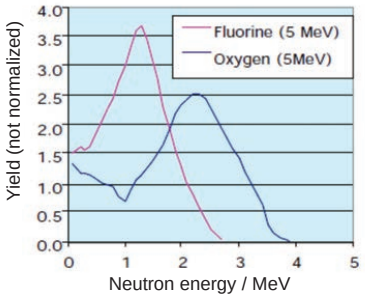

⇒ in SNF: α - decay of actinides followed by (α,n) reaction in light elements

Training material

NEUTRON EMISSION BY SPENT NUCLEAR FUEL

$$S_n(t) = \sum_k S_{n,k}(t)$$

- $S_{n,k}(t)$: contribution of radionuclide k
- $S_{n,k}(t) = (s_{sf,k} + s_{\alpha n,k})\, N_k(t)$
  - $N_k(t)$: number of nuclei of nuclide k at time t
  - $s_{sf,k}$: specific neutron emission rate of nuclide k due to **spontaneous fission**
  - $s_{\alpha,k}$: specific neutron emission rate of nuclide k due to **(α,n) reactions**

PWR UO_2 pellet (5 g)
$^{235}U/U$ = 4.8 %
burnup = 45 GWd/t

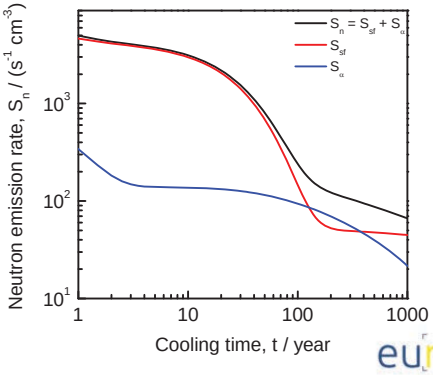

Training material

NEUTRON EMISSION BY SPENT NUCLEAR FUEL

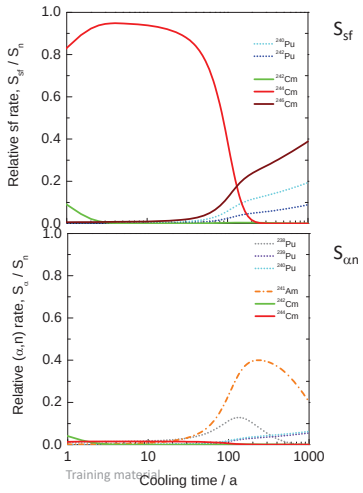

PWR UO_2 pellet (5 g)
$^{235}U/U$ = 4.8 %
burnup = 45 GWd/t

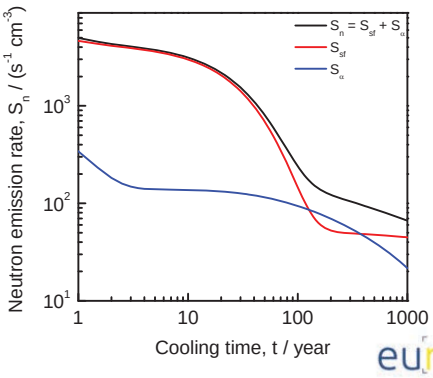

NEUTRON EMISSION BY SPENT NUCLEAR FUEL

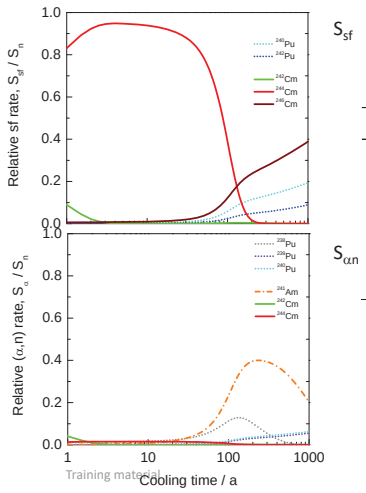

PWR UO_2 pellet (5 g)
$^{235}U/U$ = 4.8 %
burnup = 45 GWd/t

Nuclide	$T_{1/2}$	(sf) branching	<v>	S_{sf} / (s^{-1} g^{-1})
^{238}Pu	8 .774 (3) x 10^1 a	1.85 (5) x 10^{-9}	1.980 (30)	2.59 (11) x 10^3
^{240}Pu	6.561 (7) x 10^3 a	5.70 (20) x 10^{-8}	2.154 (5)	1.031 (36) x 10^3
^{242}Pu	3.73 (3) x 10^5 a	5.49 (9) x 10^{-6}	2.149 (8)	1.728 (32) x 10^3
^{242}Cm	162.86 (8) d	6.36 (14) x 10^{-8}	2.540 (20)	1.980 (46) x 10^7
^{244}Cm	**1.811 (3) x 10^1 a**	**1.36 (1) x 10^{-6}**	**2.710 (10)**	**1.107 (10) x 10^7**
^{246}Cm	4.72 (3) x 10^3 a	2.61 (4) x 10^{-6}	2.930 (30)	8.70 (13) x 10^6

Decay data from Nichols et al., INDC-2453, , INDC(NDS) – 0534, August 2008
<v> from Santi and Miller, NucL; Sci. Eng. 160 (2017) 190

GAMMA-RAY EMISSION BY SPENT NUCLEAR FUEL

$$S_\gamma(t) = \sum_k S_{\gamma,k}(E_\gamma, t)$$

^{95}Nb	35.0 d
^{95}Zr	64.0 d
^{144}Ce/^{144}Pr	284.9 d
^{106}Ru/^{106}Rh	1.02 a
^{134}Cs	2.06 a
^{154}Eu	8.8 a
^{137}Cs/^{137m}Ba	30.0 a

PWR UO_2 pellet (5 g)
^{235}U/U = 4.8 %
burnup = 45 GWd/t

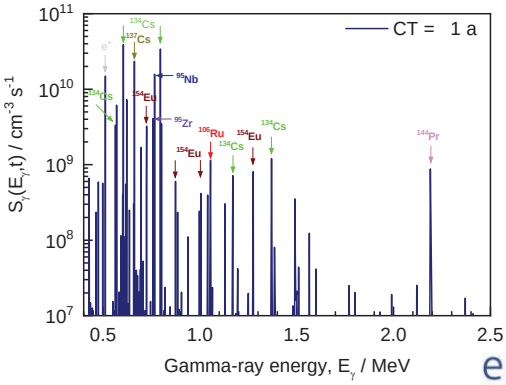

Training material

19

GAMMA-RAY EMISSION BY SPENT NUCLEAR FUEL

$$S_\gamma(t) = \sum_k S_{\gamma,k}(E_\gamma, t)$$

^{95}Nb	35.0 d
^{95}Zr	64.0 d
^{144}Ce/^{144}Pr	284.9 d
^{106}Ru/^{106}Rh	1.02 a
^{134}Cs	2.06 a
^{154}Eu	8.8 a
^{137}Cs/^{137m}Ba	30.0 a

PWR UO_2 pellet (5 g)
^{235}U/U = 4.8 %
burnup = 45 GWd/t

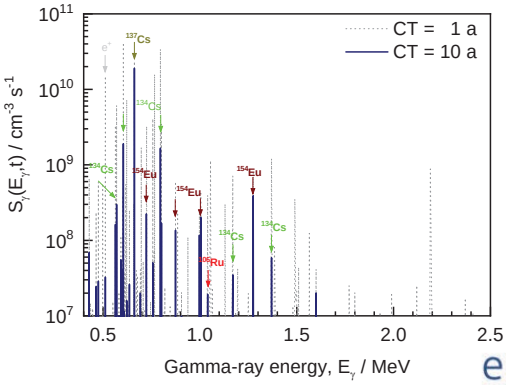

Training material

20

GAMMA-RAY EMISSION BY SPENT NUCLEAR FUEL

$$S_\gamma(t) = \sum_k S_{\gamma,k}(E_\gamma, t)$$

^{95}Nb	35.0 d
^{95}Zr	64.0 d
^{144}Ce/^{144}Pr	284.9 d
^{106}Ru/^{106}Rh	1.02 a
^{134}Cs	2.06 a
^{154}Eu	**8.8 a**
^{137}Cs/^{137m}Ba	**30.0 a**

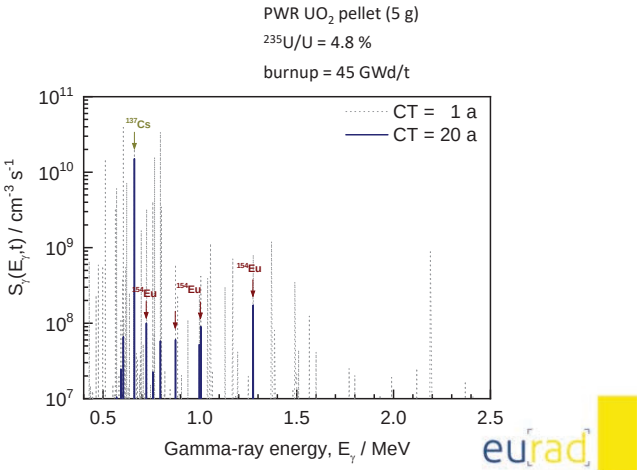

GAMMA-RAY EMISSION BY SPENT NUCLEAR FUEL

$$S_\gamma(t) = \sum_k S_{\gamma,k}(E_\gamma, t)$$

^{95}Nb	35.0 d
^{95}Zr	64.0 d
^{144}Ce/^{144}Pr	284.9 d
^{106}Ru/^{106}Rh	1.02 a
^{134}Cs	2.06 a
^{154}Eu	**8.8 a**
^{137}Cs/^{137m}Ba	**30.0 a**

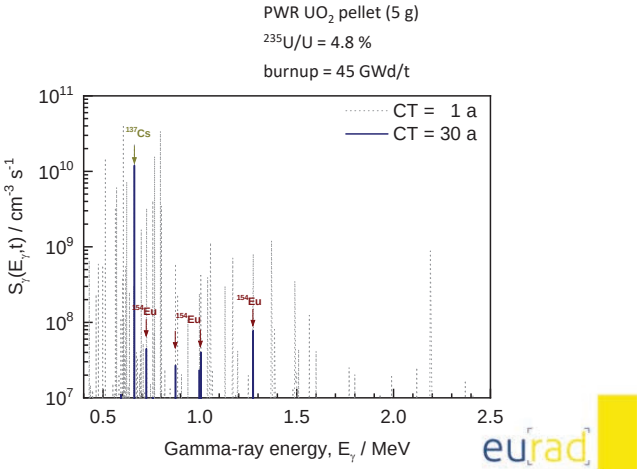

GAMMA-RAY EMISSION BY SNF: CONTRIBUTION TO THERMAL POWER

$$P_\gamma(t) = \sum_k \lambda_k N_k(t) \int E_\gamma S_{\gamma,k}(E_\gamma, t) dE_\gamma$$

^{95}Nb	35.0 d
^{95}Zr	64.0 d
^{144}Ce/^{144}Pr	284.9 d
^{106}Ru/^{106}Rh	1.02 a
^{134}Cs	2.06 a
^{154}Eu	8.8 a
^{137}Cs/^{137m}Ba	30.0 a
^{241}Am	432.6 a

PWR UO_2 pellet (5 g)
^{235}U/U = 4.8 %
burnup = 45 GWd/t

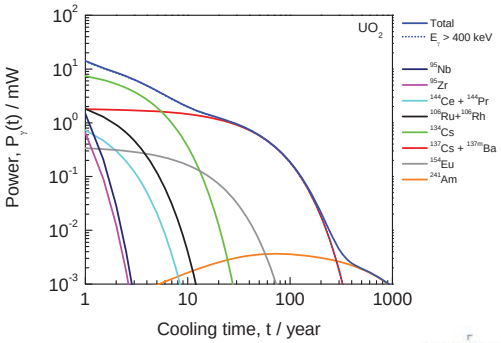

Training material

THERMAL POWER PRODUCED BY SNF

$$P(t) = \sum_k P_k(t)$$

- $P_k(t)$: contribution of radionuclide k
- $P_k(t) = p_k N_k(t)$
  - $N_k(t)$: number of nuclei of nuclide k at time t
  - p_k : specific decay heat rate of nuclide k

PWR UO_2 pellet (5 g)
^{235}U/U = 4.8 %
burnup = 45 GWd/t

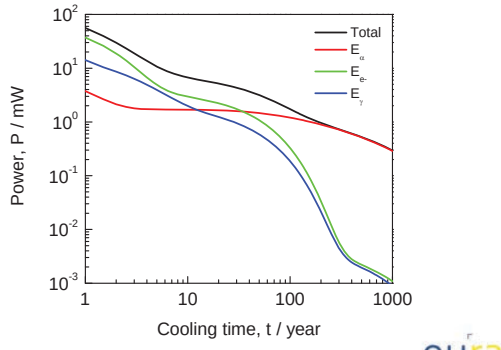

Training material

THERMAL POWER PRODUCED BY SNF

- 1 a ≤ t ≤ 10 a
  - ^{144}Ce / ^{144}Pr
  - ^{106}Ru / ^{106}Rh
  - ^{134}Cs
  - ^{90}Sr / ^{90}Y
  - ^{137}Cs / ^{137m}Ba
- 10 a ≤ t ≤ 100 a
  - ^{90}Sr / ^{90}Y
  - ^{137}Cs / ^{137m}Ba
  - ^{238}Pu
  - ^{241}Am
  - ^{244}Cm
- 100 a ≤ t
  - ^{241}Am
  - ^{238}Pu
  - ^{239,241}Pu

PWR UO_2 pellet (5 g)
^{235}U/U = 4.8 %
burnup = 45 GWd/t

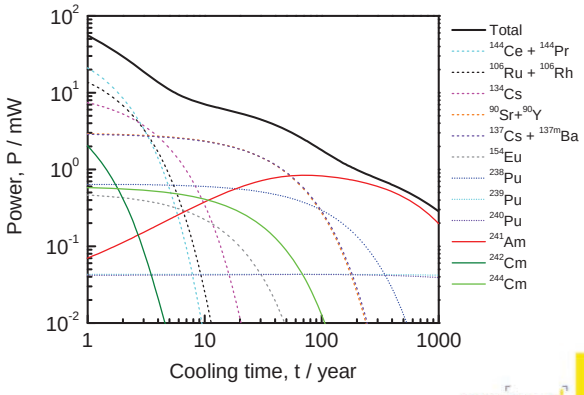

Training material

THERMAL POWER PRODUCED BY SNF

- 1 a ≤ t ≤ 10 a
  - **^{144}Ce / ^{144}Pr**
  - **^{106}Ru / ^{106}Rh**
  - **^{134}Cs**
  - ^{90}Sr / ^{90}Y
  - ^{137}Cs / ^{137m}Ba
- 10 a ≤ t ≤ 100 a
  - ^{90}Sr / ^{90}Y
  - ^{137}Cs / ^{137m}Ba
  - ^{238}Pu
  - ^{241}Am
  - ^{244}Cm
- 100 a ≤ t
  - ^{241}Am
  - ^{238}Pu
  - ^{239,241}Pu

PWR UO_2 pellet (5 g)
^{235}U/U = 4.8 %
burnup = 45 GWd/t

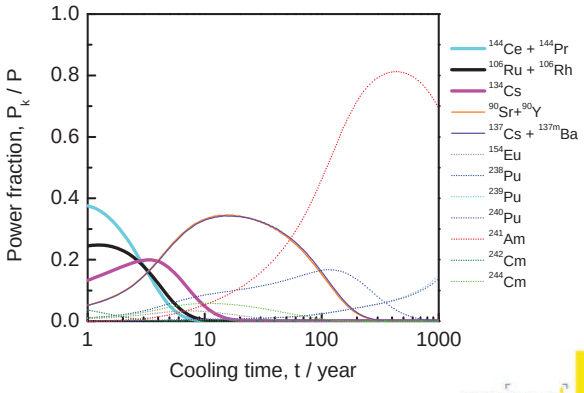

Training material

THERMAL POWER PRODUCED BY SNF

- 1 a ≤ t ≤ 10 a
  - ^{144}Ce / ^{144}Pr
  - ^{106}Ru / ^{106}Rh
  - ^{134}Cs
  - ^{90}Sr / ^{90}Y
  - ^{137}Cs / ^{137m}Ba
- 10 a ≤ t ≤ 100 a
  - **^{90}Sr / ^{90}Y**
  - **^{137}Cs / ^{137m}Ba**
  - ^{238}Pu
  - ^{241}Am
  - ^{244}Cm
- 100 a ≤ t
  - ^{241}Am
  - ^{238}Pu
  - $^{239,241}Pu$

PWR UO_2 pellet (5 g)
$^{235}U/U$ = 4.8 %
burnup = 45 GWd/t

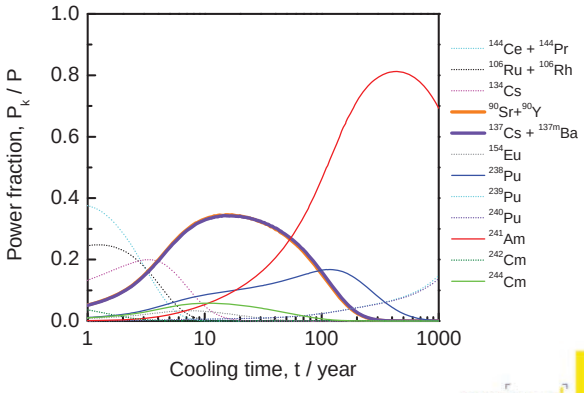

Training material

27

THERMAL POWER PRODUCED BY SNF

- 1 a ≤ t ≤ 10 a
  - ^{144}Ce / ^{144}Pr
  - ^{106}Ru / ^{106}Rh
  - ^{134}Cs
  - ^{90}Sr / ^{90}Y
  - ^{137}Cs / ^{137m}Ba
- 10 a ≤ t ≤ 100 a
  - ^{90}Sr / ^{90}Y
  - ^{137}Cs / ^{137m}Ba
  - ^{238}Pu
  - ^{241}Am
  - ^{244}Cm
- 100 a ≤ t
  - **^{241}Am**
  - ^{238}Pu
  - $^{239,241}Pu$

PWR UO_2 pellet (5 g)
$^{235}U/U$ = 4.8 %
burnup = 45 GWd/t

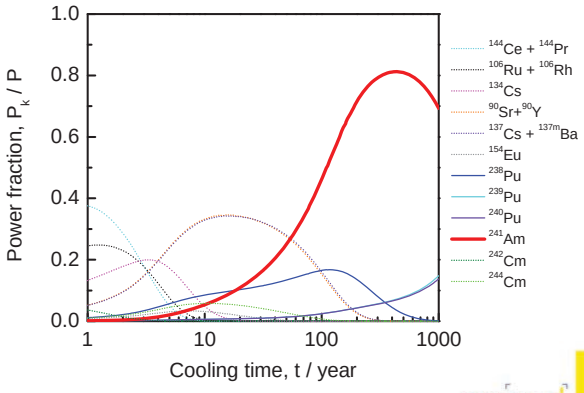

Training material

28

THERMAL POWER PRODUCED BY SNF

$$P(t) = \sum_k p_k N_k(t)$$

$N_k(t)$: number of nuclei at time t

- **$N_k(t_0)$** : number of nuclei at time t_0 with $t > t_0$
- Nuclide vector at **$t > t_0$**

$$\frac{dN_k}{dt} = \sum_{i \to k} \lambda_i N_i - \lambda_k N_k$$

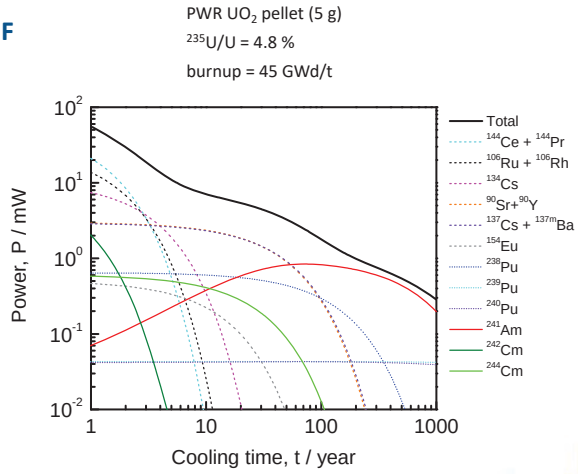

Training material

29

SNF SOURCE TERMS

Main **observables** or **source terms** of interest:

- Decay heat : H
- Neutron emission : S_n
- γ-ray emission : S_γ
- Reactivity : ^{235}U, ^{239}Pu, Fission Products (BUC)
- Fissile material : ^{235}U, ^{239}Pu
- Long-term safety : e.g. ^{14}C, ^{36}Cl, ^{79}Se, ^{94}Nb, ^{99}Tc, ^{129}I, ^{226}Ra, ^{237}Np

difficult to be **measured** directly, in particular during **industrial operation**

- Decay heat by **calorimetry** at CLAB: accurate but **long measurement times**
- Criticality safety analysis: calculations required to account for **burn-up credit** (MA, FP)
- **Prediction at long cooling times** only possible by theoretical calculations

⇒ Determined/estimated by **theoretical calculations** using a burnup code
Neutron transport + depletion/creation code

Training material

30

SNF SOURCE TERMS: NUCLIDE INVENTORY

Nuclide	Source term	CT
^{90}Sr	H, S_γ	10 a ≤ t ≤ 100 a
^{106}Ru	H	1 a ≤ t ≤ 10 a
^{134}Cs	H	1 a ≤ t ≤ 10 a
^{137}Cs	H, S_γ	10 a ≤ t ≤ 100 a
^{144}Ce	H	1 a ≤ t ≤ 10 a
^{148}Nd	*Burn-up*	*stable*
^{149}Sm	*Power*	*stable*
^{154}Eu	H, S_γ	1 a ≤ t ≤ 10 a

Nuclide	Source term	CT
^{235}U	R, S_γ	10^5 a ≤ t
^{238}U	R, S_γ	10^5 a ≤ t
^{238}Pu	H, S_γ	10 a ≤ t
^{239}Pu	R, S_γ	100 a ≤ t ≤ 10^4 a
^{240}Pu	R, S_γ	100 a ≤ t ≤ 10^4 a
^{241}Pu	H, S_γ	10 a ≤ t ≤ 100 a
^{241}Am	H	10 a ≤ t
^{242}Cm	H, S_n	1 a ≤ t ≤ 10 a
^{244}Cm	H, S_n	10 a ≤ t ≤ 100 a

H : thermal power or decay heat
S_n : neutron emission
S_γ : γ-ray emission
R : reactivity (criticality safety)

Criticality safety (Burn Up Credit, BUC):
^{95}Mo, ^{99}Tc, ^{101}Ru, ^{103}Rh, ^{109}Ag, ^{133}Cs, ^{143}Nd, ^{147,149,150,151,152}Sm, ^{155}Gd

Long term safety:
^{14}C, ^{36}Cl, ^{79}Se, ^{94}Nb, ^{99}Tc, ^{129}I, ^{226}Ra, ^{237}Np

⇒ Requires **complex nuclide inventory** which can only be obtained by **theoretical calculations**

Training material

31

BURNUP CALCULATIONS: COUPLED NEUTRON TRANSPORT – NUCLIDE DEPLETION/CREATION

Neutron transport

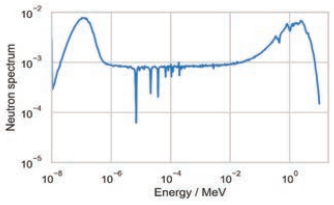

Bateman equation

$$\frac{dN_k}{dt} = Y\,N_f\,\sigma_f\,\varphi + \sum_{i\to k}\lambda_i N_i + \sum_{j\to k}\sigma_j N_j\,\varphi - (\lambda_k + \sigma_{k,a}\varphi)N_k$$

Update nuclide vector

Training material

32

PRODUCTION OF ^{137}Cs

$$\frac{dN_k}{dt} = Y\, N_f\, \sigma_f\, \varphi + \sum_{i\to k} \lambda_i N_i + \sum_{j\to k} \sigma_j N_j\, \varphi - (\lambda_k + \sigma_{k,a}\varphi) N_k$$

^{137}Cs production: only by (n,f) followed by β^- (decay of short lived precursors)

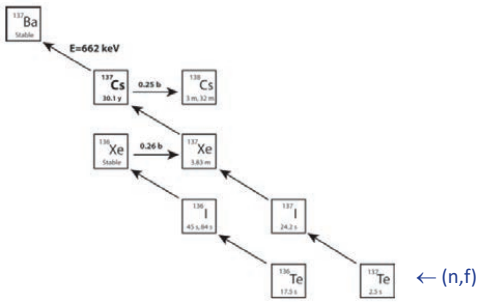

$$n + {}^{235}_{92}U \rightarrow {}^{97}_{40}Zr + {}^{137}_{52}Te + \nu_p$$

$${}^{137}_{52}Te \rightarrow {}^{137}_{53}I + e^- + \bar{\nu}_e$$

$${}^{137}_{53}I \rightarrow {}^{137}_{54}Xe + e^- + \bar{\nu}_e$$

$${}^{137}_{54}Xe \rightarrow {}^{137}_{55}Cs + e^- + \bar{\nu}_e$$

PRODUCTION OF ^{137}Cs

$$\frac{dN_k}{dt} = Y\, N_f\, \sigma_f\, \varphi + \sum_{i\to k} \lambda_i N_i + \sum_{j\to k} \sigma_j N_j\, \varphi - (\lambda_k + \sigma_{k,a}\varphi) N_k$$

^{137}Cs production: only by (n,f) followed by β^- (decay of short lived precursors)

$$N_k(t') \approx \frac{Y_c\, \sigma_f\, N_f\, \varphi}{\lambda_k + \sigma_{k,\gamma}\, \varphi}\left[1 - e^{-(\lambda_k + \sigma_{k,\gamma}\varphi)t'}\right] \qquad (\lambda_k + \sigma_{k,\gamma}\, \varphi)\, t' << 1$$

$$N_k(t') \sim Y_c\, \sigma_f\, N_f\, \varphi\, t'$$

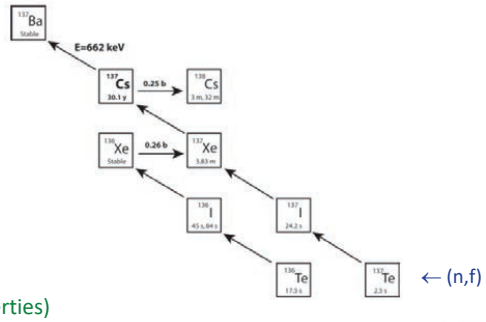

- Y_c : cumulative fission yield
- σ_f : fission cross section
- N_f : number of fissile nuclei, i.e. ^{235}U (fuel properties)
- $\varphi\, t'$: total (time integrated) neutron fluence (operation history)
- $\sigma_f\, N_f\, \varphi\, t'$: total number of fissions

BURNUP CODES: THEORETICAL CALCULATION OF SNF NUCLIDE INVENTORY AND OBSERVABLES

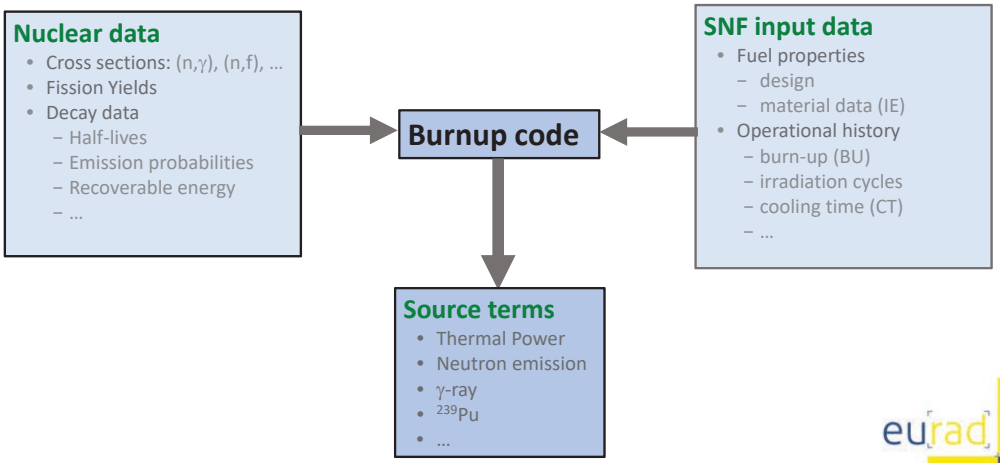

Training material

35

BURNUP CODES: THEORETICAL CALCULATION OF SNF NUCLIDE INVENTORY AND OBSERVABLES

- Burnup code: Neutron transport + nuclear fuel depletion
  - Deterministic ⇔ stochastic
  - Approach to solve the Bateman equation
  - Geometry
- Input data:
  - **Nuclear Data (ND)**
    - Cross sections
    - Fission yields
    - Decay data
    - (α,n) production yields
    - …
  - **Fuel History (FH)**
    - Fuel fabrication data (design, composition) e.g. Initial enrichment (IE)
    - Reactor operation and irradiation conditions e.g. Burnup (BU)
    - Cooling time (CT)

Burnup (BU):
time integrated power per mass of initial fuel (MWd/kg)

Training material

36

BURNUP CODES: NUCLEAR DATA

Neutron induced interaction cross sections

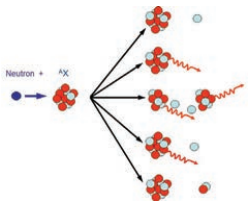

elastic scattering : (n,n)

capture: (n,γ)

fission : (n,f)

inelastic scattering : (n,n'γ)

others: e.g. (n,p), (n,α), ...

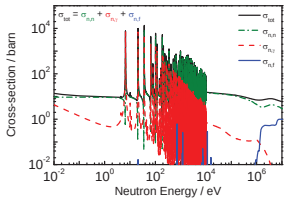

Fission process

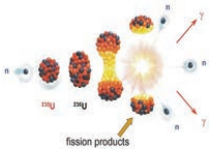

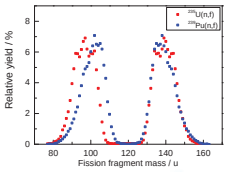

Training material

37

BURNUP CODES

- Nuclide vector $N(t_0)$ **at time t_0** after irradiation : burn-up code
  - **Nuclear Data (ND)**
    - Cross sections
    - Fission yields
    - Neutron emission probabilities
    - Decay data
  - **Fuel History (FH)**
    - Fuel fabrication data (design, composition) e.g. Initial enrichment (IE)
    - Reactor operation and irradiation conditions e.g. Burnup (BU)
    - Cooling time (CT)
- Nuclide vector **at $t > t_0$**

$$\frac{dN_k}{dt} = \sum_{i \to k} \lambda_i N_i - \lambda_k N_k$$

- Source terms **at $t > t_0$**

e.g. $P(t) = \sum_k p_k N_k(t)$

Depends on **well-known decay data**

Training material

38

GAMMA-RAY EMISSION BY SNF

$$S_\gamma(t) = \sum_k S_{\gamma,k}(E_\gamma, t)$$

^{95}Nb	35.0 d
^{95}Zr	64.0 d
^{144}Ce/^{144}Pr	284.9 d
^{106}Ru/^{106}Rh	1.02 a
^{134}Cs	2.06 a
^{154}Eu	8.8 a
^{137}Cs/^{137m}Ba	**30.0 a**

PWR UO_2 pellet (5 g)
^{235}U/U = 4.8 %
burnup = 45 GWd/t

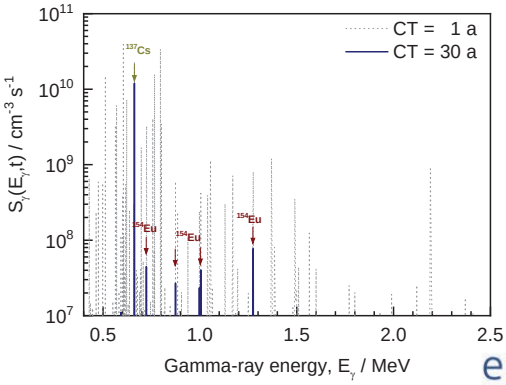

Training material

39

THERMAL POWER PRODUCED BY SNF

- 1 a ≤ t ≤ 10 a
  - ^{144}Ce / ^{144}Pr
  - ^{106}Ru / ^{106}Rh
  - ^{134}Cs
  - ^{90}Sr / ^{90}Y
  - ^{137}Cs / ^{137m}Ba
- 10 a ≤ t ≤ 100 a
  - **^{90}Sr / ^{90}Y**
  - **^{137}Cs / ^{137m}Ba**
  - ^{238}Pu
  - ^{241}Am
  - ^{244}Cm
- 100 a ≤ t
  - ^{241}Am
  - ^{238}Pu
  - ^{239,241}Pu

PWR UO_2 pellet (5 g)
^{235}U/U = 4.8 %
burnup = 45 GWd/t

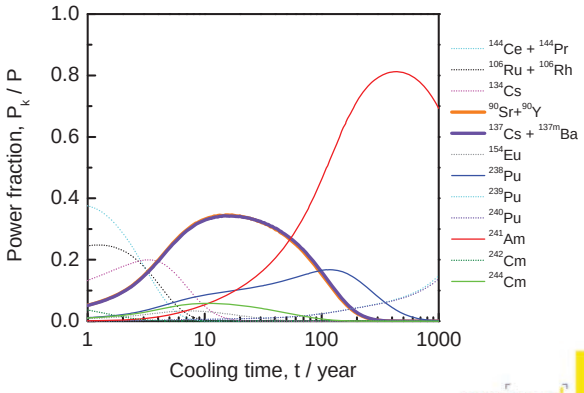

Training material

40

^{137}Cs: γ-RAY EMISSION AND THERMAL POWER

- Production :

$$N_k(t') \sim Y_c\, \sigma_f\, N_f\, \varphi\, t'$$

- Gamma-ray emission : (decay data)
  - $T_{1/2}$: 30.05 (8) a
  - $P(E_\gamma = 661.66\text{keV})$: 0.8499 (20)

- Thermal power: specific decay heat rate, $p_k = E_{dk}\, \lambda_k$ (decay data)
  - $T_{1/2}$: 30.18 (15) a
  - Q_{β^-} : 1175.63 (17) keV
  - Recoverable energy
    - Average electron + recoil energy : 247.9 (12) keV
    - $\langle E_\gamma \rangle$: 565.4 (13) keV

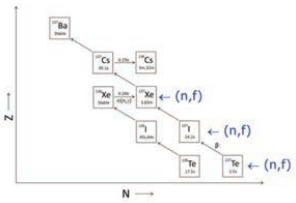

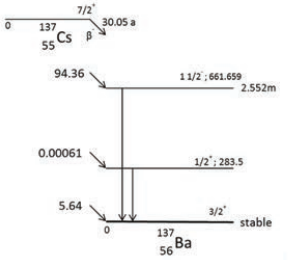

Decay data from DDEP (Decay Data Evaluation Project) : http://www.nucleide.org/DDEP.htm

^{137}Cs: PRODUCTION

$$\frac{dN_k}{dt} = Y\, N_f\, \sigma_f\, \varphi + \sum_{i \to k} \lambda_i N_i + \sum_{j \to k} \sigma_j N_j\, \varphi - (\lambda_k + \sigma_{k,a}\varphi) N_k$$

$$N_k(t') \approx \frac{Y_c\, \sigma_f\, N_f\, \varphi}{\lambda_k + \sigma_{k,\gamma}\, \varphi} \left[1 - e^{-(\lambda_k + \sigma_{k,\gamma}\varphi)t'}\right]$$

$$(\lambda_k + \sigma_{k,\gamma}\, \varphi) << 1$$

$$N_k(t') \sim Y_c\, \sigma_f\, N_f\, \varphi\, t'$$

$(\sigma_f\, N_f\, \varphi\, t')$: total number of fissions

$(\sigma_f\, N_f\, \varphi\, t') \times E_f$: time integrated reactor power = burnup (BU)

E_f = recoverable energy per fission

$\Rightarrow N_k(t_0) \propto BU$

$$N_k(t_0) \propto Y_c\, BU$$

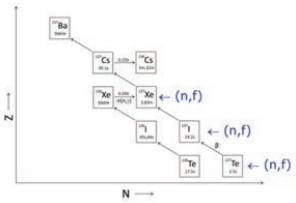

^{137}Cs production: only by (n,f) followed by β^- (decay of short lived precursors)
- Relatively long lived
- Small capture cross section

^{137}Cs: CONTRIBUTION TO THERMAL POWER

- Production : cumulative fission yields + burnup

$$N_k(t_0) \propto Y_c \, BU$$

- Thermal power after cooling time t by ^{137}Cs

$$P_k(t) = p_k \, N_k(t_0) \, e^{-\lambda_k (t-t_0)} \qquad p_k = E_{dk} \, \lambda_k$$

⇒ Nuclear data

- Y_c : cumulative fission yields
- λ_k : decay constant
- E_{dk} : recoverable energy

⇒ Operational history : BU

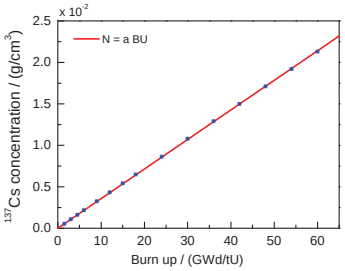

^{137}Cs: γ-RAY EMISSION AND THERMAL POWER

- Production : cumulative fission yields + burnup

$$N_k(t_0) \propto Y_c \, BU$$

- Gamma-ray emission : (decay data)
  - $T_{1/2}$: 30.05 (8) a
  - $P(E_\gamma = 661.66keV)$: 0.8499 (20)

- Thermal power: specific decay heat rate, $p_k = E_{dk} \, \lambda_k$ (decay data)
  - $T_{1/2}$: 30.18 (15) a
  - Q_{β^-} : 1175.63 (17) keV
  - Recoverable energy
    - Average electron + recoil energy : 247.9 (12) keV
    - $<E_\gamma>$: 565.4 (13) keV

Decay data from DDEP (Decay Data Evaluation Project) : http://www.nucleide.org/DDEP.htm

^{137}Cs and ^{90}Sr: CONTRIBUTION TO THERMAL POWER (UNCERTAINTY EVALUATION)

$$P_k(t) = p_k\, N_k(t_0)\, e^{-\lambda_k (t-t_0)} \qquad N_k(t_0) \propto Y_c\, BU \qquad p_k = E_{dk}\, \lambda_k$$

$$\Rightarrow \frac{u_{P_k}}{P_k} = = \sqrt{\left(\frac{u_{BU}}{BU}\right)^2 + \left(\frac{u_{Y_c}}{Y_c}\right)^2 + \left(\frac{u_{E_{dk}}}{E_{dk}}\right)^2}$$

⇒ Nuclear data
- Y_c : cumulative fission yields
- λ_k : decay constant
- E_{dk} : recoverable energy

⇒ Operational history : BU

Note:
- Contribution of ^{137}Cs and ^{90}Sr: similar
  - simple cases
  - with relatively well determined nuclear data
- Production of e.g ^{134}Cs ore complex $\propto BU^b$ with b ~ 2

$$\Rightarrow \frac{u_{N_k}}{N_k} = 2\frac{u_{BU}}{BU}$$

^{137}Cs : NUCLEAR DATA (Y_c,E_d)

			^{137}Cs			
Library	E_d / keV	Ratio	100 x Y_c	Ratio	(Y_c x E_d) / keV	Ratio
DDEP/IAEA	811.8 (18)	1	6.221 (69)	1	50.5 (6)	1
JEF-2.2	812.0 (69)	1.000 (8)	6.244 (54)	1.004 (9)	50.7 (6)	1.004 (12)
JEFF-3.1.1	**810.1 (23)**	**0.998 (3)**	**6.221 (69)**	**1.000 (11)**	**50.4 (6)**	**0.998 (11)**
JEFF-3.3	**801.8 (23)**	**0.988 (3)**	**6.090 (63)**	**0.979 (10)**	**48.8 (5)**	**0.967 (10)**
ENDF/B-VI.8	813.4 (41)	1.002 (5)	6.188 (31)	0.995 (5)	50.3 (4)	0.997 (7)
ENDF/B-VII.0	805.7 (16)	0.992 (2)	6.188 (31)	0.995 (5)	49.9 (3)	0.987 (5)
ENDF/B-VIII.0	**805.8 (18)**	**0.993 (2)**	**6.188 (31)**	**0.995 (5)**	**49.9 (3)**	**0.987 (5)**

DDEP: http://www.nucleide.org/DDEP.htm
Evaluated data libraries: https://www.oecd-nea.org/jcms/pl_39910/janis

^{90}Sr : NUCLEAR DATA (Y_c,E_d)

Library	^{90}Sr E_d / keV	Ratio	^{90}Sr 100 x Y_c	Ratio	^{90}Sr (Y_c x E_d) / keV	Ratio
DDEP/IAEA	1129.4 (14)	1	5.730 (130)	1	64.7 (15)	1
JEF-2.2	1129.6 (7)	1.000 (1)	**5.847 (188)**	**1.020 (33)**	**66.0 (21)**	**1.021 (33)**
JEFF-3.1.1	1107.8 (13)	0.981 (1)	5.729 (132)	1.000 (23)	63.5 (15)	0.981 (23)
JEFF-3.3	1127.3 (13)	0.998 (1)	**5.676 (131)**	**0.991 (23)**	**64.0 (15)**	**0.989 (23)**
ENDF/B-VI.8	1129.9 (12)	1.000 (1)	5.782 (58)	1.009 (10)	65.3 (7)	1.010 (10)
ENDF/B-VII.0	1129.4 (13)	1.000 (1)	5.782 (58)	1.009 (10)	65.3 (7)	1.009 (10)
ENDF/B-VIII.0	1128.8 (11)	0.999 (1)	**5.782 (58)**	**1.009 (10)**	**65.3 (7)**	**1.009 (10)**
Ramthum (Exp. 1967)	**1147.0 (90)**					

DDEP: http://www.nucleide.org/DDEP.htm
Evaluated data libraries: https://www.oecd-nea.org/jcms/pl_39910/janis
H. Ramthum, Proc. Symp. Standardization of radionuclides, Oct. (1966) (IAEA, 1967), p. 589

Training material

47

^{90}Sr and ^{137}Cs: NUCLEAR DATA (Y_c,E_d)

Library	^{90}Sr (E_d x Y_c) / keV	Ratio	^{137}Cs (Y_c x E_d) / keV	Ratio
DDEP/IAEA	64.7 (15)	1	50.5 (6)	1
JEF-2.2	**66.0 (21)**	**1.021 (33)**	**50.7 (7)**	**1.004 (12)**
JEFF-3.1.1	63.5 (15)	0.981 (23)	50.4 (6)	0.998 (11)
JEFF-3.3	**64.0 (15)**	**0.989 (23)**	**48.8 (5)**	**0.967 (10)**
ENDF/B-VI.8	65.3 (7)	1.010 (10)	50.3 (4)	0.997 (7)
ENDF/B-VII.0	65.3 (7)	1.009 (10)	49.9 (3)	0.987 (5)
ENDF/B-VIII.0	**65.3 (7)**	**1.009 (10)**	**49.9 (3)**	**0.987 (5)**

Ilas et al., Nucl. Eng. Des. 319 (2017) 176
u_p/P = 1.3%, is this realistic? No

Data set	Data set	Uncertainty (1σ) (%)
Modeling data	Fuel design	0.20
	Operating data	0.85
	Total	0.87
Nuclear data	Cross sections	0.88
	Fission yields	0.26
	Total	0.92
Overall effect	Total	1.27

Training material

48

NEUTRON EMISSION BY SPENT NUCLEAR FUEL

PWR UO_2 pellet (5 g)
$^{235}U/U$ = 4.8 %
burnup = 45 GWd/t

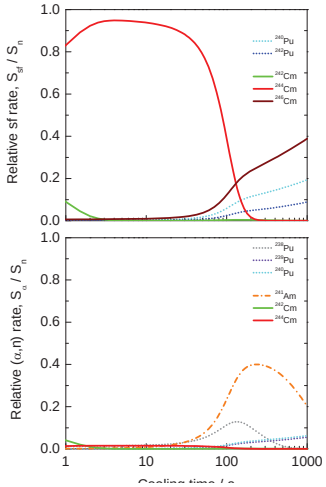

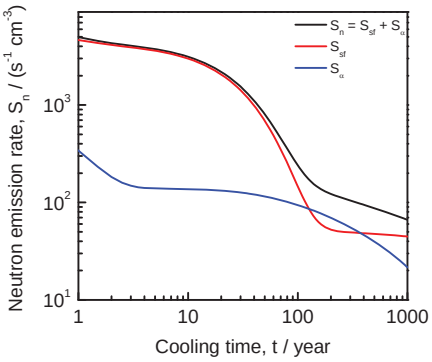

⇒ Main contribution from ^{244}Cm(sf)

^{244}Cm : NEUTRON EMISSION

- Production

$$n + {}^{238}_{92}U \xrightarrow{(n,\gamma)} {}^{239}_{92}U \xrightarrow{\beta^-} {}^{239}_{93}Np + e^- + \bar{\nu}_e$$

$${}^{239}_{93}Np \rightarrow {}^{239}_{94}Pu + e^- + \bar{\nu}_e$$

$$n + {}^{239}_{94}Pu \xrightarrow{(n,\gamma)} {}^{240}_{94}Pu$$

$$n + {}^{240}_{94}Pu \xrightarrow{(n,\gamma)} {}^{241}_{94}Pu$$

$$n + {}^{241}_{94}Pu \xrightarrow{(n,\gamma)} {}^{242}_{94}Pu$$

$$n + {}^{242}_{94}Pu \xrightarrow{(n,\gamma)} {}^{243}_{94}Pu \xrightarrow{\beta^-} {}^{243}_{95}Am + e^- + \bar{\nu}_e$$

$$n + {}^{243}_{95}Am \xrightarrow{(n,\gamma)} {}^{244}_{95}Am \xrightarrow{\beta^-} {}^{244}_{96}Cm + e^- + \bar{\nu}_e$$

Sequence of
- (n,γ) reactions (6)
- β^- decays (4)

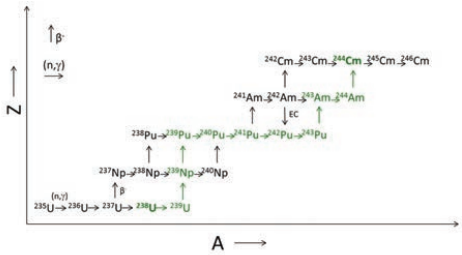

^{244}Cm : UNCERTAINTY OF INVENTORY DUE TO NUCLEAR DATA

- Production

$$n + {}^{238}_{92}U \xrightarrow{(n,\gamma)} {}^{239}_{92}U \xrightarrow{\beta^-} {}^{239}_{93}Np + e^- + \bar{\nu}_e$$

$${}^{239}_{93}Np \rightarrow {}^{239}_{94}Pu + e^- + \bar{\nu}_e$$

$$n + {}^{239}_{94}Pu \xrightarrow{(n,\gamma)} {}^{240}_{94}Pu$$

$$n + {}^{240}_{94}Pu \xrightarrow{(n,\gamma)} {}^{241}_{94}Pu$$

$$n + {}^{241}_{94}Pu \xrightarrow{(n,\gamma)} {}^{242}_{94}Pu$$

$$n + {}^{242}_{94}Pu \xrightarrow{(n,\gamma)} {}^{243}_{94}Pu \xrightarrow{\beta^-} {}^{243}_{95}Am + e^- + \bar{\nu}_e$$

$$n + {}^{243}_{95}Am \xrightarrow{(n,\gamma)} {}^{244}_{95}Am \xrightarrow{\beta^-} {}^{244}_{96}Cm + e^- + \bar{\nu}_e$$

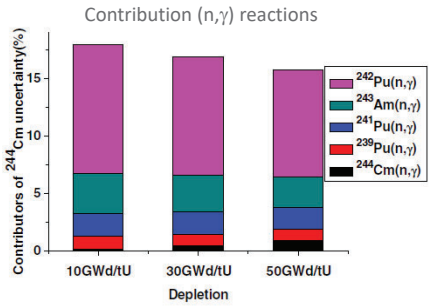

Burnup	Relative uncertainty
10 GWd/t	12.1 %
30 GWD/t	11.1 %
50 GWd/t	10.0 %

Tiejun Zu et al., Annals of Nuclear Energy 94 (2016) 399

Training material

51

^{244}Cm : UNCERTAINTY OF INVENTORY DUE TO NUCLEAR DATA

- Production

$$n + {}^{238}_{92}U \xrightarrow{(n,\gamma)} {}^{239}_{92}U \xrightarrow{\beta^-} {}^{239}_{93}Np + e^- + \bar{\nu}_e$$

$${}^{239}_{93}Np \rightarrow {}^{239}_{94}Pu + e^- + \bar{\nu}_e$$

$$n + {}^{239}_{94}Pu \xrightarrow{(n,\gamma)} {}^{240}_{94}Pu$$

$$n + {}^{240}_{94}Pu \xrightarrow{(n,\gamma)} {}^{241}_{94}Pu$$

$$n + {}^{241}_{94}Pu \xrightarrow{(n,\gamma)} {}^{242}_{94}Pu$$

$$n + {}^{242}_{94}Pu \xrightarrow{(n,\gamma)} {}^{243}_{94}Pu \xrightarrow{\beta^-} {}^{243}_{95}Am + e^- + \bar{\nu}_e$$

$$n + {}^{243}_{95}Am \xrightarrow{(n,\gamma)} {}^{244}_{95}Am \xrightarrow{\beta^-} {}^{244}_{96}Cm + e^- + \bar{\nu}_e$$

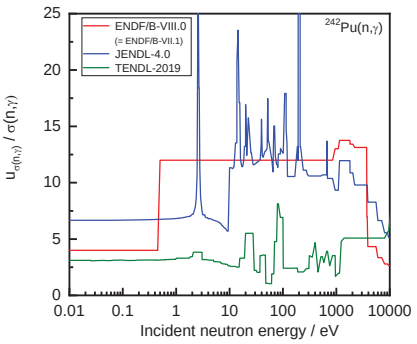

Training material

52

^{244}Cm : DIFFERENCES IN INVENTORY DUE TO NUCLEAR DATA

- Production

$$n + {}^{238}_{92}U \xrightarrow{(n,\gamma)} {}^{239}_{92}U \xrightarrow{\beta^-} {}^{239}_{93}Np + e^- + \bar{\nu}_e$$

$${}^{239}_{93}Np \rightarrow {}^{239}_{94}Pu + e^- + \bar{\nu}_e$$

$$n + {}^{239}_{94}Pu \xrightarrow{(n,\gamma)} {}^{240}_{94}Pu$$

$$n + {}^{240}_{94}Pu \xrightarrow{(n,\gamma)} {}^{241}_{94}Pu$$

$$n + {}^{241}_{94}Pu \xrightarrow{(n,\gamma)} {}^{242}_{94}Pu$$

$$n + {}^{242}_{94}Pu \xrightarrow{(n,\gamma)} {}^{243}_{94}Pu \xrightarrow{\beta^-} {}^{243}_{95}Am + e^- + \bar{\nu}_e$$

$$n + {}^{243}_{95}Am \xrightarrow{(n,\gamma)} {}^{244}_{95}Am \xrightarrow{\beta^-} {}^{244}_{96}Cm + e^- + \bar{\nu}_e$$

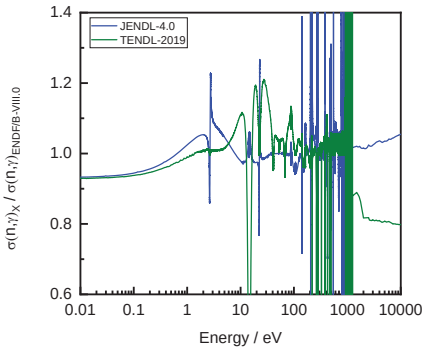

^{244}Cm : UNCERTAINTY OF INVENTORY DUE TO FUEL HISTORY

- Production

N = aBU^b
b = 6 for BU < 20 GWd/tU

$$\frac{\delta N}{N} = b\frac{\delta BU}{BU}$$

Sequence of
- (n,γ) reactions (6)
- β$^-$ decays (4)

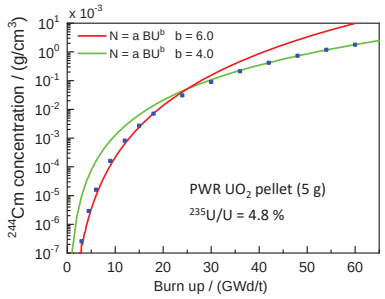

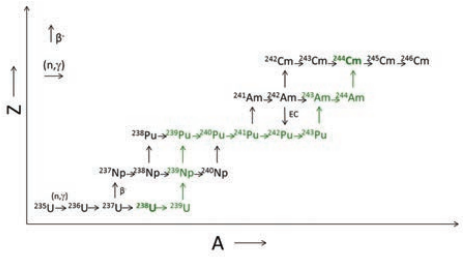

NUCLIDE INVENTORY: DESIGN AND OPERATIONAL HISTORY

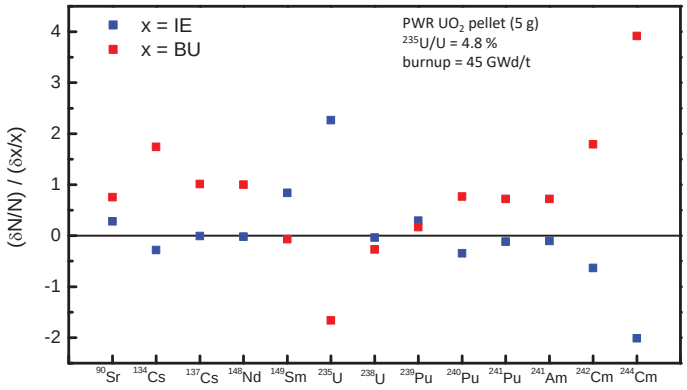

^{244}Cm : N = aBU^{b}

b ≈ 4 for BU = 45 GWd/t

$$\frac{\delta N}{N} = b\frac{\delta BU}{BU}$$

0.5 % uncertainty on BU
⇒ 2 % uncertianty on 244Cm inventory

Training material

55

SUMMARY AND CONCLUSIONS

- The main observables of interest for a safe handling, transport, intermediate storage and final disposal were identified and discussed
- A characterisation of SNF for these observables requires the inventory of some key nuclides with different characteristics
- The inventory of the key nuclides can only be obtained by theoretical calculations using burnup code which rely on a combination of neutron transport and nuclide depletion and creation calculations
- The quality of the theoretical calculations strongly depends on the quality of the nuclear data and design and irradiation history of the SNF
- Some key nuclear data (including their uncertainties) such as cumulative fission yields and neutron induced capture cross sections need to be improved to allow an accurate estimation of the main observables of interest including reliable confidence limits

Training material

56

BIBLIOGRAPHY AND REFERENCES

Spent nuclear fuel observables and key nuclides

- Broadhead et al., "Investigation of nuclide importance to functional requirements related to transport and long-term storage of LWR spent fuel", Report ORNL/TM-12742 (1995)
- Gauld et al., "Nuclide importance to criticality safety, decay heating and source terms related to transport and interim storage of high-burnup LWR fuel", Report NUREG/CR-6700, ORNL/TM-2000/284 (2001)
- Žerovnik et al. ,"Observables of interest for the characterisation of Spent Nuclear Fuel", EUR 29301 EN (2018) , JRC112361
- Schillebeeckx et al., "Characterisation of spent nuclear fuel by theoretical calculations and non-destructive analysis", see JRC114178 (2019)

Burnup codes

- Stankovskiy and Van den Eynde, "Advanced method for calculations of core burn-up, activation of structural materials and spallation products accumulation in accelerator driven system", Science and Technology of Nuclear Installations 2012 (2012) 545103
- Álvarez-Velarde, "Validation of the burn-up code EVOLCODE 2.0 with PWR experimental data and with a Sensitivity/Uncertainty analysis", Annals of Nuclear Energy 73 (2014) 175
- Leppänen et al., "The Serpent Monte Carlo code: status, development and applications in 2013", Annals of Nuclear Energy 82 (2015) 142
- Kashima et al., "Validation of burnup calculation code SWAT4 by evaluation of isotopic composition data of mixed oxide fuel irradiated in pressurized water reactor", Energy Procedia 71 (2015) 159
- Rearden and Jessee, "SCALE Code System", ORNL/TM-2005/39 Version 6.2, April 2016
- Gauld et al., "Isotopic depletion and decay methods and analysis capabilities in SCALE", Nuclear Technology 174 (2017) 169
- Ebiwonjumi et al., "Verification and validation of radiation source term capabilities in STREAM", Annals of Nulcear Energy 124 (2019) 80

BIBLIOGRAPHY AND REFERENCES

Bateman equation

- Jerzy Cetnar, "General solution of Bateman equations for nuclear transmutation", Annals of Nuclear Energy 33 (2006) 640
- Maren Vranckx, "Implementation, validation and comparison of different algorithms to solve the Bateman equations for very large systems", Thesis Msc, Univ. Gent, June 2016
- Isotalo and Aarnio, "Comparison of depletion algorithms for large systems of nuclides", Annals of Nuclear Energy 38 (2011) 261
- Maria Pusa, "Numerical methods for nuclear fuel depletion calculations", PhD Thesis, Aalto University, May 2013
- Calvin and Hart, "Architecture for the performance of nuclear fuel depletion calculations", INL/MIS-19-56187, November 2019

Nuclear data

- Nuclear data libraries at JANIS NEA, https://www.oecd-nea.org/jcms/pl_39910/janis
- Decay data, http://www.nucleide.org/DDEP.htm
- Nichols et al., "Handbook of nuclear data for safeguards: database extensions, august 2008", INDC-2453, INDC(NDS) – 0534

2.3 Neutron resonance experiments; P. Schillebeeckx, JRC Geel; Summer school on neutron detectors and related applications, Riva del Garda; 30/06 - 04/07/2022

Neutron Resonance Experiments

P. Schillebeeckx

European Commission

Joint Research Centre, Geel (BE)

Summer School on Neutron Detectors and Related Applications
Riva del Garda, 2022

Joint Research Centre

Headquarters in Brussels
and research facilities located
in 5 Member States:

- **Belgium (Geel)**
- Germany (Karlsruhe)
- Italy (Ispra)
- The Netherlands (Petten)
- Spain (Seville)

Nuclear facilities at JRC - Geel

GELINA
neutron time-of-flight facility for high-resolution neutron measurements

MONNET
tandem accelerator based fast neutron source

TARGET
nuclear target preparation laboratories

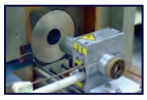

RADMET
laboratories for standardisation of radionuclide activity

HADES
low-level gamma-spectrometry laboratory

METRO
nuclear reference material and measurement facility

Operated by JRC.G.2 Unit (SN3S)
"Standards for
Nuclear Safety, Security and Safeguards"

- Nuclear data
- Radionuclide measurements
- Nuclear safeguards metrology

European Commission

Nuclear data

GELINA (this presentation)
neutron time-of-flight facility for high-resolution neutron measurements

MONNET (S. Oberstedt)
tandem accelerator based fast neutron source

TARGET
nuclear target preparation laboratories

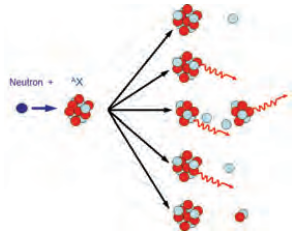

Fission process

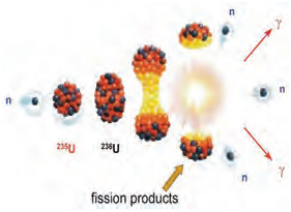

Neutron induced interaction cross sections

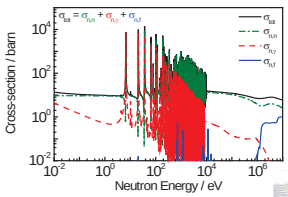

European Commission

Contents

- Neutron induced interactions: basic principles
- Neutron resonance spectroscopy
  - Neutron Time-Of-Flight measurements
  - Transmission measurements
  - Reaction cross section measurements
- Applications
  - Neutron Resonance Analysis (NRA)
  - Characterisation of Spent Nuclear Fuel (SNF)

European Commission

Nuclear data

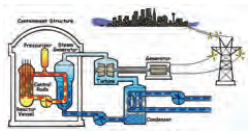

- **Nuclear data for energy technology**
  - Safety of current systems
  - Back-end: Spent Nuclear Fuel (Burn Up Credit, Decay heat, …)
  - Development of innovative systems (e.g. MYRRHA)

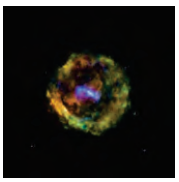

- Nuclear physics
- Nuclear medicine: diagnostics and therapy
- Nucleosynthesis and nuclear astrophysics
- Detector development
- Materials research (NAA, PGAA, Neutron Resonance Analysis, …)
- ….

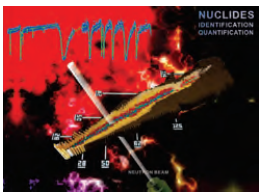

European Commission

Nuclear data: response functions of neutron detectors

- For EJ301(NE213), EJ315 type and stilbene well established
  - H(n,n)H, D(n,n)D based
- CVD diamond (Chemical Vapour Deposition)
  - Fast neutron detector
  - $^{12}C(n,p)^{12}B$, $^{12}C(n,d)^{11}B$, $^{12}C(n,\alpha)^{9}Be$, $^{12}C(n,n'3\alpha)$
- Elpasolite crystals
  - Dual mode (neutron + γ-ray detection)
  - CLYC (Cs_2LiYCl_6), CLLBC ($Cs_2LiLaBr_6Cl_6$) with ^{6}Li or ^{7}Li
  - *Thermal: $^{6}Li(n,\alpha)t$*
    Fast : $^{35}Cl(n,p)$ and $^{35}Cl(n,\alpha)$
    Also needed for sodium cooled reactor concepts
- ...

⇒ simulation of response function requires accurate cross section data (see A. Ferrari)

Diamond detector
Pillon et al., NIMA 640 (2011) 185

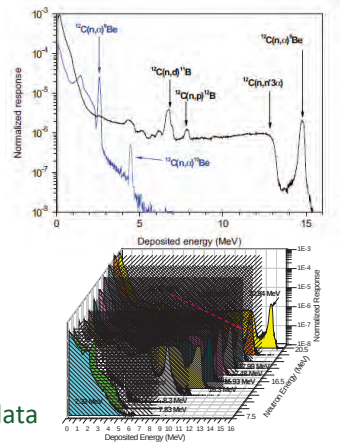

European Commission

Nuclear data: MYRRHA

"**M**ulti-purpose h**Y**brid **R**esearch **R**eactor for **H**igh-tech **A**pplications"

Nuclide	Quantity/reaction	Energy region
^{16}O	σ(n,n)	continuum (fast)
	σ(n,n)	resonance and continuum
^{56}Fe	σ(n,n')	continuum
	σ(n,γ)	resonance and continuum
^{208}Pb	σ(n,n)	resonance and continuum
	σ(n,n')	resonance and continuum
^{209}Bi	σ(n,n')	resonance and continuum
	σ(n,γ)	resonance and continuum
	$\bar{\nu}$	resonance and continuum
^{235}U	σ(n,f)	resonance and continuum
	σ(n,γ)	resonance and continuum
	σ(n,n)	continuum
^{238}U	σ(n,n')	resonance and continuum
	σ(n,γ)	resonance and continuum
^{238}Pu	σ(n,f)	resonance and continuum
	$\bar{\nu}$	continuum
^{239}Pu	χ	continuum
	σ(n,f)	continuum
	σ(n,γ)	resonance and continuum
^{240}Pu	$\bar{\nu}$	continuum
^{241}Pu	σ(n,f)	resonance and continuum
^{242}Pu	σ(n,f)	continuum

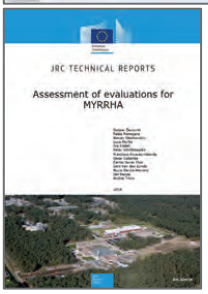

European Commission

Nuclear data: back-end of the fuel cycle

- **Criticality safety** for Spent Nuclear Fuel (SNF)
  - Original procedures : conservative based on fresh fuel (< 4%)
  - Fuel cycle extension : increase of initial enrichment (IE) and burnup (BU)

  ⇒ **Burn Up Credit (BUC)** approach:
  "Account for reactivity loss due to **(n,γ) reactions** in actinides and fission products"

- **Nuclear data** are required to **optimise**
  transport, handling, intermediate storage and **final disposal of SNF**

European Commission

Neutron transport calculations

Majority of the applications require **neutron transport** calculations
- determininistic (Boltzman)
- stochasitc (Monte Carlo),
  e.g. FLUKA, MCNP, SERPENT

relying on **neutron** interaction **cross sections**

⇒ Quality of the output depends on the quality of the nuclear data

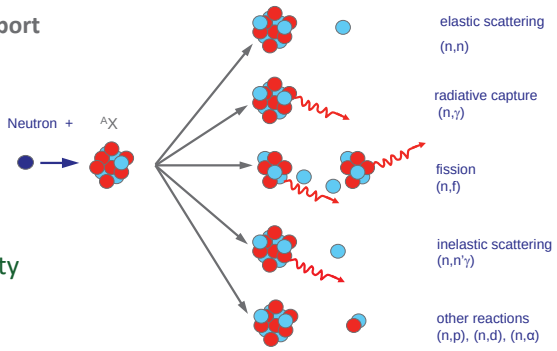

European Commission

Cross section: definition

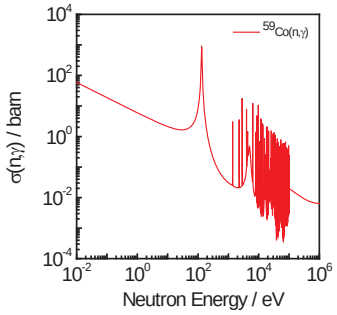

- Cross section is a quantity that is used to calculate the probability that a neutron interaction occurs:
  - symbol : σ
  - dimension : area, unit barn, 1 b = 10^{-28} m^2
- Reaction rate per target nucleus for a specific interaction (n,r) :

$$r_r = \sigma_r \varphi$$

r_r : reaction rate per nucleus (s^{-1})
φ : neutron fluence rate (s^{-1} cm^{-2})
σ_r : cross section for (n,r) reaction (cm^{-2})

Cross section: definition

Reaction: X + a → Y + b

X(a,b)Y

- Cross section $\sigma(E_a)$: **energy dependent** cross section

$$\sigma(E_a) = \int \int \frac{d^2\sigma(E_a,E_b,\Omega)}{dE_b\, d\Omega} dE_b\, d\Omega$$

E_a : kinetic energy of **incident particle** a

- **Differential** cross section (**product particle**)

$$\frac{d\sigma(E_a,E_b)}{dE_b} \qquad \frac{d\sigma(E_a,\Omega)}{d\Omega}$$

E_b : kinetic energy of product particle b

Ω : emission (solid) angle of product particle b

- **Double differential** cross section (**product particle**)

$$\frac{d^2\sigma(E_a,E_b,\Omega)}{dE_b\, d\Omega}$$

E_b and Ω

Neutron interaction cross sections: e.g. ^{238}U

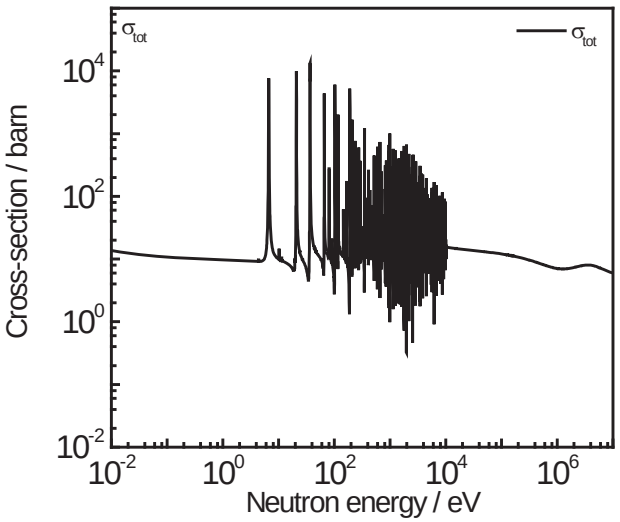

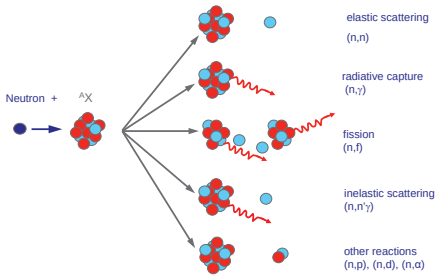

European Commission

Neutron interaction cross sections: e.g. ^{238}U

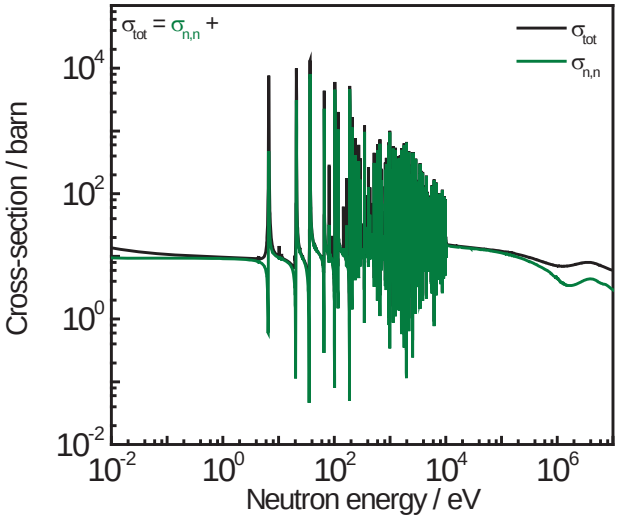

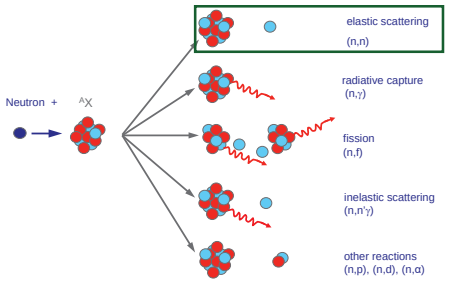

European Commission

Neutron interaction cross sections: e.g. ^{238}U

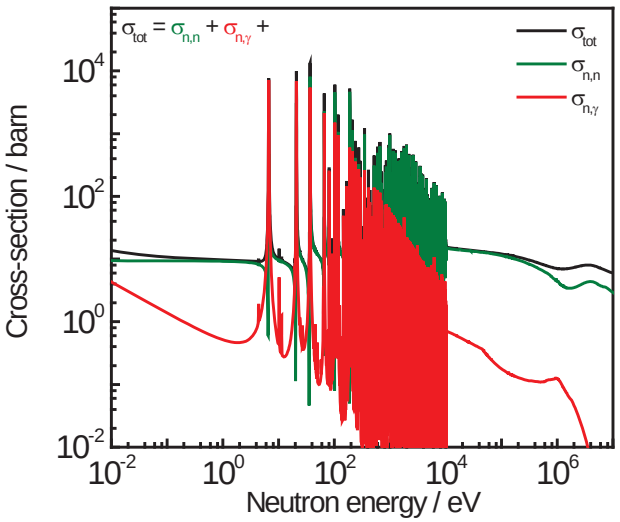

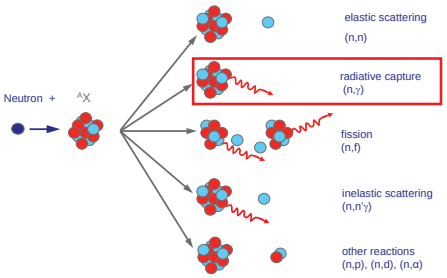

Neutron interaction cross sections: e.g. ^{238}U

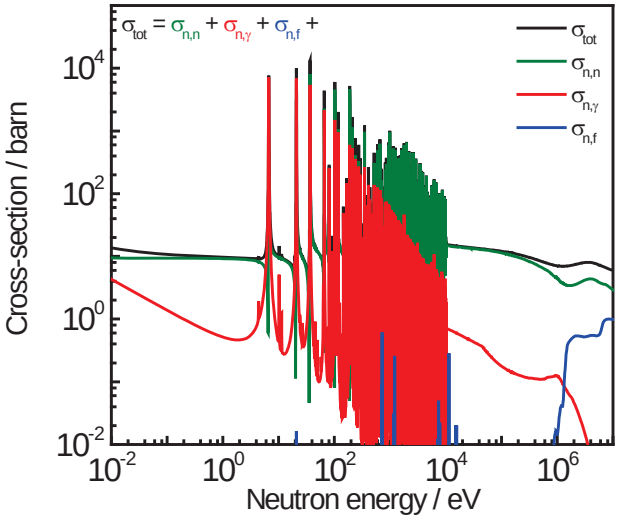

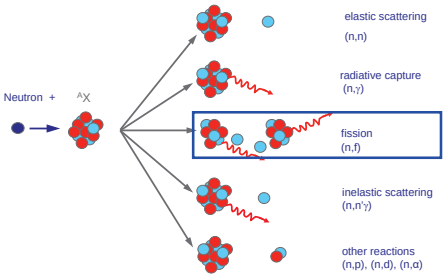

Resonance structures: compound nucleus

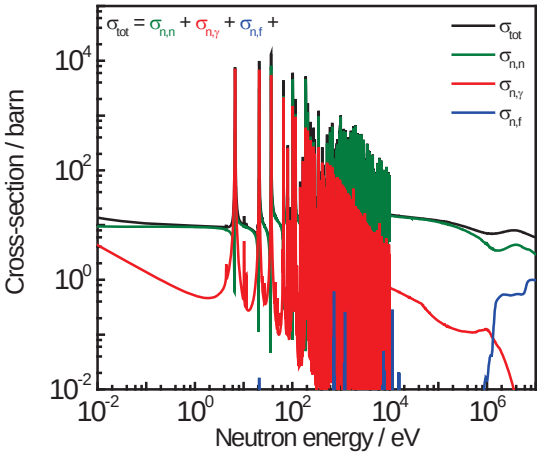

$$E^* = S_n + \frac{A}{A+1}E_n$$

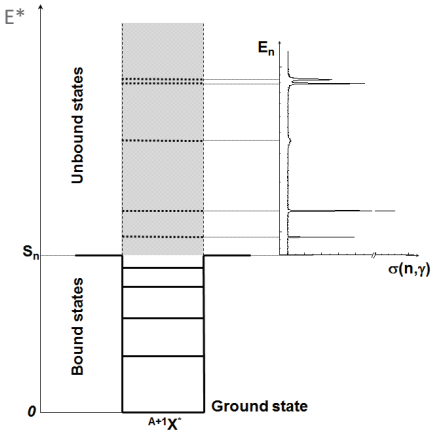

Resonance structures: compound nucleus

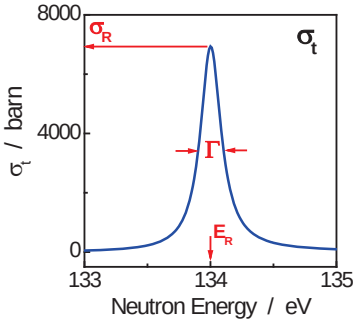

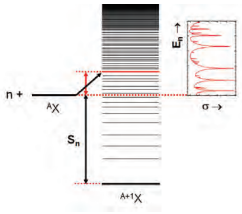

The resonant structure can be approximated by a Lorentzian shape:

with $$\sigma_{tot} \sim \frac{1}{(E_n - E_R)^2 + (\Gamma/2)^2}$$

Γ total width (FWHM)
E_R resonance energy

Heisenberg uncertainty principle

$$\Delta E\, \Delta t \geq \frac{\hbar}{2} \qquad \Gamma\, \tau \geq \frac{\hbar}{2}$$

Neutron interactions cross sections

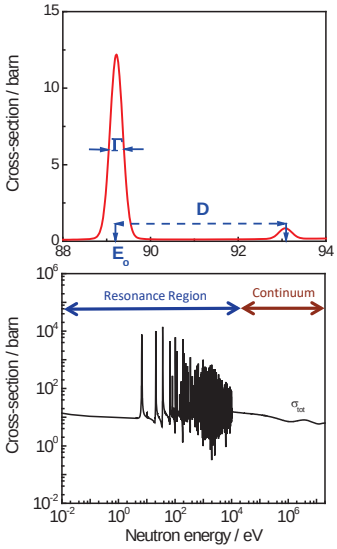

D : level distance (distance between resonances)
Γ : resonance width

Increasing E_n ↗

⇒ Level density increases : D ↘

⇒ Resonance width increases : Γ ↗

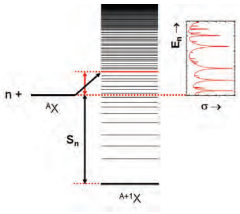

- Resonance region : D > Γ
- Continuum region : D < Γ

Neutron interaction cross sections

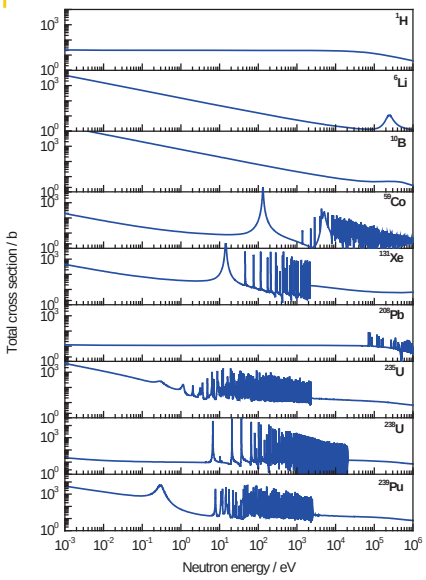

- Cross sections are different for each nuclide
- Cross sections are strongly energy dependent
  - Low energy region: 1/v dependence
  - Resonance structures
- Level density increases with increasing A
  - Except for nuclei with a magic neutron or proton number
- Upper energy of resonance region decreases with increasing A
  - Except for nuclei with a magic neutron or proton number

Neutron interaction cross sections below 20 MeV

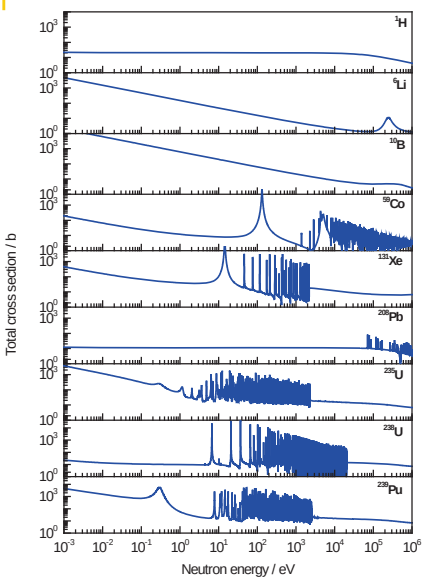

- **Theoretical cross sections** required for nuclear energy applications
  - Ensures full consistency, e.g. $\sigma_{tot} = \sum_j \sigma_j$
  - Consistency between energy regions
  - Inter- and extrapolation in regions where no data are available
  - **Doppler broadening**
- **Cross sections** for neutron induced interactions **cannot** be **predicted** by theory based on first principles
- **Cross sections** in evaluated data libraries are **parameterized** by **nuclear reaction models**

Fröhner, JEFF Report 18

Neutron interaction cross sections below 20 MeV

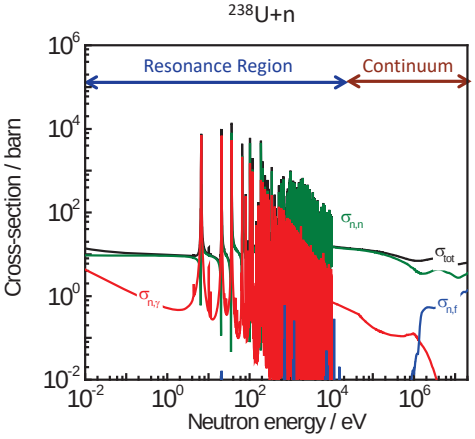

Parameterised by nuclear reaction models

Different energy regions : different theories

- Resonance region
  - R-matrix formalism
- Continuum
  - Hauser-Feshbach
  - Statistical level theories
  - Optical model
  - Pre-equilibrium thoeries
  - …

⇒ **Model parameters** determined by an **adjustment** to **experimental data**

Fröhner, JEFF Report 18

Resonance region: R – matrix formalism

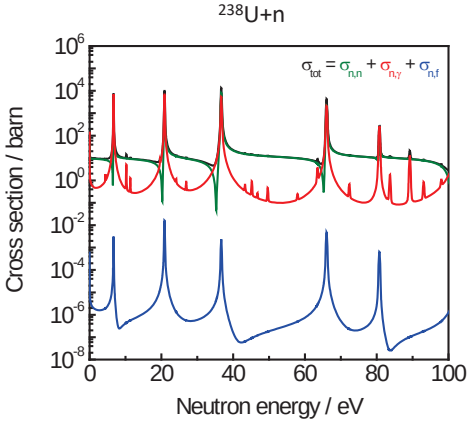

R-matrix

Lane and Thomas, Rev. Mod. Phys. 30 (1958) 257

Model parameters derived from experimental data

R and $(E_R, J^\pi, \Gamma_n, \Gamma_\gamma, \Gamma_f, \ldots)_j$

E_R	resonance energy
$\Gamma_n, \Gamma_\gamma, \Gamma_f, \ldots$	partial widths
Γ	total width
	$(\Gamma = \Gamma_n + \Gamma_\gamma + \Gamma_f \ldots)$
R	scattering radius

Partial widths $(\Gamma_n, \Gamma_\gamma, \Gamma_f, \ldots)$ reflect the probability that a specific reaction occurs

Fröhner, JEFF Report 18

Single Level Breit Wigner (SLBW) approximation

$(E_R, \Gamma_n, \Gamma_\gamma, J^\pi, R)$

g : statistical factor $g = \frac{1+2J}{2(1+2I)}$

k_n: neutron wave number

- (n, γ)

$$\sigma_\gamma(E_n) = g\frac{\pi}{k_n^2}\frac{\Gamma_n\Gamma_\gamma}{(E_n - E_R)^2 + (\Gamma/2)^2}$$

$\Rightarrow \sigma_\gamma = 0$ when $\Gamma_n = 0$

$\Rightarrow$ No resonance capture without resonance elastic scattering!

Γ_n reflects the probability to form the compound nucleus

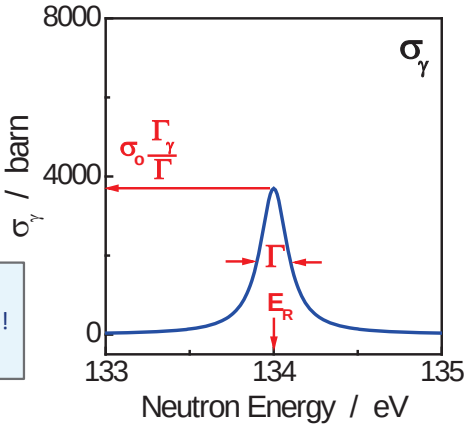

Note: resonance energy related to incident neutron energy

Fröhner, JEFF Report 18

Single Level Breit Wigner (SLBW) approximation

$(E_R, \Gamma_n, \Gamma_\gamma, J^\pi, R)$

- (n ,γ) $\sigma_\gamma(E_n) = g\frac{\pi}{k_n^2}\frac{\Gamma_n\Gamma_\gamma}{(E_n-E_R)^2+(\Gamma/2)^2}$

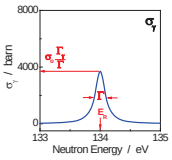

- (n,n) $\sigma_n(E_n) = g\frac{\pi}{k_n^2}\frac{\Gamma_n\Gamma_n}{(E_n-E_R)^2+(\Gamma/2)^2} + g\frac{4\pi}{k_n}\frac{\Gamma_n(E_n-E_R)R}{(E_n-E_R)^2+(\Gamma/2)^2} + 4\pi gR^2$

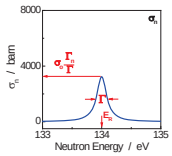

- (n,tot) $\sigma_{tot}(E_n) = g\frac{\pi}{k_n^2}\frac{\Gamma_n\Gamma}{(E_n-E_R)^2+(\Gamma/2)^2} + g\frac{4\pi}{k_n}\frac{\Gamma_n(E_n-E_R)R}{(E_n-E_R)^2+(\Gamma/2)^2} + 4\pi gR^2$

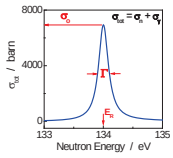

Note: resonance energy related to incident neutron energy

Fröhner, JEFF Report 18

Neutron interaction cross sections in resonance region

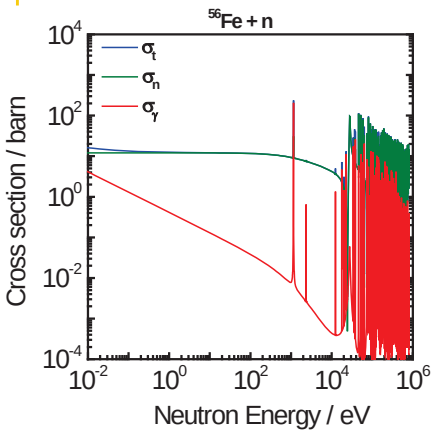

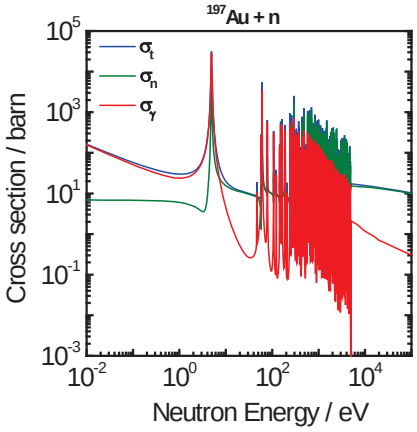

- No capture without scattering
- Relative contribution of σ_n and σ_γ to σ_{tot} may be different

Fröhner, JEFF Report 18

1/v behaviour of reaction cross section, e.g. (n,γ)

Neutron width Γ_n depends on ℓ and E_n due to centrifugal-barrier penetrability

- **s – wave ($\ell = 0$)**

$$\Gamma_n(E_n) = \Gamma_n^0 \sqrt{\frac{E_n}{1eV}} \qquad k_n = \frac{2\pi}{\lambda} = \frac{p}{\hbar}$$

1/v dependence in thermal region

$$\sigma_\gamma(E_n) = g\frac{\pi}{k_n^2}\frac{\Gamma_n\Gamma_\gamma}{(E_n - E_R)^2 + (\Gamma/2)^2}$$

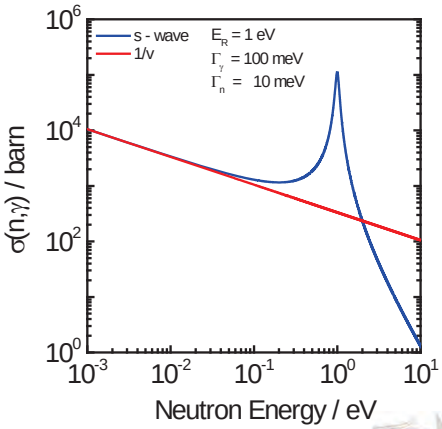

1/v behaviour of (n,n) in extreme low energy region

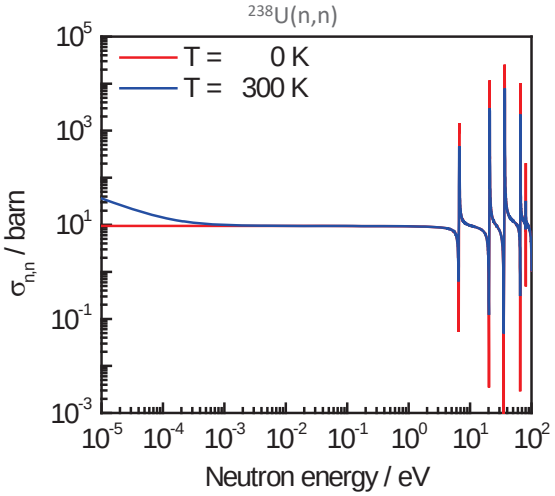

$$\bar{\sigma}(v,T) = \frac{1}{v}\int |v - V|\,\sigma(|v - V|)\,P(V)dV$$

$$\sigma(|v - V|) = k \text{ and } v << V$$

$$\Rightarrow \bar{\sigma}(v,T) \approx \frac{1}{v}\int k\,V\,P(V)dV$$

$$\Rightarrow \bar{\sigma}(v,T) = \frac{K'}{v}$$

Cross sections in data bases such as JANIS are mostly Doppler broadened

Neutron interaction cross sections in resonance region

$$\sigma_{tot}(E_n) = g\frac{\pi}{k_n^2}\frac{\Gamma_n\Gamma}{(E_n-E_R)^2+(\Gamma/2)^2} + \boxed{g\frac{4\pi}{k_n}\frac{\Gamma_n(E_n-E_R)R}{(E_n-E_R)^2+(\Gamma/2)^2}} + 4\pi gR^2$$

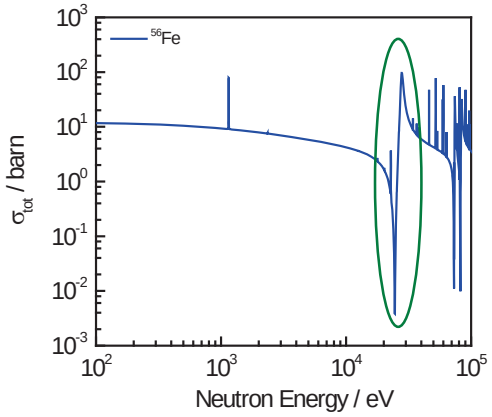

Interference term : $\ell = 0$

- Filtered neutron beams, e.g.
  - Fe + Al : 24 keV
  - Si + Ti : 144 keV
- Shielding and collimation of fast neutrons
  - several materials required

Neutron facilities: GELINA and MONNET

GELINA

MONNET

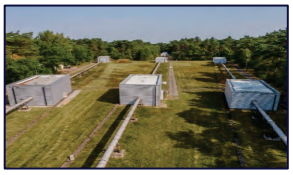

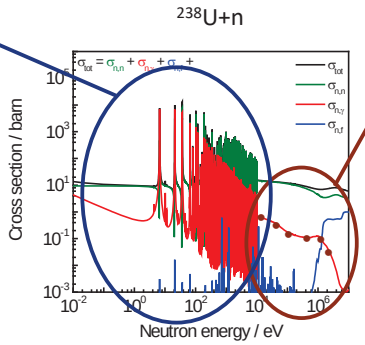

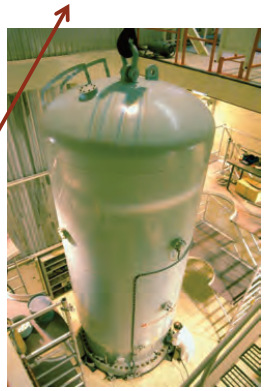

White neutron source
+
Time-of-flight (TOF)

Mono-energetic neutrons
(cp,n) reactions

MONNET

Quasi mono-energetic neutrons produced
By charged particle induced reactions

$^{7}Li(p,n)^{7}Be$	E_n: 0 - 5.3 MeV
$T(p,n)^{3}He$	E_n: 0 - 6.2 MeV
$D(d,n)^{3}He$	E_n: 1.8 - 10.1 MeV
$T(d,n)^{4}He$	E_n: 12.1 - 24.1 MeV

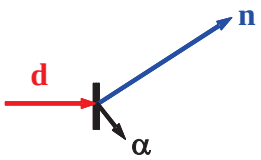

e.g. $T(d,n)^{4}He$

MONNET

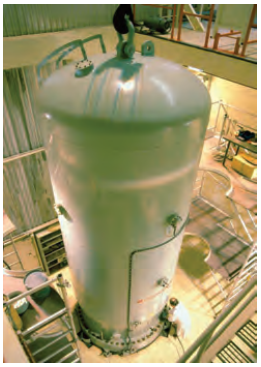

Mono-energetic neutrons
(cp,n) reactions

E.g. response functions for a EJ309 scintillator

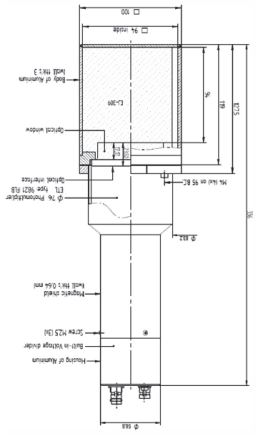

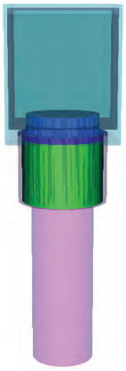

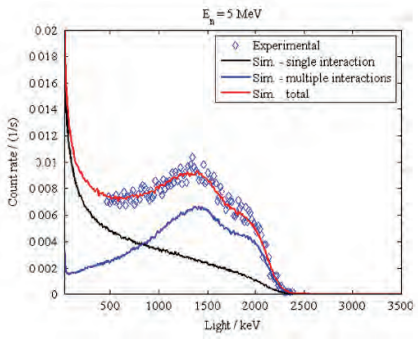

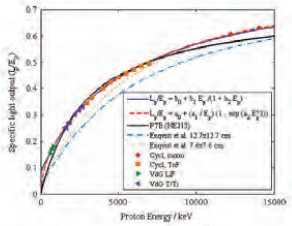

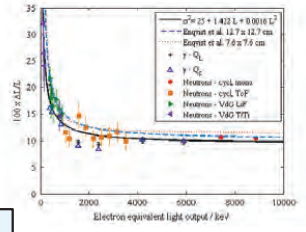

Light output functions for protons are strongly non-linear and different for each system
Require experimental verification

Tomanin et al., NIMA 756 (2014) 45

GELINA: TOF – facility

- Pulsed white neutron source
  (10 meV < E_n < 20 MeV)
- Neutron energy : time – of – flight (TOF)
- Multi-user facility: 10 flight paths (10 m – 400 m)
- Measurement stations with special equipment:
  - Total cross section measurements
  - Reaction (partial) cross section measurements

GELINA: linear accelerator

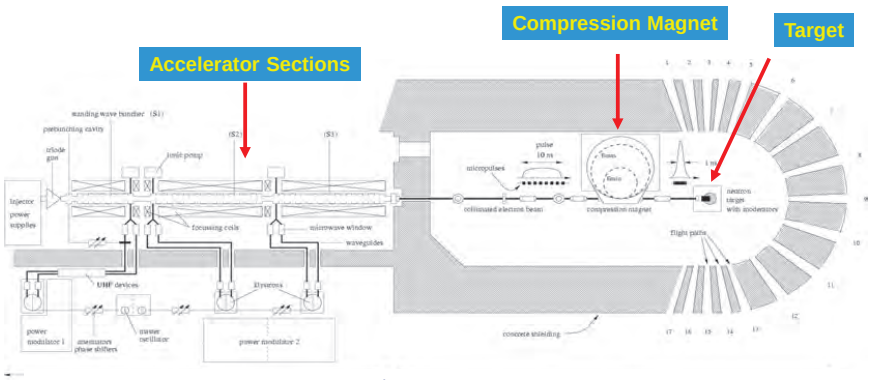

Normal operating parameters

Average Current	: 50 µA	Frequency	: 400 Hz
Average Electron Energy	: 100 MeV	Pulse Width	: 2 ns
Mean Power	: 5.0 kW	Neutron Flux	: 1 x 10^{13} 1/s

GELINA: compression magnet

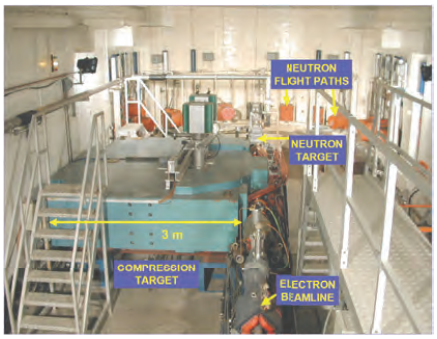

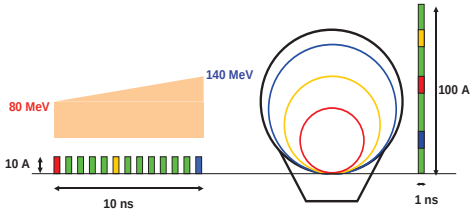

$$B\rho = \frac{p}{q};\ E \cong pc;\ q = e$$

$$\Rightarrow\ \rho = \frac{1}{B}\frac{E}{qc}$$

$$\Rightarrow\ B = \frac{2\pi}{qc^2}\frac{\Delta E}{\Delta \tau}$$

$\Delta E = 60$ MeV

$\Delta \tau = 10$ ns

⇒ compressed pulse width ~ 1 ns

GELINA: neutron production

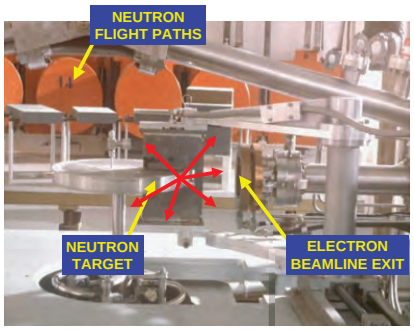

- e^- accelerated to $E_{e^-,max} \approx 140$ MeV
- Bremsstrahlung in U-target (rotating & cooled with liquid Hg)
- (γ, n), (γ, f) in U-target

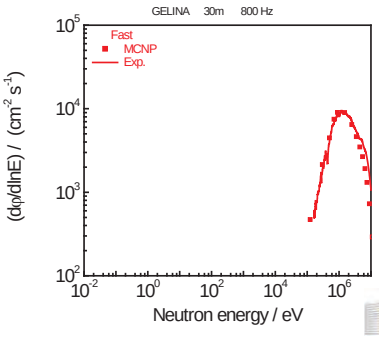

GELINA: neutron production

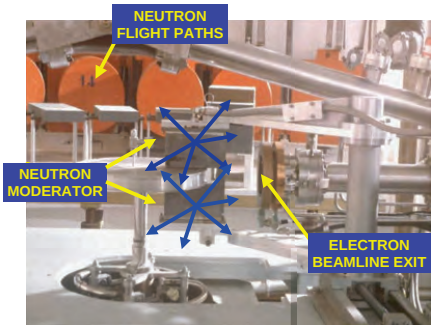

- e^- accelerated to $E_{e^-,max}$ ≈ 140 MeV
- Bremsstrahlung in U-target (rotating & cooled with liquid Hg)
- (γ , n) , (γ , f) in U-target
- Low energy neutrons by moderation (water moderator in Be-canning)

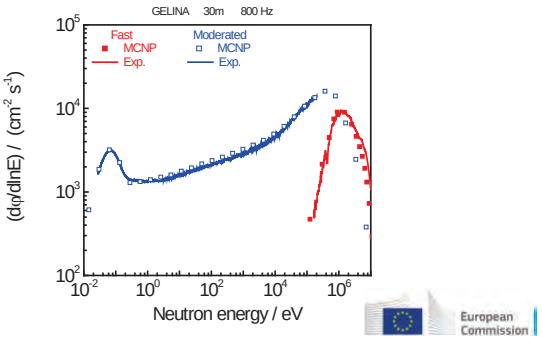

GELINA: fast and moderated neutron beam

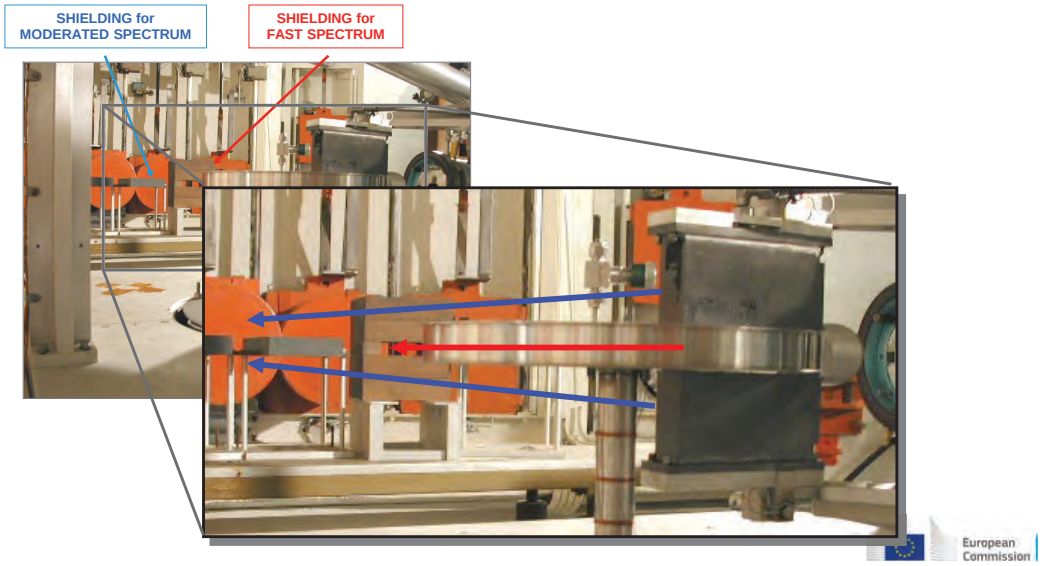

GELINA: neutron fluence moderated beam

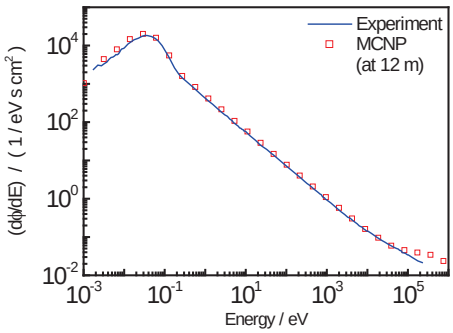

- Energy distribution ("white neutron spectrum")

  Maxwellian + 1/E

- Isotropic emission

$$\varphi(L) \propto \frac{1}{L^2}$$

Time-of-flight measurement

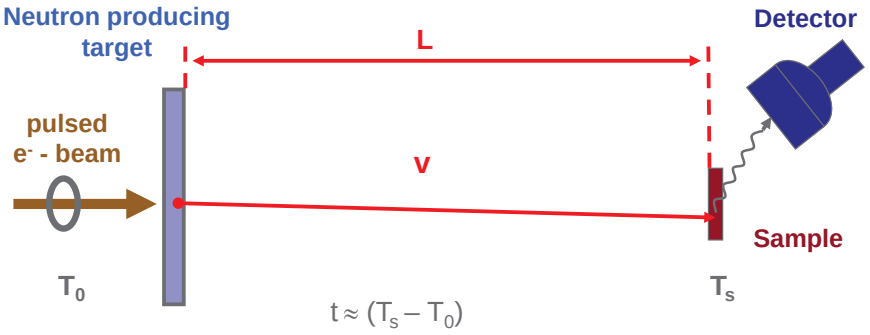

$$t \approx (T_s - T_0)$$

$$v = \frac{L}{t} \qquad \Rightarrow \quad E = mc^2(\gamma - 1) \cong \frac{1}{2}mv^2$$

Time-of-flight measurement

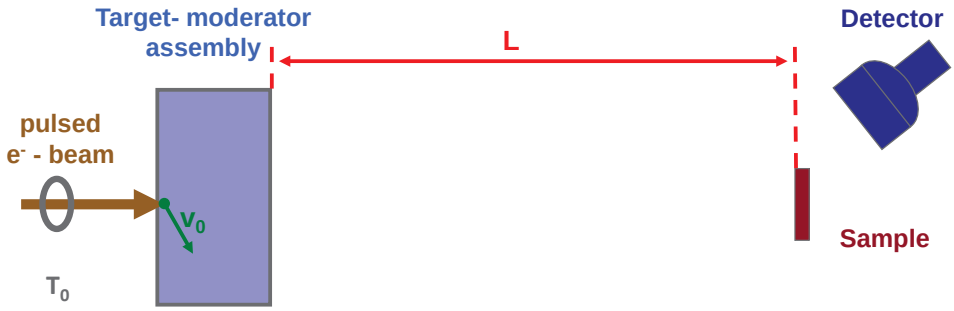

Time-of-flight measurement

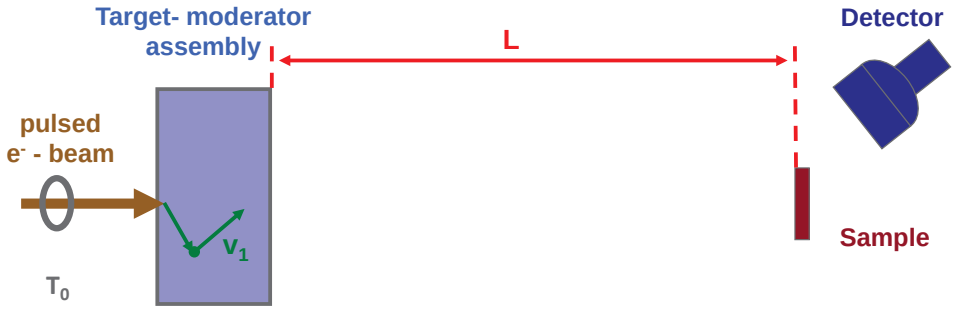

E kinetic energy before scattering
E' kinetic energy after H(n,n)H scattering

$E'_{max} = E$

$<E'> = \frac{E}{2}$

Time-of-flight measurement

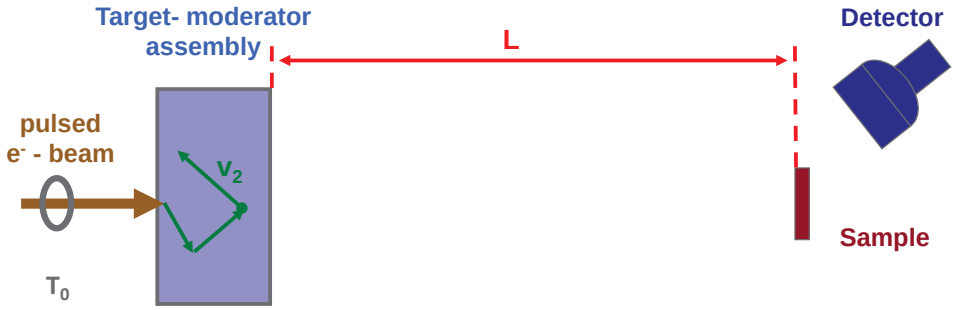

Time-of-flight measurement

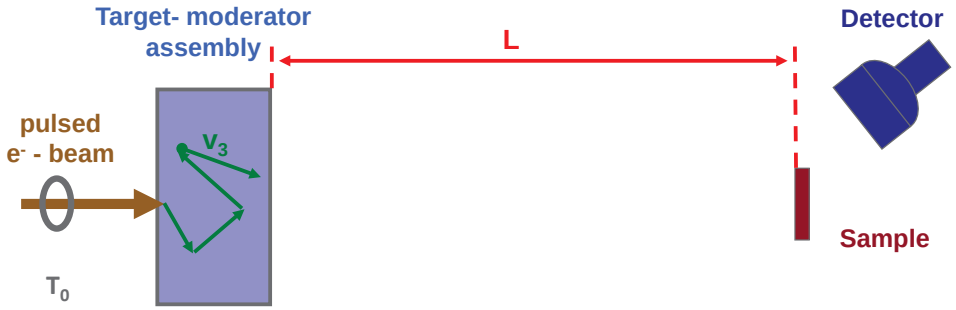

Time-of-flight measurement

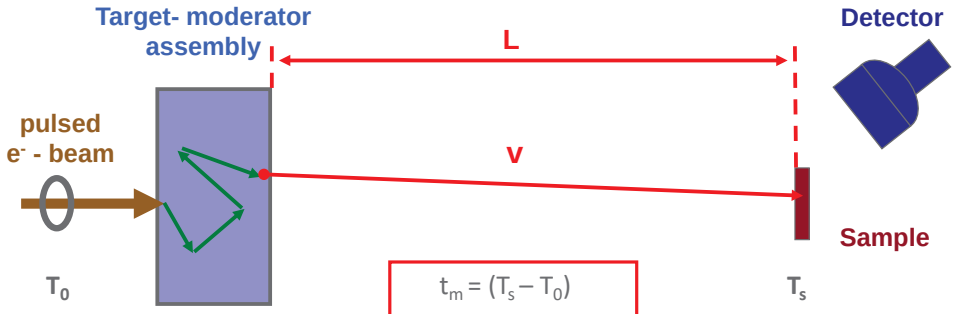

$t_m = (T_s - T_0)$

$t \neq t_m$

$v = \frac{t}{L}$

Time-of-flight measurement

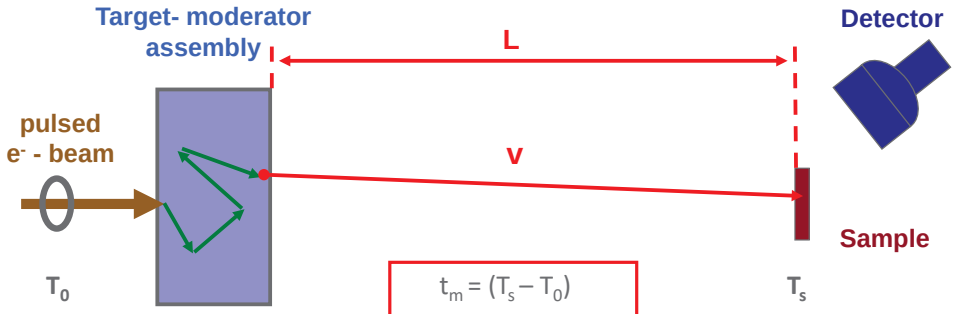

$t_m = (T_s - T_0)$

$t = t_m - (t_t + t_d)$

$v = \frac{t}{L}$

Response of time-of-flight spectrometer

$$v = \frac{t}{L} \qquad \Rightarrow E = m^2(\gamma - 1) \cong \frac{1}{2}mv^2$$

$$\frac{\Delta v}{v} = \sqrt{\frac{\Delta t^2}{t^2} + \frac{\Delta L^2}{L^2}} \qquad \Rightarrow E = \gamma(\gamma + 1)\frac{\Delta v}{v} \cong 2\frac{\Delta v}{v}$$

$$\frac{\Delta v}{v} = \frac{1}{L}\sqrt{v^2\Delta t^2 + \Delta L^2}$$

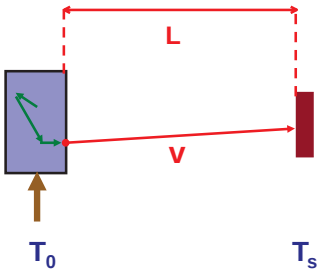

- ΔL : ~ 1 mm, independent of v (or E)
- Δt :
  - Start pulse (GELINA: $\Delta T_0 \approx 2$ ns) ΔT_0
  - Time jitter detector & electronics ΔT_s

  ⇒ *Mostly lumped into one component*

  Gaussian distribution (depending on start pulse structure)

  Independent of E (neutron energy or velocity)

$t_m = (T_s - T_0)$

$t = t_m - (t_t + t_d)$

$$v = \frac{t}{L}$$

Response of time-of-flight spectrometer

$$v = \frac{t}{L} \qquad \Rightarrow E = m^2(\gamma - 1) \cong \frac{1}{2}mv^2$$

$$\frac{\Delta v}{v} = \sqrt{\frac{\Delta t^2}{t^2} + \frac{\Delta L^2}{L^2}} \qquad \Rightarrow E = \gamma(\gamma + 1)\frac{\Delta v}{v} \cong 2\frac{\Delta v}{v}$$

$$\frac{\Delta v}{v} = \frac{1}{L}\sqrt{v^2\Delta t^2 + \Delta L^2}$$

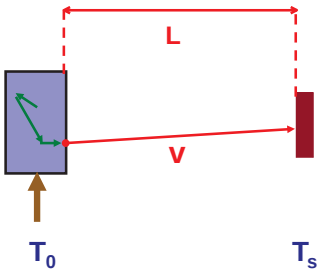

- ΔL : ~ 1 mm, independent of v (or E)
- Δt :
  - Start pulse (GELINA: $\Delta T_0 \approx 2$ ns) ΔT_0
  - Time jitter detector & electronics ΔT_s
  - Neutron transport in target - moderator Δt_t
  - Neutron transport in detector Δt_d

$t_m = (T_s - T_0)$

$t = t_m - (t_t + t_d)$

$$v = \frac{t}{L}$$

Probability distribution of t_t for GELINA

$R(t_t,E)$: TOF-response function

Probability that a neutron escaping from the moderator with an energy E spends a time t_t in the target moderator assembly

⇒ *strongly depends on neutron energy*

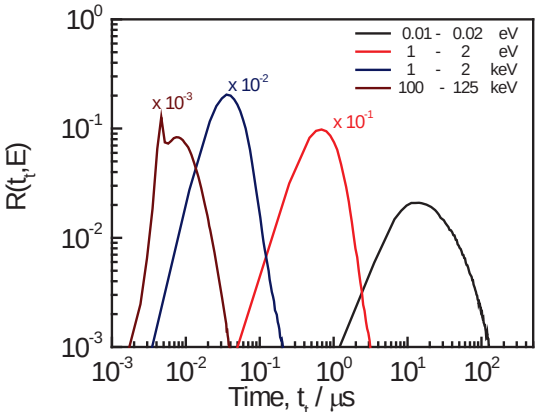

Probability distribution of t_t for GELINA

$$R(t_t, E) = R'(L_t, E)\left|\frac{dL_t}{dt_t}\right|$$

Transformation of variables :

$L_t = v\, t_t$

- **L_t : equivalent distance**
- v : neutron velocity when leaving the moderator
- t_t : time difference between neutron creation and moment it leaves the moderator

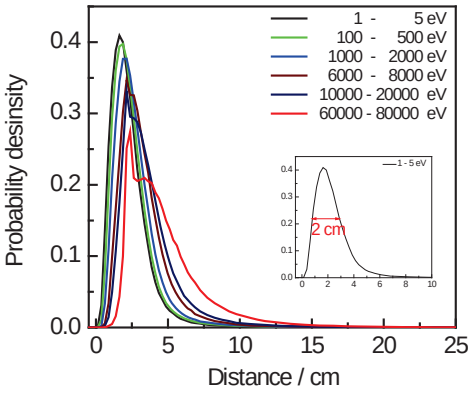

GELINA : FWHM ~ 2 cm

P(t_t, E) : photonuclear GELINA

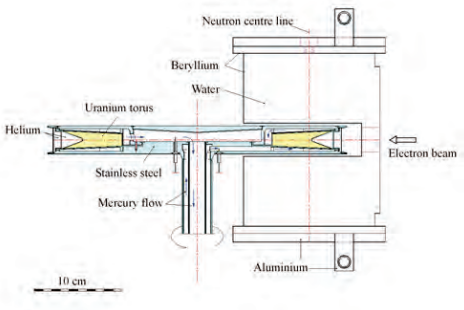

Resolution : ΔL (FWHM)
GELINA : 2 cm

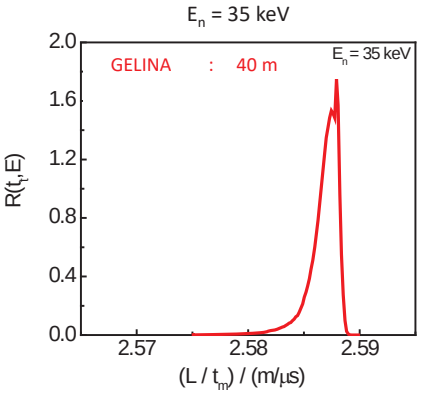

Resolution : ΔL (FWHM)
GELINA : 2 cm

P(t_t, E) : photonuclear GELINA

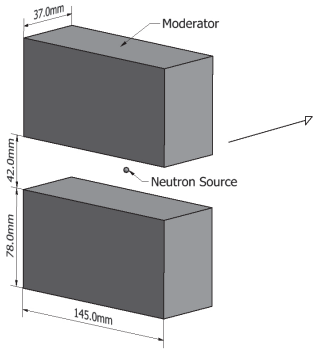

ΔL (FWHM) = 2 cm
⇒ about half of the moderator thickness

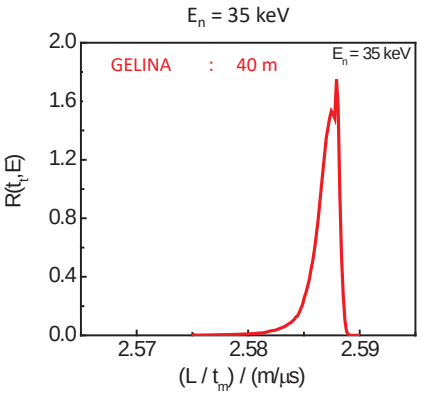

Resolution : ΔL (FWHM)
GELINA : 2 cm

P(t_t, E) : photonuclear GELINA and ORELA

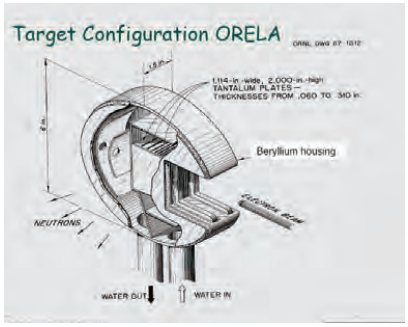

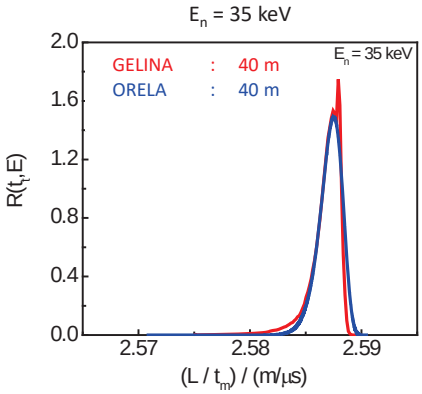

Resolution	:	ΔL (FWHM)
GELINA	:	2 cm
ORELA	:	2 cm

Neutron production at spallation sources, e.g. n_TOF, ISIS

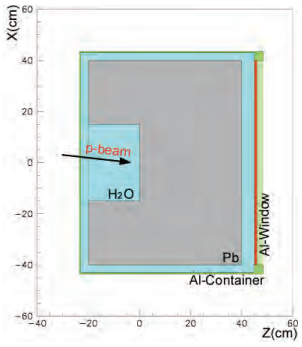

Dimensions	: 80 × 80 × 60 cm^3
Pure Lead	: 4 t
H_2O moderator	: 5 cm
Al-window	: 1.6 mm
Al-container	: 140 l

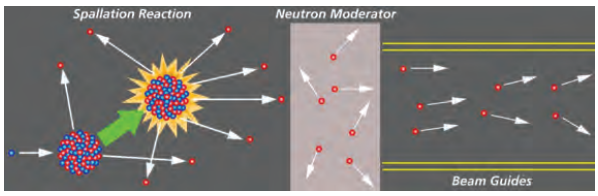

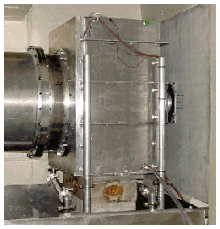

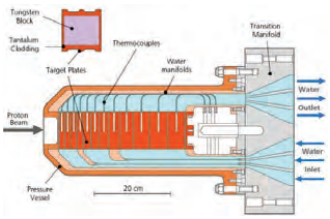

Neutron production at spallation sources, e.g. n_TOF, ISIS

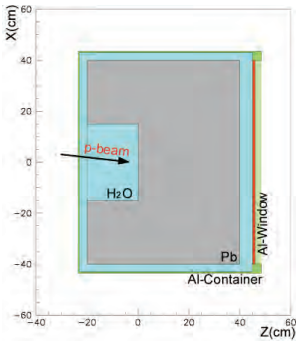

Dimensions : 80 × 80 × 60 cm³
Pure Lead : 4 t
H_2O moderator : 5 cm
Al-window : 1.6 mm
Al-container : 140 l

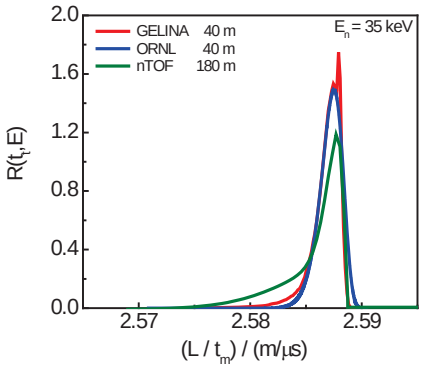

Resolution : ΔL
GELINA : 2 cm
ORELA : 2 cm
nTOF : 10 cm

Neutron production at spallation sources, e.g. n_TOF, ISIS, J-PARC

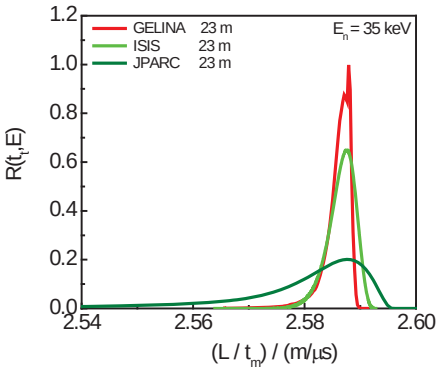

Resolution : ΔL
ISIS (INES) : 5 cm
J-PARC (MLF/ANNRI) : 12 cm
Strongly depend on target/moderator configuration (coupled/decoupled)

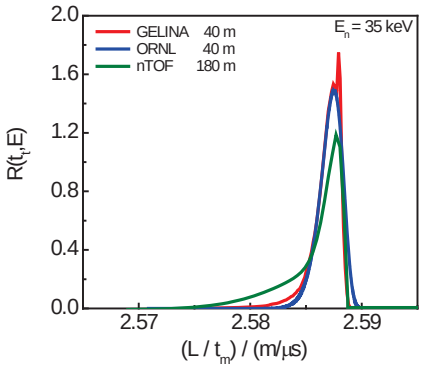

Resolution : ΔL
GELINA : 2 cm
ORELA : 2 cm
nTOF : 10 cm

GELINA - Experimental set-ups

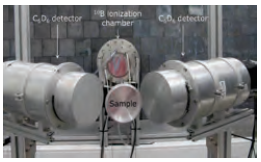

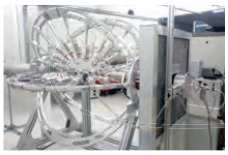

- Transmission
  - 10 m, 30 m, 50 m
- Capture
  - 10 m, 30m, 60 m
- Elastic, in-elastic scattering
  - 30 m
- In-elastic scattering (n,n'γ)
  - 30 m, 100 m
- Fission, (n,p), (n,α),
  - 10 m

European Commission

Cross section measurements

- **Transmission measurement**

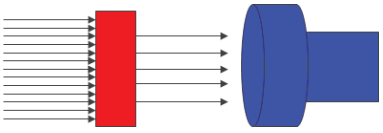

- **Reaction cross section measurement**

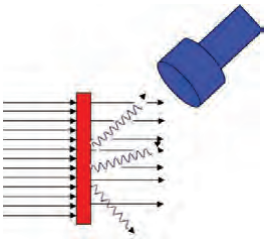

European Commission

Transmission measurement

Transmission: fraction of the beam traversing a sample without any interaction

Parallel neutron beam, perpendicular to a slab of material : **Lambert-Beer law**

Transmission
Lambert-Beer law

$$T = \frac{\varphi(d)}{\varphi(0)} = e^{-n\,\sigma_{tot}}$$

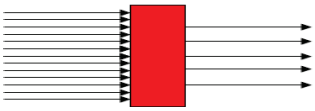

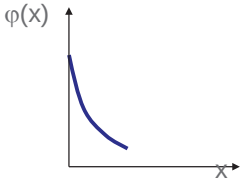

σ_{tot}: total cross section

n : areal number density
total number of atoms per unit area

Transmission measurement

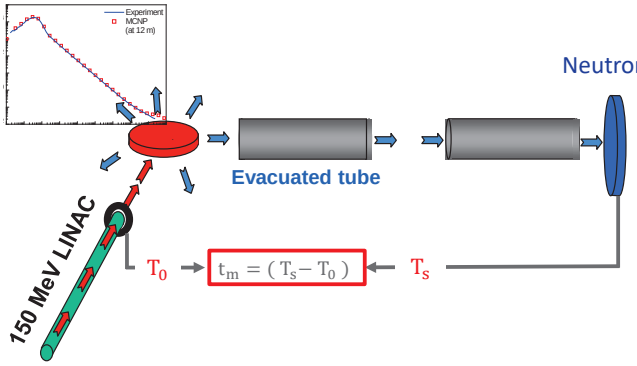

L : distance between target and detector

t_m : observed time-of-flight

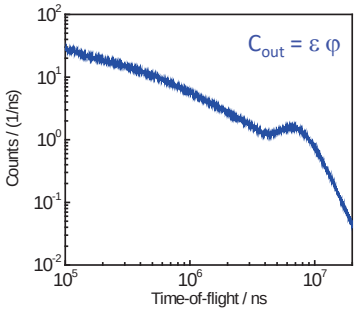

Transmission measurement

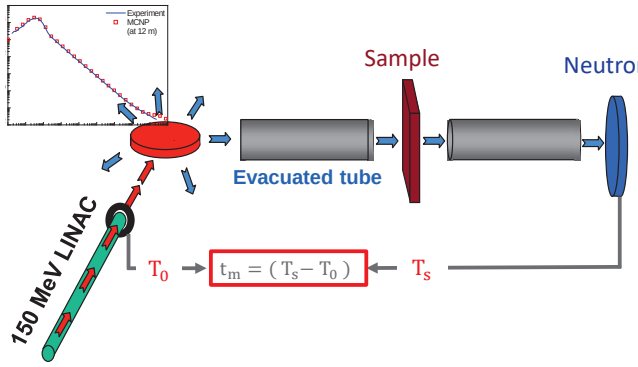

L : distance between target and detector
t_m : observed time-of-flight

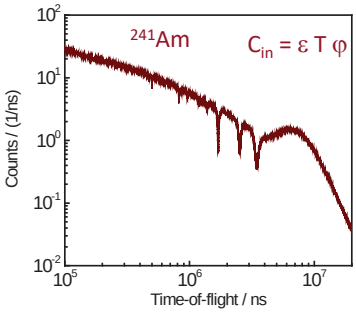

Transmission measurement

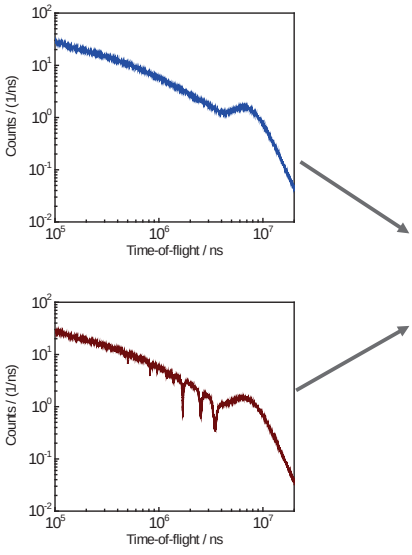

$$T_{exp} = \frac{C_{in}}{C_{out}}$$

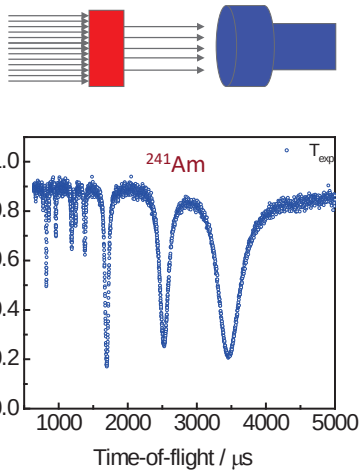

Transmission measurement

Transmission

$$T_{exp} = \frac{C_{in}}{C_{out}} \propto e^{-n\,\sigma_{tot}}$$

- Incoming neutron fluence rate cancels
- Detection efficiency cancels

⇒ Absolute measurement

⇒ Direct relation between T_{exp} and σ_{tot}

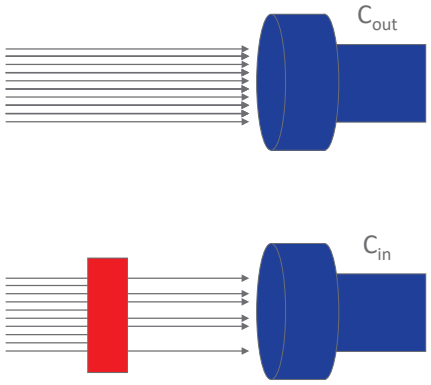

Transmission: principle

$$T_{exp} = \frac{C_{in}}{C_{out}} \propto e^{-n\,\sigma_{tot}}$$

(1) All detected neutrons passed through the sample
(2) Neutrons scattered in the target do not reach detector
(3) Sample perpendicular to parallel neutron beam
⇒ Good transmission geometry (collimation)
(4) Homogeneous target (no spatial distribution of n)

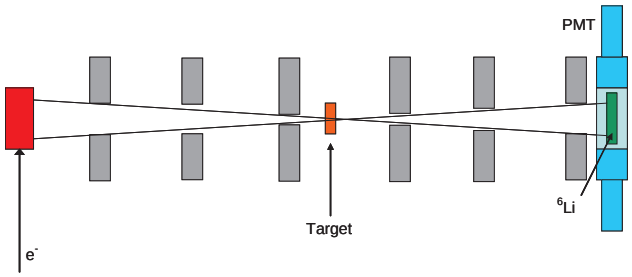

GELINA – Transmission at 10 m, 25 m and 50 m

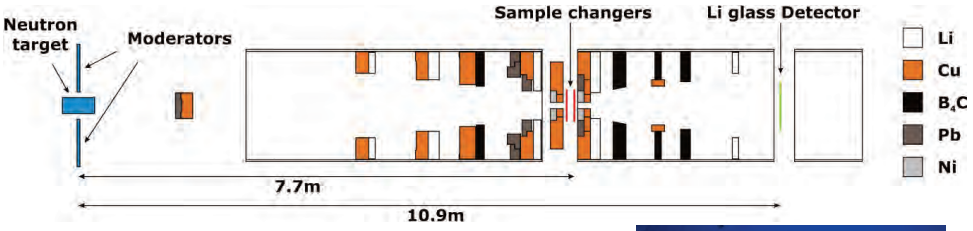

Neutron detectors

Low energy : $^{6}Li(n,t)\alpha$
Li-glass (enriched in ^{6}Li) scintillator

High energy : H(n,n)H
Plastic or NE213 type scintillator

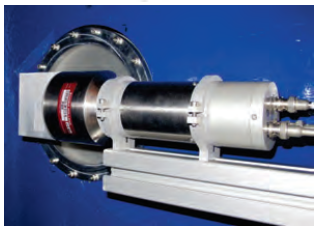

Neutron detector: TOF-response, equivalent distance

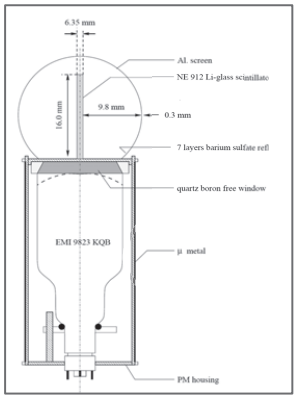

Detector thickness 6.35 mm!

Sensitive to γ-rays

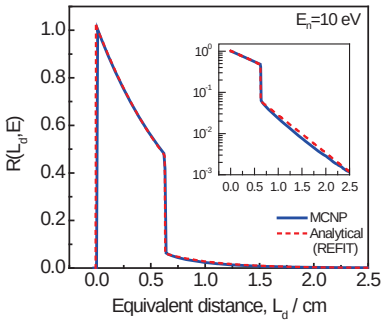

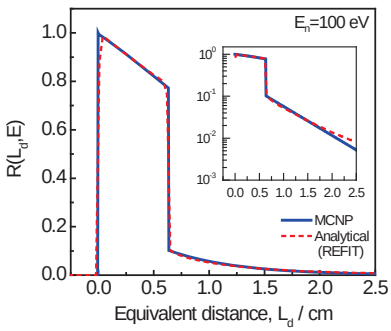

Transmission: resonance parameters for ^{241}Am + n

$$T_{exp} = N\frac{C_{in} - B_{in}}{C_{out} - B_{out}} \qquad \frac{u_{T_{exp}}}{T_{exp}} \leq 0.25\%$$

$\Rightarrow$ absolute measurement

$\Rightarrow$ no calibration measurement required

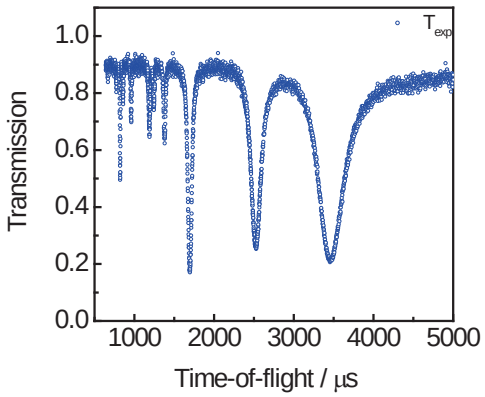

Transmission: resonance parameters for ^{241}Am + n

$$T_{exp} = N\frac{C_{in} - B_{in}}{C_{out} - B_{out}} \qquad \frac{u_{T_{exp}}}{T_{exp}} \leq 0.25\%$$

$\Rightarrow$ absolute measurement

$\Rightarrow$ no calibration measurement required

$$T_M(t_m) = \int R(t_m, E)\, e^{-n\, \bar{\sigma}_{tot}(E_n)}\, dE_n$$

$$\chi^2(\mathbf{RP}) = (T_{exp} - T_M)^T\, V_{T_{exp}}^{-1}\, (T_{exp} - T_M)$$

$R(t_m, E)$: response of TOF-spectrometer + detector

$\bar{\sigma}_{tot}$: Doppler broadened total cross section

n : areal number density
total number of atoms per unit area

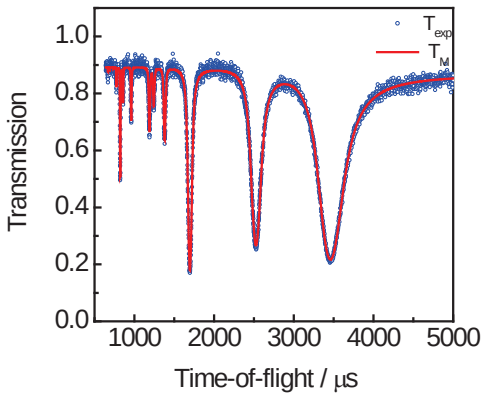

Transmission: resonance parameters for ^{241}Am + n

$$T_{exp} = N\frac{C_{in} - B_{in}}{C_{out} - B_{out}} \qquad \frac{u_{T_{exp}}}{T_{exp}} \leq 0.25\%$$

$\Rightarrow$ absolute measurement

$\Rightarrow$ no calibration measurement required

$$\chi^2(\mathbf{RP}) = (T_{exp} - T_M)^T V_{T_{exp}}^{-1} (T_{exp} - T_M)$$

Energy /eV	J/ħ	g	$g\Gamma_n$ / meV	Γ_γ / meV
0.306	3	7/12	0.0373 (2)	41.6 (4)
0.574	2	5/12	0.0629 (4)	42.1 (6)
1.271	3	7/12	0.2176 (23)	41.7 (8)

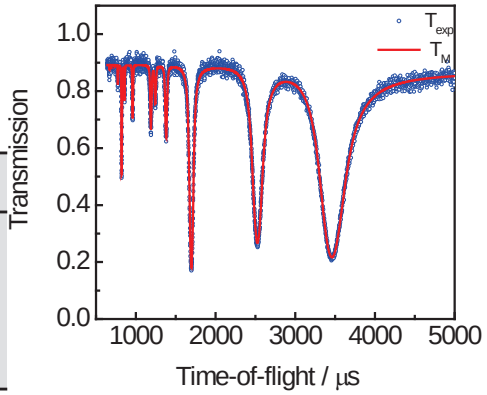

Improve nuclear data for ^{206}Pb, ^{208}Pb and ^{209}Bi (MYRRHA)

- Transmission measurements at 50 m
  - ^{209}Bi
  - ^{206,208,nat}Pb
- Capture measurements at 60 m
  - ^{209}Bi

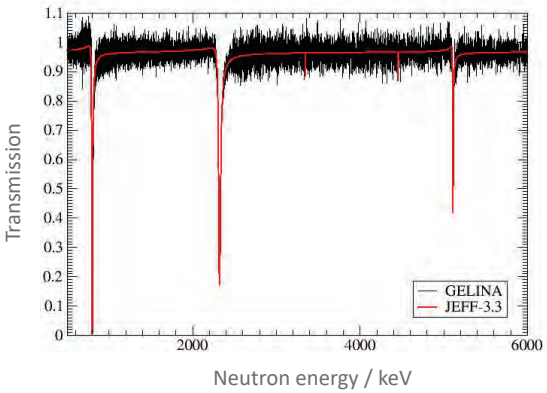

Reaction cross section measurement

Reaction yield: fraction of the beam creating a (n,r) reaction in the sample

Parallel neutron beam, perpendicular to a slab of material : Lambert-Beer law

Reaction yield

$$Y_r \cong (1 - e^{-n\,\sigma_{tot}})\frac{\sigma_r}{\sigma_{tot}}$$

$$Y_r \approx n\,\sigma_r \quad \text{for} \quad n\,\sigma_r << 1$$

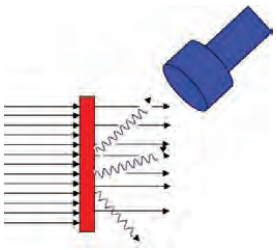

$$1 - e^{-n\,\sigma_{tot}} \cong 1 - (1 - n\,\sigma_{tot}) = n\,\sigma_{tot}$$

European Commission

Reaction cross section measurement

Reaction yield: fraction of the beam creating a (n,r) reaction in the sample

Experimental response :

$$C_r = \varepsilon_r Y_r \varphi$$

- C_r experimental response
- φ neutron fluence rate
- Y_r reaction yield
- ε_r overall detection efficiency (including solid angle)

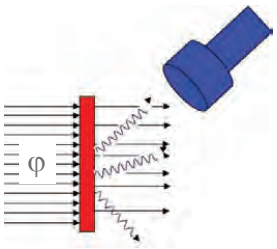

European Commission

Cross section measurements

Transmission

$$T = e^{-n\,\sigma_{tot}}$$

$$T_{exp} = \frac{C_{in}}{C_{out}}$$

- Absolute measurement
- No additional measurements

+ direct relation: $T \Leftrightarrow \sigma_{tot}$
good geometry
homogeneous sample

Reaction

$$Y_r \approx (1 - e^{-n\,\sigma_{tot}})\frac{\sigma_r}{\sigma_{tot}}$$

$$Y_{exp} = \frac{C_r}{\varepsilon_r\,\varphi}$$

- Detection efficiency
- Fluence rate: additional measurement

+ complex relation : $Y_r \Leftrightarrow \sigma_r$
$Y_r = f(\sigma_r, \sigma_{tot}\ \&\ \sigma_n)$
only for $n\sigma_{tot} << 1 : Y_r \cong n\,\sigma_r$

Cross section measurements

Transmission

$$T = e^{-n\,\sigma_{tot}}$$

$$T_{exp} = \frac{C_{in}}{C_{out}}$$

Transmission most accurate cross section measurement

$^{10}B(n,\alpha)$ from transmission: $\sigma(n_{th}, \alpha) = 3838\ (6)$ b
Axton, Nucl. Sci. Techn. 5 (1984) 609

$^{197}Au(n,\gamma)$ from transmission: $\sigma(n_{th}, \gamma) = 98.7\ (1)$ b
Dilg et al., Z. Phys. 264 (1973) 427

Reaction

$$Y_r \approx (1 - e^{-n\,\sigma_{tot}})\frac{\sigma_r}{\sigma_{tot}}$$

$$Y_{exp} = \frac{C_r}{\varepsilon_r\,\varphi}$$

- Detection efficiency
- Fluence rate: additional measurement

+ complex relation : $Y_r \Leftrightarrow \sigma_r$
$Y_r = f(\sigma_r, \sigma_{tot}\ \&\ \sigma_n)$
only for $n\sigma_{tot} << 1 : Y_r \cong n\,\sigma_r$

Neutron fluence measurements

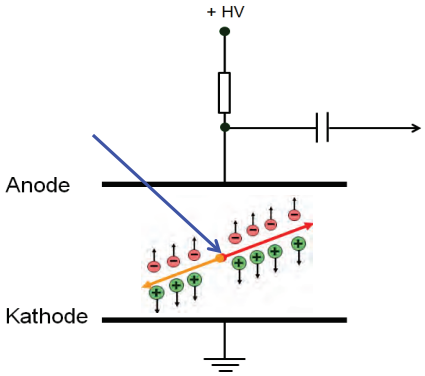

$$n + {}^{3}_{2}He \rightarrow p + {}^{3}_{1}H$$

Neutron: electrical neutral

- No direct ionisation or excitation
- *Transfer reaction is required to transform neutron energy into charged particle energy*

⇒ Transfer reaction required with well-known cross section

European Commission

Neutron fluence measurements: standard reactions

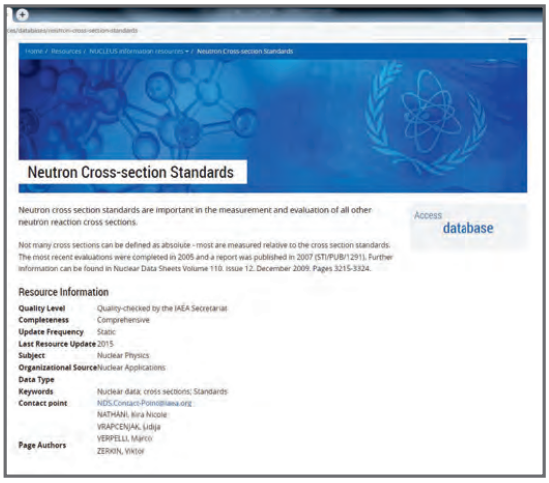

Neutron transfer reactions with an accurate cross section:

- Neutron standard and reference reactions with recommended cross sections
- https://www-nds.iaea.org/standards

European Commission

Neutron fluence measurements: standard reactions

Reaction	2200 m/s	Energy region E_{low}		E_{high}	
^{1}H(n,n)		1 keV	-	20 MeV	
^{3}He(n,p)	X	25.3 meV	-	50 keV	
^{6}Li(n,t)	X	25.3 meV	-	1 MeV	
^{10}B(n,α)	X	25.3 meV	-	1 MeV	
^{10}B(n,α$_1$γ)	X	25.3 meV	-	1 MeV	
^{nat}C(n,n)		25.3 meV	-	1.8 MeV	
^{197}Au(n,γ)	X	0.2 MeV	-	2.8 MeV	
^{235}U(n,f)	X	0.15 MeV	-	200 MeV	(1 GeV)
^{238}U(n,f)		2 MeV	-	200 MeV	(1 GeV)
^{238}U(n,γ)		150 eV	-	2.2 MeV	
^{239}Pu(n,f)		25.3 meV	-	300 MeV	
^{209}Bi(n,f)		34 MeV	-	1 GeV	
^{nat}Pb(n,f)		34 MeV	-	1 GeV	

Standard
Reference

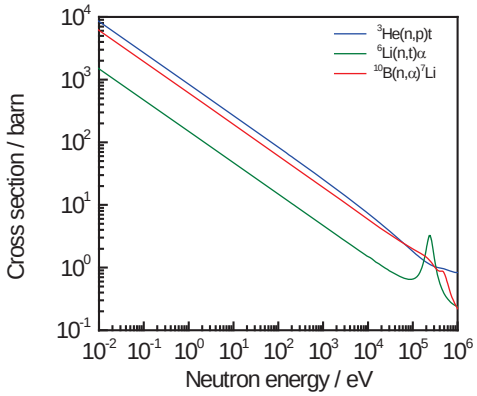

Neutron fluence measurements: standard reactions

Reaction	2200 m/s	Energy region E_{low}		E_{high}	
^{1}H(n,n)		1 keV	-	20 MeV	
^{3}He(n,p)	X	25.3 meV	-	50 keV	
^{6}Li(n,t)	X	25.3 meV	-	1 MeV	
^{10}B(n,α)	X	25.3 meV	-	1 MeV	
^{10}B(n,α$_1$γ)	X	25.3 meV	-	1 MeV	
^{nat}C(n,n)		25.3 meV	-	1.8 MeV	
^{197}Au(n,γ)	X	0.2 MeV	-	2.8 MeV	
^{235}U(n,f)	X	0.15 MeV	-	200 MeV	(1 GeV)
^{238}U(n,f)		2 MeV	-	200 MeV	(1 GeV)
^{238}U(n,γ)		150 eV	-	2.2 MeV	
^{239}Pu(n,f)		25.3 meV	-	300 MeV	
^{209}Bi(n,f)		34 MeV	-	1 GeV	
^{nat}Pb(n,f)		34 MeV	-	1 GeV	

Standard
Reference

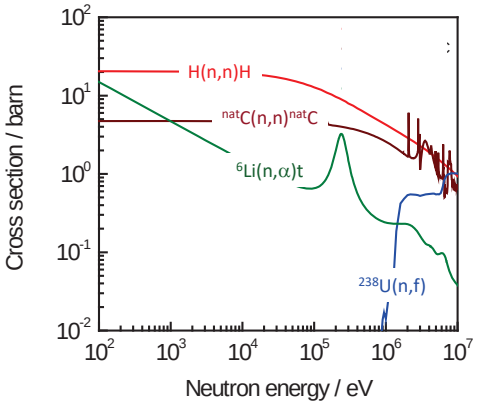

Neutron fluence measurements: standard reactions

Reaction	2200 m/s	Energy region E_{low}		E_{high}	
$^{1}H(n,n)$		1 keV	-	20 MeV	
$^{3}He(n,p)$	X	25.3 meV	-	50 keV	
$^{6}Li(n,t)$	X	25.3 meV	-	1 MeV	
$^{10}B(n,\alpha)$	X	25.3 meV	-	1 MeV	
$^{10}B(n,\alpha_1\gamma)$	X	25.3 meV	-	1 MeV	
$^{nat}C(n,n)$		25.3 meV	-	1.8 MeV	
$^{197}Au(n,\gamma)$	X	0.2 MeV	-	2.8 MeV	
$^{235}U(n,f)$	X	0.15 MeV	-	200 MeV	(1 GeV)
$^{238}U(n,f)$		2 MeV	-	200 MeV	(1 GeV)
$^{238}U(n,\gamma)$		150 eV	-	2.2 MeV	
$^{239}Pu(n,f)$		25.3 meV	-	300 MeV	
$^{209}Bi(n,f)$		34 MeV	-	1 GeV	
$^{nat}Pb(n,f)$		34 MeV	-	1 GeV	

Standard
Reference

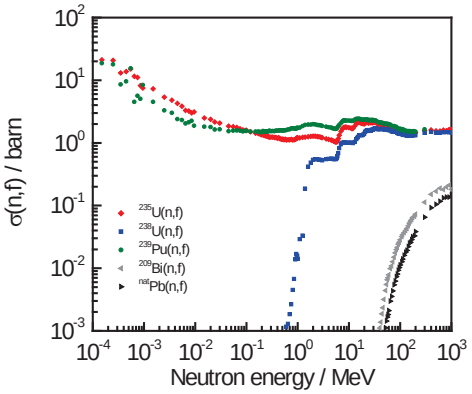

Neutron fluence measurements

Parallel plate ionisation chamber loaded with ^{235}U

standard reaction: $^{235}U(n,f)$

$\varepsilon_f \approx 1$

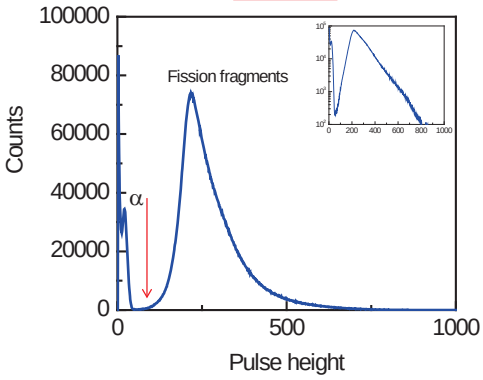

Neutron fluence measurements

Frisch-gridded ionisation chamber loaded with ^{235}U

standard reaction: $^{235}U(n,f)$

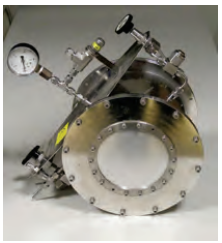

$\varepsilon_f \approx 1$

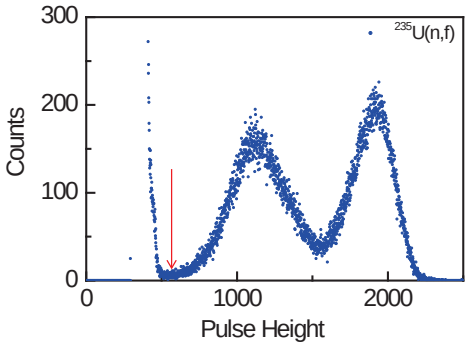

Reaction cross section measurements

$$C_r = \varepsilon_r \varphi Y_r$$

- Y reaction yield
- φ Neutron fluence rate
- ε Detection efficiency
- C response

$$Y_{r,exp} = \frac{\varepsilon_\varphi}{\varepsilon_r} \frac{C_r}{C_\varphi} Y_\varphi$$

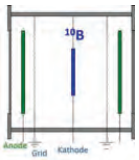

$$C_\varphi = \varepsilon_\varphi \varphi Y_\varphi$$

Reaction cross section measurements

- Absolute measurements
  - all parameters (ε_r, ε_φ) have to be determined

$$Y_{r,exp} = \frac{\varepsilon_\varphi}{\varepsilon_r}\frac{C_r}{C_\varphi}\,Y_\varphi$$

- Relative measurements based on normalisation factor N:
  - accounts for energy independent parameters (ε_r, ε_φ)
  - determined at energy where Y_r is accurately defined

$$Y_{r,exp} = N\frac{C_r}{C_\varphi}\,Y_\varphi$$

Capture cross section measurements

Efficiency to detect capture event ε_c independent of gamma-ray cascade

- Gamma-ray spectroscopy
  good resolution for E_γ e.g. Ge-detectors
- Total absorption detectors
  4π & $\varepsilon_\gamma \approx 100\%$ e.g. BaF_2
- Total energy detection principle
  $\varepsilon_\gamma \propto E_\gamma$ & $\varepsilon_\gamma << 1$ e.g. C_6D_6 scintillators

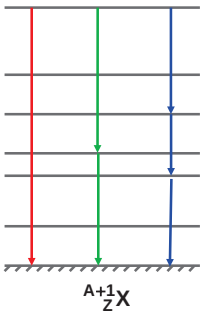

$$\Rightarrow \varepsilon_c = k\sum_i E_{\gamma,i} = k(S_n + E_n\frac{A}{1+A})$$

Schillebeeckx et al., Nuclear Data Sheets 113 (2012) 3054

GELINA – (n,γ) at 12.5 m and 60 m

- Total energy detection principle
  - C_6D_6 liquid scintillators
    (Boron free quartz window!)
  - 125º
  - Pulse Height Weighting Technique

$$C_w = \int C_c(E_d)\, WF(E_d)\, dE_d$$

$$\varepsilon_\gamma \propto E_\gamma \quad \Rightarrow \quad \varepsilon_c \propto S_n + E_n \frac{A}{1+A}$$

- Fluence rate measurements (IC)
  - $^{10}B(n,\alpha)$
  - $^{235}U(n,f)$

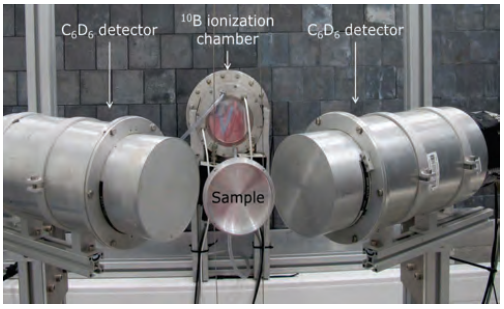

$$Y_{exp} = N \frac{C_w - B_w}{C_\varphi - B_\varphi} Y_\varphi$$

Borella et al. , NIMA 577 (2007) 626

European Commission

^{241}Am + n in RRR

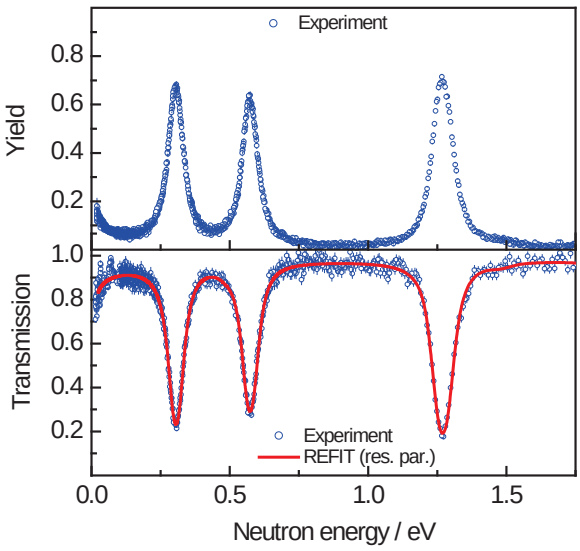

No reference cross section required

Energy /eV	J/ħ	g	$g\Gamma_n$/meV	Γ_γ/meV
0.306	3	7/12	0.0373 (2)	41.6 (4)
0.574	2	5/12	0.0629 (4)	42.1 (6)
1.271	3	7/12	0.2176 (23)	41.7 (8)

European Commission

^{241}Am + n in RRR

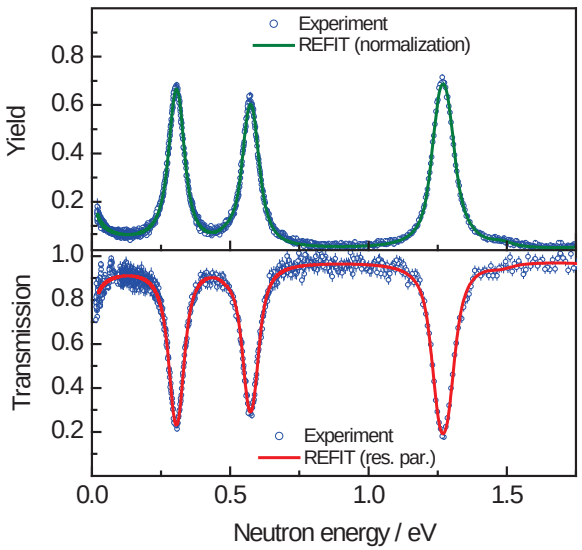

N = 1.00 (2)

No reference cross section required

Energy /eV	J/ħ	g	$g\Gamma_n$/meV	Γ_γ/meV
0.306	3	7/12	0.0373 (2)	41.6 (4)
0.574	2	5/12	0.0629 (4)	42.1 (6)
1.271	3	7/12	0.2176 (23)	41.7 (8)

^{241}Am + n in RRR

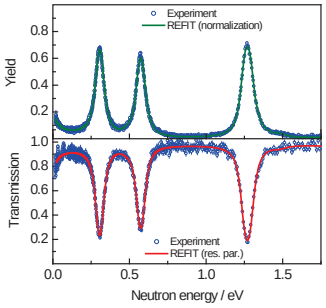

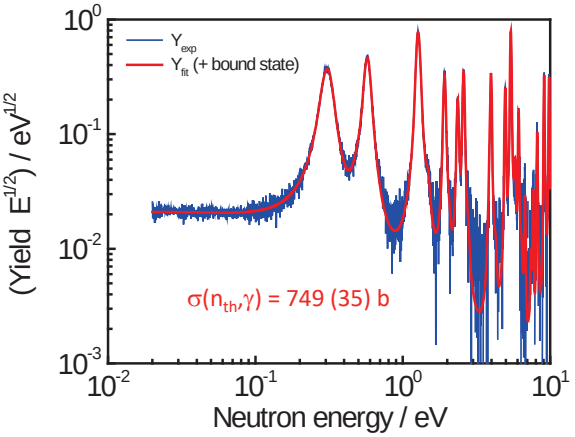

This work = 749 (35) b
JEFF-3.3 = 752.7 b

JENDL-4.0 = 684.2 b
ENDF/B-VIII.0 = 684.2 b

Lampoudis et et al., Eur. Phys. J. Plus 128 (2013) 86

^{241}Am + n in RRR

$\sigma(n_{th},\gamma)$ = 749 (35) b

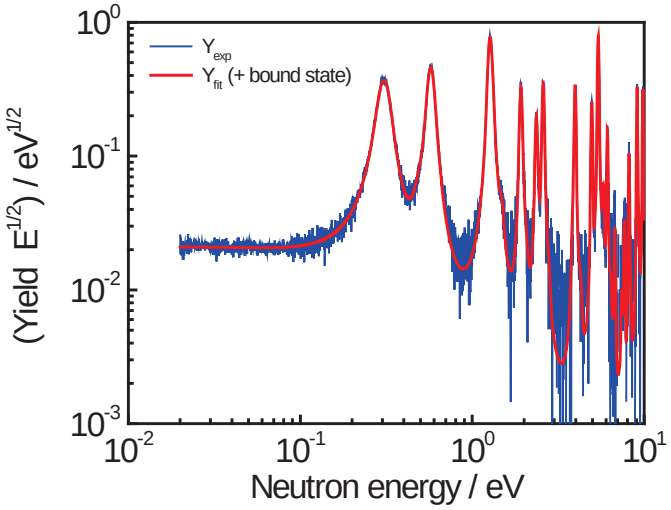

Lampoudis et et al., Eur. Phys. J. Plus 128 (2013) 86

^{241}Am + n in RRR

$\sigma(n_{th},\gamma)$ = 749 (35) b

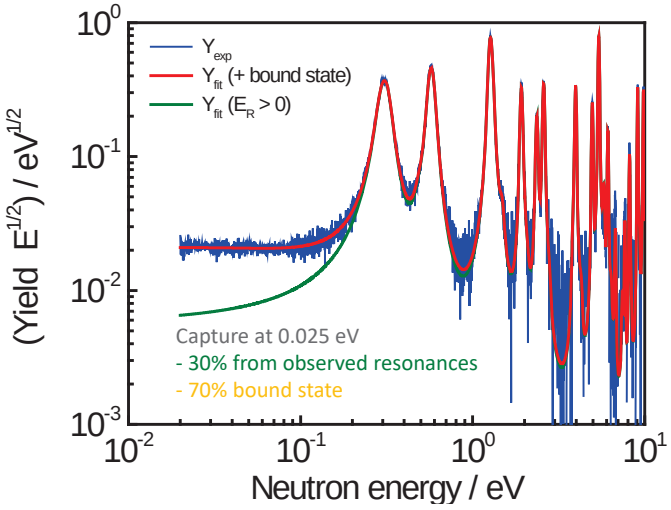

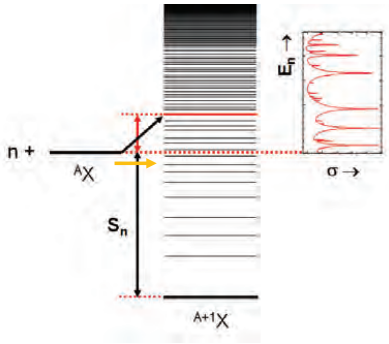

Lampoudis et et al., Eur. Phys. J. Plus 128 (2013) 86

GELINA: resonance parameters for ^{107,109}Ag + n (BUC)

Collaboration CEA (FR)

- Experiments at GELINA
  - Transmission (T) measurements at 10 m
  - Capture (C) measurements at 12.5 m
- Metallic discs of ^{nat}Ag

Thickness

- 0.06 mm T, C
- 0.126 mm T, C
- 0.25 mm T,C
- 0.5 mm T,C

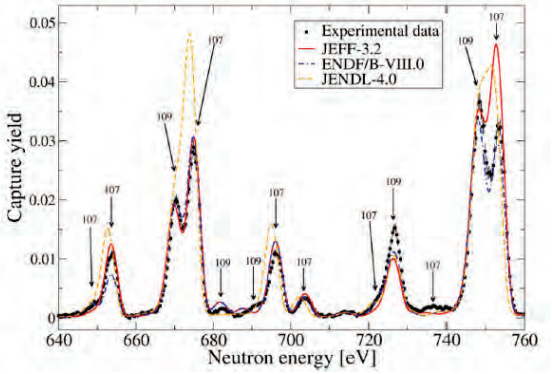

Šalamon et et al., Nucl. Instr. Meth. B446 (2019) 19

European Commission

GELINA: resonance parameters for ^{107,109}Ag + n (BUC)

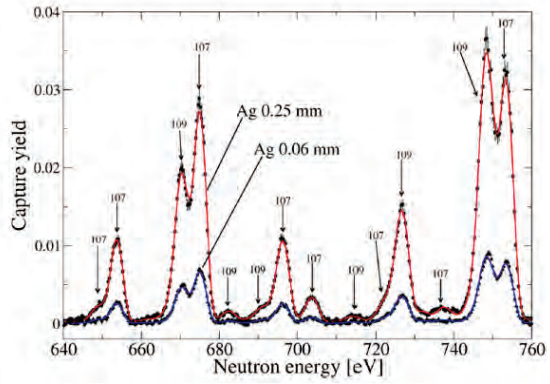

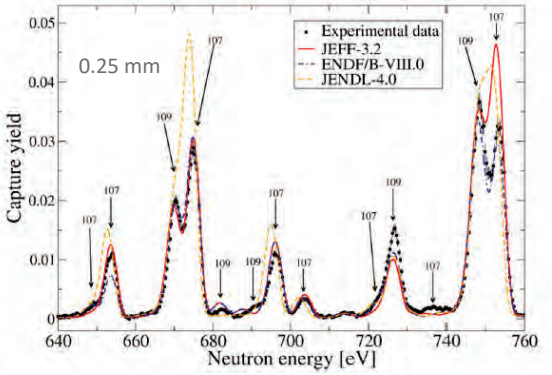

⇒ Improved RP file for ^{107,109}Ag + n

E [eV]	l	J^π	$g\Gamma_n$ [meV]	Γ_γ [meV]
5.195 (1)	0	1⁻	9.928 (9)	130.3 (2)
30.565 (1)	0	1⁻	5.533 (9)	125.5 (5)
40.342 (1)	0	1⁻	3.568 (8)	139.7 (9)
55.81 (1)	0	0⁻	9.02 (3)	131 (1)
71.06 (1)	0	1⁻	20.61 (7)	130.0 (9)
87.69 (1)	0	1⁻	4.44 (2)	128 (2)

Šalamon et et al., Nucl. Instr. Meth. B446 (2019) 19

European Commission

GELINA – ELISA (Elastic and inelastic scattering array)

(n,n) and (n,n'γ) cross sections at L = 30m
Collaboration PTB (GE)

- Neutron and γ-ray detection by
  - 16 EJ301 (NE213 equivalent)
  - 16 EJ315 (C_6D_6 based)
- (n/γ) pulse shape discrimination
- Fluence rate measurements (IC) : ^{235}U(n,f)

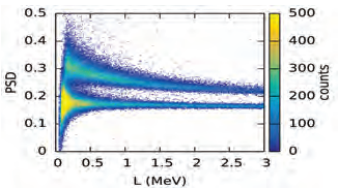

e.g. ^{nat}Fe(n,n)
Pirovano et al. Phys. Rev. C 99 (2019) 024601

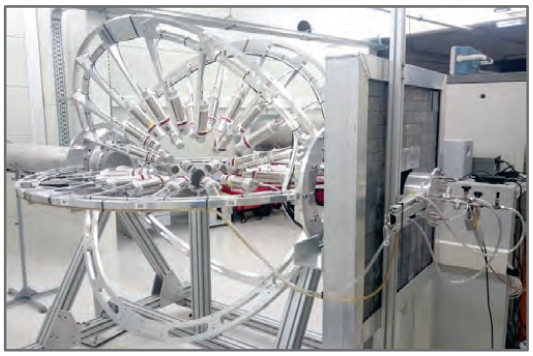

More info:
Georgios Gkatis (PhD)
Andreea Oprea

European Commission

GELINA – GAINS (Gamma Array for Inelastic Neutron Scattering)

(n,n'γ): γ-ray production cross sections at L = 100 m
Collaboration IFIN-HH (RO)

- γ-ray detection by
  - 12 HPGe detectors at 110°, 125° and 150 °
  - Digital acquisition system
- Fluence rate measurements (IC) : ^{235}U(n,f)

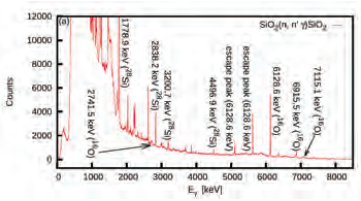

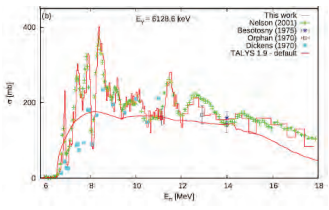

e.g. ^{16}O(n,n'γ) and ^{28}Si(n,n'γ)
Boromiza et al. Phys. Rev. C 101 (2020) 024604

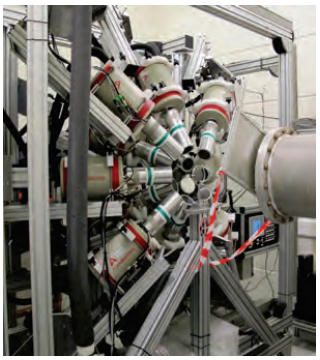

More info:
Andreea Oprea

European Commission

GELINA – Fission studies

(n,f) cross sections and
FF properties and prompt fission neutrons and γ-rays

- Fission fragments by Twin Frisch-Gridded IC
  - Fragment energy
  - Fragment masses - 2E-technique
  - Fission axis orientation
- Prompt fission neutrons
  - 12 x Scintillators (NE213 equivalent)
  - Energy : time-of-flight
- Prompt fission γ-rays
  - LaBr, CeBr scintillators

Position sensitive electrode

European Commission

Nuclear data libraries for nuclear applications

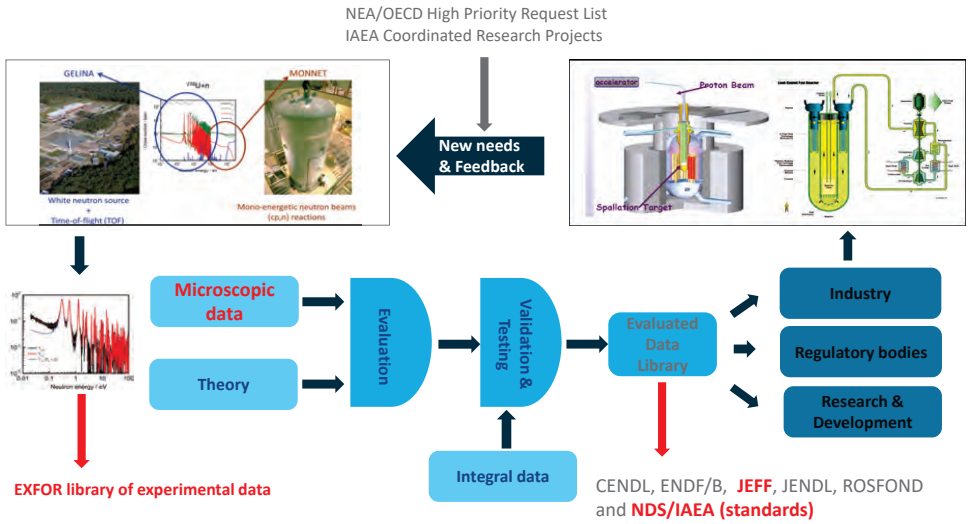

European Commission

Nuclear data services: Nuclear Energy Agency (NEA/OECD)

JANIS

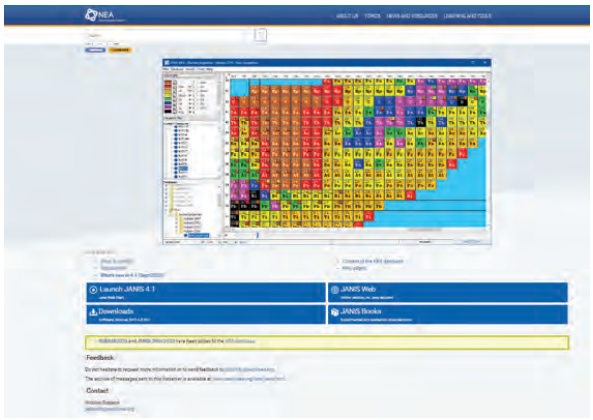

High Priority Request List

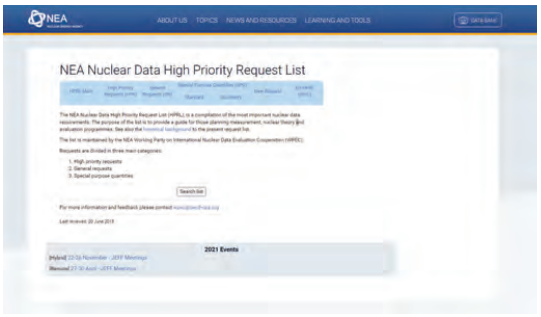

https://www.oecd-nea.org

European Commission

Neutron Resonance Analysis (NRCA & NRTA)

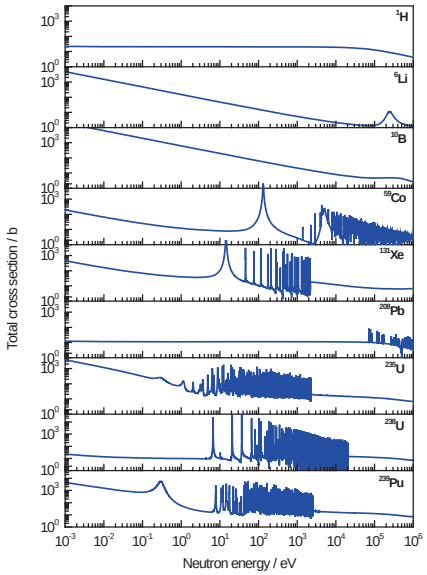

- Resonances appear at energies that are specific for each nuclide
- Position and amplitude of resonances can be used as fingerprints to
  - identify and quantify nuclides
  - elemental & isotopic composition
- Neutron Resonance Capture and Transmission Analysis (NRCA & NRTA)
  - Non-Destructive Analysis (NDA)
  - no sample preparation required
  - sensitive to almost all nuclides (except light)
  - **requirements: TOF-measurements at a white neutron source** (e.g. GELINA, LANSCE, J-PARC, ISIS)

European Commission

Cross section measurements

Total cross section

$$T \cong e^{-n\sigma_{tot}}$$

Capture cross section

$$Y_\gamma \approx (1-e^{-n\,\sigma_{tot}})\frac{\sigma_\gamma}{\sigma_{tot}}$$

Well-characterised (reference) samples

n: total number of atoms per unit area is well-known

⇓

accurate cross-sections can be determined

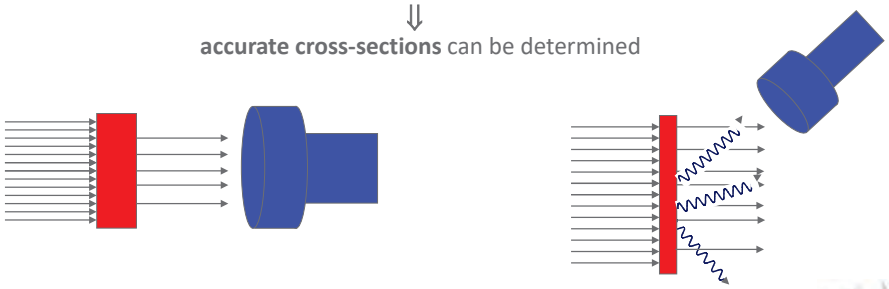

Schillebeeckx et al., Nuclear Data Sheets 113 (2012) 3054

Neutron resonance analysis (NRTA and NRCA)

NRTA

$$T \cong e^{-n\sigma_{tot}}$$

NRCA

$$Y_\gamma \approx (1-e^{-n\sigma_{tot}})\frac{\sigma_\gamma}{\sigma_{tot}}$$

Well-known cross sections

⇓

areal density can be determined

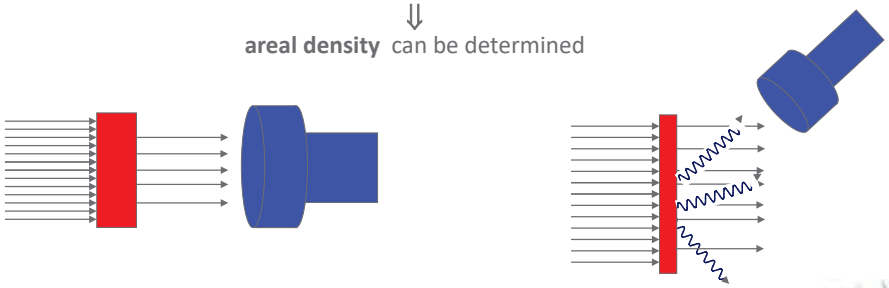

Schillebeeckx et al., Report EUR 26848-EN (2014)

Neutron Resonance Analysis

NRTA

$$T_{exp} = \frac{C_{in}}{C_{out}}$$

Resonance Shape Analysis: REFIT

$$\chi^2(n) = (T_{exp} - T_M(t,n))^T \, V_{T_{exp}}^{-1} \, (T_{exp} - T_M(t,n))$$

$$T_M(t) = \int R(t, E)\, T(E)\, dE$$

$$T(E) = e^{-n\bar{\sigma}_{tot}(E)}$$

n : areal density

total number of nuclei per unit area

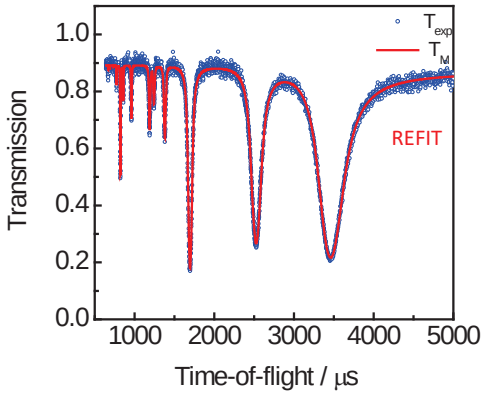

NRTA and NRCA

Transmission: areal density Cu: 0.55 (2) g/cm²

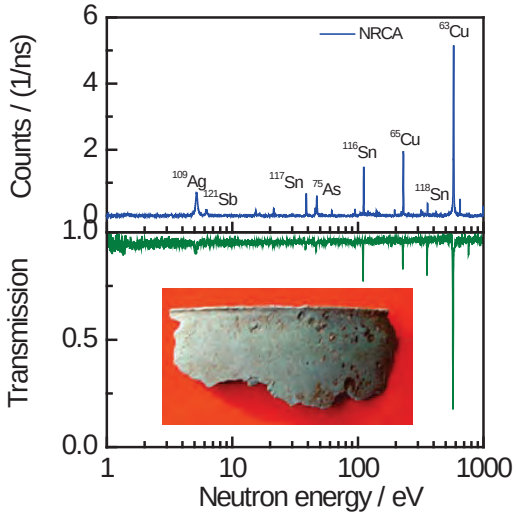

Element	Isotope	E_r / eV	wt%
Cu	^{63}Cu	579.0	77.76 (11)
	^{65}Cu	230.0	
Sn	^{112}Sn	94.8	20.85 (10)
	^{116}Sn	111.2	
	^{117}Sn	38.8	
	^{118}Sn	45.7	
	^{119}Sn	222.6	
	^{120}Sn	427.5	
	^{124}Sn	62.0	
Fe	^{56}Fe	1147.4	0.77 (1)
As	^{75}As	47.0	0.34 (1)
Sb	^{121}Sb	6.2	0.20 (2)
	^{123}Sb	21.4	
Ag	^{107}Ag	16.3	0.09 (1)
	^{109}Ag	5.2	
In	^{115}In	1.46	0.0061 (3)

Uncertainties: only counting statistics

H. Postma and P. Schillebeeckx, in Neutron Methods for Archaeology and Cultural Heritage (Springer)

NRTA and NRCA

Transmission: areal density Cu: 0.55 (2) g/cm^2

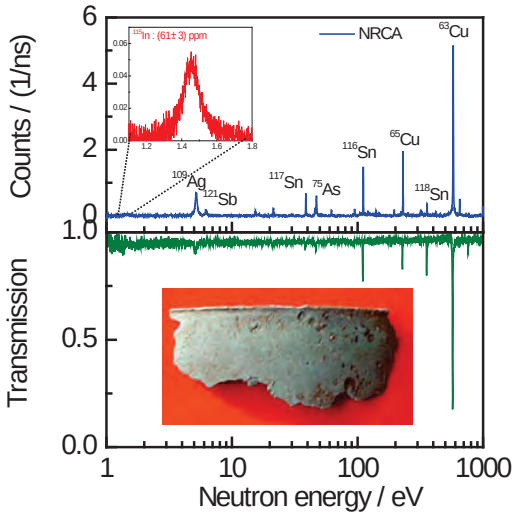

Element	Isotope	E_r/ eV	wt%
Cu	^{63}Cu	579.0	77.76 (11)
	^{65}Cu	230.0	
Sn	^{112}Sn	94.8	20.85 (10)
	^{116}Sn	111.2	
	^{117}Sn	38.8	
	^{118}Sn	45.7	
	^{119}Sn	222.6	
	^{120}Sn	427.5	
	^{124}Sn	62.0	
Fe	^{56}Fe	1147.4	0.77 (1)
As	^{75}As	47.0	0.34 (1)
Sb	^{121}Sb	6.2	0.20 (2)
	^{123}Sb	21.4	
Ag	^{107}Ag	16.3	0.09 (1)
	^{109}Ag	5.2	
In	^{115}In	1.46	0.0061 (3)

Uncertainties: only counting statistics

H. Postma and P. Schillebeeckx, in Neutron Methods for Archaeology and Cultural Heritage (Springer)

NRA ⇔ NAA & PGAA

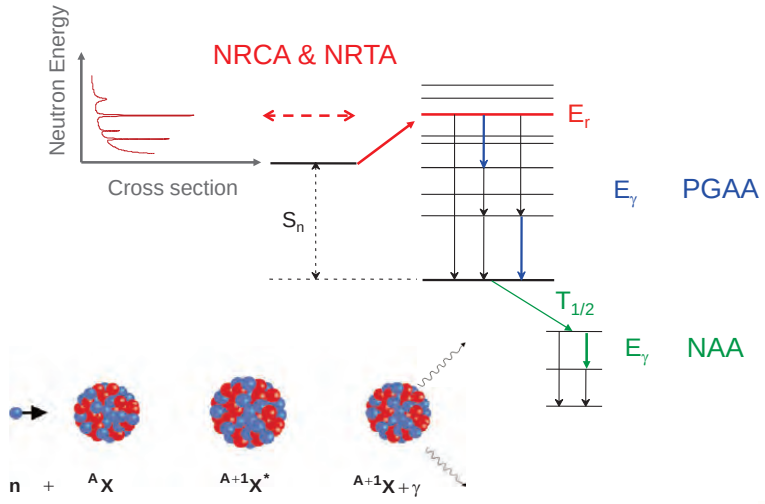

NRA ⇔ NAA & PGAA

- NRCA & NRTA
  - Pulsed white neutron beam
  - Gamma/Neutron detector: good time resolution ⇒ scintillators
- NAA
  - Intense neutron beam (irradiation in core)
  - Gamma detector: γ - ray energy resolution ⇒ Ge-detectors
- PGNAA
  - Intense neutron beam (mostly cold: Budapest, NIST, FRM-II)
  - Gamma detector: γ - ray energy resolution ⇒ Ge-detectors

NRCA ⇔ PGAA at continuous incident beam

⇒ detection of **In** is **not hindered by** strong resonances of **other elements** (e.g. Cu)

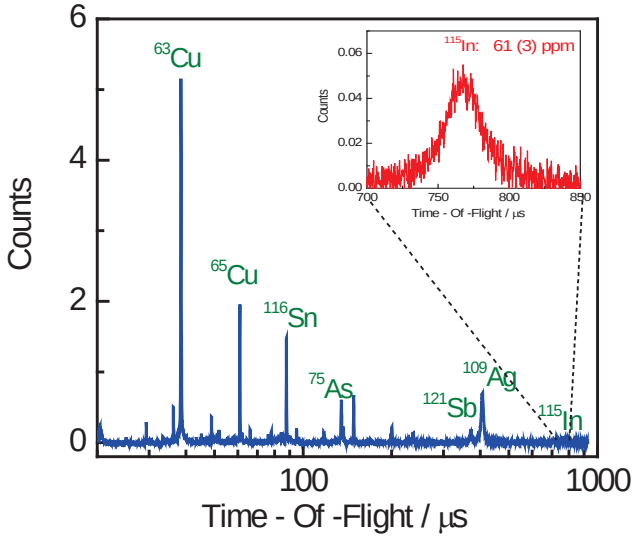

Postma et al., Czech. J. Phys. 53 (2003) A233

NRA: which elements can be detected?

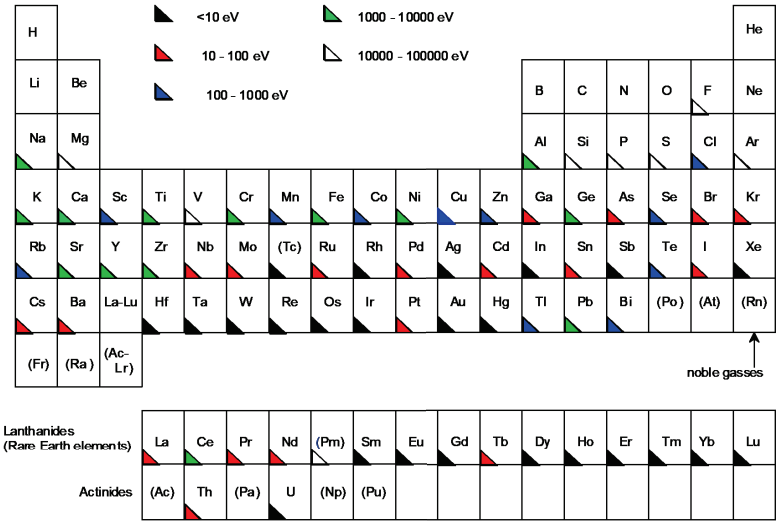

Energy region	detection limit
1 eV < E_μ < 10 eV	~ 10^{-6} (ppm)
10 eV < E_μ < 1000 eV	~ 10^{-5} - 10^{-3}
1 keV < E_μ	> 10^{-2} (%)

H. Postma and P. Schillebeeckx, in Neutron Methods for Archaeology and Cultural Heritage (Springer)

NRCA: Authenticity of Etruscan artefacts

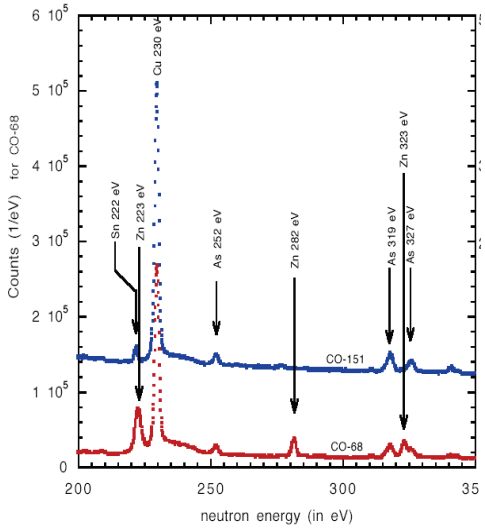

Statuettes from a collection assembled in the 18th century by count Corazzi of Cortona (It).

Now at the National Museum of Antiquities in Leiden (NL).

Postma et al., Archaeometry, 46 (2004) 635

NRCA: Authenticity of artefacts

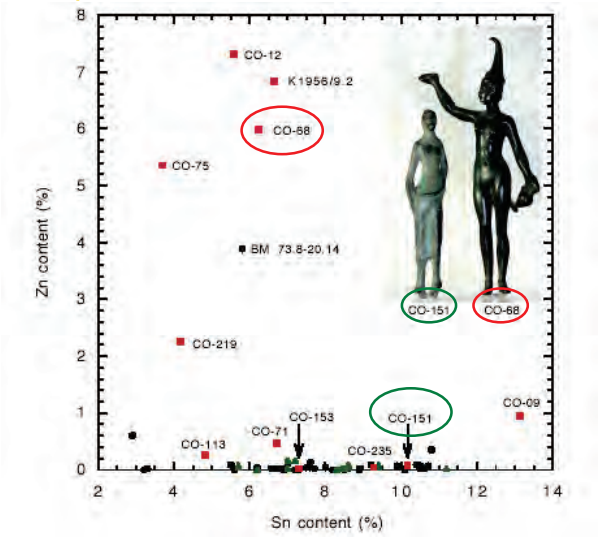

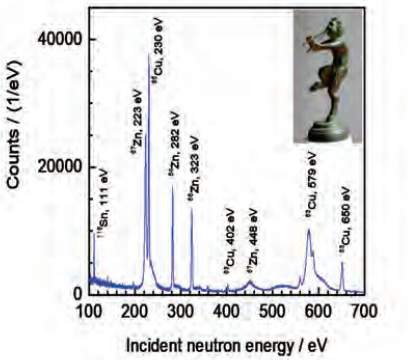

NRCA measurements at a 12.5 m station of GELINA of a figurine that is supposed to present the Greek god Pan.
Zn/Cu ratio: replica

Roman water taps: NRCA combined with Neutron Diffraction (ND)

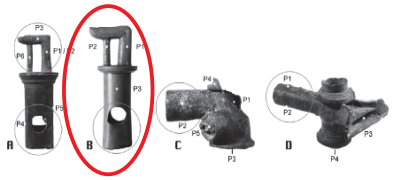

NRCA : material composition
ND : fabrication process

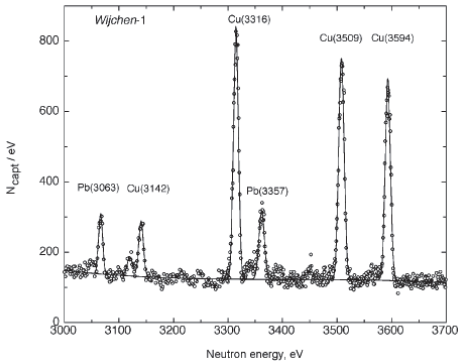

NRCA: 4.8 (5) g/cm^2 Cu

Element weight ratio	NRCA (GELINA)		Neutron diffraction (ISIS)		
			P1	P2	P3
Pb/Cu	0.335	(34)	0.415	0.337	0.402
Sn/Cu	0.0868	(25)	0.094	0.098	0.094
Zn/Cu	0.0036	(3)			
Sb/Cu	0.00167	(3)			
Fe/Cu	0.0012	(3)			
As/Cu	0.00098	(3)			
Ag/Cu	0.00096	(3)			

Schut et al., J. Radioanal. Nucl. Chem. 278 (2008) 151

NRA for cultural heritage and archaeology

Started in 2000 by a collaboration between Univ. Delft and JRC Geel initiated by **Prof. H. Postma**

† April 2021

Journal papers

Postma et al., J. Radioanal. Nucl. Chem. 248 (2001) 115
Postma et al., Czech. J. Phys. 53 (2003) A233 – A240
Postma et al., Archaeometry, 46 (2004) 635
Postma and Schillebeeckx, J. Radioanal. Nucl. Chem. 265 (2005) 297
Postma et al., Il Nuovo Cimento, 30C (2007) 105
Perego et al., J. Radioanal. Nucl. Chem. 271 (2007) 89
Postma et al., J. Radioanal. Nucl. Chem. 271 (2007) 95
Schut et al., J. Radioanal. Nucl. Chem. 278 (2008) 151
Postma et al., J. Radioanal. Nucl. Chem. 283 (2010) 641
Perelli et al., Nucl. Instr. Meth. Phys. Res. A 623 (2010) 693
Perelli et al;, J. Anal. At. Spectrom. 26 (2011) 992
Postma et al., J. Archaeol. Sci. 38 (2011) 1810
Schillebeeckx et al., J. Instrumentation, 7 (2012) C03009
Postma et al., Analecta Praehistorica Leidensia, 47 (2017) 37








European Commission

NRA for cultural heritage and archaeology

Started in 2000 by a collaboration between Univ. Delft and JRC Geel initiated by **Prof. H. Postma**

† April 2021

Chapters in books

H. Postma and P. Schillebeeckx, “Neutron resonance capture and transmission analysis”
In: Encyclopedia of analytical chemistry (chapter a9070) ,
R.A. Meyers (Ed.), John Wiley & Sons Ltd. (2009)

H. Postma and P. Schillebeeckx, “Neutron Resonance Analysis”
In: Neutron Methods for Archaeology and Cultural Heritage (chapter 12),
N. Kardjilovand G. Festa (Eds.), Springer International Publishing Switzerland (2017)

P. Schillebeeckx and H. Postma, “Neutron resonance analysis (NRA)”
In: The SAS Encyclopedia of Archaeological Sciences,
S.L. Lopez Varela (Ed.), Wiley –Blackwell (2018)

P. Schillebeeckx and H. Postma, “Neutron Resonance Analysis methods for archaeological and cultural heritage applications”
In: Handbook of Cultural Heritage Analysis (pp. 145 – 187)
S. D’Amico and V. Venuti (Eds.), Springer International Publishing Switzerland (2022)

European Commission

Characterisation of PbI_2 by NRTA at GELINA

- JRC Geel target preparation group extracted:
  - 150 g Iodine (powder) from 210 liter from **reprocessed waste** (Le Hague)
  - (1.3 g/l Iodine and 40 MBq/l)
- Sample characterisation: by mass spectrometry , NAA and **NRTA**

Fig. 3. Addition of $Pb(NO_3)_2$ to the iodide solution to precipitate lead iodide.

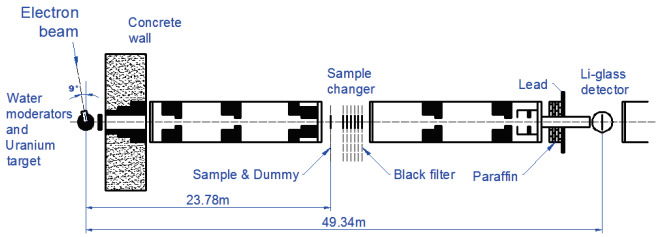

Noguere et al., Nucl. Instr. Meth. Phys. Res. A 575 (2007) 476

Characterisation of PbI_2 by NRTA at GELINA

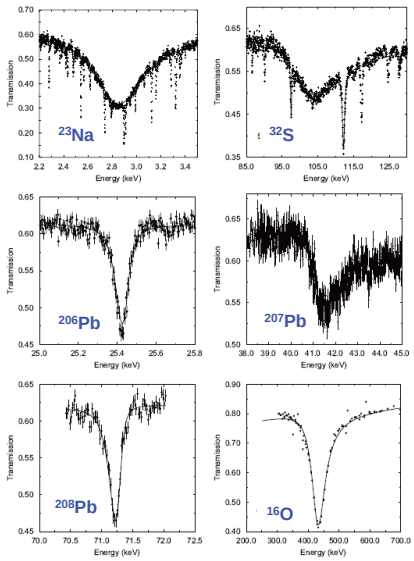

$$T_M(t_m, n) = \int R(t_m, E)\, e^{-n\,\sigma_{tot}(E)} dE$$

$$\chi^2(n) = \left(T_{exp} - T_M(t_m, n)\right)^T V_{T_{exp}}^{-1} \left(T_{exp} - T_M(t_m, n)\right)$$

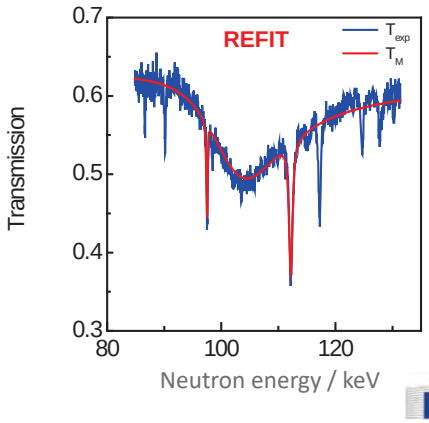

NRTA compared with NAA and ICP-MS

Element		NRTA	NAA	Mass spectrometry (PSI)
Iodine	total	20.24 (41)	19.75 (61)	19.86 (41)
	^{127}I	3.44 (5)	3.35 (10)	3.36 (8)
	^{129}I	16.80 (40)	16.40 (60)	16.50 (40)
Lead	Total	52.3 (17)	51.1 (1.8)	
	^{206}Pb	12.8 (5)		
	^{207}Pb	11.5 (1)		
	^{208}Pb	27.1 (17)		
Sulfur		5.44 (3)		
Sodium		0.72 (2)		1.0 (2)
Oxygen		13.92 (5)		14.5 (15)
Hydrogen		<0.13		0.020 (2)
Nitrogen				1.2 (4)

NRTA ↔ NAA, ICPMS :
- more elements analysed
- isotopic composition of Pb

NRTA of W sample: validation of resonance parameters

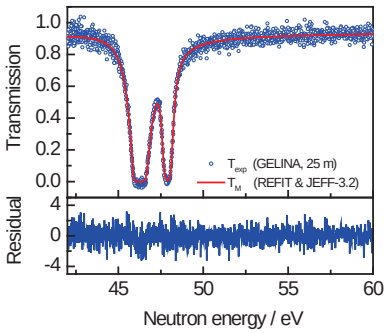

- Sample: metallic disc of ^{nat}W (1 mm thick)
  - homogeneous sample
  - areal density n : from weight and area
    ⇒ $u_n/n < 0.2\%$
- Transmission : absolute measurement
  - absolute measurement
  - methodology well understood (background, dead time correction,…)
    Schillebeeckx et al., Nuclear Data Sheets 113 (2012) 3054 – 3100
    ⇒ $u_{T_{exp}}/T_{exp} < 0.3\ \%$

⇒ NRTA: derive n_{NRTA} from the transmission data and compare with n_{REF}
⇒ one of the most accurate benchmark experiments to validate resonance parameters

NRTA of W sample: validation of resonance parameters

^{183}W

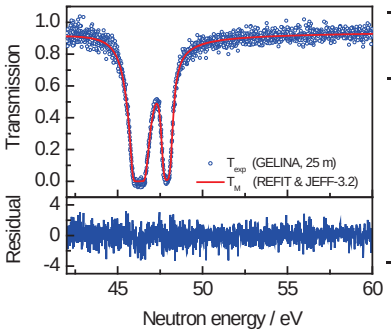

Reference		E_r = 46.26 eV Γ_n / meV	E_r = 46.26 eV Γ_γ / meV	E_r = 47.80 eV Γ_n / meV	E_r = 47.80 eV Γ_γ / meV	n_{NRTA}/n_{REF}
Lynn et al.	2002	162 (1)	72	126 (2)	72	0.983 (10)
Mughabghab	1984	140 (4)	77 (8)	108 (10)	78 (10)	1.198 (34)
Mughabghab	2006	162 (2)	77 (8)	122 (2)	78 (10)	0.992 (14)
JEFF-3.2		163.4	75.3	120.8	61.5	1.002 *(5)*
JENDL-3.3		154.0	46.0	119.0	81.0	1.113 *(5)*
ENDF/B-VII.1		154.0 (8)	46.0 (21)	119.0 (12)	81.0 (51)	1.113 (11)

$$\chi^2(n_{NRTA}) = (T_{exp} - T_M)^T V_{T_{exp}}^{-1} (T_{exp} - T_M)$$

⇒ Parameters in ENDF/B-VII.1 (JENDL-3.3) strongly biased and covariance data not reliable

Becker et al., Nuclear Data Sheets 123 (2015) 171

NRTA of PuO_2 sample: validation of resonance parameters

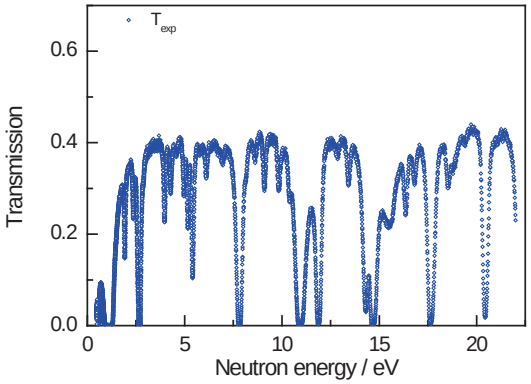

CBNM - 271

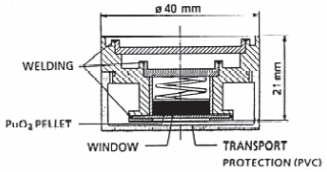

NRTA of PuO_2 sample (pressed pellet) at GELINA (CBNM – 271)

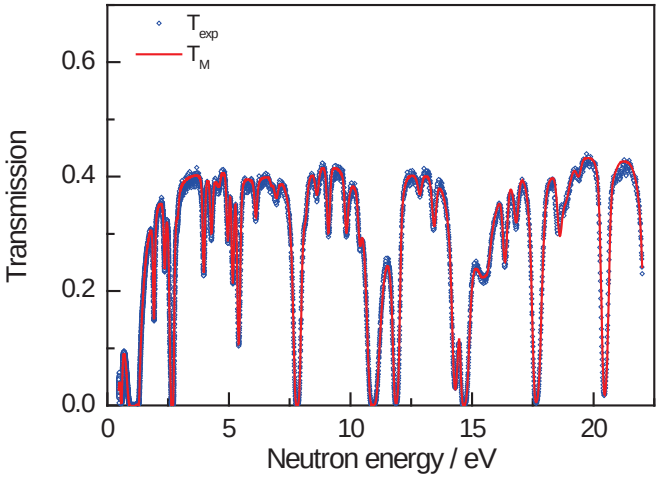

$$T_M(t_m, n) = \int R(t_m, E)\, e^{-n\,\sigma_{tot}(E)} dE$$

$$\chi^2(n) = (T_{exp} - T_M(t_m, n))^T\, V_{T_{exp}}^{-1}\, (T_{exp} - T_M(t_m, n))$$

REFIT

NRTA of PuO_2 sample (pressed pellet) at GELINA (CBNM – 271)

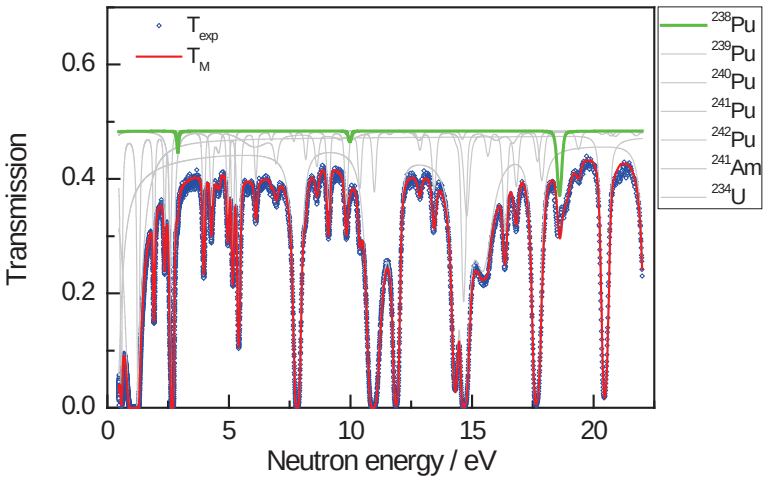

NRTA of PuO_2 sample (pressed pellet) at GELINA (CBNM – 271)

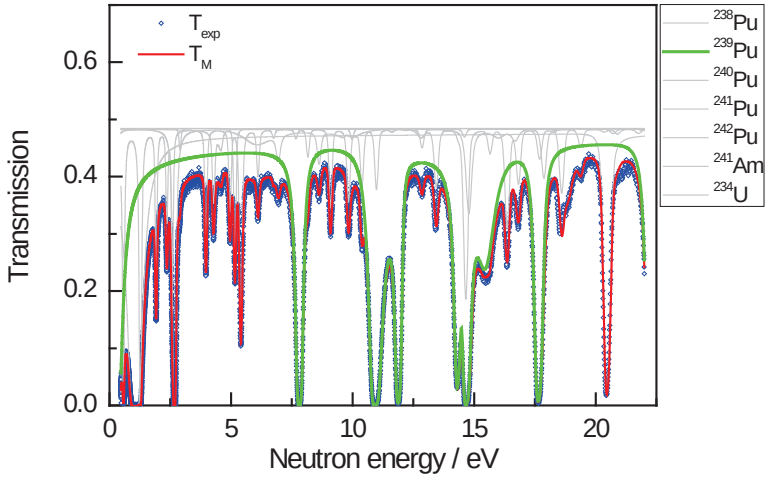

NRTA of PuO_2 sample (pressed pellet) at GELINA (CBNM – 271)

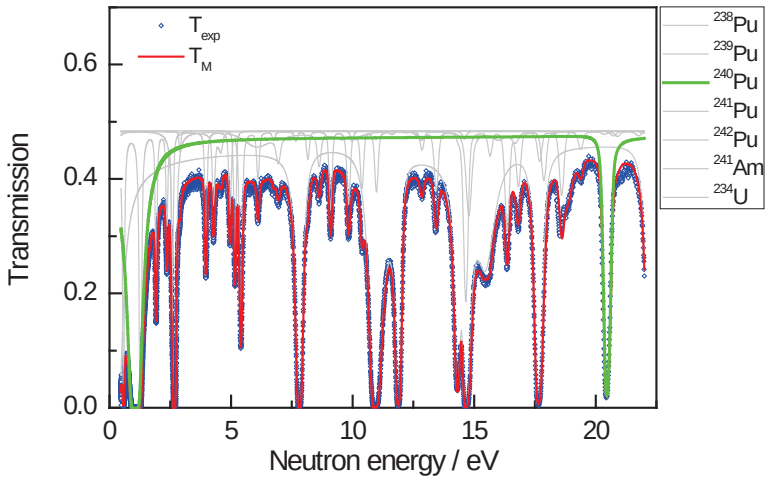

NRTA of PuO_2 sample (pressed pellet) at GELINA (CBNM – 271)

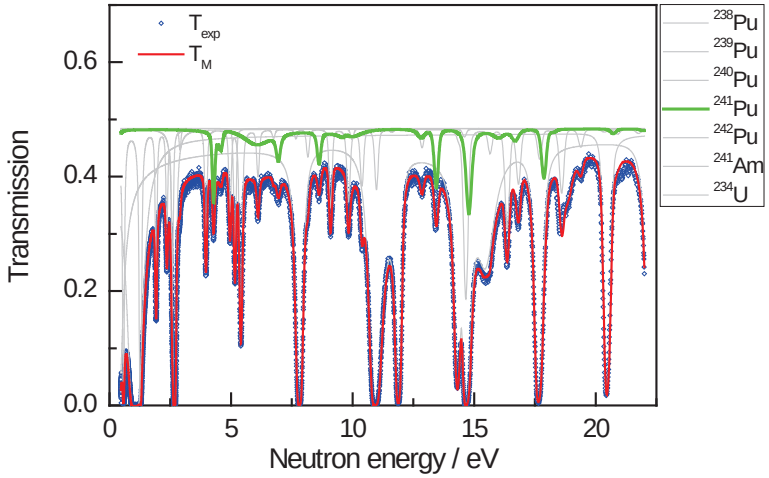

NRTA of PuO_2 sample (pressed pellet) at GELINA (CBNM – 271)

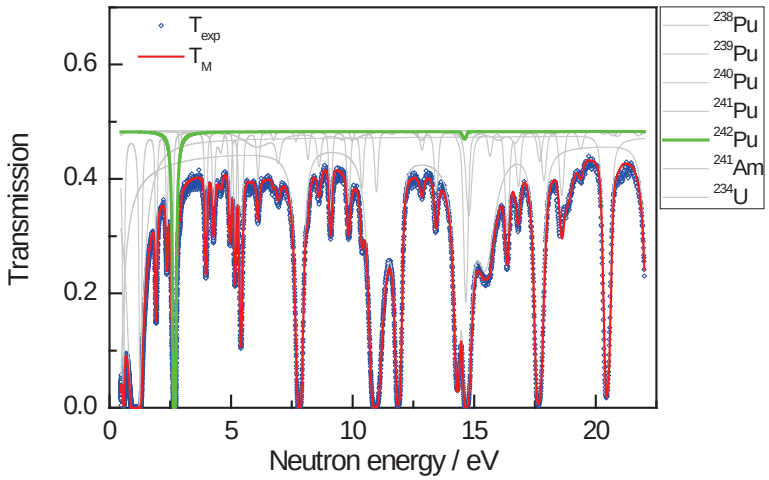

NRTA of PuO_2 sample (pressed pellet) at GELINA (CBNM – 271)

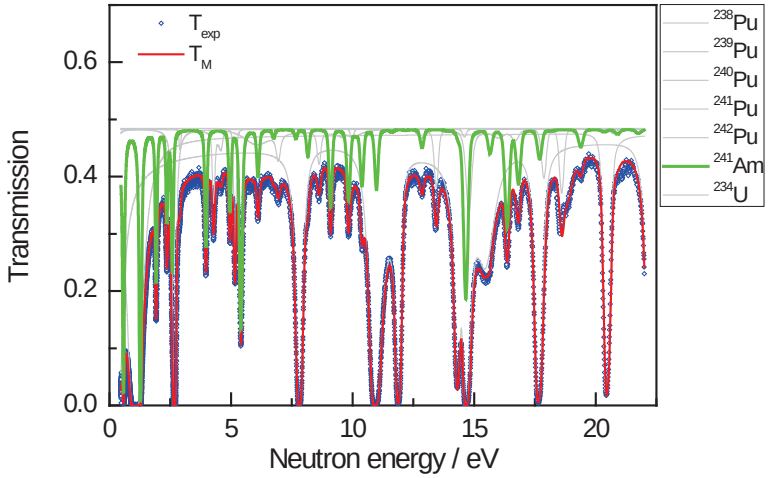

NRTA of PuO_2 sample (pressed pellet) at GELINA (CBNM – 271)

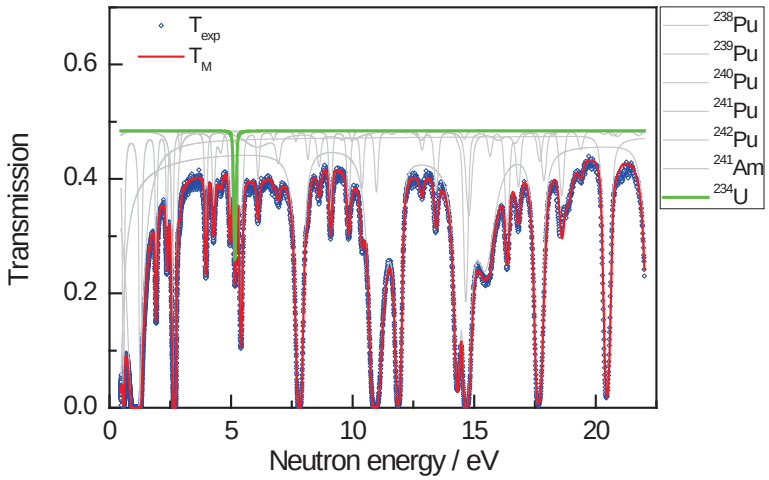

NRTA of PuO_2 sample: validation of resonance parameters

Nuclide	n_{REF}		n_{NRTA}				n_{NRTA} / n_{REF}			
			ENDF/B-VIII.0		JEFF-3.2		ENDF/B-VIII.0		JEFF-3.2	
^{238}Pu	0.009514	(20)	0.00783	(70)	0.00898	(70)	0.823	(74)	0.944	(74)
^{239}Pu	0.62603	(28)	0.62154	(90)	0.61530	(95)	0.9928	(14)	0.9829	(15)
^{240}Pu	0.25273	(24)	0.25699	(36)	0.26240	(32)	1.0169	(14)	1.0383	(13)
^{241}Pu	0.015697	(20)	0.01574	(10)	0.01577	(10)	1.0028	(64)	1.0045	(65)
^{242}Pu	0.041489	(60)	0.04334	(10)	0.04300	(10)	1.0447	(25)	1.0365	(24)
^{241}Am	0.06290	(63)	0.07236	(21)	0.06059	(20)	1.1503	(33)	0.9633	(32)
^{234}U	0.002918	(10)	0.00289	(10)	0.00287	(10)	0.989	(34)	0.982	(35)

RP in ENDF/B-VIII.0 for ^{241}Am are strongly biased: $\sigma(n,\gamma)$ underestimated

n: atomic abundance relative to total Pu
NRTA uncertainties only due to counting statistics

NRTA: MINERVE samples

Collaboration with CEA Cadarche

- MAESTRO project: determine data for FP important for BUC applications
  - Production of pellet samples
    mixture: depleted uranium + material enriched in specific FP
  - Pile oscillator measurements at MINERVE
    Validate absorption cross sections of FP and determine correction factors

- NRTA of irradiated MINERVE pellet samples at GELINA
  (part of MAESRTRO)
  - Identification and quantification of impurities
  - Validation of resonance parameters of FP

^{103}Rh
^{107,109}Ag
^{133}Cs
^{143,145}Nd
^{147,149,152}Sm,
^{151,153}Eu
^{161,162,163,164}Dy
^{168,170}Er
^{180}Hf

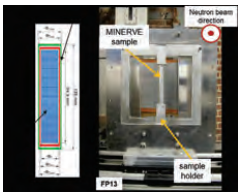

NRTA model for pellet samples

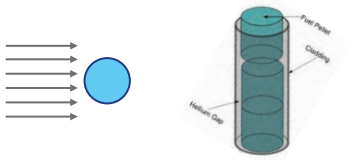

$$T(E) = f_h + (1 - f_h) \int_0^1 \frac{x}{\sqrt{1 - x^2}} e^{-\rho \sigma_{tot}(E)\, x}\, dx$$

REFIT

- x : track length (divided by 2R)
- f_h : holes fraction
- ρ : volume number density
- R : radius

Transmission through a pure Ag pellet sample

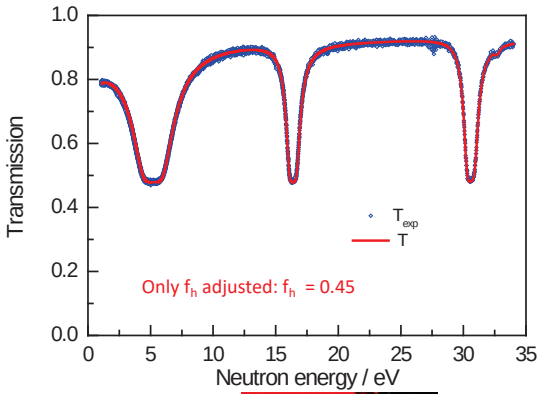

Model developed, implemented and validated at JRC Geel (S. Kopecky)

Fei Ma et al., J. Anal. At. Spectrom. 35 (2020) 478

European Commission

NRTA: MINERVE samples

- NRTA of irradiated MINERVE pellet samples at GELINA
  - Identification and quantification of impurities

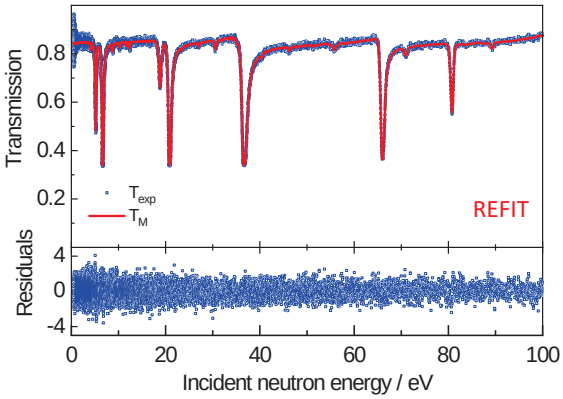

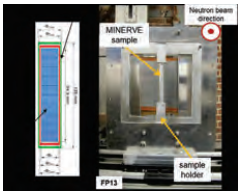

^{109}Ag

Note:

RP used result from a new evaluation for ^{107,109}Ag based on capture and transmission experiments at GELINA

Šalamon et al., Nucl. Instr. Meth. B 446 (2019) 19

European Commission

NRTA: MINERVE samples

- NRTA of irradiated MINERVE pellet samples at GELINA
  - Identification and quantification of impurities

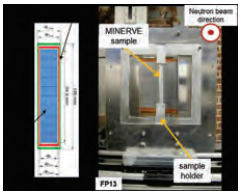

^{109}Ag

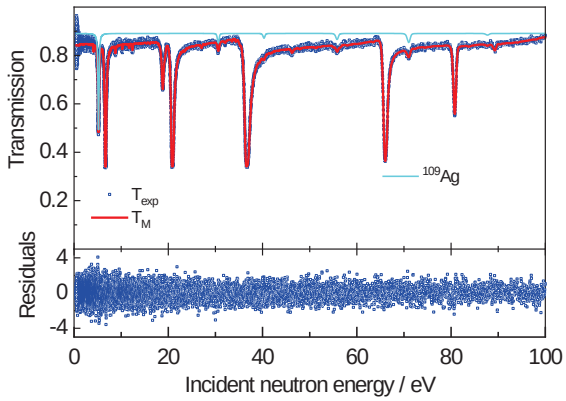

NRTA: MINERVE samples

- NRTA of irradiated MINERVE pellet samples at GELINA
  - Identification and quantification of impurities

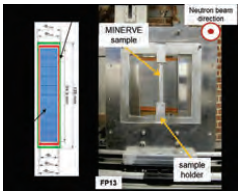

^{109}Ag

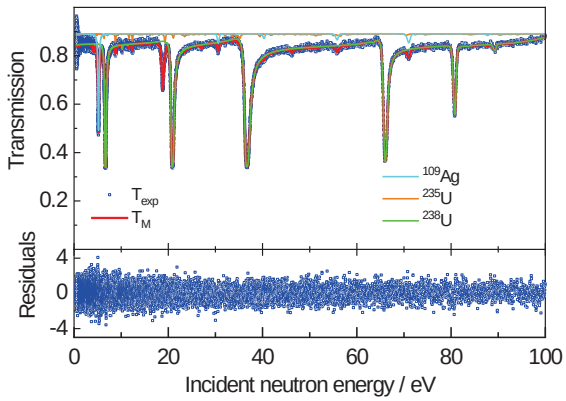

NRTA: MINERVE samples

- NRTA of irradiated MINERVE pellet samples at GELINA
  - Identification and quantification of impurities

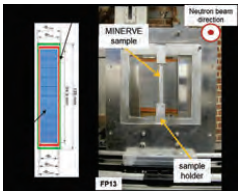

^{109}Ag

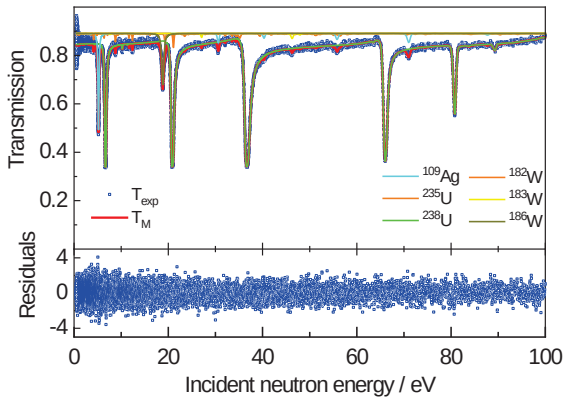

Presence of strong neutron absorber W:
Not declared by supplier

NRTA: MINERVE samples

- NRTA of irradiated MINERVE pellet samples at GELINA
  - Identification and quantification of impurities
- Presence of strong neutron absorbing elements such as W important for the interpretation pile oscillator measurements

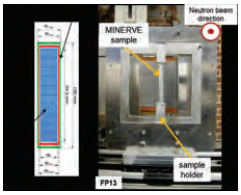

^{109}Ag

	AG9C1		AG9C2	
	ICPMS	This work	ICPMS	This work
^{109}Ag	6.30 (8) x 10^{-4}	6.03 (2) x 10^{-4}	6.82 (8) x 10^{-5}	6.54 (2) x 10^{-5}
^{235}U	8.31 (10) x 10^{-5}	8.35 (20) x 10^{-5}	8.39 (10) x 10^{-5}	8.45 (20) x 10^{-6}
^{238}U	1.119 (14) x 10^{-2}	1.126 (5) x 10^{-2}	1.129 (14) x 10^{-2}	1.136 (5) x 10^{-2}
^{182}W		1.30 (4) x 10^{-5}		6.1 (3) x 10^{-6}
^{183}W		6.6 (2) x 10^{-6}		3.1 (2) x 10^{-6}
^{186}W		1.36 (1) x 10^{-5}		6.11 (3) x 10^{-6}

10^{24} at/cm^3

Šalamon et al., J. Radioanal. Nucl. Chem. 321 (2019) 519

3D imaging (transmission)

- GELINA: high resolution, relatively low intensity
- Imaging at spallation sources: ISIS, JPARC, LANSCE, …

  E.g. Losko and Vogel, Scientific Report 12 (2022) 6648
  - LANSCE
  - Microchannel plate neutron imaging detector (^{10}B)

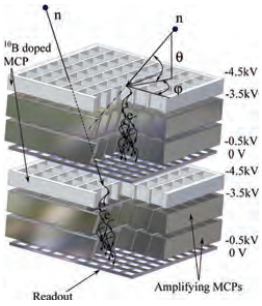

Tremsin et al., NIM 539 (2005) 278

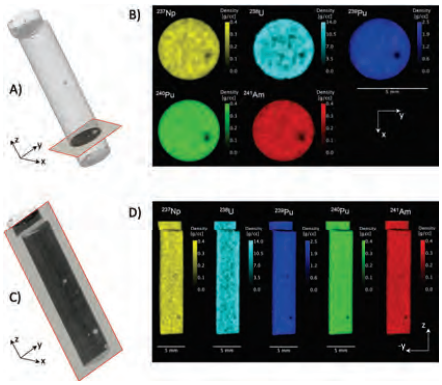

Nuclear fuel cycle

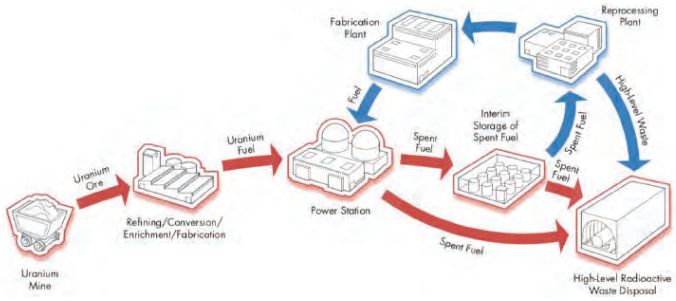

Nuclear fuel cycle (open or closed) produces waste

Open fuel cycle: final disposal of Spent Nuclear Fuel (SNF)

Open fuel cycle
Sweden : Forsmark
Finland : Onkalo

Three barriers (SKB):
- canister
- buffer (bentonite clay)
- rock

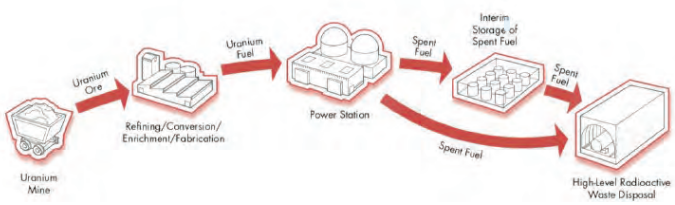

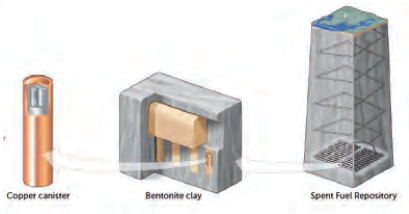

Open fuel cycle: final disposal of SNF assemblies

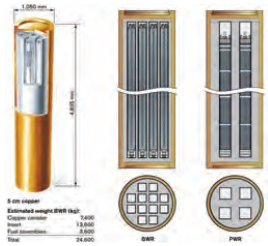

Estimate of thermal power has a substantial impact on:
- the number of canisters (Cu mining)
- ecological and financial footprint

SKB : Swedish nuclear fuel and waste management company

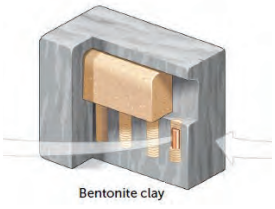

Open fuel cycle
Sweden : Forsmark

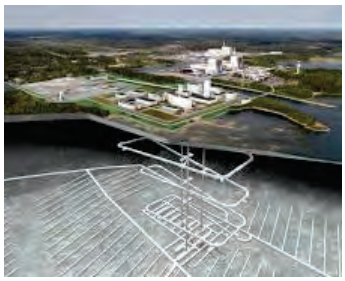

6000 canisters
12000 ton of spent fuel

Thermal power produced by SNF

- 1 a ≤ t ≤ 10 a
  - ^{144}Ce / ^{144}Pr
  - ^{106}Ru / ^{106}Rh
  - ^{134}Cs
  - ^{90}Sr / ^{90}Y
  - ^{137}Cs / ^{137m}Ba
- 10 a ≤ t ≤ 100 a
  - ^{90}Sr / ^{90}Y
  - ^{137}Cs / ^{137m}Ba
  - ^{238}Pu
  - ^{241}Am
  - ^{244}Cm
- 100 a ≤ t
  - ^{241}Am
  - ^{238}Pu
  - ^{239,241}Pu

PWR UO_2 pellet (5 g)
^{235}U/U = 4.8 %
burnup = 45 MWd/kg

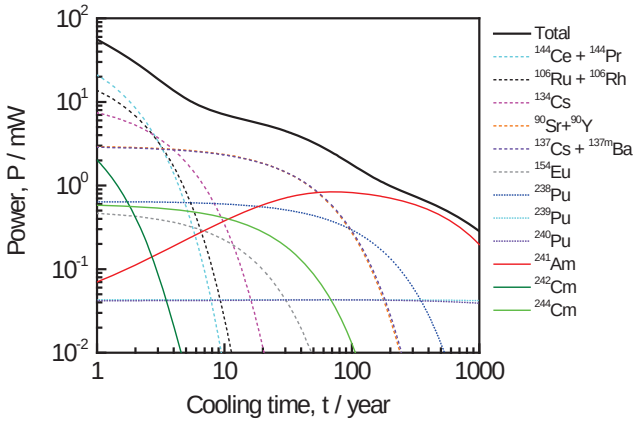

Žerovnik et al., JRC Technical Reports, EUR 29301 EN (2018)

Thermal power produced by SNF

- 1 a ≤ t ≤ 10 a
  - **^{144}Ce / ^{144}Pr**
  - **^{106}Ru / ^{106}Rh**
  - **^{134}Cs**
  - ^{90}Sr / ^{90}Y
  - ^{137}Cs / ^{137m}Ba
- 10 a ≤ t ≤ 100 a
  - ^{90}Sr / ^{90}Y
  - ^{137}Cs / ^{137m}Ba
  - ^{238}Pu
  - ^{241}Am
  - ^{244}Cm
- 100 a ≤ t
  - ^{241}Am
  - ^{238}Pu
  - ^{239,241}Pu

PWR UO_2 pellet (5 g)
^{235}U/U = 4.8 %
burnup = 45 MWd/kg

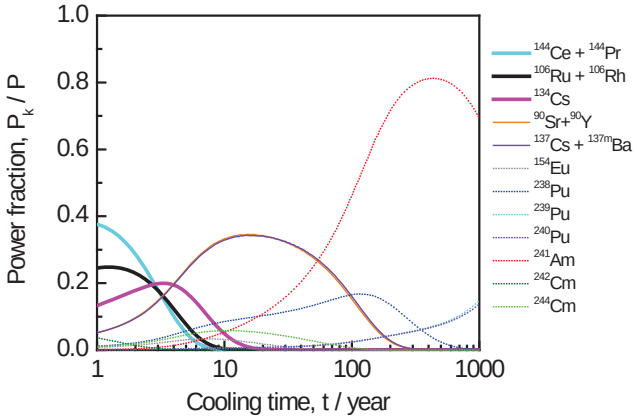

Thermal power produced by SNF

- 1 a ≤ t ≤ 10 a
  - ^{144}Ce / ^{144}Pr
  - ^{106}Ru / ^{106}Rh
  - ^{134}Cs
  - ^{90}Sr / ^{90}Y
  - ^{137}Cs / ^{137m}Ba
- 10 a ≤ t ≤ 100 a
  - **^{90}Sr / ^{90}Y**
  - **^{137}Cs / ^{137m}Ba**
  - ^{238}Pu
  - ^{241}Am
  - ^{244}Cm
- 100 a ≤ t
  - ^{241}Am
  - ^{238}Pu
  - ^{239,241}Pu

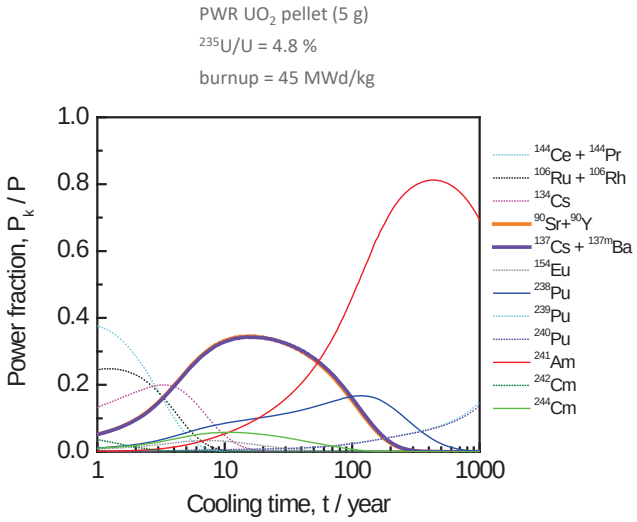

Thermal power produced by SNF

- 1 a ≤ t ≤ 10 a
  - ^{144}Ce / ^{144}Pr
  - ^{106}Ru / ^{106}Rh
  - ^{134}Cs
  - ^{90}Sr / ^{90}Y
  - ^{137}Cs / ^{137m}Ba
- 10 a ≤ t ≤ 100 a
  - ^{90}Sr / ^{90}Y
  - ^{137}Cs / ^{137m}Ba
  - ^{238}Pu
  - ^{241}Am
  - ^{244}Cm
- 100 a ≤ t
  - **^{241}Am**
  - ^{238}Pu
  - ^{239,241}Pu

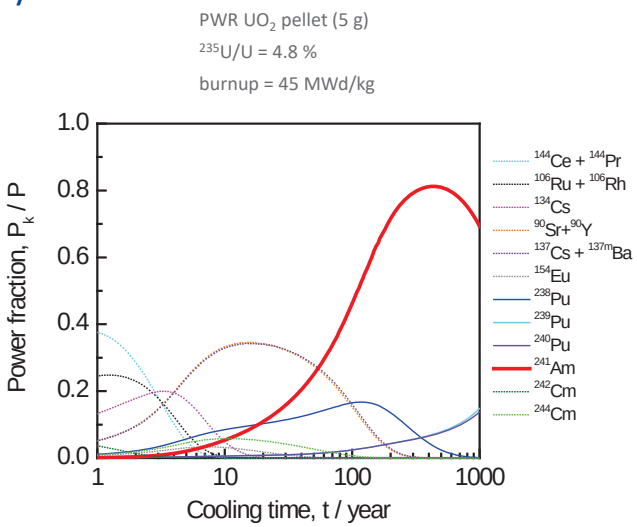

Back-end of the fuel cycle: spent fuel characterisation (SFC)

A **safe**, **secure**, **ecological** and **economic** handling, interim storage and final disposal requires that **Spent Nuclear Fuel (SNF)** is **characterised** for the main observables of interest:

- Decay heat
- Neutron emission
- γ-ray emission
- Reactivity (BurnUp Credit)
  (i.e. Fission Product (FP), actinides)
- Fissile material (Nuclear Safeguards, i.e. ^{235}U, ^{239}Pu)
- Specific nuclides (Long term safety)
  i.e. ^{14}C, ^{36}Cl, ^{79}Se, ^{94}Nb, ^{99}Tc, ^{129}I, ^{226}Ra, ^{237}Np

Spent fuel characterisation (SFC): nuclide inventory

Nuclide	Observable
^{90}Sr	H, S_γ
^{106}Ru	H
^{134}Cs	H
^{137}Cs	H, S_γ
^{144}Ce	H,
^{148}Nd	Burn-up
^{149}Sm	Power
^{154}Eu	H, S_γ

Nuclide	Observable
^{235}U	R, S_γ
^{238}U	R, S_γ
^{238}Pu	H, S_γ
^{239}Pu	R, S_γ
^{240}Pu	R, S_γ
^{241}Pu	H, S_γ
^{241}Am	H, S_γ
^{242}Cm	H, S_n
^{244}Cm	H, S_n

H : thermal power or decay heat
S_n : neutron emission
S_γ : γ-ray emission
R : reactivity (criticality safety)

⇒ Requires **complex nuclide inventory** which can only be obtained by **theoretical calculations**

Criticality safety (BUC):

^{95}Mo, ^{99}Tc, ^{101}Ru, ^{103}Rh, ^{109}Ag, ^{133}Cs, ^{143}Nd, $^{147,149,150,151,152}Sm$, ^{155}Gd

Long term safety:

^{14}C, ^{36}Cl, ^{79}Se, ^{94}Nb, ^{99}Tc, ^{129}I, ^{226}Ra, ^{237}Np

Burnup calculations

Coupled neutron transport – nuclide depletion/production

ALEPH2	(SCK CEN)
EVOLCODE	(CIEMAT)
SERPENT	(VTT)
SCALE	(ORNL)
VESTA	(IRSN)

Neutron transport

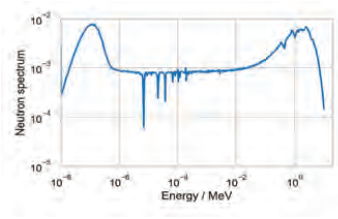

Bateman equation

$$\frac{dN_k}{dt} = Y N_f \sigma_f \varphi + \sum_{i \to k} \lambda_i N_i + \sum_{j \to k} \sigma_j N_j \varphi - (\lambda_k + \sigma_{k,a}\varphi) N_k$$

Update nuclide vector

Burnup calculations need to be validated

Nuclear data
- Cross sections: (n,γ), (n,f), …
- Fission Yields
- Decay data
  - Half-lives
  - Emission probabilities
  - Recoverable energy

Burnup code

SNF input data
- Fuel properties
  - design
  - material data (IE)
- Operational history
  - burn-up (BU)
  - cooling time (CT)
  - …

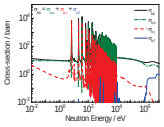

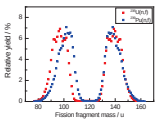

Nuclide inventory
Observables
- thermal power
- neutron emission
- γ-ray emission
- …

Burnup calculations need to be validated

Nuclear data
- Cross sections: (n,γ), (n,f), …
- Fission Yields
- Decay data
  - Half-lives
  - Emission probabilities
  - Recoverable energy

Burnup code

SNF input data
- Fuel properties
  - design
  - material data (IE)
- Operational history
  - burn-up (BU)
  - cooling time (CT)
  - …

Validate by NDA experiment
- **Neutron emission**
- NRTA: nuclide inventory
- Calorimeter at CLAB

Nuclide inventory Observables
- thermal power
- neutron emission
- γ-ray emission
- …

Neutron emission by SNF

PWR UO_2 pellet (5 g)
$^{235}U/U$ = 4.8 %
burnup = 45 GWd/t

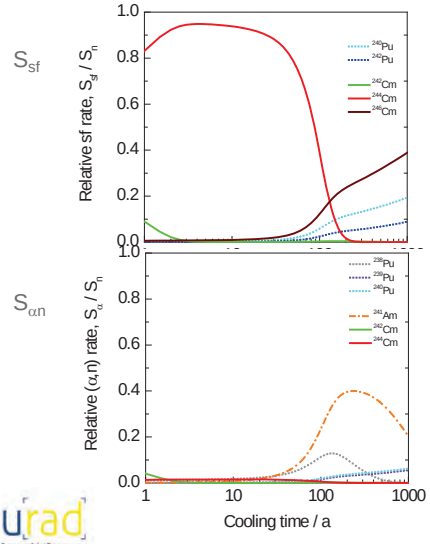

⇒ Main contribution from ^{244}Cm(sf)

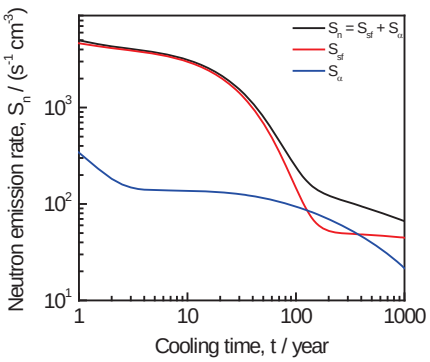

Neutron emission by SNF: spontaneous fission

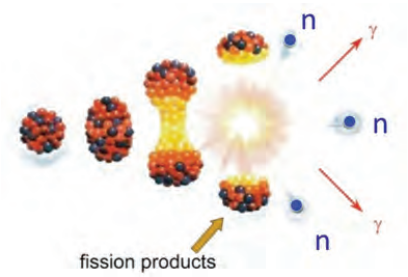

e.g. ^{240}Pu(sf), **^{244}Cm(sf)**, ^{252}Cf(sf)

Fission: nucleus splits up into fission products (FP), which are strongly :

- Prompt fission γ-rays
- **Prompt fission neutrons**

Prompt neutron emission due to spontaneous fission

Energy spectrum

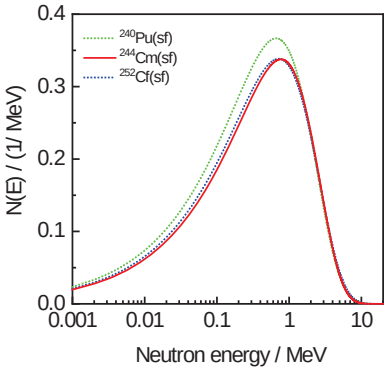

Multiplicity

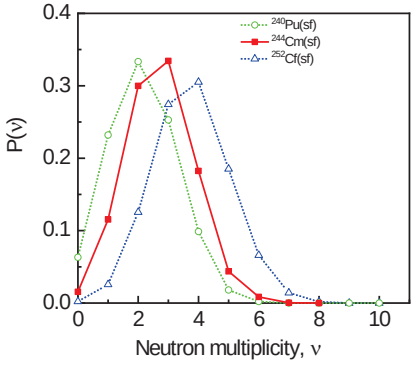

Detection of prompt fission neutrons: correlation counting

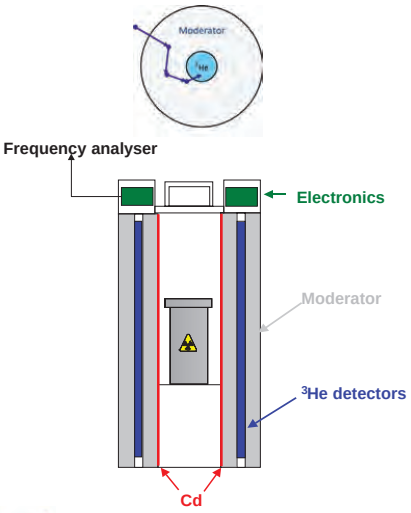

Well-known for nuclear safeguards applications

See S. Pozzi on Monday

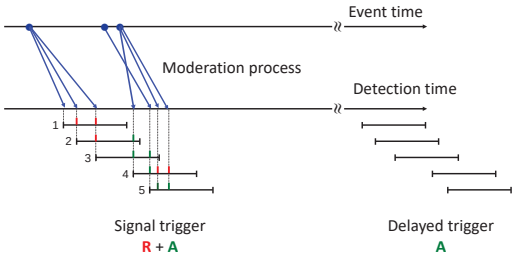

Experimental observables:

Total count rate: T

Reals count rate: R = (R+A) - A

Neutron correlation counting: Hage's point model

$$T = \varepsilon_{sf}\, \mathbf{S_{sf}}\, M\, [1 + \alpha\,]$$

$$R = \varepsilon_{sf}^{2}\, f\, \mathbf{S_{sf}}\, M^{2} \left[\frac{\nu_{sf(2)}}{\nu_{sf(1)}} + \frac{p\,\nu_{nf(2)}}{1 - p\,\nu_{nf(1)}}\,(1 + \alpha\,)\right]$$

- Neutron emission rata due to (sf) : F_s
- Relative (α,n) contribution : α
- Detection efficiency : ε
- Leakage multiplication : M
- Probability for a (n,f) reaction : p
- Factorial moments multiplicity distribution

$$\nu_{sf(j)} = \sum_{\nu=j}^{\infty} \binom{\nu}{j} P_{sf}(\nu) \qquad \nu_{nf(j)} = \sum_{\nu=j}^{\infty} \binom{\nu}{j} P_{nf}(\nu)$$

W. Hage and D.M. Cifarelli, Nucl. Sci; Eng. 89 (1985) 159

W. Hage and D.M. Cifarelli, Nucl. Instr. Meth. A236 (1985) 165

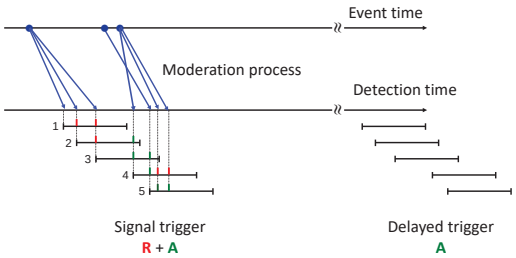

Experimental observables:

Total count rate: T

Reals count rate: R = (R+A) - A

Validation of depletion codes: neutron emission rate of SNF

NDA method to determine the neutron output of a **SNF** sample under **standard controlled area** conditions

Collaboration SCK CEN

Hot cell facility at SCK CEN

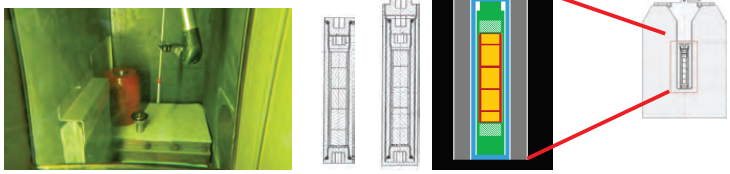

Standard controlled area

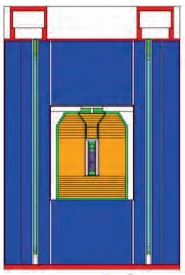

EURAD: Validation of depletion codes

- **Irradiation history** of the SNF
  - Segment (~ 50 mm) from rod D05 of FT1X57 (PWR)
  - PWR Assembly (15 x 15): 188 UO_2 rod (4.5 wt% $^{235}U/U$) and 16 $(U,Gd)O_2$ rods
  - Irradiated at Tihange 1
  - Rod used for other international project (First-Nuclides, REGAL, WETFUEL & AGAF, SF-ALE)
- **SNF** segment **sample** by **NDA**

  Part of a set of 4 samples (**REGAL project**)
  - **Radiochemical analysis (BU)**
  - Microstructural analysis
  - Leach tests (low O_2)
  - Leach tests (high O_2)

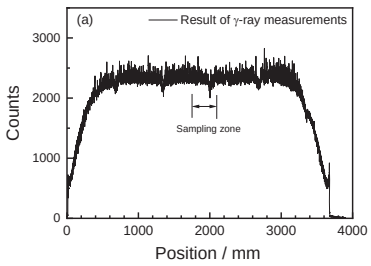

Results of radiochemical analysis

BU indicator	Date of analysis	Nuclide inventory mg/g	Cumulative fission yield (x 100)	Burnup GWd/t
^{137}Cs	10/21/2013	1.288 (28)	6.334	52.6 (11)
^{143}Nd + ^{144}Nd	02/05/2014	3.029 (32)	10.158	53.95 (56)
^{145}Nd + ^{146}Nd	02/05/2014	1.962 (21)	6.479	53.05 (56)
^{148}Nd	02/05/2014	0.534 (12)	1.724	53.3 (12)
^{150}Nd	02/05/2014	0.257 (11)	0.836	52.2 (23)
			Average:	52.78 (37)

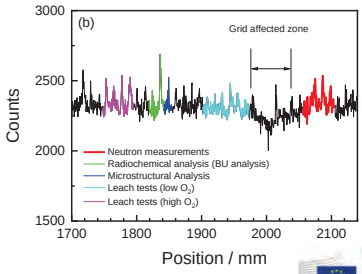

Schillebeeckx et al., JRC Technical Reports, EUR 30379 EN (2020)

Absolute neutron output of SNF segment sample: results

- SNF segment sample: characteristics

Parameter	Value
Length	52.01 (4) mm
Segment weight	42.616 (1) g
Cladding weight	6.71 (4) g
Net fuel weight	35.91 (4) g

- Neutron emission rate (exp) CT 18 a

S_{sf} = **682 (10) g^{-1} s^{-1}**

$S_{\alpha n} / S_{sf}$ = 0.036 (15)

$\rho(S_{sf}, \alpha)$ = - 0.972

- Detector calibrated with certified ^{252}Cf(sf) sources (Mn bath)
- Hage's point model

Note: neutron emission rate reflects ^{244}Cm inventory
radiochemical analysis uncertainty > 3%

Schillebeeckx et al., JRC Technical Reports, EUR 30379 EN (2020)

Absolute neutron output of SNF segment sample: code validation

Code	Library	(α,n) Method	(α,n) Library	S_{sf} / ($g^{-1}s^{-1}$)	S_{α} / ($g^{-1}s^{-1}$)	Calculation/Experiment S_{sf}	Calculation/Experiment $S_{\alpha n}$
SCALE	ENDF/B-VII.1	Y(α,n)		653	11.0	0.96	0.45
SERPENT(1)	ENDF/B-VII.1	Y(α,n)		689	14.3	1.01	0.58
SERPENT(2)	ENDF/B-VII.1	Y(α,n)		694	14.2	1.02	0.58
	ENDF/B-VIII.0	Y(α,n)		691	14.1	1.01	0.57
	JEFF-3.1.2	Y(α,n)		629	13.2	0.92	0.54
	JEFF-3.3	Y(α,n)		654	13.7	0.96	0.56
	JEFF-4T0	Y(α,n)		695	13.7	1.02	0.56
	JENDL-4.0			719	14.5	1.05	0.59
ALEPH28	ENDF/B-VIII.0	Y(α,n)		662	13.1	0.97	0.53
		σ(α,n)	TENDL2015		12.6		0.51
		σ(α,n)	JENDL_AN/500		10.6		0.43
	JEFF-3.3	Y(α,n		641	12.9	0.94	0.53
		σ(α,n)	TENDL2015		12.7		0.52
		σ(α,n)	JENDL_AN/500		10.5		0.43

All data normalised to ^{148}Nd inventory

S_{sf} = 682 (10) g^{-1} s^{-1}

$S_{\alpha n}$ / S_{sf} = 0.036 (15)

⇒ influence
- nuclear data
- burnup code

Production of ^{244}Cm

$$n + {}^{238}_{92}U \xrightarrow{(n,\gamma)} {}^{239}_{92}U \xrightarrow{\beta^-} {}^{239}_{93}Np + e^- + \bar{\nu}_e$$

$${}^{239}_{93}Np \xrightarrow{\beta^-} {}^{239}_{94}Pu + e^- + \bar{\nu}_e$$

$$n + {}^{239}_{94}Pu \xrightarrow{(n,\gamma)} {}^{240}_{94}Pu$$

$$n + {}^{240}_{94}Pu \xrightarrow{(n,\gamma)} {}^{241}_{94}Pu$$

$$n + {}^{241}_{94}Pu \xrightarrow{(n,\gamma)} {}^{242}_{94}Pu$$

$$n + {}^{242}_{94}Pu \xrightarrow{(n,\gamma)} {}^{243}_{94}Pu \xrightarrow{\beta^-} {}^{243}_{95}Am + e^- + \bar{\nu}_e$$

$$n + {}^{243}_{95}Am \xrightarrow{(n,\gamma)} {}^{244}_{95}Am \xrightarrow{\beta^-} {}^{244}_{96}Cm + e^- + \bar{\nu}_e$$

Main production root of ^{244}Cm is a sequence of
- (n,γ) reactions (6)
- β^- decays (4)

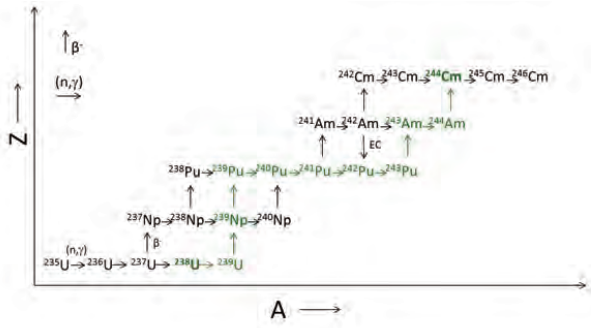

Production of ^{244}Cm

$$n + {}^{238}_{92}U \xrightarrow{(n,\gamma)} {}^{239}_{92}U \xrightarrow{\beta^-} {}^{239}_{93}Np + e^- + \bar{\nu}_e$$

$${}^{239}_{93}Np \xrightarrow{\beta^-} {}^{239}_{94}Pu + e^- + \bar{\nu}_e$$

$$n + {}^{239}_{94}Pu \xrightarrow{(n,\gamma)} {}^{240}_{94}Pu$$

$$n + {}^{240}_{94}Pu \xrightarrow{(n,\gamma)} {}^{241}_{94}Pu$$

$$n + {}^{241}_{94}Pu \xrightarrow{(n,\gamma)} {}^{242}_{94}Pu$$

$$n + {}^{242}_{94}Pu \xrightarrow{(n,\gamma)} {}^{243}_{94}Pu \xrightarrow{\beta^-} {}^{243}_{95}Am + e^- + \bar{\nu}_e$$

$$n + {}^{243}_{95}Am \xrightarrow{(n,\gamma)} {}^{244}_{95}Am \xrightarrow{\beta^-} {}^{244}_{96}Cm + e^- + \bar{\nu}_e$$

Contribution (n,γ) reactions

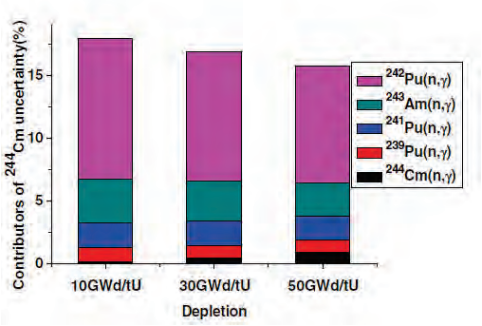

Burnup	Relative uncertainty
10 GWd/t	12.1 %
30 GWD/t	11.1 %
50 GWd/t	10.0 %

Tiejun Zu et al., Annals of Nuclear Energy 94 (2016) 399

Calculation of ^{244}Cm inventory: impact ^{242}Pu(n,γ)

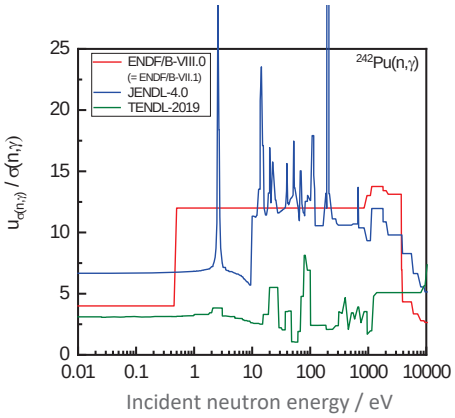

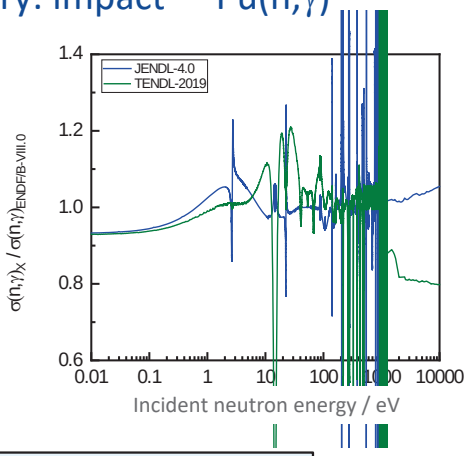

⇒ Improved evaluation for the ^{242}Pu(n,γ) cross section required
⇒ New experimental data required

Production of ^{244}Cm

$$n + {}^{238}_{92}U \xrightarrow{(n,\gamma)} {}^{239}_{92}U \xrightarrow{\beta^-} {}^{239}_{93}Np + e^- + \bar{\nu}_e$$

$${}^{239}_{93}Np \xrightarrow{\beta^-} {}^{239}_{94}Pu + e^- + \bar{\nu}_e$$

$$n + {}^{239}_{94}Pu \xrightarrow{(n,\gamma)} {}^{240}_{94}Pu$$

$$n + {}^{240}_{94}Pu \xrightarrow{(n,\gamma)} {}^{241}_{94}Pu$$

$$n + {}^{241}_{94}Pu \xrightarrow{(n,\gamma)} {}^{242}_{94}Pu$$

$$n + {}^{242}_{94}Pu \xrightarrow{(n,\gamma)} {}^{243}_{94}Pu \xrightarrow{\beta^-} {}^{243}_{95}Am + e^- + \bar{\nu}_e$$

$$n + {}^{243}_{95}Am \xrightarrow{(n,\gamma)} {}^{244}_{95}Am \xrightarrow{\beta^-} {}^{244}_{96}Cm + e^- + \bar{\nu}_e$$

Main production root of ^{244}Cm is a sequence of
- (n,γ) reactions (6)
- β$^-$ decays (4)

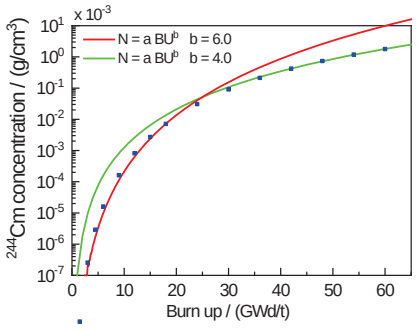

⇒ Total neutron emission extremely sensitive to BU

Burnup calculations need to be validated

Nuclear data
- Cross sections: (n,γ), (n,f), …
- Fission Yields
- Decay data
  - Half-lives
  - Emission probabilities
  - Recoverable energy

Burnup code

SNF input data
- Fuel properties
  - design
  - material data (IE)
- Operational history
  - **burn-up (BU)**
  - cooling time (CT)
  - …

Nuclide inventory
Observables
- thermal power
- neutron emission
- γ-ray emission
- …

Validate by NDA experiment
- **neutron measurements**
- γ-ray measurements

(PhD V. Solans)

Differential Die-away Self-Interrogation (DDSI)

Passive NDA: detection of neutrons emitted by SNF assembly
Developed at LANL for nuclear safeguards applications

- Neutron production
  - Primary neutrons: mainly prompt fission neutrons from ^{244}Cm(sf)
  - Prompt fission neutrons from neutron induced fission in fuel mainly after neutron moderation in the water of the pool
- Detection principle
  - ^{3}He in moderator
  - Detection of correlated neutrons: construct Ross-alpha distribution

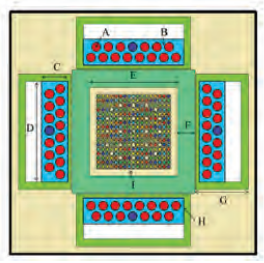

Kaplan et al., NIMA 764 (2014) 347

DDSI: Rossi-alpha distribution

1) Total counts : burn-up
2) Rossi-alpha distribution : neutron multiplication (fissile material)

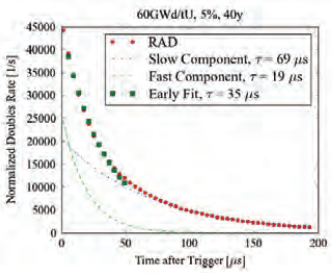

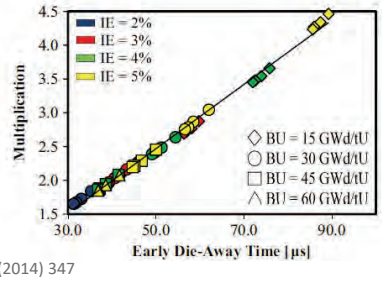

Kaplan et al., NIMA 764 (2014) 347

⇒ Poster V. Solans “Rossi-Alpha distribution analysis of DDSI data for spent nuclear fuel characterization” main objective: improve analysis procedures for DDSI

Summary and conclusions

- GELINA: TOF-facility for cross section measurements in the resonance region
- Importance of transmission measurements for an accurate determination of cross section data
- NRA: powerful tool for characterisation of objects and materials
- Improved neutron interaction cross section data are still needed for various energy and non-energy applications
- Importance of nuclear data and neutron detection for SNF characterisation

Mobility projects and access to nuclear infrastructures

- EUFRAT (open access to JRC Geel nuclear infrastructure)
  https://joint-research-centre.ec.europa.eu/knowledge-research/open-access-jrc-research-infrastructures_en
- ARIEL (Accelerator and research reactor infrastructures for education and learning)
  https://www.ariel-h2020.eu/index.php/en/call-for-proposals
- EURAD (European joint programme on radioactive waste management)
  https://euradschool.eu/application-guidelines/
- ENEN2plus
  First call mobility grants expected fall 2022

Keep in touch


EU Science Hub: ec.europa.eu/jrc


@EU_ScienceHub


EU Science Hub – Joint Research Centre


EU Science, Research and Innovation


EU Science Hub


EU science

Thank you

2.4 Spent Nuclear Fuel Characterisation, P. Schillebeeckx, JRC Geel, Training for DG-ENER EURATOM; 28/06/2023

Spent Nuclear Fuel Characterisation

Peter Schillebeeckx
JRC Directorate G, Nuclear Safety and Security
Unit G.II.5 Nuclear Data and Measurement Standards
28 June 2023, DG-ENER, Luxembourg

The project leading to this application has received funding from the European Union's Horizon 2020 research and innovation programme under grant agreement n° 847593.

CONTENTS

BACK-END OF THE FUEL CYCLE: SPENT FUEL CHARACTERISATION (SFC)

A **safe**, **secure**, **ecological** and **economic** handling, interim storage and final disposal requires that **Spent Nuclear Fuel (SNF)** is **characterised** for the main observables of interest:

- Decay heat rate (power)
- Neutron emission
- γ-ray emission
- Reactivity (BurnUp Credit)
  (i.e. Fission Product (FP), actinides)
- Fissile material (Nuclear Safeguards, i.e. ^{235}U, ^{239}Pu)
- Specific nuclides (Long term safety)
  i.e. ^{14}C, ^{36}Cl, ^{79}Se, ^{94}Nb, ^{99}Tc, ^{129}I, ^{226}Ra, ^{237}Np

OPEN FUEL CYCLE: DISPOSAL OF SPENT NUCLEAR FUEL (SNF)

Open fuel cycle
Sweden : Forsmark
Finland : Onkalo

Three barriers (SKB):
- canister
- buffer (bentonite clay)
- rock

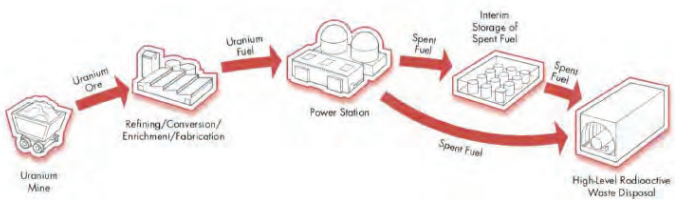

SKB : Swedish nuclear fuel and waste management company

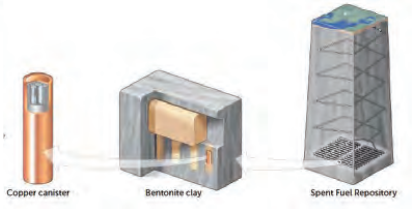

SPENT NUCLEAR FUEL (SNF) DISPOSAL EXAMPLE: SWEDISH CONCEPT

CLAB
Central Interim Storage Facility for Spent Nuclear Fuel (SNF)

CLINK
SNF encapsulation plant

SIGRID
SNF carrier

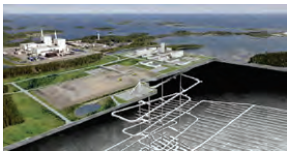

FORSMARK bedrock
SNF disposal

www.skb.com

OPEN FUEL CYCLE: DISPOSAL OF SNF ASSEMBLIES

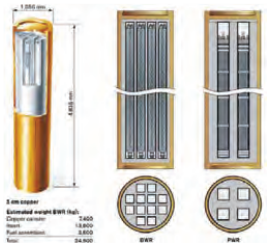

Estimate of decay heat rate (power) has a substantial impact on:
- the number of canisters (Cu mining)
- ecological and financial footprint

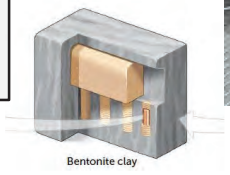

Open fuel cycle
Sweden : Forsmark

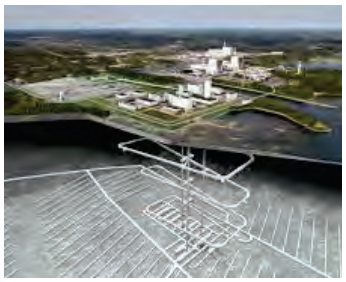

6000 canisters
12000 ton of spent fuel

www.skb.com

OPTIMISING CANISTER LOADING

Reduction of canisters and required disposal volume by

- Improved loading schemes algorithms
  e.g. Solans et al., Nucl. Eng. Des. 370 (220) 110897, reduction of 2% in number of canisters
- Improved decay power estimation
  Reduction of uncertainty of decay power estimation
  Seidl et al., Frontiers in Energy research 11 (2023) 1143312

One of the main objectives of EURAD WP8 Task 2

"Spent nuclear fuel characterisation and related uncertainty analysis"

www.skb.com

SNF MANAGEMENT : STORAGE, TRANSPORT, REPROCESSING AND DISPOSAL

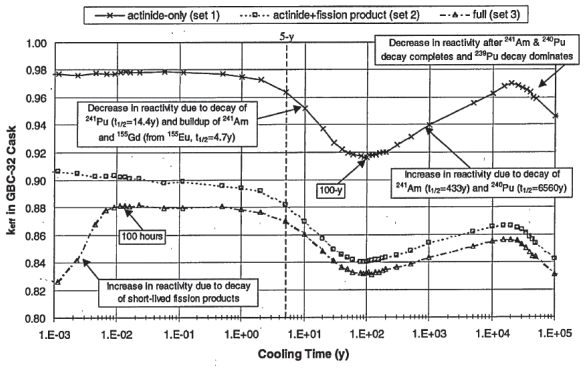

Figure 3 Reactivity behavior in the GBC-32 cask as a function of cooling time for the three classifications of burnup credit (defined in Table 1). The calculations correspond to fuel with 4.0 wt % ^{235}U initial enrichment that has accumulated 40 GWd/MTU burnup, and include an axial burnup distribution as described in Section 2.1.

Wagner and Parks, NUREG/CR-6781 (January 2003)
"Recommendations on the credit for cooling time in PWR burnup credit analysis"

Nuclear Criticality Safety (reactivity)

NEA: Woking Party (WPNCS)

- Must be guaranteed based on reliable methods
- Burn-Up Credit (NEA: Expert group EGBUC)
  - Reactivity decreases as fuel BU proceeds: reduction of fissile material and increase of neutron absorbing fission products (FP)
  - Account for this reactivity decrease for criticality safety assessments

⇒ Requires **inventory of key nuclides** and accurate neutron **absorption cross sections**

SNF CHARACTERISATION FOR THE BACK-END OF THE FUEL CYCLE

Main **observables** of interest:

- Decay heat rate (power) : H
- Neutron emission : S_n
- γ-ray emission : S_γ
- Reactivity : ^{235}U, ^{239}Pu, Fission Products (BUC)
- Fissile material : ^{235}U, ^{239}Pu
- Long-term safety : e.g. ^{14}C, ^{36}Cl, ^{79}Se, ^{94}Nb, ^{99}Tc, ^{129}I, ^{226}Ra, ^{237}Np

difficult to be **measured** directly, in particular during **industrial operation**

- Decay heat by **calorimetry** at CLAB: accurate but **long measurement times**
- Criticality safety analysis: calculations required to account for **burn-up credit** (MA, FP)
- **Prediction at long cooling times** only possible by theoretical calculations

⇒ requires knowledge of a **complex nuclide inventory** with strongly varying characteristics

SPENT NUCLEAR FUEL: NUCLIDE INVENTORY

- Fission products (FP): neutron induced fission (n,f)

  e.g. ^{90}Sr, $^{134,}\mathbf{^{137}Cs}$, ^{154}Eu, …

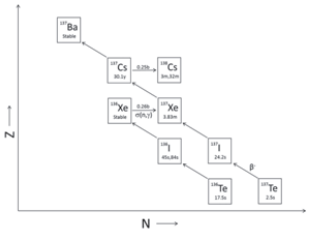

- Actinides: major and minor actinides

  e. g. ^{235}U, ^{238}U, $\mathbf{^{239}Pu}$, ^{241}Am, ^{244}Cm, …

$$\mathbf{n} + {}^{238}_{92}\mathbf{U} \xrightarrow{(n,\gamma)} {}^{239}_{92}\mathrm{U} \xrightarrow[23.5\ \mathrm{min}]{\beta^-} {}^{239}_{93}\mathrm{Np} \xrightarrow[2.36\ \mathrm{d}]{\beta^-} {}^{239}_{94}\mathbf{Pu}$$

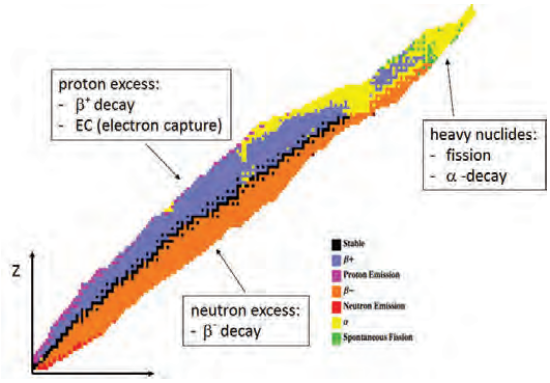

β^- - DECAY BY NEUTRON RICH NUCLIDES

Isobaric transition in which a neutron
is transformed into a proton
and an electron + anti-neutrino are emitted

$$^{A}_{Z}X \rightarrow ^{A}_{Z+1}Y^{*} + e^{-} + \bar{\nu}_e$$

$$\downarrow$$

$$^{A}_{Z+1}Y + E_\gamma$$

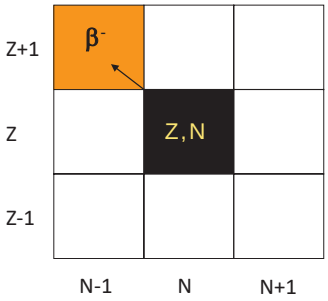

β^- - DECAY BY NEUTRON RICH NUCLIDES: e.g. ^{137}Cs

- $T_{1/2}$ = 30.05 (8) a
- Q_{β^-} = 1175.73 (17) keV

$$^{137}_{55}Cs \rightarrow ^{137}_{56}Ba^{*} + e^{-} + \bar{\nu}_e$$

$$\downarrow$$

$$^{137}_{56}Ba + E_\gamma$$

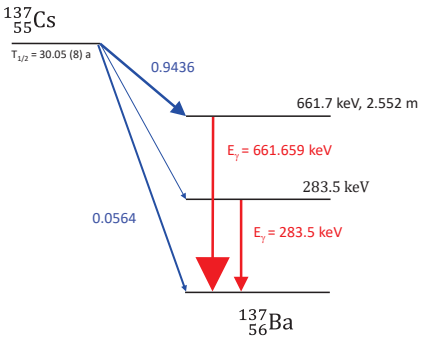

Gamma-ray emission probability: P_γ

E_γ	P_γ
661.7 keV	**0.8499 (20)**
283.5 keV	5.8 (8) x 10^{-6}

http://www.lnhb.fr/donnees-nucleaires/donnees-nucleaires-tableau/

α - DECAY

Radioactive decay in which a nucleus **emits** an **α-particle** (^{4}He nucleus) and transforms into a nucleus with 4 less nucleons (2n, 2p)

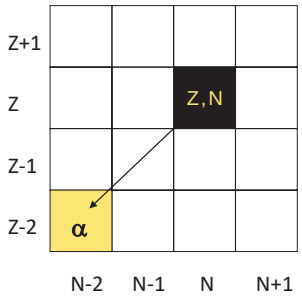

$$^{A}_{Z}X \rightarrow ^{A-4}_{Z-2}Y^{*} + \alpha$$

$$^{A-4}_{Z-2}Y + E_{\gamma}$$

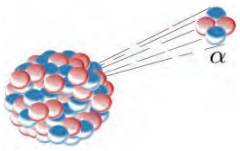

in heavy nuclei

α - DECAY BY ACTINIDES: e.g. ^{241}Am

- $T_{1/2}$ = 432.6 (6) a
- Q_{α} = 5637.82 (12) keV

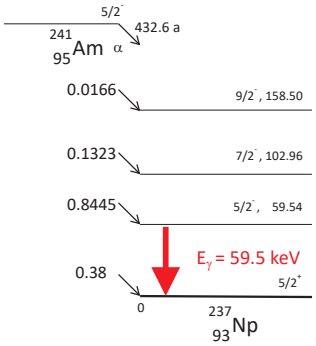

$$^{241}_{95}Am \rightarrow ^{237}_{93}Np^{*} + \alpha$$

$$^{237}_{93}Np + E_{\gamma}$$

α -particle emission probability:

E_{α}	$P(E_{\alpha})$
5388.3 keV	0.0166 (3)
5442.9 keV	0.1323 (10)
5485.6 keV	**0.8445 (10)**

http://www.lnhb.fr/donnees-nucleaires/donnees-nucleaires-tableau/

α DECAY: ^{241}AM

- $T_{1/2}$ = 432.6 (6) a

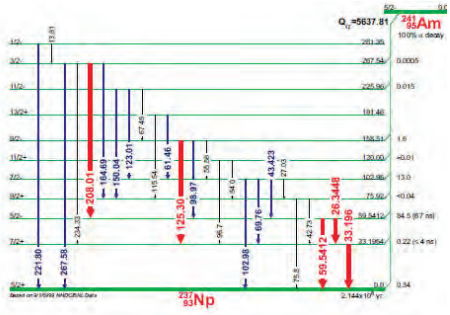

Emission of decay γ-rays

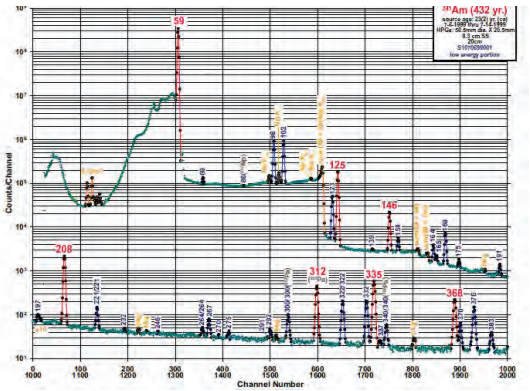

http://www.radiochemistry.org/periodictable/gamma_spectra/

SPONTANEOUS FISSION

Fission: nucleus splits up into fission products (FP)

e.g. ^{238,240,242}Pu(sf), ^{242,244,246}Cm(sf), ^{252}Cf(sf)

- FP : acceleration due to Coulomb repulsion
- FP : strongly excited, emission of
  - Prompt fission neutrons
  - Prompt fission γ-rays
- Prompt fission neutrons important for Non-Destructive Analysis (NDA)

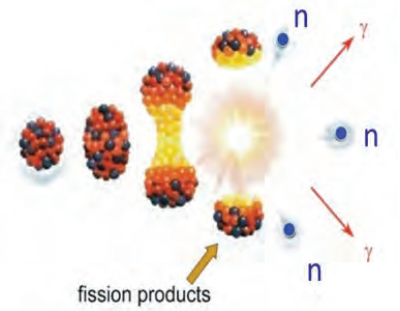

PROMPT FISSION NEUTRONS: MULTIPLICITY

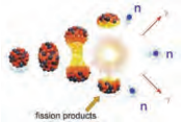

Emission of prompt fission neutrons:

- statistical process
- on average $\langle\nu\rangle = \nu_{(1)} > 1$

Nuclide	$\nu_{s(1)}$	$\nu_{s(2)}$	$\nu_{s(3)}$
^{238}Pu	2.210	1.978	0.933
^{240}Pu	2.154	1.895	0.868
^{242}Pu	2.145	1.882	0.867
^{252}Cf	3.756	5.978	5.287

$$\nu_{s(j)} = \sum_{\nu=j}^{\infty} \binom{\nu}{j} P_{s\nu}$$

Normalised factorial moments

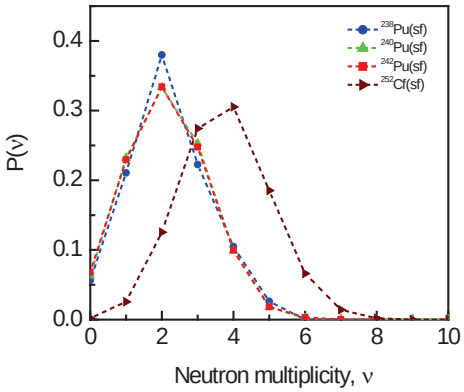

PROMPT FISSION NEUTRONS: DATA

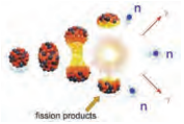

Nuclide	$T_{1/2}$	(sf) branching	<ν>	S_{sf} / (s^{-1} g^{-1})
^{238}Pu	8 .774 (3) x 10^{1} a	1.85 (5) x 10^{-9}	1.980 (30)	2.59 (11) x 10^{3}
^{240}Pu	6.561 (7) x 10^{3} a	5.70 (20) x 10^{-8}	2.154 (5)	1.031 (36) x 10^{3}
^{242}Pu	3.73 (3) x 10^{5} a	5.49 (9) x 10^{-6}	2.149 (8)	1.728 (32) x 10^{3}
^{242}Cm	162.86 (8) d	6.36 (14) x 10^{-8}	2.540 (20)	1.980 (46) x 10^{7}
^{244}Cm	1.811 (3) x 10^{1} a	1.36 (1) x 10^{-6}	2.710 (10)	1.107 (10) x 10^{7}
^{246}Cm	4.72 (3) x 10^{3} a	2.61 (4) x 10^{-6}	2.930 (30)	8.70 (13) x 10^{6}

Decay data from Nichols et al., INDC-2453, , INDC(NDS) – 0534, August 2008
<ν> from Santi and Miller, NucL; Sci. Eng. 160 (2017) 190

PROMPT FISSION NEUTRONS: ENERGY DISTRIBUTION

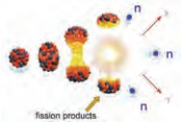

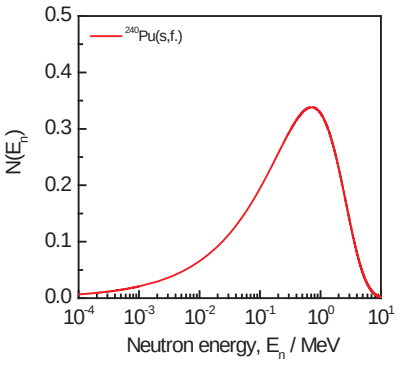

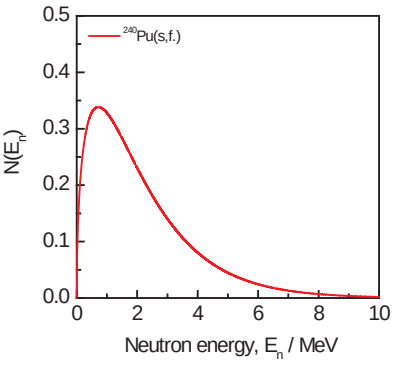

$\langle E_n \rangle \sim 2$ MeV

$N(E_n)$ can be parameterised by:

- a Maxwellian distribution in the CM system
- a Watt spectrum in the lab system

NEUTRON PRODUCTION BY (α,n) REACTIONS

- (α,n) reaction with light nuclides
  - $^{18}O(\alpha,n)^{21}Ne$
  - $^{17}O(\alpha,n)^{20}Ne$
  - $^{19}F(\alpha,n)^{22}Na$
- Neutron energy (emission)
  - O(α,n) : $\langle E_n \rangle \sim 2$ MeV
  - F(α,n) : $\langle E_n \rangle \sim 1$ MeV
- P(ν) = 1
  used to separate prompt fission neutrons from
  (α,n) neutrons in neutron correlation counting (NDA)

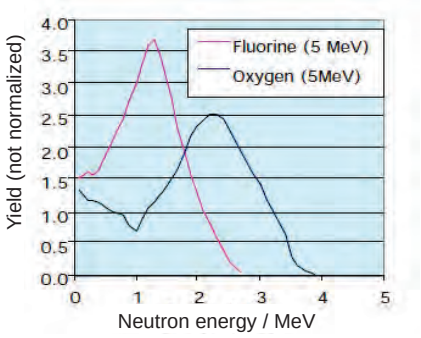

⇒ in SNF: α - decay of actinides followed by (α,n) reaction in light elements

NEUTRON PRODUCTION BY SNF

- Prompt spontaneous fission neutrons
- (α,n) reaction with light nuclides

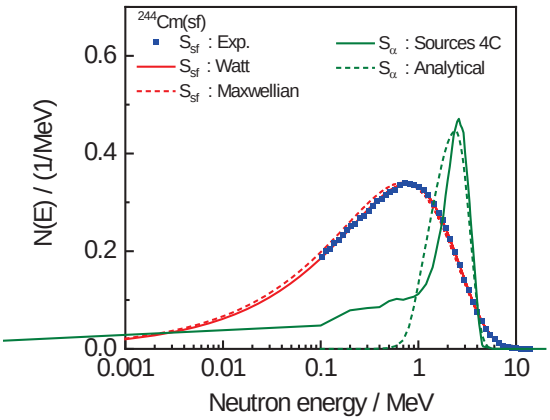

NEUTRON EMISSION BY SNF

$$S_n(t) = \sum_k S_{n,k}(t)$$

- $S_{n,k}(t)$: contribution of radionuclide k
- $S_{n,k}(t) = (s_{sf,k} + s_{\alpha n,k})\, N_k(t)$
  - $N_k(t)$: number of nuclei of nuclide k at time t
  - $s_{sf,k}$: specific neutron emission rate of nuclide k due to (sf)
  - $s_{\alpha,k}$: specific neutron emission rate of nuclide k due to (α,n) reactions

PWR UO_2 pellet (5 g)
$^{235}U/U$ = 4.8 %
burnup = 44 MWd/kg

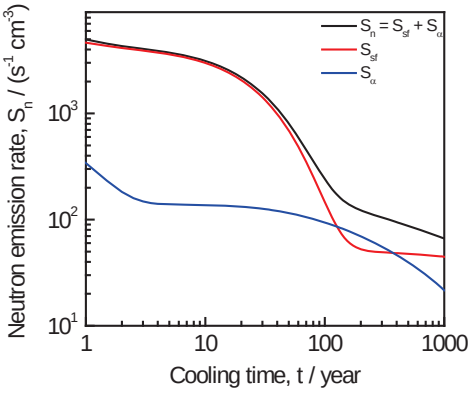

NEUTRON EMISSION BY SNF

$$S_n(t) = \sum_k (s_{sf,k} + s_{\alpha n,k})\, N_k\,(t)$$

PWR UO_2 pellet (5 g)
$^{235}U/U$ = 4.8 %
burnup = 44 MWd/kg

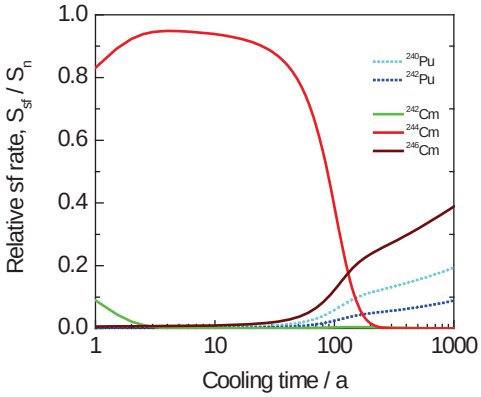

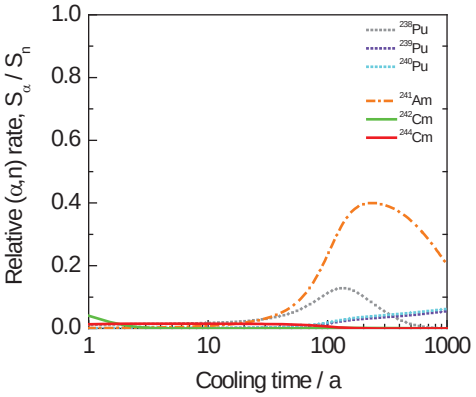

GAMMA-RAY EMISSION BY SNF

$$S_\gamma(t) = \sum_k S_{\gamma,k}(E_\gamma, t)$$

PWR UO_2 pellet (5 g)
$^{235}U/U$ = 4.8 %
burnup = 44 MWd/kg

^{95}Nb	35.0 d
^{95}Zr	64.0 d
^{144}Ce/^{144}Pr	284.9 d
^{106}Ru/^{106}Rh	1.02 a
^{134}Cs	2.06 a
^{154}Eu	8.8 a
^{137}Cs/^{137m}Ba	30.0 a

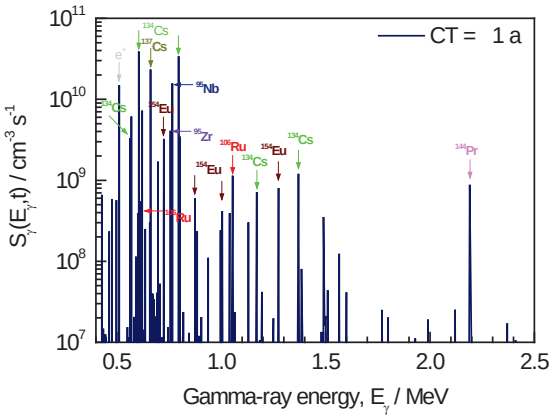

GAMMA-RAY EMISSION BY SNF

$$S_\gamma(t) = \sum_k S_{\gamma,k}(E_\gamma, t)$$

PWR UO_2 pellet (5 g)
$^{235}U/U$ = 4.8 %
burnup = 44 MWd/kg

^{95}Nb	35.0 d
^{95}Zr	64.0 d
$^{144}Ce/^{144}Pr$	284.9 d
$^{106}Ru/^{106}Rh$	**1.02 a**
^{134}Cs	**2.06 a**
^{154}Eu	**8.8 a**
$^{137}Cs/^{137m}Ba$	**30.0 a**

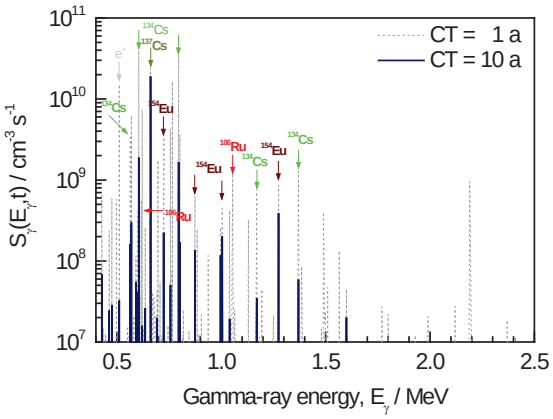

GAMMA-RAY EMISSION BY SNF

$$S_\gamma(t) = \sum_k S_{\gamma,k}(E_\gamma, t)$$

PWR UO_2 pellet (5 g)
$^{235}U/U$ = 4.8 %
burnup = 44 MWd/kg

^{95}Nb	35.0 d
^{95}Zr	64.0 d
$^{144}Ce/^{144}Pr$	284.9 d
$^{106}Ru/^{106}Rh$	1.02 a
^{134}Cs	2.06 a
^{154}Eu	**8.8 a**
$^{137}Cs/^{137m}Ba$	**30.0 a**

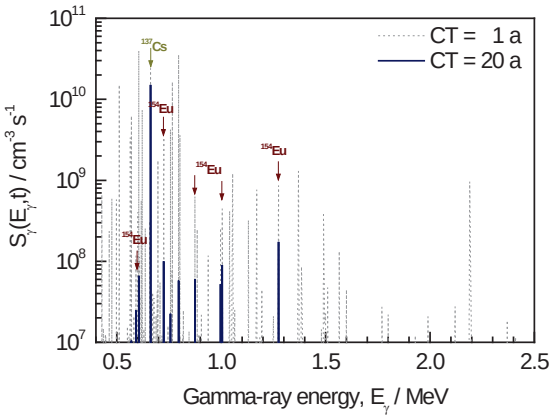

GAMMA-RAY EMISSION BY SNF

$$S_\gamma(t) = \sum_k S_{\gamma,k}(E_\gamma, t)$$

PWR UO_2 pellet (5 g)
$^{235}U/U$ = 4.8 %
burnup = 44 MWd/kg

^{95}Nb	35.0 d
^{95}Zr	64.0 d
$^{144}Ce/^{144}Pr$	284.9 d
$^{106}Ru/^{106}Rh$	1.02 a
^{134}Cs	2.06 a
^{154}Eu	**8.8 a**
$^{137}Cs/^{137m}Ba$	**30.0 a**

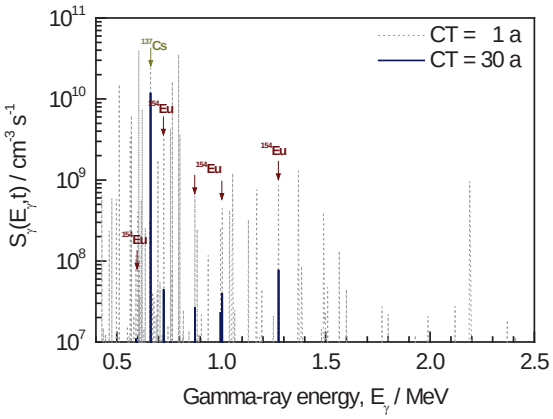

GAMMA-RAY EMISSION BY SNF: DECAY POWER

$$P_\gamma(t) = \sum_k \lambda_k N_k(t) \int E_\gamma s_{\gamma,k}(E_\gamma, t) dE_\gamma$$

PWR UO_2 pellet (5 g)
$^{235}U/U$ = 4.8 %
burnup = 44 MWd/kg

^{95}Nb	35.0 d
^{95}Zr	64.0 d
$^{144}Ce/^{144}Pr$	284.9 d
$^{106}Ru/^{106}Rh$	1.02 a
^{134}Cs	2.06 a
^{154}Eu	8.8 a
$^{137}Cs/^{137m}Ba$	30.0 a
^{241}Am	432.6 a

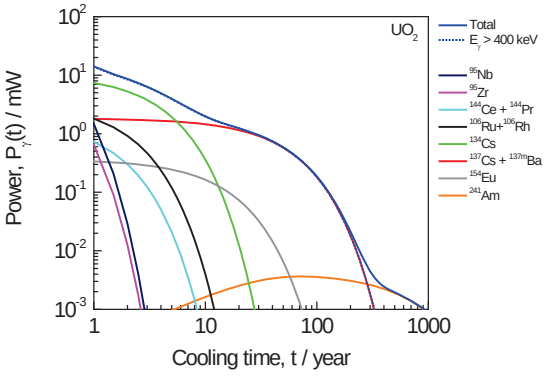

GAMMA-RAY EMISSION BY SNF: DECAY POWER

$$P_\gamma(t) = \sum_k \lambda_k N_k(t) \int E_\gamma s_{\gamma,k}(E_\gamma, t) dE_\gamma$$

Recoverable energy

PWR UO_2 pellet (5 g)
$^{235}U/U$ = 4.8 %
burnup = 44 MWd/kg

^{95}Nb	35.0 d
^{95}Zr	64.0 d
$^{144}Ce/^{144}Pr$	284.9 d
$^{106}Ru/^{106}Rh$	1.02 a
^{134}Cs	2.06 a
^{154}Eu	8.8 a
$^{137}Cs/^{137m}Ba$	30.0 a
^{241}Am	432.6 a

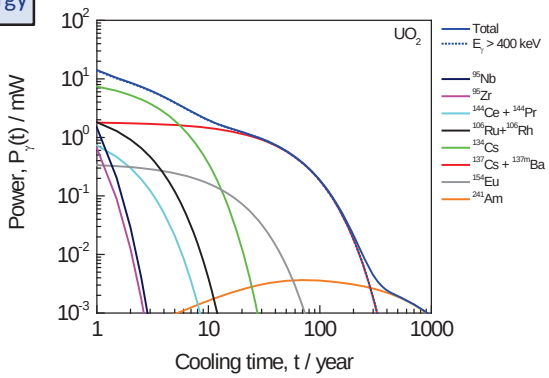

DECAY POWER PRODUCED BY SNF (RECOVERABLE)

$$P(t) = \sum_k P_k(t)$$

- $P_k(t)$: contribution of radionuclide k
- $P_k(t) = p_k N_k(t)$
  - $N_k(t)$: number of nuclei of nuclide k at time t
  - p_k : specific decay heat rate of nuclide k

PWR UO_2 pellet (5 g)
$^{235}U/U$ = 4.8 %
burnup = 44 MWd/kg

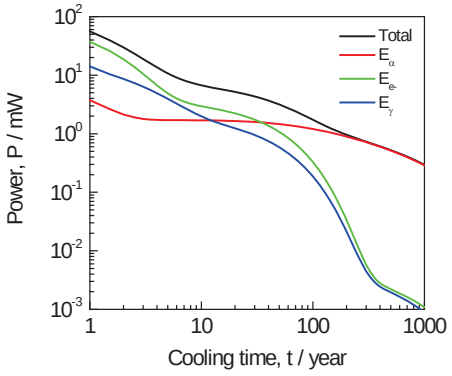

DECAY POWER PRODUCED BY SNF

- 1 a ≤ t ≤ 10 a
  - ^{144}Ce / ^{144}Pr
  - ^{106}Ru / ^{106}Rh
  - ^{134}Cs
  - ^{90}Sr / ^{90}Y
  - ^{137}Cs / ^{137m}Ba
- 10 a ≤ t ≤ 100 a
  - ^{90}Sr / ^{90}Y
  - ^{137}Cs / ^{137m}Ba
  - ^{238}Pu
  - ^{241}Am
  - ^{244}Cm
- 100 a ≤ t
  - ^{241}Am
  - ^{238}Pu
  - $^{239,241}Pu$

PWR UO_2 pellet (5 g)
$^{235}U/U$ = 4.8 %
burnup = 44 MWd/kg

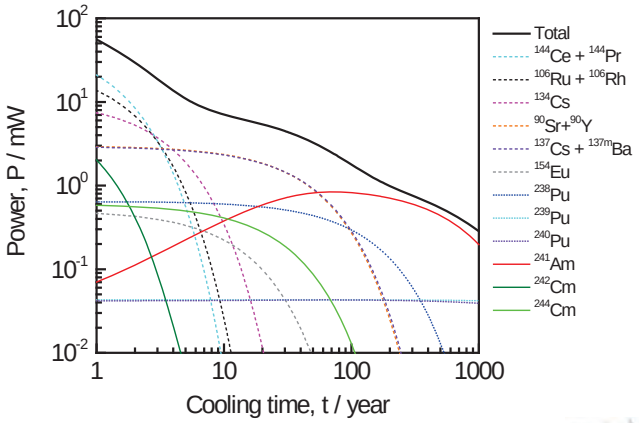

DECAY POWER PRODUCED BY SNF

- 1 a ≤ t ≤ 10 a
  - **^{144}Ce / ^{144}Pr**
  - **^{106}Ru / ^{106}Rh**
  - **^{134}Cs**
  - ^{90}Sr / ^{90}Y
  - ^{137}Cs / ^{137m}Ba
- 10 a ≤ t ≤ 100 a
  - ^{90}Sr / ^{90}Y
  - ^{137}Cs / ^{137m}Ba
  - ^{238}Pu
  - ^{241}Am
  - ^{244}Cm
- 100 a ≤ t
  - ^{241}Am
  - ^{238}Pu
  - $^{239,241}Pu$

PWR UO_2 pellet (5 g)
$^{235}U/U$ = 4.8 %
burnup = 44 MWd/kg

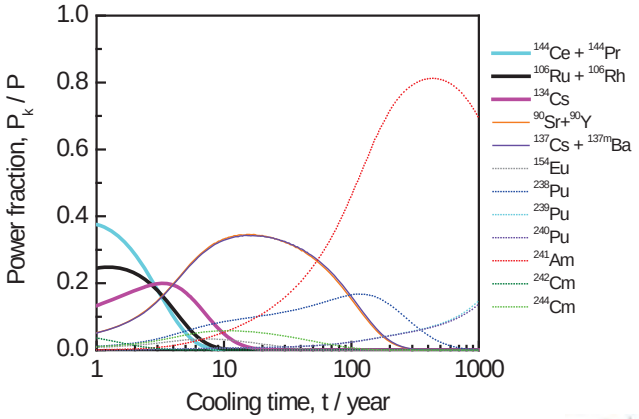

DECAY POWER PRODUCED BY SNF

- 1 a ≤ t ≤ 10 a
  - ^{144}Ce / ^{144}Pr
  - ^{106}Ru / ^{106}Rh
  - ^{134}Cs
  - ^{90}Sr / ^{90}Y
  - ^{137}Cs / ^{137m}Ba
- 10 a ≤ t ≤ 100 a
  - **^{90}Sr / ^{90}Y**
  - **^{137}Cs / ^{137m}Ba**
  - ^{238}Pu
  - ^{241}Am
  - ^{244}Cm
- 100 a ≤ t
  - ^{241}Am
  - ^{238}Pu
  - ^{239,241}Pu

PWR UO_2 pellet (5 g)
^{235}U/U = 4.8 %
burnup = 44 MWd/kg

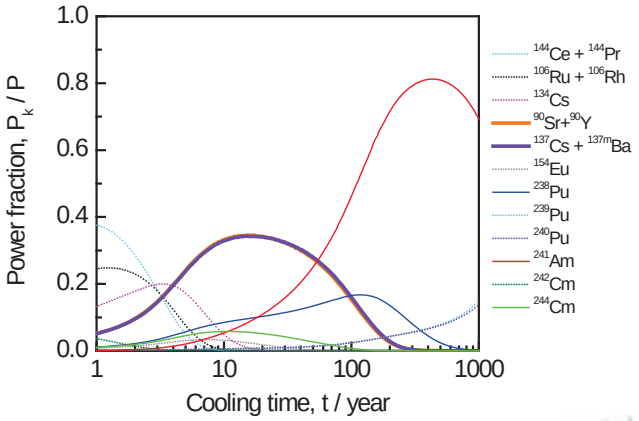

DECAY POWER PRODUCED BY SNF

- 1 a ≤ t ≤ 10 a
  - ^{144}Ce / ^{144}Pr
  - ^{106}Ru / ^{106}Rh
  - ^{134}Cs
  - ^{90}Sr / ^{90}Y
  - ^{137}Cs / ^{137m}Ba
- 10 a ≤ t ≤ 100 a
  - ^{90}Sr / ^{90}Y
  - ^{137}Cs / ^{137m}Ba
  - ^{238}Pu
  - ^{241}Am
  - ^{244}Cm
- 100 a ≤ t
  - **^{241}Am**
  - ^{238}Pu
  - ^{239,241}Pu

PWR UO_2 pellet (5 g)
^{235}U/U = 4.8 %
burnup = 44 MWd/kg

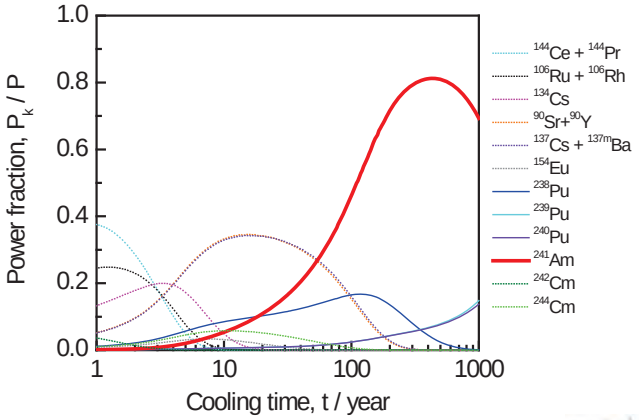

DECAY POWER PRODUCED BY SNF

PWR UO_2 pellet (5 g)
$^{235}U/U$ = 4.8 %
burnup = 44 MWd/kg

$$P(t) = \sum_k p_k N_k(t)$$

$P(t_2 > t_1)$ cannot be extrapolated from $P(t_1)$

$N_k(t)$: number of nuclei at time t

- $N_k(t_0)$: number of nuclei at time t_0 with $t > t_0$
- Nuclide vector at $t > t_0$

$$\frac{dN_k}{dt} = \sum_i \lambda_i N_i - \lambda_k N_k$$

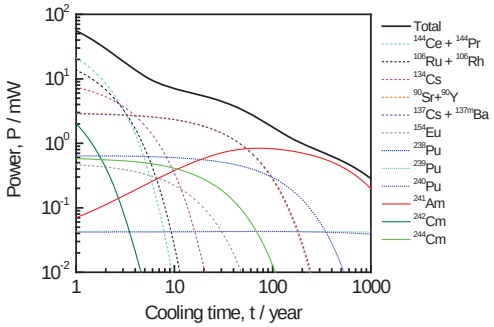

SNF SOURCE TERMS: NUCLIDE INVENTORY

Nuclide	Source term	CT
^{90}Sr	H, S_γ	10 a ≤ t ≤ 100 a
^{106}Ru	H	1 a ≤ t ≤ 10 a
^{134}Cs	H	1 a ≤ t ≤ 10 a
^{137}Cs	H, S_γ	10 a ≤ t ≤ 100 a
^{144}Ce	H	1 a ≤ t ≤ 10 a
^{148}Nd	*Burn-up*	*stable*
^{149}Sm	*Power*	*stable*
^{154}Eu	H, S_γ	1 a ≤ t ≤ 10 a

Nuclide	Source term	CT
^{235}U	R, S_γ	10^5 a ≤ t
^{238}U	R, S_γ	10^5 a ≤ t
^{238}Pu	H, S_γ	10 a ≤ t
^{239}Pu	R, S_γ	100 a ≤ t ≤ 10^4 a
^{240}Pu	R, S_γ	100 a ≤ t ≤ 10^4 a
^{241}Pu	H, S_γ	10 a ≤ t ≤ 100 a
^{241}Am	H	10 a ≤ t
^{242}Cm	H, S_n	1 a ≤ t ≤ 10 a
^{244}Cm	H, S_n	10 a ≤ t ≤ 100 a

H : decay heat rate (power)
S_n : neutron emission
S_γ : γ-ray emission
R : reactivity (criticality safety)

Nuclear safeguards
^{235}U, Pu-isotopes
Criticality safety (Burn Up Credit, BUC):
^{95}Mo, ^{99}Tc, ^{101}Ru, ^{103}Rh, ^{109}Ag, ^{133}Cs, ^{143}Nd, $^{147,149,150,151,152}Sm$, ^{155}Gd
Long term safety:
^{14}C, ^{36}Cl, ^{79}Se, ^{94}Nb, ^{99}Tc, ^{129}I, ^{226}Ra, ^{237}Np

⇒ Requires **complex nuclide inventory** which can only be obtained by **theoretical calculations**

THEORETICAL CALCULATIONS OF NUCLIDE INVENTORY

Depletion code: coupled neutron transport – nuclide depletion/creation calculations

Neutron transport

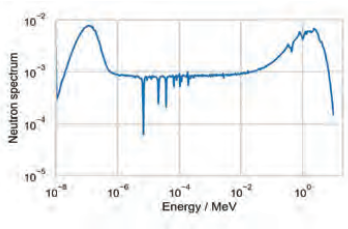

Bateman equation

$$\frac{dN_k}{dt} = Y\, N_f\, \sigma_f\, \varphi + \sum_i \lambda_i N_i + \sum_j \sigma_j N_j\, \varphi - (\lambda_k + \sigma_{k,a}\varphi) N_k$$

Update nuclide vector

EXAMPLE: PRODUCTION OF ^{137}Cs

$$n + {}^{235}_{92}U \rightarrow {}^{97}_{40}Zr + {}^{137}_{52}Te + \nu_p$$

$${}^{137}_{52}Te \rightarrow {}^{137}_{53}I + e^- + \bar{\nu}_e$$

$${}^{137}_{53}I \rightarrow {}^{137}_{54}Xe + e^- + \bar{\nu}_e$$

$${}^{137}_{54}Xe \rightarrow {}^{137}_{55}Cs + e^- + \bar{\nu}_e$$

^{137}Cs production: only by (n,f) followed by β^- -decay
(decay of short lived precursors)

- Relatively long lived
- Small capture cross section

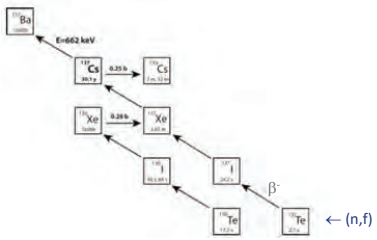

PRODUCTION OF ^{137}Cs

$$\frac{dN_k}{dt} = Y\, N_f\, \sigma_f\, \varphi + \sum_{i \to k} \lambda_i N_i + \sum_{j \to k} \sigma_j N_j\, \varphi - (\lambda_k + \sigma_{k,a}\varphi) N_k$$

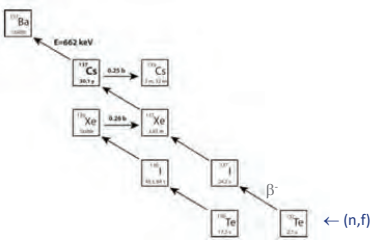

Y_c : cumulative fission yield
N_f : number of fissioning nuclei
N_i : number of nuclide i
σ_f : fission cross section
$\sigma_{j \to k}$: transmutation cross section (nuclide j to nuclide k)
$\sigma_{k,a}$: absorption cross section of nuclide k
φ : neutron fluence rate

PRODUCTION OF ^{137}Cs

$$\frac{dN_k}{dt} = Y\, N_f\, \sigma_f\, \varphi + \sum_{i \to k} \lambda_i N_i + \sum_{j \to k} \sigma_j N_j\, \varphi - (\lambda_k + \sigma_{k,a}\varphi) N_k$$

^{137}Cs production: only by (n,f) followed by β^- -decay (decay of short lived precursors)

$$N_k(t') \approx \frac{Y_c\, \sigma_f\, N_f\, \varphi}{\lambda_k + \sigma_{k,\gamma}\varphi} \left[1 - e^{-(\lambda_k + \sigma_{k,\gamma}\varphi)t'}\right]$$

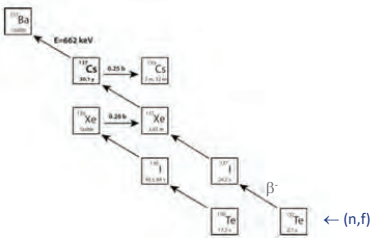

Y_c : cumulative fission yield
N_f : number of fissioning nuclei
N_i : number of nuclide i
σ_f : fission cross section
$\sigma_{j \to k}$: transmutation cross section (nuclide j to nuclide k)
$\sigma_{k,a}$: absorption cross section of nuclide k
φ : neutron fluence rate

PRODUCTION OF ^{137}Cs

$$\frac{dN_k}{dt} = Y\,N_f\,\sigma_f\,\varphi + \sum_{i\rightarrow k}\lambda_i N_i + \sum_{j\rightarrow k}\sigma_j N_j\,\varphi - (\lambda_k + \sigma_{k,a}\varphi)N_k$$

$$N_k(t') \approx \frac{Y_c\,\sigma_f\,N_f\,\varphi}{\lambda_k + \sigma_{k,\gamma}\,\varphi}\left[1 - e^{-(\lambda_k+\sigma_{k,\gamma}\varphi)t'}\right]$$

$$N_k(t') \sim Y_c\,\sigma_f\,N_f\,\varphi\,t' \qquad (\lambda_k + \sigma_{k,\gamma}\,\varphi)\,t' << 1$$

Y_c : cumulative fission yield
σ_f : fission cross section
N_f : number of fissioning nuclei, i.e. ^{235}U
$\varphi\,t'$: total (time integrated) neutron fluence
$\sigma_f\,N_f\,\varphi\,t'$: total number of fissions

^{137}Cs production: only by (n,f) followed by β^- -decay (decay of short lived precursors)

- Relatively long lived
- Small capture cross section

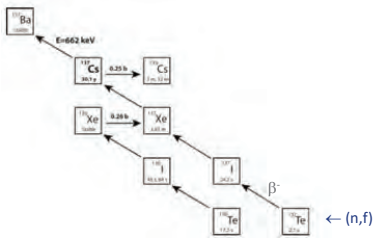

PRODUCTION OF ^{137}Cs

$$\frac{dN_k}{dt} = Y\,N_f\,\sigma_f\,\varphi + \sum_{i\rightarrow k}\lambda_i N_i + \sum_{j\rightarrow k}\sigma_j N_j\,\varphi - (\lambda_k + \sigma_{k,a}\varphi)N_k$$

$$N_k(t') \approx \frac{Y_c\,\sigma_f\,N_f\,\varphi}{\lambda_k + \sigma_{k,\gamma}\,\varphi}\left[1 - e^{-(\lambda_k+\sigma_{k,\gamma}\varphi)t'}\right]$$

$$N_k(t') \sim Y_c\,\sigma_f\,N_f\,\varphi\,t' \qquad (\lambda_k + \sigma_{k,\gamma}\,\varphi)\,t' << 1$$

$(\sigma_f\,N_f\,\varphi\,t')$: total number of fissions
E_f : energy released per fission
$(\sigma_f\,N_f\,\varphi\,t') \times E_f$: time integrated reactor power = burnup (BU)
(mostly expressed per mass of initial fuel, in MWd/kg)

$\Rightarrow N_k(t_0) \propto Y_c\,BU$ (t_0 = end of irradiation)

^{137}Cs production: only by (n,f) followed by β^- -decay (decay of short lived precursors)

- Relatively long lived
- Small capture cross section

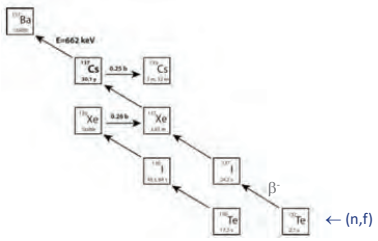

^{137}Cs: CONTRIBUTION TO DECAY HEAT RATE

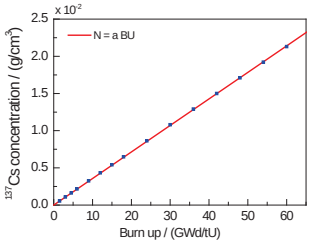

- Production at end of irradiation : cumulative fission yields + burnup

$$N_k(t_0) \propto Y_c \; BU$$

- Decay power after cooling time t by ^{137}Cs

$$P_k(t) = p_k \, N_k(t_0) \; e^{-\lambda_k (t-t_0)}$$

$$p_k = E_{dk} \, \lambda_k$$

⇒ Nuclear data
- Y_c : cumulative fission yields
- λ_k : decay constant
- E_{dk} : recoverable energy

⇒ Operational history : BU

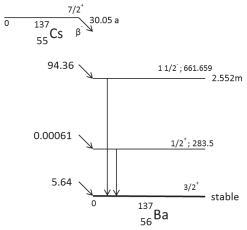

^{137}Cs : CONTRIBUTION TO THERMAL POWER (UNCERTAINTY EVALUATION)

$$P_k(t) = p_k \, N_k(t_0) \; e^{-\lambda_k (t-t_0)} \qquad N_k(t_0) \propto Y_c \; BU \qquad p_k = E_{dk} \, \lambda_k$$

$$\Rightarrow \frac{u_{P_k}}{P_k} = = \sqrt{\left(\frac{u_{BU}}{BU}\right)^2 + \left(\frac{u_{Y_c}}{Y_c}\right)^2 + \left(\frac{u_{E_{dk}}}{E_{dk}}\right)^2}$$

- Nuclear data
  - Y_c : cumulative fission yields
  - E_{dk} : recoverable energy
  - λ_k : decay constant (small uncertainty)
- Operational history : BU

Note:

Production of e.g ^{134}Cs more complex $\propto BU^b$ with b ~ 2

$$\Rightarrow \frac{u_{N_k}}{N_k} = 2\frac{u_{BU}}{BU}$$

^{137}Cs: CONTRIBUTION OF ^{235}U, ^{239}Pu AND ^{241}Pu

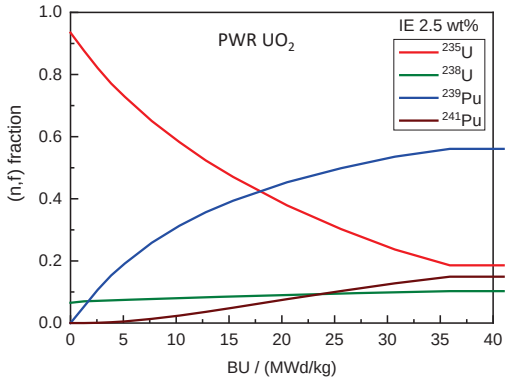

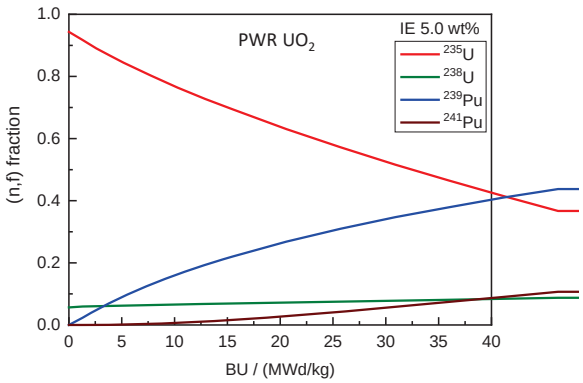

^{244}Cm PRODUCTION: COMPLEX PROCESS

$$n + {}^{238}_{92}U \xrightarrow{(n,\gamma)} {}^{239}_{92}U \xrightarrow{\beta^-} {}^{239}_{93}Np + e^- + \bar{\nu}_e$$

$${}^{239}_{93}Np \xrightarrow{\beta^-} {}^{239}_{94}Pu + e^- + \bar{\nu}_e$$

$$n + {}^{239}_{94}Pu \xrightarrow{(n,\gamma)} {}^{240}_{94}Pu$$

$$n + {}^{240}_{94}Pu \xrightarrow{(n,\gamma)} {}^{241}_{94}Pu$$

$$n + {}^{241}_{94}Pu \xrightarrow{(n,\gamma)} {}^{242}_{94}Pu$$

$$n + {}^{242}_{94}Pu \xrightarrow{(n,\gamma)} {}^{243}_{94}Pu \xrightarrow{\beta^-} {}^{243}_{95}Am + e^- + \bar{\nu}_e$$

$$n + {}^{243}_{95}Am \xrightarrow{(n,\gamma)} {}^{244}_{95}Am \xrightarrow{\beta^-} {}^{244}_{96}Cm + e^- + \bar{\nu}_e$$

Sequence of
- (n,γ) reactions (6)
- β⁻ decays (4)

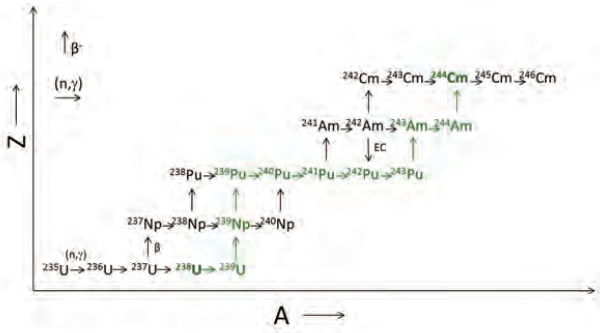

^{244}Cm PRODUCTION: COMPLEX PROCESS

^{244}Cm : $N = aBU^b$ $\quad \frac{\delta N}{N} = b\frac{\delta BU}{BU}$

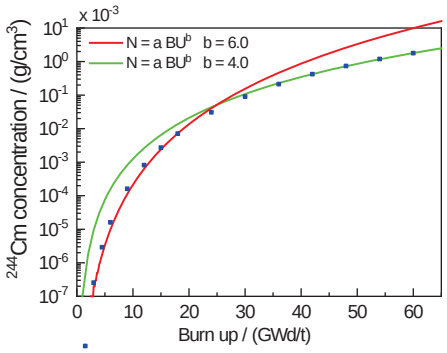

Sequence of
- (n,γ) reactions (6)
- β$^-$ decays (4)

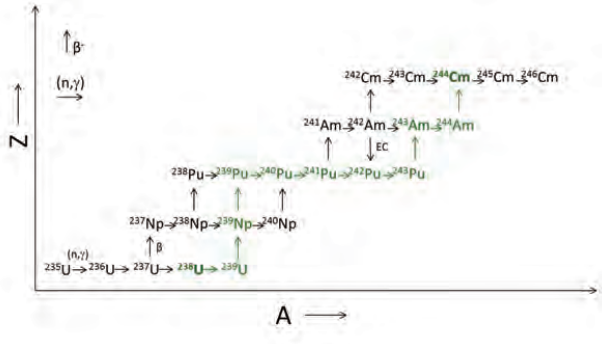

Training material

TASK 2: PRODUCE VALIDATED DEPLETION CALCULATIONS WITH REALISTIC UNCERTAINTIES

Nuclear Data (ND)
- Cross sections: (n,γ), (n,f), …
- Fission Yields
- Decay data
  - half-life
  - emission probabilities
  - recoverable energy

SNF input data
- Fuel properties
  - design
  - material data (IE)
  - …
- Operational history
  - burn-up (BU)
  - cooling time (CT)
  - …

Depletion code

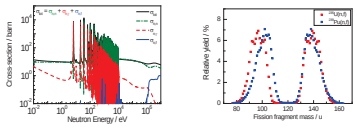

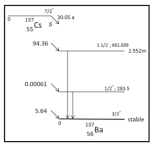

Nuclide inventory Observables
- decay heat
- neutron emission
- γ-ray emission
- …

DEPLETION CODES

- SCALE System (ORNL)
  - Neutron transport : KENO (MC) and NEWT, POLARIS (deterministic)
  - Depletion/creation module : ORIGEN
- ALEPH2 (SCK CEN)
  - Neutron transport by MCNP
- SERPENT (VTT)
- DARWIN (CEA)
- EVOLCODE (CIEMAT)

DEPLETION CODES

- Nuclide vector $N(t_0)$ **at time t_0** (end of irradiation) by depletion calculations
  - **Nuclear Data (ND)**
    - Cross sections
    - Fission yields
    - Neutron emission probabilities
    - Decay data
  - **Fuel History (FH)**
    - Fuel fabrication data (design, composition) e.g. Initial enrichment (IE)
    - Reactor operation and irradiation conditions e.g. Burnup (BU)
    - Cooling time (CT)
- Nuclide vector **at $t > t_0$**

$$\frac{dN_k}{dt} = \sum_{i \to k} \lambda_i N_i - \lambda_k N_k$$

- Observables **at $t > t_0$**

e.g. $P(t) = \sum_k p_k N_k(t)$

Depends on **well-known decay data**

BURNUP CODES: NUCLEAR DATA

Neutron induced interaction cross sections

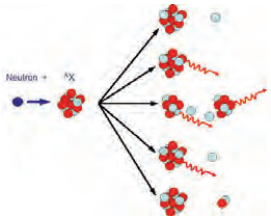

elastic scattering : (n,n)

capture: (n,γ)

fission : (n,f)

inelastic scattering : (n,n'γ)

others: e.g. (n,p), (n,α), ...

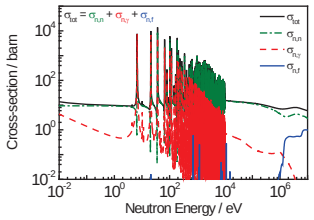

Fission process

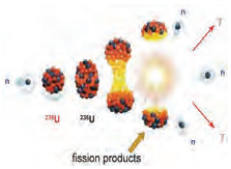

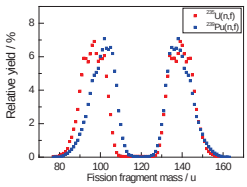

Decay data

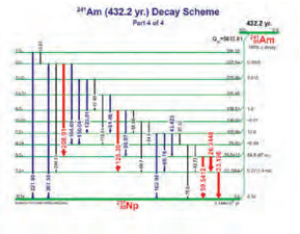

NUCLIDE INVENTORY: DESIGN AND OPERATIONAL HISTORY

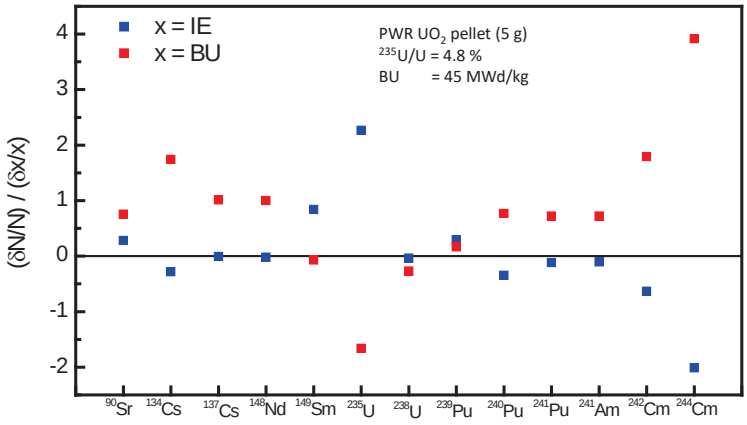

^{244}Cm : $N = aBU^b$

b ≈ 4 for BU = 45 MWd/kg

$$\frac{\delta N}{N} = b\frac{\delta BU}{BU}$$

0.5 % uncertainty on BU

⇒ 2 % uncertianty on ^{244}Cm inventory

TASK 2: PRODUCE VALIDATED DEPLETION CALCULATIONS WITH REALISTIC UNCERTAINTIES

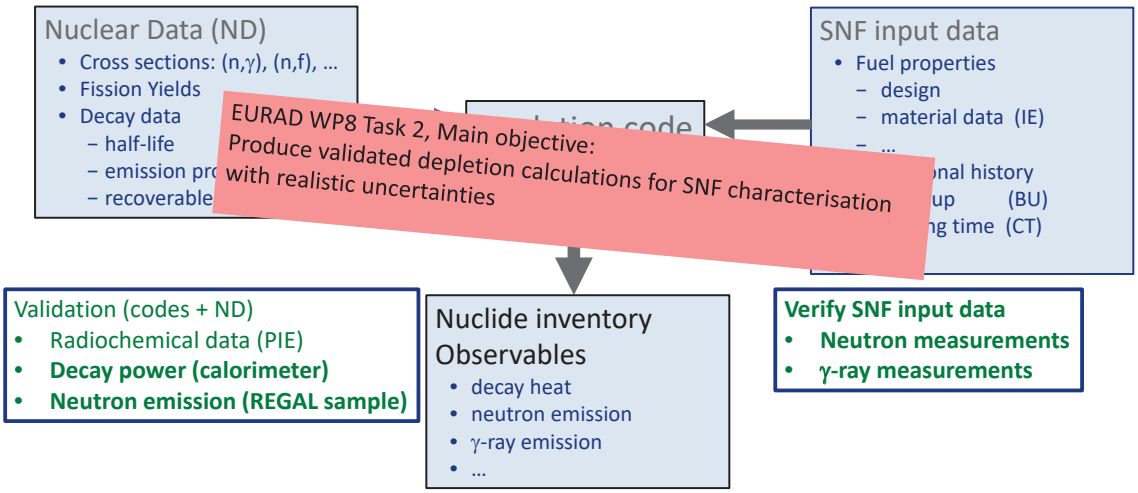

CLAB CALORIMETER

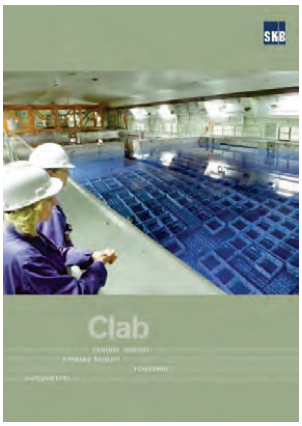

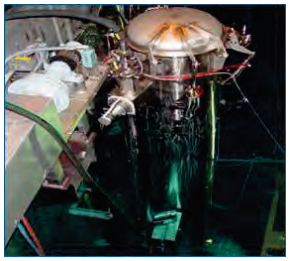

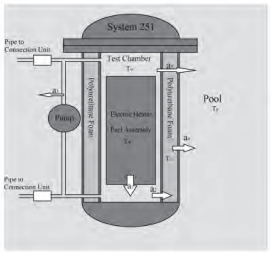

CLAB CALORIMETER: PRINIPLE

Measurement principle

- Cool down the water in calorimeter
- Stop cooling (continue circulation)

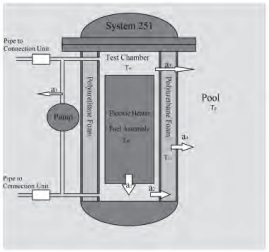

CLAB CALORIMETER: PRINIPLE

Measurement principle

- Cool down the water in calorimeter
- Stop cooling (continue circulation)
- Measure T_c and T_p
  - T_c : temperature in calorimeter
  - T_p : temperature in pool
- Determine $\Delta T = T_c - T_p$ vs time

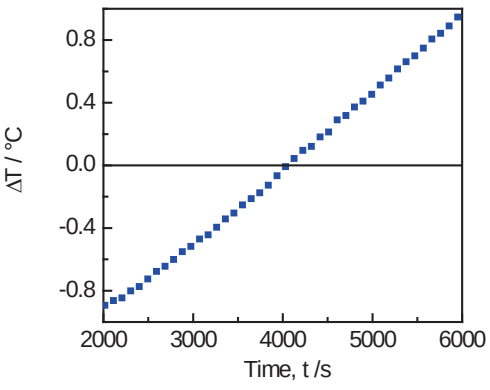

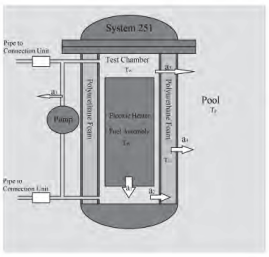

CLAB CALORIMETER: PRINCIPLE

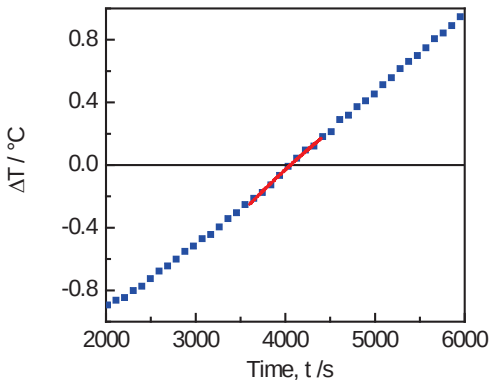

Measurement principle

- Cool down the water in calorimeter
- Stop cooling (continue circulation)
- Measure T_c and T_p
- Determine $\Delta T = T_c - T_p$ vs time
- Determine $d\Delta T/dt$ for $\Delta T = 0$

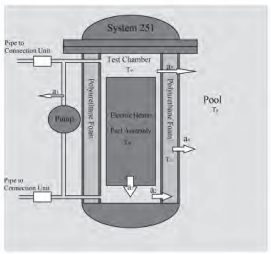

CLAB CALORIMETER: PRINCIPLE

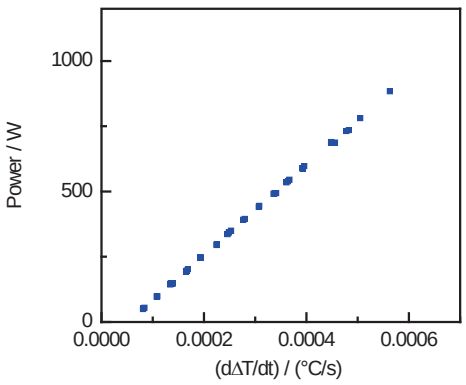

Calibration with an electrical heater

- Determine $\Delta T = T_c - T_p$ vs time
- Determine $d\Delta T/dt$ for $\Delta T = 0$ for different P

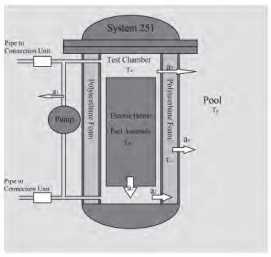

CLAB CALORIMETER: PRINCIPLE

Calibration with an electrical heater

- Determine $\Delta T = T_c - T_p$ vs time
- Determine $d\Delta T/dt$ for $\Delta T = 0$
- Fit to data: $P = a_0 + a_1\, d\Delta T/dt$

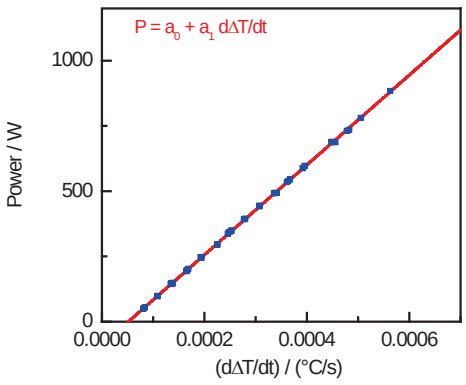

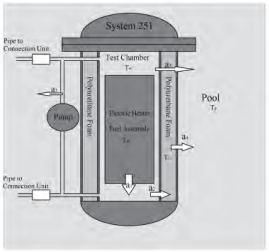

ELECTRICAL HEATER: CALIBRATION FUNCTION

Small differences partly due to differences in heat delivered by circulation pump

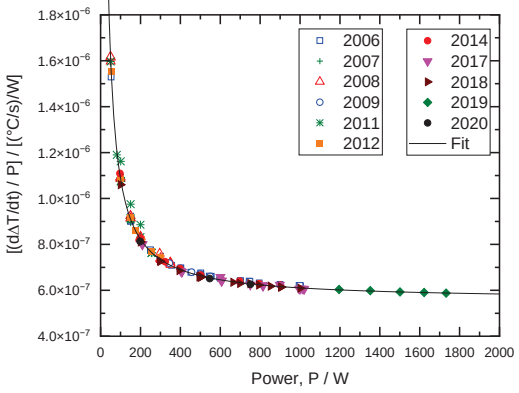

Calibration for blind test and SKB-50 data

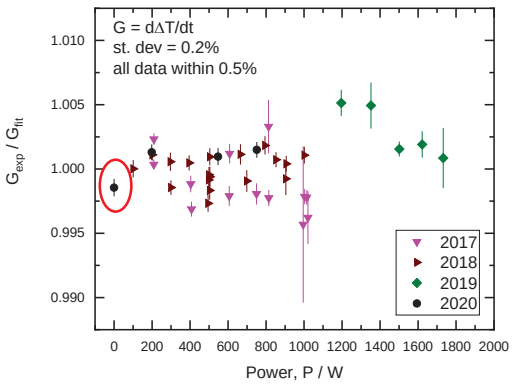

Perfect linear behaviour in whole range: from 0 W to 1800 W
Measurement without heater (heat delivered by circulation pump): fully consistent

CLAB CALORIMETER: PRINCIPLE

Spent nuclear fuel assembly

- Determine $\Delta T = T_c - T_p$ vs time
- Determine $d\Delta T/dt$ when $\Delta T = 0$
- $Q = a_0 + a_1 K\, d\Delta T/dt$
- $P = Q + P_\gamma$
  - K : correction factor due to thermal capacity difference between electrical heater and fuel assembly
  - P_γ : heat loss due to γ-rays escaping from the calorimeter

Calibration with an electrical heater

- Determine $\Delta T = T_c - T_p$ vs time
- Determine $d\Delta T/dt$ for $\Delta T = 0$
- Fit to data: $P = a_0 + a_1\, d\Delta T/dt$

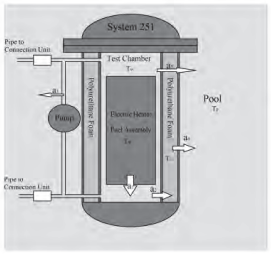

CLAB CALORIMETER: PRINCIPLE

Spent nuclear fuel assembly

- Determine $\Delta T = T_c - T_p$ vs time
- Determine $d\Delta T/dt$ when $\Delta T = 0$
- $Q = a_0 + a_1 K\, d\Delta T/dt$
- $P = Q + P_\gamma$
  - K : correction factor due to thermal capacity difference between electrical heater and fuel assembly
  - P_γ : heat loss due to γ-rays escaping from the calorimeter

- BWR: P = 140 W
  - P_γ = 3.3 W (2.4%)
  - K = 0.964
- PWR: P = 450 W
  - P_γ = 11.8 W (2.6%)
  - K = 0.915

DATA FROM CLAB CALORIMETER: SOME RESULTS

Ref.	Year	Code	Library	PWR		BWR	
				<C/E>	St. dev	<C/E>	St. dev
Ilas and Gauld	2008	SCALE 5.1	ENDF/B-V	1.011	0.012	1.003	0.025
Ilas et al.	2014	SCALE 6.1.2	ENDF/B-VII.0	1.002	0.012	0.997	0.024
Ilas and Burns	2021	SCALE 6.2.4	ENDF/B-VII.0	1.013	0.013	1.002	0.012
	2021	SCALE 6.2.4	ENDF/B-VII.1	1.008	0.012	1.009	0.024
Ilas and Burns	2022	SCALE 6.3	ENDF/B-VIII.0	1.006	0.014	1.007	0.024
Shama et al.	2022	SCALE 6.2.3	ENDF/B-VII.1	1.019	0.012	1.003	0.025
		SCALE 6.2.3 (POLARIS)	ENDF/B-VII.1	1.015	0.012	1.010	0.026
Shama et al.	2022	CASMO5		1.009	0.013	1.008	0.025
Yamamoto	2016	CASMO5	JENDL-4.0	1.016	0.013	1.001	0.024
Haeck et al.	2022	VESTA 2.1	JEFF-3.1	0.978	0.012		
		VESTA 2.1	ENDF/B-VII.0	0.996	0.012		
San-Felice et al.	2012	DARWIN	JEFF-3.1.1	0.978	0.011		

Not blind!

Normalisation not specified

Adjustments not excluded

BLIND TEST CLAB CALORIMETER

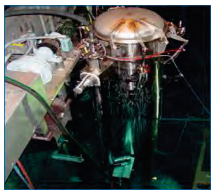

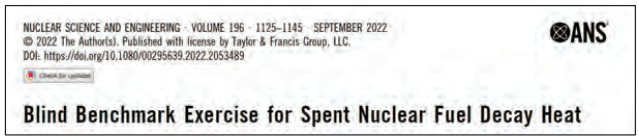
NUCLEAR SCIENCE AND ENGINEERING · VOLUME 196 · 1125–1145 · SEPTEMBER 2022
© 2022 The Author(s). Published with license by Taylor & Francis Group, LLC.
DOI: https://doi.org/10.1080/00295639.2022.2053489
ANS
Blind Benchmark Exercise for Spent Nuclear Fuel Decay Heat

- PWR assemblies
- Decay heat rate determined at CLAB

Assembly ID	BU	CT	IE	Decay heat rate	Gamma-escape
BT01	53 MWd/kg	4.5 a	3.95 wt%	1662 W	58 W
BT02	55 MWd/kg	8.6 a	3.95 wt%	1068 W	30 W
BT03	50 MWd/kg	9.8 a	3.95 wt%	895 W	21 W
BT04	51 MWd/kg	13.5 a	3.70 wt%	768 W	15 W
BT05	50 MWd/kg	21.4 a	3.60 wt%	663 W	12 W

BLIND TEST CLAB CALORIMETER: CODES + LIBRARIES

Code	Library	Appendix Section
ALEPH 2.7.2	ENDF/B-VII.1	A.I.A
APOLLO2.8/DARWIN2.3	JEFF-3.1.1	A.I.B
CASMO-4E + ORIGEN-S	JEF-2.2	A.I.C
CASMO-5 (2.03)	ENDF/B-VII.1	A.I.D
CASMO-5 (2.12.00) + SNF (1.07.02)	ENDF/B-VII.1	A.I.E
DRAGON 4.0.5	ENDF/B-VII.1	A.I.F
EVOLCODE (MCNP + ACAB)	JEFF-3.3	A.I.G
MCNP-CINDER + Nukleonika (2D)	ENDF/B-VII.1	A.I.H
Monteburns v3 + CINDER	ENDF/B-VII.1	A.I.I
MOTIVE (KENO-VI + VENTINA)	ENDF/B-VII.1	A.I.J
MOTIVE (OpenMC + VENTINA)	ENDF/B-VIII	A.I.K
MVP 3	ENDF/B-VII.1	A.I.L
MVP 3	JEFF-3.2	A.I.M
MVP 3	JENDL-4.0	A.I.N
OREST	JEF-2.2 + ENDF/B-VI	A.I.O
SCALE 6.0: ORIGEN-ARP	ENDF/B-V	A.I.P
SCALE 6.1.3: ORIGEN-ARP	ENDF/B-V	A.I.Q
SCALE 6.2.3: ORIGAMI	ENDF/B-VII.1	A.I.P
SCALE 6.2.3: Polaris	ENDF/B-VII.1	A.I.R
SCALE 6.2.3: ORIGEN	ENDF/B-VII.1	A.I.R
SCALE 6.2.3: TRITON/KENO	ENDF/B-VII.1	A.I.S
SCALE 6.2.3: TRITON/NEWT	ENDF/B-VII.1	A.I.T
SEADEP	JEFF-3.1.1	A.I.U
Serpent 2.1.29	ENDF/B-VII.1	A.I.V
Serpent 2.1.29	JEFF-3.1.1	A.I.W
Serpent 2.1.31	JEFF-3.2 + JEFF-3.1.1	A.I.X

BLIND TEST CLAB CALORIMETER: RESULTS

Assembly ID	P	CT	<C/E>	St. dev
BT01	1662 W	4.5 a	0.975	0.019
BT02	1068 W	8.6 a	0.977	0.018
BT03 (+ Gd)	895 W	9.8 a	0.967	0.019
BT04	768 W	13.5 a	0.994	0.023
BT05	663 W	21.4 a	0.979	0.021

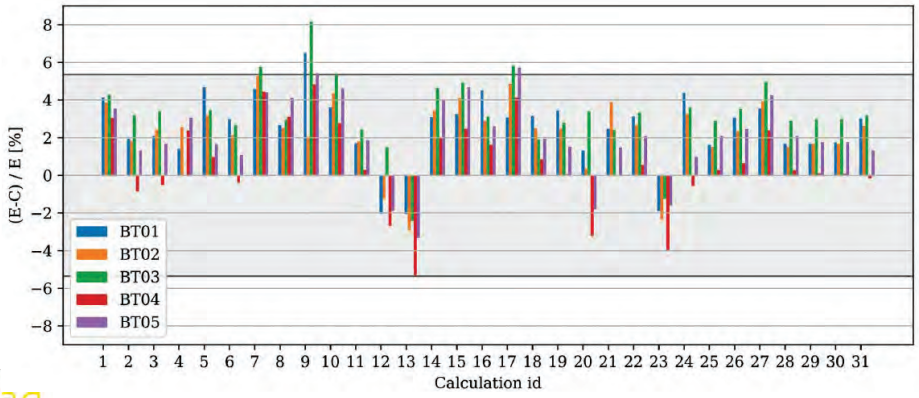

DATA FROM CLAB CALORIMETER (R-05-62)

EURAD Task 2: systematic study of published calorimeter data

Compare different codes/libraries

- Total number of fissions
- Inventory of key nuclides
- Calculate decay power using recommended decay data

Paper in preparation
Romojaro et al., SCK CEN, CEA, GRS, IRSN, JSI, JRC, NAGRA, PSI

Code	Library	PWR		BWR	
		<C/E>	St. dev	<C/E>	St. dev
SCALE	(R-05-62)	1.011	0.012	1.003	0.025
ALEPH2	JEFF-3.1.2	1.001	0.020	1.013	0.031
ALEPH2	JEFF-3.3	1.004	0.018	1.018	0.029
ALEPH2	JEFF-4T0	1.006	0.018	1.020	0.030

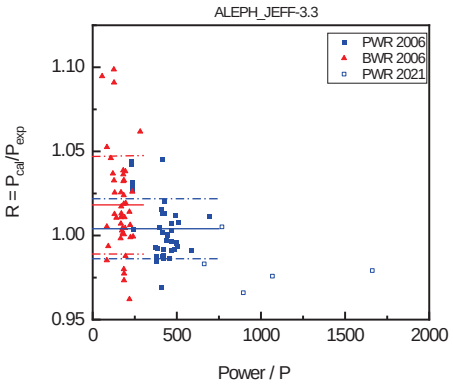

EURAD Task 2:
additional blind test exercise using SKB-50 data

^{137}Cs : CONTRIBUTION TO THERMAL POWER (UNCERTAINTY EVALUATION)

$P_k(t) = p_k\, N_k(t_0)\; e^{-\lambda_k (t-t_0)}$ $\quad N_k(t_0) \propto Y_c\, BU$ $\quad p_k = E_{dk}\, \lambda_k$

$$\Rightarrow \frac{u_{P_k}}{P_k} = = \sqrt{\left(\frac{u_{BU}}{BU}\right)^2 + \left(\frac{u_{Y_c}}{Y_c}\right)^2 + \left(\frac{u_{E_{dk}}}{E_{dk}}\right)^2}$$

- Nuclear data
  - Y_c : cumulative fission yields
  - E_{dk} : recoverable energy
  - λ_k : decay constant (small uncertainty)
- Operational history : BU

Note:

Production of e.g ^{134}Cs more complex $\propto BU^b$ with b ~ 2

$$\Rightarrow \frac{u_{N_k}}{N_k} = 2\frac{u_{BU}}{BU}$$

^{137}Cs: γ-RAY EMISSION AND DECAY HEAT RATE (POWER)

- Production : cumulative fission yields + burnup

  $N_k(t_0) \sim Y_c$ BU

- Gamma-ray emission : (decay data)
  - $T_{1/2}$: 30.05 (8) a
  - $P(E_\gamma = 661.66keV)$: 0.8499 (20)

- Specific decay heat rate, $p_k = E_{dk}\,\lambda_k$ (decay data)
  - $T_{1/2}$: 30.18 (15) a
  - Q_{β^-} : 1175.63 (17) keV
  - Recoverable energy
    - Average electron + recoil energy : 247.9 (12) keV
    - $<E_\gamma>$: 565.4 (13) keV

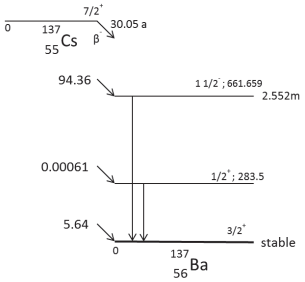

Decay data from DDEP (Decay Data Evaluation Project)
http://www.nucleide.org/DDEP.htm

^{137}Cs : NUCLEAR DATA (Y_c,E_d) FOR ^{235}U(n,f) AT THERMAL ENERGY

			^{137}Cs			
Library	E_d / keV	Ratio	100 x Y_c	Ratio	(Y_c x E_d) / keV	Ratio
DDEP/IAEA	811.8 (18)	1	6.221 (69)	1	50.5 (6)	1
JEF-2.2	812.0 (69)	1.000 (8)	6.244 (54)	1.004 (9)	50.7 (6)	1.004 (12)
JEFF-3.1.1	**810.1 (23)**	**0.998 (3)**	**6.221 (69)**	**1.000 (11)**	**50.4 (6)**	**0.998 (11)**
JEFF-3.3	**801.8 (23)**	**0.988 (3)**	**6.090 (63)**	**0.979 (10)**	**48.8 (5)**	**0.967 (10)**
ENDF/B-VI.8	813.4 (41)	1.002 (5)	6.188 (31)	0.995 (5)	50.3 (4)	0.997 (7)
ENDF/B-VII.0	805.7 (16)	0.992 (2)	6.188 (31)	0.995 (5)	49.9 (3)	0.987 (5)
ENDF/B-VIII.0	**805.8 (18)**	**0.993 (2)**	**6.188 (31)**	**0.995 (5)**	**49.9 (3)**	**0.987 (5)**

^{90}Sr and ^{137}Cs: NUCLEAR DATA (Y_c,E_d) FOR ^{235}U(n,f) AT THERMAL ENERGY

Library	^{90}Sr		^{137}Cs	
	(E_d x Y_c) / keV	Ratio	(Y_c x E_d) / keV	Ratio
DDEP/IAEA	64.7 (15)	1	50.5 (6)	1
JEF-2.2	**66.0 (21)**	**1.021 (33)**	**50.7 (7)**	**1.004 (12)**
JEFF-3.1.1	63.5 (15)	0.981 (23)	50.4 (6)	0.998 (11)
JEFF-3.3	**64.0 (15)**	**0.989 (23)**	**48.8 (5)**	**0.967 (10)**
ENDF/B-VI.8	65.3 (7)	1.010 (10)	50.3 (4)	0.997 (7)
ENDF/B-VII.0	65.3 (7)	1.009 (10)	49.9 (3)	0.987 (5)
ENDF/B-VIII.0	**65.3 (7)**	**1.009 (10)**	**49.9 (3)**	**0.987 (5)**

^{90}Sr and ^{137}Cs: NUCLEAR DATA (Y_c,E_d) FOR ^{235}U(n,f) AT THERMAL ENERGY

EPRI, PIRT, July 2020

Table 5-5
Summary of Uncertainty in Calculated Decay Heat [17] for BWR Assembly at 37 GWd/MTU Burnup and 15.6 Years' Cooling Time

Perturbed Parameter Set	Relative Uncertainty (%)
Fuel design data	0.2
Operating history data	0.8
Nuclear cross-section data	0.9
Fission yield data	0.3
Overall uncertainty	***1.3***

u_p/P = 1.3%, is this realistic? **NO**

^{90}Sr and ^{137}Cs: NUCLEAR DATA (Y_c,E_d) FOR ^{235}U(n,f) AT THERMAL ENERGY

Uncertainty only due to nuclear data > 2%

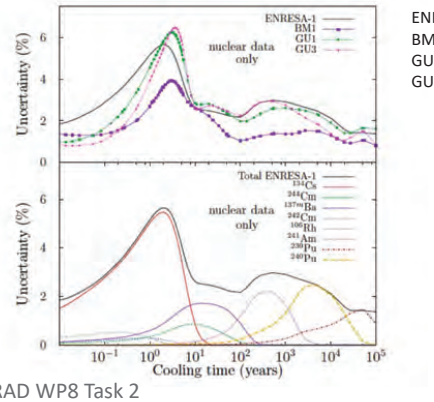

ENRESA-1: BWR
BM1 : MOX
GU1 : PWR
GU3 : PWR

EPRI, PIRT, July 2020

Table 5-5
Summary of Uncertainty in Calculated Decay Heat [17] for BWR Assembly at 37 GWd/MTU Burnup and 15.6 Years' Cooling Time

Perturbed Parameter Set	Relative Uncertainty (%)
Fuel design data	0.2
Operating history data	0.8
Nuclear cross-section data	0.9
Fission yield data	0.3
Overall uncertainty	***1.3***

u_p/P = 1.3%, is this realistic? **NO**

EURAD WP8 Task 2

Rochman et al., Annals of Nuclear Energy 160 (2021) 108539
Rochman et al., EPJ Nuclear Sci. Technolog. 7 (2021) 18
Rochman et al., EPJ Nuclear Sci. Technolog. 8 (2022) 9

UNCERTAINTY OF CALORIMETRY DATA

- Blind test paper (Jansson et al., Nucl. Sci. Eng. 196 (2022) 1125)

  5% overall uncertainty

- SKB Document R-05-62 (also used in EPRI, PRIT report)
  - PWR
    - 250 W 1.8 %
    - 900 W 1.0 %
  - BWR
    - 50 W 4.2 %
    - 350 W 1.0 %

⇒ Performance assessment and uncertainty evaluation of CLAB calorimeter is required
⇒ One of the main EURAD objectives of WP8 Task 2

Only total (combined uncertainties) are given
No separation between
- Systematic and random effects
- Correlated and uncorrelated uncertainty components

NEUTRON EMISSION: ABSOLUTE MEASUREMENTS OF SNF SEGMENT SAMPLE

Non Destructive Assay method to determine the neutron output of a **SNF** sample under **standard controlled area** conditions

Collaboration SCK CEN

Hot cell (LHMA) facility at SCK CEN

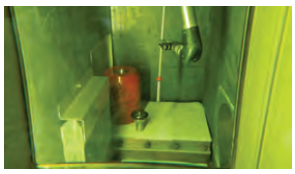

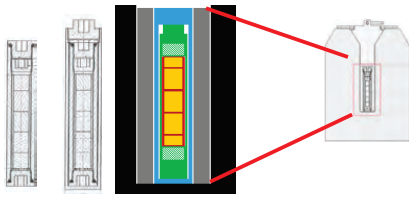

Standard controlled area

NEUTRON EMISSION: ABSOLUTE MEASUREMENTS OF SNF SEGMENT SAMPLE

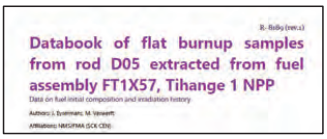

Hot cell (LHMA) facility at SCK CEN

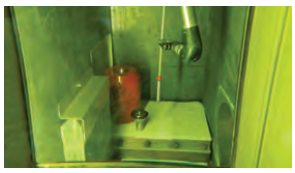

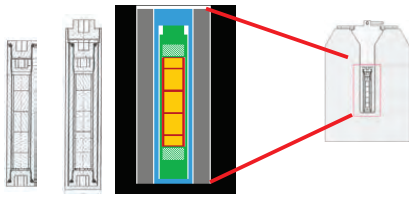

Standard controlled area

EURAD: VALIDATION OF DEPLETION CODES USING THE REGAL SAMPLE

- **Irradiation history** of the SNF
  - Segment (~ 50 mm) from rod D05 of FT1X57 (PWR)
  - PWR Assembly (15 x 15):
    188 UO_2 rod (4.5 wt% $^{235}U/U$) and 16 $(U,Gd)O_2$ rods
  - Irradiated at Tihange 1
  - Rod used for other international project
    (First-Nuclides, REGAL, WETFUEL & AGAF, SF-ALE)
- **SNF** segment **sample** by **NDA**

  Part of a set of 4 samples (**REGAL project**)
  - **Radiochemical analysis (BU)**
  - Microstructural analysis
  - Leach tests (low O_2)
  - Leach tests (high O_2)

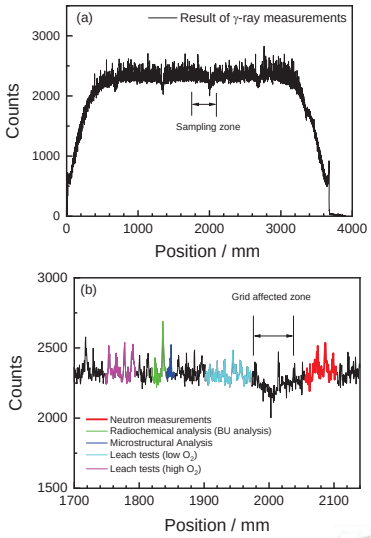

NEUTRON EMISSION: ABSOLUTE MEASUREMENTS OF SNF SEGMENT SAMPLE

- Irradiation history burnup (REGAL project)

BU indicator	Analysis date	Nuclide Inventory N_X/N_U	BU MWd/kg
^{137}Cs	21/10/2013	2.539 (55) x 10^{-3}	52.6 (11)
$^{143+144}Nd$	05/02/2014	5.701 (60) x 10^{-3}	53.95 (56)
$^{145+146}Nd$	05/02/2014	3.643 (38) x 10^{-3}	53.05 (56)
^{148}Nd	05/02/2014	0.974 (21) x 10^{-3}	53.3 (12)
^{150}Nd	05/02/2014	0.463 (21) x 10^{-3}	52.2 (23)
		Average:	52.78 (37)

- SNF segment sample: characteristics

Parameter	Value
Segment length	52.01 (4) mm
Segment weight	42.616 (1) g
Cladding weight	6.71 (4) g
Net fuel weight	35.91 (4) g

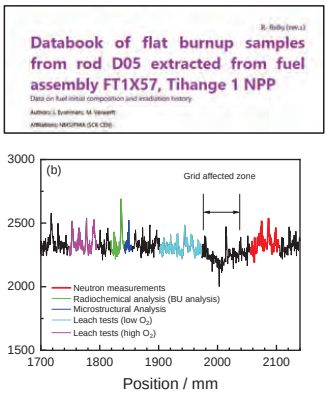

⇒ Accurate information about design and operational history

NEUTRON EMISSION MEASUREMENT: CONVENTIONAL WELL COUNTER (AWCC)

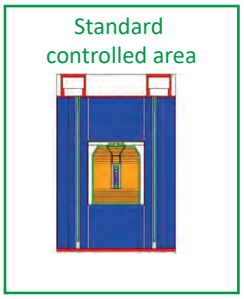

- Neutron detection
  - Modified AWCC (only internal cavity)
  - ^{3}He detectors in polyethylene
  - Detection efficiency for ^{252}Cf(sf): $\varepsilon = 0.28$
- Signal processing: shift register
  - Totals, reals and accidentals
- Data analysis: Hage's point model (JRC Ispra)

W. Hage and D.M. Cifarelli, NSE 89 (1985) 159 – 176
W. Hage and D.M. Cifarelli, NIMA 236 (1985) 165 – 177
D.M. Cifarelli and W. Hage, NIMA 251 (1986) 550 – 563

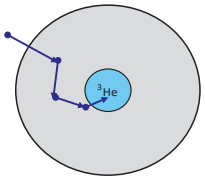

SHIFT – REGISTER: PRINCIPLE

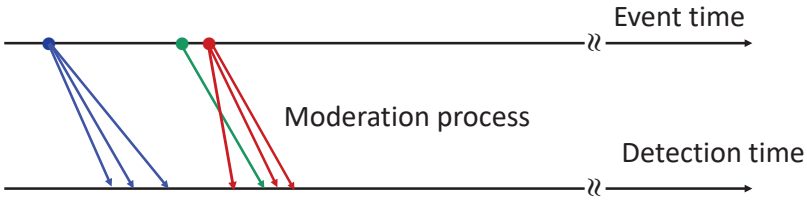

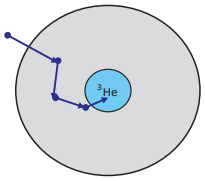

Every detected neutron will trigger the opening of two gates
- Gate close to the signal (signal trigger)
- Delayed gate

SHIFT – REGISTER: PRINCIPLE

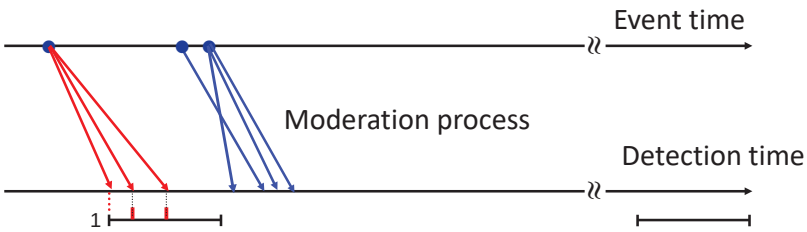

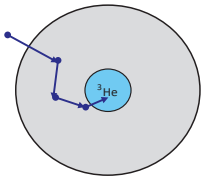

Signal trigger
R + **A**

Delayed trigger
A

SHIFT – REGISTER: PRINCIPLE

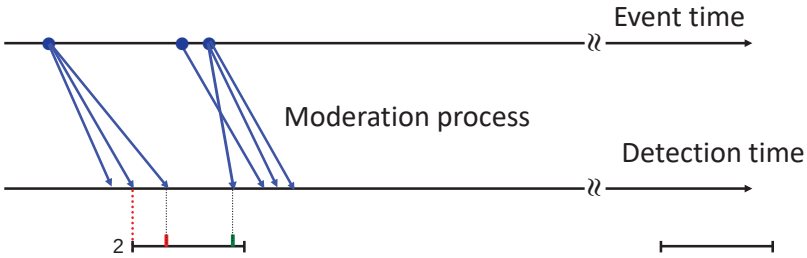

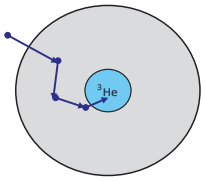

Signal trigger
R + **A**

Delayed trigger
A

SHIFT – REGISTER: PRINCIPLE

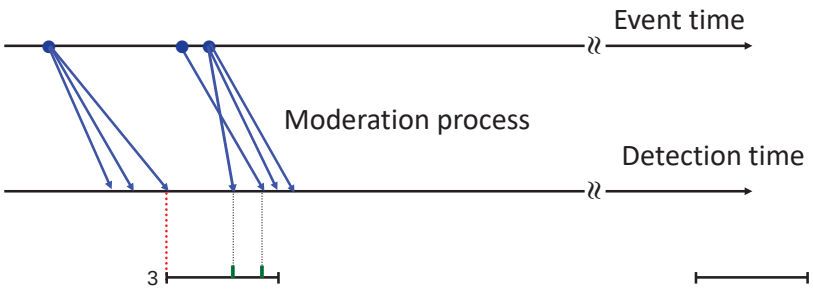

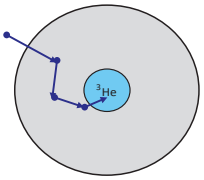

Signal trigger
R + **A**

Delayed trigger
A

SHIFT – REGISTER: PRINCIPLE

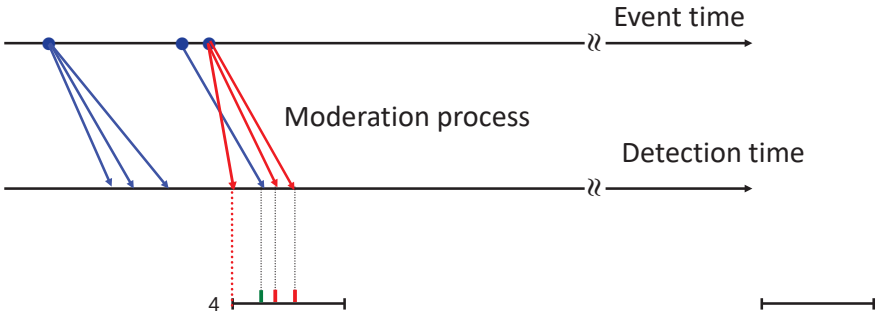

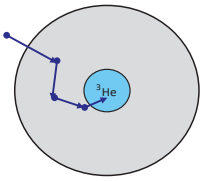

Signal trigger
R + **A**

Delayed trigger
A

SHIFT – REGISTER: PRINCIPLE

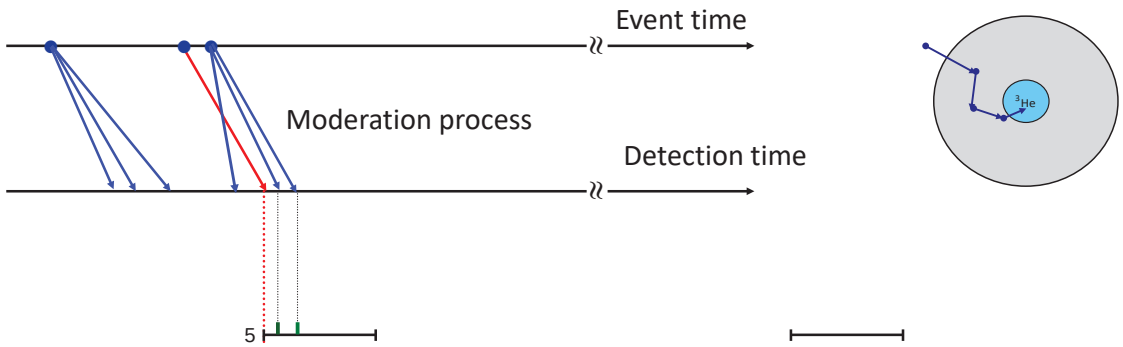

Signal trigger
R + **A**

Delayed trigger
A

SHIFT – REGISTER: PRINCIPLE

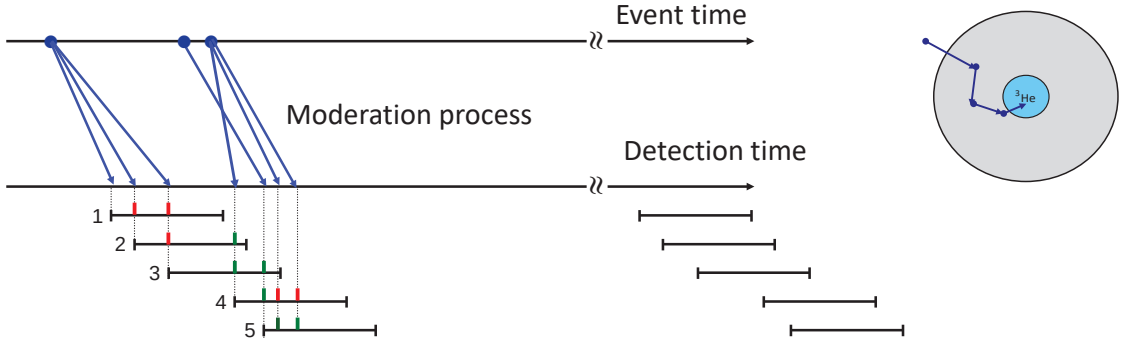

Signal trigger
R + **A**

Delayed trigger
A

SHIFT – REGISTER: PRINCIPLE

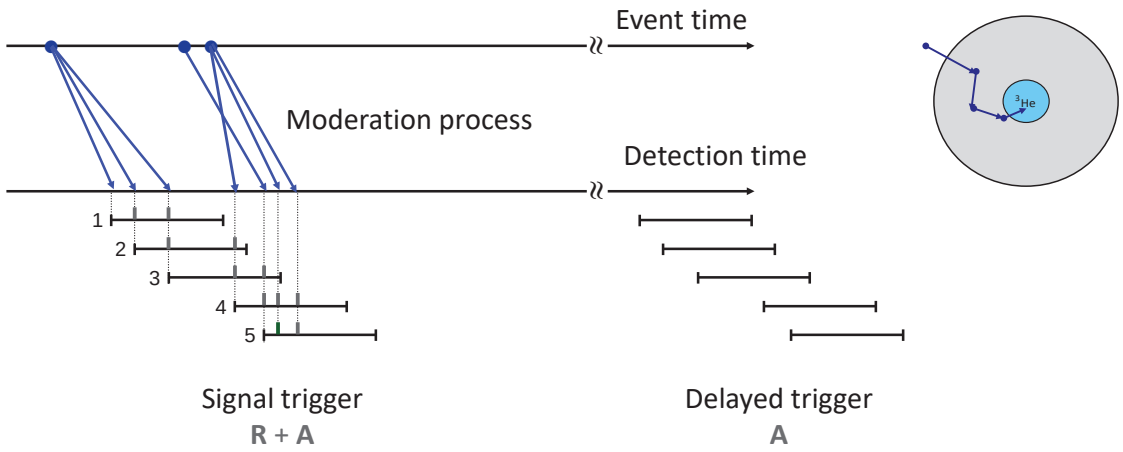

DATA ANALYSIS: HAGE'S POINT MODEL

$$\mathbf{T} = \varepsilon_{sf}\,\mathbf{S_{sf}}\,M\,[1+\alpha\,]$$

$$\mathbf{R} = \varepsilon_{sf}^{2}\,f\,\mathbf{S_{sf}}\,M^{2}\left[\frac{\nu_{sf(2)}}{\nu_{sf(1)}}+\frac{\nu_{(2)}}{\nu_{(1)}-1}\,(M-1)(1+\alpha\,)\right]$$

- Experiment
  - T : total count rate corrected for dead time and background
  - R : reals count rate corrected for dead time and background
- Detector characteristics
  - ε_{sf} : detection efficiency
  - f : gate fraction
- Nuclear data
  - $\nu_{sf(1)}$ and $\nu_{sf(2)}$: 1st and 2nd order factorial moments of P(ν) distribution for (sf)
  - $\nu_{sf(1)}$ and $\nu_{sf(2)}$: 1st and 2nd order factorial moments of P(ν) distribution for (n,f)
- Sample properties
  - **S_{sf} : production rate for prompt fission neutrons by (sf)**
  - α : ratio between neutron production rate by (α,n) and S_{sf}
  - M : neutron leakage multiplication (derived by MC simulations, M ≈ 1.006)

W. Hage and D.M. Cifarelli, NSE 89 (1985) 159 – 176
W. Hage and D.M. Cifarelli, NIMA 236 (1985) 165 – 177
D.M. Cifarelli and W. Hage, NIMA 251 (1986) 550 – 563

NEUTRON EMISSION: ABSOLUTE MEASUREMENTS OF SNF SEGMENT SAMPLE

Standard controlled area

S_{sf} = 678 (12) $s^{-1}\,g^{-1}$

α = 0.039 (18)

NEUTRON EMISSION: ABSOLUTE MEASUREMENTS OF SNF SEGMENT SAMPLE

Standard controlled area

S_{sf} = 678 (12) $s^{-1}\,g^{-1}$

α = 0.039 (18)

Uncertainty evaluation and sensitivity analysis

Uncertainty component, x_j	$\frac{u_{x_j}}{x_j}$	$\frac{u_{S_{sf},j}}{u_{S_{sf}}}$	$\frac{u_{\alpha,j}}{u_\alpha}$
Totals rate, T	0.0008	< 0.01	0.05
Reals rate, R	0.0027	0.15	0.17
Detection efficiency, ε_{sf}	0.0055	0.60	0.35
Gate fraction, f	0.0071	0.40	0.45
First order factorial moment, $\nu_{sf(1)}$	0.0037	0.20	0.25
Second order factorial moment, $\nu_{sf(1)}$	0.0120	0.67	0.80
Multiplication, M	0.0020	0.01	< 0.01

Schillebeeckx et al., Frontiers in Energy Research 11 (2023) 1162367

⇒ Improve
- detector characteristics
- nuclear data

NEUTRON EMISSION: ABSOLUTE MEASUREMENTS OF SNF SEGMENT SAMPLE

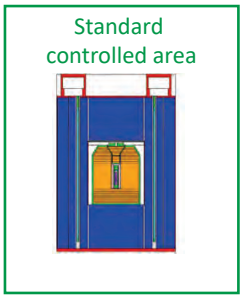

S_{sf} = 678 (12) $s^{-1}\,g^{-1}$

$S_{\alpha n} / S_{sf}$ = 0.039 (18)

Good agreement with:

Calculated from radiochemical analysis :
S_{sf} = 699 (28) $s^{-1}\,g^{-1}$

Note: uncertainty radiochemical analysis > 4%
(> factor 2)

NEUTRON EMISSION: ABSOLUTE MEASUREMENTS OF SNF SEGMENT SAMPLE

S_{sf} = 678 (12) $s^{-1}\,g^{-1}$

Code	Library	S_{calc}/S_{exp}
ALEPH2	JEFF-3.3	0.94
SCALE	ENDF/B-VII.0	0.96
Serpent2 (2.1.29)	ENDF/B-VII.0	1.01
	ENDF/B-VII.1	1.02
	ENDF/B-VIII.0	1.02
	JEFF-3.1.2	0.93
	JEFF-3.3	0.97
	JEFF-3.3 (1)	1.09
	JEFF-3.3 (2)	1.01
	JEFF-3.3 (3)	1.01
	JEFF-4T1	0.98
	JENDL-5.0	1.09

(1) $\sigma(n,\gamma)$ = 0 for ^{147}Nd
(2) $\sigma(n,\gamma)$ for ^{147}Nd from JENDL-4.0u
(3) $\sigma(n,\gamma)$ for ^{147}Nd from JEFF-4T1

NEUTRON EMISSION: ABSOLUTE MEASUREMENTS OF SNF SEGMENT SAMPLE

Code	Library	S_{calc}/S_{exp}
ALEPH2	JEFF-3.3	0.94
SCALE	ENDF/B-VII.0	0.96
Serpent2 (2.1.29)	ENDF/B-VII.0	1.01
	ENDF/B-VII.1	1.02
	ENDF/B-VIII.0	1.02
	JEFF-3.1.2	0.93
	JEFF-3.3	0.97
	JEFF-3.3 (1)	1.09
	JEFF-3.3 (2)	1.01
	JEFF-3.3 (3)	1.01
	JEFF-4T1	0.98
	JENDL-5.0	1.09

S_{sf} = 678 (12) $s^{-1}\,g^{-1}$

Uncertainty theoretical estimation

Burnup	Relative uncertainty
10 MWd/kg	12.1 %
30 MWD/kg	11.1 %
50 MWd/kg	10.0 %

Contribution mainly from : ^{242}Pu(n,γ) & ^{243}Am(n,γ)

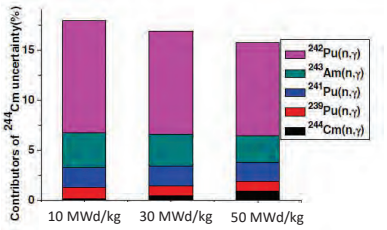

Tiejun Zu et al., Annals of Nuclear Energy 94 (2016) 399

TASK 2: PRODUCE VALIDATED DEPLETION CALCULATIONS WITH REALISTIC UNCERTAINTIES

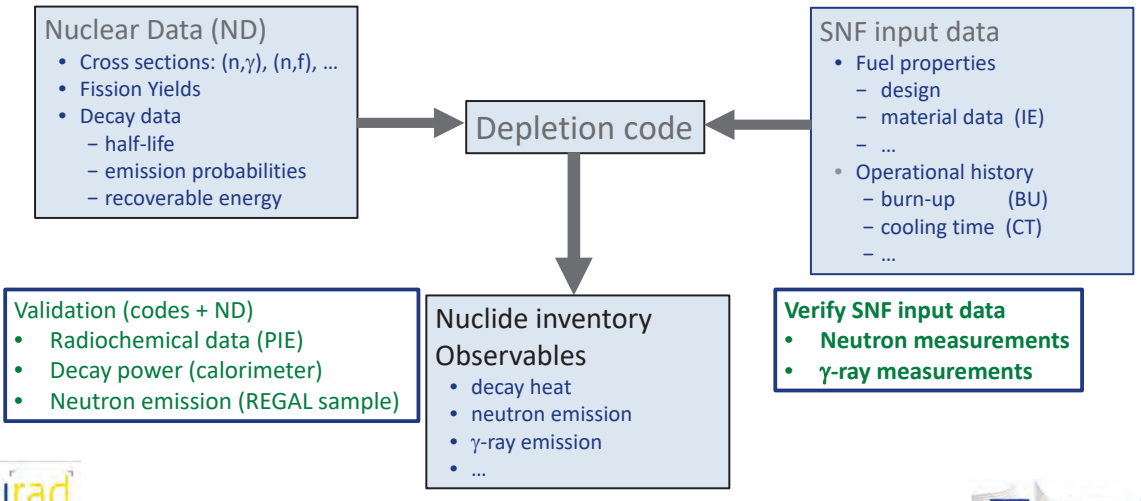

NEUTRON EMISSION RATE

N = aBU^b
b = 4 for BU > 20 MWd/kg

$$\frac{\delta N}{N} = b\frac{\delta BU}{BU}$$

⇒ Total neutron emission extremely sensitive to BU

⇒ Good BU indicator

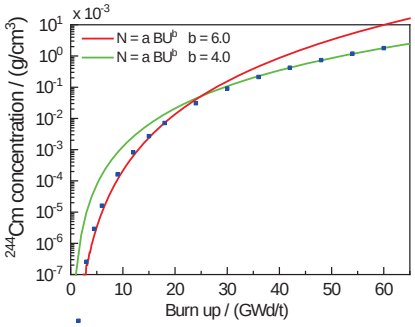

^{137}Cs

- Production : cumulative fission yields + burnup

$$N_k(t_0) \propto Y_c\ BU$$

- Decay power after cooling time t by ^{137}Cs

$$P_k(t) = p_k\ N_k(t_0)\ e^{-\lambda_k (t-t_0)}$$

$$p_k = E_{dk}\ \lambda_k$$

⇒ Nuclear data
  - Y_c : cumulative fission yields
  - λ_k : decay constant
  - E_{dk} : recoverable energy

⇒ Operational history : BU

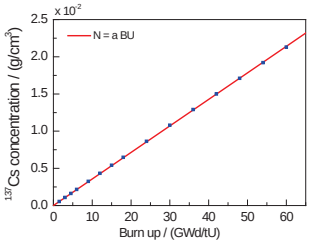

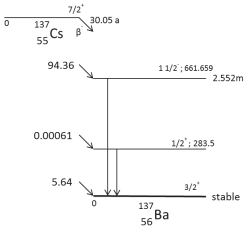

^{137}Cs USED AS BURN-UP INDICATOR

$$N_k(t) \approx Y_c \, BU$$

- N ∝ BU
  (long half-life, small σ_γ)
- Not very sensitive to IE
- Cumulative fission yields (x 100)

	^{235}U(n,f)	^{239}Pu(n,f)
^{106}Ru	0.41 (1)	4.19 (9)
^{137}Cs	**6.22 (7)**	**6.59 (8)**

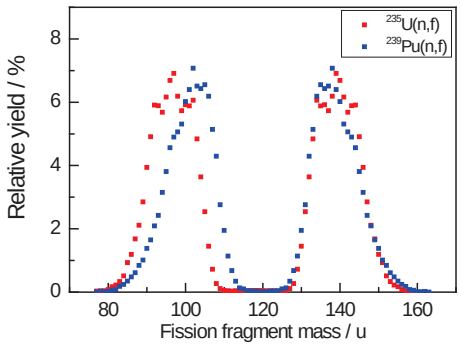

PRODUCTION OF ^{134}Cs

$$n + {}^{235}_{92}U \xrightarrow{(n,f)} {}^{100}_{40}Zr + {}^{133}_{52}Te + 3n$$

$${}^{133}_{52}Te \xrightarrow[12.4\ min]{\beta^-} {}^{133}_{53}I + e^- + \bar{\nu}_e$$

$${}^{133}_{53}I \xrightarrow[20.8\ h]{\beta^-} {}^{133}_{54}Xe + e^- + \bar{\nu}_e$$

$${}^{133}_{54}Xe \xrightarrow[5.24\ d]{\beta^-} {}^{133}_{55}Cs + e^- + \bar{\nu}_e$$

$$n + {}^{133}_{55}Cs \xrightarrow{(n,\gamma)} {}^{134}_{55}Cs$$

^{134}Cs production:
(n,f) followed by β$^-$ and (n,γ)

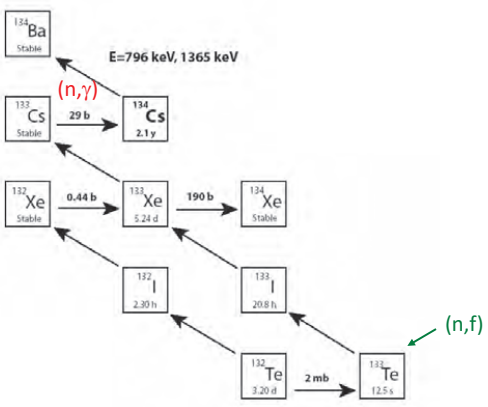

PRODUCTION OF ^{134}Cs

$N = aBU^b$
$b = 2$ for $BU < 30$ GWd/tU

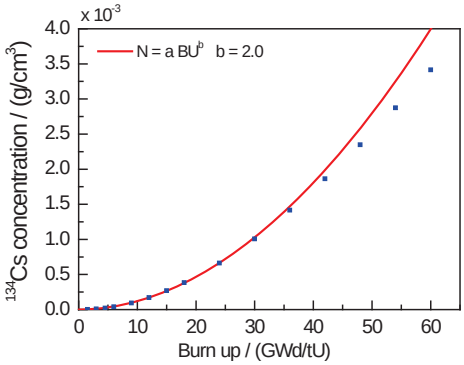

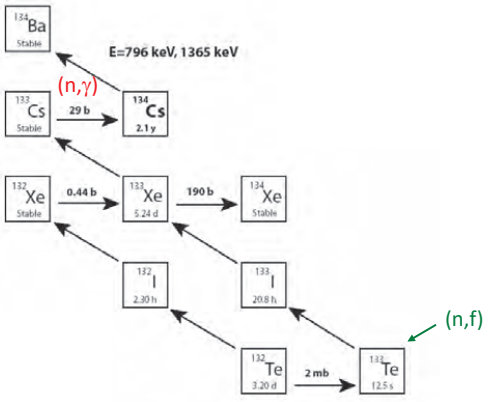

PRODUCTION OF ^{154}Eu

$N = aBU^b$
$b = 2$ for $BU < 35$ GWd/tU

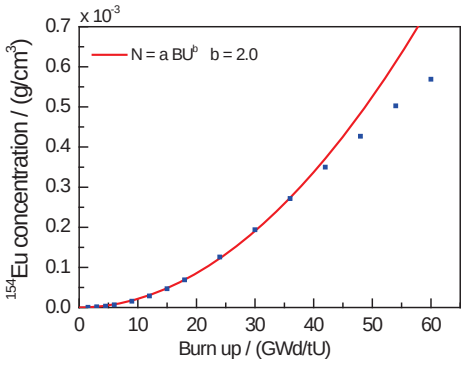

^{154}Eu production: complex
(n,f), β^- and (n,γ) from 5 mass chains

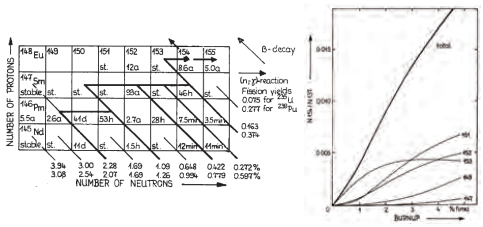

R. Berndt, Kernenergie 31 (1988) 59

EXPERIMENTS AT CLAB

- FORK detector
  - Total neutron emission
  - Total γ-ray emission
- γ-ray spectroscopy
  - HPGe detector
  - Axial scanning
- DDSI (Differential Die-away Self Interrogation)
  - MC-simulation
  - One experimental campaign (problems with device)

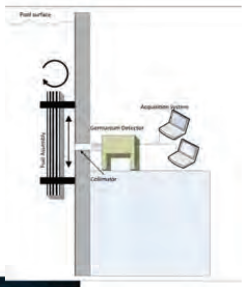

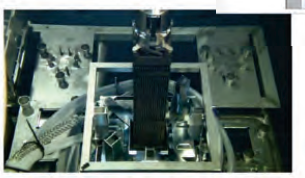

NEUTRON AND γ-RAY MEASUREMENTS: FORK DETECTOR

Passive NDA: detection of neutrons and γ-rays emitted by SNF assembly

- Neutron production
  - Primary neutrons: mainly prompt fission neutrons from ^{244}Cm(sf)
  - Neutron multiplication: neutron induced fission after neutron moderation in the pool
- Neutron detection
  - ^{235}U fission chambers (FC)
  - Fission chamber with and without Cd
  - Total neutron count rate
- γ-ray detection
  - Ionisation chamber (IC)
  - Total γ-ray dose rate measurement

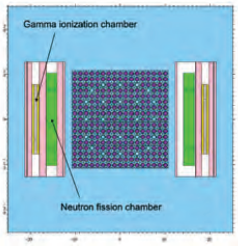

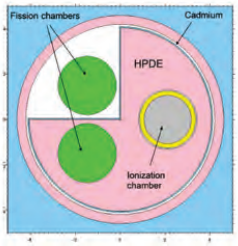

Vaccaro et al., NIMA 888 (2018) 202-217

FORK DETECTORS: THEORETICAL CALCULATIONS

- Neutron and γ-ray emission spectra by ORIGEN
  - ENDF/B-VII.1
  - ORIGEN-ARP (covers a wide range of fuel types and irradiation conditions)
  - Neutron emission spectra: SOURCES 4C
- Neutron detection response
  - Energy dependent response functions by MCNP
  - Neutron multiplication, M
    - k_∞ using macroscopic cross sections from ORIGEN
    - (1 – L) by MCNP for each assembly lattice design

$$M = \frac{1}{1 - k_\infty (1 - L)}$$

- γ-ray detection response
  - Energy-dependent response function by MCNP
  - Correction for nonlinear behaviour of IC as a function of incident dose rate determined by comparison with calculated response

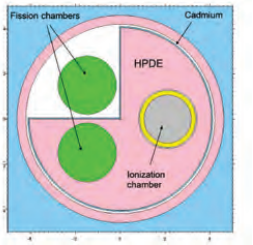

Vaccaro et al., NIMA 888 (2018) 202-217

FORK DETECTORS: RESPONSE FUNCTIONS

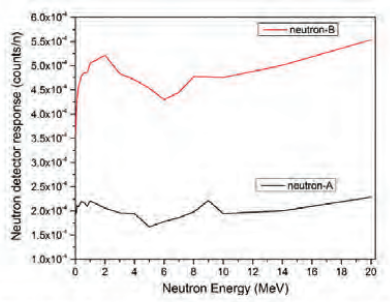

Fig. 5b. Energy-dependent response of the Fork detector neutron detectors and 17 × 17 assembly calculated by MCNP and the measurement configuration in Fig. 4a. Neutron response is counts per emitted neutron in the fuel and includes neutron multiplication in the assembly. Neutron-A represents the bare fission chamber, while neutron-B is the cadmium-covered detector.

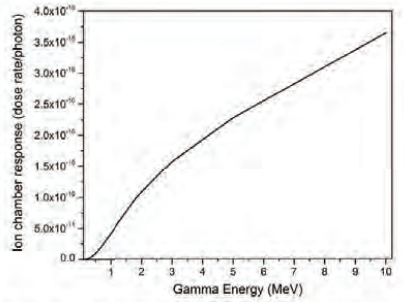

Fig. 5a. Energy-dependent response of the Fork detector gamma ionization chamber and 17 × 17 assembly calculated by MCNP and the measurement configuration in Fig. 4a. Response is dose rate per photon emitted in the fuel.

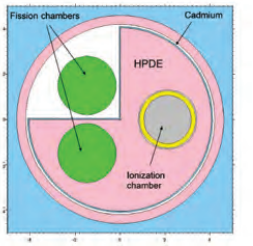

Vaccaro et al., NIMA 888 (2018) 202-217

FORK MEASUREMENTS AT CLAB

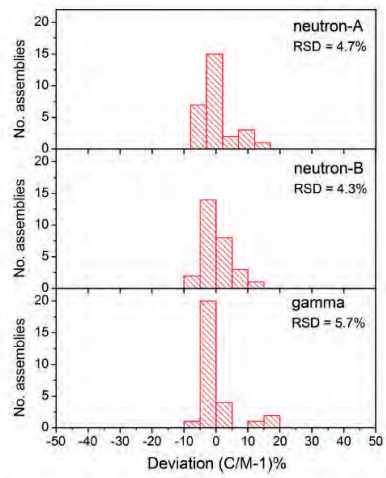

Fig. 10. Histogram distribution of the deviations between calculated (C) and measured (M) gamma, neutron-A, and neutron-B detector count rates for PWR assemblies measured at the Swedish Clab facility.

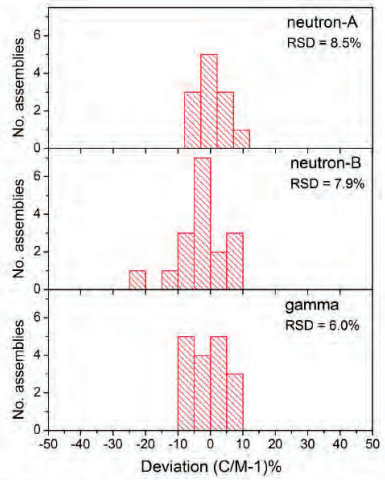

Fig. 11. Histogram distribution of the deviations between calculated (C) and measured (M) gamma, neutron-A, and neutron-B detector count rates for BWR assemblies measured at the Swedish Clab facility.

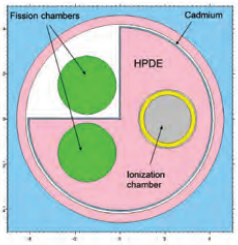

Vaccaro et al., NIMA 888 (2018) 202-217

FORK MEASUREMENTS: COMPARISON WITH CALCULATIONS

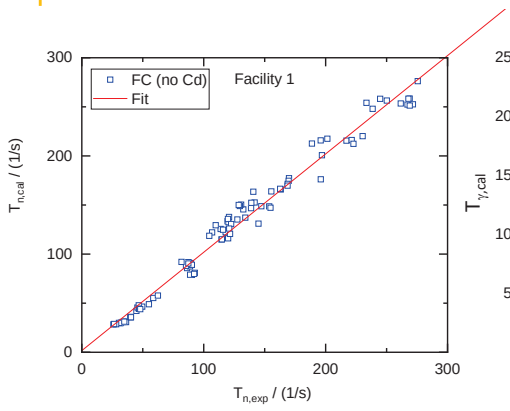

Total neutron count rate
$T_{n,exp}$: experimental
$T_{n,cal}$: calculated

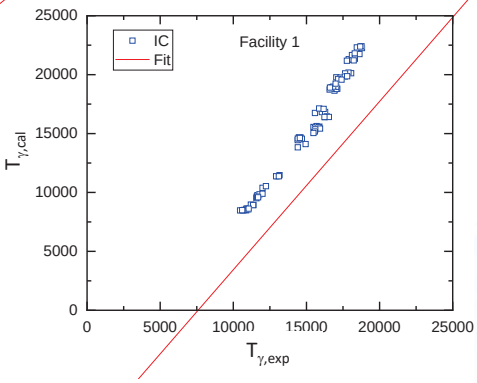

Total γ-ray response
$T_{\gamma,exp}$: experimental
$T_{\gamma,cal}$: calculated

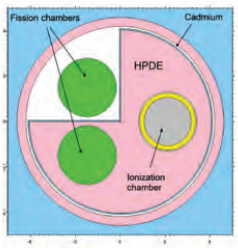

Mosconi, private communication

FORK MEASUREMENTS

Detector	Facility 1	Facility 2	Facility 3
FC (no Cd)	9.0 %	12.0 %	2.2%
FC (Cd)	9.0 %	14.0 %	2.2 %
IC	4.2 %	11.0 %	1.8 %

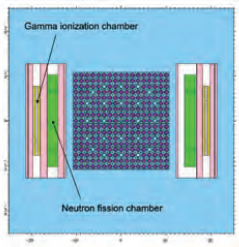

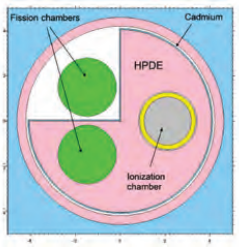

Mosconi, private communication

TASK SHEET: IMPROVE THE VERIFICATION OF SPENT FUEL WITH FORK DETECTORS

- Determine detection efficiency
  - Design and construct a reference calibration set-up
  - Perform calibration measurements with radionuclide sources, i.e. ^{244}Cm
  - Perform measurements to validate MC-calculations
- MC simulations of detector response
  - MC simulations for the reference calibration set-up
  - Verify impact of ^{10}B concentration in the pool
  - Define correction factors based on Cd/no-Cd ratio

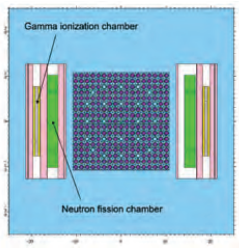

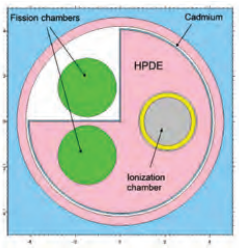

γ-RAY SPECTROSCOPIC MEASUREMENTS

- HP Ge detector
- Axial scanning

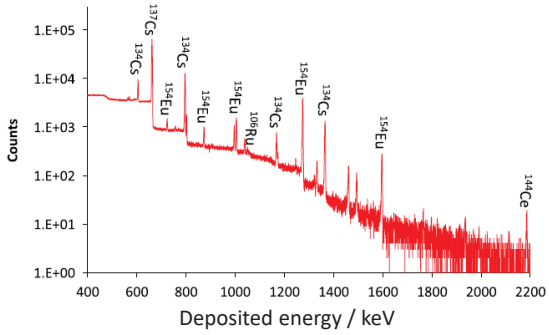

^{137}Cs: 662 keV

^{134}Cs: 605, 796, 1365 keV

^{154}Eu: 996, 1004, 1274, 1596 keV

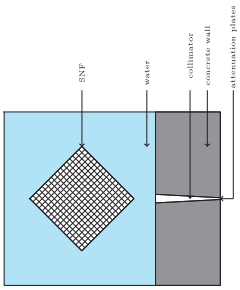

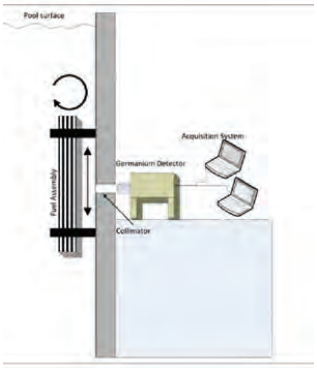

Solans et al., ANE 192 (2023) 109941
Bengtsson et al., Nucl. Techn. 208 (2022) 295
Vaccaro et al., NIMA A833 (2016) 208
Vo et al., NIMA 830 (2016) 325
Favalli et al., NIMA 820 (2016) 102

^{137}Cs ACTIVITY

$\langle A_{cal}/A_{exp} \rangle = 1.39$
St. dev A_{cal}/A_{exp} = 3.3%

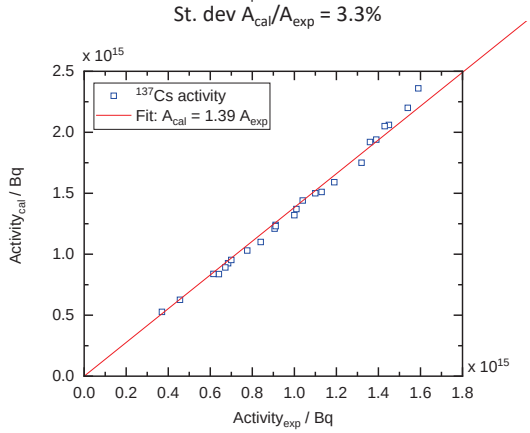

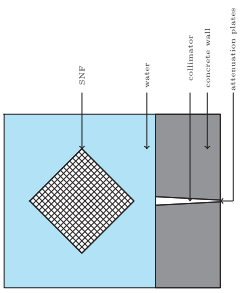

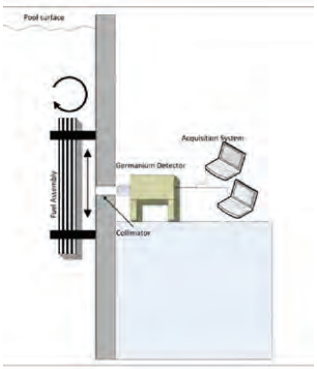

Bengtsson et al., Nucl. Techn. 208 (2022) 295

AXIAL PROFILE ^{137}CS ACTIVITY (BURNUP PROFILE)

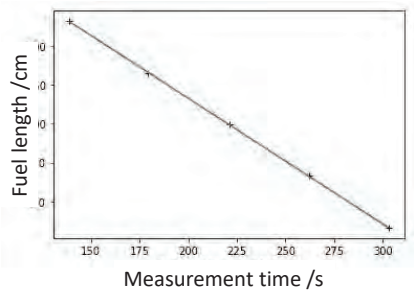

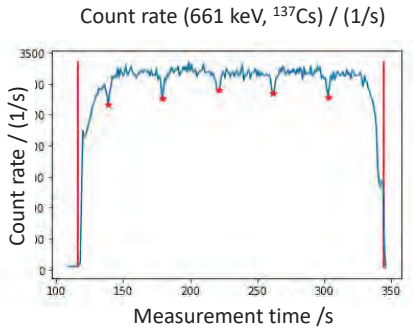

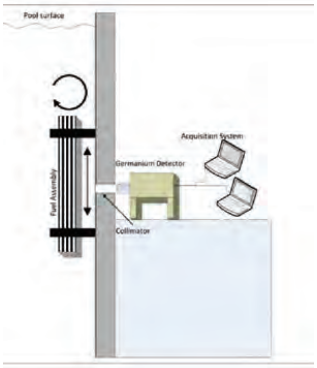

DIFFERENTIAL DIE-AWAY SELF-INTERROGATION (DDSI)

Passive NDA: detection of neutrons emitted by SNF assembly
Developed at LANL for nuclear safeguards applications

- Neutron production
  - Primary neutrons: mainly prompt fission neutrons from ^{244}Cm(sf)
  - Prompt fission neutrons from neutron induced fission in fuel mainly after neutron moderation in the water of the pool
- Detection principle
  - ^{3}He in moderator
  - Detection of **correlated neutrons**: construct **Rossi-alpha distribution**

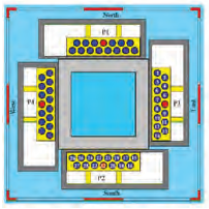

Trahan et al., NIMA 955 (2020) 163329

DDSI: ROSSI-ALPHA DISTRIBUTION

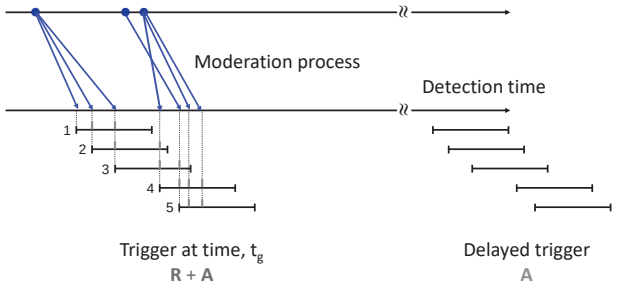

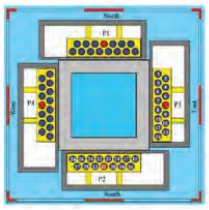

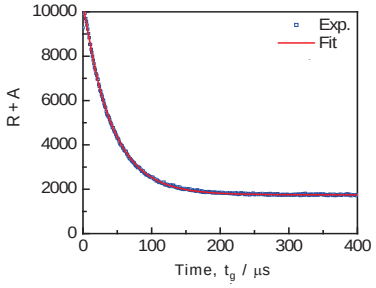

DDSI: ROSSI-ALPHA DISTRIBUTION

$$R = R_0 e^{-\frac{t}{\tau_e}}$$

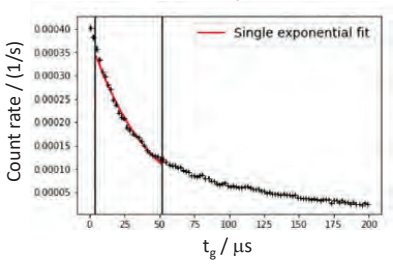

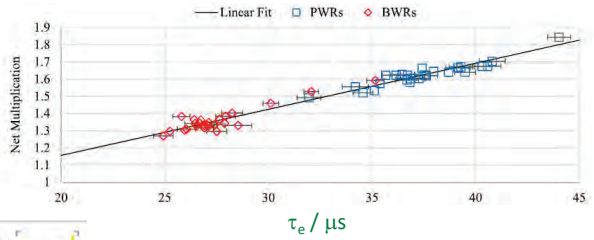

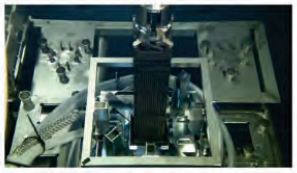

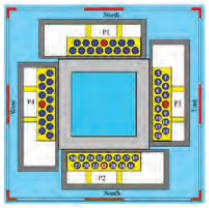

Trahan et al., NIMA 955 (2020) 163329

DDSI: ROSSI-ALPHA DISTRIBUTION

$$R = R_0 e^{-\frac{t}{\tau_e}}$$

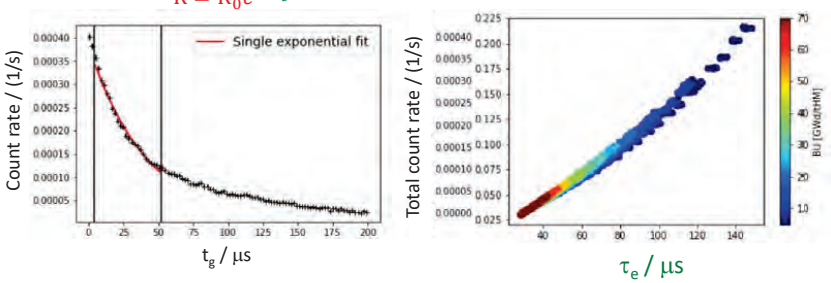

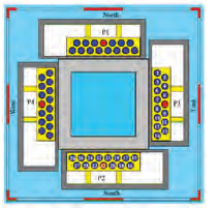

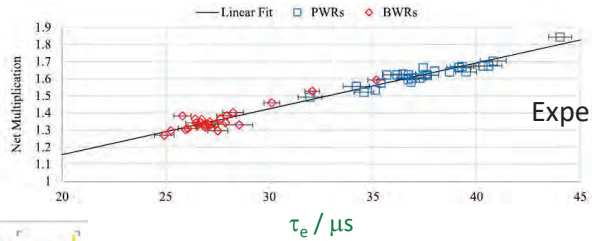

Experiments at CLAB

Trahan et al., NIMA 955 (2020) 163329

DDSI: MC SIMULATIONS

$$R = R_0 e^{-\frac{t}{\tau_e}}$$

$$R = R_{01}\, e^{-\frac{t}{\tau_f}} + R_{02}\, e^{-\frac{t}{\tau_s}}$$

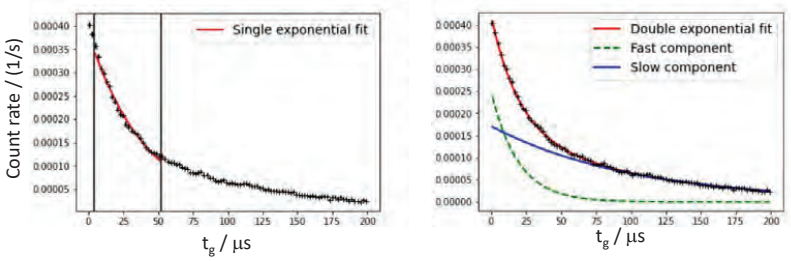

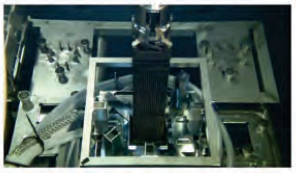

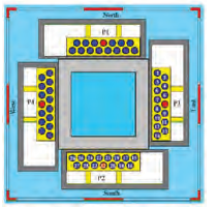

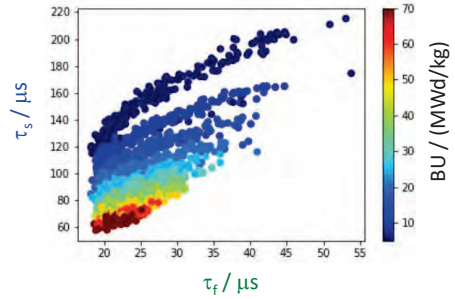

⇒ Additional information

Solans et al., IAEA Symposium, November 2022
IAEA-CN-303-137

DDSI: EXPERIMENTS AT CLAB

$R = R_0 e^{-\frac{t}{\tau_e}}$

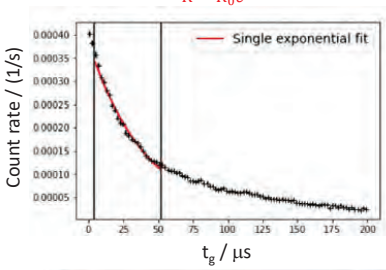

$R = R_{01}\, e^{-\frac{t}{\tau_f}} + R_{02}\, e^{-\frac{t}{\tau_s}}$

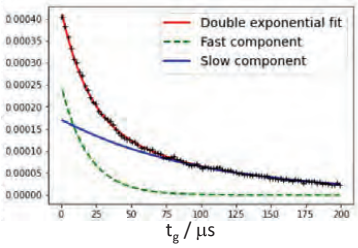

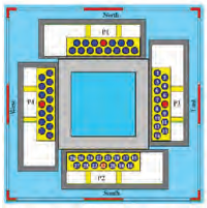

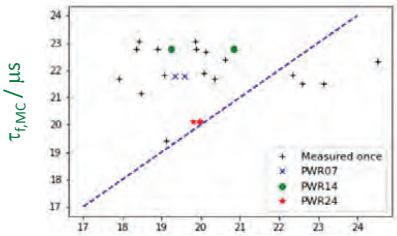

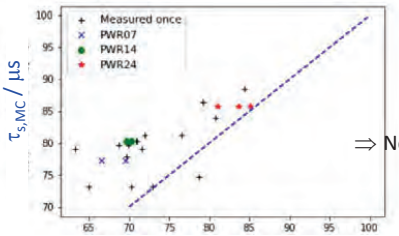

⇒ Not confirmed by experiment

Solans et al., IAEA Symposium, November 2022
IAEA-CN-303-137

FINLAND: ONKALO

Marita Mosconi

- Passive Neutron Albedo Reactivity (PNAR)
  LANL development, Tobin et al., NIMA 897 (2018) 32 - 37

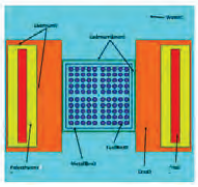

- Passive Gamma Ray Emission Tomography (PGET)
  IAEA development, Honkamaa et al., Symp. Int. Safeguards, IAEA Vienna 2014

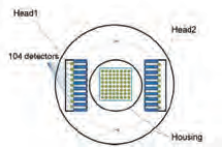

PNAR CONCEPT: RESULTS FROM MC SIMULATIONS

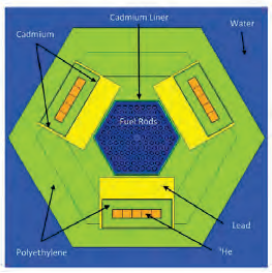

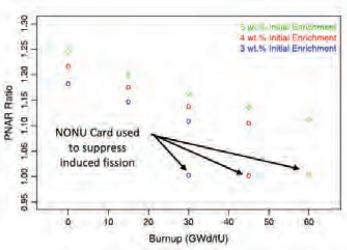

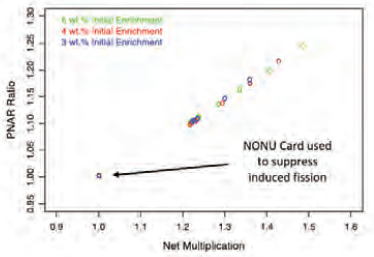

Tobin et al., NIMA 897 (2018) 32 - 37

PNAR + PGET AT ONKALO

PNAR

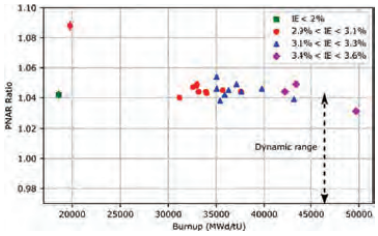

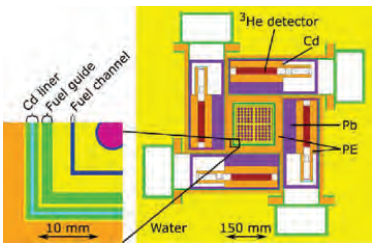

PGET

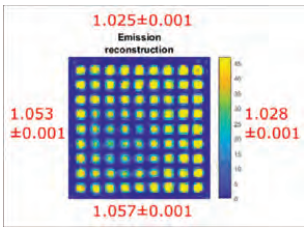

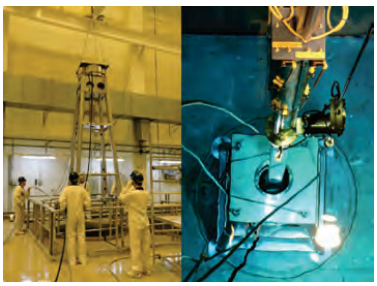

Tupasela et al., NIMA 986 (2021) 164707

BIBLIOGRAPHY

Spent nuclear fuel observables and key nuclides

- Gauld et al., "Nuclide importance to criticality safety, decay heating and source terms related to transport and interim storage of high-burnup LWR fuel", Report NUREG/CR-6700, ORNL/TM-2000/284 (2001)
- Žerovnik et al. ,"Observables of interest for the characterisation of Spent Nuclear Fuel", EUR 29301 EN (2018) , JRC112361
- Schillebeeckx et al., "Characterisation of spent nuclear fuel by theoretical calculations and non-destructive analysis", JRC114178 (2019)

Depletion codes

- Rearden and Jessee, "SCALE Code System", ORNL/TM-2005/39 Version 6.2, April 2016
- Gauld et al., "Isotopic depletion and decay methods and analysis capabilities in SCALE", Nuclear Technology 174 (2017) 169

Nuclear data

- Nuclear data libraries at JANIS NEA, https://www.oecd-nea.org/jcms/pl_39910/janis
- Decay data, http://www.nucleide.org/DDEP.htm
- Nichols et al., "Handbook of nuclear data for safeguards: database extensions, august 2008", INDC-2453, INDC(NDS) – 0534

BIBLIOGRAPHY

Non-destructive assay

Calorimeter

- SKB, "Measurements of Decay Heat in Spent Nuclear Fuel at the Swedish Interim Storage Facility", Clab, SKB Report R-05-62, December 2006
- B.D. Murphy and I.C. Gauld, "Spent Fuel Decay Heat Measurements Performed at the Swedish Central Interim Storage Facility", Report ORNL/TM-2008/016, Oak Ridge National Laboratory, Feburary 2010

Neutron

- Schillebeeckx et al., "An absolute measurements of the neutron production rate of a spent nuclear fuel sample used for depletion code validation", Frontiers in Energy Research 11 (2023) 1162367
- Schillebeeckx et al., "A non-destructive method to determine the neutron production rate of a sample of spent nuclear fuel under standard controlled area conditions", JRC Technical Report EUR 30379 EN, 2020
- Tupasela et al., "Passive neutron albedo reactivity measurements of spent fuel nuclear fuel", Nucl. Instr. Meth. A986 (2020) 164707
- Trahan et al., "Results of the Swedish spent fuel measurements field trials with the DDSI", Nucl. Instr. Meth. A955 (2020) 163329
- Tobin et al., "Measuring spent fuel assembly multiplication in borated water with a PNAR instrument", Nucl. Instr. Meth. A897 (2018) 32
- Vaccaro et al., "Advancing the FORK detector for quantitative spent nuclear fuel verification", Nucl. Instr. Meth. A888 (2018) 202

γ-ray

- Solans et al., "Spent nuclear fuel passive gamma analysis and reproducibility application to SKB-50 assemblies", Ann. Nucl. Energy 192 (2023) 109941
- Bengtsson et al., "Experimental method for the verification of calculated ^{137}Cs content in nuclear fuel assemblies", Nucl. Techn. 208 (2022) 295
- Vaccaro et al., "PWR and BWR spent fuel assembly gamma spectra measurements", Nucl. Instr. Meth. A833 (2016) 208

Thank you

EU countries

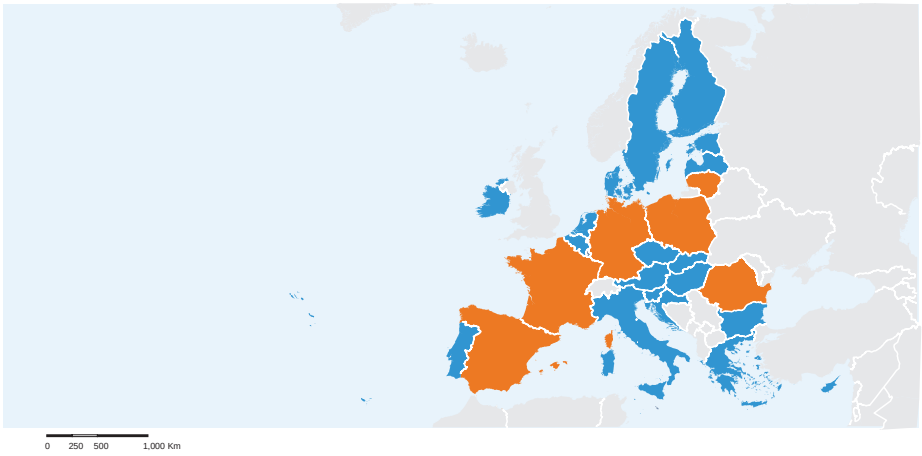

THEORETICAL CALCULATIONS OF THE NEUTRON EMISSION RATE

Code-to-code comparison (including nuclear data)
All calculations normalised to the ^{147}Nd inventory

- Verify impact ND (use one code: Serpent2)
- Verify prediction of ^{137}Cs inventory by different codes/ND libraries
- Verify prediction of BU derived from the codes/ND libraries

CODE-TO-CODE COMPARISON: ^{137}Cs, ^{244}Cm AND BU

Code	Library	^{137}Cs $N_X/N_U \times 10^{-3}$	^{137}Cs C/E	^{244}Cm $N_X/N_U \times 10^{-5}$	BU MWd/kg	^{137}Cs	^{244}Cm	BU
ALEPH2	JEFF-3.3	2.225	0.982	6.290	53.25	**0.990**	0.981	**0.983**
SCALE	ENDF/B-VII.0	2.241	0.990	6.380	54.01	0.997	0.995	0.997
Serpent2	ENDF/B-VII.0	2.285	1.009	6.633	54.37	1.016	1.035	1.004
	ENDF/B-VII.1	2.274	1.004	6.710	54.39	1.012	1.047	1.004
	ENDF/B-VIII.0	2.274	1.004	6.701	54.38	1.012	1.045	1.004
	JEFF-3.1.2	2.248	0.993	6.110	54.18	1.000	**0.953**	1.000
	JEFF-3.3	2.225	0.982	6.354	53.37	**0.990**	0.991	0.985
	JEFF-3.3 (1)	2.290	1.011	7.149	55.24	1.019	1.115	**1.020**
	JEFF-3.3 (2)	2.249	0.993	6.644	54.21	1.000	1.037	1.001
	JEFF-3.3 (3)	2.246	0.992	6.599	54.12	0.999	1.029	0.999
	JEFF-4T1	2.248	0.993	6.410	54.16	1	1	1
	JENDL-4.0u	2.301	1.016	7.009	55.07	**1.024**	1.093	1.017
	JENDL-5.0	2.253	0.995	7.194	54.97	1.002	**1.122**	1.015

(1) $\sigma(n,\gamma) = 0$ for ^{147}Nd
(2) $\sigma(n,\gamma)$ for ^{147}Nd from JENDL-4.0u
(3) $\sigma(n,\gamma)$ for ^{147}Nd from JEFF-4T1

NEUTRON EMISSION: ABSOLUTE MEASUREMENTS OF SNF SEGMENT SAMPLE

Code	Library	Ssf/ (1/sg) LIB	Ssf/ (1/sg) REC	C/E LIB	C/E REC
ALEPH2	JEFF-3.3	640.1	642.4	0.944	0.947
SCALE	ENDF/B-VII.0	653	652.1	0.963	0.962
Serpent2	ENDF/B-VII.0	683.7	678.1	1.008	1.000
	ENDF/B-VII.1	689.4	685.3	1.017	1.011
	ENDF/B-VIII.0	688.5	684.3	1.015	1.009
	JEFF-3.1.2	632.5	623.8	0.933	0.920
	JEFF-3.3	656.8	648.9	0.969	0.957
	JEFF-3.3 (1)	739.4	730.5	1.091	1.077
	JEFF-3.3 (2)	686.8	678.6	1.013	1.001
	JEFF-3.3 (3)	682.2	673.9	1.006	0.994
	JEFF-4T1	662.6	654.6	0.977	0.965
	JEFF-4T2	676.4	668.3	0.998	0.986
	JENDL-4.0u (4)		715.9		1.056
	JENDL-5.0	738.4	733.9	1.089	1.082

$S_{sf,exp} = 678\ (12)\ s^{-1}\ g^{-1}$

Overall good agreement

(1) $\sigma(n,\gamma) = 0$ for ^{147}Nd
(2) $\sigma(n,\gamma)$ for ^{147}Nd from JENDL-4.0u
(3) $\sigma(n,\gamma)$ for ^{147}Nd from JEFF-4T1
(4) No data available to calculate S_{sf}

2.5 SNF characterisation by NDA; P. Schillebeeckx, JRC Geel; School on "Nuclear data for depletion calculations; 11/09 - 15/09/2023

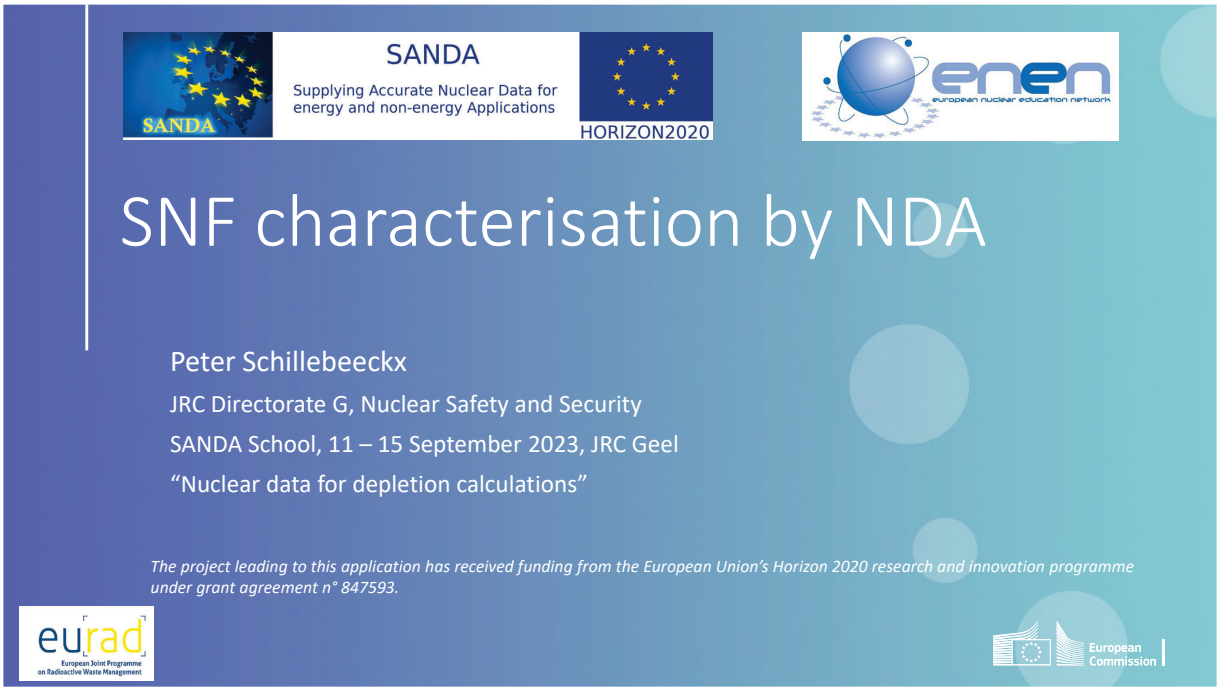

CONTENTS

- Introduction
- NDA for code validation
  - CLAB Calorimeter
  - Neutron emission measurements
  - Gamma-ray measurements
- NDA for verification of assembly properties
  - Gamma-ray measurements
  - Neutron measurements

SNF CHARACTERIZATION BY NON-DESTRUCTIVE ASSAY (NDA)

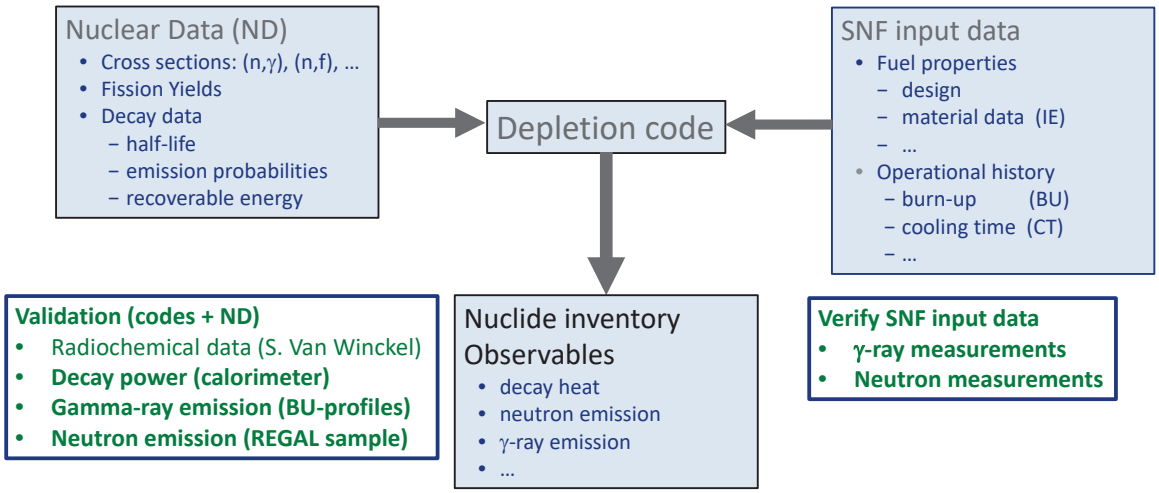

NON-DESTRUCTIVE ASSAY (NDA)

Use radiation emitted by the sample as a fingerprint to determine the properties of nuclear material

- Requirements
  - High penetration power
  - Detectable
- Radiation types
  - Charged particles (only for extreme thin samples)
  - Neutron
  - Gamma-ray
  - Heat

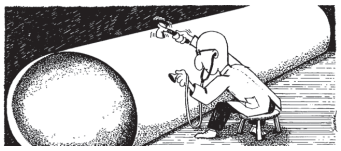

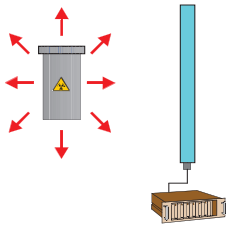

NDA: PASSIVE - ACTIVE

Passive

- Spontaneous emission
- Radioactive Decay

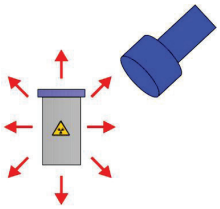

Source term: decay rate

$$S = \lambda N$$

Active

- Induced emission
- Nuclear reactions

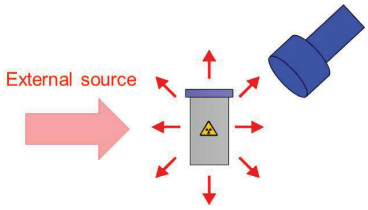

Source term : reaction yield

$$S_r = (1 - e^{-n\,\sigma_{tot}})\frac{\sigma_r}{\sigma_{tot}} + \ldots$$

CLAB CALORIMETER: DECAY HEAT

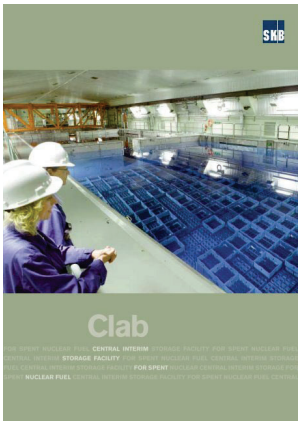

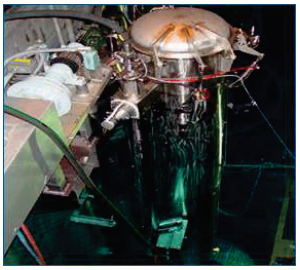

See presentations:
G. Letnar
O. Matuselanski
A. Melic
P. Romojaro

- Only operating calorimeter worldwide to determine decay power of SNF assemblies
- Extensively used to validate depletion codes, e.g.
  - Ilas and Burns, Nucl. Tech. 208 (2022) 403
    SCALE 6.2.4
  - Shama et al., Ann. Nucl. Energy 165 (2022) 108758
    ORIGE, CASMO5
  - Ebiwonjumi et al., Ann. Nucl. Energy 124 (2019) 80
    STREAM
  - Yamamoto and Iwahashi J. Nucl. Sci. Techol. 53 (2016) 2108
    ORIGEN2.2, CASMO5
  - Haeck and Ichou, EPJ Web of Conferences 146 (2017) 06012
    VESTA
  - San-Felice et al., Nucl. Technol. 184 (2013) 217
    DARWIN

DATA FROM CLAB CALORIMETER: SOME RESULTS

Ref.	Year	Code	Library	PWR		BWR	
				<C/E>	St. dev	<C/E>	St. dev
Ilas and Gauld	2008	SCALE 5.1	ENDF/B-V	1.011	0.012	1.003	0.025
Ilas et al.	2014	SCALE 6.1.2	ENDF/B-VII.0	1.002	0.012	0.997	0.024
Ilas and Burns	2021	SCALE 6.2.4	ENDF/B-VII.0	1.013	0.013	1.002	0.012
	2021	SCALE 6.2.4	ENDF/B-VII.1	1.008	0.012	1.009	0.024
Ilas and Burns	2022	SCALE 6.3	ENDF/B-VIII.0	1.006	0.014	1.007	0.024
Shama et al.	2022	SCALE 6.2.3	ENDF/B-VII.1	1.019	0.012	1.003	0.025
		SCALE 6.2.3 (POLARIS)	ENDF/B-VII.1	1.015	0.012	1.010	0.026
Shama et al.	2022	CASMO5		1.009	0.013	1.008	0.025
Yamamoto	2016	CASMO5	JENDL-4.0	1.016	0.013	1.001	0.024
Haeck et al.	2022	VESTA 2.1	JEFF-3.1	0.978	0.012		
		VESTA 2.1	ENDF/B-VII.0	0.996	0.012		
Mills and Sutton	2009	FISPIN	JEF-2.2	0.995	0.013		
		FISPIN	JEFF-3.1.1	0.985	0.012		
San-Felice et al.	2012	DARWIN	JEFF-3.1.1	0.978	0.011		

Not blind!

Adjustments not excluded

BLIND TEST CLAB CALORIMETER: CODES + LIBRARIES

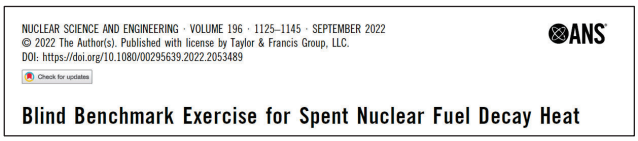
NUCLEAR SCIENCE AND ENGINEERING · VOLUME 196 · 1125–1145 · SEPTEMBER 2022

DOI: https://doi.org/10.1080/00295639.2022.2053489

Blind Benchmark Exercise for Spent Nuclear Fuel Decay Heat

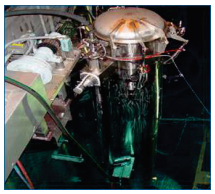

Code	Library	Appendix Section
ALEPH 2.7.2	ENDF/B-VII.1	A.I.A
APOLLO2.8/DARWIN2.3	JEFF-3.1.1	A.I.B
CASMO-4E + ORIGEN-S	JEF-2.2	A.I.C
CASMO-5 (2.03)	ENDF/B-VII.1	A.I.D
CASMO-5 (2.12.00) + SNF (1.07.02)	ENDF/B-VII.1	A.I.E
DRAGON 4.0.5	ENDF/B-VII.1	A.I.F
EVOLCODE (MCNP + ACAB)	JEFF-3.3	A.I.G
MCNP-CINDER + Nuklesnika (2D)	ENDF/B-VII.1	A.I.H
Montebumns v3 + CINDER	ENDF/B-VII.1	A.I.I
MOTIVE (KENO-VI + VENTINA)	ENDF/B-VII.1	A.I.J
MOTIVE (OpenMC + VENTINA)	ENDF/B-VIII	A.I.K
MVP 3	ENDF/B-VII.1	A.I.L
MVP 3	JEFF-3.2	A.I.M
MVP 3	JENDL-4.0	A.I.N
OREST	JEF-2.2 + ENDF/B-VI	A.I.O
SCALE 6.0: ORIGEN-ARP	ENDF/B-V	A.I.P
SCALE 6.1.3: ORIGEN-ARP	ENDF/B-V	A.I.Q
SCALE 6.2.3: ORIGAMI	ENDF/B-VII.1	A.I.P
SCALE 6.2.3: Polaris	ENDF/B-VII.1	A.I.R
SCALE 6.2.3: ORIGEN	ENDF/B-VII.1	A.I.R
SCALE 6.2.3: TRITON/KENO	ENDF/B-VII.1	A.I.S
SCALE 6.2.3: TRITON/NEWT	ENDF/B-VII.1	A.I.T
SEADEP	JEFF-3.1.1	A.I.U
Serpent 2.1.29	ENDF/B-VII.1	A.I.V
Serpent 2.1.29	JEFF-3.1.1	A.I.W
Serpent 2.1.31	JEFF-3.2 + JEFF-3.1.1	A.I.X

Assembly ID	BU	CT	IE	Decay heat rate
BT01	53 MWd/kg	4.5 a	3.95 wt%	1662 W
BT02	55 MWd/kg	8.6 a	3.95 wt%	1068 W
BT03	50 MWd/kg	9.8 a	3.95 wt%	895 W
BT04	51 MWd/kg	13.5 a	3.70 wt%	768 W
BT05	50 MWd/kg	21.4 a	3.60 wt%	663 W

BLIND TEST CLAB CALORIMETER: RESULTS

Assembly ID	P	CT	<C/E>	St. dev
BT01	1662 W	4.5 a	0.975	0.019
BT02	1068 W	8.6 a	0.977	0.018
BT03 (+ Gd)	895 W	9.8 a	0.967	0.019
BT04	768 W	13.5 a	0.994	0.023
BT05	663 W	21.4 a	0.979	0.021

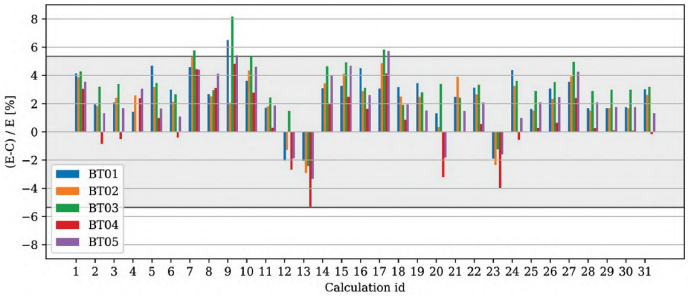

EPRI, PIRT, July 2020

Table 5-5
Summary of Uncertainty in Calculated Decay Heat [17] for BWR Assembly at 37 GWd/MTU Burnup and 15.6 Years' Cooling Time

Perturbed Parameter Set	Relative Uncertainty (%)
Fuel design data	0.2
Operating history data	0.8
Nuclear cross-section data	0.9
Fission yield data	0.3
Overall uncertainty	***1.3***

Ilas et al., Nucl. Eng. Des. 319 (2017) 176

Table 5
Decay heat uncertainty summary.

Data set	Data set	Uncertainty (1σ) (%)
Modeling data	Fuel design	0.20
	Operating data	0.85
	Total	0.87
Nuclear data	Cross sections	0.88
	Fission yields	0.26
	Total	0.92
Overall effect	Total	1.27

u_p/P = 1.3%, is this realistic?

BLIND TEST CLAB CALORIMETER: QUOTED UNCERTAINTIES

Confidence Interval (CI): 68 %

- SKB Document R-05-62 (also used in EPRI, PRIT report)
  - PWR
    - 250 W 1.8 %
    - 900 W 1.0 %
  - BWR
    - 50 W 4.2 %
    - 350 W 0.9 %
- Blind test paper (Jansson et al., Nucl. Sci. Eng. 196 (2022) 1125)
  - 5% overall uncertainty

Only total (combined uncertainties) are given
No separation between
- Systematic and random effects
- Correlated and uncorrelated uncertainty components

⇒ Performance assessment and uncertainty evaluation of CLAB calorimeter is required
⇒ One of the main EURAD objectives of WP8 Task 2

CLAB CALORIMETER: PRINCIPLE

$$C\frac{\partial T_c}{\partial t} - k\frac{\partial^2 T_c}{\partial^2 x} = \left[P - k\,(T_c - T_p)\right]$$

P : power of heat source
T_c : calorimeter temperature
T_p : pool temperature
C : heat capacity (calorimetric body)
k : heat transfer coefficient
t : time
x : position

One component heat transfer model
Equilibrium water in calorimeter and heat source
- Calorimetric body at temperature T_c
- Environment (pool) at a constant temperature T_p

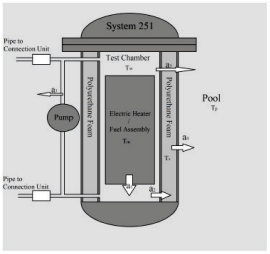

See e.g. Gunn, Nucl. Instr. Meth. 29 (1964) 1

CLAB CALORIMETER: PRINCIPLE

$$C\frac{\partial T_c}{\partial t} - k\frac{\partial^2 T_c}{\partial^2 x} = \left[P - k\,(T_c - T_p)\right]$$

P : power of heat source
T_c : calorimeter temperature
T_p : pool temperature
C : heat capacity (calorimetric body)
k : heat transfer coefficient
t : time
x : position

One component heat transfer model
Equilibrium water in calorimeter and heat source
- Calorimetric body at temperature T_c
- Environment (pool) at a constant temperature T_p

Conditions
- No spatial temperature distribution in calorimeter
- $T_c = T_p$

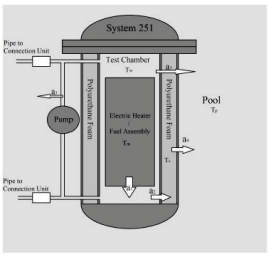

CLAB CALORIMETER: PRINCIPLE

$$C\,\frac{\partial(T_c - T_p)}{\partial t} = P \qquad \text{when } \Delta T = (T_c - T_p) = 0$$

P : power of heat source
T_c : calorimeter temperature
T_p : pool temperature
C : heat capacity (calorimetric body)
k : heat transfer coefficient
t : time
x : position

One component heat transfer model
Equilibrium water in calorimeter and heat source
- Calorimetric body at temperature T_c
- Environment (pool) at a constant temperature T_p

Conditions
- No spatial temperature distribution in calorimeter
- $T_c = T_p$

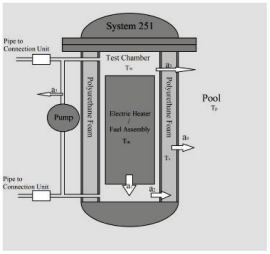

CLAB CALORIMETER: PRINCIPLE

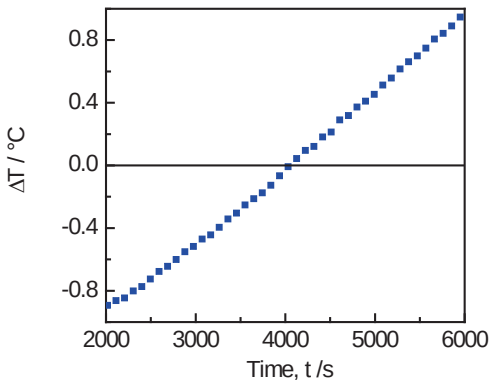

Measurement principle
- Cool down the water in calorimeter
- Stop cooling (continue circulation)
- Measure T_c and T_p
  - T_c : temperature in calorimeter
  - T_p : temperature in pool
- Determine $\Delta T = T_c - T_p$ vs time

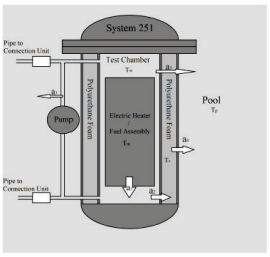

CLAB CALORIMETER: PRINCIPLE

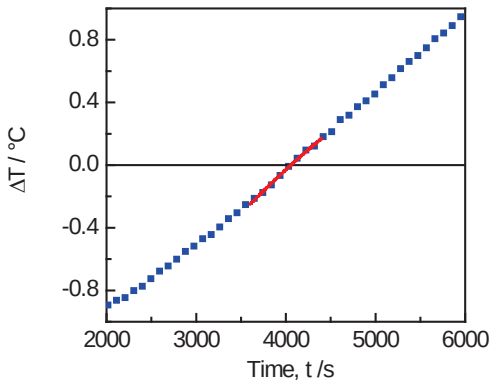

Measurement principle

- Cool down the water in calorimeter
- Stop cooling (continue circulation)
- Measure T_c and T_p
- Determine $\Delta T = T_c - T_p$ vs time
- Determine $d\Delta T/dt$ for $\Delta T = 0$

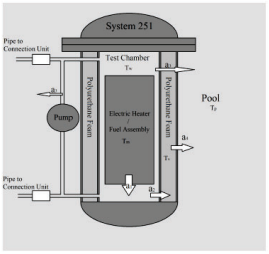

CLAB CALORIMETER: PRINCIPLE

Calibration with an electrical heater

- Determine $\Delta T = T_c - T_p$ vs time
- Determine $d\Delta T/dt$ for $\Delta T = 0$
- Fit to data: $P = a_0 + a_1\, d\Delta T/dt$

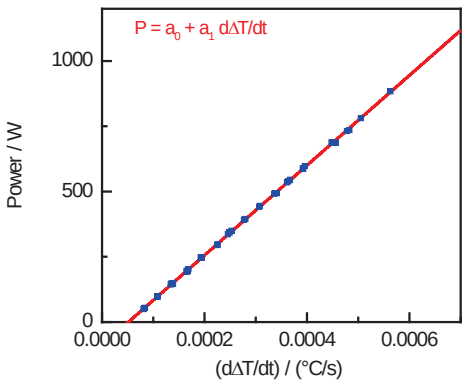

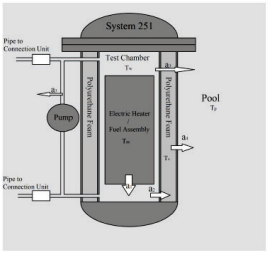

CLAB CALORIMETER: PRINCIPLE

Spent nuclear fuel assembly

- Determine $\Delta T = T_c - T_p$ vs time
- Determine $d\Delta T/dt$ when $\Delta T = 0$
- $Q = a_0 + a_1 K \, d\Delta T/dt$
- $P = Q + P_\gamma$
  - K : correction factor due to thermal capacity difference between electrical heater and fuel assembly
  - P_γ : heat loss due to γ-rays escaping from the calorimeter

Calibration with an electrical heater

- Determine $\Delta T = T_c - T_p$ vs time
- Determine $d\Delta T/dt$ for $\Delta T = 0$
- Fit to data: $P = a_0 + a_1 \, d\Delta T/dt$

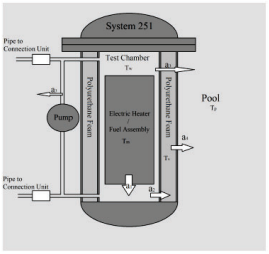

CLAB CALORIMETER: PRINCIPLE

Spent nuclear fuel assembly

- Determine $\Delta T = T_c - T_p$ vs time
- Determine $d\Delta T/dt$ when $\Delta T = 0$
- $Q = a_0 + a_1 K \, d\Delta T/dt$
- $P = Q + P_\gamma$
  - K : correction factor due to thermal capacity difference between electrical heater and fuel assembly
  - P_γ : heat loss due to γ-rays escaping from the calorimeter

Example

- BWR: P = 140 W
  - P_γ = 3.5 W (2.5 %)
  - K = 0.964
- PWR: P = 450 W
  - P_γ = 13.5 W (3.0 %)
  - K = 0.915

CLAB CALORIMETER: ANALYSIS PROCEDURE

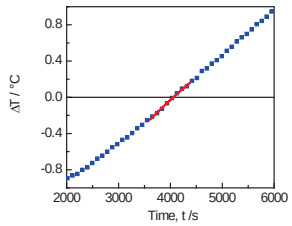

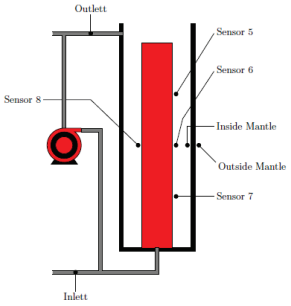

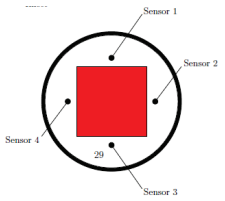

- Define temperature sensors to be used
- Define analytical function to determine temperature gradient
- Define optimum time region to fit
- Define selection criteria for high quality data

⇒ Completely independent by JRC/JSI and SKB/Vattenfall

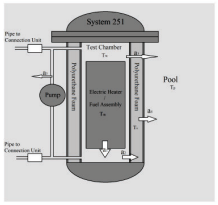

CALIBRATION BY ELECTRICAL HEATER: RESULTS JRC/JSI

Small differences partly due to differences in heat delivered by circulation pump

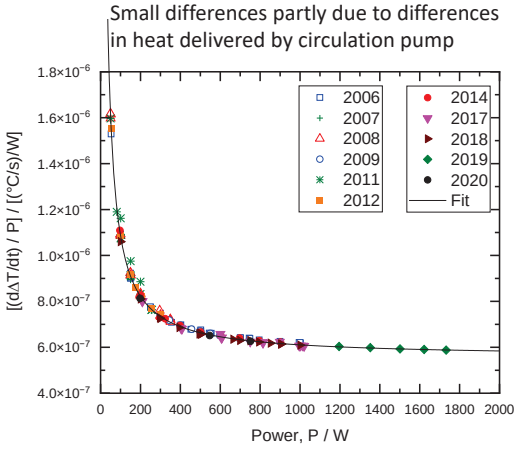

Calibration for blind test and SKB-50 data

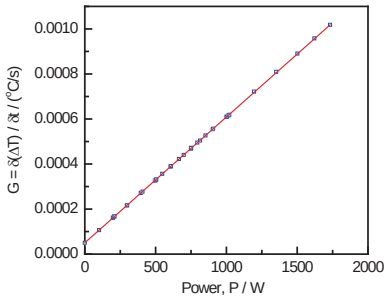

Perfect linear behaviour in whole range: from 0 W to 1800 W
No separation needed between low and high heat output as in R-05-62 report!
Offset due to heat produced by circulation pump

CALIBRATION BY ELECTRICAL HEATER: RESULTS JRC/JSI

Data within 0.5% for 95% confidence limit

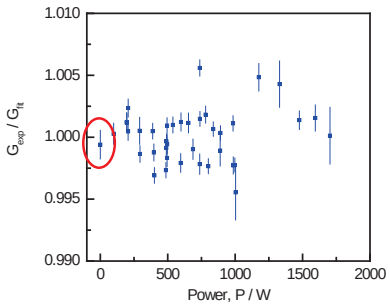

Calibration for blind test and SKB-50 data

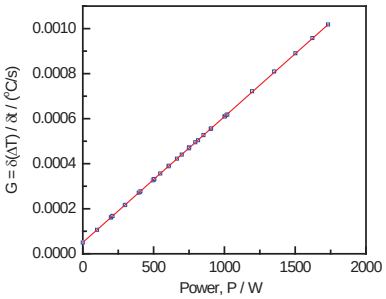

Measurement without heater: fully consistent
(heat delivered by circulation pump)

BLIND TEST: DECAY HEAT DERIVED FROM CALORIMETER DATA

Correction for difference heater and assembly : K = 0.915

Assembly ID	Decay heat derived from calorimeter measurements, P/ W			
	Blind test paper	JRC/JSI* heater correction	JRC/JSI not corrected	SKB/Vattenfall
BT01	1604	1584.0	1582.0	1580.0
BT02	1038	1022.6	1021.2	1019.3
BT03	874	859.6	858.5	857.0
BT04	753	740.8	739.8	738.8
BT05	651	640.2	639.3	638.5

Average ratio: 0.999

*includes a small bias correction on the output of the electrical heater, P = 0.182W + 1.00114 P_h

BLIND TEST: CORRECTION FOR GAMMA-RAY ESCAPE

See presentations A. Mehic and G. Letnar

- Dose rate measurements combined with analytical geometry correction
  - Blind test paper

- Gamma-ray transport simulations combined with nuclide inventory
  - SKB/Vattenfall : MCNP + CASMO
  - JRC/JSI : SERPENT + SERPENT(inventory)/MCNP(Bremstrahlung)

Assembly ID	Escaping gamma-ray energy, P_γ / W		
	Blind test paper	JRC/JSI	SKB/Vattenfall
BT01	58 (10)	49.4	49.2
BT02	30 (5)	25.3	24.7
BT03	21 (4)	20.6	20.3
BT04	15 (3)	15.0	13.8
BT05	12 (2)	12.8	11.5

Maximum difference 1.3 W

BLIND TEST: COMPARISON EXPERIMENTAL DATA

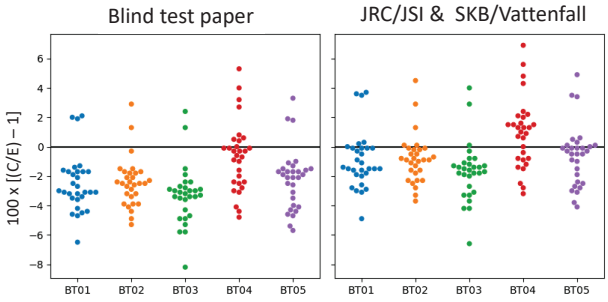

Assembly ID	CT	Average calculated	C/E	
		Blind test	Blind test Paper	JRC/JSI*
BT01	4.5 a	1620 W	0.975	0.992
BT02	8.6 a	1043 W	0.977	0.995
BT03 (+ Gd)	9.8 a	866 W	0.968	0.984
BT04	13.5 a	763 W	0.993	1.009
BT05	21.4 a	649 W	0.979	0.994

L. Fiorito

UNCERTAINTY EVALUATION: RANDOM EFFECTS

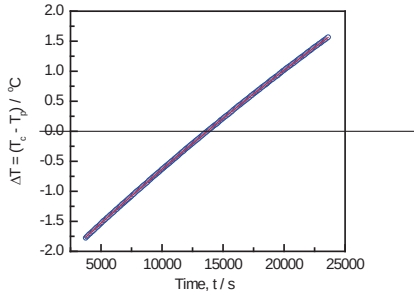

Platinum resistance thermometers (PT-100 type), with a declared uncertainty of 0.01 °C.

The measured quantity is a temperature difference!

Variance analysis from calibration data ($\chi^{2}/\nu = 1$)

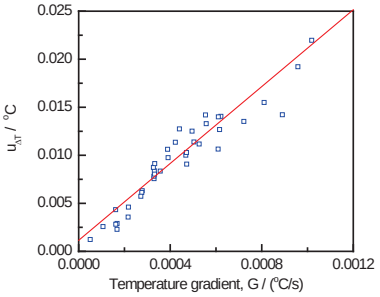

All data consistent with $u_{\Delta T} = a_0 + a_1 G$

$a_0 = 0.0015$ °C

$a_1 = 20$ s

UNCERTAINTY EVALUATION: RANDOM EFFECTS

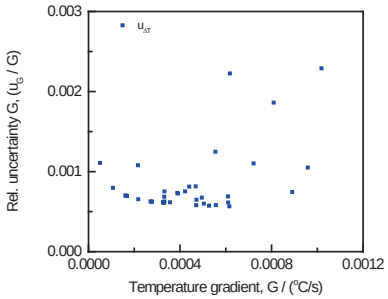

⇐

Variance analysis from calibration data ($\chi^{2}/\nu = 1$)

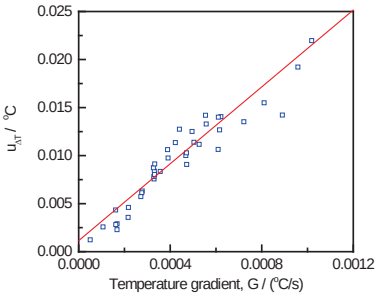

All data consistent with $u_{\Delta T} = a_0 + a_1 G$

$a_0 = 0.0015$ °C

$a_1 = 20$ s

UNCERTAINTY EVALUATION: RANDOM EFFECTS

$$C\,\frac{\partial T_c}{\partial t} = \left[P - k\,(T_c - T_p)\right]$$

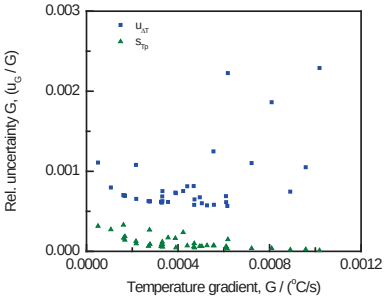

⇐

Pool temperature variations

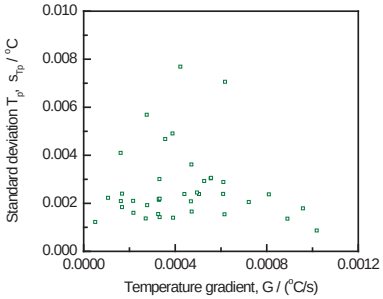

UNCERTAINTY EVALUATION: RANDOM EFFECTS

Uncertainty on temperature difference
Temperature variations in pool

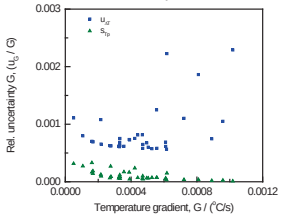

Variations in heater output

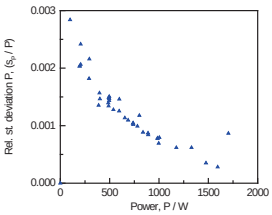

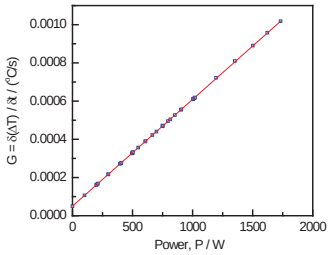

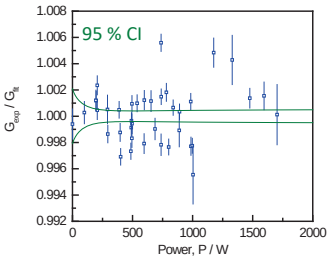

UNCERTAINTY EVALUATION: RANDOM EFFECTS

Uncertainty on temperature difference
Temperature variations in pool

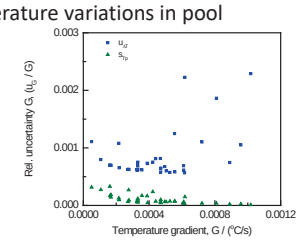

Variations in heater output

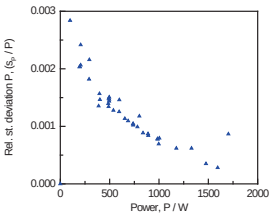

Scatter of data cannot be explained by propagating the uncertainty of random effects
⇒ All data suffer from a 0.25% (CI 68%) additional uncertainty due to hidden effect

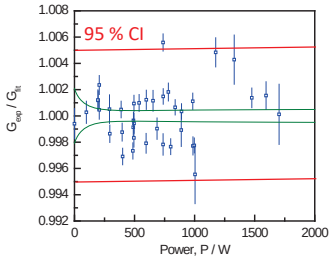

UNCERTAINTY EVALUATION: SYSTEMATIC EFFECTS (ELECTRICAL HEATER)

- Power meter (ION7600) of electrical heater is calibrated by an accredited service using an independent reference instrument
- Calibration data shows that the power P_h derived by the ION7600 suffers from a small bias effect
  ⇒ correction: $P = c_o + c_1 P_h$ (c_o = 0.182 W and c_1 = 1.00114)
- 95% confidence interval after correction
  - 0.60 % at 0 W
  - 0.13 % at 2000 W

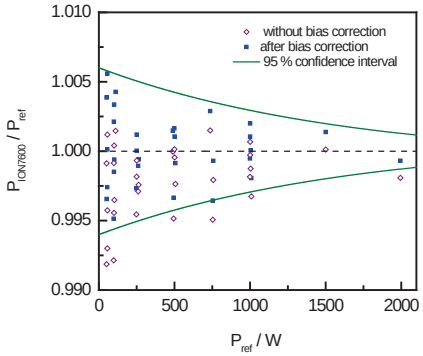

UNCERTAINTY EVALUATION: SYSTEMATIC EFFECTS (ELECTRICAL HEATER)

- Loss of the power provided by the calibration unit due to cables outside the calorimeter
  The heat loss is estimated from the length and electrical resistance per unit length
  - Outside
    - Length: 2 x 20 m
    - Resistance per unit length: 0.012 Ω/m
  - Inside (heating cable in calorimeter)
    - Length: 261 m
    - Resistance per unit length: 0.10 Ω/m

  ⇒ Power loss fraction: 26.1/(26.1 + 0.48) = 0.982

- No uncertainty data provided
  ⇒ uncertainty evaluation based on least significant figure combined with rectangular distributions

- Probability distribution of correction factor can be approximated by a Gaussian distribution with
  - mean : 0.982
  - standard deviation : 0.00135

UNCERTAINTY EVALUATION FUEL ELEMENT

- Systematic effects
  - Heat loss in cables
  - Bias on power meter of heater

  Combined uncertainty

Power	100 x s_P/P	95% CI
0	0.34	0.67
1000	0.20	0.40
2000	0.15	0.30

  - Calibration constants (negligible)
  - + 0.25% (1 st. dev) for hidden effect

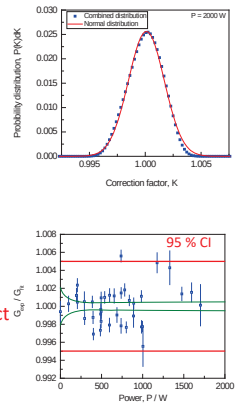

- Random effects
  - Uncertainty temperature difference
  - Pool temperature variations

  (negligible)

CORRECTION FACTOR: HEATER - ASSEMBLY

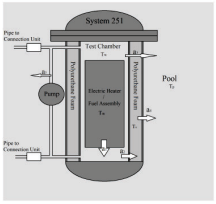

Present correction factor: based on one component heat transfer model (for PWR K = 0.915).
Verify by a three component heat transfer model

$$C_m \frac{dT_m}{dt} = -a_1(T_m - T_w) + Q_m$$

$$C_w \frac{dT_W}{dt} = a_1(T_m - T_w) - a_2(T_w - T_s) - a_3(T_w - T_p) + Q_w + a_c(T_w - T_c)$$

$$C_s \frac{dT_S}{dt} = a_2(T_w - T_s) - a_4(T_s - T_p)$$

Index:
- m : metal (heater or assembly)
- w : water
- s : structure
- p : pool

Parameters/variables
- T : temperature
- C : heat capacity
- a : heat transfer coefficient
- Q : heat source

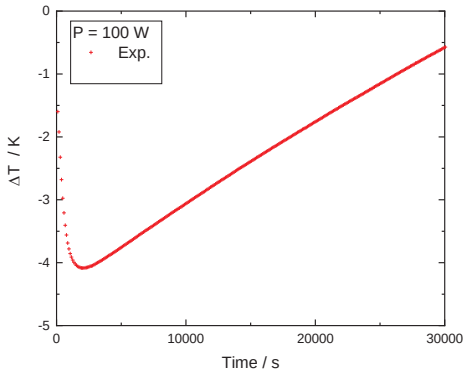

CORRECTION FACTOR: HEATER - ASSEMBLY

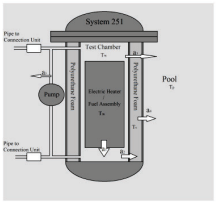

Present correction factor: based on one component heat transfer model (for PWR K = 0.915).
Verify by a three component heat transfer model

$$C_m \frac{dT_m}{dt} = -a_1(T_m - T_w) + Q_m$$

$$C_w \frac{dT_W}{dt} = a_1(T_m - T_w) - a_2(T_w - T_s) - a_3(T_w - T_p) + Q_w + a_c(T_w - T_c)$$

$$C_s \frac{dT_S}{dt} = a_2(T_w - T_s) - a_4(T_s - T_p)$$

Index:
- m : metal (heater or assembly)
- w : water
- s : structure
- p : pool

Parameters/variables
- T : temperature
- C : heat capacity
- a : heat transfer coefficient
- Q : heat source

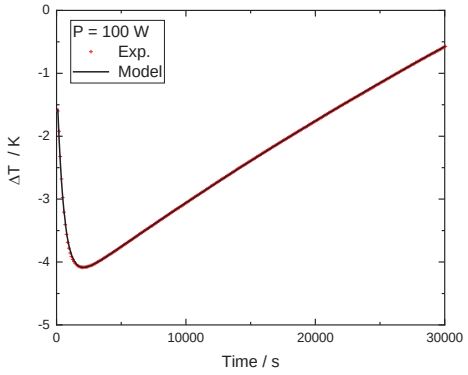

CORRECTION FACTOR: HEATER - ASSEMBLY

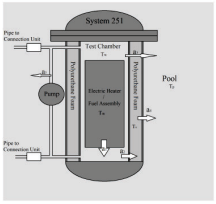

Present correction factor: based on one component heat transfer model

Verify by a three component heat transfer model

$$C_m \frac{dT_m}{dt} = -a_1(T_m - T_w) + Q_m$$

$$C_w \frac{dT_w}{dt} = a_1(T_m - T_w) + a_2(T_s - T_p) + Q_w + a_c(T_w - T_c)$$

$$C_s \frac{dT_S}{dt} = a_2(T_w - T_s) - a_4(T_s - T_p)$$

Work in progress

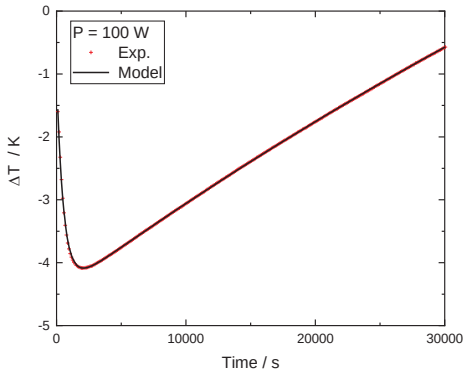

Index:
- m : metal (heater or assembly)
- w : water
- s : structure
- p : pool

Parameters/variables
- T : temperature
- C : heat capacity
- a : heat transfer coefficient
- Q : heat source

CLAB CALORIMETER: CONCLUSIONS

- Decay power from CLAB calorimeter are valuable (high quality) data for code validation
  - Measurement process and analysis procedures of CLAB calorimeter are well understood
  - Some previous results suffer from a bias effect
  - Uncertainty evaluation in progress
    - Preliminary estimation (95% confidence limit) : < 2%
    - ***Main task: evaluate factor to correct for difference heater – assembly***
- Performance of present calorimeter can be improved:
  - Control characteristics of cables of the heater (length, resistivity, etc..)
  - Regular calibration of heater with reference instrument
  - Improved operational procedure, e.g.
    - Minimum cooling temperature
    - Perform long measurements to verify K based on steady-state condition

NDA: GAMMA-RAY SPECTROSCOPY

Used as part of Radiochemical analysis of PIE data (see presentation S. Van Winckel)

NDA: Direct measurements (no chemistry)

- Axial BU profile determination (presentation K. Govers, J. Kirkegaard)
  - e.g. Govers et al., Technical Report – BLG – 1142, April 2019, "Characterization of Belgian Spent Fuel Assemblies"
- Determination of nuclide inventory ratios
  - e.g. Caruso et al., ($^{134}Cs/^{137}Cs$, $^{134}Cs/^{154}Eu$ ratios (comparison with HPLC-MC-ICP-MS) (Nucl. Instr. Meth. A 589 (2008) 425)
    High-performance liquid chromatography coupled to inductively coupled plasma – Mass spectrometry
- Tomography: material properties
  - e.g. Caruso et al., J. Nucl. Sci. Techn. 45 (2008) 828
    Holcombe et al., Nucl. Instr. Meth. A 837 (2016) 99

NDA: GAMMA-RAY SPECTROSCOPY FOR CODE VALIDATION

Axial BU profile determination

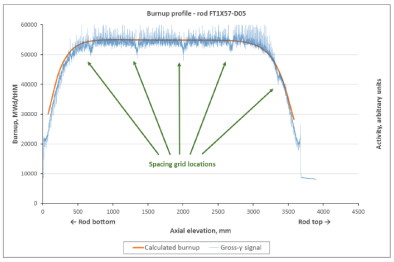

Figure 44 Calculated burnup axial profile for the same fuel rod as in Figure 43. The measured gross-gamma scan, dominated by the Cs-137 signal and, hence, roughly proportional to the burnup is superimposed. Spacer grid positions are easily identified on the activity signal, as they induce a local loss of power (loss of moderation).

Spent nuclear fuel rod

- rod D05 of FT1X57 (PWR)
- PWR Assembly (15 x 15):
  188 UO_2 rod (4.5 wt% $^{235}U/U$) and 16 $(U,Gd)O_2$ rods
- Irradiated at Tihange 1
- Rod used for other international project
  (First-Nuclides, REGAL, WETFUEL & AGAF, SF-ALE)

Govers et al., Technical Report – BLG – 1142, April 2019,
"Characterization of Belgian Spent Fuel Assemblies"

NEUTRON EMISSION: ABSOLUTE MEASUREMENTS OF SNF SEGMENT SAMPLE

Non Destructive Assay method to determine the neutron output of a **SNF** segement sample under **standard controlled area** conditions

Collaboration SCK CEN

Hot cell (LHMA) facility at SCK CEN

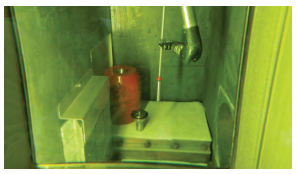

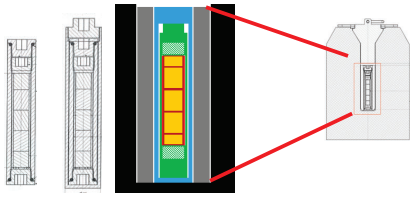

Standard controlled area

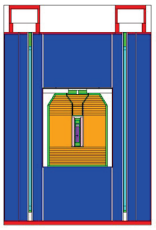

NEUTRON EMISSION: ABSOLUTE MEASUREMENTS OF SNF SEGMENT SAMPLE

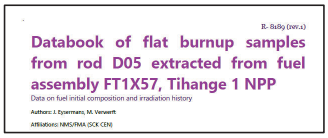

Hot cell (LHMA) facility at SCK CEN

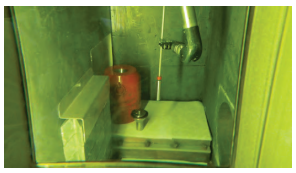

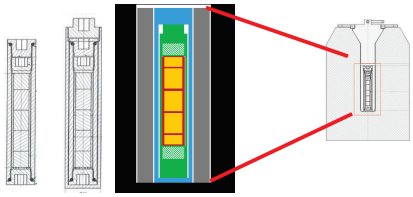

Standard controlled area

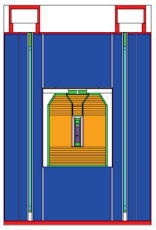

EURAD: VALIDATION OF DEPLETION CODES USING THE REGAL SAMPLE

- **Irradiation history** of the SNF
  - Segment (~ 50 mm) from rod D05 of FT1X57 (PWR)
  - PWR Assembly (15 x 15):
    188 UO_2 rod (4.5 wt% $^{235}U/U$) and 16 $(U,Gd)O_2$ rods
  - Irradiated at Tihange 1
  - Rod used for other international project
    (First-Nuclides, REGAL, WETFUEL & AGAF, SF-ALE)
- **SNF** segment **sample** by **NDA**

  Part of a set of 4 samples (**REGAL project**)
  - **Radiochemical analysis (BU)**
  - Microstructural analysis
  - Leach tests (low O_2)
  - Leach tests (high O_2)

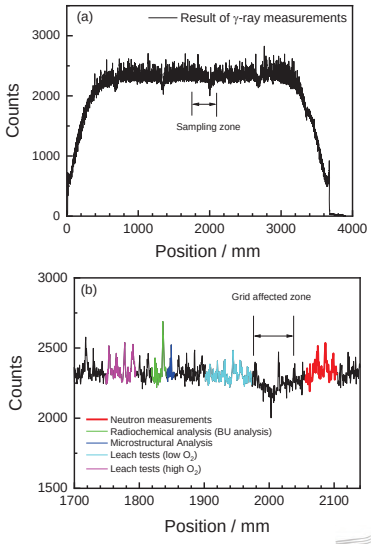

NEUTRON EMISSION: ABSOLUTE MEASUREMENTS OF SNF SEGMENT SAMPLE

- Irradiation history burnup (REGAL project)

BU indicator	Analysis date	Nuclide Inventory N_X/N_U	BU MWd/kg
^{137}Cs	21/10/2013	2.539 (55) x 10^{-3}	52.6 (11)
$^{143+144}Nd$	05/02/2014	5.701 (60) x 10^{-3}	53.95 (56)
$^{145+146}Nd$	05/02/2014	3.643 (38) x 10^{-3}	53.05 (56)
^{148}Nd	05/02/2014	0.974 (21) x 10^{-3}	53.3 (12)
^{150}Nd	05/02/2014	0.463 (21) x 10^{-3}	52.2 (23)
			Average: 52.78 (37)

Govers et al., EPJ Nucl. S&T, 8 (2022) 18

- SNF segment sample: characteristics

Parameter	Value
Segment length	52.01 (4) mm
Segment weight	42.616 (1) g
Cladding weight	6.71 (4) g
Net fuel weight	35.91 (4) g

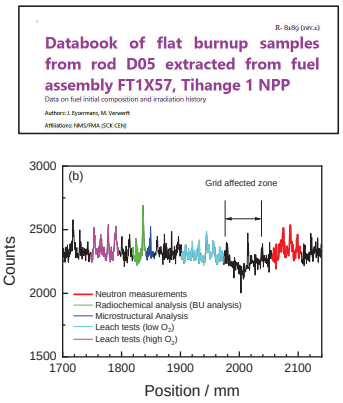

⇒ Accurate information about design and operational history

NEUTRON EMISSION MEASUREMENT: CONVENTIONAL WELL COUNTER (AWCC)

Standard controlled area

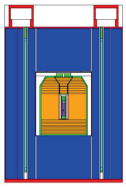

- Neutron detection
  - Modified AWCC (only internal cavity)
  - ^{3}He detectors in polyethylene
  - Detection efficiency for ^{252}Cf(sf): $\varepsilon = 0.28$
- Signal processing: shift register
  - Totals, reals and accidentals
- Data analysis: Hage's point model (JRC Ispra)

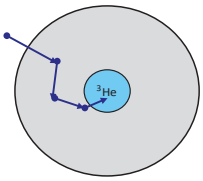

W. Hage and D.M. Cifarelli, NSE 89 (1985) 159 – 176
W. Hage and D.M. Cifarelli, NIMA 236 (1985) 165 – 177
D.M. Cifarelli and W. Hage, NIMA 251 (1986) 550 – 563

SHIFT – REGISTER: PRINCIPLE

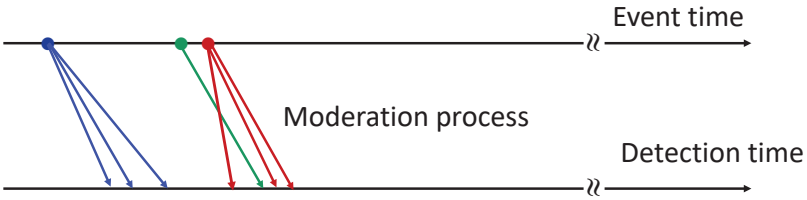

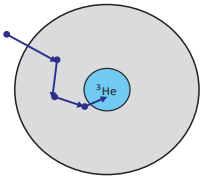

Every detected neutron will trigger the opening of two gates
- Gate close to the signal (signal trigger)
- Delayed gate

SHIFT – REGISTER: PRINCIPLE

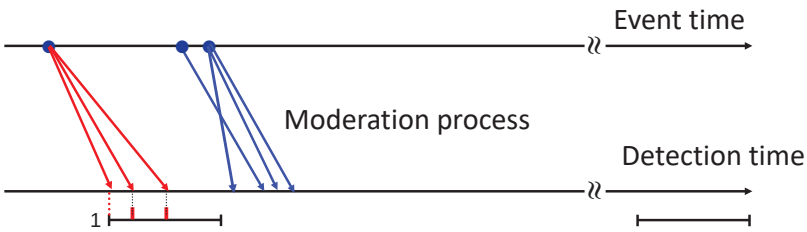

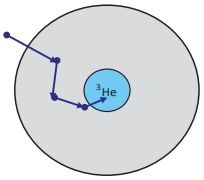

Signal trigger
R + **A**

Delayed trigger
A

SHIFT – REGISTER: PRINCIPLE

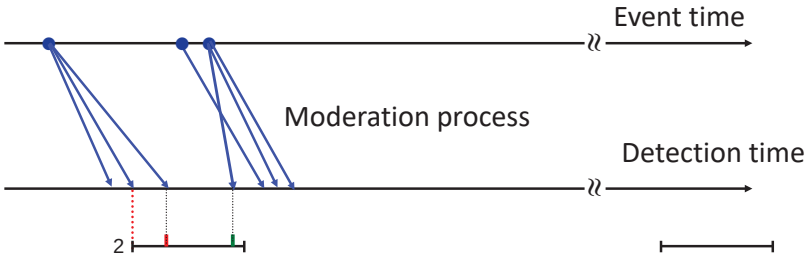

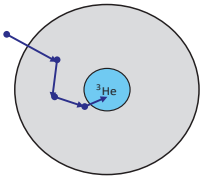

Signal trigger
R + **A**

Delayed trigger
A

SHIFT – REGISTER: PRINCIPLE

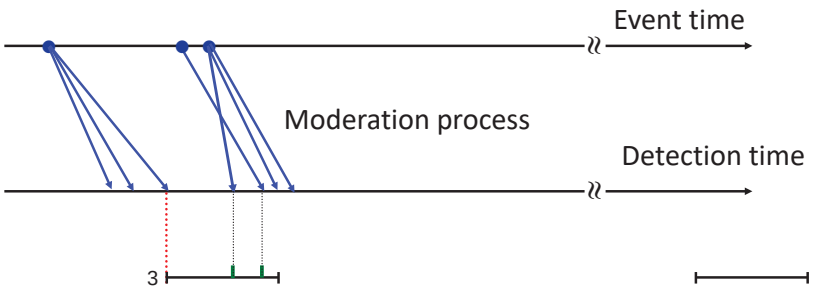

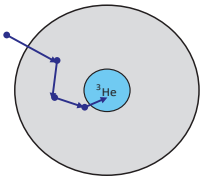

Signal trigger
R + **A**

Delayed trigger
A

SHIFT – REGISTER: PRINCIPLE

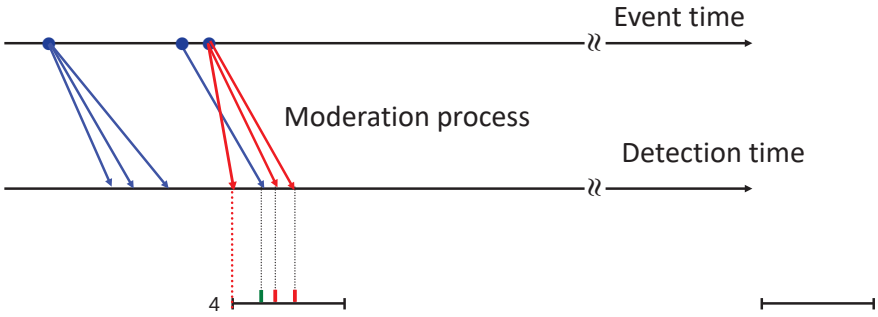

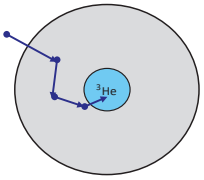

Signal trigger
R + **A**

Delayed trigger
A

SHIFT – REGISTER: PRINCIPLE

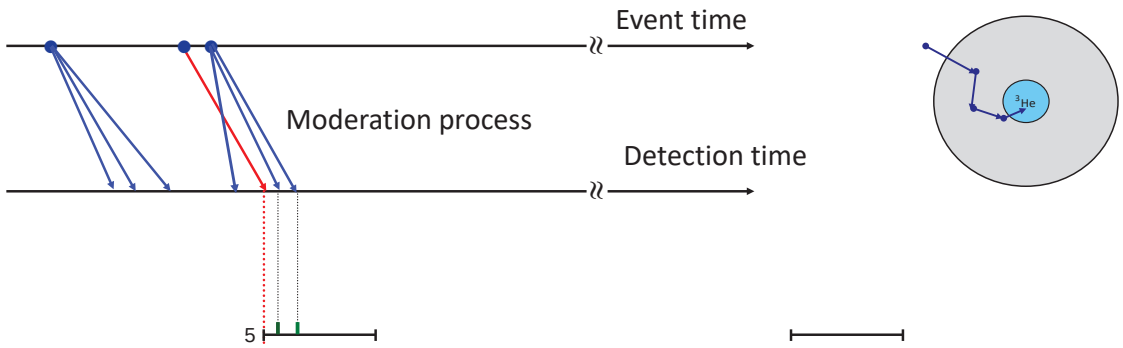

Signal trigger
R + **A**

Delayed trigger
A

SHIFT – REGISTER: PRINCIPLE

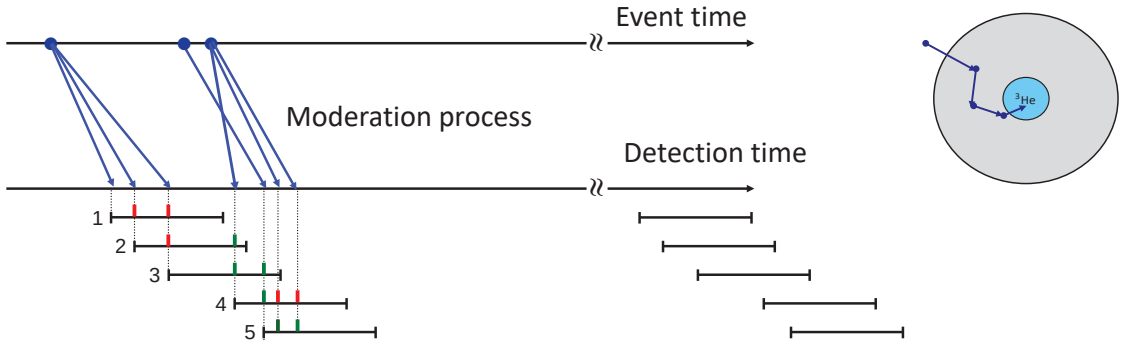

Signal trigger
R + **A**

Delayed trigger
A

SHIFT – REGISTER: PRINCIPLE

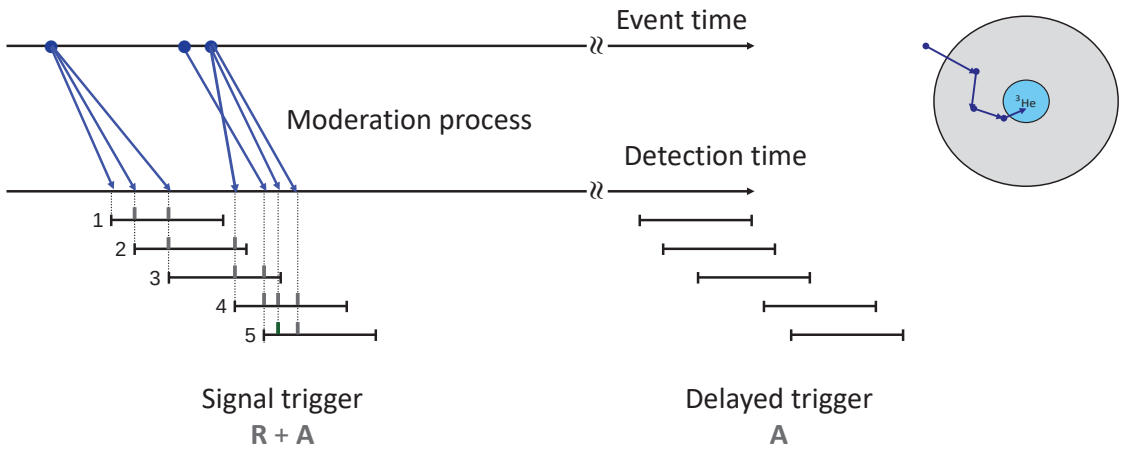

DATA ANALYSIS: HAGE'S POINT MODEL

$$\mathbf{T} = \varepsilon_{sf}\,\mathbf{S_{sf}}\,M\,[1+\alpha]$$

$$\mathbf{R} = \varepsilon_{sf}^{2}\,f\,\mathbf{S_{sf}}\,M^{2}\left[\frac{\nu_{sf(2)}}{\nu_{sf(1)}} + \frac{\nu_{(2)}}{\nu_{(1)}-1}\,(M-1)(1+\alpha)\right]$$

- Experiment
  - T : total count rate corrected for dead time and background
  - R : reals count rate corrected for dead time and background
- Detector characteristics
  - ε_{sf} : detection efficiency
  - f : gate fraction
- Nuclear data
  - $\nu_{sf(1)}$ and $\nu_{sf(2)}$: 1st and 2nd order factorial moments of P(ν) distribution for (sf)
  - $\nu_{sf(1)}$ and $\nu_{sf(2)}$: 1st and 2nd order factorial moments of P(ν) distribution for (n,f)
- Sample properties
  - **S_{sf} : production rate for prompt fission neutrons by (sf)**
  - α : ratio between neutron production rate by (α,n) and S_{sf}
  - M : neutron leakage multiplication (derived by MC simulations, M ≈ 1.006)

W. Hage and D.M. Cifarelli, NSE 89 (1985) 159 – 176
W. Hage and D.M. Cifarelli, NIMA 236 (1985) 165 – 177
D.M. Cifarelli and W. Hage, NIMA 251 (1986) 550 – 563

NEUTRON EMISSION: ABSOLUTE MEASUREMENTS OF SNF SEGMENT SAMPLE

Standard controlled area

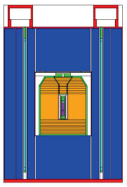

S_{sf} = 678 (12) $s^{-1}\,g^{-1}$

α = 0.039 (18)

Uncertainty evaluation and sensitivity analysis

Uncertainty component, x_j	$\frac{u_{x_j}}{x_j}$	$\frac{u_{S_{sf},j}}{u_{S_{sf}}}$	$\frac{u_{\alpha j}}{u_\alpha}$
Totals rate, T	0.0008	< 0.01	0.05
Reals rate, R	0.0027	0.15	0.17
Detection efficiency, ε_{sf}	0.0055	0.60	0.35
Gate fraction, f	0.0071	0.40	0.45
First order factorial moment, $\nu_{sf(1)}$	0.0037	0.20	0.25
Second order factorial moment, $\nu_{sf(1)}$	0.0120	0.67	0.80
Multiplication, M	0.0020	0.01	< 0.01

⇒ Improve
- detector characteristics
- nuclear data

Schillebeeckx et al., Frontiers in Energy Research 11 (2023) 1162367

NEUTRON EMISSION: ABSOLUTE MEASUREMENTS OF SNF SEGMENT SAMPLE

Standard controlled area

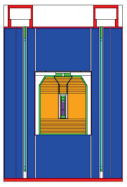

S_{sf} = 678 (12) $s^{-1}\,g^{-1}$

$S_{\alpha n} / S_{sf}$ = 0.039 (18)

Good agreement with:

Calculated from radiochemical analysis :
S_{sf} = 699 (28) $s^{-1}\,g^{-1}$

Note: uncertainty radiochemical analysis > 4%
(> factor 2)

NEUTRON EMISSION: ABSOLUTE MEASUREMENTS OF SNF SEGMENT SAMPLE

Code	Library	C/E LIB
ALEPH2	JEFF-3.3	0.944
SCALE	ENDF/B-VII.0	0.963
Serpent2 (2.1.29)	ENDF/B-VII.0	1.008
	ENDF/B-VII.0	1.017
	ENDF/B-VII.0	1.015
	JEFF-3.1.2	0.933
	JEFF-3.3	0.969
	JEFF-3.3 (1)	1.091
	JEFF-3.3 (2)	1.013
	JEFF-3.3 (3)	1.006
	JEFF-4T1	0.977
	JEFF-4T2	0.998
	JENDL-4.0u (4)	
	JENDL-5.0	1.089

S_{sf} = 678 (12) $s^{-1} g^{-1}$

All calculations normalised to produce the same ^{148}Nd inventory

Importance of normalization
(1) σ(n,γ) = 0 for ^{147}Nd
(2) σ(n,γ) for ^{147}Nd from JENDL-4.0u
(3) σ(n,γ) for ^{147}Nd from JEFF-4T1

NEUTRON EMISSION: ABSOLUTE MEASUREMENTS OF SNF SEGMENT SAMPLE

Code	Library	C/E LIB
ALEPH2	JEFF-3.3	0.944
SCALE	ENDF/B-VII.0	0.963
Serpent2 (2.1.29)	ENDF/B-VII.0	1.008
	ENDF/B-VII.0	1.017
	ENDF/B-VII.0	1.015
	JEFF-3.1.2	0.933
	JEFF-3.3	0.969
	JEFF-3.3 (1)	1.091
	JEFF-3.3 (2)	1.013
	JEFF-3.3 (3)	1.006
	JEFF-4T1	0.977
	JEFF-4T2	0.998
	JENDL-4.0u (4)	
	JENDL-5.0	1.089

S_{sf} = 678 (12) $s^{-1} g^{-1}$

Uncertainty theoretical estimation

Burnup	Relative uncertainty
10 MWd/kg	12.1 %
30 MWD/kg	11.1 %
50 MWd/kg	10.0 %

Contribution mainly from : ^{242}Pu(n,γ) & ^{243}Am(n,γ)

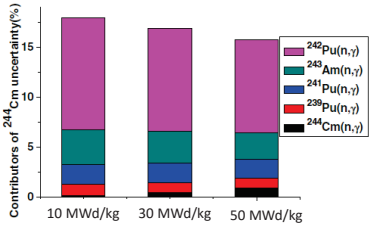

Tiejun Zu et al., Annals of Nuclear Energy 94 (2016) 399

NEUTRON EMISSION: DECAY DATA AND NU-BAR

Code	Library	S_{sf}/(1/gs) LIB	S_{sf}/(1/gs) REC	LIB/REC
ALEPH2	JEFF-3.3	640.1	642.4	0.996
SCALE	ENDF/B-VII.0	653.0	652.1	1.001
Serpent2 (2.1.29)	ENDF/B-VII.0	683.7	678.1	1.008
	ENDF/B-VII.0	689.4	685.3	1.006
	ENDF/B-VII.0	688.5	684.3	1.006
	JEFF-3.1.2	632.5	623.8	1.014
	JEFF-3.3	656.8	648.9	1.012
	JEFF-3.3 (1)	739.4	730.5	1.012
	JEFF-3.3 (2)	686.8	678.6	1.012
	JEFF-3.3 (3)	682.2	673.9	1.012
	JEFF-4T1	662.6	654.6	1.012
	JEFF-4T2	676.4	668.3	1.012
	JENDL-4.0u (4)		715.9	
	JENDL-5.0	738.4	733.9	1.006

REC (recommended data)

Decay data : DDEP
http://www.lnhb.fr/ddep_wg/

Neutron emission data: Santi and Muller
Nucl. Sci. Eng. 160 (2008) 199

NEUTRON EMISSION: DECAY DATA AND NU-BAR

Nuclide	Decay constant, λ / (1/s)		(sf) branching		nu-bar	
	ENDF/REC	JEFF/REC	ENDF/REC	JEFF/REC	ENDF/REC	JEFF/REC
^{238}U	1.0000	1.0000	1.0018	1.0018	1.0101	1.0101
^{238}Pu	1.0004	1.0005	1.0054	1.0054	1.0091	1.0091
^{240}Pu	1.0000	0.9997	1.0000	1.0000	0.9986	0.9986
^{242}Pu	0.9986	0.9986	1.0000	1.0000	0.9963	0.9963
^{242}Cm	0.9995	0.9996	0.9591	0.9591	0.9953	0.9953
^{244}Cm	0.9999	1.0061	1.0147	1.0147	0.9917	0.9917
^{246}Cm	0.9921	0.9970	0.9996	0.9996	1.0061	1.0061

- Differences not only due to neutron emission
- Largest difference between (sf) branching values
- Compensation effect for neutron emission of ^{244}Cm(sf)

NEUTRON EMISSION RATE

$N = aBU^b$
$b = 4$ for $BU > 20$ MWd/kg

$$\frac{\delta N}{N} = b\frac{\delta BU}{BU}$$

⇒ Total neutron emission extremely sensitive to BU

⇒ Good BU indicator

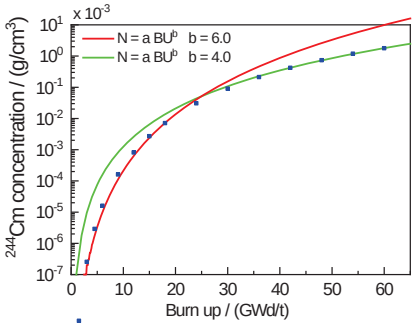

NEUTRON MEASUREMENTS: CONCLUSIONS

Neutron emission (sensitive to BU)

- Neutron measurements presented in this work is a valuable method for code validation
- Neutron measurements can be used to verify the BU of an SNF assembly in industrial conditions

Nuclear data:

- Recommended decay and neutron emission data not always adopted in evaluated data libraries
- ^{241}Pu(n,γ) and ^{243}Am(n, γ) cross sections require a re-evaluation (use of available experimental data)
- P(ν) of ^{244}Cm(sf) needs to be improved
- ^{147}Nd(n,γ) cross section in JEFF-3.3 and ENDF/B-VIII.0 are too high (important for normalisation of PIE data)
- Fission yields for ^{148}Nd in JENDL-5.0 are too low

TASK 2: PRODUCE VALIDATED DEPLETION CALCULATIONS WITH REALISTIC UNCERTAINTIES

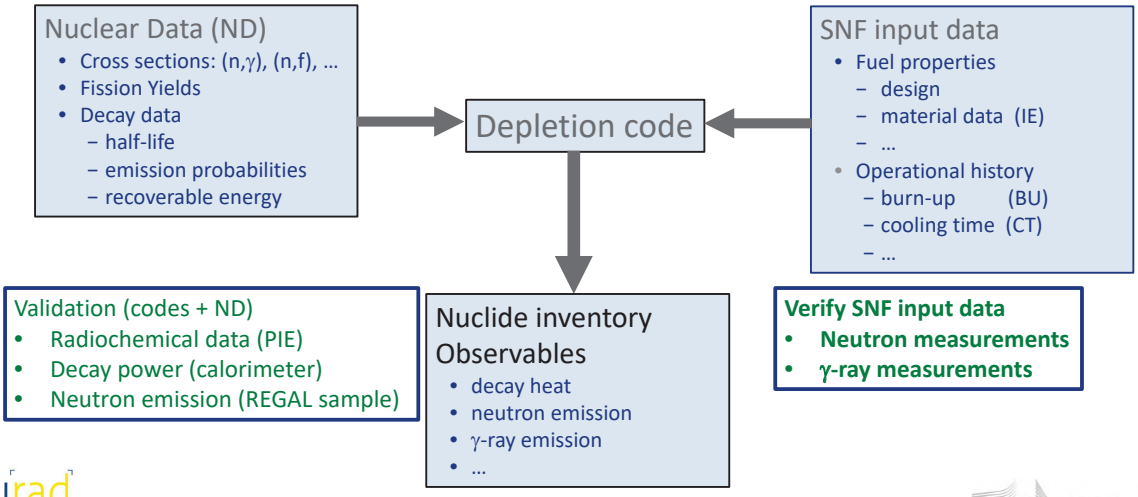

NDA FOR CHARACTERISATION OF FUEL ASSEMBLIES

- γ-ray spectroscopy
  - HPGe detector
  - Axial scanning
- FORK detector
  - Total neutron emission
  - Total γ-ray emission

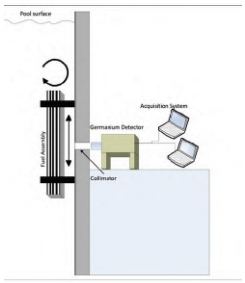

- DDSI (Differential Die-away Self Interrogation)
- PNAR (Passive Neutron Albedo Reactivity)

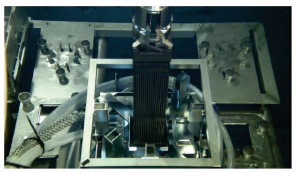

γ-RAY SPECTROSCOPIC MEASUREMENTS

- HP Ge detector
- Axial scanning

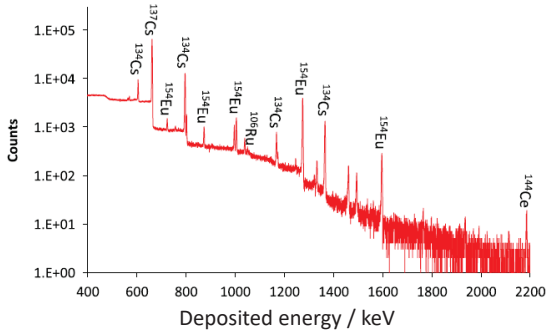

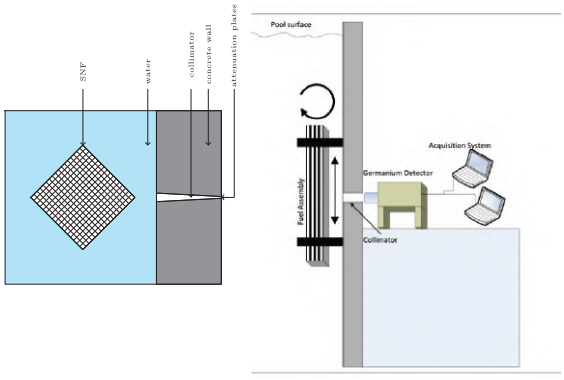

Solans et al., ANE 192 (2023) 109941
Bengtsson et al., Nucl. Techn. 208 (2022) 295
Vaccaro et al., NIMA A833 (2016) 208
Vo et al., NIMA 830 (2016) 325
Favalli et al., NIMA 820 (2016) 102

^{137}Cs: 662 keV
^{134}Cs: 605, 796, 1365 keV
^{154}Eu: 996, 1004, 1274, 1596 keV

^{137}Cs ACTIVITY

$\langle A_{cal}/A_{exp} \rangle = 1.39$
St. dev A_{cal}/A_{exp} = 3.3%

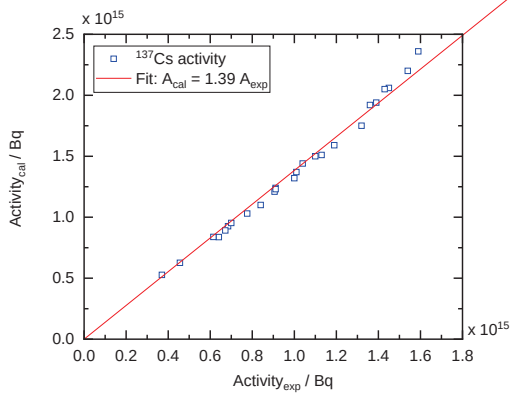

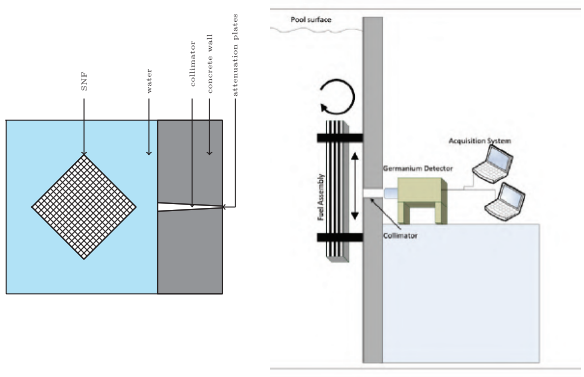

Bengtsson et al., Nucl. Techn. 208 (2022) 295

AXIAL PROFILE ^{137}CS ACTIVITY (BURNUP PROFILE)

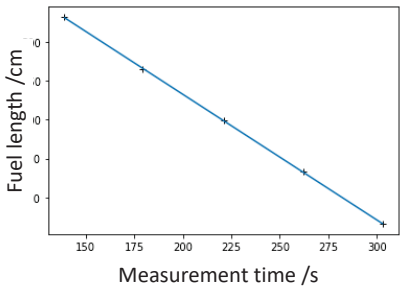

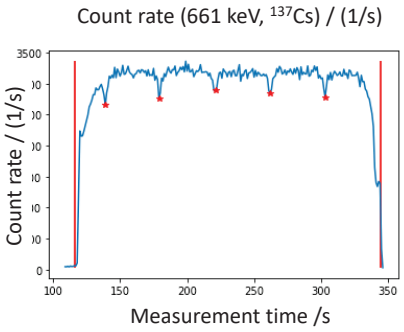

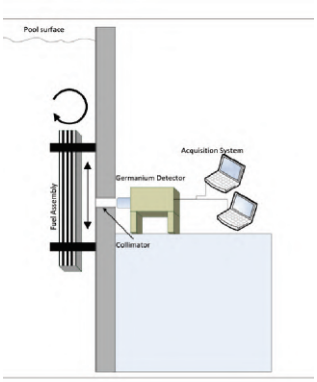

NEUTRON AND γ-RAY MEASUREMENTS: FORK DETECTOR

Passive NDA: detection of neutrons and γ-rays emitted by SNF assembly

- Neutron detection
  - ^{235}U fission chambers (FC)
  - Fission chamber with and without Cd
  - Total neutron count rate
- γ-ray detection
  - Ionisation chamber (IC)
  - Total γ-ray dose rate measurement

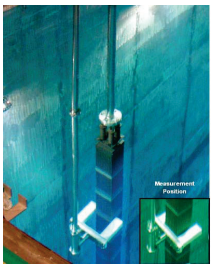

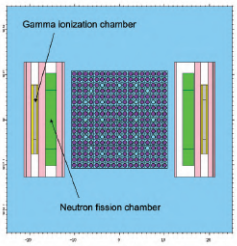

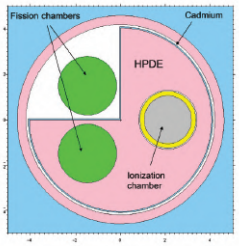

Vaccaro et al., NIMA 888 (2018) 202-217

FORK MEASUREMENTS AT CLAB

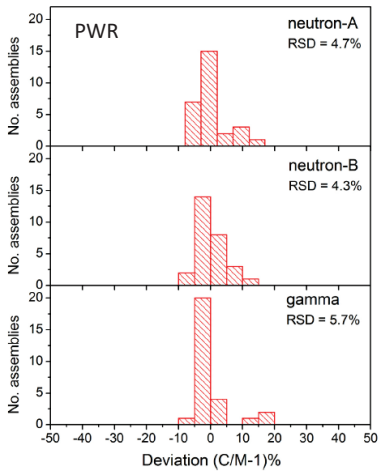

Fig. 10. Histogram distribution of the deviations between calculated (C) and measured (M) gamma, neutron-A, and neutron-B detector count rates for PWR assemblies measured at the Swedish Clab facility.

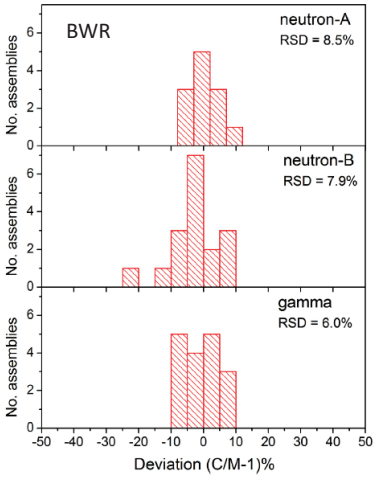

Fig. 11. Histogram distribution of the deviations between calculated (C) and measured (M) gamma, neutron-A, and neutron-B detector count rates for BWR assemblies measured at the Swedish Clab facility.

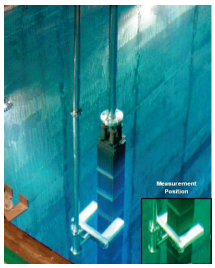

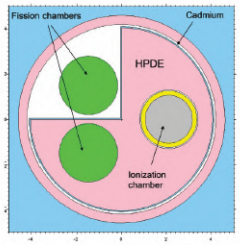

Vaccaro et al., NIMA 888 (2018) 202-217

DIFFERENTIAL DIE-AWAY SELF-INTERROGATION (DDSI)

Passive NDA: detection of neutrons emitted by SNF assembly
Developed at LANL for nuclear safeguards applications

- Neutron production
  - Primary neutrons: mainly prompt fission neutrons from ^{244}Cm(sf)
  - Prompt fission neutrons from neutron induced fission in fuel mainly after neutron moderation in the water of the pool
- Detection principle
  - ^{3}He in moderator
  - Detection of **correlated neutrons**: construct **Rossi-alpha distribution**

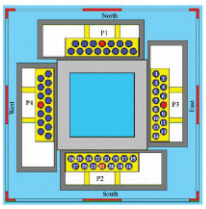

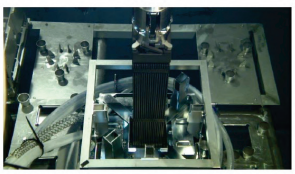

Trahan et al., NIMA 955 (2020) 163329

DDSI: ROSSI-ALPHA DISTRIBUTION

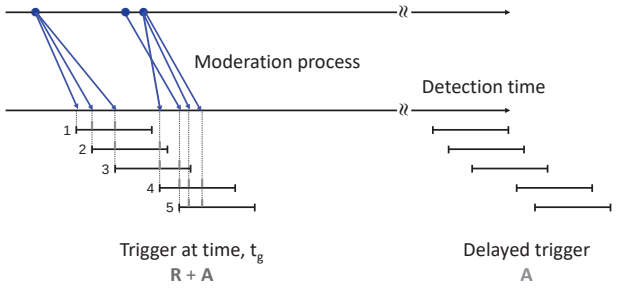

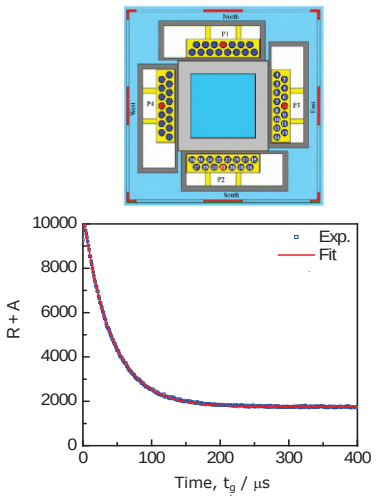

DDSI: ROSSI-ALPHA DISTRIBUTION

$$R = R_0 e^{-\frac{t}{\tau_e}}$$

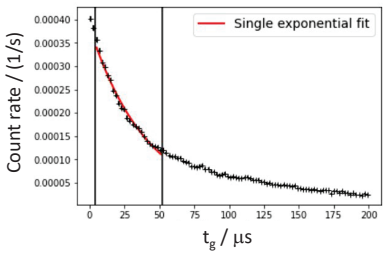

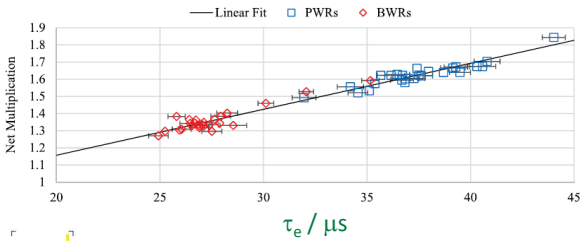

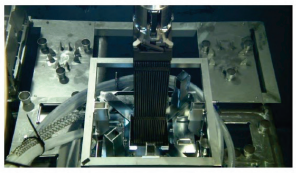

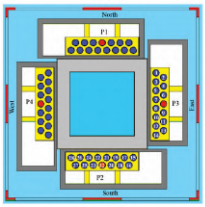

Trahan et al., NIMA 955 (2020) 163329

DDSI: ROSSI-ALPHA DISTRIBUTION

$$R = R_0 e^{-\frac{t}{\tau_e}}$$

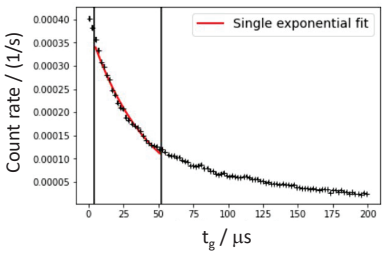

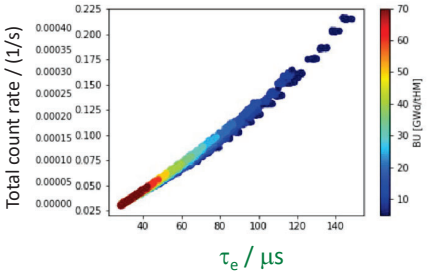

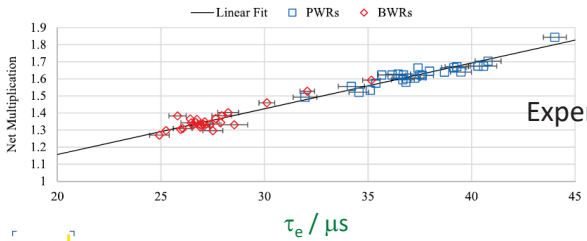

Experiments at CLAB

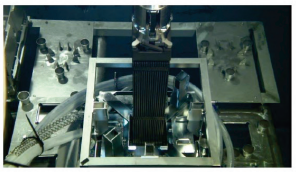

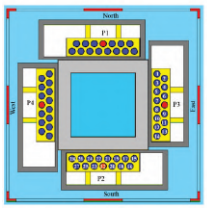

Trahan et al., NIMA 955 (2020) 163329

DDSI: MC SIMULATIONS

$$R = R_0 e^{-\frac{t}{\tau_e}}$$

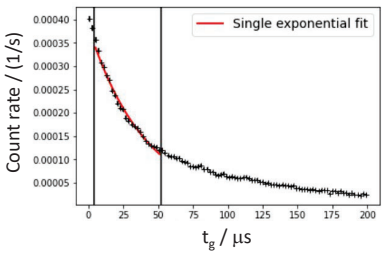

$$R = R_{01}\, e^{-\frac{t}{\tau_f}} + R_{02}\, e^{-\frac{t}{\tau_s}}$$

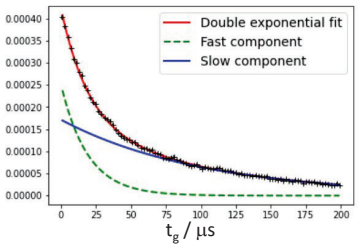

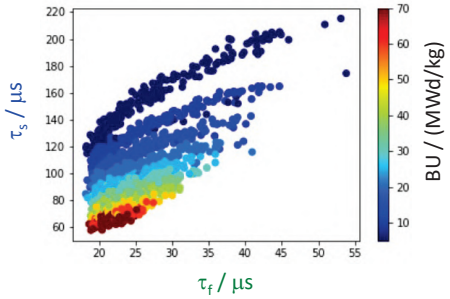

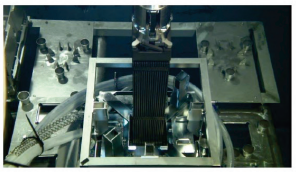

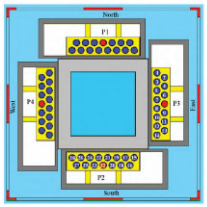

⇒ Additional information

Solans et al., IAEA Symposium, November 2022
IAEA-CN-303-137

DDSI: EXPERIMENTS AT CLAB

$R = R_0 e^{-\frac{t}{\tau_e}}$

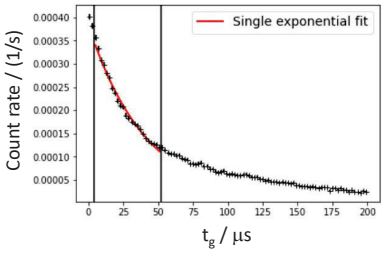

$R = R_{01}\, e^{-\frac{t}{\tau_f}} + R_{02}\, e^{-\frac{t}{\tau_s}}$

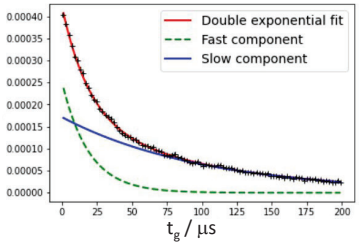

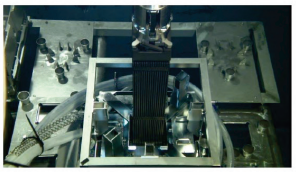

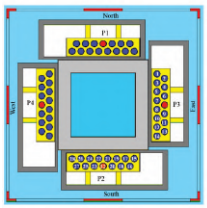

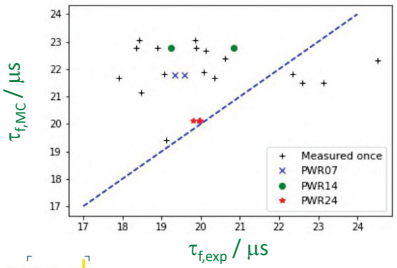

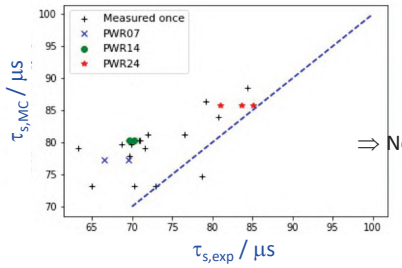

⇒ Not confirmed by experiment

Solans et al., IAEA Symposium, November 2022
IAEA-CN-303-137

FINLAND: ONKALO

Marita Mosconi

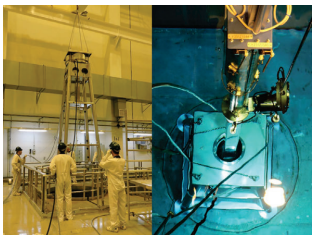

- Passive Neutron Albedo Reactivity (PNAR)
  LANL development, Tobin et al., NIMA 897 (2018) 32 - 37

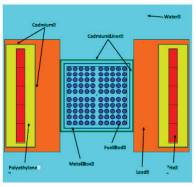

- Passive Gamma Ray Emission Tomography (PGET)
  IAEA development, Honkamaa et al., Symp. Int. Safeguards, IAEA Vienna 2014

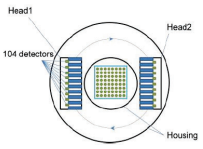

CONCLUSIONS

- NDA for code validation
  - Calorimeter at CLAB: ideal instrument to validate code performance for decay power prediction
  - Neutron correlation measurements is a valuable method to validate code performance for neutron emission predication and an alternative to radiochemical methods to determine the ^{244}Cm inventory
  - ND need to be improved to use neutron emission as BU indicator

- NDA of SNF assemblies
  - Methods based on neutron and gamma-ray emission detection require improvement

CONTRIBUTORS

F. Johansson	(SKB)
J. Kirkegaard	(Vattenfall)
S. Kopecky	(JRC Geel)
G. Letnar	(JSI)
A. Mehic	(SKB)
B. Pedersen	(JRC Ispra)
P. Romojaro	(SCK CEN)
V. Solans	(UU)
M. Verwerft	(SCK CEN)
G. Žerovnik	(JSI)

The school has been funded by the Euratom Research and Training Programme 2014-2018 under Grant Agreement No. 847552 (SANDA) and by ENEN2plus

BIBLIOGRAPHY

GUM: Guide to the expression of Uncertainty in Measurement

- Evaluation of measurements data (JCGM 100:2008(E))
- Supplement 1 – Propagation of distribution using a Monte Carlo method (JCGM 101:2008)
- Supplement 2 – Extension to any number of quantities (JCGM 102:2011)
- An introduction to the "GUM" and related documents (JCGM 104:2009)
- Guide to the expression of uncertainty in measurement Part 6: Developing and using measurement models (JCGM GUM-6:2020)

VIM: International Vocabulary of Metrology

- VIM – Basic and general concepts and associated terms (JCGM 200:2012)

https://www.bipm.org/en/committees/jc/jcgm/publications

Spent nuclear fuel observables and key nuclides

- Gauld et al., "Nuclide importance to criticality safety, decay heating and source terms related to transport and interim storage of high-burnup LWR fuel", Report NUREG/CR-6700, ORNL/TM-2000/284 (2001)
- Žerovnik et al. ,"Observables of interest for the characterisation of Spent Nuclear Fuel", EUR 29301 EN (2018) , JRC112361
- Schillebeeckx et al., "Characterisation of spent nuclear fuel by theoretical calculations and non-destructive analysis", JRC114178 (2019)

Nuclear data

- Nuclear data libraries at JANIS NEA, https://www.oecd-nea.org/jcms/pl_39910/janis
- Decay data, http://www.nucleide.org/DDEP.htm
- Nichols et al., "Handbook of nuclear data for safeguards: database extensions, august 2008", INDC-2453, INDC(NDS) – 0534

BIBLIOGRAPHY

Non-destructive assay of SNF

Calorimeter

- SKB, "Measurements of Decay Heat in Spent Nuclear Fuel at the Swedish Interim Storage Facility", Clab, SKB Report R-05-62, December 2006
- B.D. Murphy and I.C. Gauld, "Spent Fuel Decay Heat Measurements Performed at the Swedish Central Interim Storage Facility", Report ORNL/TM-2008/016, Oak Ridge National Laboratory, Feburary 2010

Neutron

- Schillebeeckx et al., "An absolute measurements of the neutron production rate of a spent nuclear fuel sample used for depletion code validation", Frontiers in Energy Research 11 (2023) 1162367
- Schillebeeckx et al., "A non-destructive method to determine the neutron production rate of a sample of spent nuclear fuel under standard controlled area conditions", JRC Technical Report EUR 30379 EN, 2020
- Tupasela et al., "Passive neutron albedo reactivity measurements of spent fuel nuclear fuel", Nucl. Instr. Meth. A986 (2020) 164707
- Trahan et al., "Results of the Swedish spent fuel measurements field trials with the DDSI", Nucl. Instr. Meth. A955 (2020) 163329
- Tobin et al., "Measuring spent fuel assembly multiplication in borated water with a PNAR instrument", Nucl. Instr. Meth. A897 (2018) 32
- Vaccaro et al., "Advancing the FORK detector for quantitative spent nuclear fuel verification", Nucl. Instr. Meth. A888 (2018) 202

γ-ray

- Solans et al., "Spent nuclear fuel passive gamma analysis and reproducibility application to SKB-50 assemblies", Ann. Nucl. Energy 192 (2023) 109941
- Bengtsson et al., "Experimental method for the verification of calculated ^{137}Cs content in nuclear fuel assemblies", Nucl. Techn. 208 (2022) 295
- Vaccaro et al., "PWR and BWR spent fuel assembly gamma spectra measurements", Nucl. Instr. Meth. A833 (2016) 208

Thank you

NRAS school: 13 – 17 May 2024
ENEN2+

EU countries

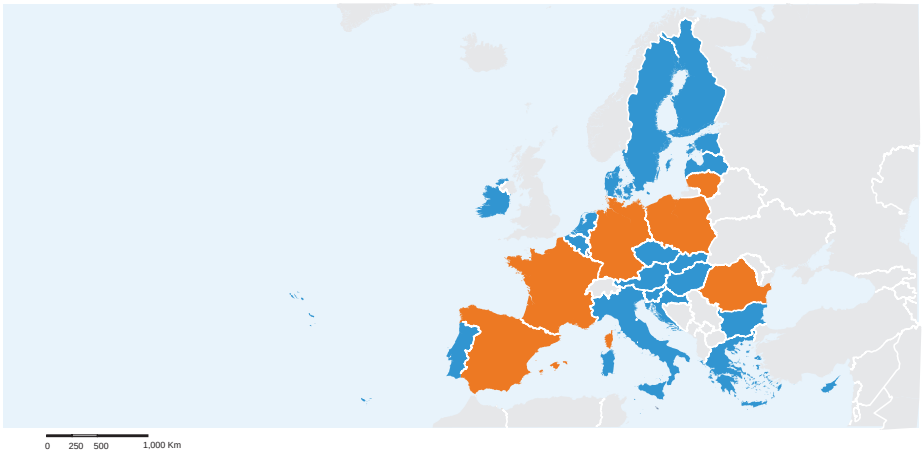

2.6 Observables of interest (in spent fuel); G. Žerovnik, JSI-; School on "Nuclear data for depletion calculations"11/09 - 15/09/2023

SANDA

Supplying Accurate Nuclear Data for energy and non-energy Applications

OBSERVABLES OF INTEREST (IN SPENT FUEL)

P. Schillebeeckx, G. Žerovnik

The school has been funded by the Euratom Research and Training Programme 2014-2018 under Grant Agreement No. 847552 (SANDA).

CONTENTS

NUCLEAR FUEL CYCLE

Nuclear fuel cycle (open or closed) produces waste

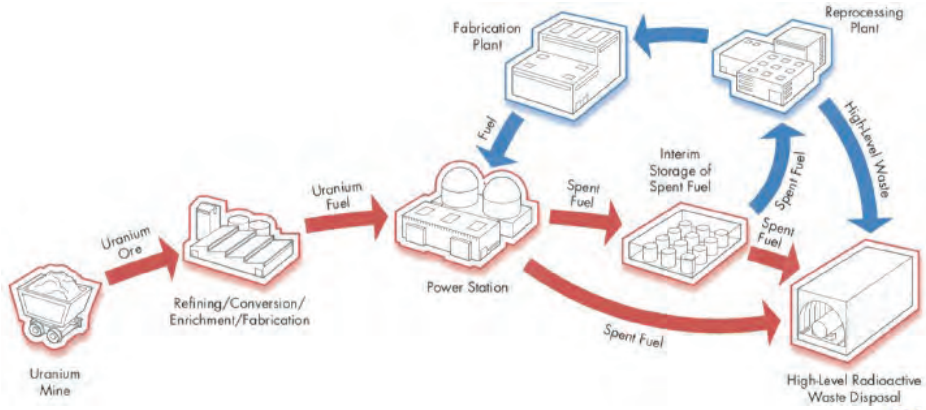

Training material

SNF CHARACTERISATION

An accurate characterisation of **Spent Nuclear Fuel** (SNF) is required for a **safe**, **ecological** and **cost effective** operation of the facilities involved in **SNF management** (transport**,** storage, handling, reprocessing and disposal):



- Decay heat : H
- Neutron emission : S_n
- γ-ray emission : S_γ
- Reactivity : ^{235}U, ^{239}Pu, Fission Products (BUC)
- Fissile material : ^{235}U, ^{239}Pu
- Long-term safety : e.g. ^{14}C, ^{36}Cl, ^{79}Se, ^{94}Nb, ^{99}Tc, ^{129}I, ^{226}Ra, ^{237}Np

- A reliable determination of these observables including **realistic uncertainties** requires a **good understanding** of the underlying physics **process**
- **Difficult** to be **measured** directly, in particular during **industrial operation**

Training material

SPENT NUCLEAR FUEL: NUCLIDE INVENTORY

- Fission products (FP): neutron induced fission (n,f)

  e.g. ^{90}Sr, ^{99}Tc, **^{137}Cs**, ^{154}Eu, …

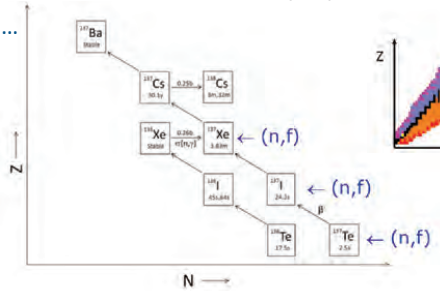

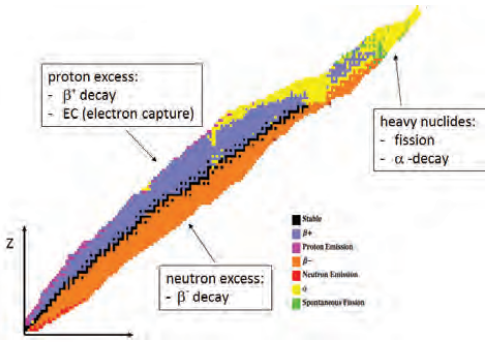

- Actinides: neutron induced capture (n,γ)

  e. g. ^{235}U, **^{238}U**, **^{239}Pu**, ^{241}Am, ^{244}Cm, …

$$n + {}^{238}_{92}U \xrightarrow{(n,\gamma)} {}^{239}_{92}U \xrightarrow[23.5\ min]{\beta^-} {}^{239}_{93}Np \xrightarrow[2.36\ d]{\beta^-} {}^{239}_{94}Pu$$

Training material

eurad 5

β⁻ - DECAY BY NEUTRON RICH NUCLIDES

Radioactive decay in which neutron is transformed into proton and electron + anti-neutrino are emitted

$$^{A}_{Z}X \rightarrow {}^{A}_{Z+1}Y^{*} + e^{-} + \bar{\nu}_e$$

$$\downarrow$$

$$^{A}_{Z+1}Y + E_\gamma$$

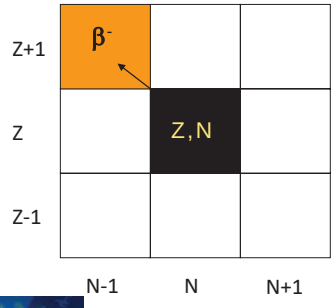

Anti-neutrino kinetic energy is not recoverable!

Training material

eurad 6

β^- - DECAY BY NEUTRON RICH NUCLIDES: e.g. ^{137}Cs

- $T_{1/2}$ = 30.05 (8) a
- Q_{β^-} = 1175.73 (17) keV

$$A = \lambda N = N \frac{\ln 2}{T_{1/2}}$$

$$P = \lambda N E_{rec}$$

$$E_{rec} = \sum_i P_{\gamma i} E_{\gamma i} + \langle E_{e-} \rangle < Q_{\beta-}$$

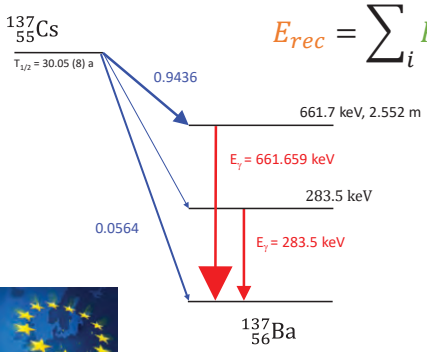

$$^{137}_{55}\mathrm{Cs} \rightarrow {}^{137}_{56}\mathrm{Ba}^* + \mathrm{e}^- + \bar{\nu}_\mathrm{e}$$

$$\downarrow$$

$$^{137}_{56}\mathrm{Ba} + E_\gamma$$

Gamma-ray emission probability: P_γ

E_γ	P_γ
661.7 keV	**0.8499 (20)**
283.5 keV	5.8 (8) × 10^{-6}

http://www.nucleide.org/DDEP_WG/Nuclides/Cs-137_tables.pdf

More in presentation by Mark Kellet

Training material

α - DECAY

Radioactive decay in which nucleus **emits α-particle** (^{4}He nucleus) and transforms into nucleus with 4 less nucleons (2n, 2p)

$$^{A}_{Z}X \rightarrow {}^{A-4}_{Z-2}\mathrm{Y}^* + \alpha$$

$$\downarrow$$

$$^{A-4}_{Z-2}\mathrm{Y} + E_\gamma$$

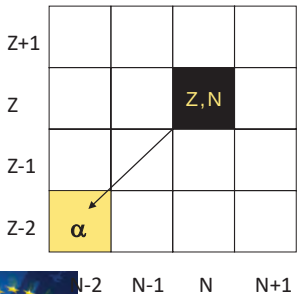

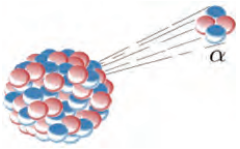

in heavy nuclei

Training material

α - DECAY BY ACTINIDES: e.g. ^{241}Am

- $T_{1/2}$ = 432.6 (6) a
- Q_α = 5637.82 (12) keV

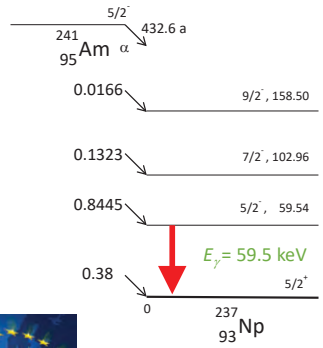

$$^{241}_{95}\mathrm{Am} \rightarrow {}^{237}_{93}\mathrm{Np}^{*} + \alpha$$
$$\downarrow$$
$$^{237}_{93}\mathrm{Np} + E_\gamma$$

α -particle emission probability:

E_α	P_α
5388.3 keV	0.0166 (3)
5442.9 keV	0.1323 (10)
5485.6 keV	**0.8445 (10)**

http://www.nucleide.org/DDEP_WG/Nuclides/Am-241_tables.pdf

$$E_{rec} = \sum_i P_{\gamma i} E_{\gamma i} + \sum_j P_{\alpha j} E_{\alpha j} = Q_\alpha$$

Training material

9

SPONTANEOUS FISSION

Fission: nucleus splits up into fission products (FP)

e.g. ^{238,240,242}Pu(sf), ^{242,244,246}Cm(sf), ^{252}Cf(sf)

- FP: acceleration due to Coulomb repulsion

- FP: strongly excited, emission of
  - Prompt fission neutrons (PFN)
  - Prompt fission γ-rays (PFG)

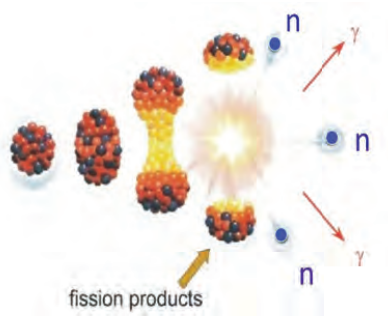

$$S_n = \lambda_{SF}\, N\langle\nu\rangle = \lambda\, x_{SF}\, N\langle\nu\rangle$$
$$P = \lambda_{SF}\, NE_{rec} = \lambda\, x_{SF}\, NE_{rec}$$

$$E_{rec} = \langle\nu\rangle\langle E_n\rangle + \langle\nu_\gamma\rangle\langle E_\gamma\rangle + \langle E_{rec,fp}\rangle$$

Prompt fission neutrons important for Non-Destructive Assay (NDA)

Training material

10

PROMPT FISSION NEUTRONS: MULTIPLICITY AND ENERGY

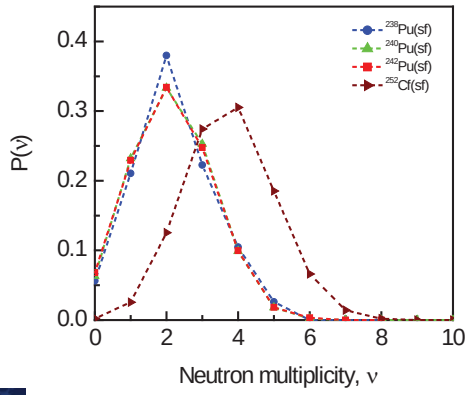

Emission of prompt fission neutrons:

- statistical process
- $\langle \nu \rangle > 1$

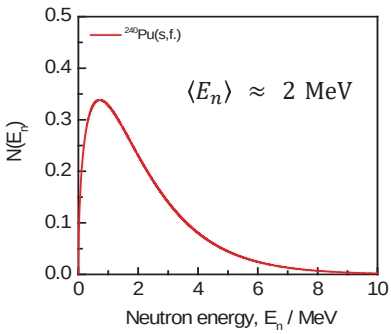

PROMPT FISSION NEUTRONS: EMISSION PROBABILITY

Nuclide	$T_{1/2}$ / a	Main decay mode	(sf) branch x 100	<ν>	$S_{n,sf}$ ($s^{-1}g^{-1}$)
^{238}U	4.468 10^{9}	α	5.45 10^{-5}	1.990	1.35 10^{-2}
^{238}Pu	**87.74**	**α**	**1.85 10^{-7}**	**2.21**	**2592**
^{239}Pu	24110	α	3.1 10^{-10}	2.219	2.18 10^{-2}
^{240}Pu	**6561**	**α**	**5.7 10^{-6}**	**2.154**	**1023**
^{241}Pu	14.29	β⁻	5.74 10^{-13}	2.27	4.5 10^{-2}
^{242}Pu	**373500**	**α**	**5.49 10^{-4}**	**2.145**	**1725**
^{241}Am	432.6	α	4.30 10^{-10}	2.46	1.3
^{242}Cm	**0.446**	α	6.36 10^{-4}	2.54	**2.10 10^{7}**
^{244}Cm	**18.1**	α	1.37 10^{-4}	2.72	**1.08 10^{7}**
^{252}Cf	**2.645**	**α**	**3.10**	**3.757**	**2.31 10^{12}**

NEUTRON PRODUCTION BY (α,n) REACTIONS

Additional neutron source, $S_{n,\alpha}$

SNF: α - decay of actinides followed by (α,n) reaction in light elements

- (α,n) reactions
  - $^{18}O(\alpha,n)^{21}Ne$
  - $^{17}O(\alpha,n)^{20}Ne$
  - $^{19}F(\alpha,n)^{22}Na$
- Neutron energy (emission)
  - O(α,n) : $<E_n> \sim 2$ MeV
  - F(α,n) : $<E_n> \sim 1$ MeV
- $\nu \equiv 1$
  used to separate prompt fission neutrons from (α,n) neutrons in neutron correlation counting (NDA)

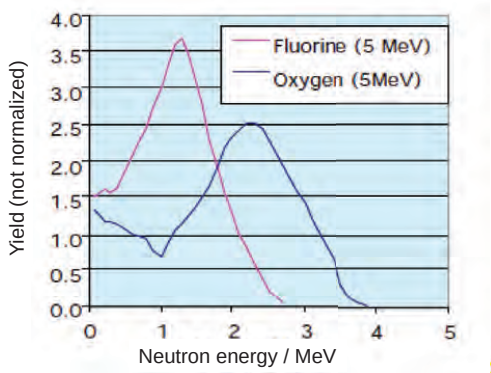

SPENT NUCLEAR FUEL: DEFINITIONS

- Initial enrichment (IE)
  - amount of ^{235}U relative to the total amount of U (or actinides) in the fresh fuel
  - $^{235}U/U$ mostly expressed in wt.%
- Cooling time (CT)
  - Time period since the end of neutron irradiation
- Burnup (BU)
  - Measure of the total energy production

    $E_{tot} \approx E_{rec,f} \times N_f$

    E_{tot} : total energy

    $E_{rec,f}$: energy per fission

    N_f : total number of fission events
  - Mostly defined as: total energy divided by total amount of actinides in initial fuel in MWd/kg (time integrated power/amount of initial fuel)

NEUTRON EMISSION BY SPENT NUCLEAR FUEL

$$S_n(t) = \sum_k S_{n,k}(t)$$

- $S_{n,k}(t)$: contribution of radionuclide k
- $S_{n,k}(t) = (s_{sf,k} + s_{\alpha n,k})\, N_k(t)$
  - $N_k(t)$: number of nuclei of nuclide k at time t
  - $s_{sf,k}$: specific neutron emission rate of nuclide k due to **spontaneous fission**
  - $s_{\alpha,k}$: specific neutron emission rate of nuclide k due to **(α,n) reactions**

PWR UO_2 pellet (5 g)
$^{235}U/U$ = 4.8 wt%
burnup = 45 MWd/kg

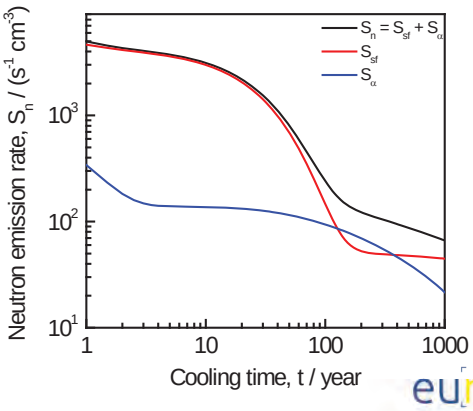

NEUTRON EMISSION BY SPENT NUCLEAR FUEL

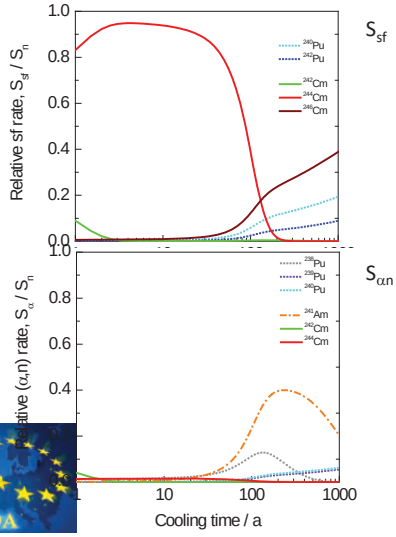

PWR UO_2 pellet (5 g)
$^{235}U/U$ = 4.8 wt%
burnup = 45 MWd/kg

⇒ Main contribution from ^{244}Cm(sf)

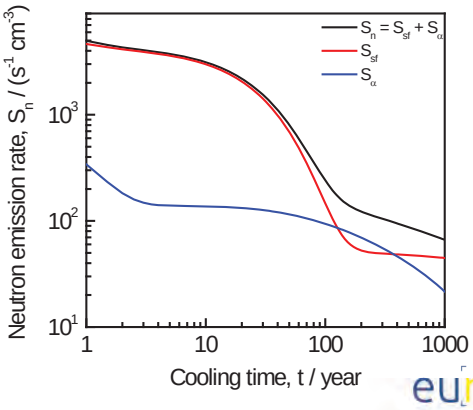

^{244}Cm PRODUCTION: A COMPLEX PROCESS

^{244}Cm : N = aBU^{b}

b ≈ 4 for BU = 45 MWd/kg

$$\frac{\delta N}{N} = b\frac{\delta BU}{BU}$$

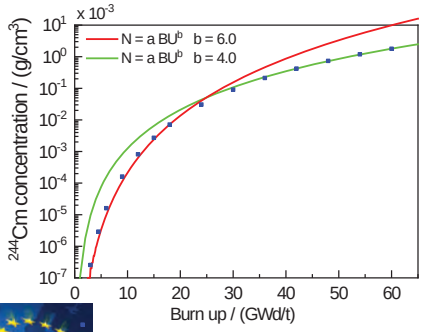

$$s_n = \frac{\ln 2}{T_{1/2}}\, x_{SF}\, \langle\nu\rangle = 4.5(1) \times 10^{-15}\ \mathrm{s}^{-1}$$

Sequence of
- (n,γ) reactions (6)
- β$^-$ decays (4)

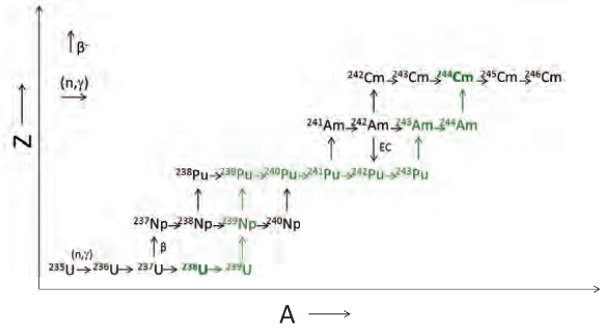

- $T_{1/2} = 18.11\ (3)$ Ref.: Nudat2; Singh and Browne, Nucl. Data Sheets 109 (2008) 2439
- $x_{SF} = 1.38(4) \times 10^{-6}$ Ref.: JEFF-3.3; Plompen et al., Eur. Phys. J. A 56 (2020) 181
- $\langle\nu\rangle = 2.6875$ Ref.: JEFF-3.3

GAMMA-RAY EMISSION BY SNF

$$S_\gamma(t) = \sum_k S_{\gamma,k}(E_\gamma, t)$$

^{95}Nb	35.0 d
^{95}Zr	64.0 d
^{144}Ce/^{144}Pr	284.9 d
^{106}Ru/^{106}Rh	1.02 a
^{134}Cs	2.06 a
^{154}Eu	8.8 a
^{137}Cs/^{137m}Ba	30.0 a

PWR UO_2 pellet (5 g)

^{235}U/U = 4.8 wt%

burnup = 45 MWd/kg

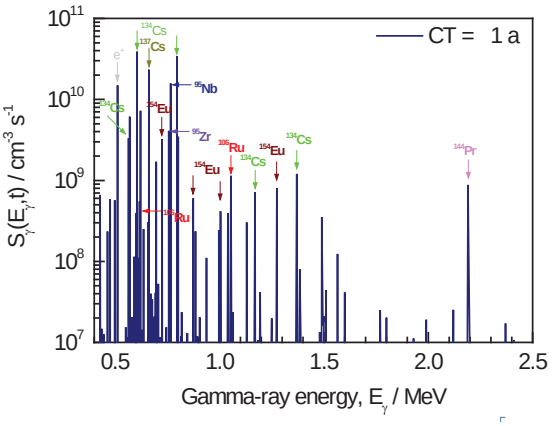

GAMMA-RAY EMISSION BY SNF

$$S_\gamma(t) = \sum_k S_{\gamma,k}(E_\gamma, t)$$

^{95}Nb	35.0 d
^{95}Zr	64.0 d
^{144}Ce/^{144}Pr	284.9 d
^{106}Ru/^{106}Rh	**1.02 a**
^{134}Cs	**2.06 a**
^{154}Eu	**8.8 a**
^{137}Cs/^{137m}Ba	**30.0 a**

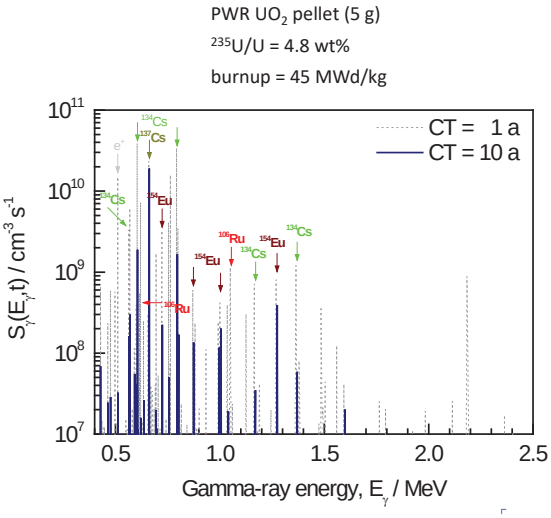

Training material

19

GAMMA-RAY EMISSION BY SNF

$$S_\gamma(t) = \sum_k S_{\gamma,k}(E_\gamma, t)$$

^{95}Nb	35.0 d
^{95}Zr	64.0 d
^{144}Ce/^{144}Pr	284.9 d
^{106}Ru/^{106}Rh	1.02 a
^{134}Cs	2.06 a
^{154}Eu	**8.8 a**
^{137}Cs/^{137m}Ba	**30.0 a**

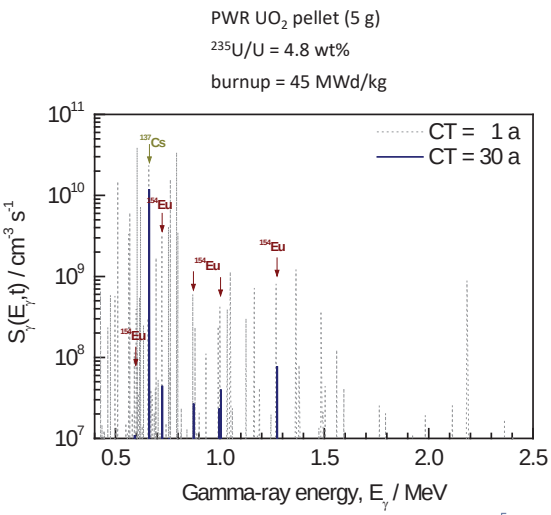

Training material

20

GAMMA-RAY EMISSION: DECAY HEAT RATE (POWER)

$$P_\gamma(t) = \sum_k \lambda_k N_k(t) \int E_\gamma s_{\gamma,k}(E_\gamma, t) dE_\gamma$$

^{95}Nb	35.0 d
^{95}Zr	64.0 d
^{144}Ce/^{144}Pr	284.9 d
^{106}Ru/^{106}Rh	1.02 a
^{134}Cs	2.06 a
^{154}Eu	8.8 a
^{137}Cs/^{137m}Ba	30.0 a
^{241}Am	432.6 a

PWR UO_2 pellet (5 g)
^{235}U/U = 4.8 wt%
burnup = 45 MWd/kg

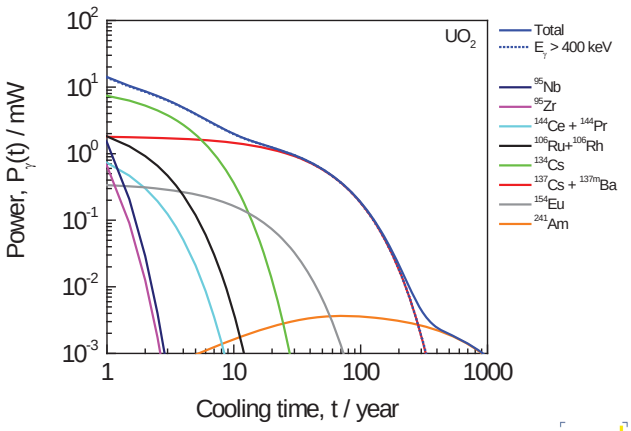

DECAY POWER PRODUCED BY SNF

$$P(t) = \sum_k P_k(t)$$

- $P_k(t)$: contribution of radionuclide k
- $P_k(t) = p_k N_k(t) = \lambda_k E_{rec,k} N_k(t)$
  - $N_k(t)$: number of nuclei of nuclide k at time t
  - p_k : specific decay heat rate of nuclide k

PWR UO_2 pellet (5 g)
^{235}U/U = 4.8 wt%
burnup = 45 MWd/kg

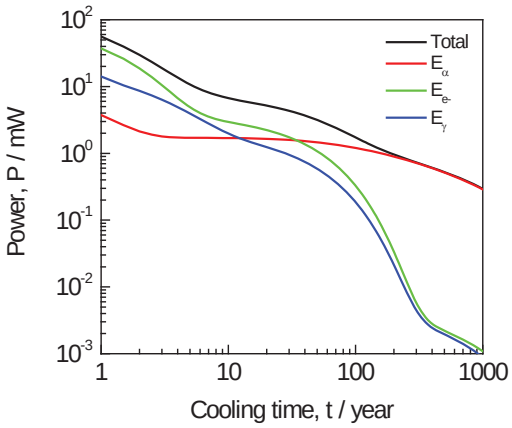

DECAY POWER PRODUCED BY SNF

- 1 a ≤ t ≤ 10 a
  - **^{144}Ce / ^{144}Pr**
  - **^{106}Ru / ^{106}Rh**
  - **^{134}Cs**
  - ^{90}Sr / ^{90}Y
  - ^{137}Cs / ^{137m}Ba
- 10 a ≤ t ≤ 100 a
  - ^{90}Sr / ^{90}Y
  - ^{137}Cs / ^{137m}Ba
  - ^{238}Pu
  - ^{241}Am
  - ^{244}Cm
- 100 a ≤ t
  - ^{241}Am
  - ^{238}Pu
  - ^{239,241}Pu

PWR UO_2 pellet (5 g)
^{235}U/U = 4.8 wt%
burnup = 45 MWd/kg

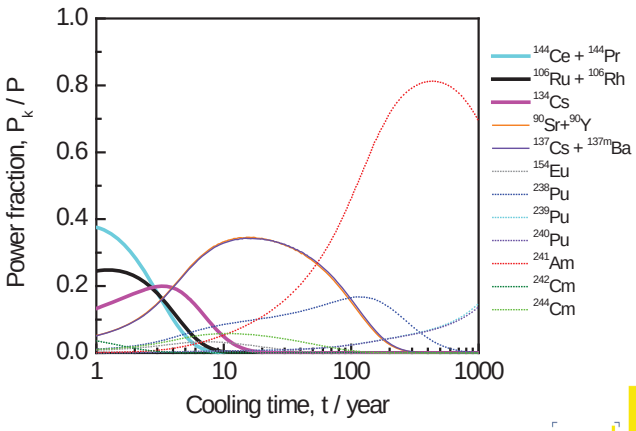

Training material

DECAY POWER PRODUCED BY SNF

- 1 a ≤ t ≤ 10 a
  - ^{144}Ce / ^{144}Pr
  - ^{106}Ru / ^{106}Rh
  - ^{134}Cs
  - ^{90}Sr / ^{90}Y
  - ^{137}Cs / ^{137m}Ba
- 10 a ≤ t ≤ 100 a
  - **^{90}Sr / ^{90}Y**
  - **^{137}Cs / ^{137m}Ba**
  - ^{238}Pu
  - ^{241}Am
  - ^{244}Cm
- 100 a ≤ t
  - ^{241}Am
  - ^{238}Pu
  - ^{239,241}Pu

PWR UO_2 pellet (5 g)
^{235}U/U = 4.8 wt%
burnup = 45 MWd/kg

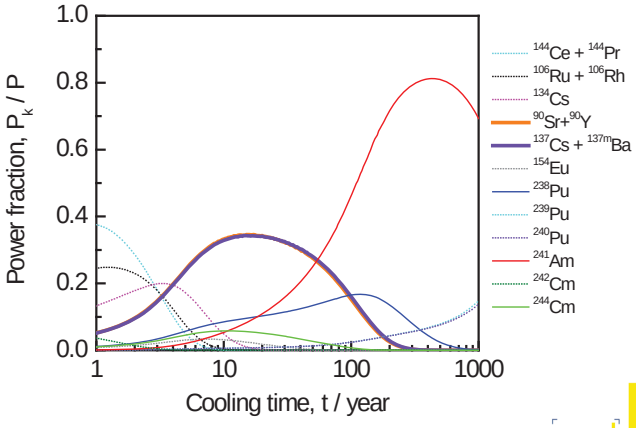

Training material

DECAY POWER PRODUCED BY SNF

- 1 a ≤ t ≤ 10 a
  - ^{144}Ce / ^{144}Pr
  - ^{106}Ru / ^{106}Rh
  - ^{134}Cs
  - ^{90}Sr / ^{90}Y
  - ^{137}Cs / ^{137m}Ba
- 10 a ≤ t ≤ 100 a
  - ^{90}Sr / ^{90}Y
  - ^{137}Cs / ^{137m}Ba
  - ^{238}Pu
  - ^{241}Am
  - ^{244}Cm
- 100 a ≤ t
  - **^{241}Am**
  - ^{238}Pu
  - $^{239,241}Pu$

PWR UO_2 pellet (5 g)
$^{235}U/U$ = 4.8 wt%
burnup = 45 MWd/kg

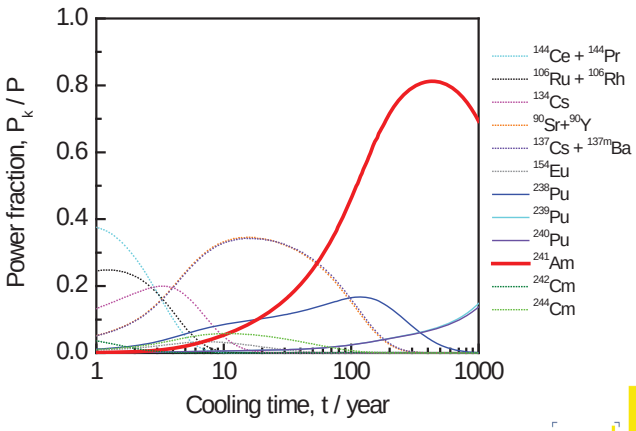

Training material

25

^{134}Cs: PRODUCTION

^{134}Cs production:
(n,f) followed by β^- and (n,γ)

$$n + {}^{235}_{92}U \xrightarrow{(n,f)} {}^{100}_{40}Zr + {}^{133}_{52}Te + 3n$$

$${}^{133}_{52}Te \xrightarrow[12.4\ min]{\beta^-} {}^{133}_{53}I + e^- + \bar{\nu}_e$$

$${}^{133}_{53}I \xrightarrow[20.8\ h]{\beta^-} {}^{133}_{54}Xe + e^- + \bar{\nu}_e$$

$${}^{133}_{54}Xe \xrightarrow[5.24\ d]{\beta^-} {}^{133}_{55}Cs + e^- + \bar{\nu}_e$$

$$n + {}^{133}_{55}Cs \xrightarrow{(n,\gamma)} {}^{134}_{55}Cs$$

More in presentation by Daniel Cano Ott

$N = aBU^b$
$b = 2$ for $BU < 30$ GWd/tU

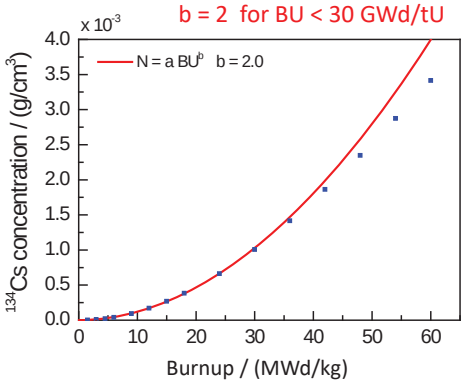

Training material

26

^{90}Sr: PRODUCTION

^{90}Sr production:
(n,f) followed by β$^-$

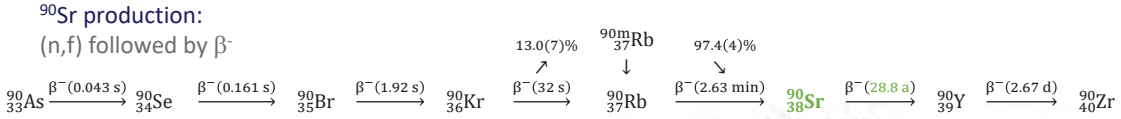

- Significantly different ^{235}U and ^{239}Pu fission yields:
→ non-linearity vs. BU

	CFY (JEFF-3.3)
^{235}U(n_{th},f)	**0.0568(13)**
^{238}U(n_f,f)	0.0320(14)
^{239}Pu(n_{th},f)	**0.0208(6)**
^{241}Pu(n_{th},f)	0.0146(4)

More in presentation by Olivier Serot

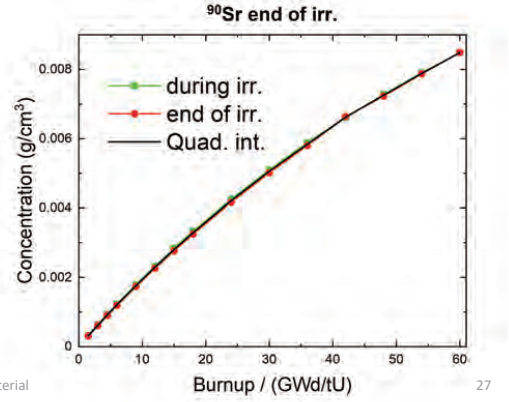

FISSION FRACTIONS OF ^{235}U, ^{239}Pu AND ^{241}Pu

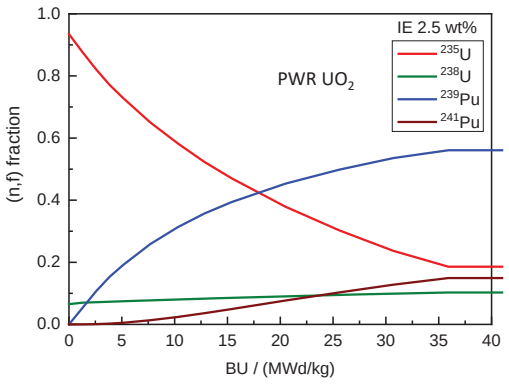

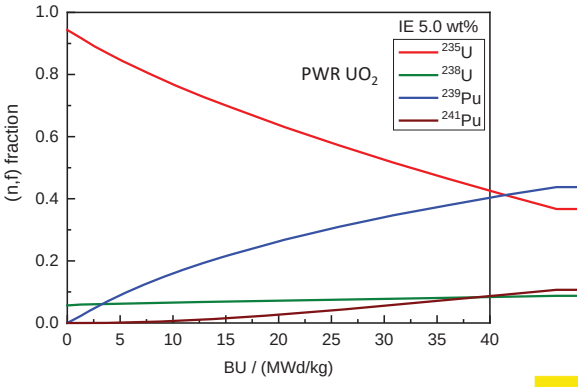

SNF SOURCE TERMS: NUCLIDE INVENTORY

Nuclide	Source term	CT
^{90}Sr	H, S_γ	10 a ≤ t ≤ 100 a
^{106}Ru	H	1 a ≤ t ≤ 10 a
^{134}Cs	H	1 a ≤ t ≤ 10 a
^{137}Cs	H, S_γ	10 a ≤ t ≤ 100 a
^{144}Ce	H	1 a ≤ t ≤ 10 a
^{148}Nd	*Burn-up*	*stable*
^{149}Sm	*Power*	*stable*
^{154}Eu	H, S_γ	1 a ≤ t ≤ 10 a

Nuclide	Source term	CT
^{235}U	R, S_γ	10^5 a ≤ t
^{238}U	R, S_γ	10^5 a ≤ t
^{238}Pu	H, S_γ	10 a ≤ t
^{239}Pu	R, S_γ	100 a ≤ t ≤ 10^4 a
^{240}Pu	R, S_γ	100 a ≤ t ≤ 10^4 a
^{241}Pu	H, S_γ	10 a ≤ t ≤ 100 a
^{241}Am	H	10 a ≤ t
^{242}Cm	H, S_n	1 a ≤ t ≤ 10 a
^{244}Cm	H, S_n	10 a ≤ t ≤ 100 a

H : thermal power or decay heat
S_n : neutron emission
S_γ : γ-ray emission
R : reactivity (criticality safety)

Criticality safety (Burn Up Credit, BUC):

^{95}Mo, ^{99}Tc, ^{101}Ru, ^{103}Rh, ^{109}Ag, ^{133}Cs, ^{143}Nd, ^{147,149,150,151,152}Sm, ^{155}Gd

Long term safety:

^{14}C, ^{36}Cl, ^{79}Se, ^{94}Nb, ^{99}Tc, ^{129}I, ^{135}Cs, ^{226}Ra, ^{237}Np

⇒ Requires **complex nuclide inventory** which can only be obtained by **theoretical calculations**

Training material

DEPLETION CALCULATIONS/CODES

Coupled neutron transport – nuclide depletion/creation

Neutron transport

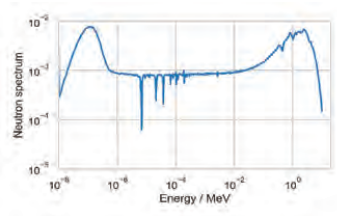

Bateman equation

$$\frac{dN_k}{dt} = Y\, N_f\, \sigma_f\, \varphi + \sum_{i \to k} \lambda_i N_i + \sum_{j \to k} \sigma_j N_j\, \varphi - (\lambda_k + \sigma_{k,a}\varphi) N_k$$

Update nuclide vector

- ALEPH2
- CASMO
- DARWIN
- EVOLCODE
- SERPENT
- SCALE
- STREAM
- VESTA
- …

Training material

DEPLETION CODES: THEORETICAL CALCULATION OF SNF NUCLIDE INVENTORY AND OBSERVABLES

Nuclear data
- Cross sections: (n,γ), (n,f), …
- Fission yields, neutron multiplicities and spectra
- Radioactive decay data
  - half-life
  - emission probabilities
  - recoverable energy

Depletion code

SNF input data
- Fuel properties
  - design
  - material data (IE)
  - …
- Operational history
  - burn-up (BU)
  - cooling time (CT)
  - …

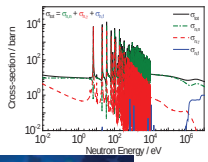

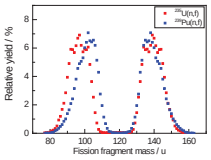

Nuclide inventory Observables
- decay heat
- neutron emission
- γ-ray emission
- …

More in presentation by Gert Van den Eynde

Training material

31

EXPERIMENTAL DATA TO VALIDATE DEPLETION CODES

- Results of analytical methods (destructive chemical and radiochemical analysis)
- Calorimetry data (assembly)
- Neutron emission measurements

In addition, an accurate knowledge of the design and operational history is required

Training material

32

ANALYTICAL METHODS FOR SNF ASSAY DATA

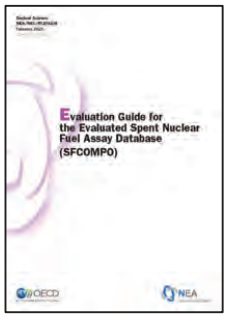

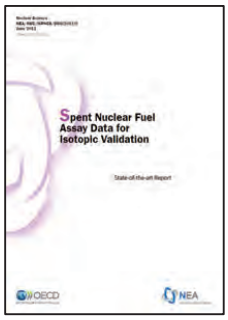

Post-Irradiation Experiments (PIE)

Complex process including different steps:

- Sampling and sample dissolution
- Separation
  linked to measurement technique, e.g. ICPMS)
- Measurement
  - Radiometric (α- and γ-spectrometry, Liquid Scintillation Counting (α- and β-emitters))
  - Mass spectrometry

$\Rightarrow$ Data collected in SFCOMPO database

More in presentations by:
- **Steven Van Winckel (experiment)**
- **Kevin Govers (use of ND)**

VALIDATION OF CALCULATIONS: CLAB CALORIMETER

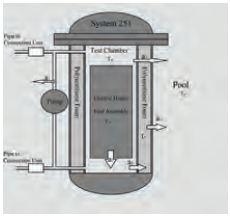

- Only operating calorimeter worldwide to determine decay power of SNF assemblies
- Extensively used to validate depletion codes, e.g.
- Blind Test on decay heat:

Assembly ID	P	CT	<C/E>	St. dev
BT01	1662 W	4.5 a	0.975	0.019
BT02	1068 W	8.6 a	0.977	0.018
BT03 (+ Gd)	895 W	9.8 a	0.967	0.019
BT04	768 W	13.5 a	0.994	0.023
BT05	663 W	21.4 a	0.979	0.021

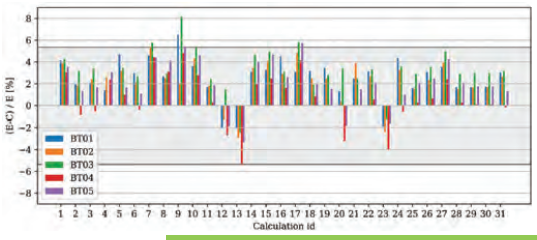

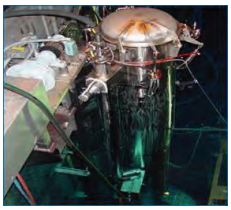

More in presentations by:
- **Peter Schillebeeckx (experiment)**
- **Pablo Romojaro (use of ND)**

IMPORTANCE OF NEUTRON EMISSION ESTIMATION FOR SNF MANAGEMENT

^{244}Cm : $N = aBU^b$

$b \approx 4$ for $BU = 45$ MWd/kg

$$\frac{\delta N}{N} = b\frac{\delta BU}{BU}$$

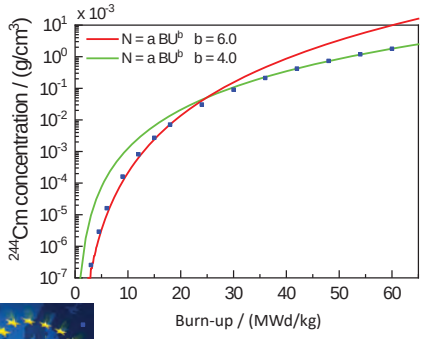

- Use neutron emission as a BU indicator to improve the operational input for depletion calculations
- For nuclear safeguards authorities using neutron emission as a signature for the fissile material
- Neutron dose

More in presentation by Peter Schillebeeckx

SUMMARY AND CONCLUSIONS

- The main observables of interest for a safe handling, transport, storage and disposal of SNF were identified and discussed
- A characterisation of SNF for these observables requires the inventory of some key nuclides with different characteristics
- The inventory of some key nuclides can only be obtained by theoretical calculations using depletion codes
- The quality of the theoretical calculations strongly depends on the quality of the nuclear data and design and operational history of the SNF
- Some key nuclear data such as cumulative fission yields and neutron induced capture cross sections need to be improved to allow a more accurate estimation of the main observables of interest

LEARNING OUTCOMES

After the completion of this training lesson, the participants should be able to

- identify the observables that are important for the transport, handling, storage and disposal of spent nuclear fuel
- identify key nuclides determining these observables
- identify the different components involved in the theoretical calculations of the observables
- understand the importance of nuclear data and design characteristics and operational history of the fuel for an accurate theoretical estimation of the observables
- realise the need of accurate experimental data to validate theoretical calculations

KEY WORDS

- Actinides
- Alpha-decay
- Bateman equation
- Beta-decay
- Burnup
- Cooling time
- Cross section
- Decay heat
- Decay power
- Depletion codes
- Disposal
- Fission product
- Fission yields
- Gamma-ray emission
- Initial enrichment
- Irradiation history
- Light water reactor
- Neutron emission
- Neutron reactions
- Neutron induced capture reaction
- Neutron induced fission reaction
- Neutron transport
- Nuclear data
- Pressurised water reactor
- Recoverable energy
- Spent nuclear fuel
- Spontaneous fission

ADDITIONAL BIBLIOGRAPHY AND REFERENCES

Spent nuclear fuel observables and key nuclides

- Broadhead et al., "Investigation of nuclide importance to functional requirements related to transport and long-term storage of LWR spent fuel", Report ORNL/TM-12742 (1995)
- Gauld et al., "Nuclide importance to criticality safety, decay heating and source terms related to transport and interim storage of high-burnup LWR fuel", Report NUREG/CR-6700, ORNL/TM-2000/284 (2001)
- Žerovnik et al. ,"Observables of interest for the characterisation of Spent Nuclear Fuel", EUR 29301 EN (2018) , JRC112361
- Schillebeeckx et al., "Characterisation of spent nuclear fuel by theoretical calculations and non-destructive analysis", see JRC114178 (2019)

Depletion codes

- Stankovskiy and Van den Eynde, "Advanced method for calculations of core burn-up, activation of structural materials and spallation products accumulation in accelerator driven system", Science and Technology of Nuclear Installations 2012 (2012) 545103
- Álvarez-Velarde, "Validation of the burn-up code EVOLCODE 2.0 with PWR experimental data and with a Sensitivity/Uncertainty analysis", Annals of Nuclear Energy 73 (2014) 175
- Leppänen et al., "The Serpent Monte Carlo code: status, development and applications in 2013", Annals of Nuclear Energy 82 (2015) 142
- Kashima et al., "Validation of burnup calculation code SWAT4 by evaluation of isotopic composition data of mixed oxide fuel irradiated in pressurized water reactor", Energy Procedia 71 (2015) 159
- Rearden and Jessee, "SCALE Code System", ORNL/TM-2005/39 Version 6.2, April 2016
- Gauld et al., "Isotopic depletion and decay methods and analysis capabilities in SCALE", Nuclear Technology 174 (2017) 169
- Ebiwonjumi et al., "Verification and validation of radiation source term capabilities in STREAM", Annals of Nuclear Energy 124 (2019) 80

ADDITIONAL BIBLIOGRAPHY AND REFERENCES

Radiochemical analysis and validation of depletion codes

- DE Scatena-Wachsel, "Radiochemical analysis methodology for uranium depletion measurements", Report LM-06K140, January 2007
- Gauld et al., "Uncertainties in Predicted Isotopic Compositions for High Burnup PWR Spent Nuclear Fuel", Report NUREG/CR-7012, ORNL/TM-2010/41, January 2011
- OECD/NEA, "Spent Nuclear Fuel Assay Data for Isotopic Validation, State-of-the-art Report", Nuclear Science, NEA/NSC/WPNCS/DOC(2011)5, June 2011
- OECD/NEA, "Evaluation Guide for the Evaluated Spent Nuclear Fuel Assay Database (SFCOMPO)", Nuclear Science, NEA/NSC/R(2015)8, February 2016G. Ilas,"Review of Experimental Assay Data for PWR Spent Fuel", Report ORNL/SPR-2019/1143, April 2019

Non-destructive assay

- SKB, "Measurements of Decay Heat in Spent Nuclear Fuel at the Swedish Interim Storage Facility", Clab, SKB Report R-05-62, December 2006
- B.D. Murphy and I.C. Gauld, "Spent Fuel Decay Heat Measurements Performed at the Swedish Central Interim Storage Facility", Report ORNL/TM-2008/016, Oak Ridge National Laboratory, Feburary 2010
- Schillebeeckx et al., "A non-destructive method to determine the neutron production rate of a sample of spent nuclear fuel under standard controlled area conditions", JRC Technical Report EUR 30379 EN, 2020

Nuclear data

- Nuclear data libraries at JANIS NEA, https://www.oecd-nea.org/jcms/pl_39910/janis
- Decay data, http://www.nucleide.org/DDEP.htm
- Nichols et al., "Handbook of nuclear data for safeguards: database extensions, august 2008", INDC-2453, INDC(NDS) – 0534

Keep in touch

EU Science Hub
joint-research-centre.ec.europa.eu

@EU_ScienceHub
EU Science Hub – Joint Research Centre
EU Science, Research and Innovation
EU Science Hub
@eu_science

Thank you

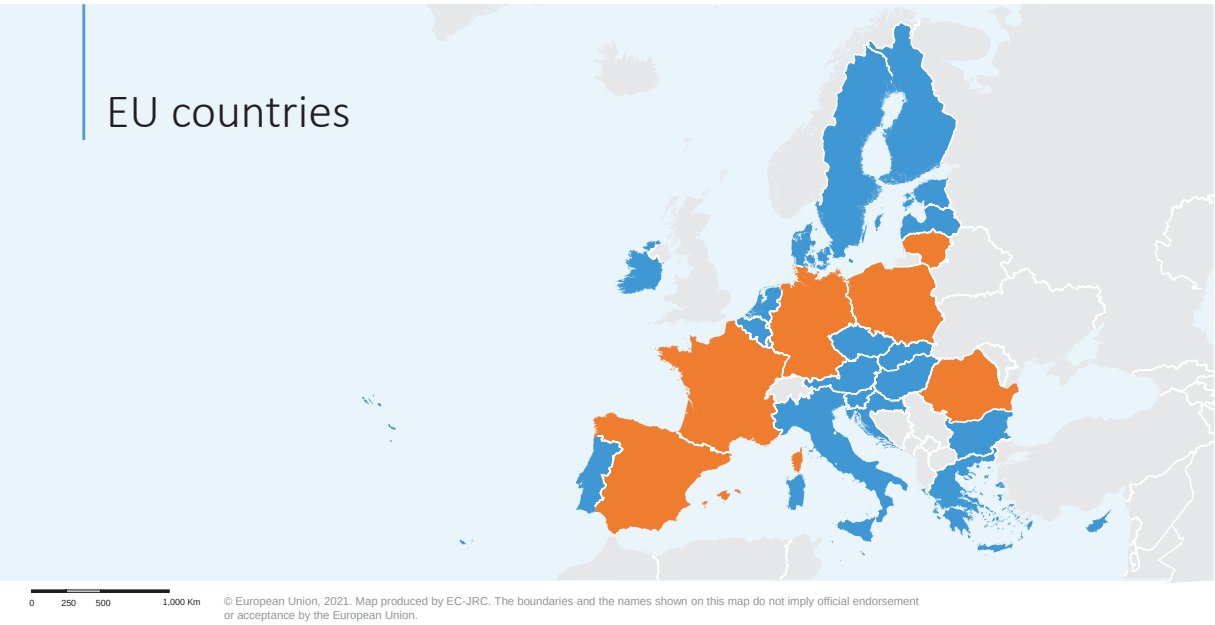
EU countries
0 250 500 1,000 Km
© European Union, 2021. Map produced by EC-JRC. The boundaries and the names shown on this map do not imply official endorsement or acceptance by the European Union.

3. Internal meeting

- Dry Storage Accidents; IDOM; SFC Annual Meeting 2022; 20/09/2022
- Spectroscopic investigation of fission and activation products in irradiated light water reactor fuels; T. König, R. Dagan, K. Dardenne, M. Herm, V. Metz, T. Pruessmann, J. Rothe, D. Schild, A. Walschburger, H. Geckeis; WP8 SFC Annual Meeting 2023; 11/01/2023

3.1 Dry Storage Accidents; IDOM; SFC Annual Meeting 2022; 20/09/2022

EURAD SFC

IDOM - Dry Storage Accidents, Risk Assessment Methodology

Carlos Pérez – 20 September 2022

This project has received funding from the European Union's Horizon 2020 research and innovation programme under grant agreement N°847593

INDEX

BACKGROUND

IDOM is an Spanish firm providing Consulting, Engineering and Architecture professional services for clients including NPPs, WMOs, and TSOs like CIEMAT. It takes part in EURAD WP8 Task 4 as a LTP of CIEMAT.

OVERALL OBJECTIVE

The overall objective of IDOMs work is to establish the influence of the SNF parameters or the degradation phenomena that may be present in it during accidents of Dry Storage Systems.

APPROACH

To meet the proposed objective, an initial methodology has been established, which could be applicable later to particular cases.

In addition, the initial methodology has been extended and made more specific to the national case through the Spanish perspective. This is, from the Spanish regulatory point of view and the fuel types and Dry Storage Systems available in Spain.

IIT-004
Risk Assessment Methodology
November 2020.

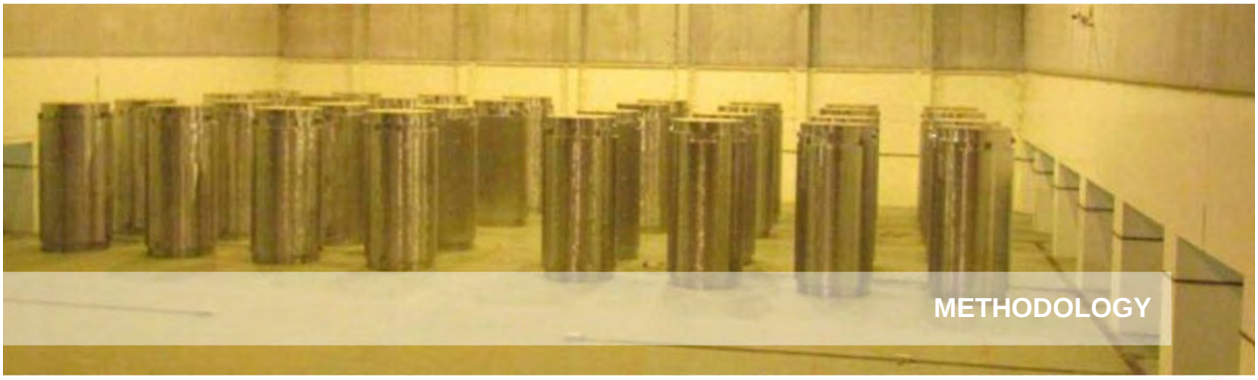

METHODOLOGY

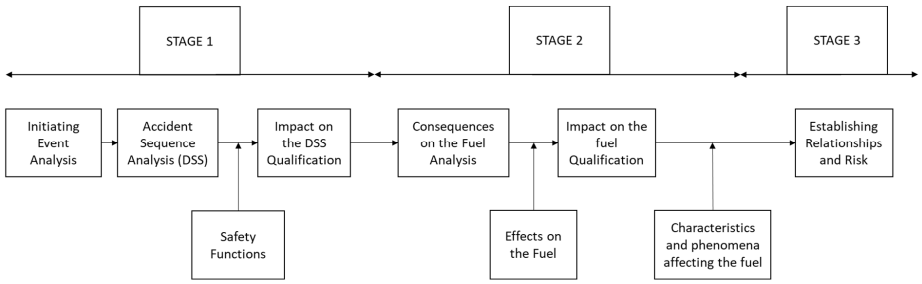

METHODOLOGY

STAGE 1 – Dry Storage System Analysis

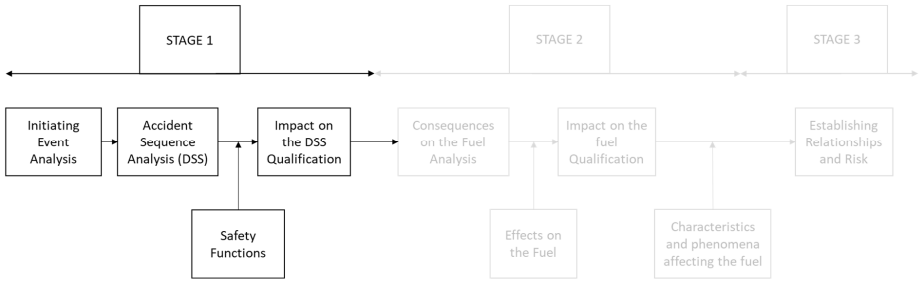

METHODOLOGY

STAGE 2 – Spent Nuclear Fuel

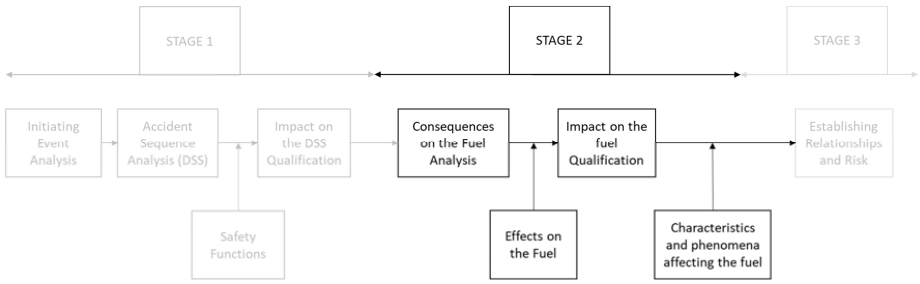

METHODOLOGY

STAGE 3 – Establishing Relationships

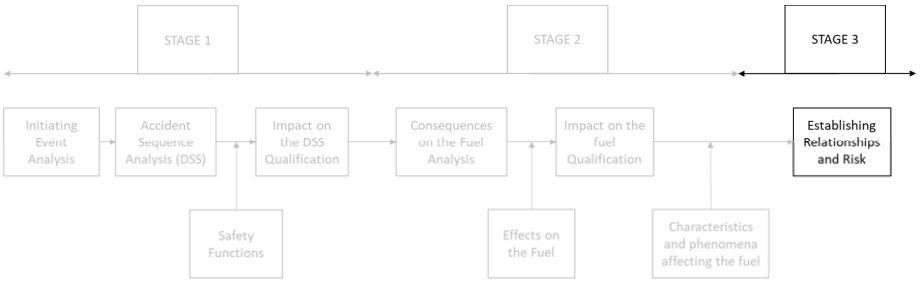

DEVELOPMENT OF THE WORK

STAGE 1 – Storage System Analysis

Scoping

Fuel Types in the scope:

- **BWR**
- **PWR**

Dry Storage Systems in the scope:

- **Canister + Overpack**
- **Dual Purpose Cask**

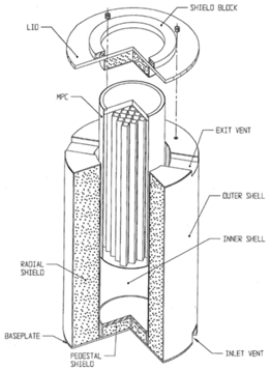

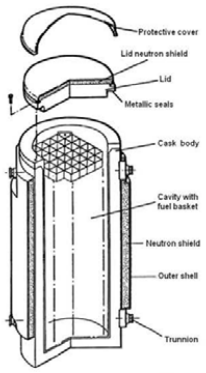

20 September 2022 SFC Annual Meeting 13

DEVELOPMENT OF THE WORK

STAGE 1 – Storage System Analysis

What can be found in references by DSS designers and regulators?

Tip over
Drop
Flood
Fire
Explosion
Lightning
Earthquake
Loss of Shielding
Adiabatic Heatup
Tornado
Missiles generated by natural phenomena
…

20 September 2022 SFC Annual Meeting 14

DEVELOPMENT OF THE WORK

STAGE 1 – Storage System Analysis

Accident Sequence Analysis

Initiating Events	Accident	Consequences to de DSS
Earthquake	Tip over	Loss of Shielding
Handling device failure	Drop	Lid ovalization
Damm breach / Tsunami	Flood	
Transfer vehicicle fire	Fire	Adiabatic Heatup
On / off-site explosion	Explosion	
Electrical storm	Lightning	
Tornado	Missiles generated by natural phenomena	Loss of Shielding

DEVELOPMENT OF THE WORK

STAGE 1 – Storage System Analysis

Accident Sequence Analysis – Cask Tip-Over Example

Initiating Events	Accident	Consequences to de DSS
• Tornado / hurricane winds • Missiles generated by natural phenomena • Flooding (water drag) • Earthquake • Lifting device failure	Tip-Over	• Overstress and deformation of certain structural components (e.g., shell, lids, bolting, support channels, etc.). • Overstress and deformation of basket plates. • Localized decrease in shielding material thickness. • General temperature increase due to horizontal reorientation. • CRUD detachment.

DEVELOPMENT OF THE WORK

STAGE 1 – Storage System Analysis

How do we evaluate the severity of an accident from the DSS point of view?

SAFETY FUNCTIONS

- Criticality Control (CC)
- Structural Support (SS)
- Heat Transfer (HT)
- Confinement (CF)
- Radiation Shielding (RS)
- Retrievability (RT)

Severity from the DSS point of view is established as the sum of the number of compromised Safety Functions.
(0 to 6)

0	1	2	3	4	5	6

DEVELOPMENT OF THE WORK

STAGE 1 – Storage System Analysis

Accident Sequence Analysis – Cask Tip-Over Example

Consequences to de DSS

- Overstress and deformation of certain structural components (e.g., shell, lids, bolting, support channels, etc.).
  (CF, SS, RT, HT)
- Overstress and deformation of basket plates.
  (CC, SS, HT, RT)
- Localized decrease in shielding material thickness.
  (RS)
- General temperature increase due to horizontal reorientation.
  (HT)
- CRUD detachment.
  (No consequences to the DSS)

Total number of compromised Safety Functions:

(CF, SS, RT, HT, RS, CC) -> **6**

SEVERITY FROM THE DSS POINT OF VIEW:

6

DEVELOPMENT OF THE WORK

STAGE 1 – Storage System Analysis

Accident Sequence Analysis – Lightning Example

Consequences to de DSS

- Local temperature increase in the point of impact under allowable limits.

(No consequences to the DSS)

Total number of compromised Safety Functions:

(None) -> **0**

SEVERITY FROM THE DSS POINT OF VIEW:

0

DEVELOPMENT OF THE WORK

STAGE 2 – Consequences in the Spent Fuel Analysis

How does an accident affect the fuel?

- Normally, DSS documentation does not go into detail regarding the effects of an accident in the fuel.
- Consequences in the container can be seen as the initiating events for the effects in the fuel.

Examples:

- Accelerations in the container -> Accelerations in the fuel -> Induced buckling or flexion
- Fire in the container -> Loss of heat transfer -> Cladding temperature increase
- Flooding in the container -> Change in moderation conditions

DEVELOPMENT OF THE WORK

STAGE 2 – Consequences in the Spent Fuel Analysis

Consequences in the Fuel - Cask Tip-Over Example

- The fuel might suffer deformations and damages due to the accelerations induced on it, grid-to-rod fretting, or it might be crushed and hit by violent contact with the components of the DSS (basket plates) or other fuel assemblies.
- Rearrangement of the fuel assemblies within the storage system basket, both from the DSS horizontal reorientation and the deformation of the basket plates.
- CRUD detachment.

DEVELOPMENT OF THE WORK

STAGE 2 – Consequences in the Spent Fuel Analysis

How do we evaluate the severity of an accident from the SNF point of view?

- **Mechanical Effects (ME):**
  - Cladding failure, either with breached (punctured) or damaged rods
  - Rod / assembly deformation without cladding failure
  - Changes to the assembly axial alignment without cladding failure
- **Thermal Effects (TE):**
  - Heating of the cladding
  - Repeated heating and cooling cycles
- **Criticality Effects (CE):**
  - Any effect that will result in a variation of the effective neutron multiplication factor k_{eff}

Severity from the SNF point of view is established as the sum of the number of Effects on the fuel.
(0 to 3)

0	1	2	3

DEVELOPMENT OF THE WORK

STAGE 2 – Consequences in the Spent Fuel Analysis

Consequences in the Fuel - Cask Tip-Over Example

- The fuel might suffer deformations and damages due to the accelerations induced on it, grid-to-rod fretting, or it might be crushed and hit by violent contact with the components of the DSS (basket plates) or other fuel assemblies.
  (ME, TE, CE)
- Rearrangement of the fuel assemblies within the storage system basket, both from the DSS horizontal reorientation and the deformation of the basket plates.
  (TE, CE)
- CRUD detachment.
  (No effects from the Safety Point of view)

Total number of Effects:

(ME, TE, CE) -> **3**

SEVERITY FROM THE SNF POINT OF VIEW:

3

DEVELOPMENT OF THE WORK

Summary of Results

- Tip-Over
- Drop
- Fire
- Explosion
- Lightning
- Object Impact
- Flooding
- Burial Under Debris
- Extreme Temperature Changes
- Supplemental Cooling System Failure
- Blockage of Air Inlets

Accident Severity from the DSS and the SNF points of view

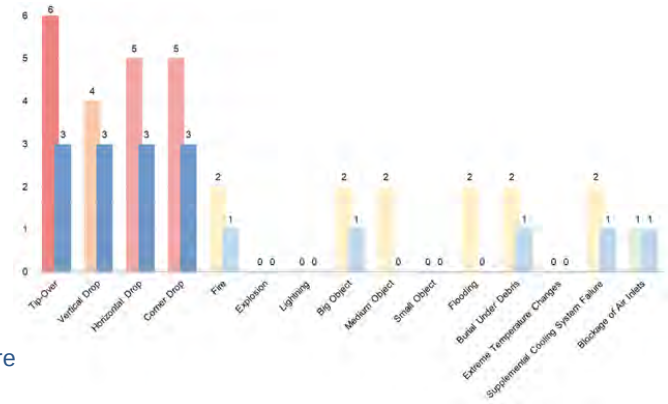

DEVELOPMENT OF THE WORK

Accident Severity Evaluation Conclusions

- The severity of an accident in the DSS in not necessarily related to the severity in the SNF, as it can be seen in the case of flooding or medium object impact.
- Accidents involving movement of the DSS (Tip-Over and Drop) can have the greatest effect on the fuel, which confirm the prioritisation of their analyses.
- A number of analyses that are not of great relevance from the DSS nor SNF damage point of view are identified (explosion, lightning, small object or extreme temperature changes).

NEXT STEPS

STAGE 2 (Continuation)

Review of documentation and references applicable to LWR fuel, identifying the most common degradation mechanisms, classifying them and establishing their applicability or likehood of occurrence based on operating parameters, e.g.:

- Burnup (+- 45 Gwd/MTU)
- Cooling time in spent fuel pool
- Dry Storage time (extended 20+ years)
- Temperatures during the loading of the Dry Storage System

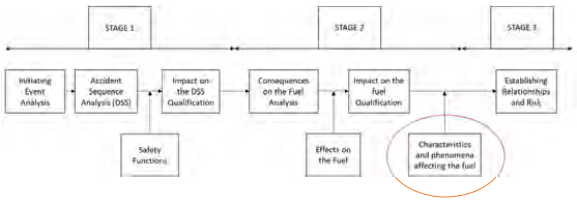

20 September 2022 SFC Annual Meeting 27

Thank you!

3.2 Spectroscopic investigation of fission and activation products in irradiated light water reactor fuels; T. König, R. Dagan, K. Dardenne, M. Herm, V. Metz, T. Pruessmann, J. Rothe, D. Schild, A. Walschburger, H. Geckeis; WP8 SFC Annual Meeting 2023; 11/01/2023

Spectroscopic investigation of fission and activation products in irradiated light water reactor fuels

EURAD SFC Annual Meeting 2023, Wettingen

T. König*, R. Dagan, K. Dardenne, M. Herm, V. Metz, T. Pruessmann, J. Rothe, D. Schild, A. Walschburger and H. Geckeis
Karlsruhe Institute of Technology (KIT), Institute for Nuclear Waste Disposal (INE), P.O. Box 3640, 76021 Karlsruhe Germany

This project has received funding from the European Union's Horizon 2020 research and innovation programme under grant agreement N°847593

Outline

- **Introduction:**
- **Experimental:**
  - Examined fuel types – *High burn-up UO_X and mixed oxide (MOX) fuel*
  - Spectroscopic analysis – *Interaction layer between fuel and cladding*
    - *SEM-EDX and XPS analysis*
    - *XAS analysis*
- **Summary**

Spent Nuclear Fuel (SNF)

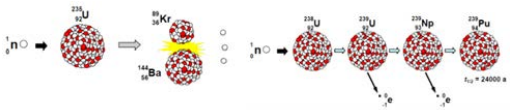

- **Composition of SNF (4.0% ^{235}U, 52 GWd/t_{HM}) utilised in a light water reactor (LWR) for ~ 4 years:**
  - **93.4% UO_2 matrix:**
    92% ^{238}U, < 1% ^{235}U, < 0.5% ^{236}U
  - **1.2% transuranium isotopes / actinides:**
    1% ^{239}Pu, ^{240}Pu, ^{241}Pu, ^{237}Np > ^{244}Cm > ^{241}Am, etc.
  - **5.4% fission products:**
    1.7% ^{79}Se, ^{90}Sr, $^{135, 137}Cs$, ^{129}I, etc.
    1.6% lanthanides
    1.3% ε-phases (^{99}Tc, ^{109}Pd, etc.)
    0.8% fission gases (krypton, xenon)
  - **Activation products:**
    e.g. ^{14}C, ^{93}Zr, ^{36}Cl ➡ **^{35}Cl (n,γ) ^{36}Cl**

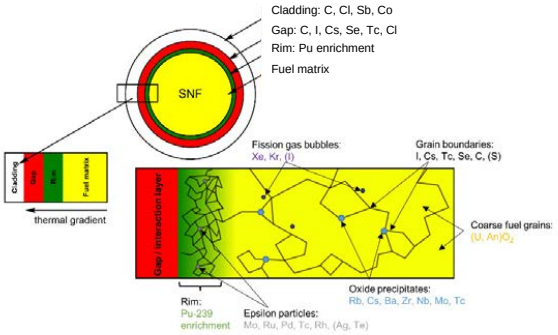

➡ **Heterogenous distribution of radionuclides.**

Source: Hippler, *Reaktorchemie*, Leibniz Universität Hannover (2004).

Interaction layer between fuel and cladding

- **Cross section of a nuclear fuel pellet:**

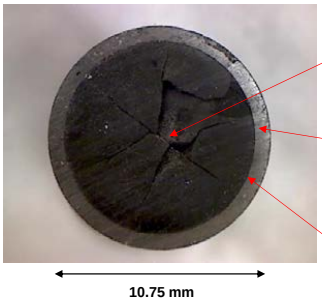

Pellet: Radial cracks due to temperature gradient during irradiation; migration pathways for radionuclides in the SNF pellet.

Cladding: Built-up of an external ZrO_2 layer due to primary circuit water corrosion; thin ZrO_2 layer on the inner side due to Zr / UO_2 reactions.

Gap: Closed at burn-ups > 40 GWd/t_{HM}; Formation of an **interaction layer.**

➡ **Possibility of transport of volatile fission and activation products to the cladding during irradiation and subsequent chemical reactions between fuel and cladding!**

Dry interim storage

- **Interim dry storage of used fuel assemblies in dual-purpose casks:**
  - Dual-purpose cask (e.g. CASTOR®) guarantees **shielding of radiation**, as well as a temporary, **safe enclosure of radionuclides.**
  - **Decay heat** dissipated by air circulation.
  - **However, final repositories in many countries not operational yet.**

→ **Necessity of prolonged interim storage until construction and commissioning of a final repository site!**

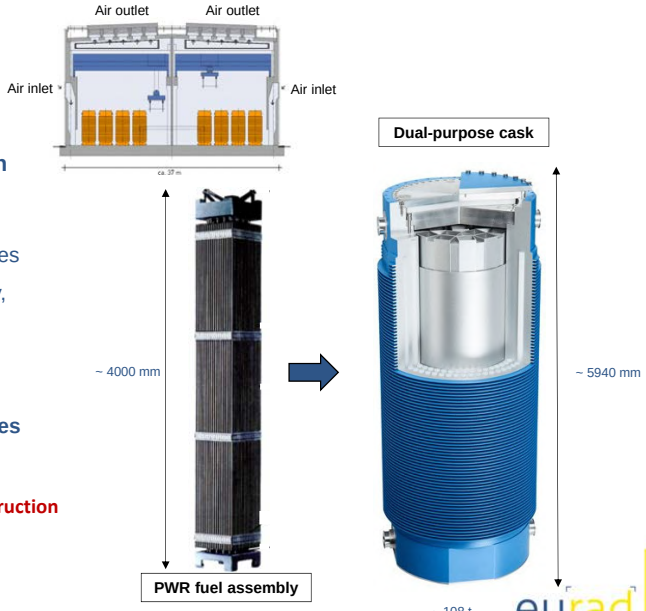

Sources: GNS, CASTOR® V/19, *Nuclear Engineering International* (2003). EnBW Kraftwerk AG

Dry interim storage

- **Interim dry storage of used fuel assemblies in dual-purpose casks:**
  - Dual-purpose cask guarantees **shielding of radiation**, as well as a temporary, **safe enclosure of radionuclides.**
  - Interim storage of irradiated fuel assemblies is **licensed for only 40 years.**
  - **Final repository not available until at least 2050 and emplacement of the last fuel assemblies decades later!**

- Several phenomena affect the cladding integrity during interim storage:
  - **Increase in pressure** due to swelling of the pellet and ongoing α-decays.
  - **Irradiation damage of cladding** via α-decays.
  - Cracking due to **hydride re-orientation**.

$$Zr + 2\,H_2O \rightarrow ZrO_2 + 2\,H_2$$

  - **Corrosion of cladding induced by fission and activation products.**

→ **Formation of agglomerates on the inner side of the cladding due to thermal gradient in SNF and possibility of halogen induced stress corrosion cracking**.

Final disposal

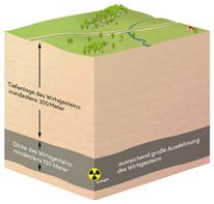

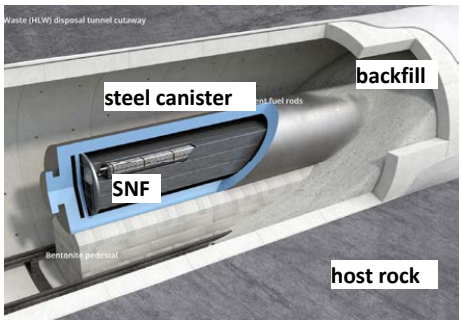

- **Deep geological disposal:**
  - Multibarrier concept: technical (e.g. waste matrix, cladding), geo-technical (e.g. buffer, backfill) and geological barriers (e.g. host rock, overburden).
  - Oxygen trapped in deep geological repository after its closure will be consumed e.g. by bacteria, reducing minerals and aerobic corrosion of outer layers of waste canisters.
  - Subsequently, ground water in contact with metallic canisters leads to anaerobic corrosion of metals, mainly corrosion of iron.
  - H_2 pressure build-up ≥ 50 bar in repository.

➡ **Safety analyses require profound knowledge on the occurence and chemical behaviour of long-lived and dose relevant radionuclides (e.g. ^{36}Cl, ^{129}I, ^{135}Cs).**

https://www.grimsel.com/gts-information/waste-disposal-overview/the-engineered-barrier-system (02.11.2021).
https://www.einblicke.de/fileadmin/images/magazin/Einblicke_6/Kriterien_zur_Endlagersuche.jpg (04.04.2022).

Open questions

- **In which condition is the fuel-cladding interface during interim storage and will it impact the integrity of the cladding?**
- **In which chemical speciation are possible cladding degrading elements such as chlorine or iodine present in SNF and cladding?**

➡ **Reducing uncertainties on degradation processes.**

SNF specimens

Fuel rod segment N0204, irradiated in the pressurised water reactor Gösgen (CH):

- Fuel type: **UO_X**, initial 3.8% ^{235}U enrichment (NIKUSI).
- Cladding alloy: **Zircaloy-4**.
- Full power days: 1226 days in 4 cycles.
- Average linear power: 260 W/cm.
- Average burn-up: **50.4 GWd/t_{HM}**.
- Decay time: ~ 32 years.

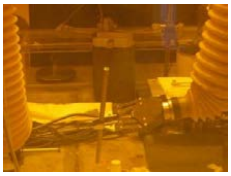

Fuel rod 5810, irradiated in the pressurised water reactor Obrigheim (DE):

- Fuel type: **MOX**, initial 3.2% Pu_{fiss} enrichment (OCOM).
- Cladding alloy: **Zircaloy-4**.
- Full power days: 1157 days in 4 cycles.
- Average linear power: 200 W/cm.
- Average burn-up: **38.0 GWd/t_{HM}**.
- Decay time: ~ 36 years.

Preparation of the SNF specimens

- Segmentation of the SNF specimens in specially equipped laboratories (hot cells).
- Use of a cutting machine Isomet® Low Speed Saw (*11-1180, Buehler Ltd*).
- Equipped with a diamond wafering blade Isomet® (*11-4254 Buehler Ltd*).
- Mechanical defueling of SNF specimens:
  - Fuel fragments.
  - Zircaloy cladding segments.

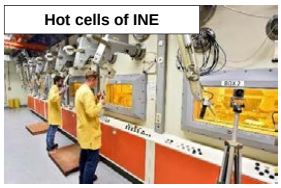

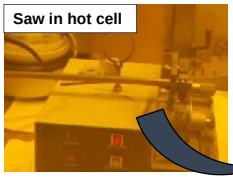

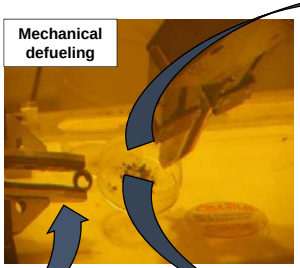

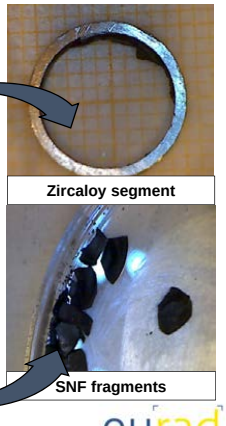

Spectroscopic measurements

- Preparation of fuel fragments and Zircaloy segments for spectroscopic analyses:
  - Scanning electron microscopy coupled with energy dispersive X-ray spectroscopy (**SEM-EDX**)
  - X-ray Photoelectron spectroscopy (**XPS**)
  - X-ray absorption spectroscopy (**XAS**)

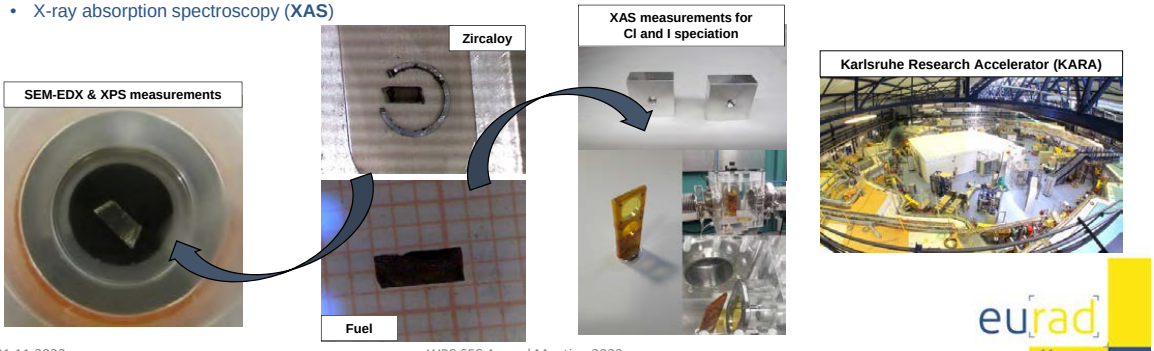

Spectroscopic measurements: SEM-EDX and XPS

- **SEM-EDX:**
  - Measurements were performed by use of a Quanta 650 FEG.
  - Accelerating voltage: 15 kV; beam current: 1 nA
  - **Information depth in range of few µm.**
- **XPS:**
  - Measurements performed on an ULVAC-PHI VersaProbe II spectrometer.
  - Mg Kα (E = 1253.6 eV) and Al Kα (E = 1486.7 eV) radiation sources.
  - **Information depth in range of few nm**.

All samples for SEM-EDX and XPS were treated in an ultrasonic bath prior to measurement.

INE-Beamline and CAT-ACT station at the KIT light source

- **INE-Beamline** fully operational since October 2005 (2nd dedicated beamline for radioactive materials in Europe).
- **CAT-ACT station** fully operational since fall 2016.
- Energy range 2.1 – 55 keV, bending magnet (INE-Beamline) or superconductin wiggler source (CAT-ACT).

Both stations are licensed for working with 10^6 the exemption limit and up to 200 mg of fissile ^{235}U and ^{239}Pu within a double containment.

01.11.2023 WP8 SFC Annual Meeting 2023 13

Spectroscopic analysis – SEM-EDX

- Zircaloy in contact with spent UO_x / MOX fuel:
  - **SEM-EDX:** Cl, Te, I, Cs, Fe, Zr, Ba, U.

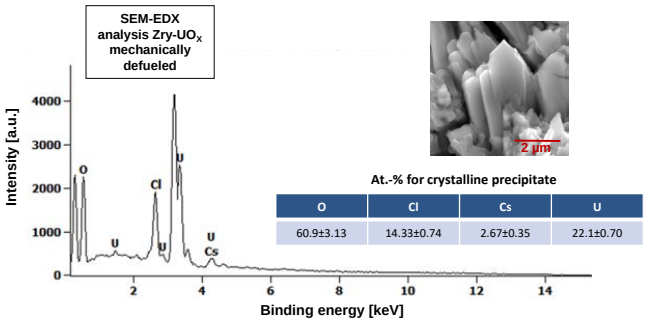

At.-% for crystalline precipitate

O	Cl	Cs	U
60.9±3.13	14.33±0.74	2.67±0.35	22.1±0.70

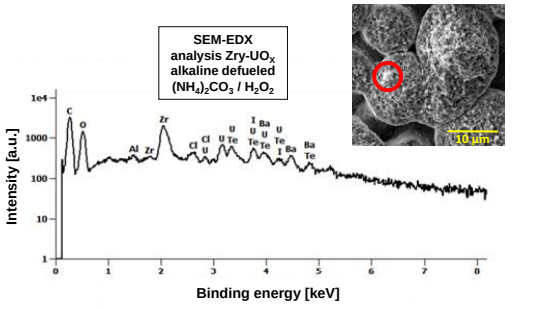

At.-% for agglomerates on alkaline defueled cladding

C	O	Al	Cl	Zr	Te	I	Ba	U
51.1±1.1	34.4±1.4	0.4±0.1	0.8±0.2	6.0±0.2	2.7±0.5	1.9±0.5	1.2±0.2	1.4±0.1

01.11.2023 WP8 SFC Annual Meeting 2023 14

Spectroscopic analysis – XPS

- **XPS analysis confirms Chlorine in oxidation state -I as Chloride (Cl^-):**
  - Binding energy $Clp_{3/2}$ for metal chlorides: ~198.5 – 199 eV.
  - All spectra superposed by minor intensity of U $5p_{3/2}$.

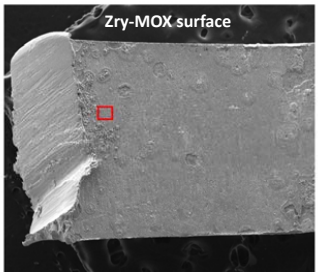

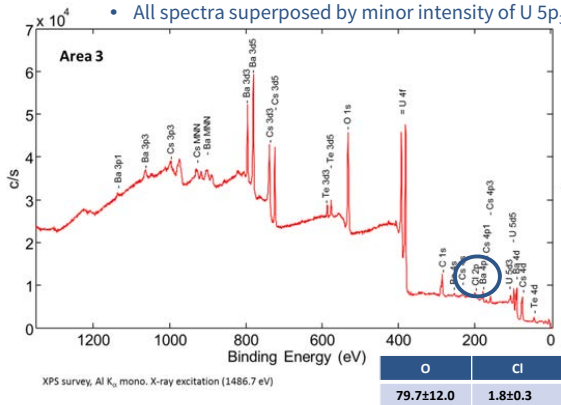

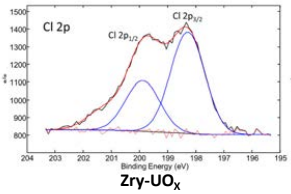

Zry-UO_x

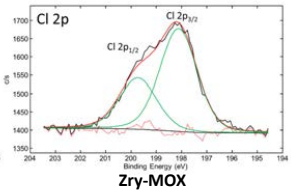

Zry-MOX

At.-% for analysed Zry-MOX area

O	Cl	Cd	Te	Cs	Ba	U
79.7±12.0	1.8±0.3	0.2±0.1	1.0±0.2	4.3±0.6	5.7±0.9	7.3±1.1

Spectroscopic analysis – XAS

- Knowledge on the chlorine (and iodine) inventory and speciation in fuel and Zircaloy afflicted with large uncertainties.
- Initial maximum impurity assumptions of up to 25 ppm Cl in the fuel and 20 ppm Cl in Zircaloy-4 cladding [HÄK19].
- First ever XAS measurements for chlorine (and iodine) speciation in fuel and cladding. ⟹ Complex mixed phases in case of chlorine.

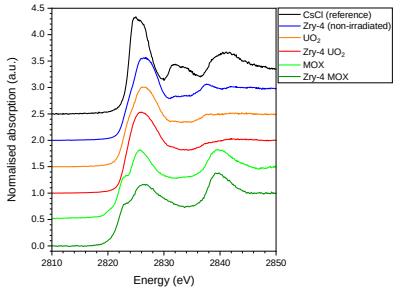

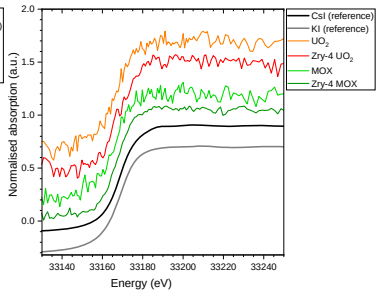

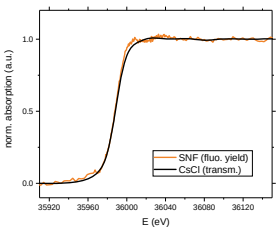

[HÄK19] S. Häkkinen, *Impurities in LWR fuel and structural materials*, VTT, Finland (2019).

Spectroscopic analysis – XAS

- Initial analysis confirms results obtained by E. Curti et al.* (PSI, SNF bulk sample obtained by FIB): Se is present as Se(-II) in UO_2 lattice replacing oxygen.
- Se K-EXAFS point to U in the first Se coordination sphere.
- Selenium (same as tellurium) are reacting strongly with zirconium-based cladding tubes.
- **However**, in presence of caesium, formation of Cs-selenides / Cs-tellurides is thermodynamically preferred, reducing reactions with the cladding.

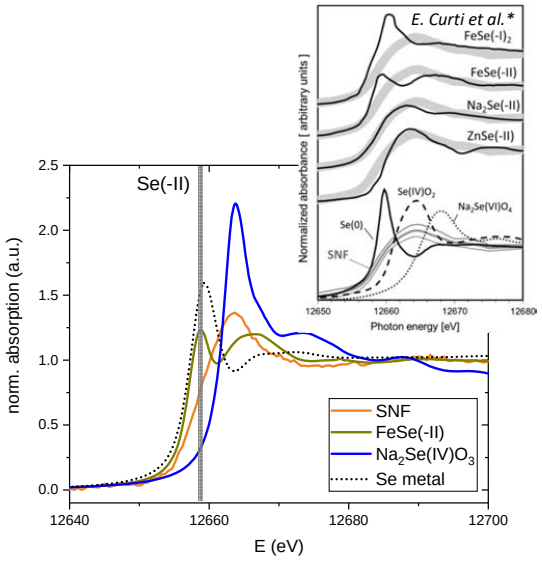

** E. Curti et al., Environ. Sci.: Processes Impacts 17, 2015, E. Curti et al., Journal of Nuclear Materials 453, 2014*

Spectroscopic analysis – XAS

- Measurements in UOX fuel: Mo K, Ru K, Pd K, Tc K, Te K – Rh hampered due to Rh coated mirrors!

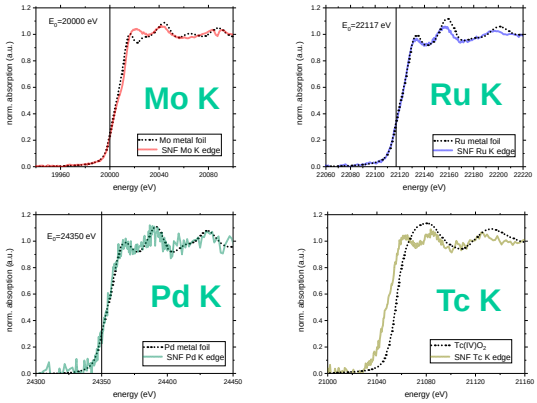

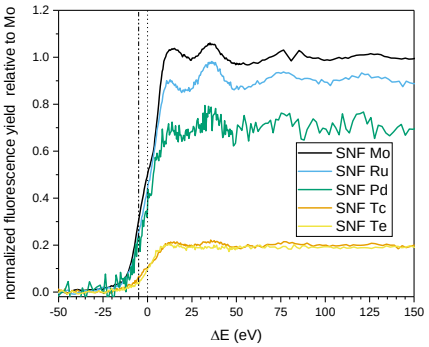

Measurements on MOX (38.0 GWd/t_{HM}) were performed. Data analysis ongoing.

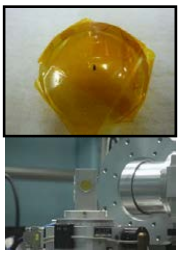

element	at%	calc.
Mo	**0.324**	**0.324**
Ru	0.223	0.203
Pd	0.135	0.114
Tc	0.056	0.072
Te	0.017	0.040

Summary

- **First ever measurements of Cl *K*- and I *K*-edge** in high active waste specimens (SNF and Zircaloy).
- Agglomerates in interaction layer consist, amongst others, of halogen-rich mixed phases **(Cl and I)**, as well as Cs, Te, Ba, U and Pu.
- However: **For profound statement on cladding integrity**, experiments for mechanical stability (e.g. nanoindentation) are necessary.

Femto-Indenter FT-104
Soon to be established in controlled area of KIT-INE

Acknowledgements

- **E. González-Robles (IdISBa)**
- **V. Krepper (KIT-INE)**
- **S. Schmitt (KIT-INE)**
- **K. Hardock (KIT-INE)**
- **Beamline-Staff (KIT-IBPT)**

European Joint Programme on Radioactive Waste Management

This work received funding from the European Union's Horizon 2020 research and innovation programme under grant agreement No 847593

Thank you for your kind attention

4. Participation to a Conference

- Verification and validation of MCNP/CINDER burnup capabilities; S. Panizo, CIEMAT; 46th Annual Meeting of the Spanish Nuclear Society; 06 - 08/10/2021
- Evaluating Peak Area Uncertainties in Connection to Passive Gamma Measurements of Spent Nuclear Fuel; V. Solans, UU; TopFuel conference, Santander, Spain; 24 -28/10/2021
- Spent Fuel Characterization to Support NPP Krško Spent Fuel Dry Storage Project; M. Kromar, JSI; 13th International Conference of the Croatian Nuclear Society; 05 - 08/06/2022
- Passive neutron and gamma technique for spent nuclear fuel characterisation; V. Solans, UU; IAEA CRP spent fuel characterization ; 22 – 23/09/2022
- Recent Spent Fuel Research at VTT; S. Häkkinen, P. Juutilainen, L. Vaara, R. Tuominen; Nuclear Science and Technology Symposium 2022 (SYP2022); 27/05/2021
- Rossi-Alpha distribution analysis of DDSI data for spent nuclear fuel investigation ; V. Solans, UU; Symposium on International Safeguards: Reflecting on the Past and Anticipating the Future; 31/10-04/11/2022

4.1 Verification and validation of MCNP/CINDER burnup capabilities; S. Panizo, CIEMAT; 46th Annual Meeting of the Spanish Nuclear Society; 06 - 08/10/2021

Verification and validation of MCNP/CINDER burnup capabilities

Impact evaluation of the nuclear data library *cinder.dat*

Sonia Panizo Prieto, Francisco Álvarez-Velarde, Daniel Cano Ott.

CIEMAT – Unidad de Innovación Nuclear.

Sonia.Panizo@ciemat.es

GOBIERNO DE ESPAÑA MINISTERIO DE CIENCIA E INNOVACIÓN Ciemat Centro de Investigaciones Energéticas, Medioambientales y Tecnológicas

Granada 2021 46 REUNIÓN ANUAL SOCIEDAD NUCLEAR ESPAÑOLA

Introduction

- The characterization of spent nuclear waste is essential for its safe management given that it is the source of decay heat, neutron emission and gamma emission, coming from unstable isotopes.
- The EU EURAD (European Joint Programme on Radioactive Waste Management) project includes a Work Package devoted to Spent Fuel Characterization and Evolution Until Disposal, where this work is framed.
- Burn-up calculations are needed for this characterization. They are based on the coupling of codes for neutronics and isotopic evolution with the irradiation. Tools dedicated to burn-up are usually validated using the SFCOMPO database (available at the OECD/NEA).
- This work includes the validation of two burn-up codes, EVOLCODE and MCNP/CINDER, with light water reactor experimental data from the SFCOMPO database, and their verification when both use the same basic neutron library.

MCNP/CINDER & EVOLCODE

- MCNP: general-purpose Monte Carlo N-Particle code that simulates neutron, photon and electron transport.
- CINDER: burnup code that calculates the isotopic inventory evolution of irradiated materials. It uses a self-contained library file, cinder.dat, that includes fission yields, decay data and cross-sections distributed among 63 energy groups.
- EVOLCODE: burnup code developed at CIEMAT that incorporates neutron transport and depletion evolution, by means respectively of MCNP and ORIGEN or ACAB codes. It also incorporates a predictor/corrector method.

$$\frac{dN}{dt} = -N_m(t)\beta_m + Y_m + \sum N_k(t)P_{k\to m}$$

$N_m(t)$: atomic density of isotope "m"
β_m: transmutation probability of isotope "m"
Y_m: production rate of isotope "m"
$P_{k\to m}$: transmutation probability of isotope "k" to "m"

$$\vec{\nabla}\cdot\vec{J}(\vec{r}) + \Sigma_a(\vec{r})\phi(\vec{r}) = s'''(\vec{r}) + \nu\Sigma_f(\vec{r})\phi(\vec{r})$$

$\vec{\nabla}\cdot\vec{J}(\vec{r})$ dV: neutrons in dV that escape without interaction
$\Sigma_a(\vec{r})\phi(\vec{r})$dV: captured neutrons in dV
$s'''(\vec{r})$dV: neutrons from external source in dV
$\nu\Sigma_f(\vec{r})\phi(\vec{r})$dV: neutrons produced by fission in dV

Takahama-3

- Takahama-3. Japanese light water reactor (LWR) operated by Kansai Electric Power Company (KEPCO).
- Three fuel rods of the assembly NT3G23 from Takahama-3 which are referred to as SF95, SF96 and SF97, were reproduced in both codes, MCNP and EVOLCODE.
- SF95-5 fuel pin selected – EURAD. Single model includes cladding and moderator.

Fuel assembly NT3G23 from Takahama-3.

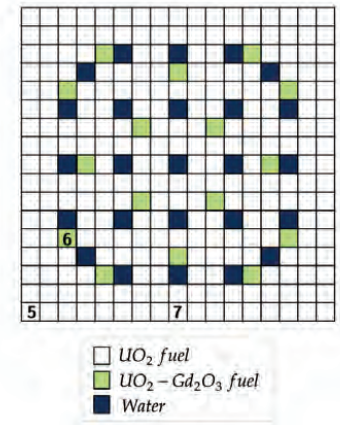

Operating history of SF95 fuel rod in Takahama-3.

Beginning	Ending	Days	Status
26/01/1990	15/02/1991	385	Burnup
15/02/1991	14/05/1991	88	Cool
14/05/1991	19/06/1992	402	Burnup

Results - actinides

	C/E	
	MCNP/CINDER	EVOLCODE
U-234	0.91	0.91
U-235	1.03	1.04
U-236	1.01	0.99
U-238	1	1
Pu-238	1.12	1.15
Pu-239	1.12	1.14
Pu-240	1.07	1.07
Pu-241	1.07	1.09
Pu-242	1	1
Am-241	1.12	1.09
Am-242m	-	1.29
Am-243	1.04	1.09
Cm-242	1.03	1.04
Cm-243	1.01	1.05
Cm-244	1.17	1.24
Cm-245	1.4	1.52
Cm-246	1.73	1.86

The (C/E) values show a good agreement between calculations and experimental values for the actinides.

- For the uranium isotopes: 3-4% difference for ^{235}U and even better agreement for ^{236}U and ^{238}U.
- Largest discrepancies between the simulations and the experimental data: $^{244,245,246}Cm$.
- Relevant discrepancies for ^{238}Pu and ^{239}Pu.

7th October 2021 46ª Reunión Anual SNE 5

Results - fission products

The fission products also show a good agreement except for ^{125}Sb and ^{154}Eu.

	C/E	
	MCNP/CINDER	EVOLCODE
Cs-137	0.97	0.96
Cs-134	0.98	0.98
Eu-154	1.13	1.25
Ce-144	0.97	0.96
Sb-125	2.07	2.26
Ru-106	1.09	1.13
Nd-142	0.88	0.91
Nd-143	0.97	0.98
Nd-144	0.96	0.95
Nd-145	0.97	0.98
Nd-146	1	1.01
Nd-148	1	0.99
Nd-150	0.99	1

7th October 2021 46ª Reunión Anual SNE 6

Results - ^{154}Eu

The discrepancy in this isotope comes from the thermal ^{239}Pu cumulative fission product yields for **^{153}Eu** between JEFF-3.3 and ENDF/B-VI:

FY (cumulative)	ENDF/B-VI	JEFF-3.3
Pu-239	$3.61 \cdot 10^{-3}$	$5.90 \cdot 10^{-3}$

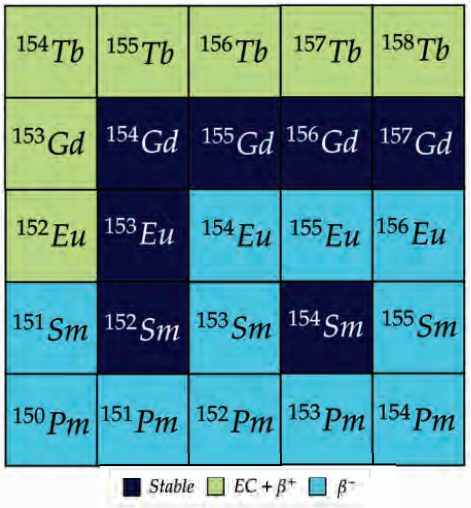

Library *cinder.dat* in MCNP

MCNP supersedes all the **cross-section** data in cinder.dat for those isotopes and reactions with transport information.

No information about **fission yields** is updated from the transport data file.

This has been verified using the SF95-5 model with a single burn-up step of 120 days to ease the subsequent analysis.

To this end, three calculations have been performed, replacing in cinder.dat information from the JEFF-3.3 data:

- XS: Only the cross-sections are replaced.
- XS+FY: The cross-sections and the fission product yields are replaced.
- XS+FY+HL: Cross-sections, fission product yields and half-life data are replaced.

Isotope	XS	XS + FY	XS + FY + HL
U-233	-1.50 %	-0.50 %	-0.50 %
U-234	0.00 %	0.00 %	0.00 %
U-235	0.00 %	0.00 %	0.00 %
U-236	0.00 %	0.00 %	0.00 %
U-238	0.00 %	0.00 %	0.00 %
Np-237	-0.10 %	-0.10 %	-0.10 %
Pu-238	-0.10 %	-0.20 %	-0.10 %
Pu-239	0.00 %	0.00 %	0.00 %
Pu-240	0.00 %	-0.10 %	-0.10 %
Pu-241	0.00 %	-0.20 %	-0.20 %
Pu-242	0.00 %	-0.20 %	-0.30 %
Sr-88	0.00 %	0.20 %	0.20 %
Sr-90	0.10 %	-2.00 %	-2.00 %
Mo-95	0.00 %	0.00 %	-0.10 %
Tc-99	0.10 %	0.20 %	0.20 %
Ru-101	0.00 %	0.20 %	0.20 %
Ru-106	0.00 %	2.70 %	2.70 %
Rh-103	0.00 %	1.90 %	1.90 %
Ag-109	0.10 %	**-21.80 %**	-21.80 %
Sb-125	0.00 %	**-18.80 %**	-18.80 %
I-129	0.00 %	**27.80 %**	27.80 %
Cs-133	0.10 %	-0.60 %	-0.60 %
Cs-134	-1.10 %	-1.90 %	-1.90 %
Cs-137	0.00 %	-1.70 %	-1.70 %
Ce-144	0.10 %	-7.20 %	-7.20 %

Isotope	XS	XS + FY	XS + FY + HL
Nd-142	-0.10 %	0.00 %	0.00 %
Nd-143	0.10 %	-0.20 %	-0.20 %
Nd-144	0.00 %	-6.80 %	-6.80 %
Nd-145	0.10 %	0.70 %	-
Nd-146	0.10 %	0.30 %	-0.20 %
Nd-148	0.00 %	2.50 %	2.50 %
Nd-150	0.00 %	0.70 %	0.70 %
Pm-147	0.00 %	0.20 %	0.10 %
Sm-147	0.00 %	0.20 %	0.10 %
Sm-148	**34.60 %**	34.70 %	34.60 %
Sm-149	-0.60 %	-5.50 %	-5.50 %
Sm-150	-0.20 %	-4.90 %	-4.90 %
Sm-151	0.10 %	1.90 %	2.00 %
Sm-152	0.00 %	-2.30 %	-2.30 %
Sm-153	0.10 %	-7.20 %	-7.20 %
Eu-151	0.10 %	2.00 %	-3.10 %
Eu-153	0.00 %	-7.70 %	-7.70 %
Eu-154	-0.70 %	**-12.10 %**	-7.30 %
Eu-155	0.00 %	-1.80 %	-1.80 %
Gd-154	-2.10 %	-11.10 %	-7.40 %
Gd-155	0.00 %	-1.90 %	-3.50 %
Gd-156	0.00 %	-8.40 %	-8.30 %
Gd-157	0.00 %	-7.90 %	-7.90 %
Gd-158	0.00 %	**-16.90 %**	-16.90 %

Results - ^{148}Sm

There is a **lack of cross-section** data in JEFF-3.3 for **capture in ^{147}Pm** leading to ^{148M}Pm, one of the parents of ^{148}Sm (with a half-life of 41.3 d, larger than the ground ^{148}Pm, with 5.37 d), allowing an extra accumulation of ^{148}Sm with JEFF-3.3.

Isotope	XS	XS + FY	XS + FY + HL
Sm-148	**34.60 %**	34.70 %	34.60 %

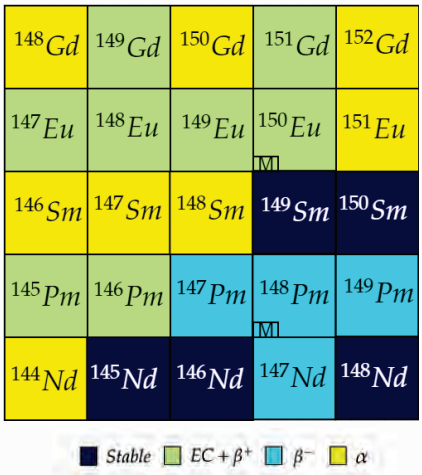

Results - ^{109}Ag

Isotope	XS	XS + FY	XS + FY + HL
Ag-109	0.10 %	-21.80 %	-21.80 %

The discrepancy in this isotope comes from the cumulative fission product yields in JEFF-3.3, which are smaller than in ENDF/B-VI for the most relevant tables. ^{239}Pu is the largest contributor.

FY (cumulative)	ENDF/B-VI	JEFF-3.3
U-235	$3.12 \cdot 10^{-4}$	$2.85 \cdot 10^{-4}$
U-238	$2.52 \cdot 10^{-3}$	$1.62 \cdot 10^{-3}$
Pu-239	$1.48 \cdot 10^{-2}$	$1.11 \cdot 10^{-2}$

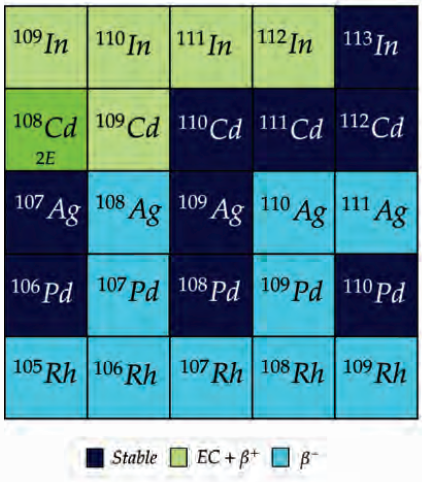

Results - ^{129}I

Isotope	XS	XS + FY	XS + FY + HL
I-129	0.00 %	27.80 %	27.80 %

The discrepancy in this isotope comes from the cumulative fission product yields in JEFF-3.3, which are smaller than in ENDF/B-VI for the most relevant tables. ^{235}U is responsible for the 90% production.

FY (cumulative)	ENDF/B-VI	JEFF-3.3
U-235	$5.43 \cdot 10^{-3}$	$8.14 \cdot 10^{-3}$

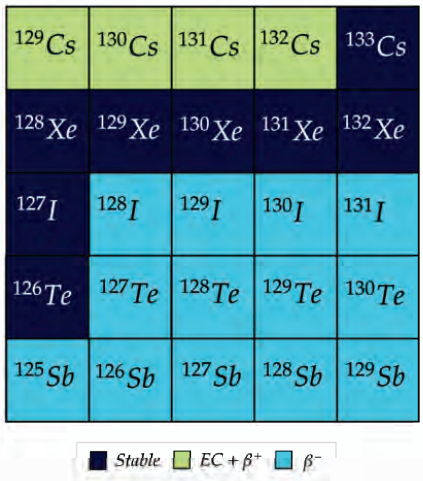

Results - ^{125}Sb

Isotope	XS	XS + FY	XS + FY + HL
Sb-125	0.00 %	-18.80 %	-18.80 %

Again, the discrepancy in this isotope comes from the cumulative fission product yields. The 80% of its mass appears as cumulative fission yield from the ^{238}U fast fission table.

FY (cumulative)	ENDF/B-VI	JEFF-3.3
U-238	$4.85 \cdot 10^{-4}$	$2.10 \cdot 10^{-4}$

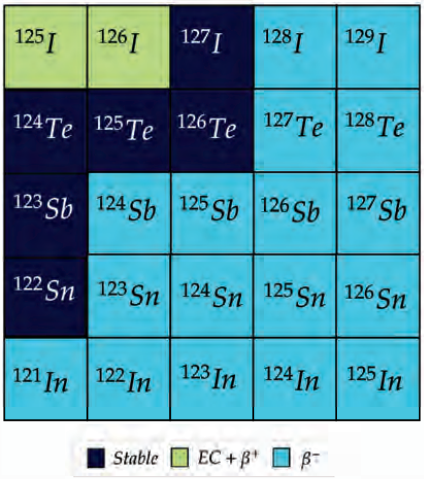

Results - ^{158}Gd

Isotope	XS	XS + FY	XS + FY + HL
Gd-158	0.00 %	-16.90 %	-16.90 %

The discrepancy comes from two different sources.

- Discrepancy ~7000 b between ENDF and JEFF in capture cross-section of ^{157}Gd (sufficiently small).
- Formation of ^{158}Gd as fission product and again discrepancies come from the cumulative fission product yields.

FY (cumulative)	ENDF/B-VI	JEFF-3.3
U-238	$3.29 \cdot 10^{-5}$	$1.96 \cdot 10^{-5}$

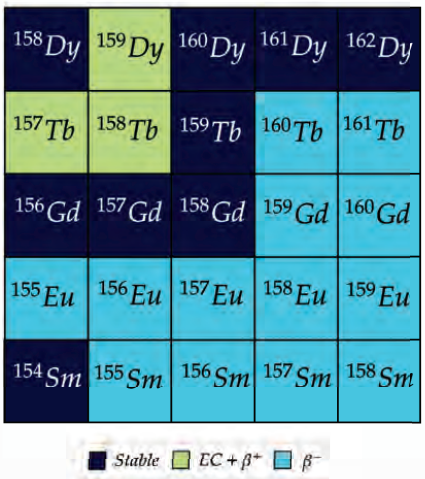

Conclusions

- General good agreement between calculations with EVOLCODE and MCNP/CINDER and experimental values have been obtained for a simple model of the Takahama-3 benchmark.
- Some severe discrepancies in the fission products between codes led to a more in-depth study of the MCNP and CINDER coupling.
  - Identification of an inconsistent use of cinder.dat in MCNP.
- The replacement of data from JEFF-3.3 in cinder.dat has a substantial impact is for some of the fission products, especially in the case of the fission yield data substitution.
- It is necessary to create a new version of the cinder.dat library replacing all the data by JEFF-3.3 data if coherent estimations are desired.

7th October 2021 46ª Reunión Anual SNE 15

4.2 Evaluating Peak Area Uncertainties in Connection to Passive Gamma Measurements of Spent Nuclear Fuel; V. Solans, UU; TopFuel conference, Santander, Spain; 24 -28/10/2021

EVALUATING PEAK AREA UNCERTAINTIES IN CONNECTION TO PASSIVE GAMMA MEASUREMENTS OF SPENT NUCLEAR FUEL

V. SOLANS[1], H. SJÖSTRAND[1], P. JANSSON[1], S. GRAPE[1], P. SCHILLEBEECKX[2], A. SJÖLAND[3,4]

[1] *Uppsala University,* [2] *JRC-Geel,* [3] *Swedish Nuclear Fuel and Waste Management Company* [4] *Lund University*

UPPSALA UNIVERSITET

Virginie Solans
PhD student
Uppsala University
virginie.solans@physics.uu.se

Objective

In this study, the objective is to estimate the uncertainty in the peak area determination of those radionuclides from the SNFs using results of passive gamma-ray measurements. In particular the uncertainty coming from the parameters of the models will be investigated, and compared for the different models.

Fitted models

The signal part of the full-energy peak is here proposed to be described using a Gaussian function and a tailing function.

Gaussian function

$$P(x) = a_1 \cdot exp(-(x-\mu)^2/\sigma^2) \quad (1)$$

Tailing function

$$T(x) = a_3 \cdot (exp(B(x-\mu))) \cdot (1 - exp((-1/\sigma^2)(x-\mu)^2)) \cdot \delta \quad (2)$$

Background function

$$B(x) = a_2 \cdot erfc((x-\mu)/\sigma) + constant \quad (3)$$

where a_1, a_2 and a_3 are scale parameters, μ is the mean value of the Gaussian peak, and σ is related to the width of the peak. δ takes the value 1 when $x < \mu$ and 0 when x is above μ. x are the channels of the spectrum (proportional to the energy deposited).

Numerical integration

Numerical integration using best fitted model, NI_{BFM}

For this method the background is simultaneously fitted together with the peak. I.e., the background level is determined from the best fitted model (the model that fits the data the best between the one with or without the tailing term).

Numerical integration fitting background using only edge channels, NI_E

In this method, a sequential fit of the peak and the background is performed. First the full spectrum is fitted. Subsequently, the parameters defining the the full energy peak are fixed. Finally, the background parameters ($erfc$ function and constant value) are fitted using only the edge channels. By first defining the peak and subsequently fitting the background in a region where the spectrum is dominated by the background, a better fit to the background can be obtained. Since the NI (Numerical Integration) methods only need a good method to define the background level, this method is considered to be best practise and is the reference method for the paper.

Peak area evaluation and uncertainty

$$\text{Area uncertainty} = \sqrt{J_{\text{Area}} * J_{\text{Parameters}} * Cov * J^T_{\text{Parameters}} * J^T_{\text{Area}}} \quad (4)$$

where Cov is the covariance matrix of the parameters of the fit given by the "fit" function of the lmfit package in Python. $J_{\text{Parameters}}$ is the Jacobian of the fitted model with respect to the parameters of the fit. J_{Area} is the Jacobian of the function that described the peak area, with respect to the predicted count per channel. This is one of the methods that can be used to account for a non-perfect parameterisation of the data.

To compute the uncertainty for the numerical integration methods, it was decided to use again Eq. 4, and the square root of the total area:

$$\text{Area uncertainty} = \sqrt{(\sqrt{\text{total area}})^2 + (\text{uncertainty from Eq.4})^2} \quad (5)$$

For the numerical method NI_E, the ratio between the $\sqrt{\text{total area}}$ and the uncertainty from Eq.5 is compared. In average, the $\sqrt{\text{total area}}$ is 1.43 higher than the uncertainty from Eq.4. The minimum ratio in the 166 spectra measured on 42 assemblies at Clab, is 1.08, and the maximum ratio is 1.63. Therefore in all the spectrum the $\sqrt{\text{total area}}$ component of the uncertainty is the bigger.

Results

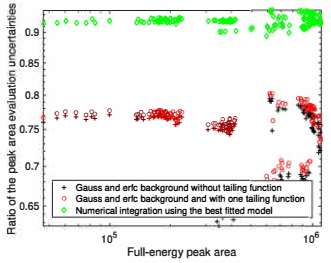

Fig. 1: Ratio of the full-energy peak area uncertainty for all models with respect to the numerical integration using only the edges (NI_E).

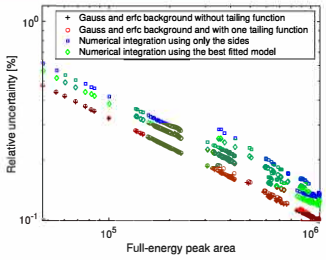

Fig. 2: Relative uncertainty of the full-energy peak area uncertainty for all models

The relative uncertainty decreases when the full-energy peak area, because the counting statistics improves (mainly the term $\sqrt{\text{total area}}$). At maximum the uncertainty is 0.6% for the reference model, and 0.2% in average. The relative uncertainty can be fitted to a exponential relation depending on the full-energy peak area which is: Relative uncertainty [%] $= (\text{Full-energy peak area})^{-0.4844} \cdot 112.1$.

Conclusion

On average, the numerical integration gives higher uncertainties than the other methods tested in this study on the full-energy peak area after subtraction of the background. However other methods such as the fitted models has uncertainties that cannot be trusted for $\chi^2_\nu >> 1$. Therefore this method (integration using only the edges, IN_E) should be used in similar cases.

Acknowledgement

The project leading to this paper has received funding from the European Union's Horizon 2020 research and innovation programme under grant agreement No 847593.

4.3 Spent Fuel Characterization to Support NPP Krško Spent Fuel Dry Storage Project; M. Kromar, JSI; 13th International Conference of the Croatian Nuclear Society; 05 - 08/06/2022

Spent Fuel Characterization to Support NPP Krško Spent Fuel Dry Storage Project

Marjan Kromar, Jan Malec
"Jožef Stefan" Institute
Andrej Kavčič
Nuclear Power Plant Krško

13th International Conference of the Croatian Nuclear Society
Zadar, Croatia, June 5-8, 2022

2/40

OUTLINE

- Introduction
- Fuel manufacturing and irradiation data
- Determination of the suitable calculation tools and models
- Sensitivity analysis
- Fuel segmentation
- Conclusions

Introduction

- Currently, all spent fuel in the NPP Krško (NEK) is stored in the spent fuel pool located in the fuel handling building of the plant.
- NEK decided to implement inherently safer dry storage solution.
- Spent Fuel Dry Storage (SFDS) project - the building with Holtec International HI-STORM FW casks.
- Jožef Stefan Institute (JSI) is supporting NPP Krško SFDS project together with the Faculty of Electrical Engineering and Computing (FER), University of Zagreb.
- JSI is providing independent spent fuel characterization data together with validated procedures and calculation tools.

Fuel manufacturing and irradiation data

- NEK database maintained by FAR code - “as built” fuel manufacturing data (provided by the fuel manufacturer Westinghouse Electric Company) and measurements performed at the plant.
- JSI database maintained by calculation performed by CORD-2 system - “as built” data periodically sent from NEK to JSI.
- Harmonization of both databases - the following FA parameters were compared:
  - mass,
  - enrichment,
  - number of BPRs,
  - number of IFBA rods,
  - burnup.

Fuel manufacturing and irradiation data

- All FAs inserted into the core up to the cycle 31 were considered. Burnup comparison was performed for the first 30 cycles.
- Comparison has shown a few minor differences, which were resolved by inspection of original documents from NEK archive.
- Final FAs burnup reported in the FAR (obtained from INCORE measurements) and FASLIB (obtained from CORD-2 calculations) agree well. All values are within 3.5 %.

Determination of the fuel parameter space

- Determination of the suitable fuel parameters range covering entire spent fuel variations is needed to define valid parameter space.
- FASLIB database was used, since it contains calculated data required for the sensitivity analysis such as burnup distribution, various temperatures, moderator density, specific power, soluble boron concentrations etc.
- Data are listed for 10 axial layers with relative thicknesses (1, 1, 2, 4, 4, 4, 4, 2, 1, 1), where the unit is 15.24 cm (6 inch). Special attention is needed for the first and last axial periphery region, where masses and enrichments differ significantly (axial blankets) compared to the central regions for the Vantage5 fuel.

Determination of the fuel parameter space

- Relative large parameter variations occurred during the plant operation of almost 40 years.

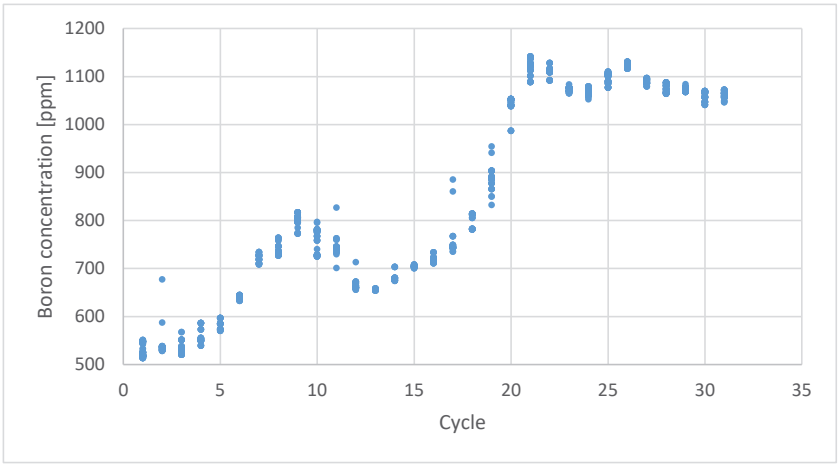

Average soluble boron concentration

Determination of the fuel parameter space

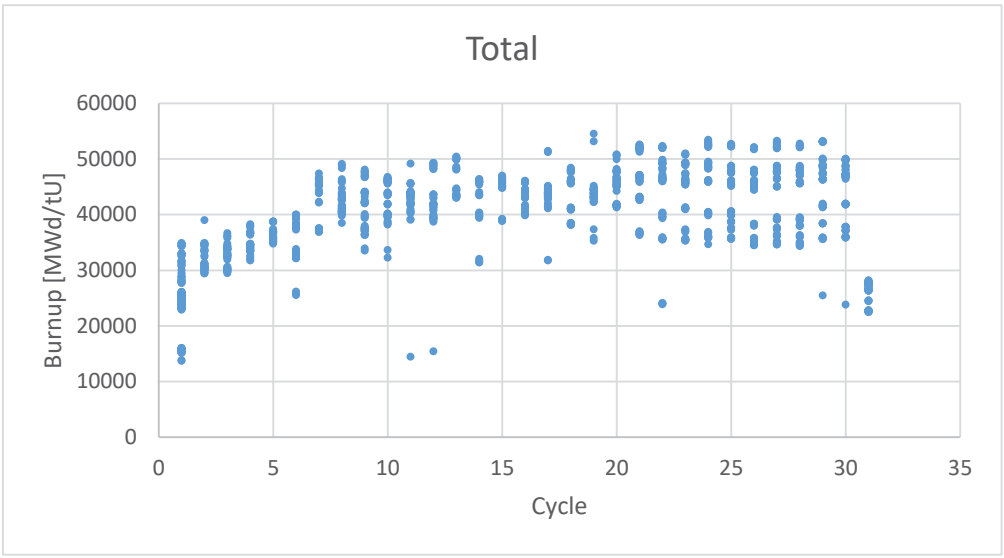

Total fuel assembly burnup

Determination of the fuel parameter space

9/40

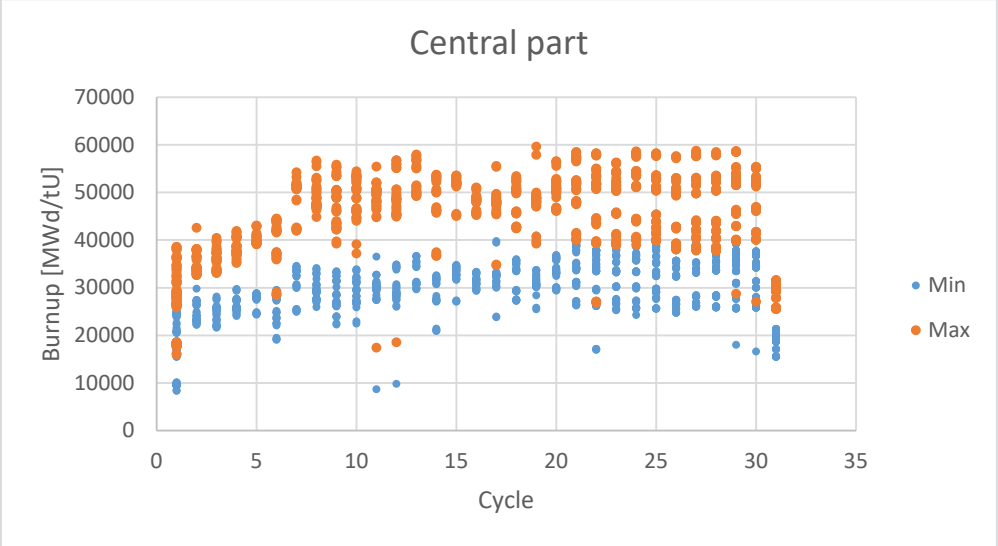

Minimal and maximal burnup values of central regions

Determination of the fuel parameter space

10/40

Fuel parameters range

Parameter	**Range**
Fuel enrichment	0.7 % - 5 %
Maximal burnup, max. difference	60000 MWd/tU, 24000 MWd/tU
Burnup range	36000 MWd/tU - 60000 MWd/tU
Fuel temperature	600 K – 1100 K
Moderator density	0.655 g/cm^3 (601.91 K)-0.755 g/cm^3 (558.56 K)
Boron concentration	500 ppm -1200 ppm
Specific power	15 W/gU - 65 W/gU
Number of rods in BPR absorbers	0 - 16
Number of IFBA rods	0 - 116

Determination of the suitable calculation tools and models

- SCALE code system has been selected for the spent fuel characterization, while the Serpent2 code served as an independent supplementary tool to validate prepared SCALE models. Both code systems are widely used and are thoroughly validated.
- The TRITON/NEWT module from the SCALE package has been used in the analysis, since for now more contemporary POLARIS is not capable to provide ORIGEN binary one-group reaction coefficients library files (.f33). SCALE version 6.2.4 with internal 56 energy group library v7-56 based on the ENDF/B-VII.1 evaluated nuclear data files has been applied.
- Version 2.1.29 of the Monte Carlo code Serpent2 and the continuous energy cross section library in ACE format, based also on the ENDF/B-VII.1 evaluated nuclear data files has been used for the validation.

NPP Krško fuel model validation

- A typical FA with 4.95 % enrichment and no IFBA rods was selected as a test case. A reference 2-D case scenario (infinite in axial direction) with periodic boundary conditions in lateral direction consists of the following reactor operational parameters:
    1. Fuel temperature 900 K,
    2. Moderator temperature 580.46 K with density 0.70871 g/cm^3,
    3. Soluble boron concentration of 1000 ppm.
- Parameters are close to the average operational parameters applied in the last NPP Krško cycles.
- Decay heat, fuel activity, photon and neutron source term after burnup of 60000 MWd/tU were examined.

NPP Krško fuel model validation

13/40

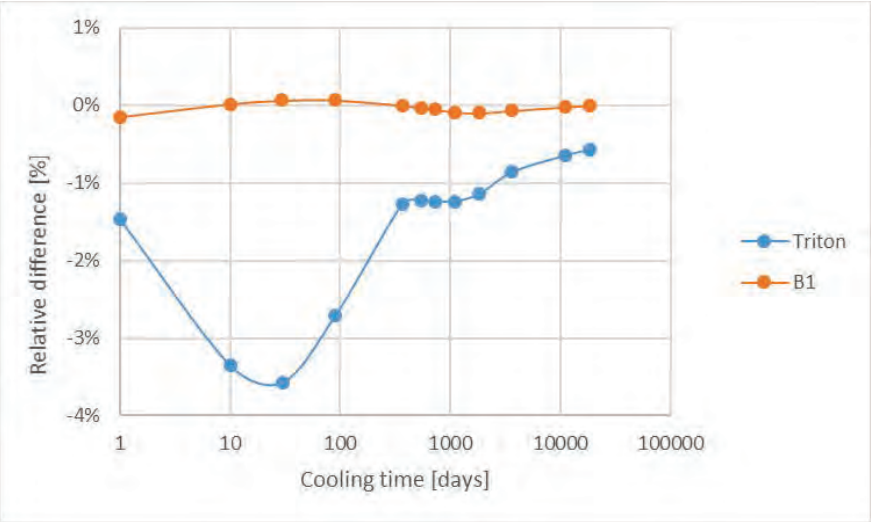

Relative differences of the decay heat – DH; Triton: $(DH_{SCALE} - DH_{Serpent})/ DH_{Serpent}$, B1: $(DH_{B1} - DH_{SCALE})/DH_{SCALE}$

NPP Krško fuel model validation

14/40

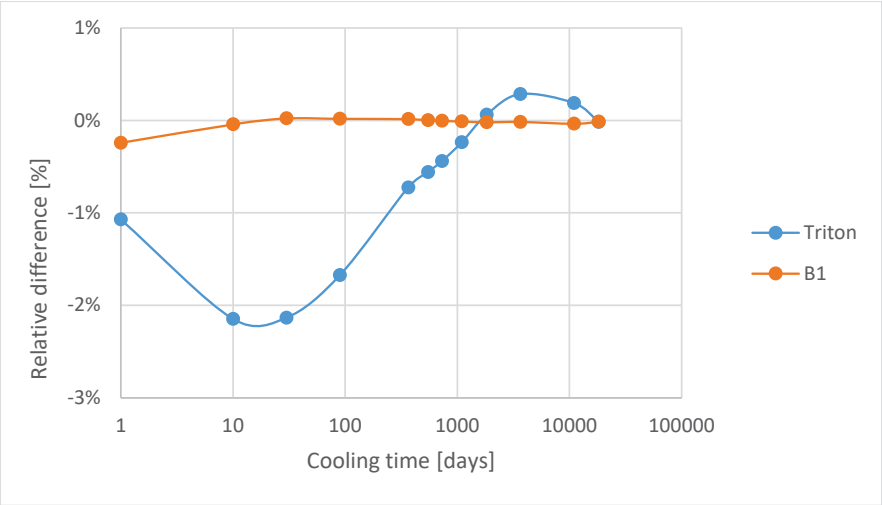

Relative differences of the activity – A; Triton: $(A_{SCALE} - A_{Serpent})/ A_{Serpent}$, B1: $(A_{B1} - A_{SCALE})/A_{SCALE}$

Origami model validation

- The use of the TRITON/NEWT sequence for the characterization of the more than 1400 considered FAs would be impractical, since a single depletion run takes around 2 hours on the PC with the Intel I7 processor.
- Fortunately, the TRITON/NEWT module is capable to provide ORIGEN binary one-group reaction coefficients library .f33 files. These library files are sufficient to determine isotopic composition during the fuel irradiation (solution of Bateman equations) avoiding the need of time-consuming neutron transport calculation.
- However, the calculation sequence has to be validated.

Origami model validation

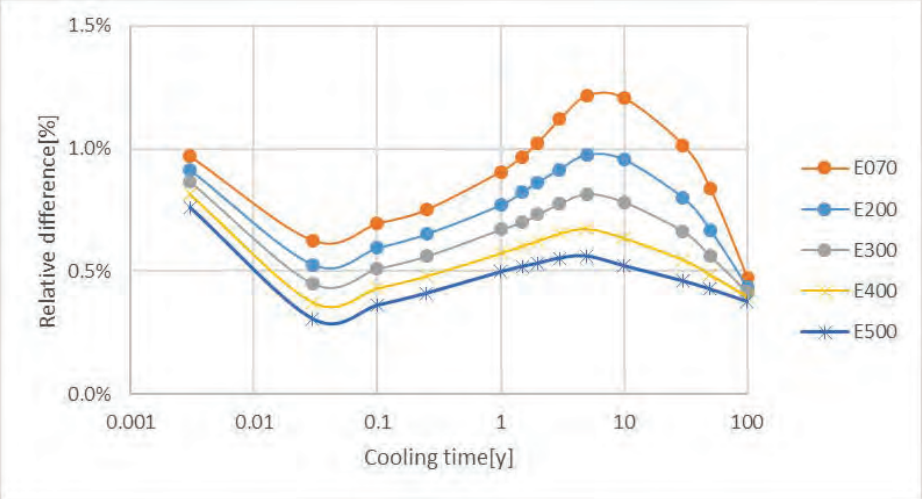

Relative differences of the ORIGAMI decay heat compared to the TRITON/NEWT results

Origami model validation

17/40

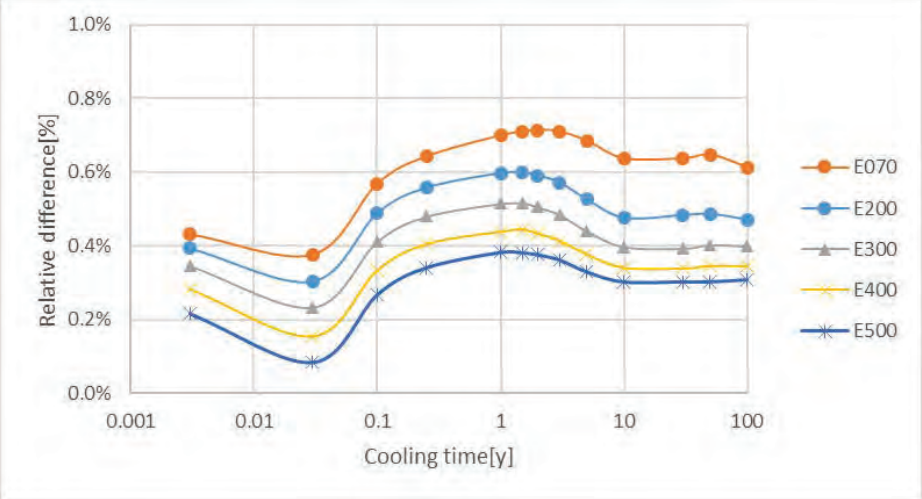

Relative differences of the ORIGAMI activities compared to the TRITON/NEWT results

Origami model validation

18/40

- Closer examination has revealed that the observed differences are due to the neutron capture reactions.
- Namely, in the FA non-fuel materials (e.g., structural materials) are also present. These materials contribute to the overall power production due to the energy produced by the neutron capture. For a given value of the total assembly power, this reduces the power from the fuel mass and thus slightly alter the fuel burnup and isotopics.
- The problem is that this contribution is case dependant and varies with enrichment, burnup, etc. The factor of the energy contributed to the fuel itself varies from 0.986 (enrichment 0.7 %) to the 0.997 (enrichment 5 %) for the presented cases.

Origami model validation

19/40

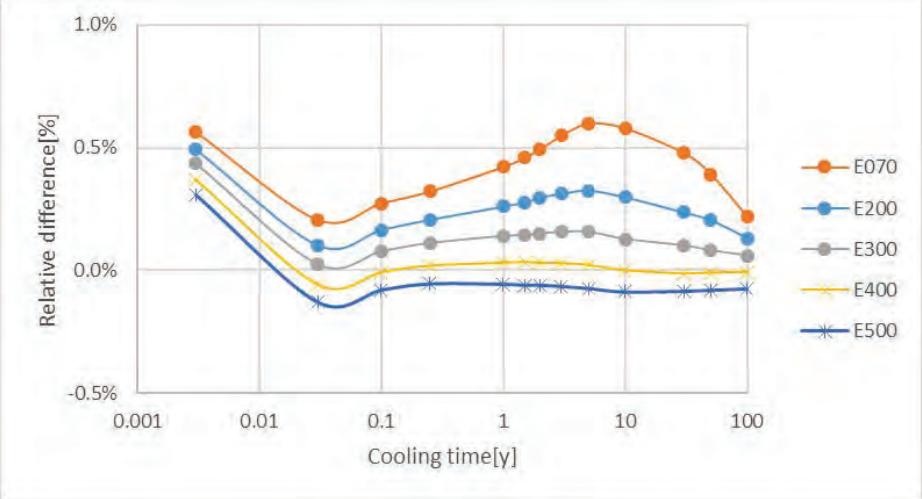

Relative differences of the ORIGAMI decay heat compared to the TRITON/NEWT results, neutron capture correction factor 0.996

Origami model validation

20/40

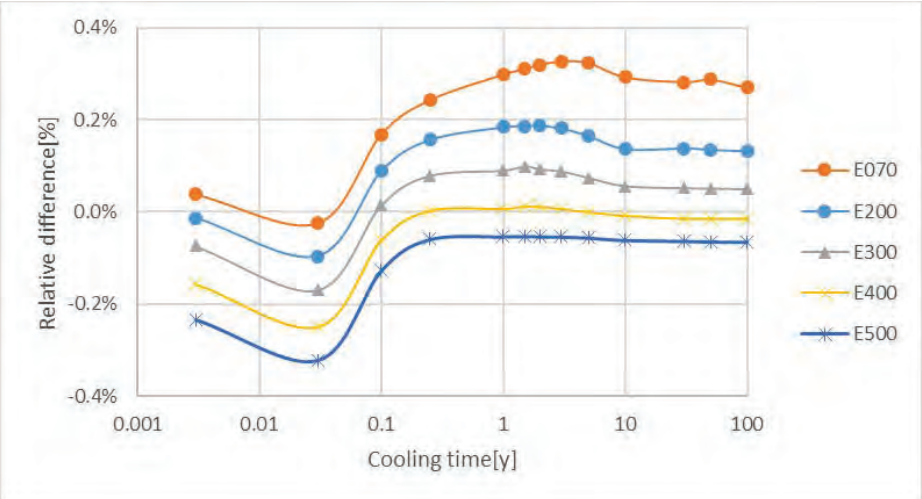

Relative differences of the ORIGAMI activities compared to the TRITON/NEWT results, neutron capture correction factor 0.996

Sensitivity analysis

- Sensitivity analysis defines response of the parameter variation on the observables and can be used to determine conservative approach, when explicit parameter consideration in the characterization process is not reasonable or viable, and define basic uncertainties due to propagation of uncertainties in each parameter and selected process.

- In the evaluation of the averaging process, non-linearity of the sensitivity coefficients should be examined also. Namely, calculations are usually performed at some averaged parameters value. It is not self-evident that such averaging process would yield also an averaged result.

Sensitivity analysis

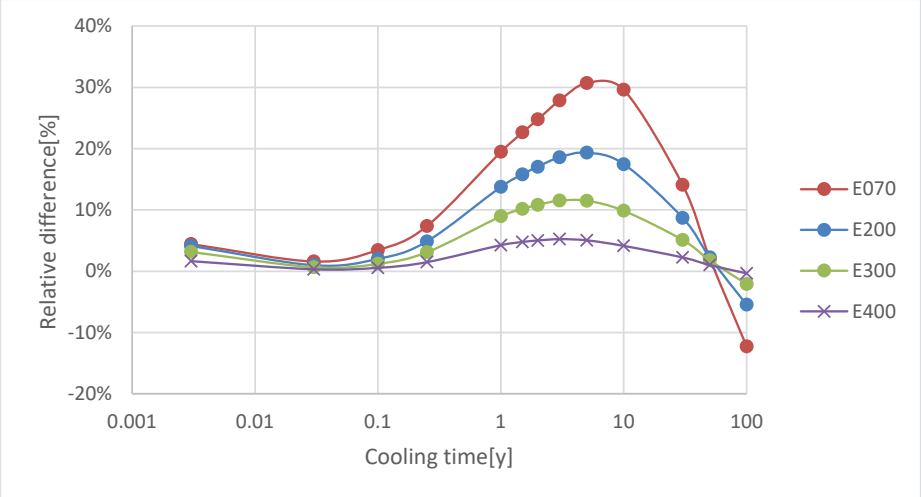

Impact of the fuel enrichment on the decay heat

Sensitivity analysis

23/40

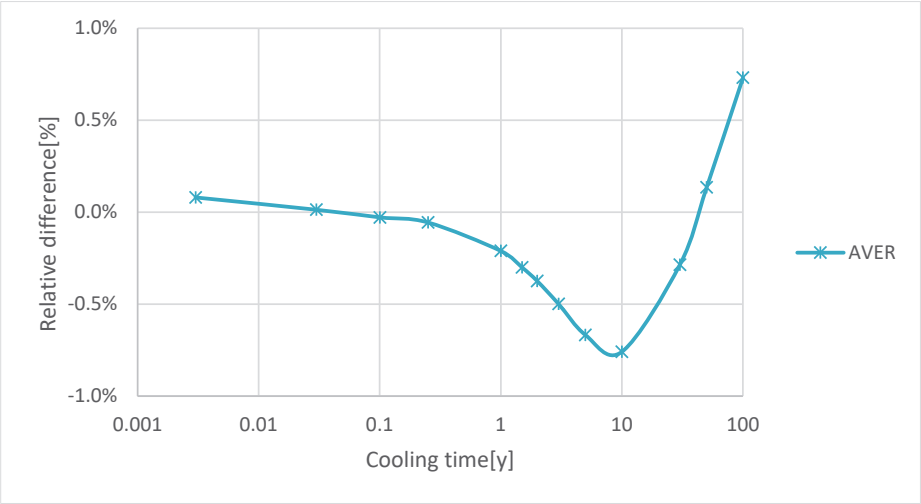

Impact of the ±1 % enrichment averaging on the decay heat

Sensitivity analysis

24/40

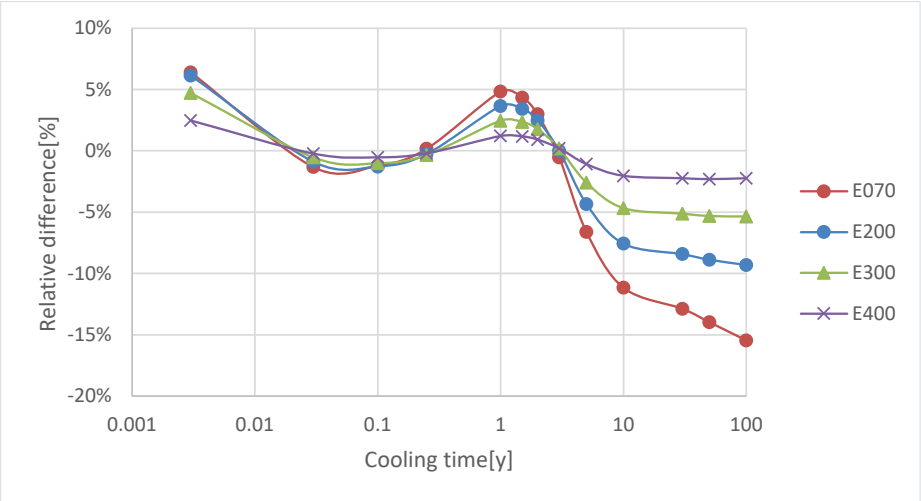

Impact of the fuel enrichment on the activity

Sensitivity analysis

25/40

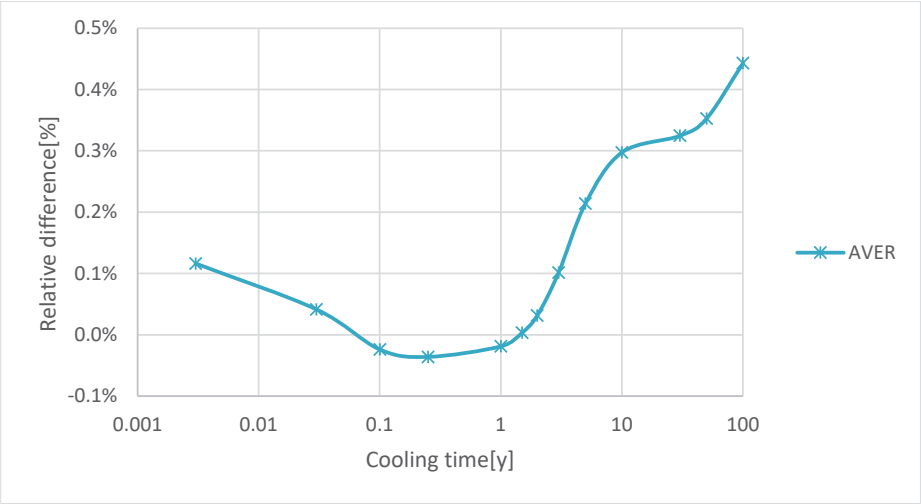

Impact of the ±1 % enrichment averaging on the activity

Sensitivity analysis

26/40

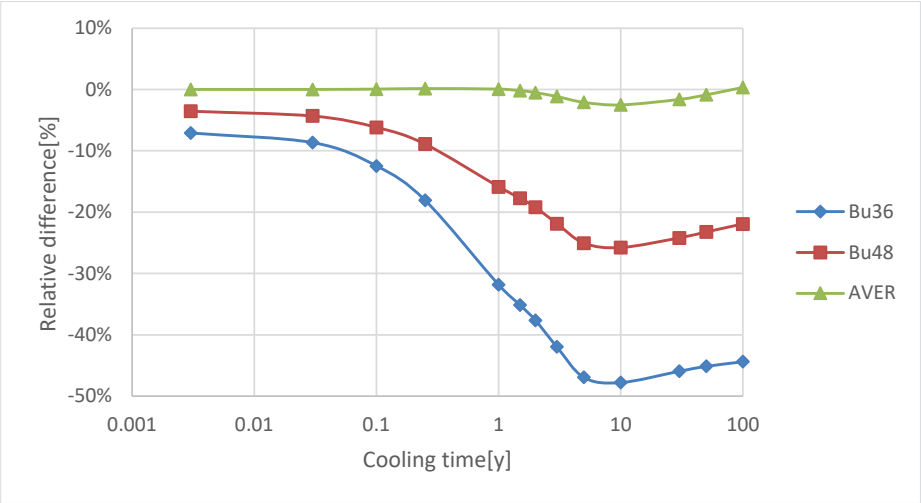

Impact of the fuel burnup on the decay heat

Sensitivity analysis

27/40

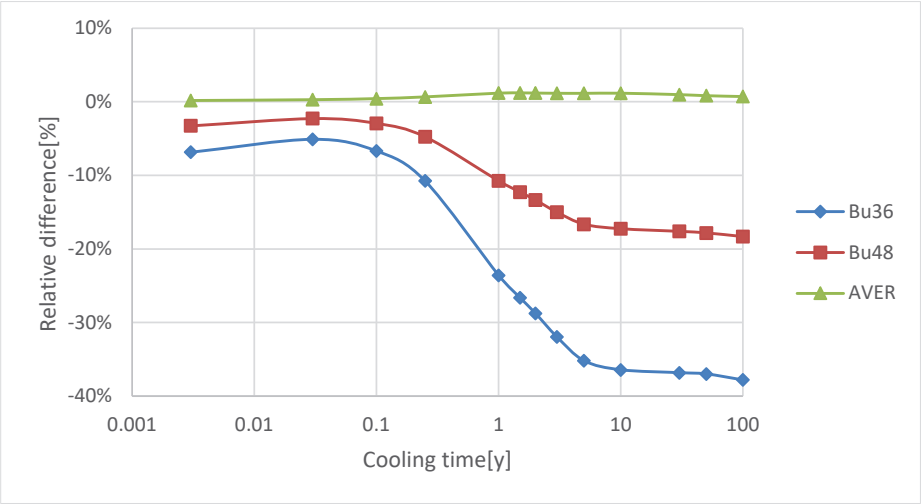

Impact of the fuel burnup on activity

Sensitivity analysis

28/40

- Impact of all other parameters has been evaluated in the project.
- Due to programming and execution time constraints in ORIGAMI, only limited number of variables can be explicitly taken into account in the interpolation of the .f33 files.
- All others will have to be covered in some conservative manner. The final decision has yet to be made.

Fuel segmentation

- Performed sensitivity analysis has determined impact of individual parameters on the specific spent fuel observable.
- Unfortunately, averaging process yields to over prediction in some cases and under prediction in others, with possible opposite trends in different observables.
- It is very hard to identify the most important ones for all cases. The final result is a mixture of individual contributions.
- The most accurate approach would be to take all 10 axial regions explicitly. However, such approach is time consuming. It would take more than 3 years of the CPU time to calculate 1400 FAs with the TRITON/NEWT sequence. Even ORIGAMI would require several days of calculation.
- Some kind of homogenization is therefore necessary.

Fuel segmentation

- It seems natural to explore axial blankets, since there are large material heterogeneities present.
- To get a proper feeling, a few typical cases have been evaluated:
  - A – standard FA without axial blankets (cycles 1-7)
  - B – FA with natural uranium axial blankets (cycles 7-16)
  - C – FA with annular axial blankets (from cycle 16 onward)

Fuel segmentation

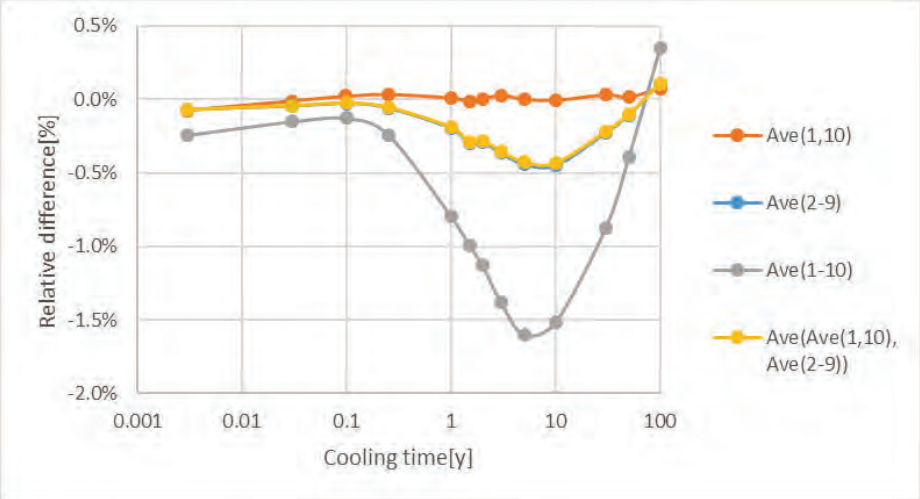

Impact of the homogenization on decay heat – case A

Fuel segmentation

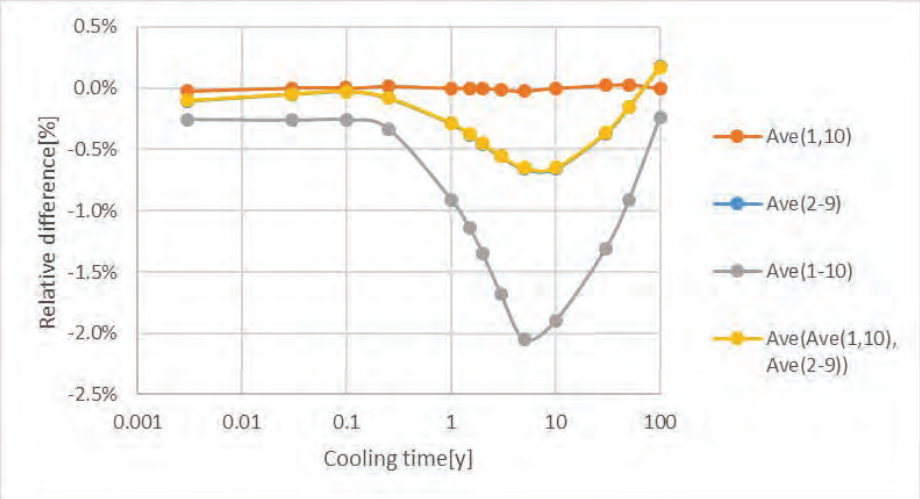

Impact of the homogenization on decay heat – case B

Fuel segmentation

33/40

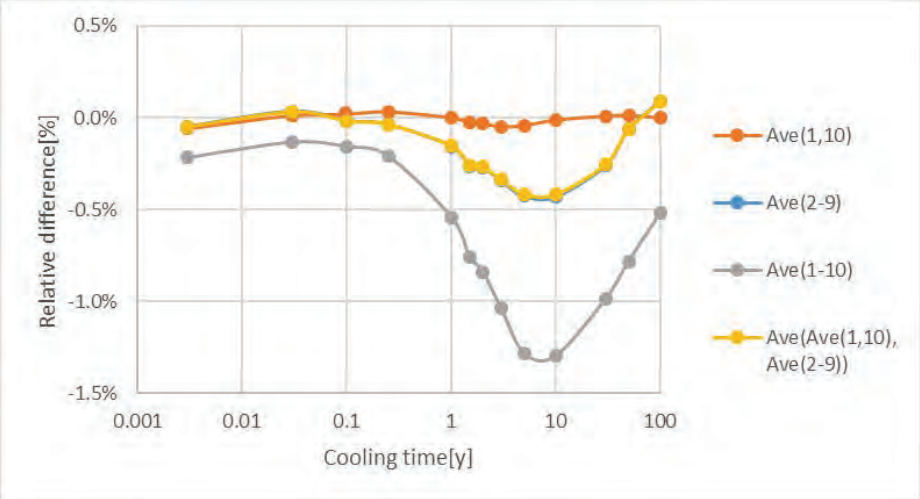

Impact of the homogenization on decay heat – case C

Fuel segmentation

34/40

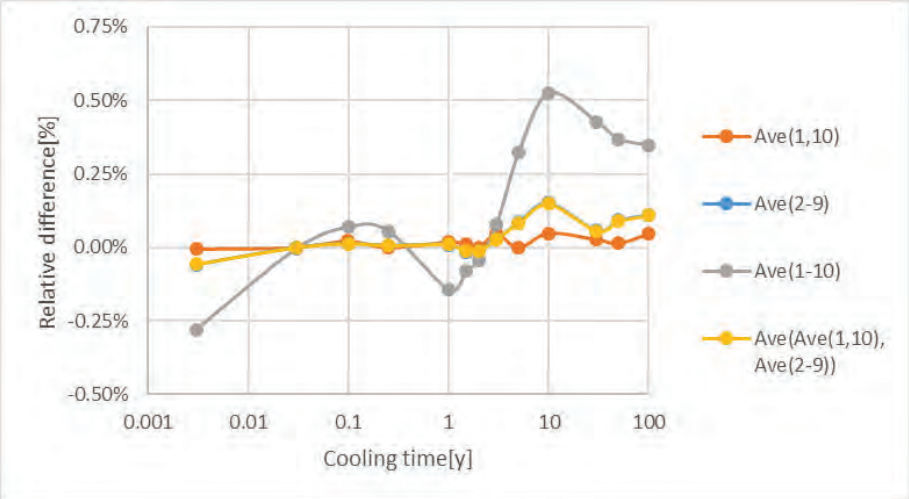

Impact of the homogenization on activity – case A

Fuel segmentation

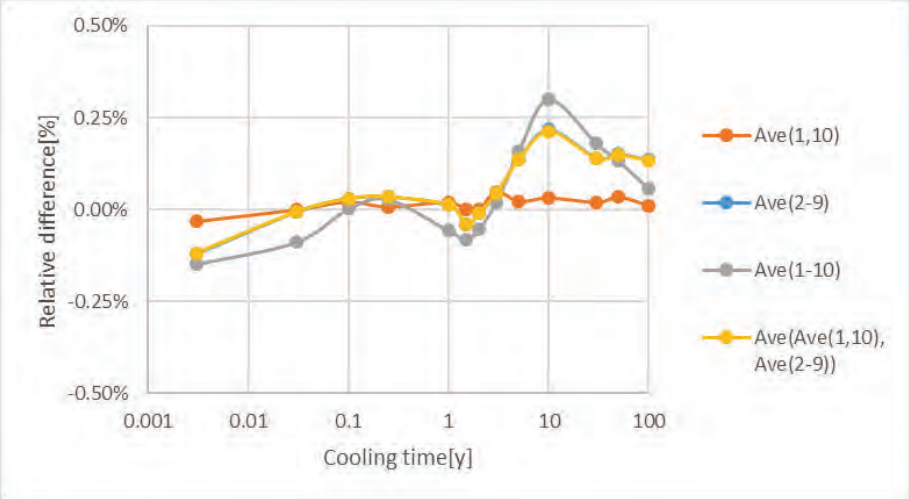

Impact of the homogenization on activity – case B

Fuel segmentation

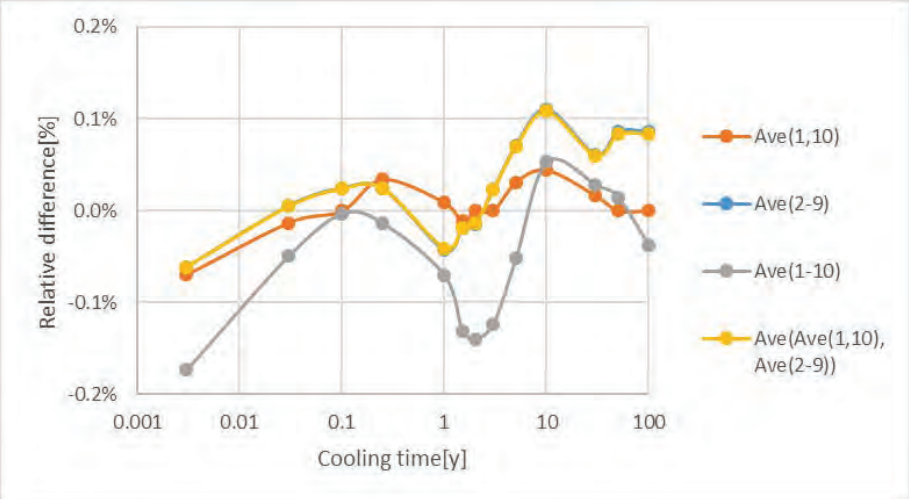

Impact of the homogenization on activity – case C

Conclusion

- Activities performed at JSI to support NPP Krško Spent Fuel Dry Storage project are presented in this report.
- In the initial phase of the project, FAR and FASLIB fuel assembly databases have been harmonized. Validated data from the FASLIB database served to analyse fuel manufacturing and irradiation data.
- TRITON/NEWT calculation model has been validated by the comparison of the predictions obtained from the stochastic neutron transport code Serpent2.
- Results obtained by both codes are in good agreement. For the time period of 1 year – 50 years decay heat differences are less than 1.3 %, in activity 1 %, while neutron and photon emissions are inside 5 % and 2 % respectively.

Conclusion

- ORIGAMI model running on the TRITON/NEWT binary one-group reaction coefficients library (.f33 files) has been validated. The importance of the energy produced by the neutron capture has been stressed to reduced observed differences.
- NPP Krško spent fuel sensitivity study has been accomplished based on the developed TRITON/NEWT model and fuel predetermined parameters range.
- It seems that fuel burnup and enrichment are the most influential parameters in the calculation of observables.

Conclusion

39/40

- In the evaluation of the averaging process, non-linearity of the sensitivity coefficients was examined also.
- The effect is mainly noticeable for the enrichment and burnup, where the decay heat prediction might be several % too low, if unsuitable segmentation is performed.
- A few FA cases based on the real data have been analyzed to demonstrate reasonable axial discretization.
- Planned activities are gradually coming to successful conclusion contributing to the safe and economical spent fuel dry storage on the NPP Krško site.

40/40

Thank you for your attention!

Questions?

13th International Conference of the Croatian Nuclear Society Zadar, Croatia, June 5-8, 2022

4.4 Passive neutron and gamma technique for spent nuclear fuel characterisation; V. Solans, UU; IAEA CRP spent fuel characterization; 22 – 23/09/2022

PASSIVE NEUTRON AND GAMMA TECHNIQUE FOR SPENT NUCLEAR FUEL CHARACTERISATION

Virginie SOLANS (Uppsala University)
Henrik Sjöstrand, Sophie Grape, Erik Branger (UU)
Alessandro Borella, Riccardo Rossa (SCK CEN)
Peter Schillebeeckx (JRC), Anders Sjöland (SKB)

This project has received funding from the European Union's Horizon 2020 research and innovation programme 2014-2018 under grant agreement N°847593

September 2022 IAEA CRP 1

UPPSALA UNIVERSITY

- **Spent nuclear characterization for the geological repository (EURAD)**

- **Safeguards**
  - sophie.grape@physics.uu.se

- **Fuel performance modelling**
  - henrik.sjostrand@physics.uu.se

- **Gamma tomography**
  - peter.andersson@physics.uu.se

2

EURAD GOALS

Ā **In deep geological repositories, spent nuclear fuel needs to be characterized:**

- Reactivity
- Decay heat
- Gamma's and neutron's dose
- Safeguards parameters

Ā **Before encapsulation, need to verify (update), the fuel parameters calculated by the state of the art codes.**

Ā **Experimental mesurements:**

- Calorimetric measurements
- **Gamma-ray scans**
- **Neutron measurements**

SUMMARY

Ā **Gamma measurements**

- Ā Reproducibility measurement
- Ā Intrinsic self-calibration

Ā **Neutron measurements**

- Ā Fit Rossi-alpha distribution with double exponential fit
- Ā Predict BU and IE

SKB50

- Set of 25 BWR and 25 PWR assemblies
- Used in Swedish reactors
- Various burnup, initial enrichment, cooling time, manufacturers
- Gamma scans
- Calorimetric measurements
- Neutron measurements
- Chosen around 2013-2014

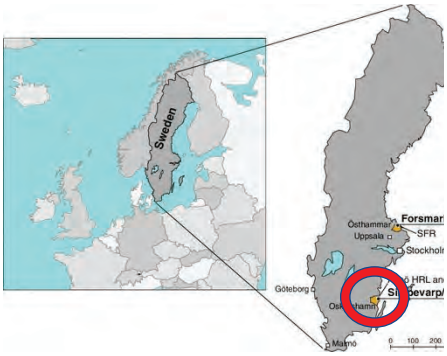

Image reference: Andersson, J., Skagius, K., Winberg, A. *et al.* Site-descriptive modelling for a final repository for spent nuclear fuel in Sweden. *Environ Earth Sci* **69,** 1045–1060 (2013). https://doi.org/10.1007/s12665-013-2226-1

DIFFERENT CAMPAIGNS

- **Campaign 1**
  - Done in 2014
  - Static measurement
- **Campaign 2**
  - Done in 2014
  - Axial measurement
- **Campaign 3**
  - Done in 2016-2019
  - Axial measurement

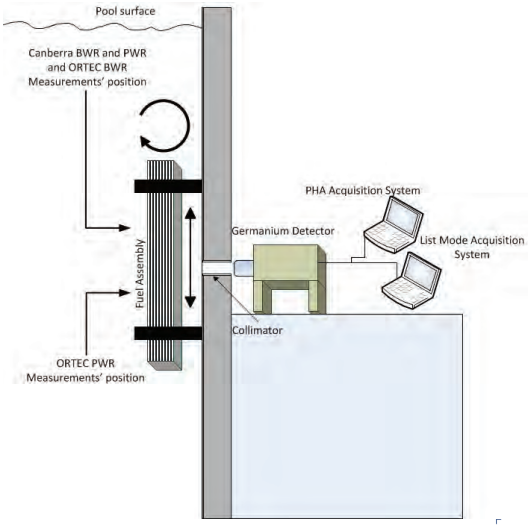

Image reference: S. Vaccaro, et Al., PWR and BWR spent fuel assembly gamma spectra measurements, Nuclear Instruments and Methods in Physics Research Section A: Accelerators, Spectrometers, Detectors and Associated Equipment, Volume 833,2016

SPECTRUM

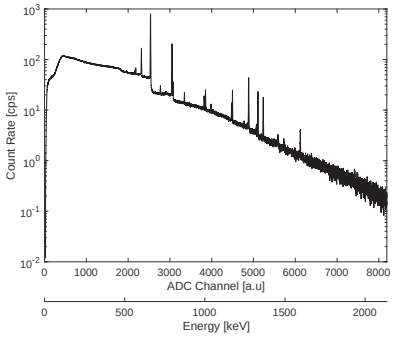

V. Solans, et Al. evaluating peak area uncertainties in connection to passive gamma measurements of spent nuclear fuel, TopFuel Conference 2021

From SNF's spectrum it is possible to extract the count rate (by numerical integration):

Cs-137, 662 keV $T_{1/2}$ =30y

Cs-134, 996 keV $T_{1/2}$ =2.1y
1004 keV
1274 keV
1596 keV

Eu-154, 605 keV $T_{1/2}$ =8.6y
796 keV
1365 keV

COUNT RATE

Comparing count rate between different campaigns have several challenges :

- Attenuation plates
- Detector efficiency
- Position of the fuel with respect to the detector
- ...

Use of the intrinsic self calibration method

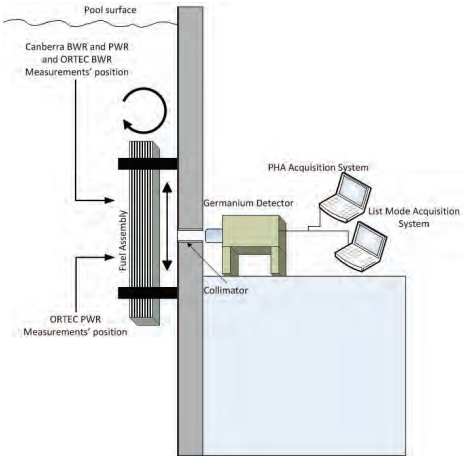

Image reference: S. Vaccaro, et Al., PWR and BWR spent fuel assembly gamma spectra measurements, Nuclear Instruments and Methods in Physics Research Section A: Accelerators, Spectrometers, Detectors and Associated Equipment, Volume 833,2016

INTRINSIC SELF-CALIBRATION

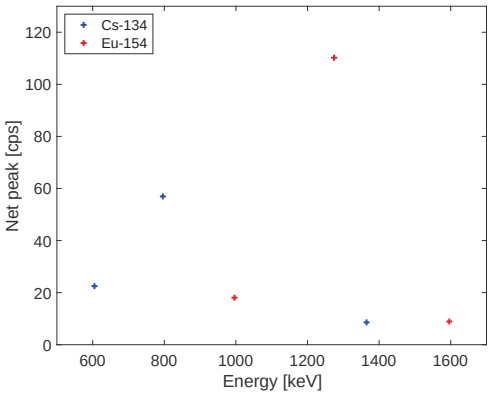

9

INTRINSIC SELF-CALIBRATION

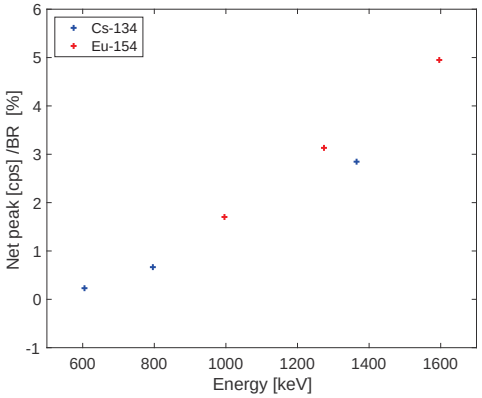

10

INTRINSIC SELF-CALIBRATION

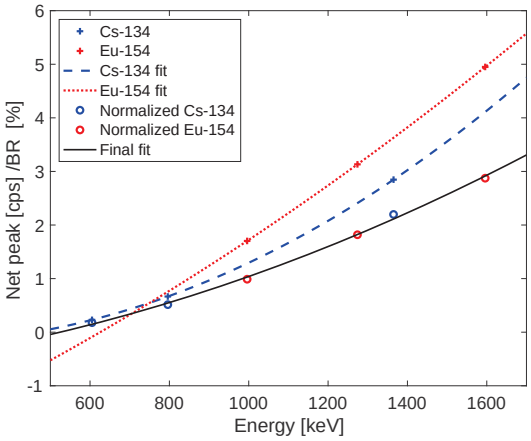

Multiple peaks for a singles/multiple radionuclides:

- **Self calibration possible**
- **Remove dependence on the detector and geometry**
- **Cs-134/Cs 137 and Eu-154/Cs-137 can be determined independently of knowledge of the campaign details**

RESULTS – SELF CALIBRATION

- **Even if the measurement conditions were different between the campaigns, mean deviation between campaigns obtained were:**
- **With self-calibration**
  - 1.4% for Cs-137
  - 2.3% for Eu-154/Cs-137
  - 1.9% for Cs-134/Cs-137
- **Without self-calibration**
  - 1.4% for Cs-137
  - 8.1% for Eu-154/Cs-137
  - 4.0% for Cs-134/Cs-137

RESULTS - REPRODUCIBILITY

- **Standard deviation of the best determined peak:**
  - The standard deviation in the inter-campaign reproducibility for the best-determined gamma peaks is between 2 and 3%.

13

DIFFERENTIAL DIE-AWAY SELF INTERROGATION INSTRUMENT (DDSI)

- **Passive instrument developed and built in LANL**
- **Use neutron from Cm244 to interrogate the assembly**
- **Detect neutrons in coincidence (Rossi-alpha distribution)**

- **56 ^{3}He tubes detect thermal neutrons**
- **Polyethylene to slow down neutrons**
- **Lead to reduce gamma-ray dose rate**

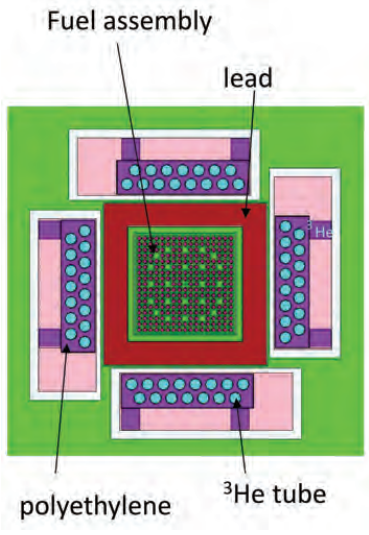

Image courtesy of Li Balkeståhl

14

ROSSI-ALPHA DISTRIBUTION (RAD)

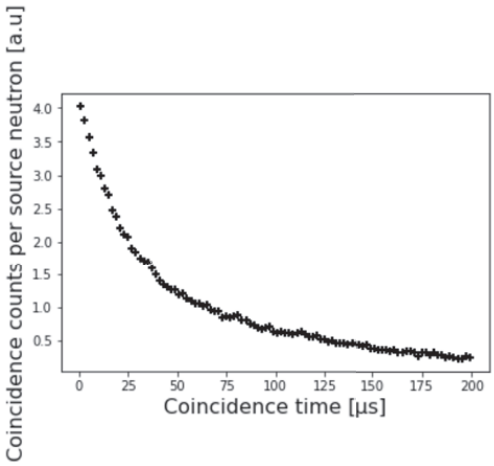

- Rossi-alpha distribution (RAD)
- Time correlation for coincident neutrons
- Each neutron as start
- Total number of neutrons detected is also an outcome of the DDSI

15

DOUBLE EXPONENTIAL

- A fast and a slow component
- Fast is not only direct detection or fast multiplication
- Slow is neutrons that have time to thermalized before fission

$$RAD_{double}(t) = A_{fast} \cdot exp(-\tau_{fast}\, t) + A_{slow} \cdot exp(-\tau_{slow}\, t)$$

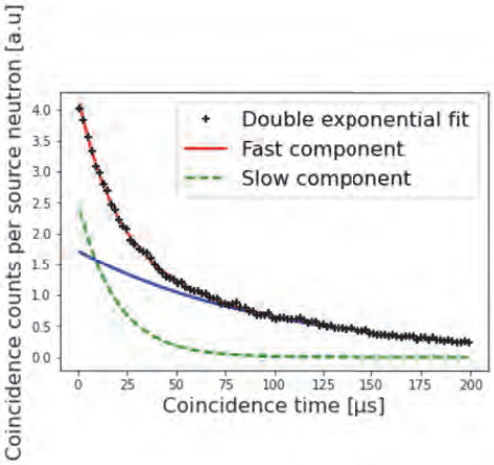

Increase in absorbers will decrease the fission chain therefore will lead to a smaller slow component

16

TAU FAST VERSUS TAU SLOW

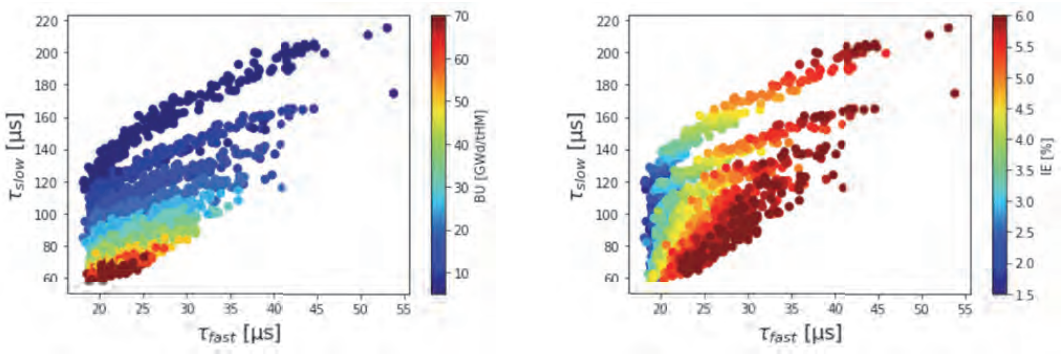

Indication that there is more information

Same data point with different colouring indicating BU or IE

MODEL

- **Use a KNN model**
  - Trained on the simulated dataset
  - Tested on the simulated dataset and the experimental data

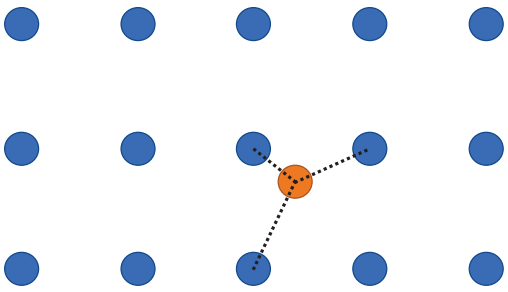

Average of the 3 closet neighbours

DATASETS

Simulated dataset

- 2536 samples (from a pincell model)
- 17x17 PWR fuel
- BU ranges from 5 to 70 GWd/tHM
- IE from 1.5% to 6% (alternating 0.3% and 0.2% steps)
- CT from 0 to 70 y (with intermediate CTs at 2.5, 5, 7.5, 10, 12.5, 15, 20, 30, 40, 55 y)

Experimental data

- SKB 50 PWR 17x17 SNFs ranges from 19 to 48 GWd/tHM, and IE goes from 2.1 to 3.94%. The cooling time at the time of the measurement of the SNFs was between 6.3 and 30.4 years.

RESULTS

RMSE	BU [GWd/tHM]	IE [%]
Test set simulation	4.51	0.284
Experimental After KNN	11.85	0. 963

EXPERIMENTAL RESULTS

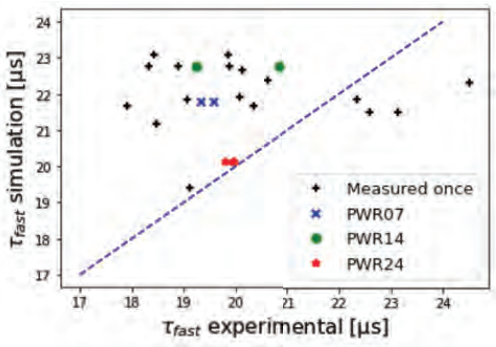

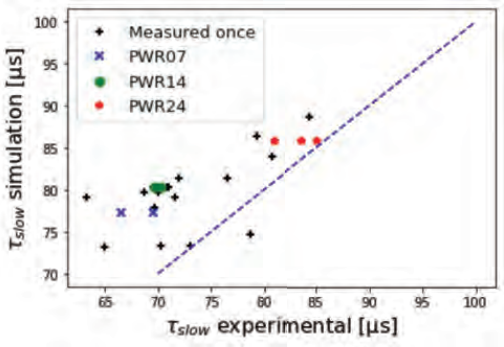

Dotted line is the unity line

RESULTS

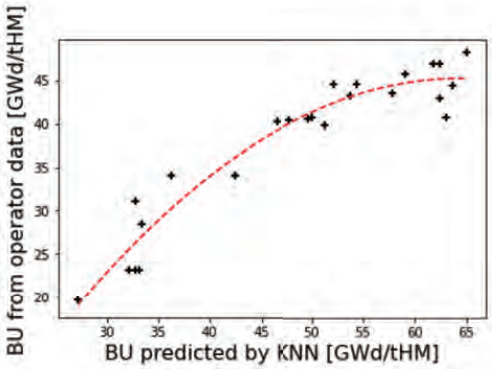

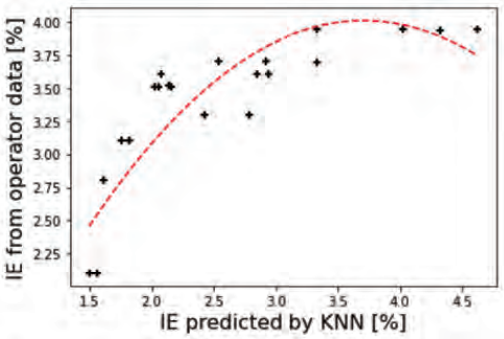

RESULTS

RMSE	BU [GWd/tHM]	IE [%]
Test set simulation	4.51	0.284
Experimental After KNN	11.85	0. 963
Experimental After fit	2.65	0.324
Simulated set after fit	2.45	0.640

CONCLUSION

Gamma measurement:

- Ā Reproducibility of the SKB50 measurement campaigns has been investigated between 1.4 to 2.3 %
- Ā Intrinsic self calibration for the experimental gamma measurements applied to the SKB-50

Neutron measurement:

- Ā Predict BU and IE using KNN enabled by the double exponential fit
- Ā Improve the prediction capability using polynomial fit

For the future, focus on predicting decay heat using gamma and neutron measurements

4.5 Recent Spent Fuel Research at VTT; S. Häkkinen, P. Juutilainen, L. Vaara, R. Tuominen; Nuclear Science and Technology Symposium 2022 (SYP2022); 27/05/2021

VTT

Outline

- Motivation and overview
- Results in selected topics
- Nuclear data uncertainty propagation
- Key take aways and future work

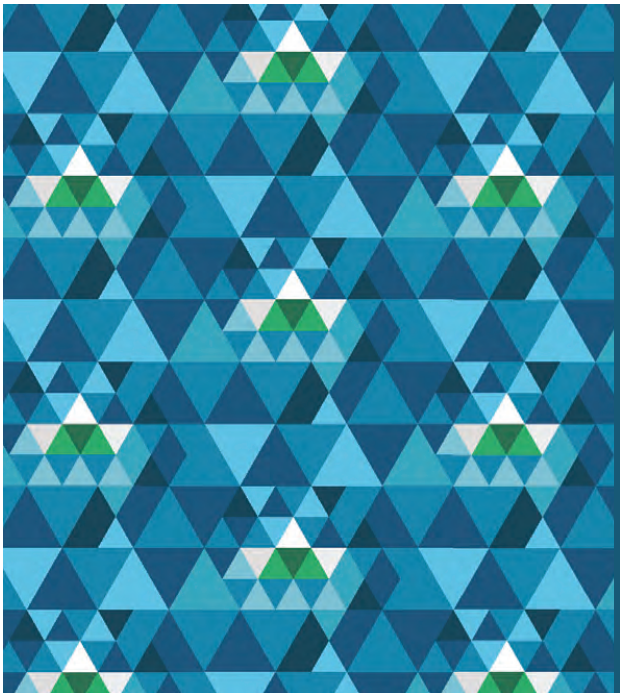

Motivation and overview

Motivation

- Knowledge of spent fuel (SNF) properties is important for safe handling and final disposal
  - Decay heat and reactivity → volume of repository space
  - Nuclide inventories → radiation protection, dose estimates
- Computational determination of decay heat involves several uncertainty sources
- SNF properties are also dependent on fuel type, enrichement and burnup
- At VTT, these uncertainties have been studied using the Monte Carlo reactor physics code Serpent 2 [1]

[1] Leppänen, J., et al. (2015) "The Serpent Monte Carlo code: Status, development and applications in 2013." Ann. Nucl. Energy, 82 (2015) 142-150.

Recent spent fuel studies at VTT

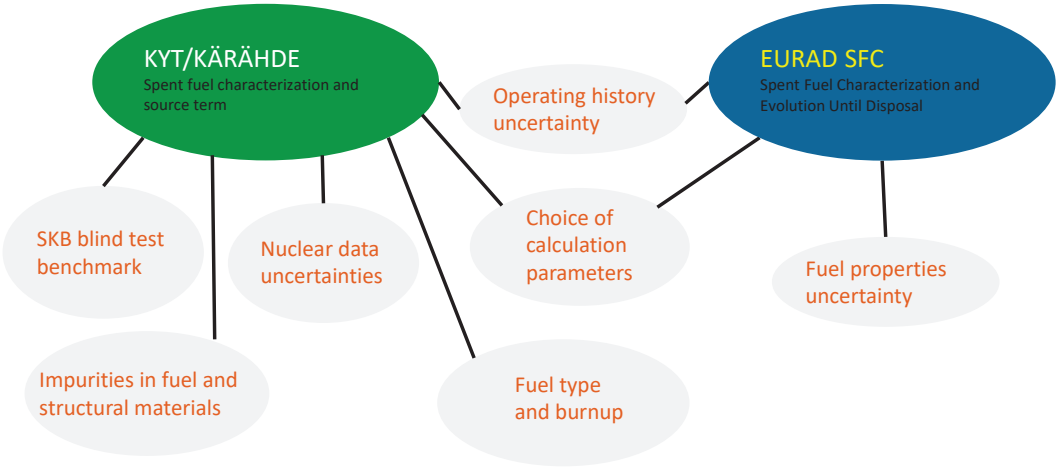

27/10/2022 VTT – beyond the obvious

VTT

Simplifications in operating history

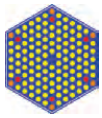

- Boron concentration, assembly power and coolant temperature and density were averaged over three cycles.
- Averaging assembly power overestimates activity, decay heat and photon emission rate 64 – 78 % right after irradiation.
- After 10 years the effect is < 1 %
- Effect on spontaneous fission rate and the studied nuclides (C-14, Cl-36, Mo-93, Ag-108m, I-129, U-233, U-235, Pu-239, Pu-241) is mostly below 1.5 %

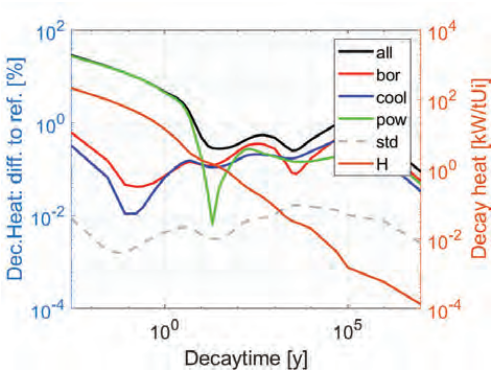

27.10.2022 VTT – beyond the obvious 7

VTT

Choice of calculation parameters

- Studied calculation parameters:
  - Depletion zone division
  - Depletion step length
  - Doppler-broadening rejection correction (DBRC)
  - Unresolved resonance probability table sampling
  - Energy-dependent branching ratios
- Maximum effects (depletion zone division)
  - Decay heat 0.6 % at 7 y
  - Photon emission rate 1.1 % at ~7000 y
  - Spontaneous fission rate 8 % at ~400 y
- Neglecting DBRC
  - non-negligible effect on some heavier nuclides
  - Maximum effect on DH and PE ~0.5 %

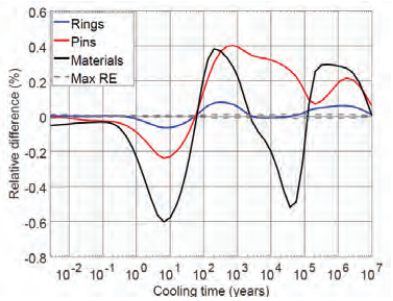

Decay heat

27.10.2022 VTT – beyond the obvious 8

Uncertainty analysis of one sample in a 6x6 BWR assembly

Parameter	Average	RSD [%]
Moderator density	0.759 g/cm^3	2
Power density	18.84 W/gU	1.7
Fuel temperature	923 K	2
Water temperature	549 K	1
Void$_1$	50 %	6.7 (Δvoid = ±10 %)
Void$_2$	50 %	1.3 (Δvoid = ±2 %)
Fuel density	10.5 g/cm^3	0.3
Fuel radius	0.612 cm	0.01
^{234}U enrichment (in ^{235}U)	0.65	0.1 (Δ^{234}U = ±0.25 %)
^{235}U enrichment	2.53	0.7 (Δ^{235}U = ±0.05 %)
^{238}U content	85.92	0.7
Burnup (assembly)	22.627	2

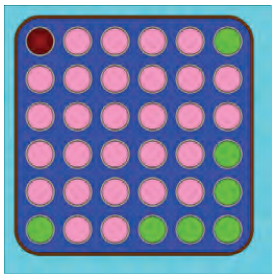

$$\sigma_{calc,i}^2 = \sigma_i^2 + \sigma_{MC}^2$$

$$\sigma_{tot}^2 = \sum_{i=1}^{n} \sigma_i^2$$

Decay heat uncertainty of the BWR sample

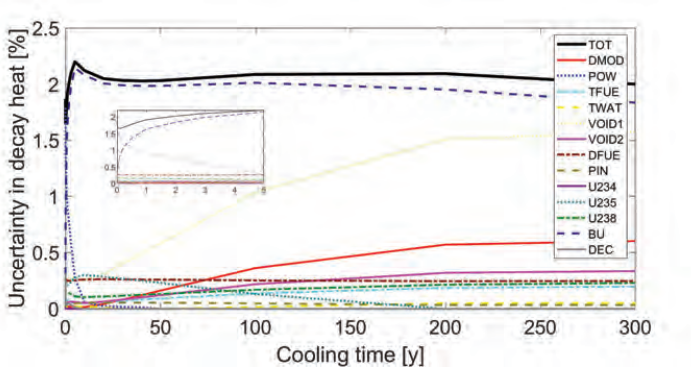

TOT	–	Total uncertainty (void$_2$ = ±2 %)
DMOD	–	Moderator density
POW	–	Power density
TFUE	–	Fuel temperature
TWAT	–	Water temperature
VOID1	–	Void$_1$ = ±10 %
VOID2	–	Void$_2$ = ±2 %
DFUE	–	Fuel density
PIN	–	Fuel radius
U234	–	^{234}U enrichment
U235	–	^{235}U enrichment
U238	–	^{238}U content
BU	–	Burnup
DEC	–	Decay data

Impact of fuel type and burnup on decay heat

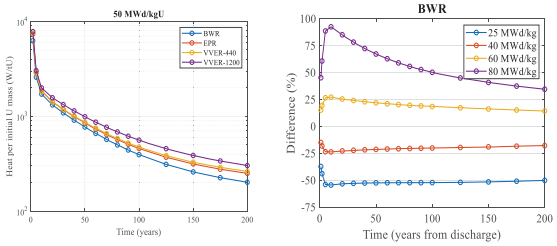

- Difference to 50 MWd/kgU

Top decay heat contributors 5 y (top) and 100 y (below) after irradiation

BWR	%	EPR	%	VVER-440	%	VVER-1200	%
Y90	27.7	Cs134	27.2	Cs134	27.9	Cs134	25.4
Ba137m	27.2	Ba137m	24.5	Y90	25.2	Y90	24.2
Cs134	24.9	Y90	23.2	Ba137m	25.1	Ba137m	23.2
Cm244	10.2	Cm244	13.7	Rh106	11.4	Pu238	16.9
Rh106	10.0	Rh106	11.4	Cm244	10.3	Rh106	10.4

Nuclides	% (BWR)	% (EPR)	% (VVER-440)	% (VVER-1200)
Am241	40.0	44.8	46.4	39.1
Pu238	22.8	23.6	22.6	**34.8**
Ba137m	16.3	14.1	13.6	11.4
Y90	15.0	12.1	12.4	10.7
Pu240	5.9	5.4	5.0	4.0

27.10.2022 VTT – beyond the obvious 11

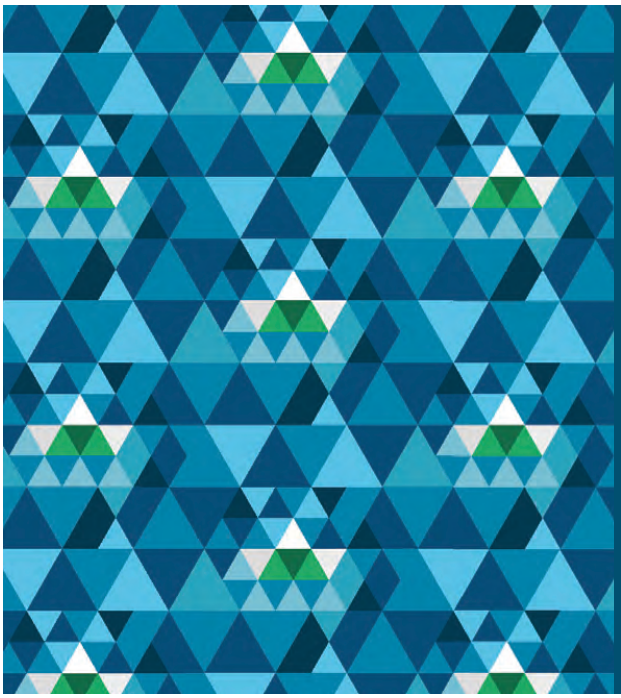

Nuclear data uncertainty propagation

27.10.2022 VTT – beyond the obvious 12

Key Idea

- Create hundreds of randomized nuclear data files for many nuclides
  - New nuclear data is produced from nuclear models and experimental data: No need to resort to covariance data.
  - The data is produced with TALYS and a few satellite programs = T6 [2]
- Assign a random combination of the random data files for a Serpent run
  - Repeat hundreds of times and compile uncertainty in the output with an appropriate statistic

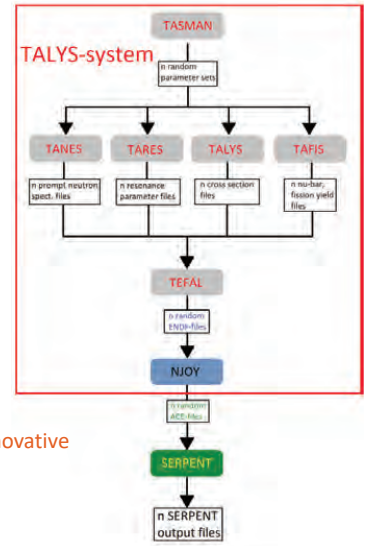

[2] A.J. Koning et al. (2019) "TENDL: Complete Nuclear Data Library for innovative Nuclear Science and Technology". In: Nuclear Data Sheets 155, 1-55.

Current state

- 500 files for 88 nuclides have been produced for 0 K, 300 K, 600K, 900 K and 1200 K temperatures
- Random fission yield files have been included
  - Adopted from TENDL – website
- Scripts for file processing, TALYS/Serpent environment initialization, data visualization etc. have been set up.
- It is now straightforward to propagate data uncertainties through Serpent, although computationally expensive.

Significant Uncertainties in Actinide Concentrations

Uncertainty in decay heat > 3.5 % due to nuclear data when cooling time >15 y

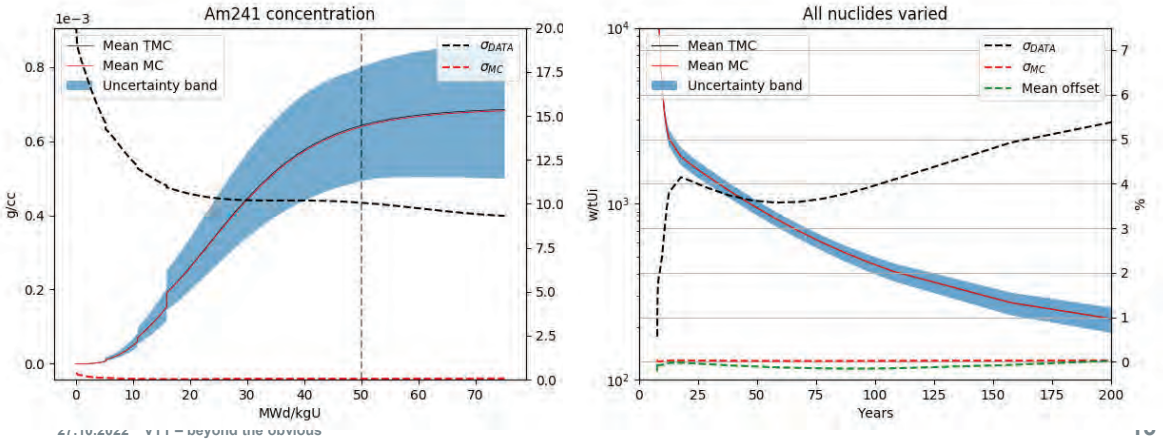

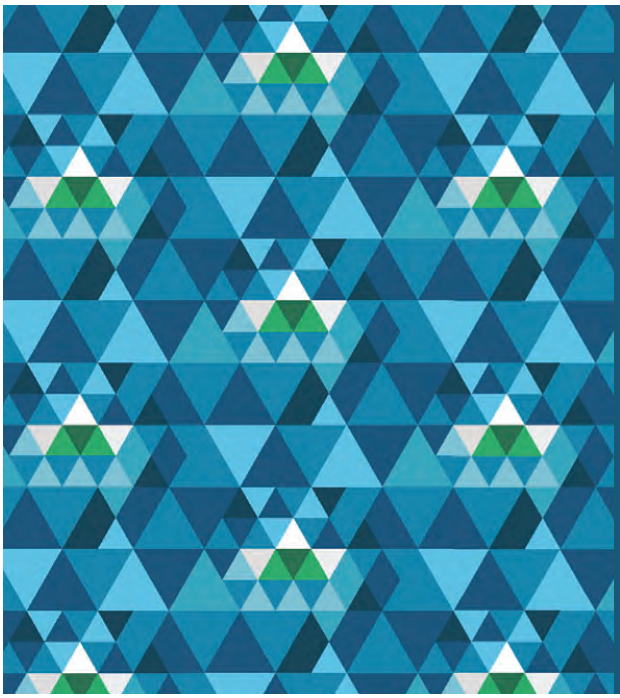

Key take aways and future work

Key take aways

- Approximations in power density should be avoided, when dealing with ”fresh” SNF (cooling time < 10 y).
- Pin-wise depletion zone division should be used in burnup calculations and Gd pins should be further divided in radial rings.
- DBRC should not be neglected. Use on U isotopes and ^{239}Pu and ^{240}Pu is mainly sufficient.
- Significant sources of uncertainty for BWR assembly calculations
  - Nuclear data
  - Burnup
  - (Void fraction and moderator density)
- Using recycled uranium significantly increases decay heat from SNF

27.10.2022 VTT – beyond the obvious 17

Future work

- Full libraries and random nuclear data files with T6
- Expanding from 2D assembly calculations to 3D full core
  - Serpent – Ants sequence (Kraken computational framework [3])
- Participation in activities of NEA subgroup on decay heat

[3] Leppänen, J., et al. (2022) "Current Status and On-Going Development of VTT's Kraken Core Physics Computational Framework" Energies, 15, 876, https://doi.org/10.3390/en15030876.

27.10.2022 VTT – beyond the obvious 18

Selected publications

- International Journal publications
  1. Tuominen R., Valtavirta V. (2022), "The Effect of Serpent 2 Calculation Parameters on Evaluated Spent Nuclear Fuel Source Term", Journal of Nuclear Engineering and Radiation Science, 8(4), [044503], https://doi.org/10.1115/1.4051445 .
  2. Häkkinen S. (2022), "Impact of Approximations in Operating History Data on Spent Fuel Properties with Serpent 2", Journal of Nuclear Engineering and Radiation Science, 8(4), 041901. [NERS-21-1015]. https://doi.org/10.1115/1.4051444.
  3. Jansson P., et.al. (2022), " Blind Benchmark Exercise for Spent Nuclear Fuel Decay Heat", Nuclear Science and Engineering, 196, pp.1125-1145, https://doi.org/10.1080/00295639.2022.2053489 .
  4. Rochman D., et.al., "On the estimation of nuclide inventory and decay heat: a review from the EURAD Eurpean project", Frontiers in Energy Research. (submitted in 2022).
- Conference articles
  1. Rintala A., "Evaluating the Effect of Decay and Fission Yield Data Uncertainty on Spent Nuclear Fuel Source Term Using Serpent 2", In Proc. 28th International Conference Nuclear Energy for New Europe, Paper No. 602, Portorož, Slovenia, 2019.
  2. Juutilainen P., Häkkinen S., "Impact of Fuel Type and Discharge Burnup on Source Term", In Proc. 28th International Conference Nuclear Energy for New Europe, Paper No. 906, Portorož, Slovenia, 2019.
  3. Rintala A., " Evaluating the Effect of Decay and Fission Yield Data Uncertainty on BWR Spent Nuclear Fuel Source Term", In Proc. 29th International Conference Nuclear Energy for New Europe, Paper No. 1506, Portorož, Slovenia, 2020.
  4. Tuominen R., Valtavirta V., "The Effect of Serpent 2 Calculation Parameters on Evaluated Spent Nuclear Fuel Source Term", In Proc. 29th International Conference Nuclear Energy for New Europe, Paper No. 1503, Portorož, Slovenia, 2020.
  5. Häkkinen S., "Impact of Approximations in Operating History Data on Spent Fuel Properties with Serpent 2", In Proc. 29th International Conference Nuclear Energy for New Europe, Paper No. 1505, Portorož, Slovenia, 2020.
- Research reports
  1. Rintala A., "Evaluating the effect of decay and fission yield data uncertainty on spent nuclear fuel source term using Serpent 2 – continued study", VTT Research Report, VTT-R-00209-20, 2020.
  2. Rintala A., "Separate effect of decay and fission yield data uncertainty on spent nuclear fuel source term", VTT Research Report, VTT-R-00106-21, 2021.
  3. Juutilainen P., "Effect of burnable absorber rods and U-235 enrichment on EPR UO2 fuel assembly source term with Serpent 2", VTT-R-00242-21, 2021.
  4. Häkkinen S., "Gundremmingen-A assembly B23 sample I2680 depletion calculation with Serpent 2", VTT Research Report, VTT-R-00631-21, 2021.
  5. Häkkinen S., "Sensitivity and uncertainty analysis of Gundremmingen-A assembly B23 sample I2680 depletion calculation with Serpent 2", VTT Research Report, VTT-R-00632-21, 2021.
- Thesis
  1. Vaara L., "Nuclear Data Uncertainty Propagation in Total Monte-Carlo Method", M.Sc. Thesis, Aalto University, 2022.
  2. Vaara L., "Impurity-generated impact on the characteristics of spent nuclear fuel", Special Assignment, Aalto University, 2020.

Acknowledgements

- This work has received funding from the Finnish Research Programme on Nuclear Waste Management KYT2022.
- This work has received funding from the European Union's Horizon 2020 research and innovation programme under grant agreement N°847593.

VTT

beyond the obvious

Silja Häkkinen
silja.hakkinen@vtt.fi

4.6 Rossi-Alpha distribution analysis of DDSI data for spent nuclear fuel investigation; V. Solans, UU; Symposium on International Safeguards: Reflecting on the Past and Anticipating the Future; 31/10-04/11/2022

Rossi-Alpha distribution analysis of DDSI data for spent nuclear fuel investigation

Virginie Solans
Uppsala University (UU)
virginie.solans@physics.uu.se
S. Grape (UU), H. Sjöstrand (UU), E. Branger (UU),P. Schillebeeckx (JRC), A. Borella (SCK CEN), R. Rossa (SCK CEN), A. Sjöland (SKB)

ABSTRACT

- Aim: Predict burnup (BU) and initial enrichment (IE) from differential die-away self-interrogation (DDSI) instrument response
- Fit a double exponential fit to the Rossi-alpha distribution (RAD), describing neutrons detected in coincidence, for both simulated and experimental data
- Enhance prediction using a polynomial fit between predicted values and operator data

INTRODUCTION

- Safety, operational and safeguards parameters need to be verified with NDA measurements.
- The differential die-away self-interrogation (DDSI) instrument is a passive neutron measurement technique
- Investigate if a double exponential fit to the RAD (Fig 1) can provide additional information about the fuel compared to a single exponential fit

$$RAD_{double}(t) = A_{fast} \cdot exp(-\tau_{fast}\, t) + A_{slow} \cdot exp(-\tau_{slow}\, t)$$

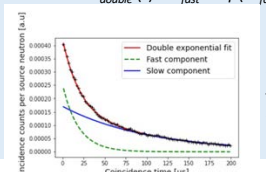

Fig 1. RAD for a simulated PWR SNF having BU= 10 GWd/tHM, IE= 1.5% and CT= 50 y

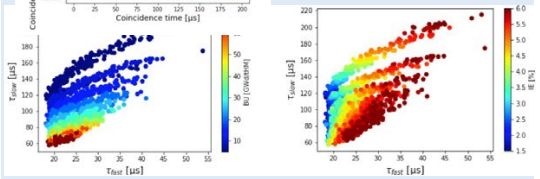

Fig 2. τ_{fast} and τ_{slow} depending on the BU (left) and IE (right) for the simulated dataset.

DESCRIPTION OF THE DATA

SIMULATED DATASET

- 2536 samples of 17x17 PWR fuel, obtained with Serpent 2 and MCNP
  BU: (5 to 70 GWd/tHM), IE: (1.5% to 6%), CT: (0 to 70 y)

EXPERIMENTAL DATASET

- 20 PWR 17x17 SNFs from the SKB-50 fuel set, irradiated in Swedish reactors
- BU: (19 to 48 GWd/tHM), IE: (2.1 %to 3.94%), CT: (6.3 to 30.4 y).

COMPARING DATASETS

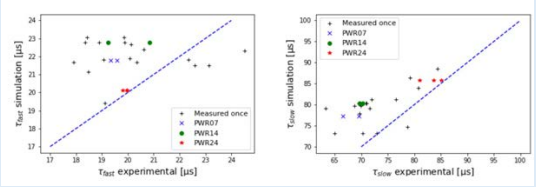

Fig 3. τ_{fast} (left) and τ_{slow} (right) calculated from the simulated and experimental data. The dashed line is the unity line.

RESULTS

PREDICTING MODEL

- *k*NN trained on simulated data, tested on simulated and experimental data using 10-fold cross validation
- Correcting for bias in experimental predictions (which is due to the fuels being fully depleted) using a calibration (Fig. 4) improves the prediction capability.

RMSE for predictions with	BU [GWd/tHM]	IE [%]
Simulated data	4.51	0.284
Experimental data	11.86	0.963
Experimental data and calibration	2.65	0.324
Simulated data and calibration	2.69	0.104

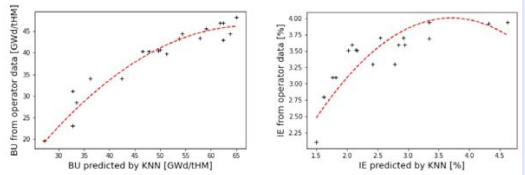

Fig 4. Operator declared BU (left) and IE (right) versus kNN predicted quantities. The red curve is a polynomial fit of degree 2.

CONCLUSION

- It is possible to predict BU and IE using a double exponential fit on the Rossi-alpha distribution.

ACKNOWLEDGEMENTS

The project leading to this poster presentation has received funding from the European Union's Horizon 2020 research and innovation program under grant agreement No 847593.

#IAEASG2022

5. Participation to a Workshop

- Fuel properties characterisation and related uncertainty analysis (EURAD/SFC/Task 2); P. Schillebeeckx, JRC Geel; Spent Fuel Workshop 2019, Ghent, Belgium; 15/11/2019
- Fuel properties characterisation and related uncertainty analysis; P. Schillebeeckx, JRC Geel; ESARDA Final Disposal Working Group Meeting, SCK CEN, Mol; 06 - 07/02/2020
- Predicting the Bias in Calculations of Spent Nuclear Fuel Characteristics; A. Shama, NAGRA; Workshop on Machine Learning in Nuclear Science and Technology, Madrid, Spain (online); 27/05/2021
- Chemical and spectroscopic investigations on the distribution of radionuclides in fuel-cladding interfaces of irradiated high burn-up UOX and MOX fuels; R. Dagan, T. König et al., KIT; Safety of Extended Dry Storage; 01 – 03/06/2022
- Experimentelle und numerische Bestimmungen des Radionuklidinventars von abgebrannten Kernbrennstoffen als eine Grundlage für die vorläufige Sicherheitsuntersuchung (vSU); R. Dagan, T. König et al., KIT; Tage der Standortauswahl; 08 - 10/06/2022
- Passive gamma and neutron measurements for characterization of spent nuclear fuel; V. Solans, UU; 31th Spent Fuel Workshop; 19 – 21/10/2022
- Characterisation of spent nuclear fuel for a typical PWR; G. Žerovnik, JSI; 31th Spent Fuel Workshop; 19 – 21/10/2022
- Impact of Some 3-D Modelling Effects on the Spent Fuel Characterization; ; 31th Spent Fuel Workshop; 19 – 21/10/2022
- Burnup credit application in CONSTOR SNF cask criticality analysis for RBMK-1500 fuel; R.Plukiene, FTMC; 31th Spent Fuel Workshop; 19 – 21/10/2022

5.1 Fuel properties characterisation and related uncertainty analysis (EURAD/SFC/Task 2); P. Schillebeeckx, JRC Geel; Spent Fuel Workshop 2019, Ghent, Belgium; 15/11/2019

Task 2: Fuel properties characterisation and related uncertainty analysis

Volker Metz KIT
Dimitri Rochman PSI
Peter Schillebeeckx JRC Geel
Marcus Seidl PEL
Marc Verwerft SCK•CEN

Participants:

CIEMAT, CPST, CTU (SURAO), ENRESA, ENUSA, JRC, JSI, KIT, LEI, NAGRA, PEL, PSI, SCK•CEN, SKB, SSTC NRS, TUS, VTT, UU

SNF - Gent, 15/11/2019

SFC: Spent Fuel Characterization and Evolution Until Disposal

- Task 1: S/T coordination, state-of-the-art and training material
- **Task 2: Fuel properties characterisation and related uncertainty analysis**
- Task 3: Behaviour of nuclear fuel and cladding after discharge
- Task 4: Accident scenario and consequence analysis
- Task 5: Civil Society interaction

SNF - Gent, 15/11/2019

Spent Nuclear Fuel (SNF) intermediate storage or final disposal

A **safe**, **secure**, **ecological** and **economic** transport**,** storage and final disposal requires that **SNF** is **characterised** for the main source terms of interest:

- Decay heat : H
- Neutron emission : S_n
- γ-ray emission : S_γ
- Reactivity : R
- Fissile material : Nuclear Safeguards
  i.e. ^{235}U, ^{239}Pu
- Specific nuclides : Long term safety
  e.g. ^{14}C, ^{79}Se, ^{94}Nb, ^{99}Tc, ^{129}I, ^{226}Ra

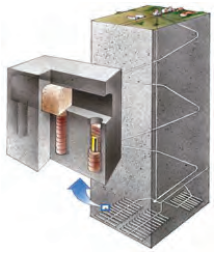

SNF - Gent, 15/11/2019

European Commission

Characterisation of SNF

Main **source terms** of interest:

- Decay heat : H
- Neutron emission : S_n
- γ-ray emission : S_γ
- Reactivity : ^{235}U, ^{239}Pu, Fission Products (BUC)
- Fissile material : ^{235}U, ^{239}Pu
- Long-term safety : e.g. ^{14}C, ^{79}Se, ^{94}Nb, ^{99}Tc, ^{129}I, ^{226}Ra

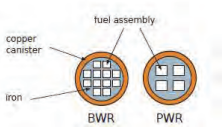

difficult to be measured directly, in particular during industrial operation

- Decay heat by calorimetry at CLAB: accurate but long measurement times
- Criticality safety analysis: calculations required to account for burn-up credit (MA, FP)

⇒ Determined/estimated by **theoretical calculations** using a burnup code
Neutron transport + depletion/creation code (see L. Fiorito)

SNF - Gent, 15/11/2019

European Commission

e.g. decay heat of SNF

Decay heat rate: $H(t) = \sum_j H_j(t)$

- $H_j(t)$: contribution of radionuclide j

  $H_j(t) = h_j N_j(t)$

  – h_j : specific decay heat rate of nuclide j

  – $N_j(t)$: number of nuclei of nuclide j at time t

- $N_j(t = t_0)$ known at $t = t_0$ (after irradiation)

  – $N_j(t > t_0)$ can be predicted accurately

  $N_j(t) = N_j(t_0)\, e^{-\lambda_j (t-t_0)}$

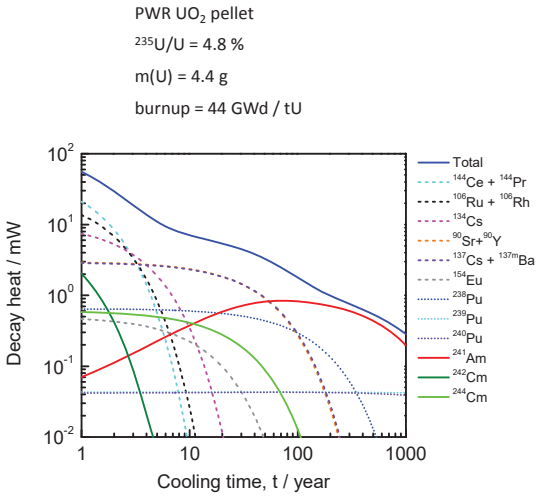

⇒ accurate nuclide vector $N_j(t_0)$ at t_0 is required from burn-up codes

European Commission

e.g. decay heat of SNF

Decay heat rate: $H(t) = \sum_j H_j(t)$

- $H_j(t)$: contribution of radionuclide j

  $H_j(t) = h_j N_j(t)$

  – h_j : specific decay heat rate of nuclide j

  – $N_j(t)$: number of nuclei of nuclide j at time t

- $N_j(t = t_0)$ known at $t = t_0$ (after irradiation)

  – $N_j(t > t_0)$ can be predicted accurately

  $N_j(t) = N_j(t_0)\, e^{-\lambda_j (t-t_0)}$

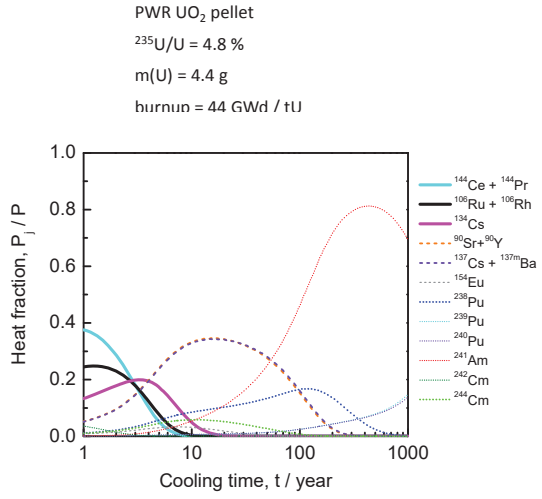

⇒ **accurate nuclide vector $N_j(t_0)$** at t_0 is required from **burn-up codes**

SNF - Gent, 15/11/2019

European Commission

Task 2: Fuel properties characterisation and related uncertainty analysis

- **Subtask 2.1 (Theory)** co-ordinator PSI
  Theoretical study of SNF source terms (assess and improve performance)
- **Subtask 2.2 (NDA)** co-ordinator SCK•CEN
  Develop, improve and demonstrate NDA methods/systems for SNF characterisation
- **Subtask 2.3 (Cladding)** co-ordinator KIT
  Calculate and determine experimentally the inventory of activation and fission products in cladding material
- **Subtask 2.4 (Final procedures)** co-ordinator KIT (PEL)
  Define and verify procedures to determine the source terms of SNF with realistic confidence limits

SNF-Task 2, SKB (07/08/2019)

European Commission

Subtask 2.1: Theoretical study of SNF source term

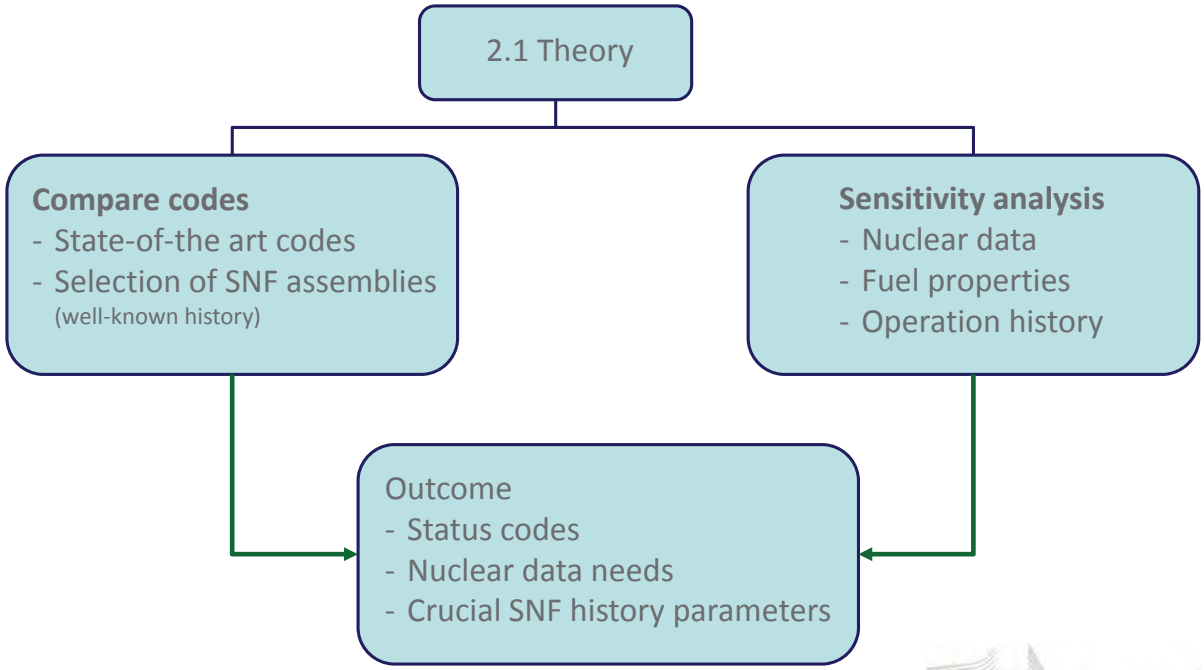

SNF - Gent, 15/11/2019

European Commission

Subtask 2.1 – Code comparison

- NAGRA : SCALE
- JSI : SCALE, DRAGON, (MCNP/FISPACT)
- PSI : CASMO
- VTT : SERPENT
- JRC Geel : SERPENT
- CIEMAT : MCNP/ACAB
- SCK•CEN : MCNP/ALEPH-2

Subtask 2.1 – SNF assemblies for code comparison

- 3 **PWR** assemblies
  - SF95-5 from the Takahama-3 reactor (UO_2 assembly, 30 MWd/kgU, 2 cycles, 4.1 %). Details in **SFCOMPO**
  - BM1 from the ARIANE campaign (MOX assembly, 45-47 MWd/kgU, 5 cycles, 4.2 % fissile). Details in **ARIANE** public report
  - GU1 from the ARIANE campaign (UO_2 assembly, 60 MWd/kgU, 4 cycles, 3.5 %). Details in **ARIANE** public report
- 2 **BWR** assemblies
  - KLU1 from the MALIBU campaign (UO_2 assembly, 60 MWd/kgU, 7 cycles, 3.9 %). Details **publicly available** 01/2020
  - Gundremmingen-7 sample (UO_2, 25 MWd/kgU, 4 cycles, 2.5 %). Details in **SFCOMPO**
- **Subtask 2.2**
  - ENRESA (BWR)
  - **SKB-50** campaign + blind test SKB: 2 PWR assemblies
  - **Reference pellet (REGAL)** (PWR UO_2 , 4.25 %, 50 MWd / kgU)

Subtask 2.1: Sensitivity and covariance analysis

- Nuclear data
  - Cross sections
  - Fission yields
  - Decay data (emission probabilities, recoverable energy per reaction/decay)
- Fuel properties: geometry and material data
  - Initial enrichment
  - …
- Operational history
  - Burn-up
  - Cooling time
  - Influence of neighbouring assemblies
  - Albedo boundary conditions
  - …
- Computational
  - Method (stochastic/deterministic)
  - Model (2D/3D, boundary conditions, etc.)
  - Numerical approximations (depletion time steps, depletion zones, etc.)

⇒ Recommendations for improvement and realistic uncertainty limits

Sensitivity analysis: e.g. $^{242,\ 244}$Cm production in MOX

- MOX, Borella et al. MC 2017, Jeju, Korea
  - PWR: 17 x 17
  - Single pin model

$$S_{N\sigma} = \frac{\partial N/N}{\partial \sigma/\sigma}$$

- Production : σ(n,γ)
  - ^{242}Cm : 2.5 % ^{241}Am(n,γ), ^{242m}Am(n,γ)
  - ^{244}Cm : 10 % ^{242}Pu(n,γ), ^{243}Am(n,γ)

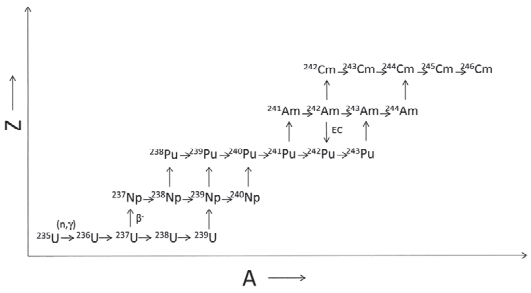

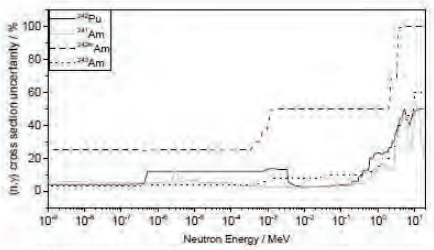

Fig. 4. Relative uncertainties of some of the considered radiative capture cross sections.

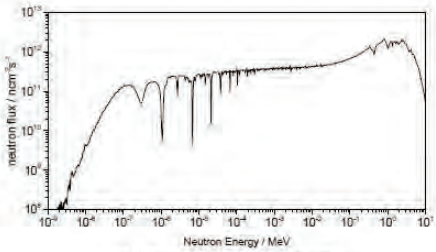

Fig. 5. Neutron flux spectrum in the studied model.

Sensitivity analysis: initial enrichment and burnup

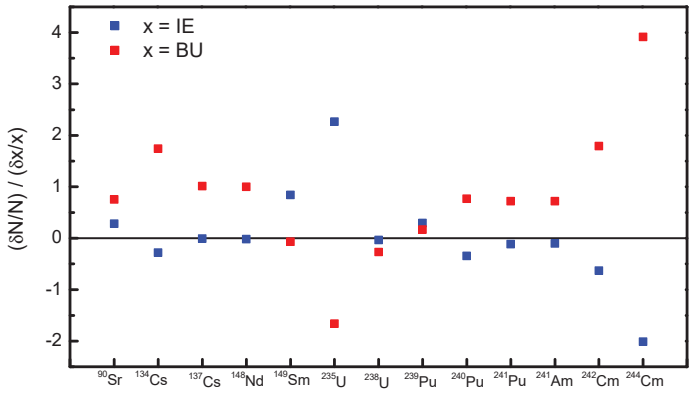

PWR UO_2

$^{235}U/U$ = 4.8 %

burnup = 50 MWd/kgU

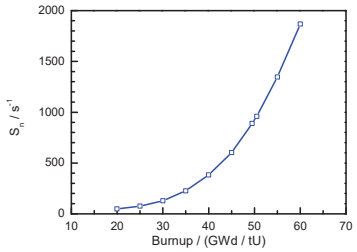

Subtask 2.2: NDA methods/systems for SNF characterisation

- **Innovative NDA** methods to characterise **small samples**
  - Validate codes (alternative to radiochemical analysis)
  - Production of a reference pellet
- **NDA** methods to characterise **fuel assemblies** (SKB-50)
  - Validate codes
  - Improve theoretical predictions during industrial routine operation
- Study new detectors
  - CLYC, *CVD*
- *Radiochemical analysis of BWR samples*

⇒ input to 2.1 and 2.4

SNF - Gent, 15/11/2019

NDA methods to characterise small samples

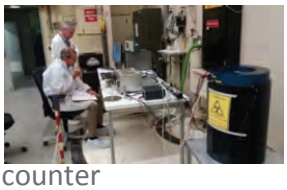

- **Neutron emission rate** of a SNF pellet
  - Non-destructive method to determine ^{244}Cm content
  - Measurements in conventional controlled area conditions
  - First measurements at SCK•CEN Mol using an existing neutron counter developed and calibrated at JRC finalised
  - Improved/optimised neutron counter under development at JRC Ispra (optimised to apply Hage's point model)

- **Nuclide vector** of SNF pellet by **NRTA**
  - Non-destructive; no chemical analysis
  - Absolute measurement
  - Measurements at GELINA facility of JRC Geel

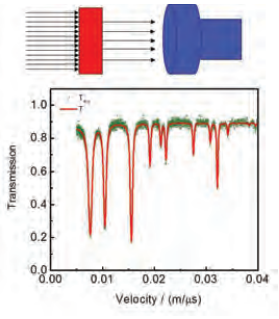

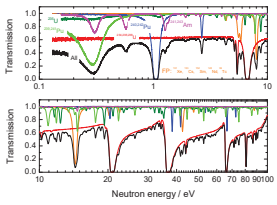

European Commission

Reference spent nuclear fuel pellet

- Material: **REGAL project**
  - Well-known production and irradiation history
  - γ-ray scan of fuel pin
  - Neighbouring pellets: analysed by radio-chemistry

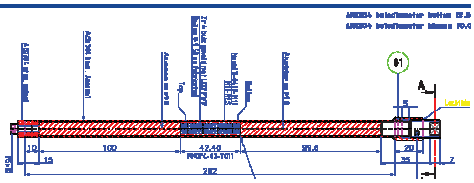

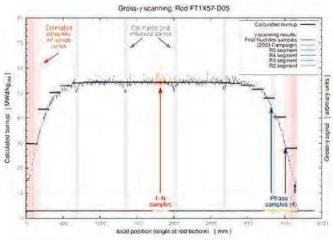

- NDA measurements on **reference SNF pellet**
  - γ-ray spectroscopy
  - **Neutron emission rate**
  - **NRTA: nuclide inventory (GELINA)**

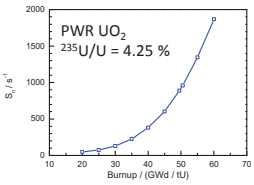

PWR UO_2
$^{235}U/U = 4.25$ %
burnup = 50 GWd / tU

European Commission

Fuel assemblies: calorimeter at CLAB

Improve and assess performance of calorimeter

- Performance assessment
  - Understand measurement method (analytic model)
  - Dedicated experiments to apply ANOVA and MLE

    ANOVA : Analysis Of Variance
    MLE : Maximum Likelihood Estimate (Bayesian approach)
- Calibration
  - Difference electrical heater ⇔ nuclear fuel
  - Heat losses due to escaping γ-rays

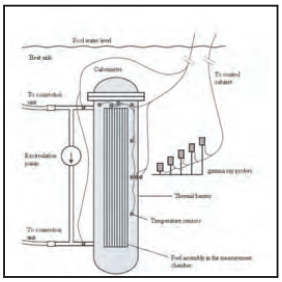

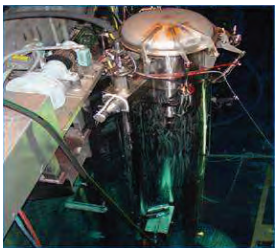

⇒ **Reference instrument** for code validation (SKB-50 input for 2.1 and 2.4)

⇒ Objective: decay heat ~ 2%

European Commission

Fuel assemblies: DDSI and DDA (LANL development, NGSI)

Improve/extend data analysis of DDA and DDSI (part of the SKB-50 project)

- Differential Die Away Self-Interrogation (DDSI, passive) *A.C. Trahan, LA-UR_16_20026*

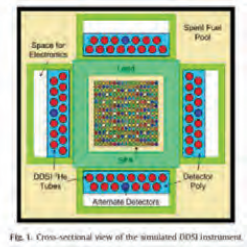

Fig. 1. Cross-sectional view of the simulated DDSI instrument.

- Differential Die Away (DDA, active) *V. Henzl, LANL-UR-123025*

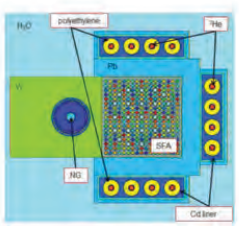

European Commission

Fuel assemblies: DDSI and DDA (LANL development)

Improve/extend data analysis of DDA and DDSI

- Differential Die Away Self-Interrogation (DDSI, passive) *A.C. Trahan, LA-UR_16_20026*

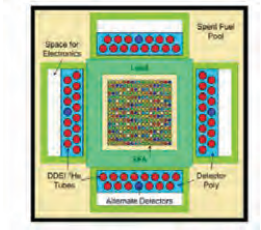

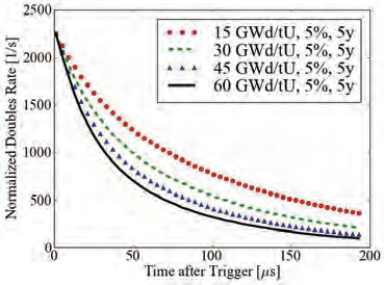

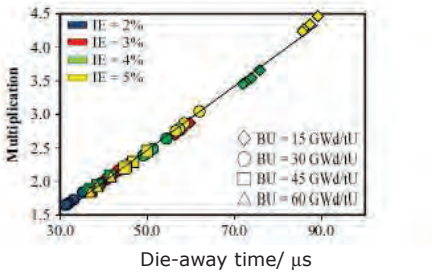

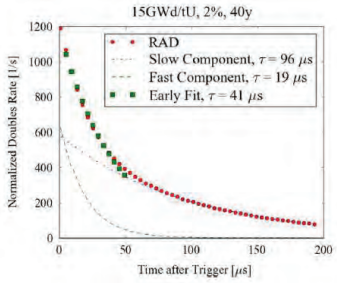

Optimise the use of data:

- Analyse the full Rossi-Alpha distribution
- Determine source strength: ^{244}Cm

European Commission

Fuel assemblies: DDSI and DDA (LANL development)

Improve/extend data analysis of DDA and DDSI

- Differential Die Away (DDA, active) *V. Henzl, LANL-UR-123025*

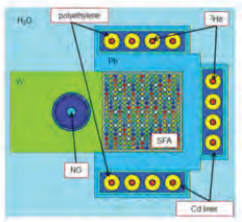

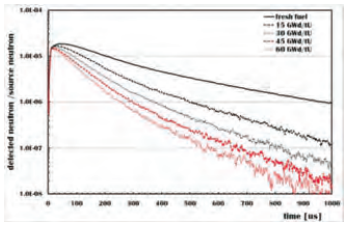

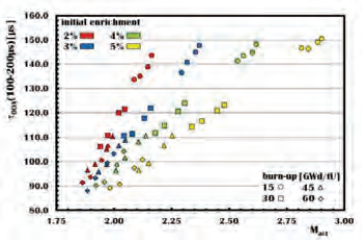

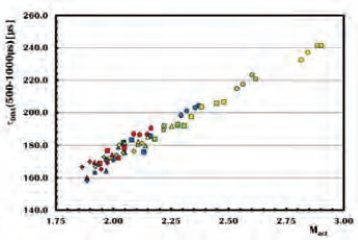

European Commission

Subtask 2.3 – Inventory of activation products and FP in cladding

- Preparation of three irradiated samples for further analysis (2 types)
  - Cladded pellets of UO_2 (50 GWd/t_{HM}) and MOX (38 GWd/t_{HM}) irradiated in a PWR
  - Plenum cladding from a UO_2 (50 GWd/tHM) rod segment irradiated in a PWR
- Experimental determination of nuclide inventory: radiochemical analysis
  - FP + ^{14}C and ^{36}Cl
- Validate and improve theoretical calculations of nuclide inventory

European Commission

Subtask 2.4: Final objective

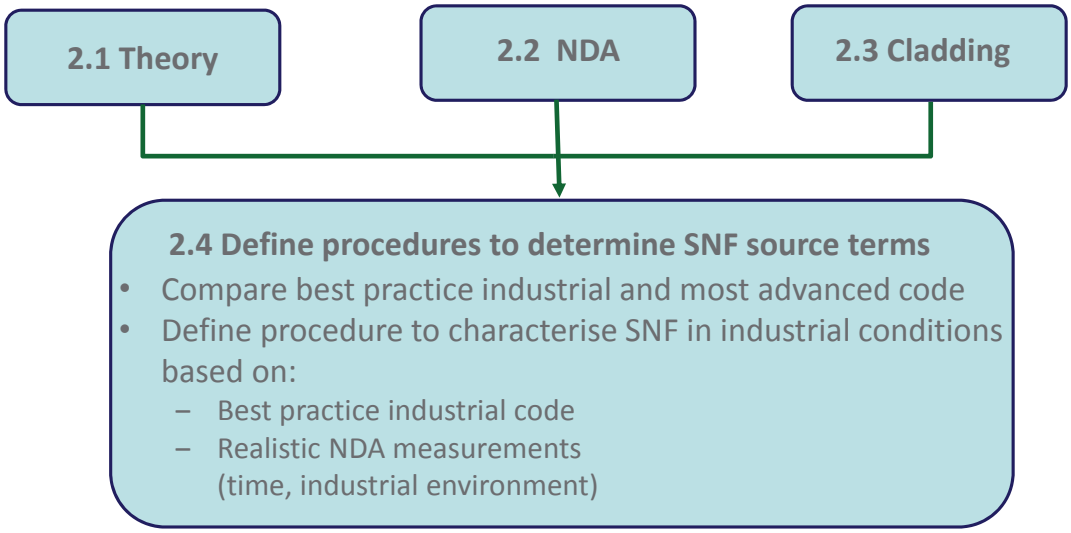

European Commission

Thank you for the attention

- EURAD project (SNF characterisation)
  - PhD position at Uppsala University
    https://www.uu.se/en/about-uu/join-us/details/?positionId=300024
  - NUGENIA
    http://nugenia.org/call-for-mobility-grants-open/

European Commission

5.2 Fuel properties characterisation and related uncertainty analysis; P. Schillebeeckx, JRC Geel; ESARDA Final Disposal Working Group Meeting, SCK CEN, Mol; 06 - 07/02/2020

European Joint Programme on Radioactive Waste Management

Spent Fuel Characterization and evolution until disposal

Task 2: Fuel properties characterisation and related uncertainty analysis

Ron Dagan	KIT
Dimitri Rochman	PSI
Peter Schillebeeckx	**JRC Geel (co-ordinator)**
Marcus Seidl	PEL
Marc Verwerft	SCK•CEN

Partners:

CIEMAT, CPST, CTU (SURAO), ENRESA, ENUSA, JRC, JSI, KIT, LEI, NAGRA, PEL, PSI, SCK•CEN, SKB, SSTC NRS, TUS, VTT, UU

ESARDA, 6 - 7 february 2020, SCK CEN Mol (BE)

European Commission

Spent Nuclear Fuel (SNF) intermediate storage or final disposal

A **safe**, **secure**, **economic** and **ecological** transport**,** storage and final disposal requires that **SNF** is **characterised** for the main source terms of interest:

- Decay heat
- Neutron emission
- γ-ray emission
- Reactivity (burnup credit)
  nuclides with high neutron absorption cross section)
- Fissile material (Safeguards)
  i.e. ^{235}U, ^{239}Pu
- Specific long-lived radionuclides (Long term safety)
  e.g. ^{14}C, ^{79}Se, ^{94}Nb, ^{99}Tc, ^{129}I, ^{226}Ra

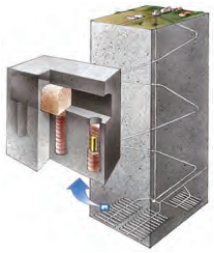

ESARDA, 6 - 7 february 2020, SCK CEN Mol (BE)

European Commission

Neutron emission by SNF

$$S_n(t) = \sum_k S_{n,k}(t)$$

- $S_{n,k}(t)$: contribution of radionuclide k
- $S_{n,k}(t) = (s_{sf,k} + s_{\alpha n,k})\, N_k(t)$
  - $N_k(t)$: number of nuclei of nuclide k at time t
  - $s_{sf,k}$: specific neutron emission rate of nuclide k due to sf
  - $s_{\alpha,k}$: specific neutron emission rate of nuclide k due to (α,n) reactions

PWR UO_2 pellet (5 g)
$^{235}U/U$ = 4.8 %
burnup = 44 GWd/t

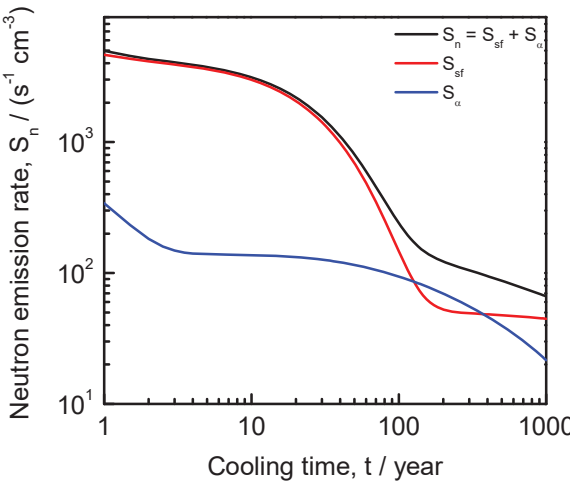

European Commission

Neutron emission by SNF

$$S_n(t) = \sum_k (s_{sf,k} + s_{\alpha n,k}) N_k(t)$$

PWR UO_2 pellet (5 g)
$^{235}U/U$ = 4.8 %
burnup = 44 GWd/t

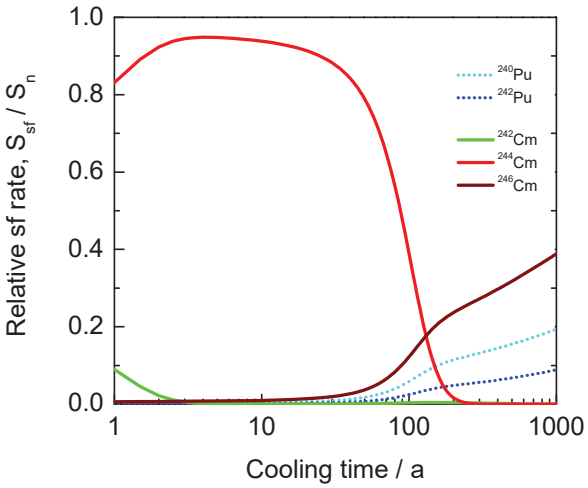

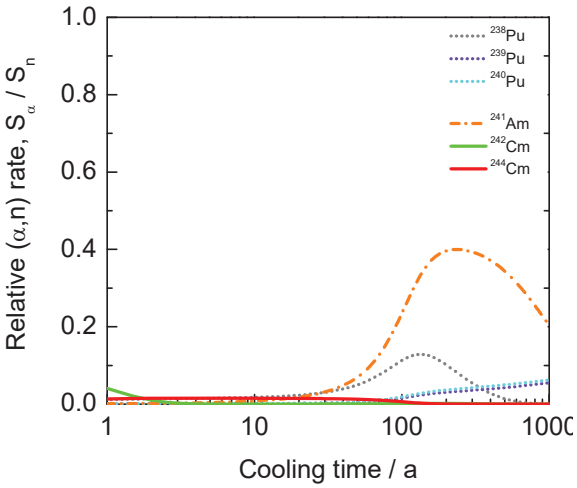

European Commission

Gamma-ray emission by SNF

$$S_\gamma(t) = \sum_k S_{\gamma,k}(E_\gamma, t)$$

PWR UO_2 pellet (5 g)
$^{235}U/U$ = 4.8 %
burnup = 44 GWd/t

^{95}Nb	35.0 d
^{95}Zr	64.0 d
$^{144}Ce/^{144}Pr$	284.9 d
$^{106}Ru/^{106}Rh$	1.02 a
^{134}Cs	2.06 a
^{154}Eu	8.8 a
$^{137}Cs/^{137m}Ba$	30.0 a

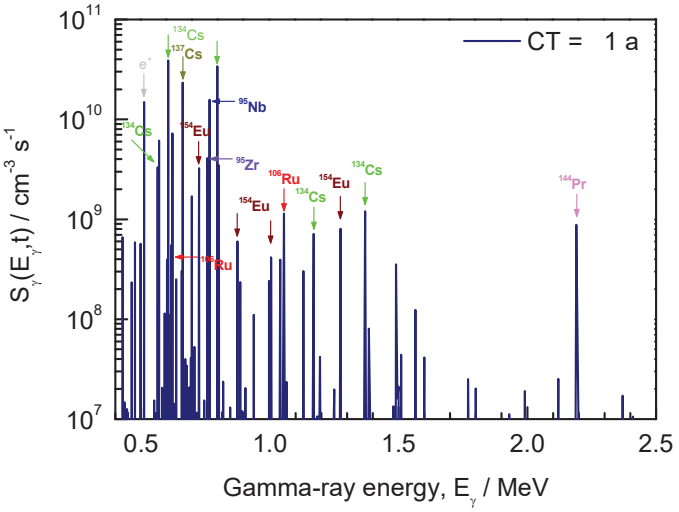

European Commission

Gamma-ray emission by SNF

$$S_\gamma(t) = \sum_k S_{\gamma,k}(E_\gamma, t)$$

PWR UO_2 pellet (5 g)
$^{235}U/U$ = 4.8 %
burnup = 44 GWd/t

^{95}Nb	35.0 d
^{95}Zr	64.0 d
$^{144}Ce/^{144}Pr$	284.9 d
$^{106}Ru/^{106}Rh$	1.02 a
^{134}Cs	2.06 a
^{154}Eu	8.8 a
$^{137}Cs/^{137m}Ba$	30.0 a

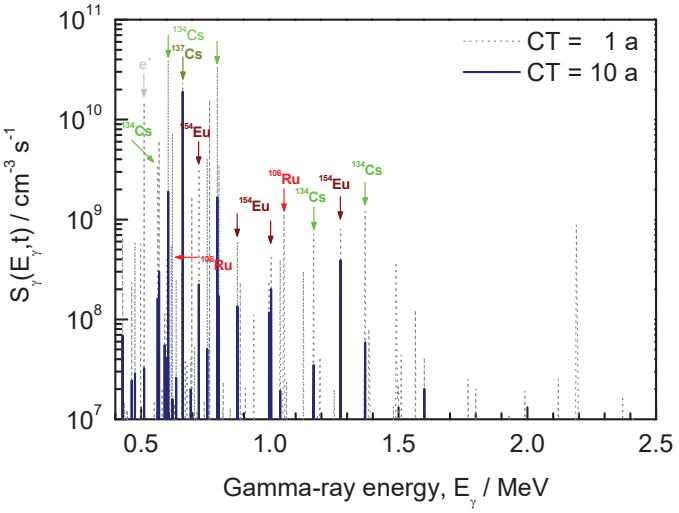

European Commission

Gamma-ray emission by SNF

$$S_\gamma(t) = \sum_k S_{\gamma,k}(E_\gamma, t)$$

PWR UO_2 pellet (5 g)
$^{235}U/U$ = 4.8 %
burnup = 44 GWd/t

^{95}Nb	35.0 d
^{95}Zr	64.0 d
$^{144}Ce/^{144}Pr$	284.9 d
$^{106}Ru/^{106}Rh$	1.02 a
^{134}Cs	2.06 a
^{154}Eu	**8.8 a**
$^{137}Cs/^{137m}Ba$	**30.0 a**

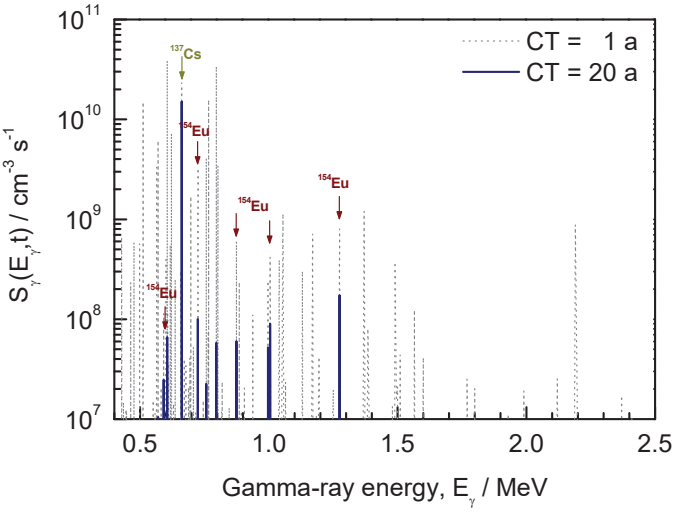

Gamma-ray emission by SNF

$$S_\gamma(t) = \sum_k S_{\gamma,k}(E_\gamma, t)$$

PWR UO_2 pellet (5 g)
$^{235}U/U$ = 4.8 %
burnup = 44 GWd/t

^{95}Nb	35.0 d
^{95}Zr	64.0 d
$^{144}Ce/^{144}Pr$	284.9 d
$^{106}Ru/^{106}Rh$	1.02 a
^{134}Cs	2.06 a
^{154}Eu	**8.8 a**
$^{137}Cs/^{137m}Ba$	**30.0 a**

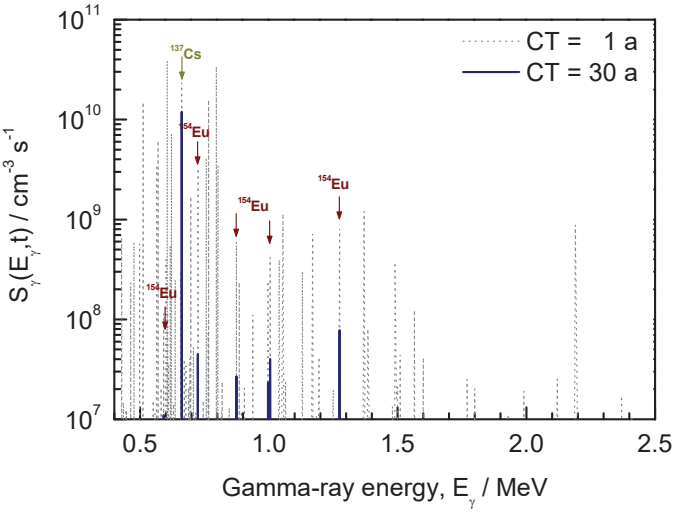

ESARDA, 6 - 7 february 2020, SCK CEN Mol (BE)

Characterisation of SNF

Main **source terms** of interest:

- Decay heat : H
- Neutron emission : S_n
- γ-ray emission : S_γ
- Reactivity : ^{235}U, ^{239}Pu, ^{241}Am, Fission Products (BUC)
- Fissile material : ^{235}U, ^{239}Pu
- Long-term safety : e.g. ^{14}C, ^{79}Se, ^{94}Nb, ^{99}Tc, ^{129}I, ^{226}Ra

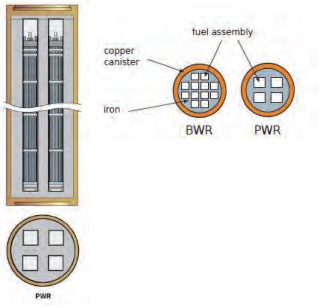

Contributions of nuclides with different characteristics

Difficult to be measured directly, in particular during industrial operation

e.g. decay heat by calorimetry at CLAB: accurate but long measurement times

⇒ Estimated by **theoretical calculations** using a burnup code

European Commission

$(N_k(t_0), k = 1, \ldots, n)$: by theoretical calculations

Coupled neutron transport – nuclide depletion/creation calculation

Neutron transport

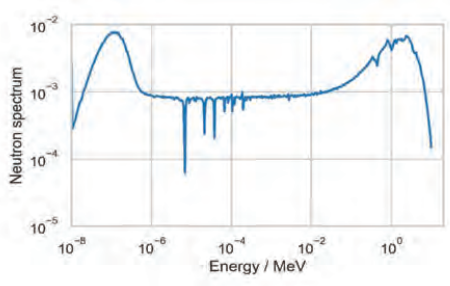

Bateman equation

$$\frac{dN_k}{dt} = Y\, N_f\, \sigma_f\, \varphi + \sum_i \lambda_i N_i + \sum_j \sigma_j N_j\, \varphi - (\lambda_k + \sigma_{k,a}\varphi) N_k$$

Update nuclide vector

ESARDA, 6 - 7 february 2020, SCK CEN Mol (BE)

European Commission

SFC – Task 2 (structure)

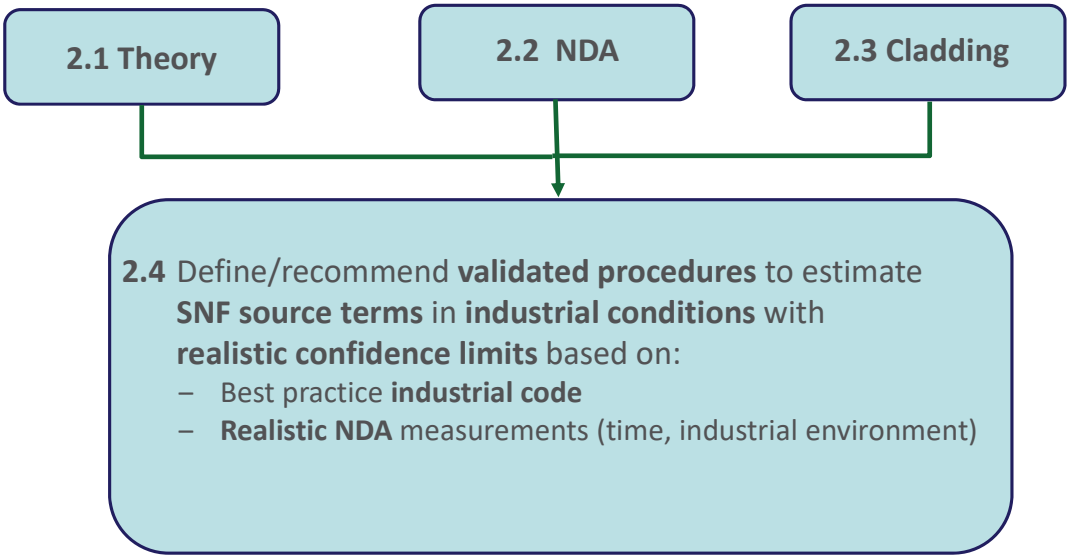

SFC- Task 2: Code comparison

- CIEMAT : EVOLCODE (MCNP)
- JRC Geel : SERPENT, SCALE
- JSI : SCALE, DRAGON
- KIT : MCNP-CINDER
- NAGRA : SCALE
- PSI : CASMO
- SCK CEN : ALEPH-2 (MCNP)
- VTT : SERPENT

ESARDA, 6 - 7 february 2020, SCK CEN Mol (BE)

Sensitivity and Uncertainty (S/U) analysis

- Input data:
  - **Nuclear Data (ND)**
    - Cross sections (neutron interactions)
    - Fission yields
    - Neutron emission probabilities
    - Decay data
  - **Fuel History (FH)**
    - Fuel properties (design, composition) e.g. Initial enrichment (IE)
    - Reactor operation and irradiation conditions e.g. Burnup (BU)
    - Cooling time (CT)

BurnUp (BU):
time integrated power per mass of initial fuel (MWd/kg)
$\propto$ *total number of fission x energy per fission event*

- Computational
  - Method: stochastic/deterministic
  - Model (2D/3D, boundary conditions, …)
  - Numerical approximations (depletion time steps, depletion zones, …)

European Commission

S/U analysis: ^{244}Cm production

$$\frac{dN_k}{dt} = Y\, N_f\, \sigma_f\, \varphi + \sum_i \lambda_i N_i + \sum_j \sigma_j N_j\, \varphi - (\lambda_k + \sigma_{k,a}\varphi) N_k$$

$N = aBU^b$

$b = 6$ for BU < 20 GWd/t

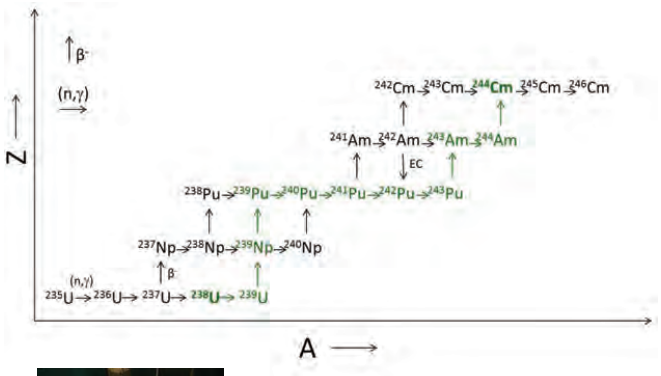

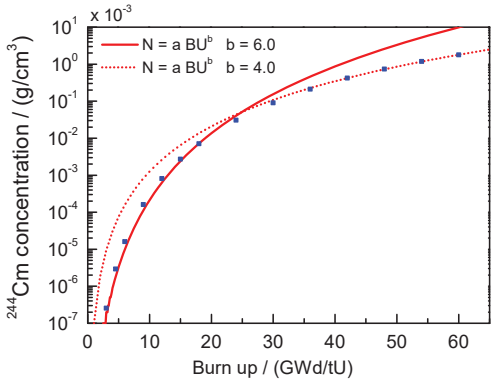

⇒ ^{244}Cm : burnup indicator

⇒ Neutron emission rate : burnup indicator

ESARDA, 6 - 7 february 2020, SCK CEN Mol (BE)

European Commission

S/U analysis: estimation of ^{244}Cm inventory

$$\frac{dN_k}{dt} = Y\, N_f\, \sigma_f\, \varphi + \sum_i \lambda_i N_i + \sum_j \sigma_j N_j\, \varphi - (\lambda_k + \sigma_{k,a}\varphi) N_k$$

Ref.	Library	Reactor	Fuel	BU GWd/t	IE wt%	^{244}Cm
Rochman	ENDF/B-VII.0	PWR	UO_2	10	4.1	18.7 %
	ENDF/B-VII.0	PWR	UO_2	20	4.1	16.9 %
	ENDF/B-VII.0	PWR	UO_2	30	4.1	15.5 %
	ENDF/B-VII.0	PWR	UO_2	40	4.1	14.1 %
Zwermann	SCALE-6.1	PWR	UO_2	40	4.1	8.5 %
Leary	ENDF/B-VII.1	PWR	UO_2	54	3.4	9.6 %
Rochman	ENDF/B-VII.1	PWR	UO_2	54	3.4	9.1 %
Rochman	ENDF/B-VII.1	PWR	UO_2	40	4.1	9.7 %

^{244}Cm inventory prediction production
- uncertainty due to nuclear data : ~10%
- due to ^{242}Pu(n,γ), ^{243}Am(n,γ)

⇒ Systematic study for key nuclides

⇒ Improve nuclear data
- Input HPRL NEA/OECD
- Input to SANDA (DG-RTD)
  https://cordis.europa.eu/project/id/847552
  Supplying Accurate Nuclear Data for energy and non-energy Applications

European Commission

Innovative NDA methods/systems for SNF characterisation

- **Innovative NDA** methods to characterise **pin segments**
  - **Validate codes** (alternative to radiochemical analysis)
  - Production of a reference pellet
- **NDA** methods to characterise **fuel assemblies** (SKB-50)
  - Improve theoretical source term predictions during industrial routine operation
    Improve fuel history data: e.g. BU
  - Validate codes
- Study **new detectors**
  - CLYC, *CVD*

ESARDA, 6 - 7 february 2020, SCK CEN Mol (BE)

European Commission

NDA methods to characterise pin segments

- **Neutron emission rate** of a SNF pin segment
  (collaboration SCK CEN – JRC Geel, Ispra)
  - Non-destructive method to determine ^{244}Cm content
  - Measurements in conventional controlled area conditions
    Hage's point model, JRC Ispra (B. Pedersen)

- **Nuclide vector** of SNF pin segment by **NRTA**
  (collaboration SCK CEN – JRC Geel)
  - **Non-destructive**; no chemical analysis
  - **Absolute** measurement (no calibration)
  - Measurements at **GELINA** facility of JRC Geel

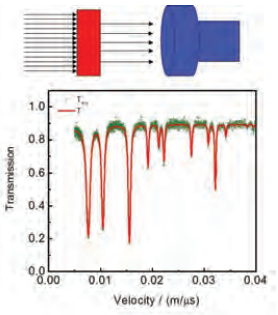

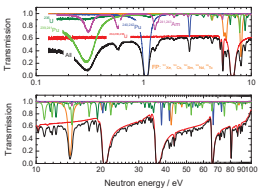

European Commission

Experiments at CLAB: SKB-50

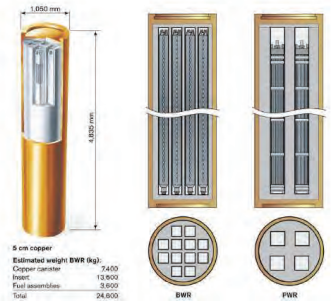

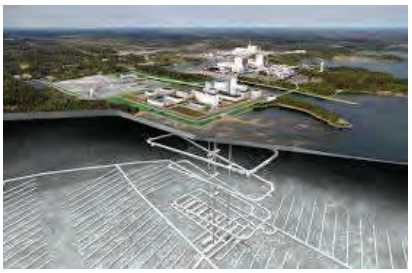

Installed systems

- Calorimeter
- Gamma-ray spectroscopic scanner

Testing of advanced systems (LANL)

- Differential Die-Away Self-Interrogation (DDSI)
- Differential Die-Away (DDA)

European Commission

Calorimeter at CLAB

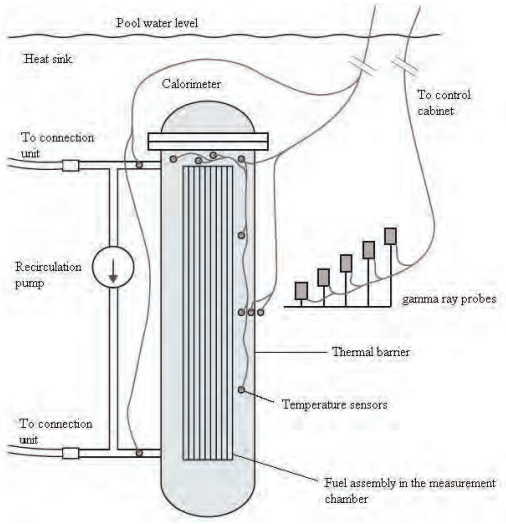

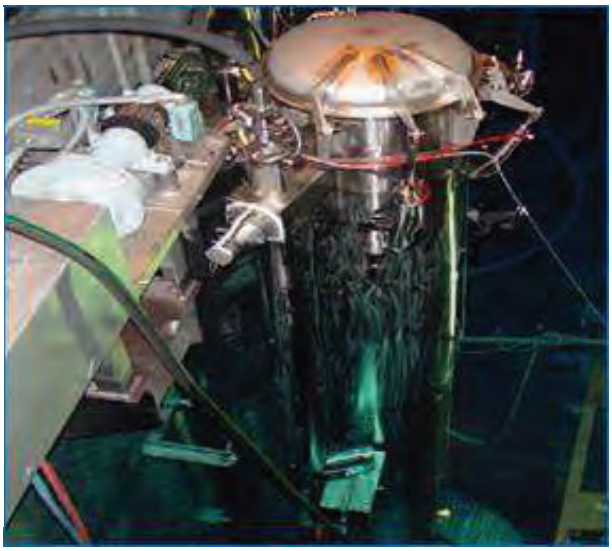

⇒ Target value uncertainty ≤ 2%
⇒ Reference instrument for decay heat of SNF

ESARDA, 6 - 7 february 2020, SCK CEN Mol (BE)

European Commission

Gamma-ray spectroscopic scanning system at CLAB

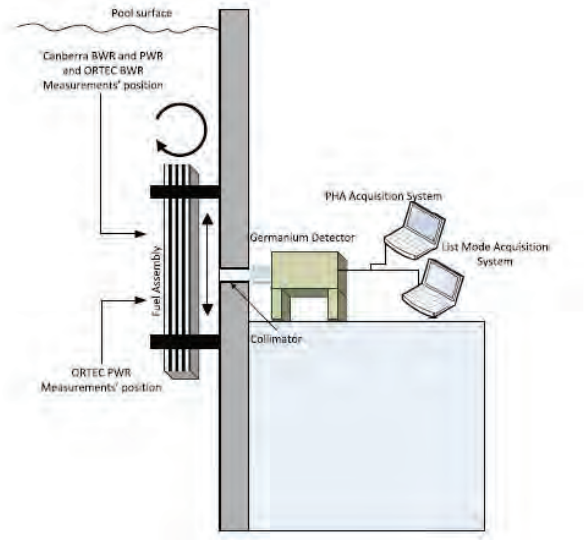

Vaccaro et al. NIMA 830 (2016) 325

^{134}Cs, ^{137}Cs, ^{154}Eu

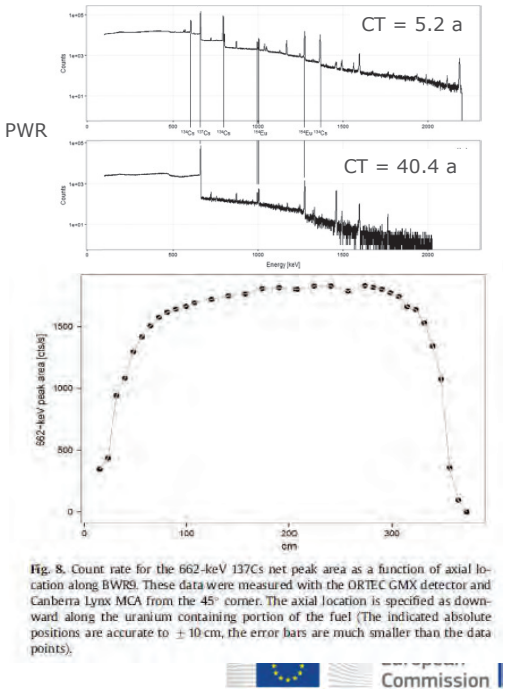

Fig. 8. Count rate for the 662-keV 137Cs net peak area as a function of axial location along BWR8. These data were measured with the ORTEC GMX detector and Canberra Lynx MCA from the 45° corner. The axial location is specified as downward along the uranium containing portion of the fuel (The indicated absolute positions are accurate to ± 10 cm, the error bars are much smaller than the data points).

ESARDA, 6 - 7 february 2020, SCK CEN Mol (BE)

European Commission

Fuel assemblies: DDSI and DDA at CLAB (LANL development, NGSI)

- Differential Die Away Self-Interrogation (DDSI, passive)

A.C. Trahan, LA-UR_16_20026 Kaplan et al., NIMA 764 (2014) 347 - 351

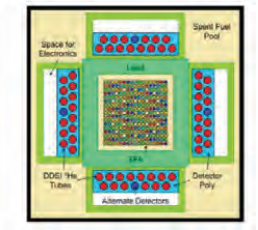

⇒ Optimise data analysis procedures for source term determination (not only safeguards)

- Differential Die Away (DDA, active)

V. Henzl, LANL-UR-123025

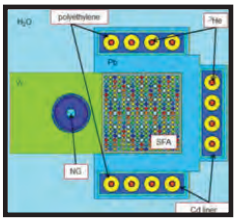

European Commission

Fuel assemblies: Finland

- Passive Neutron Albedo Reactivity (PNAR, NGSI)

LANL development, Tobin et al., NIMA 897 (2018) 32 - 37

Tobin et al., ESARDA bulletin 56 (2018) 12 - 18

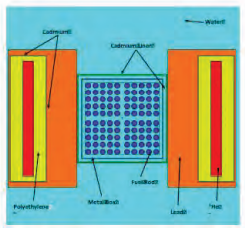

- Passive Gamma Ray Emission Tomography (PGET)

IAEA development, Honkamaa et al., Symp. Int. Safeguards, IAEA Vienna 2014

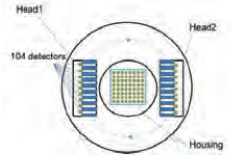

European Commission

EURAD-SFC (4 years project)

Define/recommend **validated procedures** to estimate **SNF source terms** (including fissile material) in **industrial conditions** with **realistic confidence limits** based on:

- Best practice **industrial code**
- **Realistic NDA** measurements (time, industrial environment)

European Commission

- EURAD project (SNF characterisation)
  - https://www.ejp-eurad.eu/about-eurad
  - NUGENIA, http://nugenia.org/call-for-mobility-grants-open/
- ARIEL
  support for open access, scientific visits, training early researchers, …
  - www.ariel-h2020.eu
- JRC Geel open access
  - https://ec.europa.eu/jrc/en/research-facility/open-access

ESARDA, 6 - 7 february 2020, SCK CEN Mol (BE)

European Commission

5.3 Predicting the Bias in Calculations of Spent Nuclear Fuel Characteristics; A. Shama, NAGRA; Workshop on Machine Learning in Nuclear Science and Technology, Madrid, Spain (online); 27/05/2021

PAUL SCHERRER INSTITUT PSI

Ahmed Shama :: PhD Student (EPFL/LRS, PSI/LRT)

Predicting the Bias in Calculations of Spent Nuclear Fuel Characteristics

27 May 2021

Workshop on ML in Nuclear Science and Technology Applications

Background and Motivation

- SNF characterization relies on calculations (measurements are extremely expensive, difficult)
- A question arises: How can we be sure about these calculations?
- Validation is required *a priori,* modelling benchmarks which have their characteristics measured, and comparing calculations to measurements (e.g., $C - E$ or C/E)
  - Limited measurements (e.g., ~300 SNF decay heat measurement worldwide) and actual SNF are ~13,000 SNF in Switzerland alone
  - Benchmarks cover ranges of SNF properties, area-of-applicability (AOA), and realistic SNF calculations usually have different properties
- We need to predict the bias (i.e., predictive modeling), by comparison with validation benchmarks

In criticality safety, methods are established

ANS-8.17: Criticality Safety Criteria for the Handling, Storage, and Transportation of LWR Fuel Outside Reactors

ANS-8.24: Validation of neutron transport methods for nuclear criticality safety calculations

[Broadhead et. al., 2004]

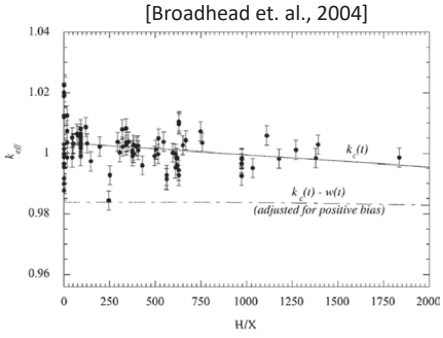

Seite 2

Overview of this work

Research Questions:

- Could the bias be predicted for SNF properties (decay heat and nuclide concentration) given a set of validation benchmarks?
- What properties would be informative into these predictions?
- What are the assumptions of these predictions?

$$C - E = f(X) + \varepsilon$$

Hypotheses:

- Bias prediction is based on neutronically similar benchmarks → Neighborhood-based schemes
- Integral SNF properties, such as spectral index, burnup, and correlations could be informative toward the bias prediction

Seite 3

Research Steps

1. **Collecting data:** SNF validation benchmarks (calculations and measurements)
2. **Extracting features:** sensitivity analysis and uncertainty propagation
3. **Application of data-driven techniques (novelty of this work):** Machine Learning models and algorithms

Seite 4

Research Steps

1. **Collecting data:** SNF validation benchmarks (calculations and measurements)

Decay heat labelled-data

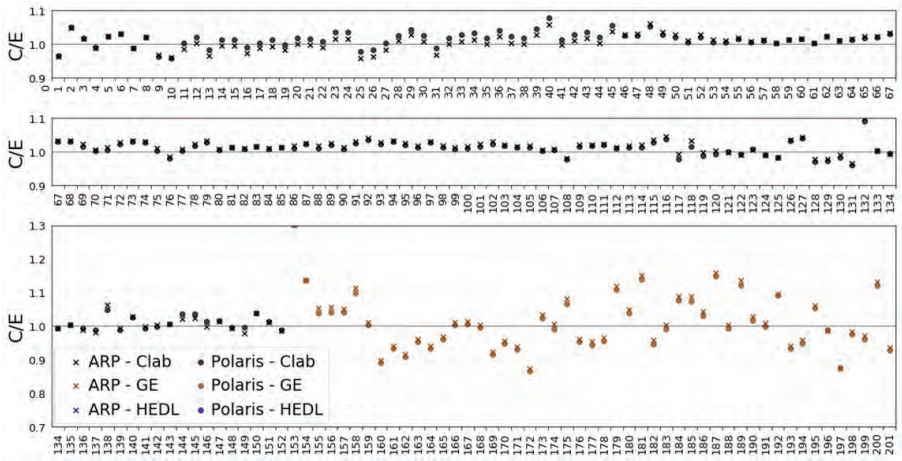

Seite 5

Research Steps

1. Collecting data: SNF validation benchmarks (calculations and measurements)
2. **Extracting features:** sensitivity analysis and uncertainty propagation

$$S_{C,x} = \frac{\partial C/C}{\partial x/x}$$

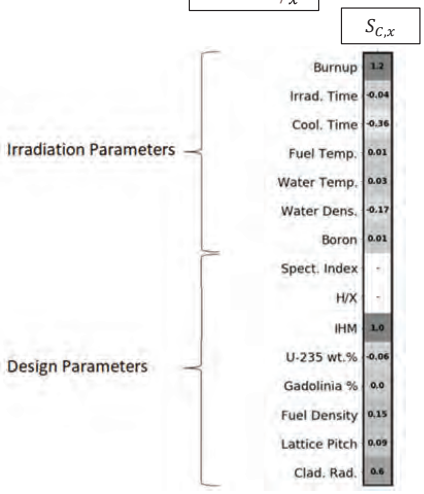

$$\rho_{ij} = \frac{1}{N-1}\sum_{k=1}^{N}\frac{(DH^i{}_k - \overline{DH_i})(DH^j{}_k - \overline{DH_j})}{\sigma_i\,\sigma_j}$$

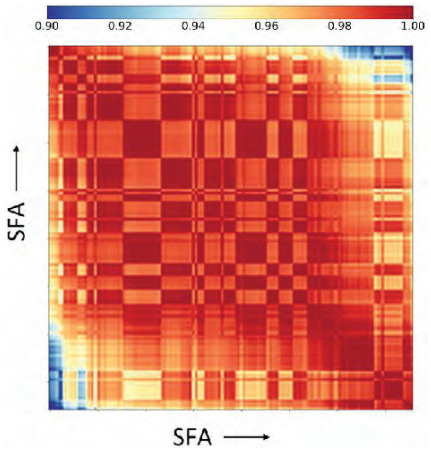

Seite 6

Research Steps

1. **Collecting data:** SNF validation benchmarks (calculations and measurements)
2. **Extracting features:** sensitivity analysis and uncertainty propagation

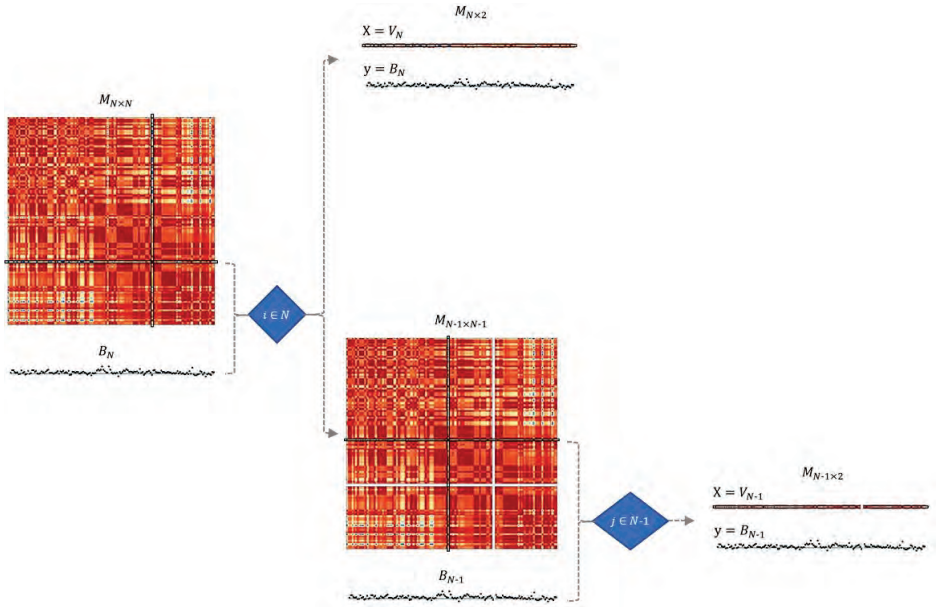

Research Steps

1. **Collecting data:** SNF validation benchmarks (calculations and measurements)
2. **Extracting features:** sensitivity analysis and uncertainty propagation
3. **Application of data-driven techniques (novelty of this work):** Machine Learning models and algorithms

$$C - E = f(X) + \varepsilon$$

Hypotheses

– Bias prediction is based on neutronically similar benchmarks

– Integral SNF properties, such as spectral index (*SI*) correlations between benchmarks, could be informative toward the bias predictions

Linear Model (~ criticality safety)

$LM\ with\ cutoffs$: $B_{(\rho=1)} = I_{\rho > co}(\rho)\beta\rho$

Neighborhood-based Schemes

$KKNN$: $B_{(\rho=1)} = \sum_{k=1}^{K} w_k B_k$

RF: $B_{(\rho=1)} = \frac{1}{N}\sum_{n=1}^{N}\left(\sum_{\rho \in [C/O,\,1]} w_n B_\rho\right)$

Results : Decay Heat

- Comparing predictions to observations (Features: SI or Correlations)
- Statistical testing, Kolmogorov–Smirnov test, testing whether model-predicted biases originate from the same distribution as observed ones at *p*-value = 0.05

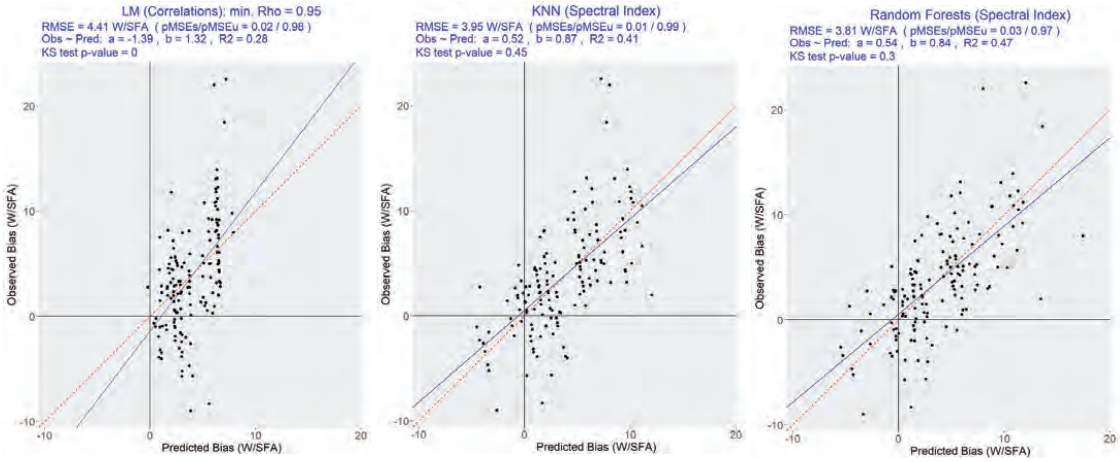

Seite 9

Summary

- SNF calculations are being validated (i.e., decay heat and nuclide concentration)
- Machine Learning models are being analyzed for their predictive performance, comparing bias model predictions to observed ones
- We have shown that the bias could be predicted from validation data (benchmarks), meaning we could support activities such as license applications, and decisions on safety margins
- Neighborhood based schemes (neutronically similar benchmarks) predict biases statistically similar to observed ones
- The models rely only on few SNF features, namely:
  - Spectral index (neutron flux)
  - Correlation between benchmarks
- **Ongoing work:** bias prediction for other quantities, i.e., actinides conc. (U-235 and Pu-239) and a fission product (Cs-137), using also neighborhood-based schemes and SNF features measuring similarities

Seite 10

Seite 11

Appendix : Validation

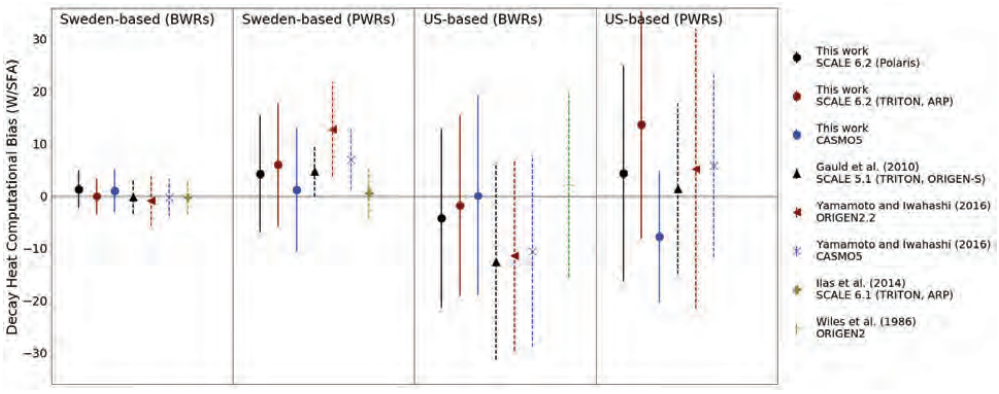

Seite 12

Appendix : Selecting Benchmarks

$$H_0: C_P \text{ or } C_O \text{ or } C_C = E$$

$$H_a: C_P \text{ and } C_O \text{ and } C_C \neq E$$

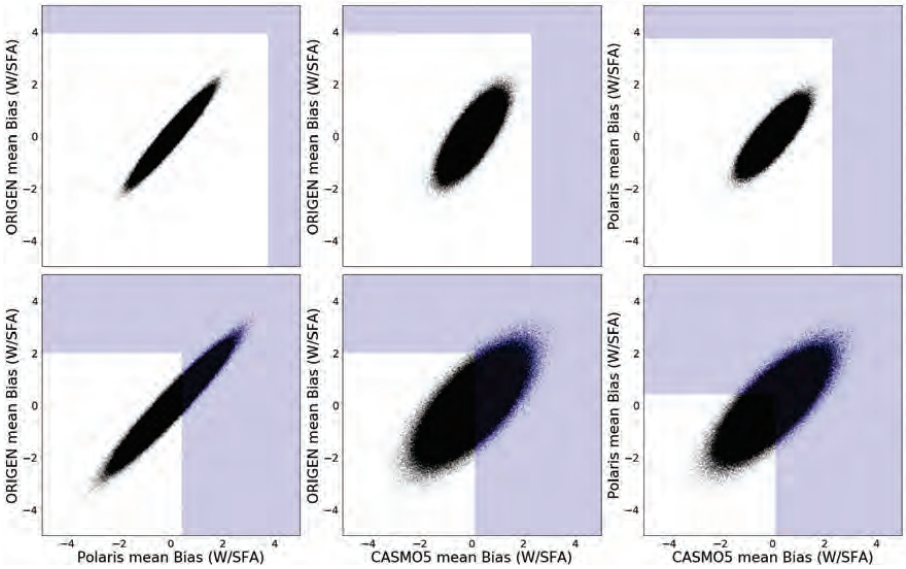

Seite 13

Appendix : Spectral Index

$$SI_i = \frac{\emptyset_{E>0.625\,eV}}{\emptyset_{total}}$$

$$SI = \frac{\sum_1^n (BU_i \times SI_i)}{\sum_1^n (BU_i)}$$

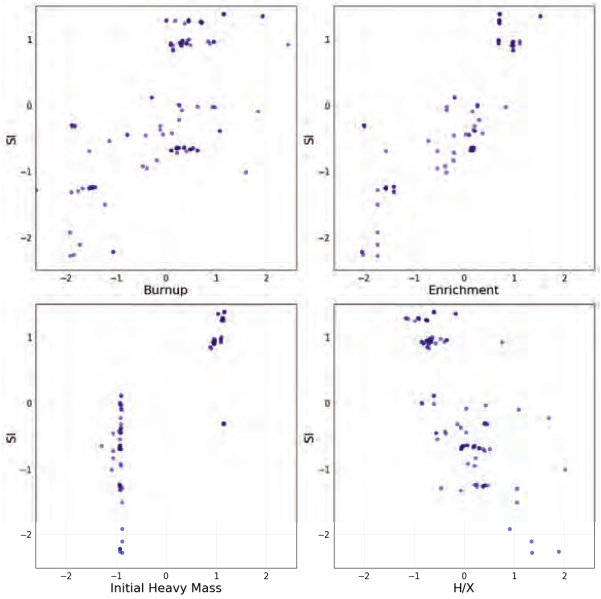

Seite 14

Appendix : Final Models

Table. Test errors of the applied models along with fractions of the explained variances.

Design Matrix	Model	MAE ± 1σ (W/SFA)	R^2
Spectral Index	RF	2.94 ± 2.42	0.47
	KNN	3.01 ± 2.56	0.41
	KKNN	2.97 ± 2.40	0.46
Correlation	RF	2.99 ± 2.67	0.44
	KNN	3.35 ± 2.69	0.32
	KKNN	3.49 ± 2.60	0.30

Seite 15

Appendix : Ongoing Activities

Bias prediction for other quantities, i.e., concentration of actinides (U-235 and Pu-239) and a fission product (Cs-137), using neighborhood-based schemes and SNF features measuring similarities

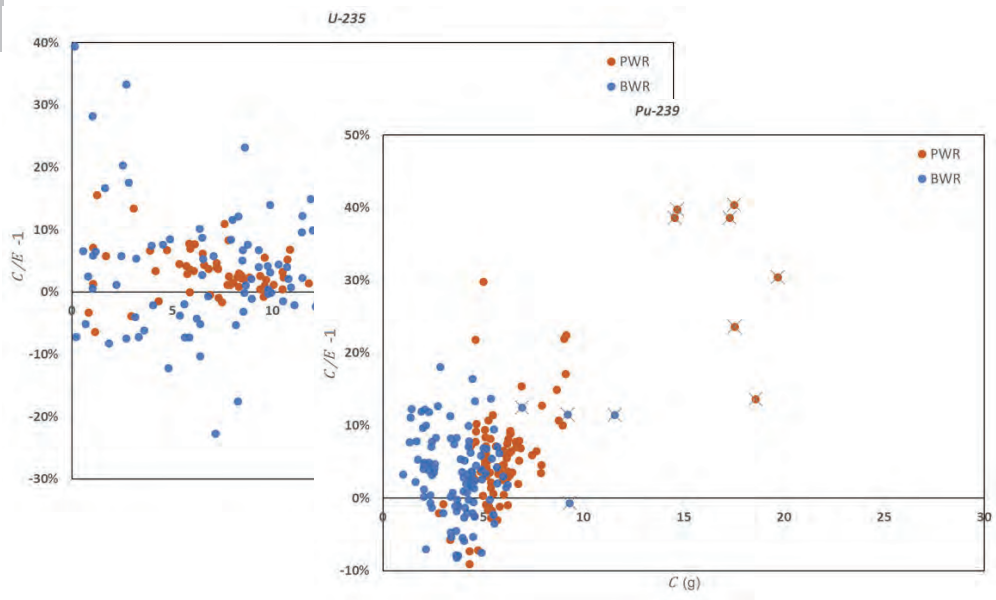

Seite 16

5.4 Chemical and spectroscopic investigations on the distribution of radionuclides in fuel-cladding interfaces of irradiated high burn-up UOX and MOX fuels; R. Dagan, T. König et al., KIT; Safety of Extended Dry Storage; 01 – 03/06/2022

Karlsruhe Institute of Technology

Institut für Nukleare Entsorgung

1980 - 2020 INE - 40 Institut für Nukleare Entsorgung

Chemical and spectroscopic investigations on the distribution and enrichment of radionuclides in fuel-cladding interfaces of irradiated high burn-up UO_X and MOX fuels

T. König*, R. Dagan, K. Dardenne, M. Herm, V. Metz, T. Pruessmann, J. Rothe, D. Schild, A. Walschburger and H. Geckeis

Karlsruhe Institute of Technology (KIT), Institute for Nuclear Waste Disposal (INE), P.O. Box 3640, 76021 Karlsruhe Germany

KIT – The Research University in the Helmholtz Association

*koenig.tobias@kit.edu

www.kit.edu

Outline

Karlsruhe Institute of Technology

- **Introduction:**
  - Nuclear fuel – *From cradle to grave*
- **Experimental:**
  - Examined fuel types – *High burn-up UO_X and MOX fuel*
  - Radionuclide analysis – *Inventory determination of spent nuclear fuel*
  - Spectroscopic analysis – *Interaction layer between fuel and cladding*
  - Model systems – *Experiments on the formation of agglomerates and corrosion of the reaction layer*
- **Summary**

Nuclear fission in Light Water Reactors

- **Neutron induced fission of fissile material** (^{235}U, ^{239}Pu, etc.):
  - Generation of neutrons ➡ **Maintaining the chain reaction**.
  - Built-up of fission products ➡ **2 – 3 fragments per fission**.
  - Neutron capture reactions ➡ **Built-up of transuranic isotopes (Np, Pu, etc.) & activation products (^{14}C, ^{36}Cl).**
- **Burn-up** as definition of fuel utilisation:

  ➡ **Produced energy per mass initial heavy metal atom [GWd/t_{HM}].**

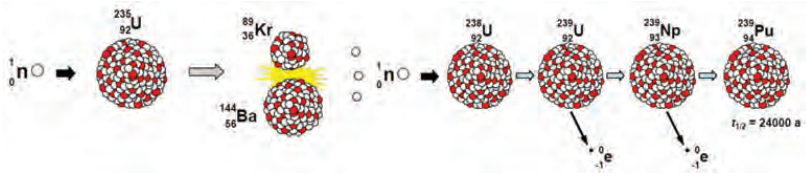

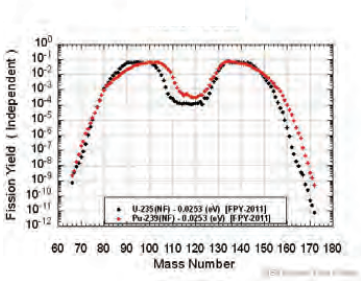

Spent Nuclear Fuel (SNF)

- Composition of SNF (4.0% ^{235}U, 52 GWd/t_{HM}) utilised in a light water reactor (LWR) for ~ 4 years:
  - **93.4% UO_2 matrix:**

    92% ^{238}U, < 1% ^{235}U, < 0.5% ^{236}U
  - **1.2% transuranium isotopes / actinides:**

    1% ^{239}Pu, ^{240}Pu, ^{241}Pu, ^{237}Np > ^{244}Cm > ^{241}Am, etc.
  - **5.4% fission products:**

    1.7% ^{90}Sr, $^{135, 137}$Cs, ^{129}I, etc.

    1.6% lanthanides

    1.3% ε-phases (^{99}Tc, ^{109}Pd, etc.)

    0.8% fission gases (krypton, xenon)
  - **Activation products:**

    e.g. ^{14}C, ^{93}Zr, ^{36}Cl ➡ **^{35}Cl (n,γ) ^{36}Cl**

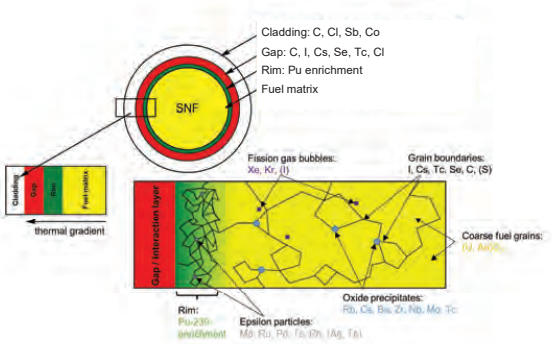

➡ **Heterogenous distribution of radionuclides.**

Source: Hippler, Reaktorchemie, Leibniz Universität Hannover

From cradle to grave | Materials and methods | Radionuclide analysis | Spectroscopic analysis | Summary

Interaction layer between fuel and cladding

- **Cross section of a nuclear fuel pellet:**

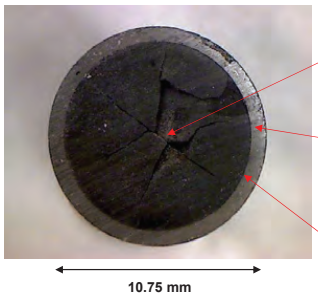

Pellet: Radial cracks due to temperature gradient during irradiation; migration pathways for radionuclides in the SNF pellet.

Cladding: Built-up of an external ZrO_2 layer due to primary circuit water corrosion; thin ZrO_2 layer on the inner side due to Zr / UO_2 reactions.

Gap: Closed at burn-ups > 40 GWd/t_{HM}; Formation of an **interaction layer.**

➡ **Possibility of transport of volatile fission and activation products to the cladding during irradiation and subsequent chemical reactions between fuel and cladding!**

From cradle to grave | Materials and methods | Radionuclide analysis | Spectroscopic analysis | Summary

Interim storage in Germany

- **Interim dry storage** of used fuel assemblies in dual-purpose casks:
  - Dual-purpose cask guarantees **shielding of radiation**, as well as a temporary, **safe enclosure of radionuclides.**
  - Interim storage of irradiated fuel assemblies is **licensed for only 40 years.**
  - **Final repository not available until at least 2050 and emplacement of the last fuel assemblies decades later!**

➡ **Necessity of a prolonged interim storage of 65 – 100 years and conditioning of fuel assemblies from dual-purpose cask to final repository waste container!**

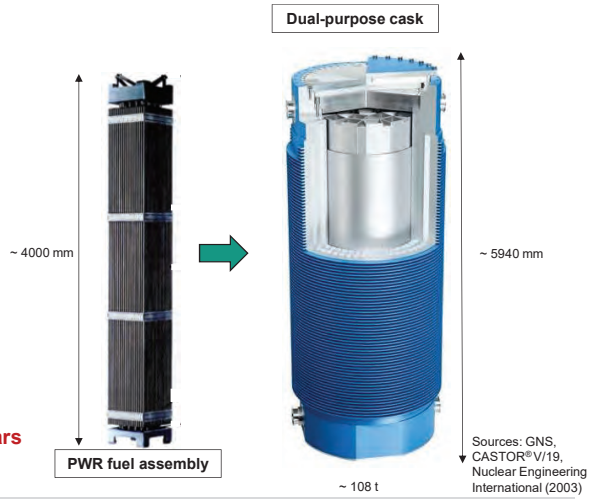

From cradle to grave | Materials and methods | Radionuclide analysis | Spectroscopic analysis | Summary

Interim storage in Germany

- **Interim dry storage** of used fuel assemblies in dual-purpose casks:
  - Dual-purpose cask guarantees **shielding of radiation**, as well as a temporary, **safe enclosure of radionuclides.**
  - Interim storage of irradiated fuel assemblies is **licensed for only 40 years.**
  - **Final repository not available until at least 2050 and emplacement of the last fuel assemblies decades later!**

- Several phenomena affect the cladding integrity during interim storage:
  - **Increase in pressure** due to swelling of the pellet and ongoing α-decays.
  - **Irradiation damage of cladding** via α-decays.
  - Cracking due to **hydride re-orientation**.

$$Zr + 2\,H_2O \longrightarrow ZrO_2 + 2\,H_2$$

  - **Corrosion of cladding induced by fission and activation products.**

→ **Formation of agglomerates on the inner side of the cladding due to thermal gradient in SNF and possibility of halogen induced stress corrosion cracking.**

From cradle to grave | Materials and methods | Radionuclide analysis | Spectroscopic analysis | Summary

Final disposal in Germany

- Deep geological disposal:
  - **3 different lithologies** (clay, salt or crystalline rock) are under investigation.
  - **Safe enclosure for long timescale** needs to be guaranteed (1 million years).

Safety analyses require profound knowledge on the occurence and chemical behaviour of long-lived and dose relevant radionuclides (e.g. ^{36}Cl, ^{129}I, ^{135}Cs)

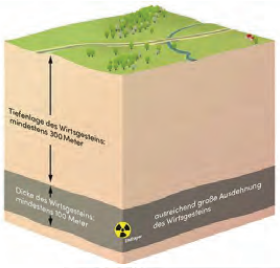

Source: https://www.einblicke.de/fileadmin/images/magazin/Einblicke_6/Kriterien_zur_Endlagersuche.jpg (aufgerufen am 04.04.2022)

[FLA18]: D. Flamikova, V. Necas, *Creation of Reference Biosphere Model for Safety Assessment of Deep Geological Repository*, AIP Conference Proceedings 1996, 020009 (2018).

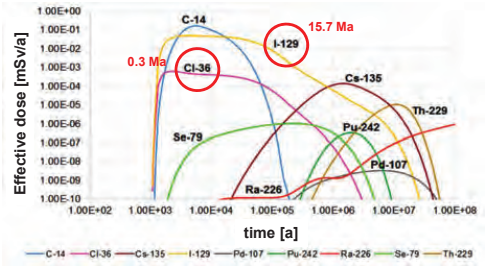

Open questions

- If, after breaching of the (geo-) technical barriers, water intrusion appears, **^{36}Cl and ^{129}I are quickly immobilised from the SNF**! In which concentration and chemical form are ^{36}Cl and ^{129}I present in used nuclear fuel rods?
  - **Quantification and localisation of the repository relevant and mobile isotopes ^{36}Cl and ^{129}I in SNF and cladding.**
  - **Comparison of experimental determined radionuclide concentrations to expected inventory data derived from calculations.**

  ⇒ **Reducing uncertainties on inventory data.**
- In which condition is the fuel-cladding interface during interim storage?
  - **In which chemical speciation are possible cladding degrading elements such as chlorine or iodine present in SNF and cladding?**
  - **Is a halogen induced pitting corrosion possible at temperatures prevailing during interim dry storage?**

  ⇒ **Reducing uncertainties on degrading processes.**

SNF specimens

Fuel rod segment N0204, irradiated in the pressurised water reactor Gösgen (CH):

- Fuel type: **UO_X**, initial 3.8% ^{235}U enrichment.
- Cladding alloy: Zircaloy-4.
- Full power days: 1226 days in 4 cycles.
- Average linear power: 260 W/cm.
- Average burn-up: **50.4 GWd/t_{HM}**.
- Decay time: ~ 32 years.

Fuel rod 5810, irradiated in the pressurised water reactor Obrigheim (DE):

- Fuel type: **MOX**, initial 3.2% Pu_{fiss} enrichment.
- Cladding alloy: Zircaloy-4.
- Full power days: 1157 days in 4 cycles.
- Average linear power: 200 W/cm.
- Average burn-up: **38.0 GWd/t_{HM}**.
- Decay time: ~ 35 years.

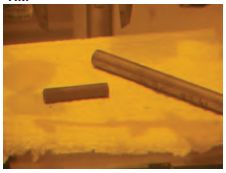

From cradle to grave | Materials and methods | Radionuclide analysis | Spectroscopic analysis | Summary

Preparation of the SNF specimens

- Segmentation of the SNF specimens in specially equipped laboratories (**hot cells**) due to the high dose rate!
- Selective sampling in order to analyse local radionuclide enrichments:
  - Fragments from central position **("CORE")**.
  - Fragments from peripheral position **("RIM")**.
  - **Zircaloy cladding segments.**


Hot cells of INE

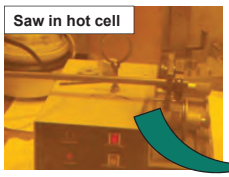
Saw in hot cell

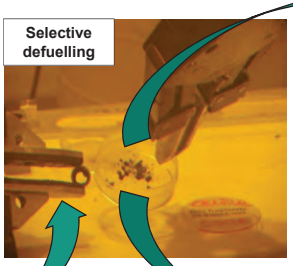
Selective defuelling

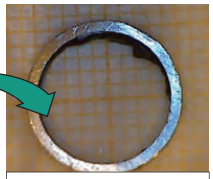
Zircaloy segment


SNF fragments

From cradle to grave | Materials and methods | Radionuclide analysis | Spectroscopic analysis | Summary

Radiochemical analytic & numerical calculations

- **Acidic and alkaline digestions of Zircaloy and fuel specimens** in HF / H_2SO_4, HNO_3 / HCl or $(NH_4)_2CO_3$ / H_2O_2:
  - **γ-spectrometry:** ^{241}Am, $^{134, 137}$Cs, ^{125}Sb, $^{154, 155}$Eu, ^{60}Co, **^{129}I**.
  - **Liquid scintillation counting (LSC): ^{129}I, ^{36}Cl**, ^{90}Sr. ➡ **High purity of samples necessary!**
  - **ICP-MS:** $^{235, 238}$U, ^{237}Np, $^{239, 240}$Pu, ^{241}Am, ^{244}Cm.
  - **Gas-MS:** Kr- and Xe-isotopes.
- **Calculations of the radionuclide inventory** with **MCNP Code** for neutron flux and **CINDER module** for burn-up calculations:
  - Numerical calculations for the respective fuel assemblies, reactor types and irradiation conditions.
  - Radionuclide concentrations in central and peripheral part of pellets.


Digestions in autoclaves for fission gas determination

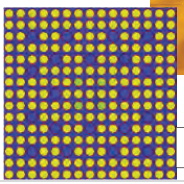
Simulations of the fuel assemblies

From cradle to grave | Materials and methods | Radionuclide analysis | Spectroscopic analysis | Summary

Spectroscopic measurements

- Preparation of fuel fragments and Zircaloy segments for analyses by **SEM-EDX / -WDX**, and **XAS** at the **KIT Light Source**. ➡ **Enormous radiation protection measures necessary!**
  - Samples for **examination of the chemical composition**.
  - Samples for **speciation measurements**.

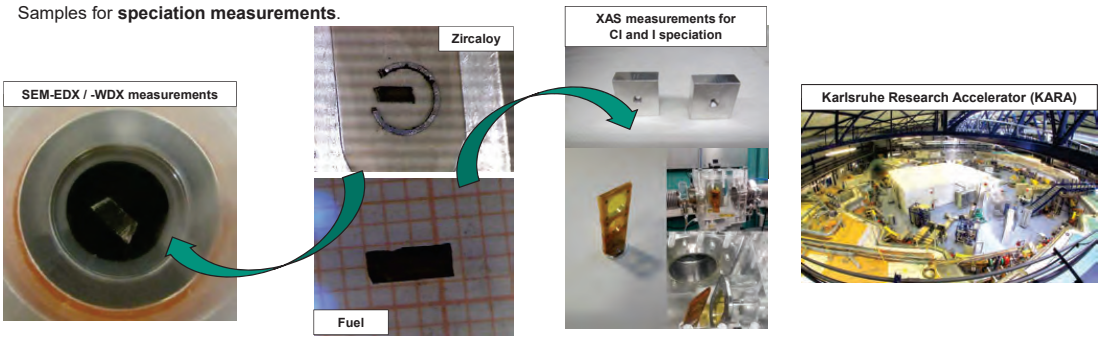

From cradle to grave | Materials and methods | Radionuclide analysis | Spectroscopic analysis | Summary

Radionuclide analysis – Separation of ^{36}Cl and ^{129}I

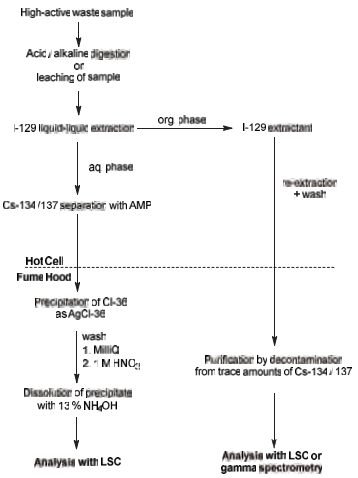

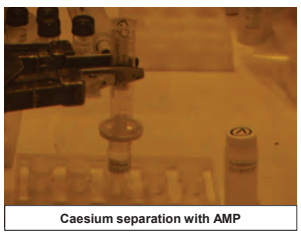
Caesium separation with AMP

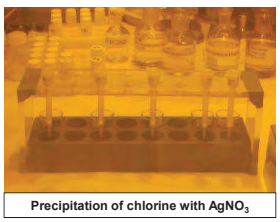
Precipitation of chlorine with $AgNO_3$

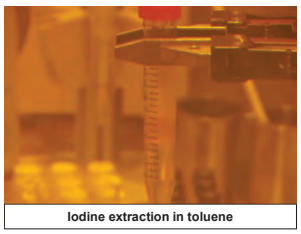
Iodine extraction in toluene

Chemical yield chlorine = 94±2%

Chemical yield iodine = 93±3%

Good yields despite complex matrices and working in highly contaminated areas!

From cradle to grave | Materials and methods | Radionuclide analysis | Spectroscopic analysis | Summary

Radionuclide analysis – ^{36}Cl in SNF and Zircaloy

^{36}Cl inventories	SNF		Zircaloy cladding	
Specimen	UO_X 50.4 GWd/t_{HM} [Bq/t_{HM}]	MOX 38.0 GWd/t_{HM} [Bq/t_{HM}]	UO_X 50.4 GWd/t_{HM} [Bq/t_{HM}]	MOX 38.0 GWd/t_{HM} [Bq/t_{HM}]
experimental	$3.62(\pm0.54)\times10^8$	$5.80(\pm0.87)\times10^8$	$6.32(\pm0.28)\times10^8$	$5.33(\pm0.24)\times10^8$
calculated	4.73×10^8	3.68×10^8	6.57×10^8	5.23×10^8
ratio (exp/calc)	0.77 ± 0.12	1.58 ± 0.24	0.96 ± 0.04	1.02 ± 0.05

^{35}Cl (n,γ) ^{36}Cl

- Numerical calculations based on literature data assuming 15 ppm ^{35}Cl precursor in SNF and Zircaloy [HÄK19].
- Experimental activity inventories in good agreement with calculations.

[HÄK19] S. Häkkinen, *Impurities in LWR fuel and structural materials*, VTT, Finland (2019).

→ First ever analysis of ^{36}Cl in PWR fuel rod components!

From cradle to grave | Materials and methods | Radionuclide analysis | Spectroscopic analysis | Summary

Radionuclide analysis – Fission products

- Determination of the fission product inventory in SNF fragments originating from the fuel-cladding interaction layer and comparison with MCNP calculations.
- No significant differences between **UO_X (50.4 GWd/t_{HM})** and **MOX (38.0 GWd/t_{HM})** fuel.

Comparison MOX and UO_X SNF [Bq/t_{HM}]

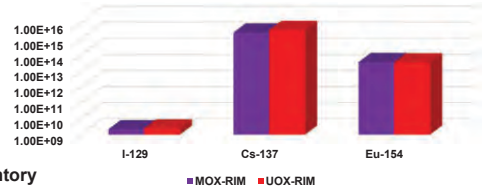

Comparison of ^{129}I inventory [Bq/t_{HM}]

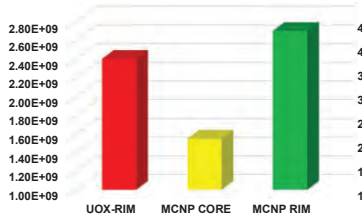

Comparison of ^{137}Cs inventory [Bq/t_{HM}]

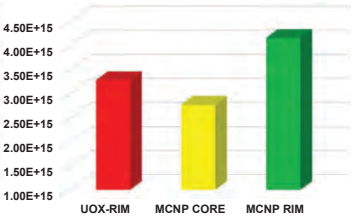

→ Elevated ^{129}I and ^{137}Cs activity due to enrichment effect at the cladding interface, originating from the higher local burn-up and transport of iodine along a thermal gradient in SNF pellet.

From cradle to grave | Materials and methods | Radionuclide analysis | Spectroscopic analysis | Summary

Radionuclide analysis – Actinides

- Experimentally derived and calculated inventory data for different regions in fuel pellet of actinides.
- MOX fuel shows elevated activity of minor actinides compared to UO_X fuel due to initial enrichment with Pu.

Comparison MOX and UO_X fuel [Bq/t_{HM}]

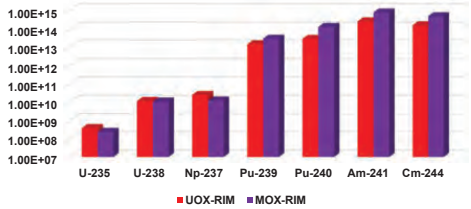

Comparison of actinide inventory [Bq/t_{HM}]

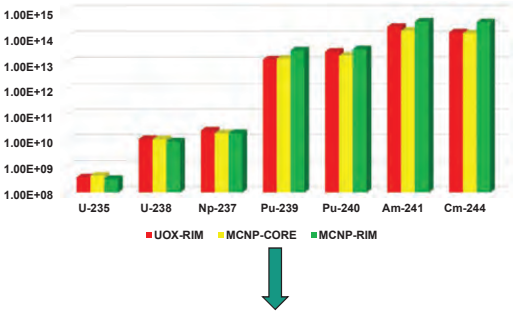

Knowledge on the amount of transuranium isotopes is of importance for calculations on α-radiation induced damage of the cladding tube during interim storage.

From cradle to grave | Materials and methods | Radionuclide analysis | Spectroscopic analysis | Summary

Spectroscopic analysis – SEM-EDX / -WDX

- **Zircaloy in contact with spent UO_x / MOX fuel:**
  - **SEM-EDX:** Cl, Te, I, Cs, Fe, Zr, Ba, U.
  - **XPS:** Cl, Te, Cs, Fe, Zr, Ba, U.

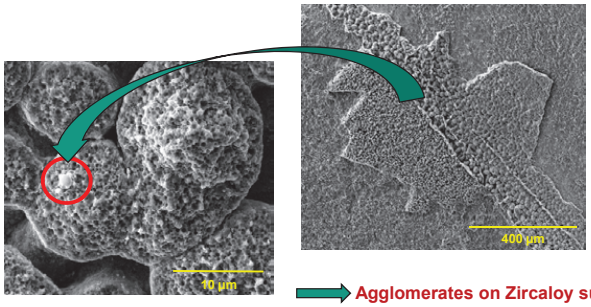

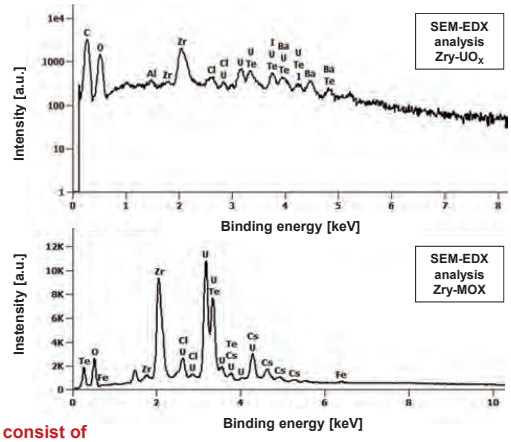

Agglomerates on Zircaloy surface consist of U-O-Zr-Cs-Cl-I rich phases.

From cradle to grave | Materials and methods | Radionuclide analysis | Spectroscopic analysis | Summary

Spectroscopic analysis – XAS

- Knowledge on the chlorine (and iodine) inventory and speciation in fuel and Zircaloy **afflicted with large uncertainties**.
- Initial maximum impurity assumptions of up to **25 ppm Cl in the fuel and 20 ppm Cl in Zircaloy-4 cladding**.
- **First ever XAS measurements for chlorine (and iodine) speciation** in fuel and cladding. ➡ **Complex mixed phases**.

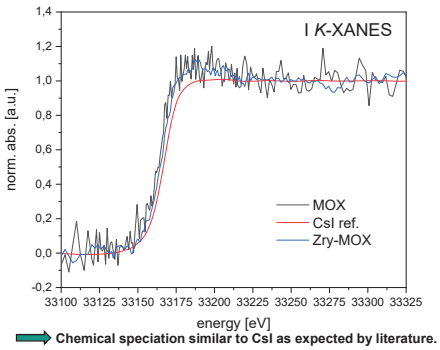

➡ **Chemical speciation similar to CsI as expected by literature.**

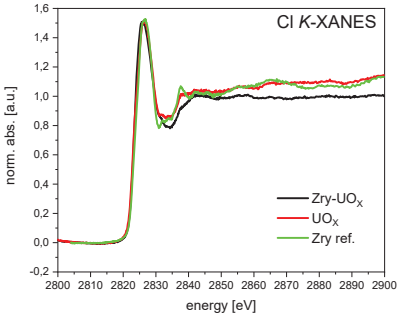

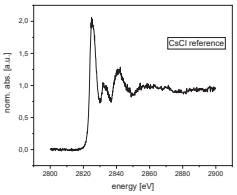

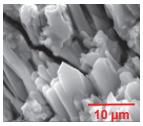

➡ **Yet unknown chlorine species; mixed phase consisting of U-Zr-O-Cs-Cl.**

From cradle to grave | Materials and methods | Radionuclide analysis | Spectroscopic analysis | Summary

Spectroscopic analysis – Model systems

- Laboratory experiments for formation of agglomerates and pitting corrosion under simulated interim dry storage conditions:
  - **Caesium halides in contact with Zircaloy and UO_2 pellet** under Ar atmosphere.
  - **Reduction of temperature over 3 months from** 400°C to room temperature.
  - Subsequent analysis with SEM-EDX and XPS.

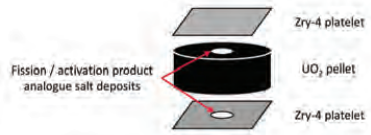

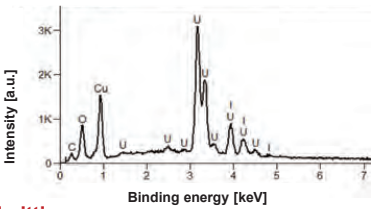

➡ **Validation of mixed phases formation and pitting corrosion at T < 400°C!**

Formation of halogen-rich agglomerates

Halogen-induced pitting corrosion

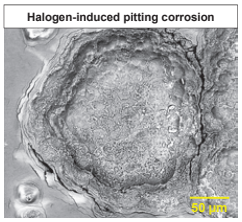

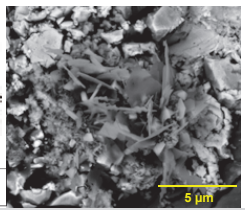

Summary

- **Radionuclide analysis:**
  - Development of separation method for **^{36}Cl and ^{129}I in high active waste specimens**.
  - **First ever analysis of ^{36}Cl inventory** in PWR fuel rod components.
  - **Verification** of iodine enrichment in interaction layer between fuel and cladding.
  - Good agreement between calculated and experimentally determined radionuclide inventory data.
- **Spectroscopic analysis:**
  - **First ever measurements of Cl *K*- and I *K*-edge** in high active waste specimens (SNF and Zircaloy).
  - Agglomerates in interaction layer consist, amongst others, of halogen-rich mixed phases **(Cl and I)**, as well as Cs, Te, Ba, U and Pu.
  - **Validation of agglomerate-formation and pitting corrosion at T < 400°C under laboratory conditions**.

Acknowledgements

- E. Bohnert (KIT-INE)
- M. Böttle (KIT-INE)
- M. Fuss (KIT-INE)
- F. Geyer (KIT-INE)
- C. Walschburger (KIT-INE)
- A. Fried (KIT-INE)
- E. Soballa (KIT-INE)
- V. Krepper (KIT-INE)
- S. Schmitt (KIT-INE)
- M. Große (KIT-IAM)
- D. Papaioannou (JRC-KRU)

This project has received funding from the European Union's Horizon 2020 research and innovation programme under grant agreement N°847593

Thank you for your kind attention and stay healthy!

5.5 Experimentelle und numerische Bestimmungen des Radionuklidinventars von abgebrannten Kernbrennstoffen als eine Grundlage für die vorläufige Sicherheitsuntersuchung (vSU); R. Dagan, T. König et al., KIT; Tage der Standortauswahl; 08 - 10/06/2022

Experimentelle und numerische Bestimmungen des Radionuklidinventars von abgebrannten Kernbrennstoffen als eine Grundlage für die vSU

T. König, R. Dagan, M. Herm, V. Metz, A. Walschburger und H. Geckeis

Karlsruher Institut für Technologie, Institut für Nukleare Entsorgung, P.O. Box 3640, 76021, Karlsruhe, Deutschland

koenig.tobias@kit.edu

Einleitung

In den vorläufigen Sicherheitsuntersuchungen (vSU) wird gemäß § 27 StandAG das Endlagersystem in seiner Gesamtheit betrachtet und hinsichtlich seiner Sicherheit bewertet, wobei abdeckende Annahmen zur Menge, Art und Eigenschaften der radioaktiven Abfälle herangezogen werden [BGB17]. Hierbei sind die zu betrachtenden Radionuklidinventare der Ausgangspunkt für die Bewertung des sicheren Einschlusses der Abfälle und Dosisabschätzungen in den vSU [BGE22]. Neben den Inventaren sind die chemische Speziation und lokale Verteilung der Radionuklide entscheidend für deren Mobilisierung aus den Abfällen.

In unserer Studie bestimmen wir experimentell die Radionuklidinventare von UO_X (Abbrand 50,4 GWd/t_{HM}) bzw. Mischoxid (MOX) (Abbrand 38,0 GWd/t_{HM}) Brennstabsegmenten, welche in Leistungsreaktoren eingesetzt wurden. Die gemessenen Radionuklidaktivitäten werden mit Inventarberechnungen, die wir mit den Programmen MCNP / CINDER und webKORIGEN ermitteln, verglichen. Aufgrund der relativ hohen Mobilität von ^{36}Cl und ^{129}I unter Endlagerbedingungen, liegt das Hauptaugenmerk unserer Untersuchungen auf den Inventaren und der Verteilung der beiden Aktivierungs- und Spaltprodukte.

Kernbrennstoffe

Brennstabsegment N0204, bestrahlt im Druckwasserreaktor, DWR Gösgen:

Brennstofftyp: **UO_X** mit 3,8% ^{235}U Anreicherung.
Hüllrohr: Zircaloy-4.
Volllasttage: 1226 Tage in 4 Zyklen.
Durchschnittliche lineare Leistung: 260 W/cm.
Durchschnittlicher Abbrand: **50,4 GWd/t_{HM}**.
Abklingzeit: ~ 32 Jahre.

Brennstab 5810, bestrahlt im Druckwasserreaktor, DWR Obrigheim:

Brennstofftyp: **MOX** mit 3,2% Pu_{fiss} Anreicherung.
Hüllrohr: Zircaloy-4.
Volllasttage: 1157 Tage in 4 Zyklen.
Durchschnittliche lineare Leistung: 200 W/cm.
Durchschnittlicher Abbrand: **38,0 GWd/t_{HM}**.
Abklingzeit: ~ 35 Jahre.

Endlagerung von abgebranntem Kernbrennstoff

Tiefengeologische Endlagerung:

- **3 unterschiedliche Gesteinsarten** (Ton-, Salz- und Kristallingestein) werden in Betracht gezogen.
- **Sicherer Einschluss über langen Zeitraum** muss gewährt werden (1 Million Jahre).

Sicherheitsbewertung erfordert grundlegende Kenntnisse über das Vorkommen und chemisches Verhalten von langlebigen und dosisrelevanten Radionukliden (z. ^{36}Cl, ^{129}I, ^{135}Cs)

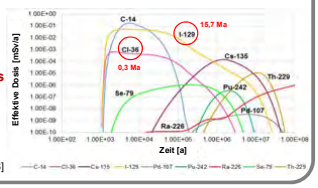

Quellen: BASE, [FLA18]

Radionuklidinventarbestimmung

Saurer und alkalischer Aufschluss von Zircaloy- sowie Brennstoffproben aus dem **zentralen und Randbereich der Pellets** in HF / H_2SO_4, HNO_3 / HCl, $(NH_4)_2CO_3$ / H_2O_2:

- **Neuentwickelte Abtrennungsmethode für ^{36}Cl und ^{129}I aus hochradioaktiven Proben.**
- **γ-Spektrometrie:** ^{241}Am, $^{134, 137}Cs$, ^{125}Sb, $^{154, 155}Eu$, ^{60}Co, ^{129}I.
- **Flüssigszintillationsmessung:** ^{129}I, ^{36}Cl, ^{90}Sr, ^{241}Pu.
- **ICP-MS:** $^{235, 238}U$, ^{237}Np, $^{239, 240, 242}Pu$, $^{241, 243}Am$, $^{244, 245, 246}Cm$.
- **Gas-MS:** Kr- und Xe-Isotope.

Berechnungen des Radionuklidinventars mittels **webKORIGEN** sowie **MCNP Code** für Neutronenfluss und **CINDER Modul** für Abbrand-Berechnungen:

- Numerische Berechnungen für die jeweiligen Brennstoffanordnungen, Reaktortypen und Bestrahlungsbedingungen.
- Radionuklidkonzentrationen im **zentralen und Randbereich des Pellets**.

^{36}Cl Inventar in Kernbrennstoff und Hüllrohr

^{36}Cl Inventare	Kernbrennstoff [Bq/t_{HM}]		Zircaloy-Hüllrohr [Bq/t_{HM}]	
Probe	UO_X 50,4 GWd/t_{HM}	MOX 38,0 GWd/t_{HM}	UO_X 50,4 GWd/t_{HM}	MOX 38,0 GWd/t_{HM}
Experimentell	$3,62(\pm0,54)\times10^8$	$5,80(\pm0,87)\times10^8$	$6,32(\pm0,28)\times10^8$	$5,33(\pm0,24)\times10^8$
Berechnet	$4,73\times10^8$	$3,68\times10^8$	$6,57\times10^8$	$5,23\times10^8$
Verhältnis (exp/ber)	0,77 ± 0,12	1,58 ± 0,24	0,96 ± 0,04	1,02 ± 0,05

➡ **Numerische Berechnungen auf Grundlage von Literaturdaten, ausgehend von 15 ppm ^{35}Cl Precursor in KBS und Hüllrohr [HÄK19].**

➡ **Erstmalige Analyse von ^{36}Cl in DWR-Brennstoffkomponenten!**

^{129}I Inventar in Kernbrennstoff

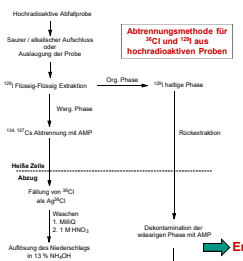

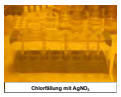

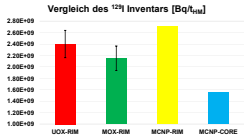

➡ **Erhöhte ^{129}I Aktivität durch einen Anreicherungseffekt an der Hüllrohrgrenzfläche auf Grund des höheren lokalen Abbrands und dem Transport von Iod entlang eines thermischen Gradienten im Pellet.**

Zusammenfassung

- **Abtrennungsmethode für ^{36}Cl und ^{129}I aus hochradioaktiven Proben entwickelt.**
- **Erstmalige Analyse des ^{36}Cl Inventars in DWR-Brennstoffkomponenten.**
- **Nachweis von Iod-reichen Anreicherungen in der Wechselwirkungsschicht zwischen KBS und Zircaloy-Hüllrohr.**
- **Gute Übereinstimmung zwischen Berechnungen und experimentell bestimmten Radionuklidinventardaten für etliche Isotope wie ^{36}Cl, ^{129}I und ^{137}Cs; jedoch auch Abweichungen ersichtlich bei z. B. ^{60}Co, ^{235}U, ^{245}Cm.**

Quellen

- [BGB17] Bundesgesetzblatt I S. 1074, Gesetz zur Suche und Auswahl eines Standortes für ein Endlager für hochradioaktive Abfälle, Deutschland (2017).
- [BGE22] Bundesgesellschaft für Endlagerung, *Methodenbeschreibung zur Durchführung der rvSU gemäß EndlSiUntV*, BGE, Deutschland (2022).
- [FLA18] D. Flamikova, V. Necas, Creation of Reference Biosphere Model for Safety Assessment of Deep Geological Repository, AIP Conf. Proceed. 1996, 020009 (2018).
- [HÄK19] S. Häkkinen, *Impurities in LWR fuel and structural materials*, VTT, Finnland (2019).

KIT – Die Forschungsuniversität in der Helmholtz-Gemeinschaft

This project has received funding from the European Union's Horizon 2020 research and innovation programme under grant agreement N°847593

www.kit.edu

5.6 Passive gamma and neutron measurements for characterization of spent nuclear fuel; V. Solans, UU; 31th Spent Fuel Workshop; 19 – 21/10/2022

PASSIVE GAMMA AND NEUTRON MEASUREMENTS FOR CHARACTERIZATION OF SPENT NUCLEAR FUEL.

Virginie SOLANS (Uppsala University)
Henrik Sjöstrand, Sophie Grape, Erik Branger (Uppsala University)
Alessandro Borella, Riccardo Rossa (SCK CEN)
Peter Schillebeeckx (JRC), Anders Sjöland (SKB & Lund University)

This project has received funding from the European Union's Horizon 2020 research and innovation programme 2014-2018 under grant agreement N°847593

September 2022 IAEA CRP 1

EURAD GOALS

- **In deep geological repositories, spent nuclear fuel needs to be characterized:**
  - Reactivity
  - Decay heat
  - Gamma's and neutron's dose
  - Safeguards parameters

- **Before encapsulation the fuel parameters need to be determined**
  - calculated by the state of the art codes
    - emphasis on uncertainties
  - verify (update) with experimental measurements.
- **Experimental mesurements:**
  - Calorimetric measurements
  - **Gamma-ray scans**
  - **Neutron measurements**

2

GOALS

Ā **Neutron measurements (DDSI)**

Ā Predict BU and IE

Ā **Gamma measurements**

Ā Cs-137, Cs-134/Cs-137, Eu-154/Cs-137 -> BU indicators, verify predicted isotopic composition

A neutron and a gamma measurement techniques are planned to be used for all SNFs at the encapsulation plant in Sweden

SKB50

- Set of 25 BWR and 25 PWR assemblies
- Used in Swedish reactors
- Various burnup, initial enrichment, cooling time,manufacturers
- Gamma scans
- Calorimetric measurements
- Neutron measurements
- Chosen around 2013-2014

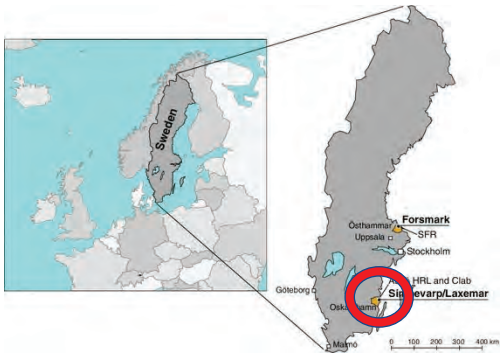

Image reference: Andersson, J., Skagius, K., Winberg, A. *et al.* Site-descriptive modelling for a final repository for spent nuclear fuel in Sweden. *Environ Earth Sci* **69,** 1045–1060 (2013). https://doi.org/10.1007/s12665-013-2226-1

DIFFERENTIAL DIE-AWAY SELF INTERROGATION INSTRUMENT (DDSI)

- Passive instrument developed and built in LANL
- Use neutron from Cm244 to interrogate the assembly
- Detect neutrons in coincidence (Rossi-alpha distribution)

- 56 ^{3}He tubes detect thermal neutrons
- Polyethylene to slow down neutrons
- Lead to reduce gamma-ray dose rate

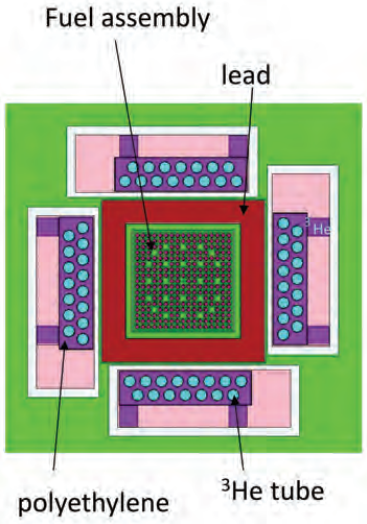

Image courtesy of Li Balkeståhl

ROSSI-ALPHA DISTRIBUTION (RAD)

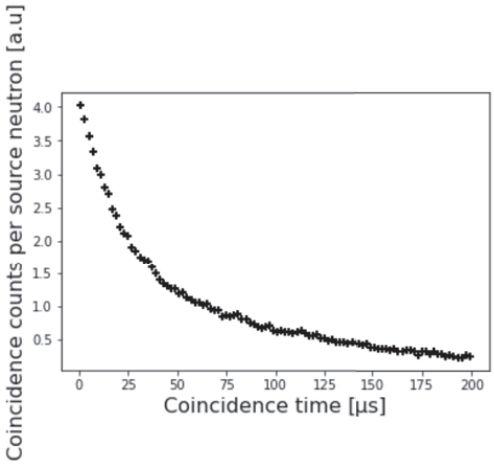

Output of the DDSI:

- Rossi-alpha distribution (RAD) describing neutrons detected in coincidence
- Total number of neutrons detected

DOUBLE EXPONENTIAL

- **A fast and a slow component**
- **Fast is not only direct detection or fast multiplication**
- **Slow is neutrons that have time to thermalized before fission**

$$RAD_{double}(t) = A_{fast} \cdot exp(-\tau_{fast} t) + A_{slow} \cdot exp(-\tau_{slow} t)$$

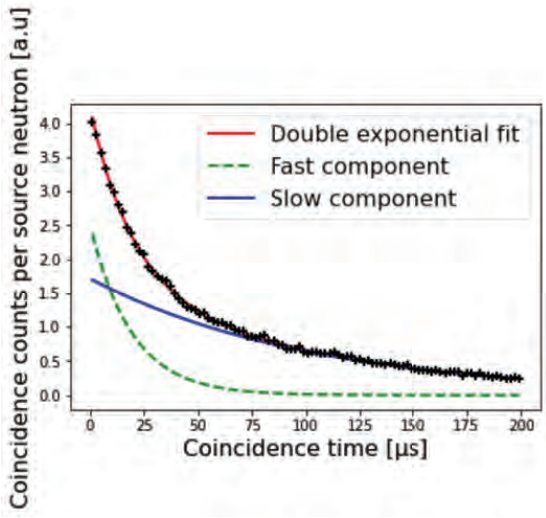

Increase in **absorbers decrease** the fission chain ⟶ **lower** amplitudes and a **shorter** slow component

Increase in **fissile content increase** the fission chain ⟶ **larger** amplitudes and a **longer** slow component

TAU FAST VERSUS TAU SLOW

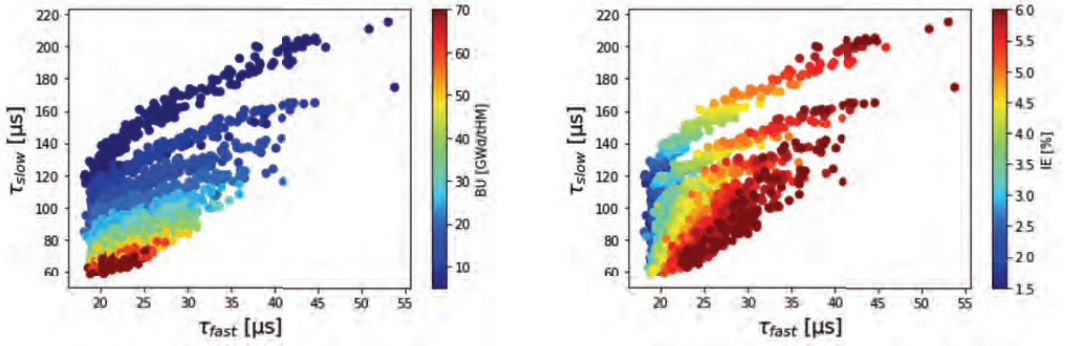

Indication that there is more information

Same data point with different colouring indicating BU or IE

MODEL

Ã **Use a KNN model**

- Ã Trained on the simulated dataset
- Ã Tested on the simulated dataset and the experimental data

Input:
Ã τ_{fast}
Ã τ_{slow}
Ã Ratio amplitude

Output:
Ã IE
Ã BU

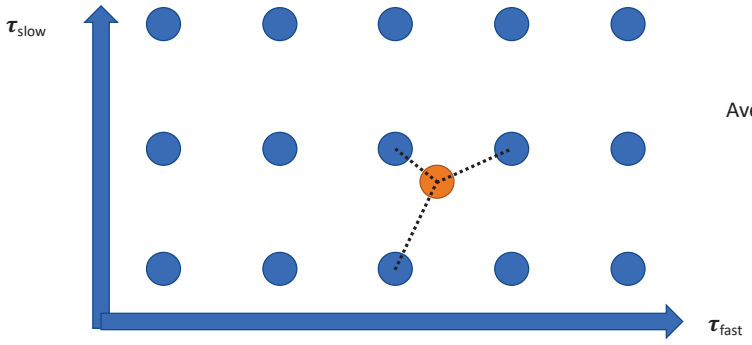

Average of the 3 closet neighbours

RESULTS

RMSE	BU [GWd/tHM]	IE [%]
Test set simulation	4.51	0.284
Experimental after KNN	11.86	0. 963
Experimental after bias correction	2.65	0.324

GAMMA MEASUREMENTS

Date Event

DIFFERENT CAMPAIGNS

- **Campaign 1**
  - Done in 2014
  - Static measurement
- **Campaign 2**
  - Done in 2014
  - Axial measurement
- **Campaign 3**
  - Done in 2016-2019
  - Axial measurement

Different detectors, attenuation plates, …

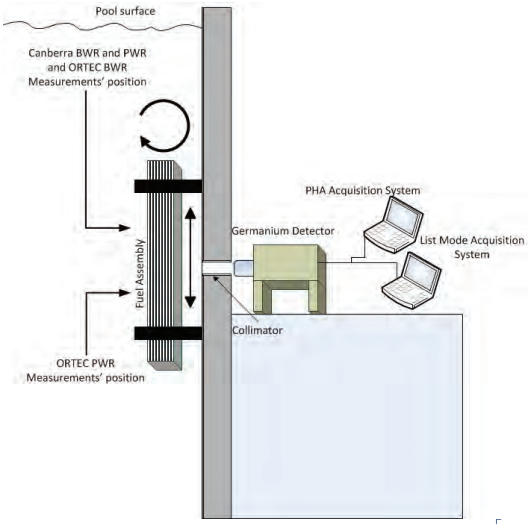

Image reference: S. Vaccaro, et Al., PWR and BWR spent fuel assembly gamma spectra measurements, Nuclear Instruments and Methods in Physics Research Section A: Accelerators, Spectrometers, Detectors and Associated Equipment, Volume 833,2016

INTRINSIC SELF-CALIBRATION

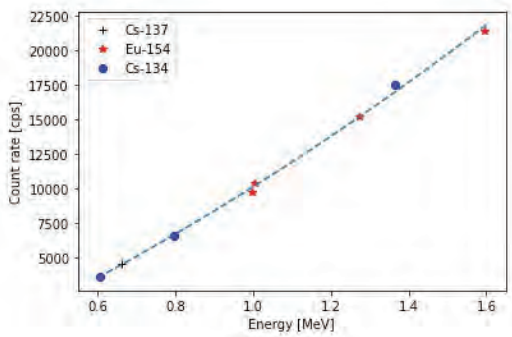

5 parameters to optimized : a, b, c, R_1 and R_2

$$\begin{cases} C_{Cs-137}/BR_{Cs-137} = (a \cdot E^2 + b \cdot E + c) \\ C_{Es-154}/BR_{Eu-154} = (a \cdot E^2 + b \cdot E + c) \cdot R_1 \\ C_{Cs-134}/BR_{Cs-134} = (a \cdot E^2 + b \cdot E + c) \cdot R_2 \end{cases}$$

RESULTS – SELF CALIBRATION

- **Even if the measurement conditions were different between the campaigns, mean deviation between campaigns obtained were:**
- **With self-calibration**
  - 2.3% for Eu-154/Cs-137
  - 1.9% for Cs-134/Cs-137

  } High reproducibility!
- **Without self-calibration**
  - 1.4% for Cs-137
  - 8.1% for Eu-154/Cs-137
  - 4.0% for Cs-134/Cs-137

RESULTS - REPRODUCIBILITY

- **Standard deviation of the best determined peak:**
  - The standard deviation in the inter-campaign reproducibility for the best-determined gamma peaks is between 2 and 3%.

CONCLUSION

Neutron measurement:

- Only 17x17 PWRs assemblies
- Rossi alpha distribution from the DDSI instrument has been analysed with a double exponential fit
- BU and IE are predicted using a *k*NN algorithm

Gamma measurement:

- HPGe detectors
- Intrinsic self calibration for the experimental gamma measurements applied to the SKB-50
- Reproducibility of the SKB50 measurement campaigns has been investigated between 1.4 to 2.3 %
- The standard deviation in the inter-campaign reproducibility for the best-determined gamma peaks is between 2 and 3%.

APPENDIX

EXPERIMENTAL RESULTS

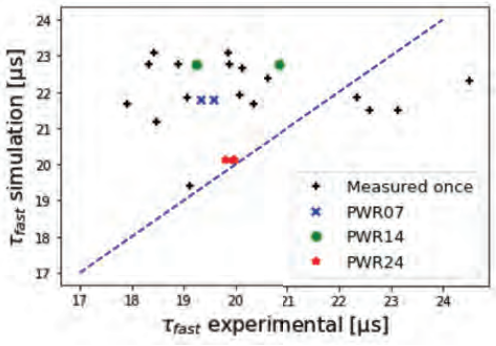

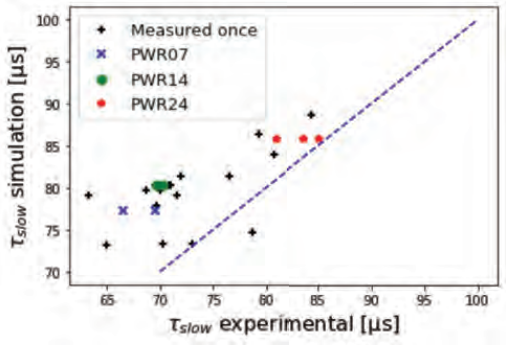

Dotted line is the unity line

RESULTS

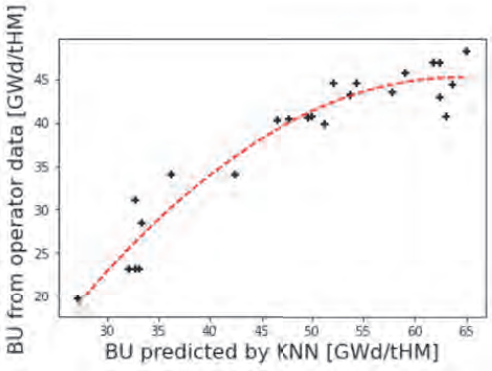

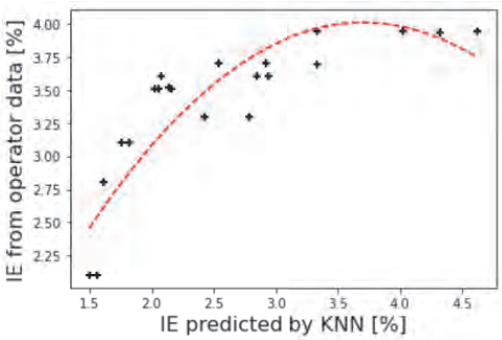

RESULTS

RMSE	BU [GWd/tHM]	IE [%]
Test set simulation	4.51	0.284
Experimental After KNN	11.86	0. 963
Experimental After fit	2.65	0.324
Simulated set After fit	2.69	0.104

5.7 Characterisation of spent nuclear fuel for a typical PWR; G. Žerovnik, JSI; 31th Spent Fuel Workshop; 19 – 21/10/2022

Characterisation of spent nuclear fuel for a typical PWR

Žerovnik, G.[1,*], Cabezas, M.[2], Čalič, D.[1], Fiorito, L.[2], Kromar, M.[1], Romojaro, P.[2], Schillebeeckx, P.[3] and Stankovskiy, A.[2]

[1] Jožef Stefan Institute (JSI). Ljubljana, Slovenia

[2] Belgian Nuclear Research Centre (SCK CEN). Mol, Belgium

[3] European Commission, Joint Research Centre Geel (JRC Geel). Geel, Belgium

* gasper.zerovnik@ijs.si

Overview

- Motivation
- Main contributors to NDA observables
- Depletion code comparison
- Sensitivity/uncertainty analysis
- Neutron emission measurements
- Conclusions

Spent Nuclear Fuel (SNF) storage or disposal

A **safe**, **secure**, **ecological** and **economic** storage and final disposal requires that **SNF** is **characterised** for the main observables of interest:

- Decay heat
- Neutron emission
- γ-ray emission
- Reactivity

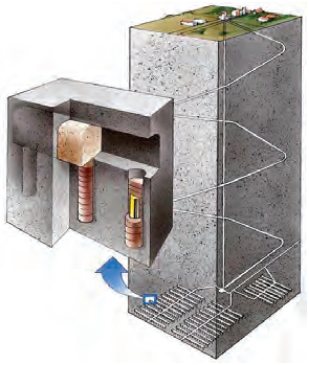

Research funded by EU project EURAD

Decay heat of SNF: main contributing nuclides

Decay heat rate: $H(t) = \sum_j H_j(t)$

- 1 a ≤ t_c ≤ 10 a
  - **^{144}Ce / ^{144}Pr**
  - **^{106}Ru / ^{106}Rh**
  - **^{134}Cs**
  - ^{90}Sr / ^{90}Y & ^{137}Cs / ^{137m}Ba
- 10 a ≤ t_c ≤ 100 a
  - **^{90}Sr / ^{90}Y & ^{137}Cs / ^{137m}Ba**
  - ^{238}Pu
  - ^{241}Am
  - ^{244}Cm
- 100 a ≤ t_c
  - **^{241}Am**
  - ^{238}Pu
  - ^{239,241}Pu

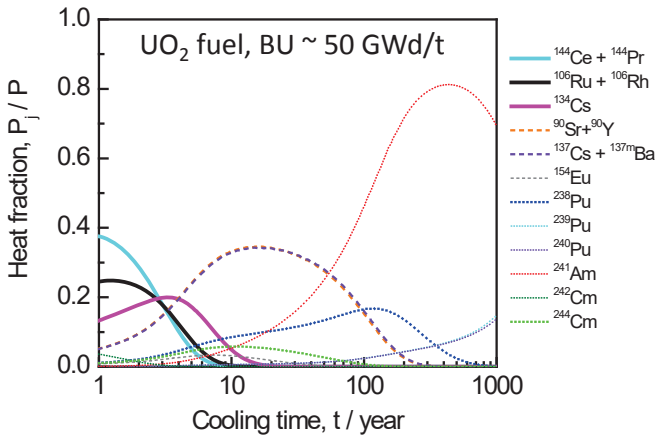

γ-ray emission by SNF: main contributing nuclides

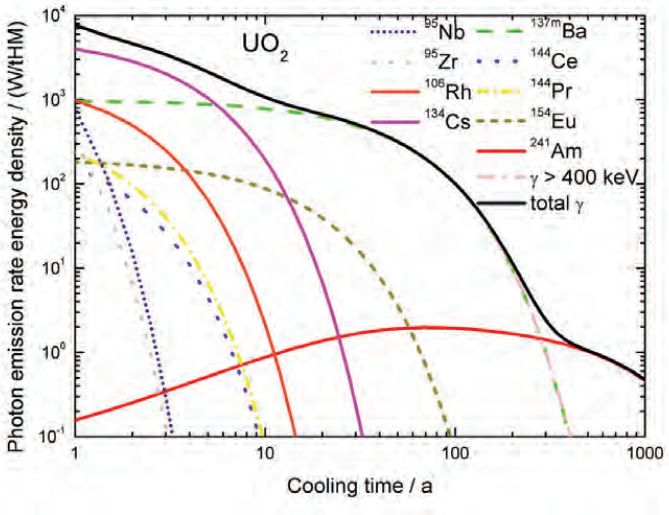

Photon emission rate energy density:

$$H_\gamma(t) = \sum_j H_{\gamma,j}(t) = \sum_j N_j(t)\,\lambda_j E_{\gamma,j}$$

= Contribution of γ-rays to decay heat

- 1 a ≤ *t* ≤ 10 a
  - **^{134}Cs**
  - ^{137}Cs / **^{137m}Ba**
  - ^{106}Ru / **^{106}Rh**
- 10 a ≤ *t* ≤ 300 a
  - ^{137}Cs / **^{137m}Ba**
  - **^{154}Eu**
  - ^{241}Am
- 300 a ≤ *t*
  - **^{241}Am**
  - ^{137}Cs / ^{137m}Ba

Neutron emission of SNF: main contributing nuclides

Neutron emission rate:

$$S_n(t) = \sum_j S_{n,j}(t)$$

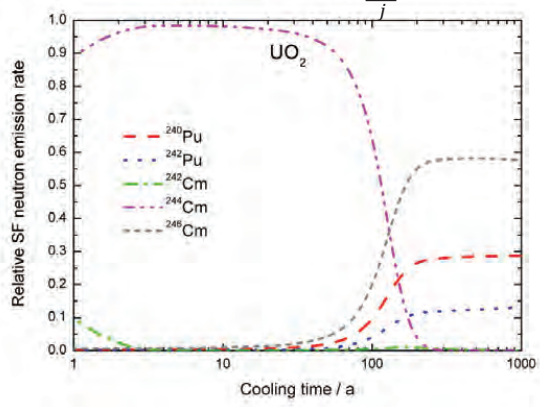

Contribution from SF dominating!

- for cooling time < 100 a, (α ,n) rate at least 10× lower than SF n. emission rate

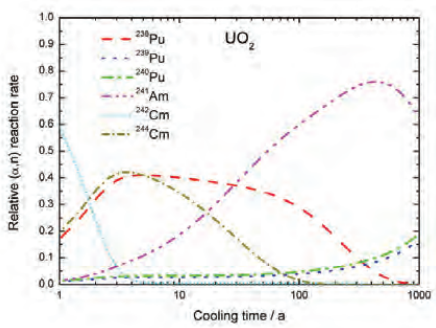

$S_n(t)$ ⇒ **sensitive to ^{244}Cm production**

Code comparison: definition of the study case

2D PWR 17×17, reflective boundary conditions. Zircaloy-4, 4% enriched UO_2 fuel, 4 × 300 d fuel cycles, cooling periods 30 d. Fuel radius 4.095 mm, clad inner/outer radii 4.18/4.75 mm, rod pitch 12.6 mm.

Simplified operating conditions:

- Power levels 50, 50, 40 and 30 MW/tHM during each cycle.
- Coolant density 0.655 kg/cm^3, constant boron level 800 ppm.
- Fuel density (95% theoretical density): 10.4 g/cm^3.
- Constant *T*: fuel and gap: 900 K; coolant and cladding: 600 K.

Numerical approximations:

- 4 equi-volume radial depletion zones
- Time steps per cycle: 1 d, 10 d, 14 d, 3 × 25 d, 2 × 50 d.

Codes: Serpent (v2.1.29), Aleph2, SCALE/Polaris, DRAGON4

Nuclear data library: ENDF/B-VII.1

Code comparison: nuclide vector @ t_c = 5 a

Output: **nuclide vector** and derived quantities (observables of interest)

Code Nuclide	Serpent c_0/(g/tHM)	ALEPH2 c /(g/tHM)	$\Delta c/c_0$	SCALE c /(g/tHM)	$\Delta c/c_0$	Dragon c /(g/tHM)	$\Delta c/c_0$
^{90}Sr	678.56(2)	678.86	0.04%	675.43	-0.46%	679.08	0.08%
^{134}Cs	43.86(2)	43.68	-0.43%	41.11	-6.28%	43.64	-0.51%
^{137}Cs	1638.0(0)	1640.2	0.13%	1643.2	0.32%	1639.8	0.11%
^{235}U	7109.9(14)	7064.5	-0.64%	7283.3	2.44%	7119.6	0.14%
^{238}Pu	426.44(18)	426.55	0.03%	429.22	0.65%	434.35	1.85%
^{239}Pu	6747.4(18)	6786.5	0.58%	6947.2	2.96%	6825.4	1.16%
^{240}Pu	3065.2(13)	3044.1	-0.69%	2976.3	-2.90%	3056.1	-0.30%
^{241}Pu	1556.7(6)	1561.8	0.33%	1608.5	3.33%	1570.8	0.91%
^{242}Pu	970.92(30)	967.77	-0.32%	990.42	2.01%	963.26	-0.79%
^{241}Am	499.66(17)	499.79	0.03%	516.77	3.43%	503.06	0.68%
^{244}Cm	109.38(8)	108.80	-0.52%	102.37	-6.41%	106.86	-2.32%

DH sensitivity to operational parameters

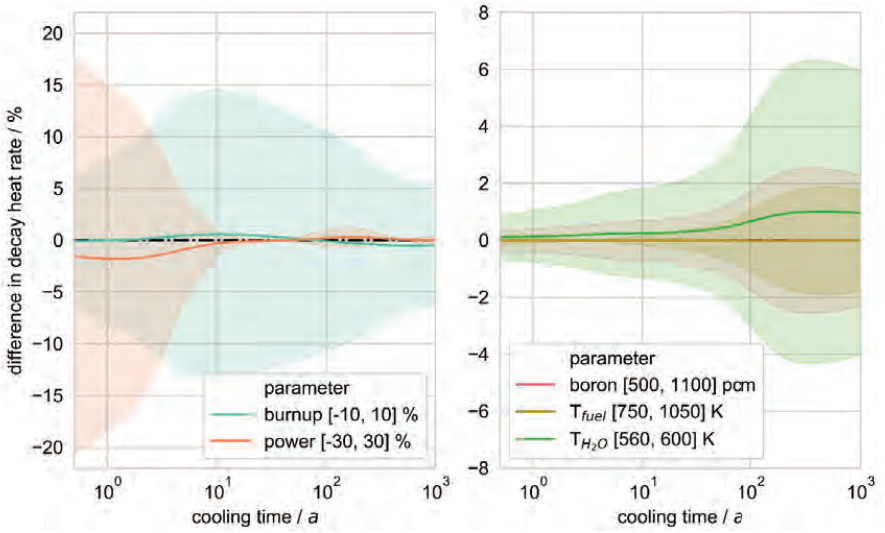

Sensitivity of NDA observables

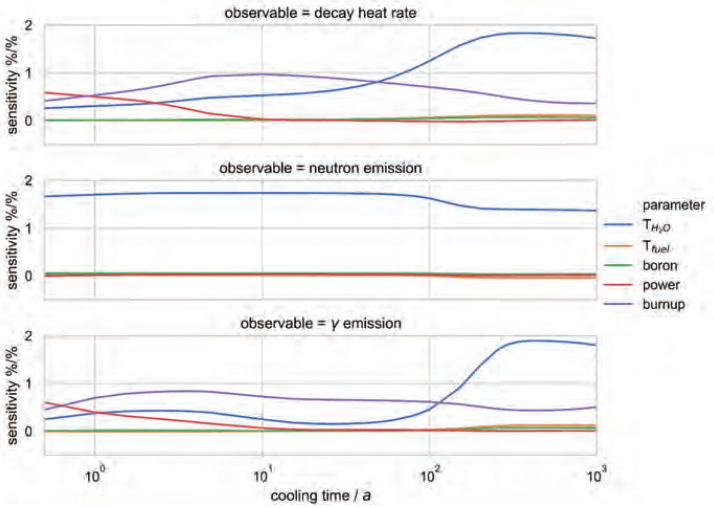

Prompt fission neutron detection

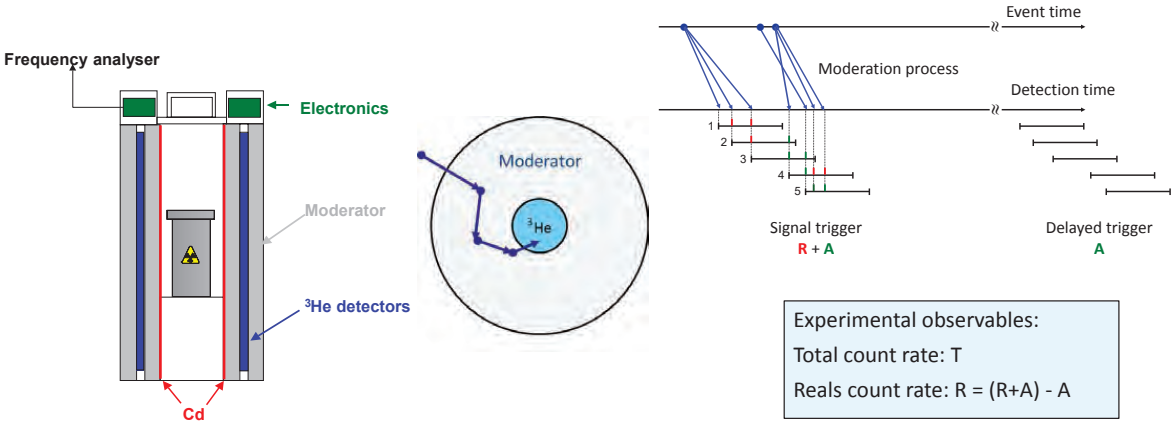

Experimental observables:
Total count rate: T
Reals count rate: R = (R+A) - A

Neutron correlation counting: Hage's point model

- Neutron emission rata due to (sf) : S_{sf}
- Relative (α,n) contribution : α
- Detection efficiency : ε
- Leakage multiplication : M
- Probability for a (n,f) reaction : p
- Factorial moments multiplicity distribution

$$\nu_{sf(j)} = \sum_{\nu=j}^{\infty} \binom{\nu}{j} P_{sf}(\nu) \qquad \nu_{nf(j)} = \sum_{\nu=j}^{\infty} \binom{\nu}{j} P_{nf}(\nu)$$

$$T = \varepsilon_{sf} \mathbf{S_{sf}} M [1 + \alpha]$$

$$R = \varepsilon_{sf}^2 f \mathbf{S_{sf}} M^2 \left[\frac{\nu_{sf(2)}}{\nu_{sf(1)}} + \frac{p \nu_{nf(2)}}{1 - p \nu_{nf(1)}} (1 + \alpha) \right]$$

W. Hage and D.M. Cifarelli, Nucl. Sci; Eng. 89 (1985) 159
W. Hage and D.M. Cifarelli, Nucl. Instr. Meth. A236 (1985) 165

Neutron output of SNF segment sample

Code	Library	(α,n) Method	(α,n) Library	S_{sf} / ($g^{-1}s^{-1}$)	S_α / ($g^{-1}s^{-1}$)	Calculation/Experiment S_{sf}	Calculation/Experiment $S_{\alpha n}$
SCALE	ENDF/B-VII.1	Y(α,n)		653	11.0	0.96	0.45
SERPENT(1)	ENDF/B-VII.1	Y(α,n)		689	14.3	1.01	0.58
SERPENT(2)	ENDF/B-VII.1	Y(α,n)		694	14.2	1.02	0.58
	ENDF/B-VIII.0	Y(α,n)		691	14.1	1.01	0.57
	JEFF-3.1.2	Y(α,n)		629	13.2	0.92	0.54
	JEFF-3.3	Y(α,n)		654	13.7	0.96	0.56
	JEFF-4T0	Y(α,n)		695	13.7	1.02	0.56
	JENDL-4.0			719	14.5	1.05	0.59
ALEPH28	ENDF/B-VIII.0	Y(α,n)		662	13.1	0.97	0.53
		σ(α,n)	TENDL2015		12.6		0.51
		σ(α,n)	JENDL_AN/500		10.6		0.43
	JEFF-3.3	Y(α,n		641	12.9	0.94	0.53
		σ(α,n)	TENDL2015		12.7		0.52
		σ(α,n)	JENDL_AN/500		10.5		0.43

All data normalised to ^{148}Nd inventory

REGAL sample (UO_2): NPP Tihange

experimental:

S_{sf} = 682 (10) g^{-1} s^{-1}

$S_{\alpha n}$ / S_{sf} = 0.036 (15)

⇒ influence
- nuclear data
- burnup code

Production of ^{244}Cm

Main production root of ^{244}Cm is a sequence of
- (n,γ) reactions (6)
- β^- decays (4)

$$n + {}^{238}_{92}\mathrm{U} \xrightarrow{(n,\gamma)} {}^{239}_{92}\mathrm{U} \xrightarrow{\beta^-} {}^{239}_{93}\mathrm{Np} + e^- + \bar{\nu}_e$$

$${}^{239}_{93}\mathrm{Np} \xrightarrow{\beta^-} {}^{239}_{94}\mathrm{Pu} + e^- + \bar{\nu}_e$$

$$n + {}^{239}_{94}\mathrm{Pu} \xrightarrow{(n,\gamma)} {}^{240}_{94}\mathrm{Pu}$$

$$n + {}^{240}_{94}\mathrm{Pu} \xrightarrow{(n,\gamma)} {}^{241}_{94}\mathrm{Pu}$$

$$n + {}^{241}_{94}\mathrm{Pu} \xrightarrow{(n,\gamma)} {}^{242}_{94}\mathrm{Pu}$$

$$n + {}^{242}_{94}\mathrm{Pu} \xrightarrow{(n,\gamma)} {}^{243}_{94}\mathrm{Pu} \xrightarrow{\beta^-} {}^{243}_{95}\mathrm{Am} + e^- + \bar{\nu}_e$$

$$n + {}^{243}_{95}\mathrm{Am} \xrightarrow{(n,\gamma)} {}^{244}_{95}\mathrm{Am} \xrightarrow{\beta^-} {}^{244}_{96}\mathrm{Cm} + e^- + \bar{\nu}_e$$

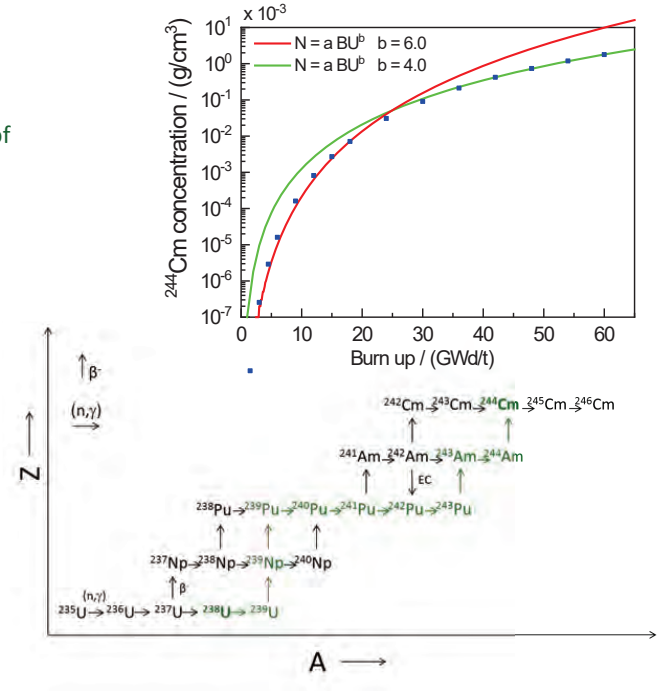

Production of Cs isotopes

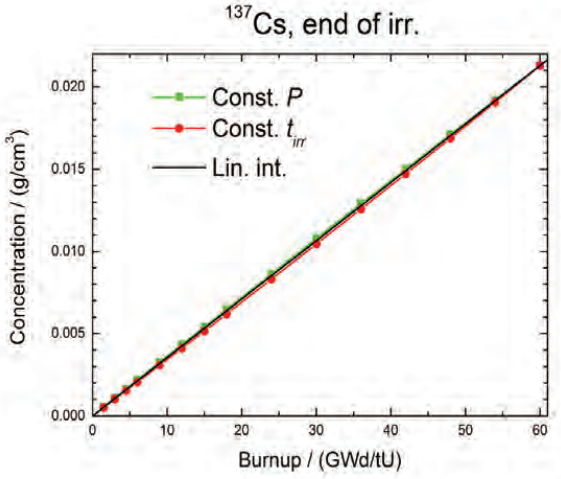

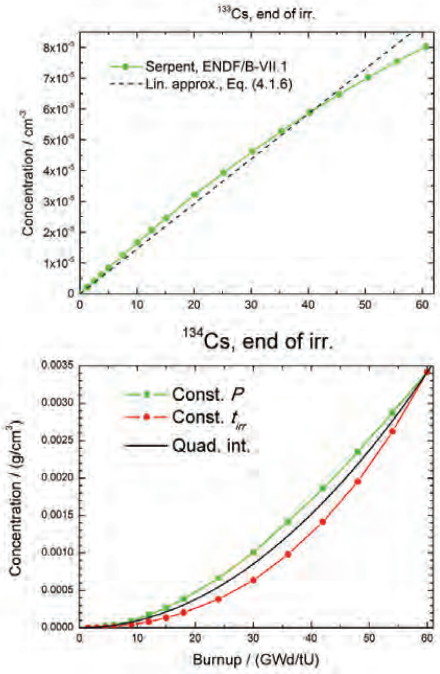

Conclusions

- NDA: powerful tool for SNF characterisation
- Few nuclides contributing to NDA observables at a fixed cooling time
- NDA observables are very sensitive to moderator temperature (density)
- Both deterministic and stochastic codes give consistent results for SNF
- Importance of nuclear data and neutron detection for SNF characterisation
- BU/irradiation time dependence of some nuclides described by simple analytical functions

5.8 Impact of Some 3-D Modelling Effects on the Spent Fuel Characterization; 31th Spent Fuel Workshop; 19 – 21/10/2022

Impact of Some 3-D Modelling Effects on the Spent Fuel Characterization

Marjan Kromar, Dušan Čalič

„Jožef Stefan“ Institute, Slovenia

31st Spent Fuel Workshop

Barcelona, October 19-21, 2022

Content

- Introduction/motivation
- 3-D case
- Impact of the fuel grids
- Fuel segmentation – real case
- Conclusions

Introduction / motivation

- Spent fuel characterization:
  - ➢ Reactor core simulators such as VERA-CS and CASMO5/SIMULATE/SNF, where detail observables distributions are obtained directly from the 3-D reactor core depletion.
  - ➢ Codes capable of specific 2-D or 3-D depletion on the fuel assembly level, such as TRITON/NEWT from the SCALE package or the Monte Carlo code Serpent2.

Introduction / motivation

- The first approach is more straightforward, but requires significant computer resources.
- For industrial applications, the second approach is more commonly used.
- In this approach, the fuel assemblies are divided into few independent regions (domains), which leads to additional uncertainties resulting from this process.
  - Spectral end-effects are not accounted for.
  - In domains the average fuel input parameters such as the fuel burnup, temperature, moderator density, etc. are used.
  - However, characterization observables (decay heat) do not depend linearly on the input parameters. Therefore, the segmentation of the fuel has a noticeable effect on the accuracy of the whole process.

Introduction / motivation

NPP Krško, Westinghouse 2-loop PWR, 16×16 fuel

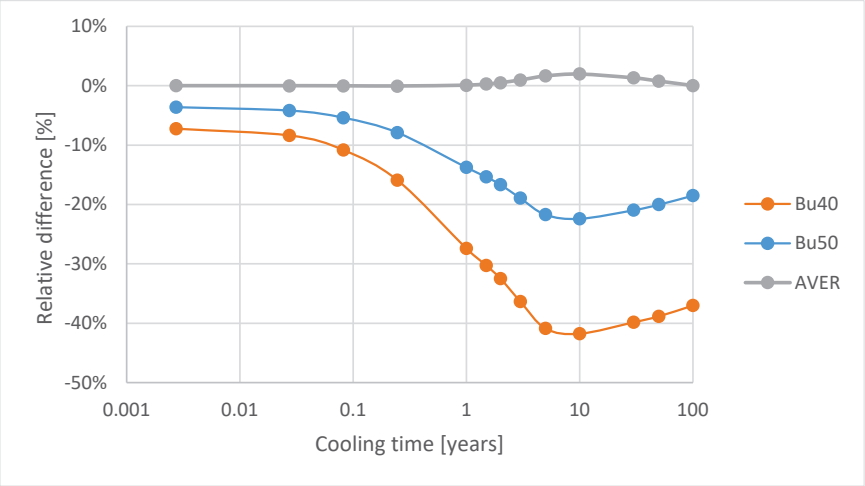

Impact of the fuel burnup on the decay heat
(relative difference to the 60 MWd/kgU, averaging process)

Introduction / motivation

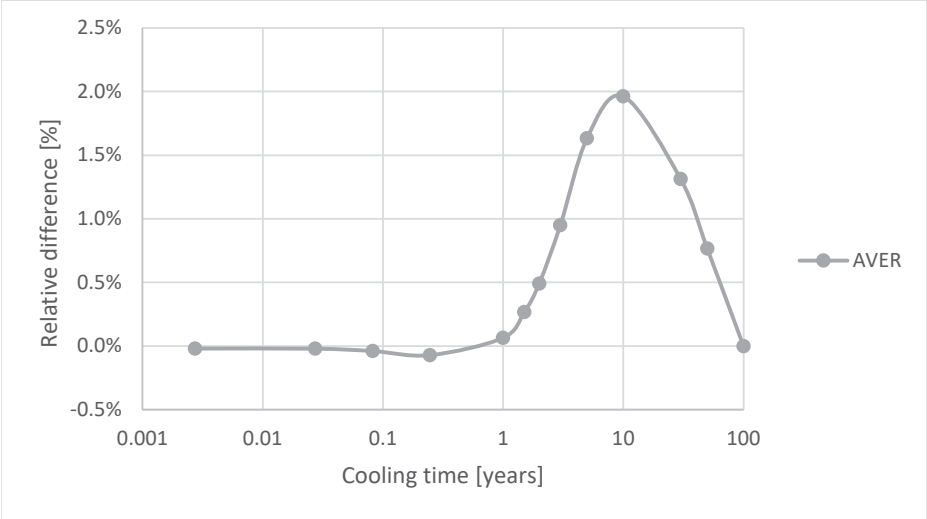

Deficiency of the ±10 MWd/kgU averaging process

3-D case

7/21

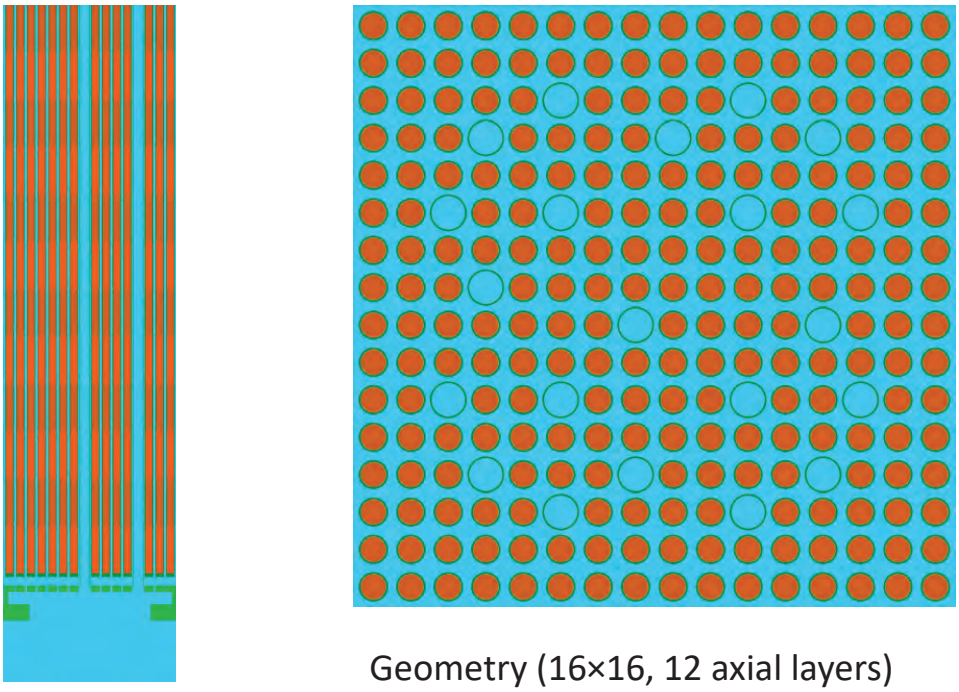

Geometry (16×16, 12 axial layers)

3-D case

8/21

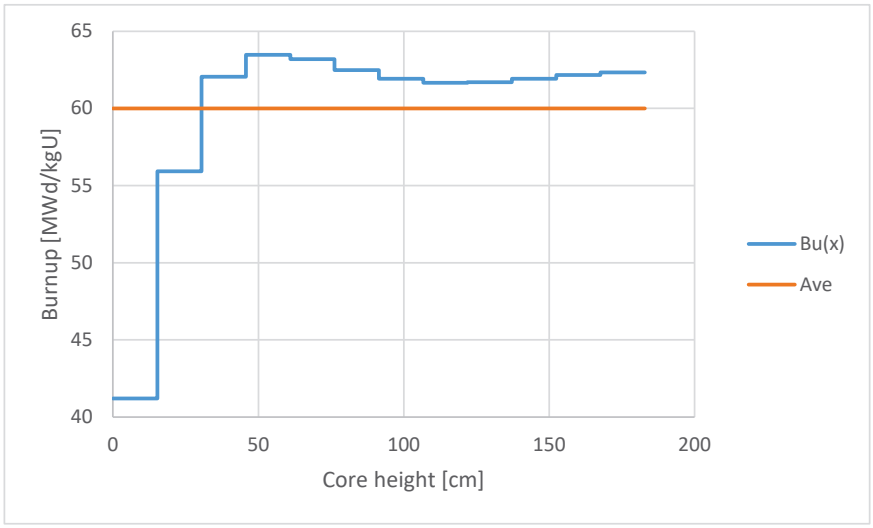

Burnup profile after irradiation of 60 MWd/kgU at averaged HFP conditions

3-D case

9/21

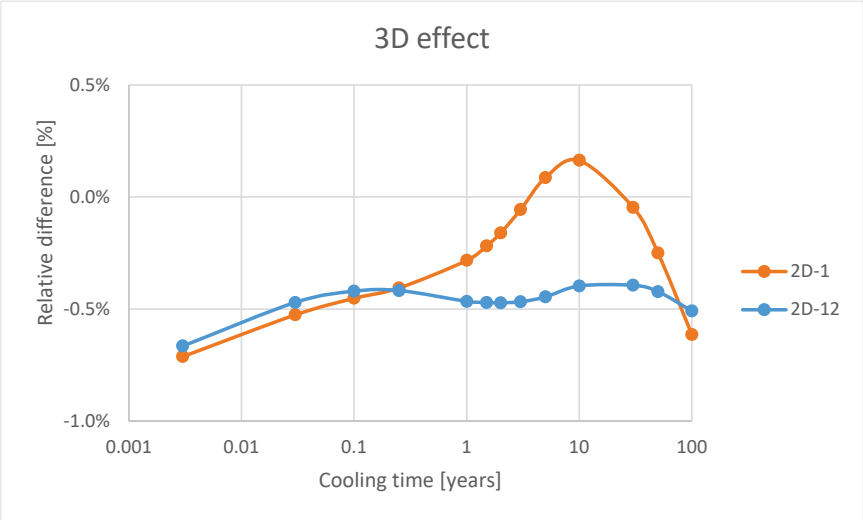

Decay heat relative difference (3-D vs. various 2-D)

3-D case

10/21

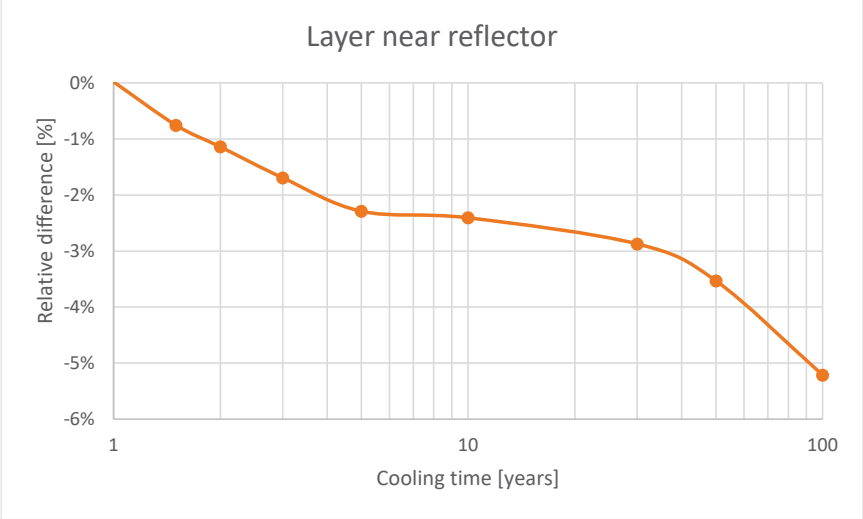

Decay heat relative difference in the layer closest to the axial reflector (3-D vs. 2-D)

Grid impact

- The effect of the NPP Krško Inconel-718 grids on the decay heat was investigated

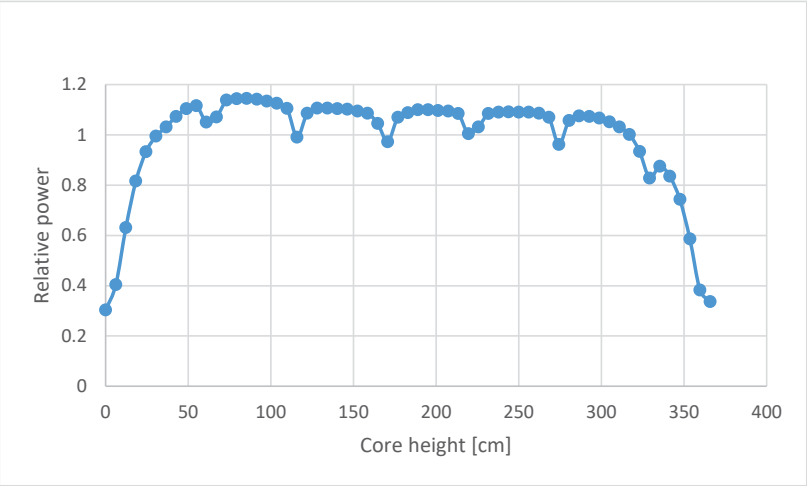

Effect of the grids on the power distribution

Grid impact

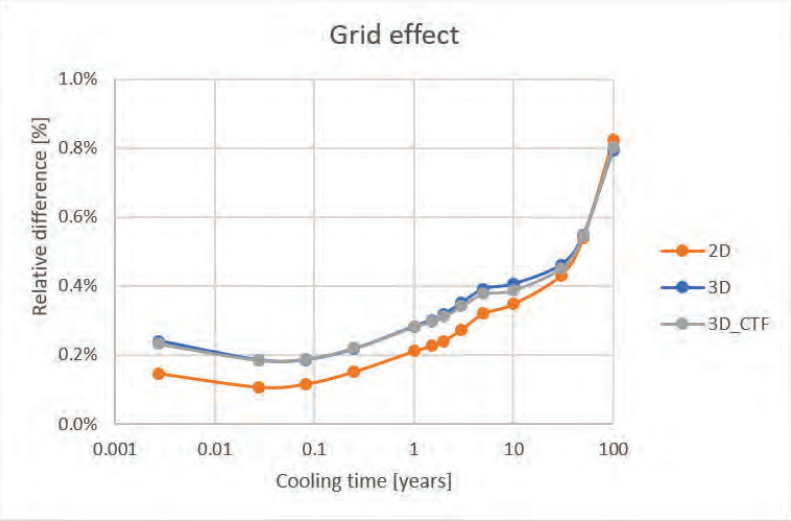

Effect of the grids on the decay heat

Grid impact

13/21

- The total grid impact is less than 1 %.
- 2-D and 3-D approaches give very similar results confirming suitability of the axial smearing approximation.
- Impact of power feedback effects is negligible.

Fuel segmentation – real case

14/21

- NPP Krško fuel - ~1400 fuel assemblies
- Operational database (Bu, T, P …) available on 10 axial layers from CORD-2 simulator
- Relative thicknesses (1, 1, 2, 4, 4, 4, 4, 2, 1, 1), where the unit is 15,24 cm (6 inch)
- The most accurate approach would be to take all 10 axial regions treated in FA database explicitly.
- However, such approach is time consuming. It would take more than 3 years of the CPU time to calculate 1400 FAs with the TRITON/NEWT sequence. Even ORIGAMI would require several days of calculation.
- Some kind of homogenization is therefore necessary.

Fuel segmentation – real case

- Fuel segmentation process should correctly represent axial profiles.
- It seems natural to explore axial blankets first, since there are large material heterogeneities and large flux gradients present.
- To get a proper feeling, a few typical cases have been evaluated:
  - A – standard FA without axial blankets (cycles 1-7)
  - B – FA with natural uranium axial blankets (cycles 7-16)
  - C – FA with slightly enriched annular axial blankets (from cycle 16 onward)

Fuel segmentation – real case

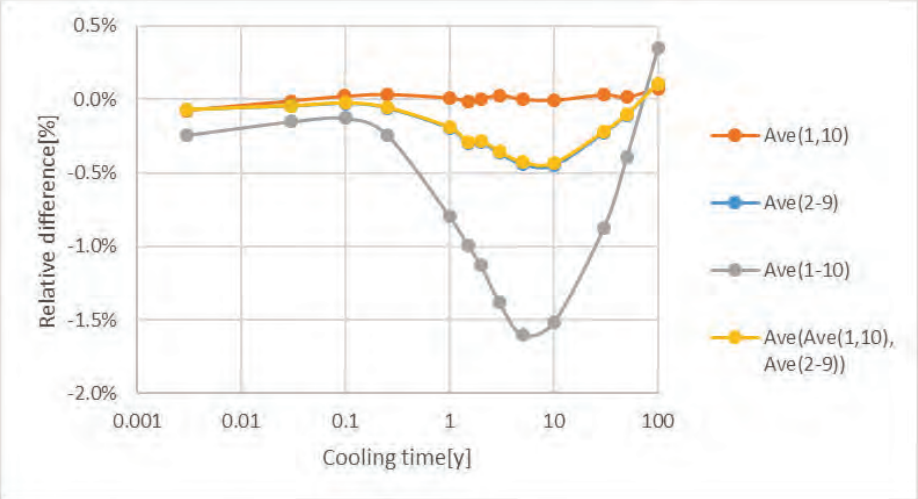

Impact of the homogenization on the decay heat – case A

Fuel segmentation – real case

17/21

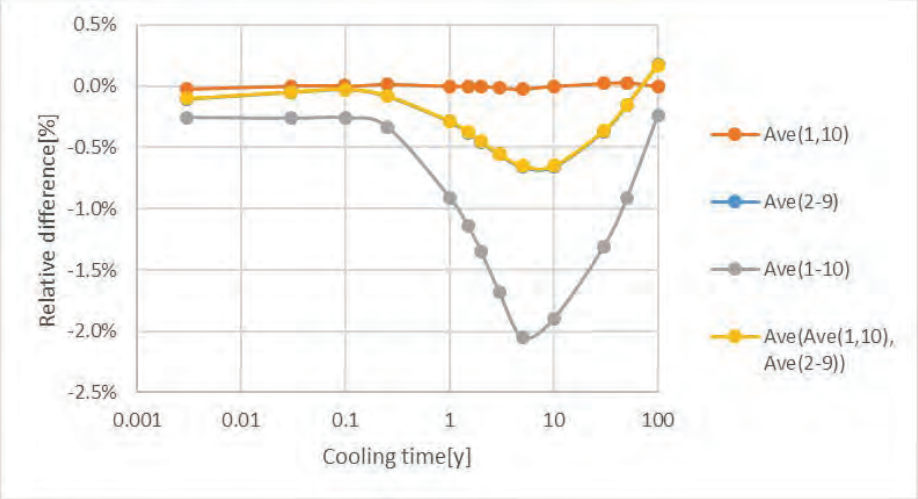

Impact of the homogenization on the decay heat – case B

Fuel segmentation – real case

18/21

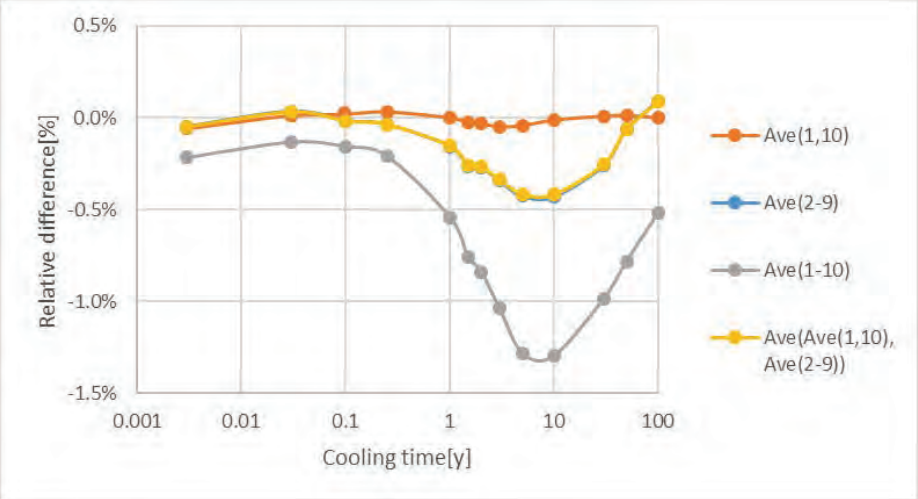

Impact of the homogenization on the decay heat – case C

Conclusion

- Differences between 3-D and 2-D computational models were evaluated.
- Sufficiently fine fuel segmentation can preclude discrepancies coming from the averaging process.
- To properly account spectral end-effects 3-D approach is needed.
- Impact of the Inconel grids can be covered by the material smearing in axial direction.
- A few FA cases based on the real data have been analyzed to demonstrate reasonable axial discretization.

Acknowledgements

- Authors acknowledge the financial support from the Slovenian Research Agency (research core funding No. P2-0073).
- Some of the underlying research was performed within the Euratom Research and Training Program under Grant Agreement No. 847593 (EURAD project).

Thank you for your attention!

Questions?

5.9 Burnup credit application in CONSTOR SNF cask criticality analysis for RBMK-1500 fuel; R. Plukiene, FTMC; 31th Spent Fuel Workshop; 19 – 21/10/2022

FIZINIŲ IR TECHNOLOGIJOS MOKSLŲ CENTRAS

Burnup credit application in CONSTOR SNF cask criticality analysis for RBMK-1500 fuel

V. Barkauskas, **R. Plukienė** and A. Plukis

Center for Physical Sciences and Technology,
Department of Nuclear Research,
Vilnius, Lithuania

31st Spent Fuel Workshop | 19-21 October 2022

Content

FIZINIŲ IR TECHNOLOGIJOS MOKSLŲ CENTRAS

- Current status - Lithuania
- Criticality safety and Burnup credit application
- Modeling of RBMK fuel composition
- CONSTOR RBMK-1500/M2 cask k_{eff} calculations
- Results and burnup credit application possibilities

31st Spent Fuel Workshop | 19-21 October 2022

Current status: Ignalina NPP

Location: Far north-east corner of Lithuania. Immediately bordering Latvia and Belarus

Design: 2 × RBMK-1500 water-cooled, graphite-moderated channel-type power reactors

Capacity: Intended to supply NW region of former USSR (not Lithuania). After independence, one unit could produce 80% of Lithuanian electricity demand

Operation:
Unit 1 commissioned Dec 1983 / closed Dec 2004
Unit 2 commissioned Aug 1987 / closed Dec 2009

https://am.lrv.lt/uploads/am/documents/files/INPP%2BDecom%2B2021-04-12eng.pdf

31st Spent Fuel Workshop | 19-21 October 2022

Current status: SNF

Spent nuclear fuel	Fuel Assemblies	21,571 item

- By now storage of SNF is realized at interim storage facility at Ignalina NPP site for 50 years:
  - ✓ #1 SNF storage contains 118 containers works from 1999;
  - ✓ #2 SNF storage facility for ~200 containers started at 2020 (146 stored already).

31st Spent Fuel Workshop | 19-21 October 2022

Current status: SNF storage casks

- 3 types of SNF storage casks (GNB (Germany)) are used:
  - ✓ CASTOR (metal)
  - ✓ CONSTOR (reinforced concrete)
  - ✓ New type CONSTOR RBMK-1500/M2 with 80% increased capacity for RBMK-1500 SNF

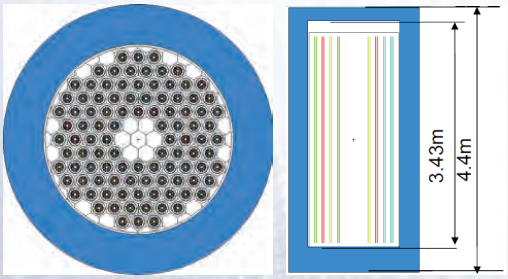

MCNP model of CASTOR container: 102 half-assemblies bundles

31st Spent Fuel Workshop | 19-21 October 2022

CONSTOR M2/RBMK-1500 cask

- transport and storage container CONSTOR M2/RBMK-1500 consist of: cylindrical basket 32M (stainless steal) and 454 mm thick ring basket (made of aluminum alloy)
- Modeling of accident scenario: H_2O in all cavities, FA standard (design) configuration.

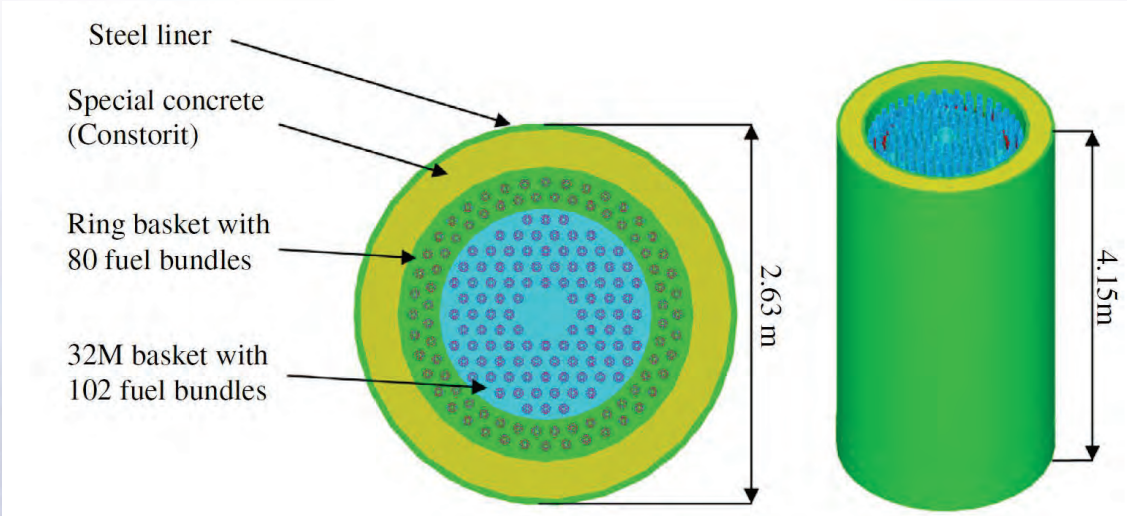

SCALE 6.1 model of CONSTOR® RBMK-1500/M2 SNF cask

31st Spent Fuel Workshop | 19-21 October 2022

Criticality safety

- According to the Lithuanian national regulations the k_{eff} shall not exceed 0.95 during normal operation and postulated accident scenarios.
- Goal : to ensure sub-criticality of system with fissile materials (k_{eff}<0.95)
- Fissile isotopes – ^{235}U, ^{239}Pu, ^{241}Pu, etc.
- Safety justifications are based on conservative assumption of fresh fuel
- In case of different SNF burnup, the conservatism may be too high -> the cost of storage systems increases
- Burn-up credit (BUC) approach calculations takes into account the reduced SNF reactivity due to depletion of fissile isotopes and accumulation of neutron absorbing isotopes during fuel burn-up

31st Spent Fuel Workshop | 19-21 October 2022

Example: Reactivity behavior in the GBC-32 cask as a function of cooling time for fuel with 4.0% ^{235}U initial enrichment and 40 GWd/MTU burnup

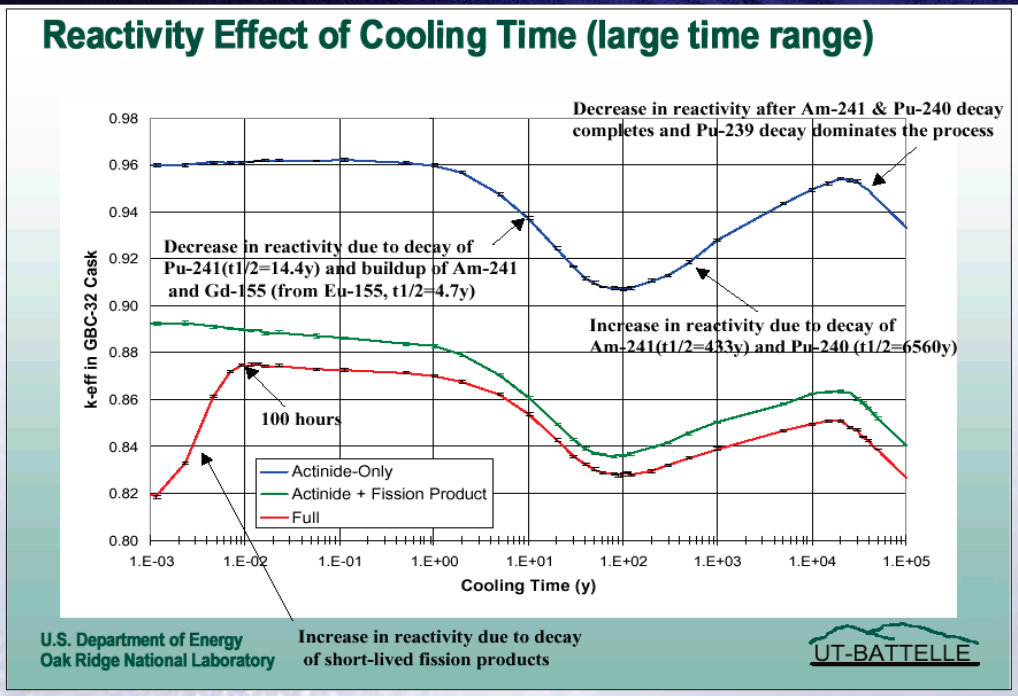

Ref. [NRC-2012-0100]

31st Spent Fuel Workshop | 19-21 October 2022

K_{eff} calculation assumptions

- SCALE6.1: STARBUCKS (ORIGEN-ARP, CENTRM, KENO VI, ENDF/B-VII.0 238 energy group data library),
- Mirror boundary conditions were applied for 2.64-2.64 4.52m cask surrounding cuboid.
- A triangular pitch of 125 mm between fuel bundles (centered in its position tube of 102 mm outer demeter with 2 mm thick wall).
- 2.0% and 2.8% ^{235}U enrichment RBMK fuel mixture composition and 0 (fresh fuel assumption) – 22.5 GWd/tU burn-up
- 5 years cooling time was used
- horizontal burn-up profile uniform but axial burn-up profile taken into account : "end-effect" – slightly higher criticality for the upper fuel bundle profile due to water density varying from 0.8 to 0.2 g/cm^3.
- uniform water density distribution from 0.1 to 1.0 g/cm^3
- conservative uniform temperature of 100^{o}C (conservative accident scenario)

31st Spent Fuel Workshop | 19-21 October 2022

K_{eff} evaluation for BUC

Ref.[IAEA-TECDOC-1241]

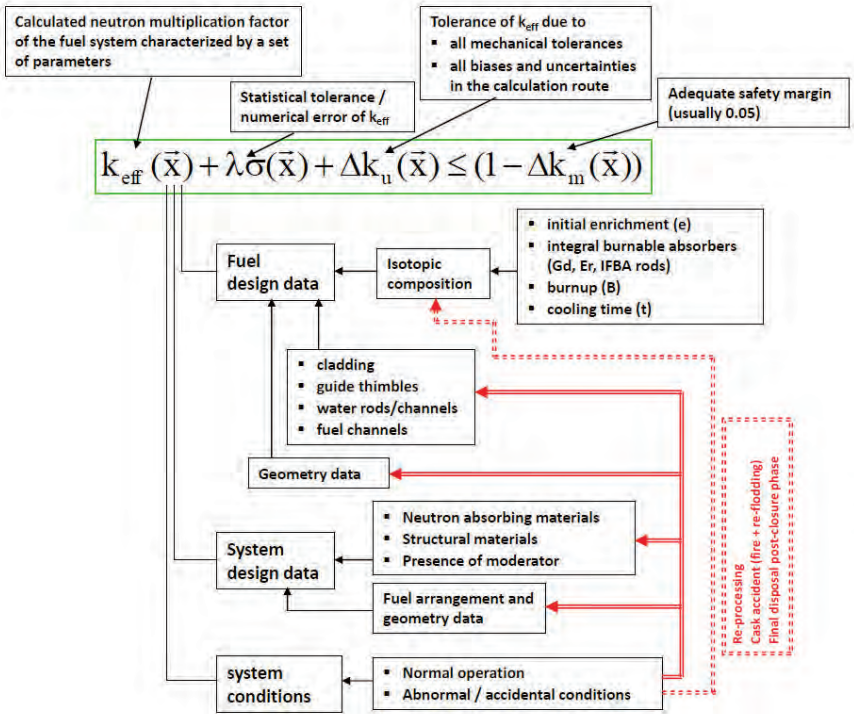

31st Spent Fuel Workshop | 19-21 October 2022

Burnup credit calculation

- Actinide-only approach: fuel with most important actinides ($^{234-236}$U, ^{238}U, $^{238-242}$Pu, $^{241-243}$Am, ^{237}Np) were included in keff calculation
- Fission product case for BUC additionally includes: ^{95}Mo, ^{99}Tc, ^{101}Ru, ^{103}Rh, ^{109}Ag, ^{133}Cs, ^{143}Nd, ^{145}Nd, ^{147}Sm, $^{149-152}$Sm, ^{153}Eu,^{155}Gd and $^{166-168}$Er, ^{170}Er.

31st Spent Fuel Workshop | 19-21 October 2022

RBMK SNF - Pre-generated ARP libraries for fast burn-up inventory modeling

- ~7 m length fuel assembly with 18 fuel elements
- 14 fuel assemblies and 2 control rods segment with infinitive lattice approach
- SCALE6.1:
  - TRITON with NEWT ir ORIGEN-S
  - ORIGEN-ARP (Automatic Rapid Processing)
  - ENDF/B-VII nuclear data library
  - One group cross-section libraries for non-erbium fuel with 2 % enrichment and 2.4 % (with 0.41 % mass of Er_2O_3), 2.6 % (0.5 % Er_2O_3) and 2.8 % (0.6 % Er_2O_3) enrichment fuel

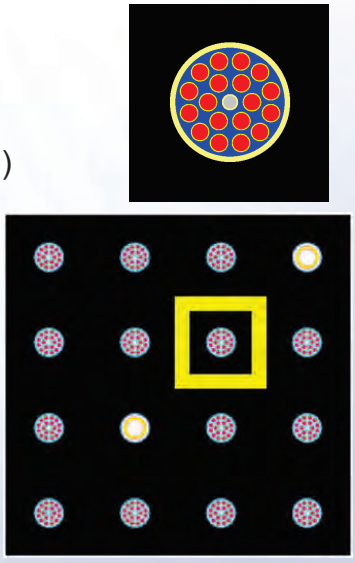

31st Spent Fuel Workshop | 19-21 October 2022

Validation of RBMK SNF one group cross-section libraries

Very few experimental data:

- KORENKOV, A. G., et al. Destructive Analysis Determination of Neutron Emission from Spent RBMK Fuel, Atomic Energy, 2002, Vol. 93, No. 4, p. 815-822 (only some of actinides present in 22 2% of samples)
- MAKAROVA, T. P., et al. Destructive Analysis of the Nuclide Composition of Spent Fuel of WWER-440, WWER-1000, and RBMK-1000 Reactors, Radiochemistry, 2008, Vol. 50, No. 4, p. 414-426. (2% enrichment fuel, only two burnup cases)

Modeling of RBMK fuel:

- Plukienė, R., et al., Numerical sensitivity study of irradiated nuclear fuel evolution in the RBMK reactor, Lithuanian journal of physics. ISSN 1648-8504. Vol. 49, no. 4 (2009), p. 461-469
- Šmaižys, A., et al. Numerical modelling of radionuclide inventory for RBMK irradiated nuclear fuel, Nuclear Engineering and Design, 2014, Vol. 277, p. 28–35.

Validation of nuclear data libraries (1)

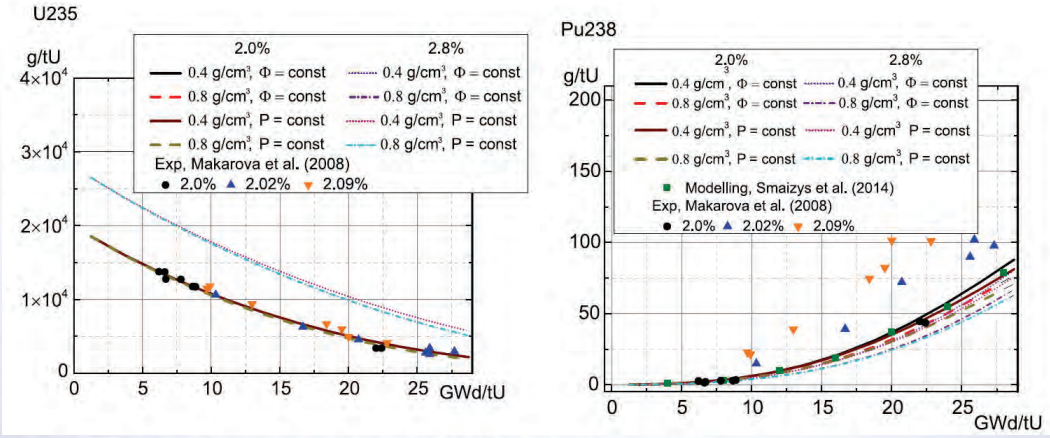

- The comparison shows an acceptable agreement between the values obtained using created one-group cross-section libraries and experimental data as well as point depletion calculations.
- The exception was observed only for ^{238}Pu, which was caused by the initial composition of nuclear fuel (most probably presence of ^{236}U the parent nuclide of ^{237}Np which is obtained through the activation)

Validation of nuclear data libraries (2)

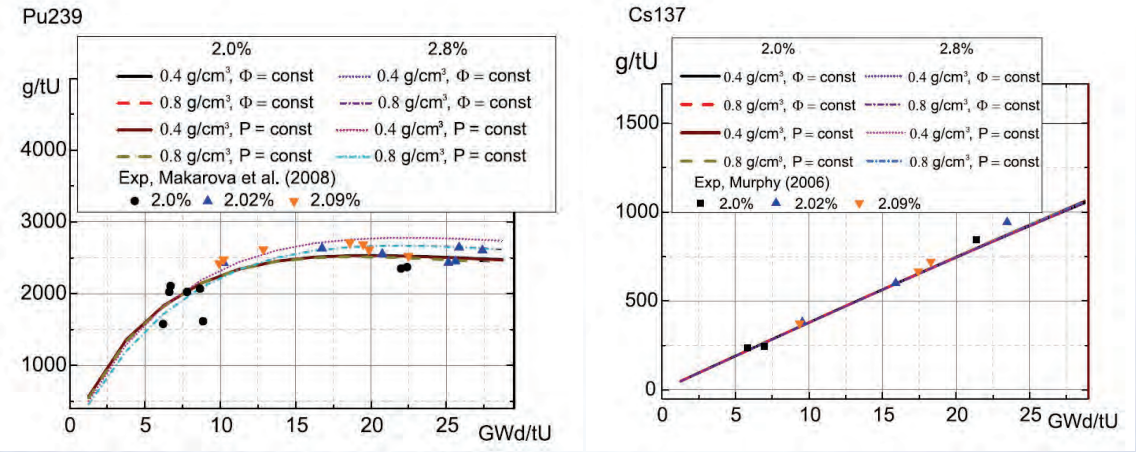

- Agreement of the experimental data and the calculated values is satisfactory for other plutonium isotopes – the difference between the experimental and calculated values is 5–6% for ^{239}Pu, 5–25% (the highest difference for low burn-up) for ^{240}Pu, 5–15% for ^{241}Pu and 5–19% for ^{242}Pu, as well as for FP (^{137}Cs).
- At the highest modelled burn-up (29 GWd/tU) the isotopic composition differences between 2 and 2.8% enrichment fuel burn-up for actinides important to BUC applications vary from 11 to 52%

k_{eff} as a function of water density in the CONSTOR® RBMK-1500/M2 storage cask (1)

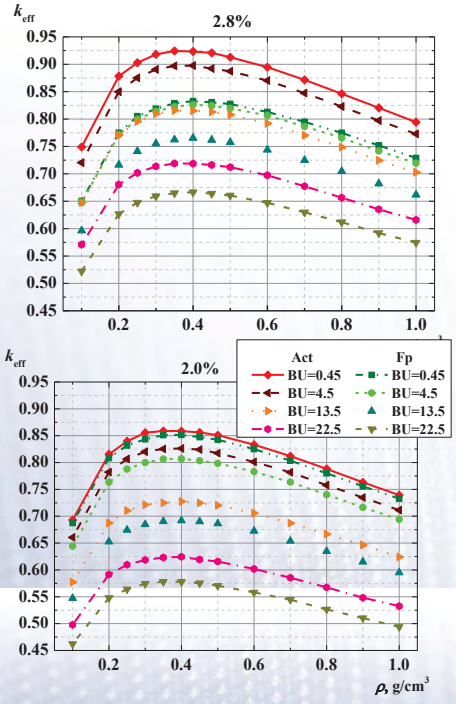

k_{eff} as a function of water density
inside SNF cask cavities
for various burn-up 2.8% and 2.0% enrichment fuel
taking into account
actinide-only (Act) and fission products (Fp)
including burnable absorber erbium

Most critical conditions region is identified:
0.3-0.5 g/cm^3 water density inside CONSTOR.

Neutron absorption rate (R) spectra inside CONSTOR® RBMK-1500/M2 storage cask (2)

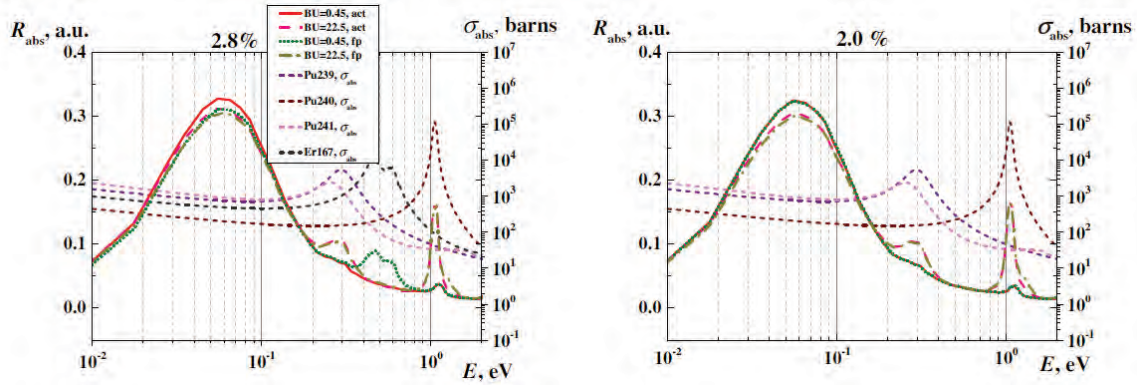

Neutron absorption rate (R ~Φ*σ_{abs}) spectra inside SNF cask in case of 0.35 g/cm^3 water density for 2.8% and 2.0% enrichment fuel. Pu neutron absorption cross sections on the right for information.

Most critical conditions: low burn-up (0.45 GWd/tU) SNF.

Isotopic composition differences for 2% and 2.8% enrichment SNF at CONSTOR® RBMK-1500/M2 storage cask (3)

Isotopic composition differences for actinides between 2% and 2.8% enrichment fuel at 29GWd/tU burn-up

Nuclide	$(N_{2.8}-N_{2.0})/N_{2.8}$
^{234}U	32%
^{236}U	23%
^{238}Pu	-28%
^{239}Pu	11%
^{240}Pu	-15%
^{241}Pu	11%
^{242}Pu	-36%
^{237}Np	15%
^{241}Am	-40%
^{243}Am	-52%
^{242}Cm	-27%
^{244}Cm	-60%

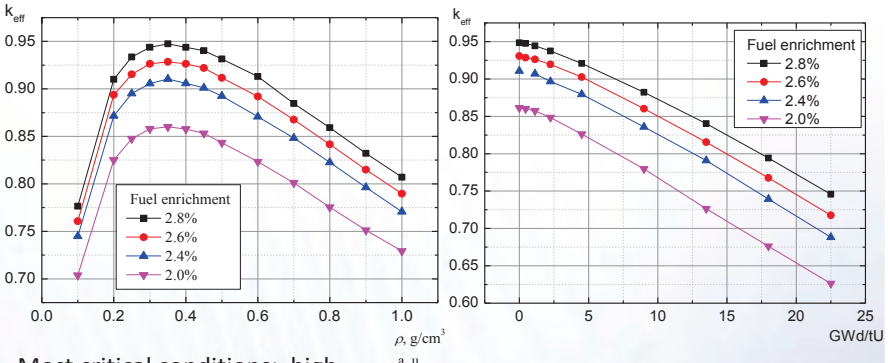

Most critical conditions: high enrichment (2.8%), low burn-up (0.45 GWd/tU) of SNF and 0.3-0.5 g/cm^3 water density.

Neutron spectra for 2.8% enrichment fuel at low 0.45 GWd/tU burn-up at different water density in the cask.

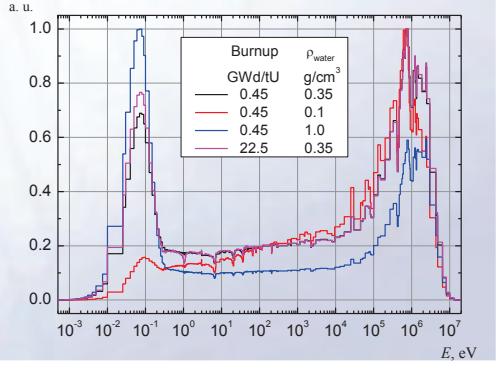

k_{eff} calculations of 2.8% enrichment RBMK-1500 SNF at CONSTOR® RBMK-1500/M2 storage cask (4)

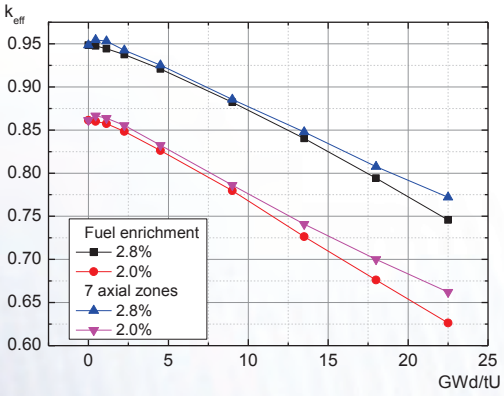

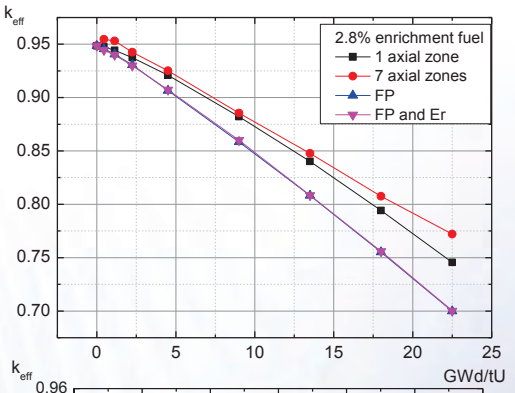

The marginal cases: less reactive 2.0% enrichment and most reactive case (2.8% enrichment, multiple (z=7) zones, actinide only case) was analyzed more exactly.

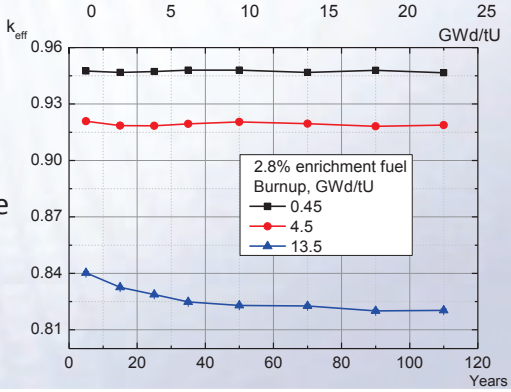

31st Spent Fuel Workshop | 19-21 October 2022

Conclusions

- Criticality calculations of CONSTOR® RBMK-1500/M2 storage cask were performed using pre-generated ORIGEN-ARP SNF libraries and STARBUCKS BUC evaluation tool from SCALE 6.1 code package.
- Worst condition k_{eff}=0.924±0.003 (>0.95) with 2.8% ^{235}U SNF enrichment using actinides only approach at 0.45GWd/tU. In case of FP and Er k_{eff} decreases due to ^{167}Er, which burns at higher burnups.
- k_{eff}=0.859 of 2.0% ^{235}U SNF enrichment fresh fuel is due to less fissile material.
- Non-uniform uranium depletion is responsible for end effect in RBMK-1500 SNF whereas build-up of plutonium has no significant effect.
- Most critical conditions region is identified: 0-3 GWd/tU burn-up fuel and 0.3-0.5 g/cm^3 water density inside SNF.

31st Spent Fuel Workshop | 19-21 October 2022

Thank you for attention!

ACNOWLEDGEMENTS

This work was performed as part of WP8 Spent Fuel Characterization and Evolution Until Disposal (SFC) of Euratom research and training programme 2018-2020 under grant agreement No 847593 to fulfill the objective to provide contributions to operational safety concepts for fuel handling at SNF packaging facilities by using state-of-the-art characterization techniques for spent nuclear fuel during its evolution from reactor unloading until disposal.

31st Spent Fuel Workshop | 19-21 October 2022

6. Participation to an Event other than a Conference or a Workshop

- Effect of modelling parameters on calculated PWR spent fuel observables; G. Žerovnik, JRC; Serpent User Meeting 2020; 29/10/2020
- Fuel properties characterisation and related uncertainty analysis: overview, status and planning; P. Schillebeeckx, JRC Geel; 1st research coordination meeting on the CRP on spent fuel characterisation; 06 - 10/12/2021
- Neutron resonance analysis and applications to material characterisation; P. Schillebeeckx, JRC Geel; LANL P/T Colloquium, April 2022; 28/04/2022
- Untersuchung des Radionuklidinventars und chemischer Wechselwirkungsprozesse an der Grenzfläche zwischen Kernbrennstoff und Zircaloy-Hüllrohr von bestrahlten LWR-Brennstoffproben; R. Dagan, T. König et al., KIT; BGZ Studierendentag; 05 – 06/05/2022
- SFC Task 2: Fuel properties characterisation and related uncertainty analysis (summary and status); P. Schillebeeckx, JRC Geel; IAEA CRP spent fuel characterization ; 22 – 23/09/2022
- Performance assessment and uncertainty evaluation of the clab calorimeter; P. Schillebeeckx, JRC Geel; WPNCS Subgroup 12 meeting; 01/12/2022

6.1 Effect of modelling parameters on calculated PWR spent fuel observables; G. Žerovnik, JRC; Serpent User Meeting 2020; 29/10/2020

Effect of modelling parameters on calculated PWR spent fuel observables

G. Žerovnik, D. Čalič, L. Fiorito, A. Hernandez Solis, B. Kos, M. Kromar, P. Romojaro, A. Stankovskiy

EC-JRC Geel, Retieseweg 111, B-2440 Geel
SCK•CEN, Boeretang 200, B-2400 Mol
Jožef Stefan Institute, Jamova cesta 39, SI-1000 Ljubljana

gasper.zerovnik@ec.europa.eu

Modelling uncertainties

- Modelling, computational, numerical?
- Uncertainties, biases, errors?
- Types of modelling uncertainties?

Modelling uncertainties: Monte Carlo vs. deterministic

Monte Carlo n. transport

- Continuous energy
- Continuous direction
- Continuous time (e.g. for n. kinetics)
- Space continuum (particle tracking)
- Counting statistics from n. history

Deterministic n. transport

- Energy intervals (multi-group)
- Solid angle discretization (S_n) or polynomial expansion (P_n)
- Discretization of the time variable
- Discretization of the spatial variables
- „Exact“ solution (except round-off)

sck cen

Modelling uncertainties: Monte Carlo vs. deterministic

Monte Carlo n. transport

- Continuous energy
- Continuous direction
- Continuous time (e.g. for n. kinetics)
- Space continuum (particle tracking)
- Counting statistics from n. history

Deterministic n. transport

- Energy intervals (multi-group)
- Solid angle discretization (S_n) or polynomial expansion (P_n)
- Discretization of the time variable
- Discretization of the spatial variables
- „Exact“ solution (except round-off)

- **Apart from counting statistics, are there any other souces of numerical error in continuous enegy MC particle transport codes?**

sck cen

Modelling uncertainties: Monte Carlo vs. deterministic

Monte Carlo n. transport

- Continuous energy
- Continuous direction
- Continuous time (e.g. for n. kinetics)
- Space continuum (particle tracking)
- Counting statistics from n. history

Deterministic n. transport

- Energy intervals (multi-group)
- Solid angle discretization (S_n) or polynomial expansion (P_n)
- Discretization of the time variable
- Discretization of the spatial variables
- „Exact“ solution (except round-off)

- **Apart from counting statistics, are there any other souces of numerical error in continuous enegy MC particle transport codes?**
- **YES:**
  - **Discretization of thermal scattering data (e.g. Serpent 2.1.29 → fixed in 2.1.32)**
  - **Ignoring Doppler Broadening Rejection Correction (DBRC) (e.g. MCNP)**
  - **Energy release per fission proportional to atomic mass (e.g. Serpent before v. 2.1.31)**
  - **etc.**

European Commission

sck cen

Modelling uncertainties: depletion vs. n. transport

MC neutron transport

- Continuous energy
- Continuous direction
- Continuous time (e.g. for n. kinetics)
- Space continuum (particle tracking)
- Counting statistics from n. history

Material depletion by n. irradiation

- Reaction rates from continous *E*
- Not needed for depletion (4π int.)
- Depletion time steps
- Depletion geometric zones
- Counting statistics from n. history

Additional modelling uncertainties:

- Model simplifications (e.g. 2D)
- Physical approximations (e.g. no DBRC)
- Energy deposition model (fission; all n reactions; n+γ)

European Commission

sck cen

Types of modelling uncertainties

- Counting statistics
- **Discretization**
  - **Independent variables**
  - **Conditions (e.g. temperature, density)**
- Physical approximations
- Simplifications (e.g. 3D→2D, boundary conditions)
- Round-off (negligible in double precision for well-conditioned problems)

Discretization parameters

Independent variables:

- Irradiation time steps:
  - Depletion solver (i.e. mathematical method used to solve Bateman equations)
  - Implicit/explicit
  - Interpolation/extrapolation scheme
  - Substeps
- Depletion geometrical zones:
  - Radial zones within pin (to model „rim effect“)
  - Pins grouped in separate zones (to account for asymmetry, e.g. due to boundary conditions)
  - Axial zones (in 3D model or 2D slices with different irradiation conditions)
  - Azimuthal regions within pin (not studied, probably negligible effect?)

Conditions:

- Fuel temperature profiles: radial, axial (negligible)
- Moderator axial density and temperature profiles

SNF observables

Main studied observables:

- Decay heat rate : H
- Neutron emission rate : S_n
- γ-ray emission rate : S_γ

Possible to measure, but different difficulties...

⇒ Determined/estimated by **theoretical calculations**

⇒ Summation formula starting from **nuclide vector**

Decay heat of SNF: main contributing nuclides

Decay heat rate: $H(t) = \sum_j H_j(t)$

- 1 a ≤ t_c ≤ 10 a
  - **^{144}Ce / ^{144}Pr**
  - **^{106}Ru / ^{106}Rh**
  - **^{134}Cs**
  - ^{90}Sr / ^{90}Y & ^{137}Cs / ^{137m}Ba
- 10 a ≤ t_c ≤ 100 a
  - **^{90}Sr / ^{90}Y & ^{137}Cs / ^{137m}Ba**
  - ^{238}Pu
  - ^{241}Am
  - ^{244}Cm
- 100 a ≤ t_c ≤ 1000 a
  - **^{241}Am**
  - ^{238}Pu
  - ^{239,241}Pu

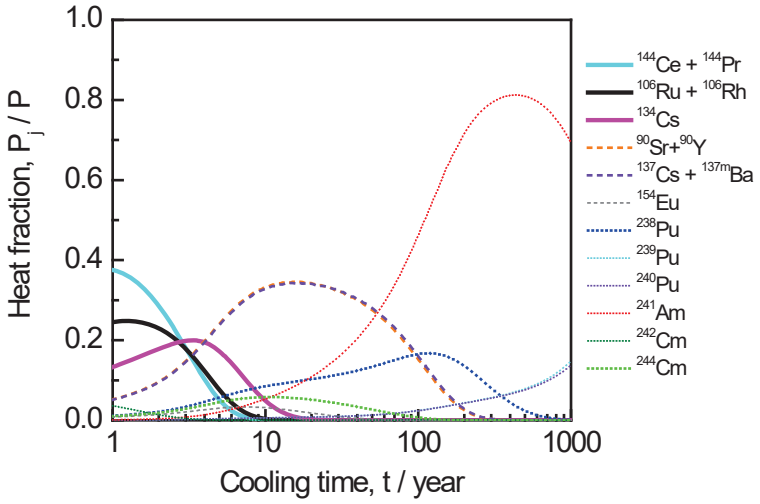

Neutron emission of SNF: main contributing nuclides

Neutron emission rate:

$$S_n(t) = \sum_j S_{n,j}(t)$$

Contribution from SF dominating!

- for cooling time < 100 a, **(α,n) rate** at least 10× lower than SF n. emission rate

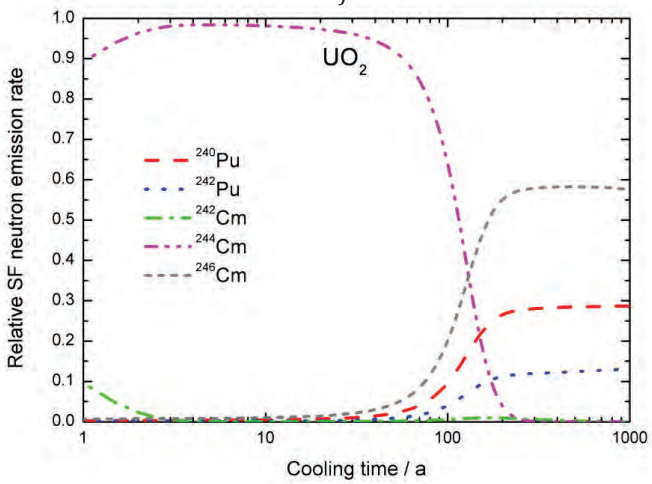

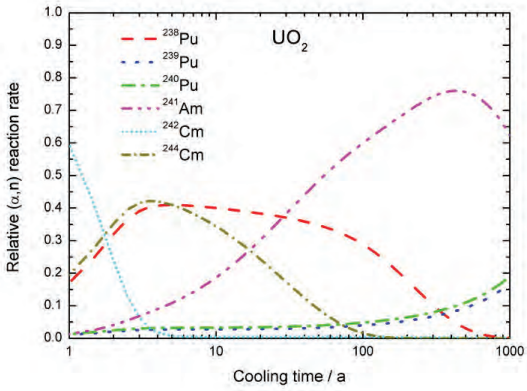

$S_n(t) \Rightarrow$ **sensitive to ^{244}Cm production**

European Commission

sck cen

γ-ray emission by SNF: main contributing nuclides

Photon emission rate energy density:

$$H_\gamma(t) = \sum_j H_{\gamma,j}(t) = \sum_j N_j(t)\,\lambda_j E_{\gamma,j}$$

= Contribution of γ-rays to decay heat

- 1 a ≤ t_c ≤ 10 a
  - **^{134}Cs**
  - ^{137}Cs / **^{137m}Ba**
  - ^{106}Ru / **^{106}Rh**
- 10 a ≤ t_c ≤ 300 a
  - ^{137}Cs / **^{137m}Ba**
  - **^{154}Eu**
  - ^{241}Am
- 300 a ≤ t_c ≤ 1000
  - **^{241}Am**
  - ^{137}Cs / ^{137m}Ba

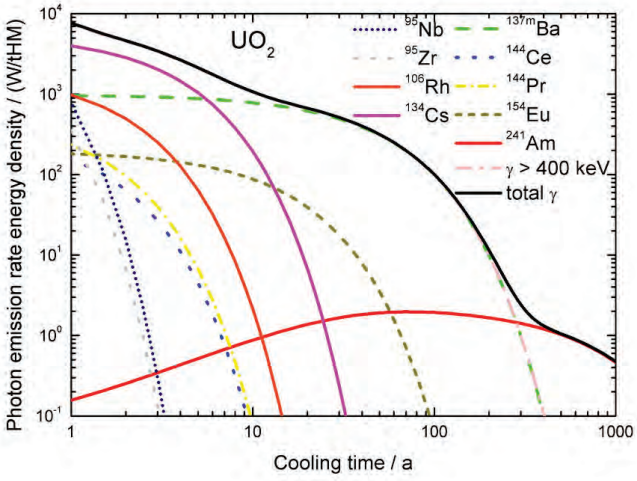

European Commission

sck cen

Definition of the study case

2D PWR 17×17, Zircaloy-4, 4% enriched UO_2 fuel, 4 × 300 d fuel cycles, cooling periods 30 d. Fuel radius 4.095 mm, clad inner/outer radii 4.18/4.75 mm, rod pitch 12.6 mm.

Simplified operating conditions:

- Power levels 50, 50, 40 and 30 MW/tHM during each cycle.
- Coolant density 0.655 kg/cm^3, constant boron level 800 ppm.
- Fuel density (95% theoretical density): 10.4 g/cm^3.
- Constant *T*: fuel and gap: 900 K; coolant and cladding: 600 K.

Numerical approximations (ref. model):

- 4 equi-volume radial depletion zones
- Time steps per cycle: 1 d, 10 d, 14 d, 3 × 25 d, 2 × 50 d
- reflective boundary conditions

Code: Serpent (v2.1.29/30)

Nuclear data library: ENDF/B-VII.1

European Commission

sck cen

Counting statistics: nuclide vector at cooling time 5 a

No. of neutron histories: 2.5 × 10^6 (5000 n. in 500 active cycles)

Count. stat. unc.: estimated from **50 runs** with different random seeds

Nuclide	c_0/(g/tHM)	σ_c/c_0	Nuclide	c_0/(g/tHM)	σ_c/c_0
^{90}Sr	678.56 (2)	0.003%	^{238}Pu	426.44 (18)	0.04%
^{133}Cs	1621.7 (1)	0.01%	^{239}Pu	6747.4 (18)	0.03%
^{134}Cs	43.86 (2)	0.04%	^{240}Pu	3065.2 (13)	0.04%
^{137}Cs	1638.0 (0)	0.001%	^{241}Pu	1556.7 (6)	0.04%
^{148}Nd	567.92 (6)	0.01%	^{242}Pu	970.92 (30)	0.03%
^{235}U	7109.9 (14)	0.02%	^{241}Am	499.66 (17)	0.03%
^{238}U	920116 (4)	0.0004%	^{244}Cm	109.38 (8)	0.08%

European Commission

sck cen

Actinide production chains

Actinide production processes: $R_j = \sum_i \phi \, \sigma_{fi} \gamma_{ij}$

- Radioactive decay
  - **β-decay**
  - Isomeric transition
  - α-decay
- Nuclear reactions:
  - **Neutron capture**
  - Other reactions:
    - (n,2n)
    - (n,α)
    - (n,p)
    - etc.

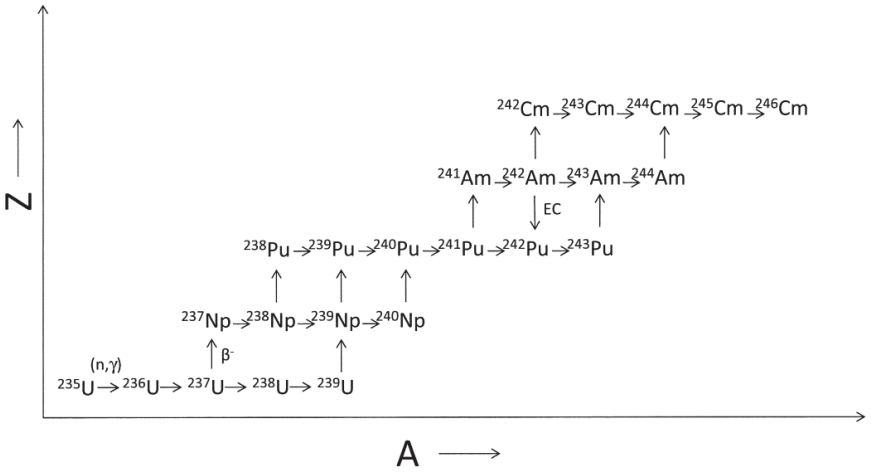

European Commission

sck cen

Irradiation time discretization

Reference model:

- Time steps per cycle: 1 d, 10 d, 14 d, 3 × 25 d, 4 × 50 d
- Depletion solver: CRAM order 14
- Predictor/corrector: linear extrapolation/linear interpolation
- Substeps: 10/10

Time step with longest time steps within 0.2% for ^{244}Cm:

- 1 d, 10 d, 14 d, 25 d, 50 d, 2 × 100 d

The optimal time step scheme is problem dependent. The findings are only valid for specific fuel type and power density range (only valid for PWR UO_2 fuel and not valid e.g. for MOX fuel!).

European Commission

sck cen

Depletion zone discretization: pin level, radial

- Burn card: equi-volume
- Div card: equi-thickness
- Manual: 2 zones to study the ring effect

No. of radial zones	1	2	4 (ref.)	6	8	10	1+1 (ring)
^{244}Cm / ref.	0.984	0.994	1	0.999	1.002	1.002	0.997
^{241}Am / ref.	1.002	1.000	1	1.000	1.000	1.000	1.001
^{239}Pu / ref.	1.005	1.002	1	1.000	0.999	1.000	1.001

European Commission

sck cen

Depletion zone discretization: assembly level; boundary conditions

Reference model:

- 17 × 17 pins
  - 264 equal fuel pins
  - 25 empty positions (for CR)
- All pins grouped in a single depletion zone
- 4 radial (equi-volume) zones
- Reflective boundary conditions

Separate pin treatment study:

- As a function of boundary conditions (1-group albedo)
- Optimal pin grouping?
- Effect on observables

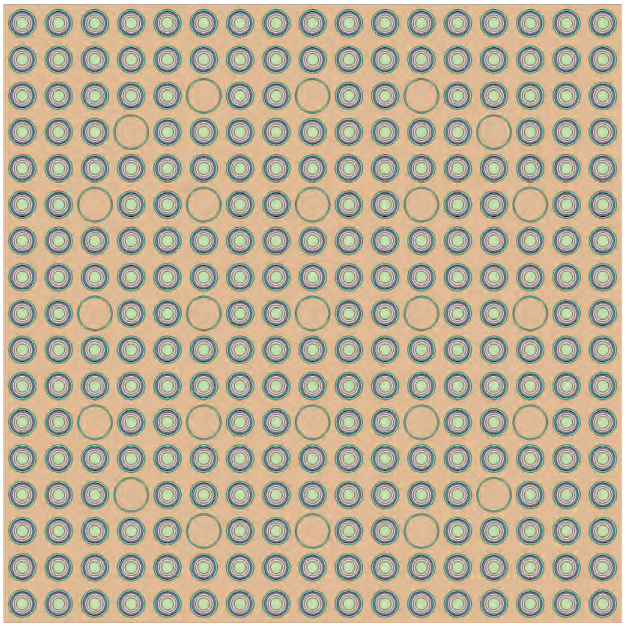

European Commission

sck cen

Pin grouping: by „feeling“

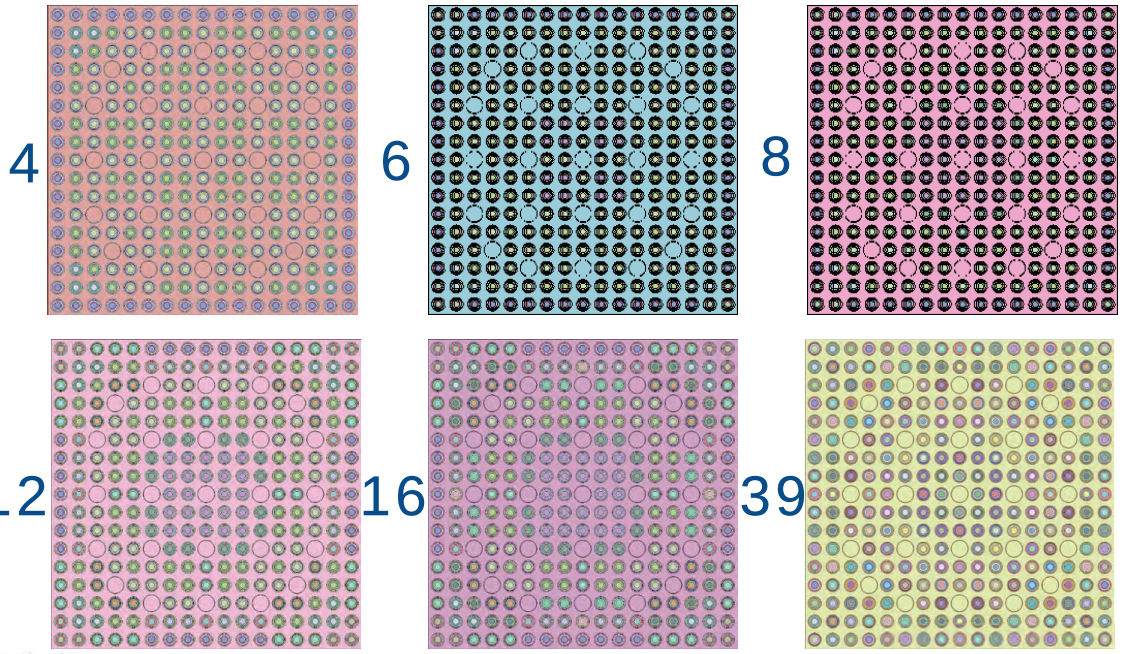

European Commission

sck cen

Pin burnup distributions

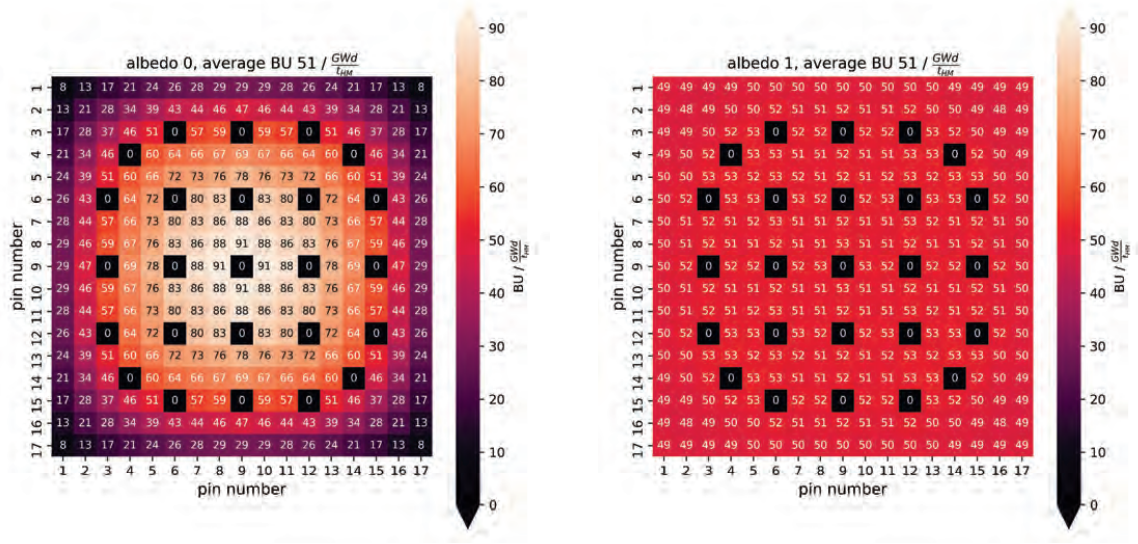

European Commission

sck cen

Pin grouping: by burnup, separated by 10 GWd/tHM

a=1
2 zones

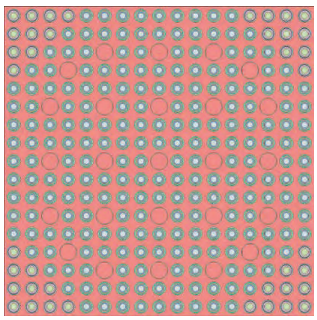

a=0.8
4 zones

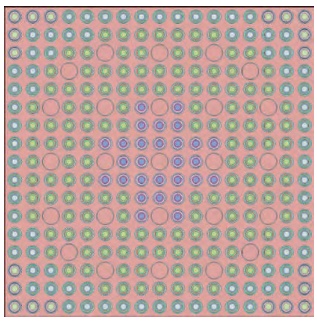

a=0.5
6 zones

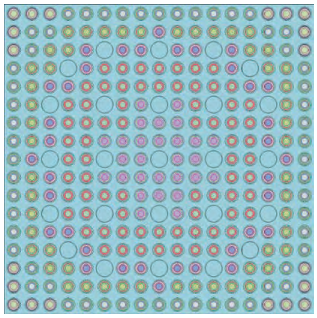

a=0
10 zones

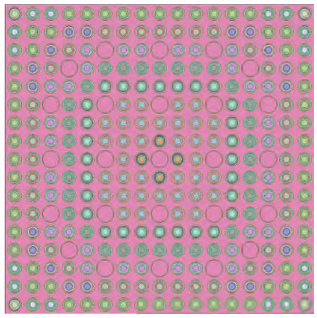

European Commission

sck cen

Separate pin treatment: results (decay heat rate at 5 a cooling)

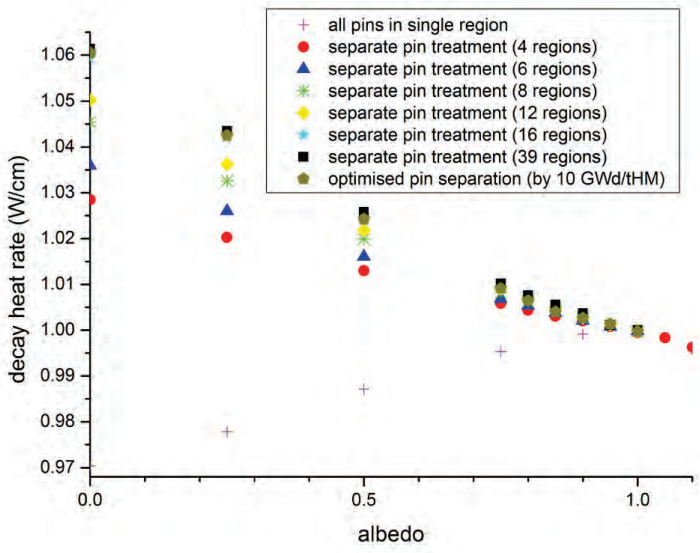

European Commission

sck cen

Separate pin treatment: results (^{244}Cm – n. emission)

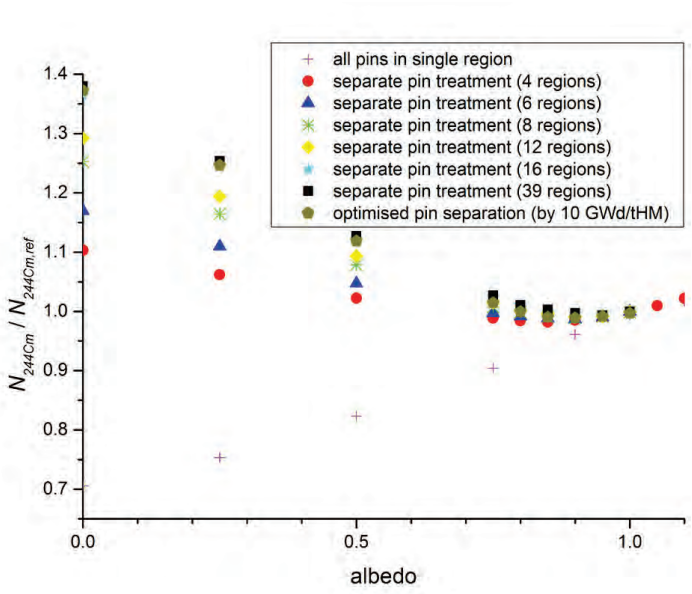

Irradiation conditions: fuel temperature profile

T_f: 4 equi-volume radial regions @ different T
Ref. case: T independent of radial position

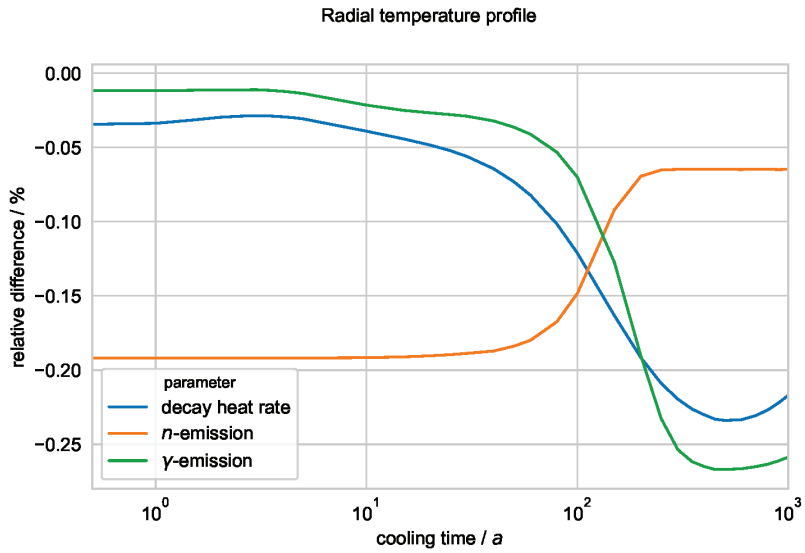

Irradiation conditions: moderator density and temperature

Moderator temperature profile in a typical PWR:

- Bottom: ~560 K (ρ = 0.752 g/cm^3 @ 15.5 MPa)
- Top: ~600 K (ρ = 0.661 g/cm^3 @ 15.5 MPa)
- 2D slices at different conditions: **T effect small, ρ effect large**

Nucl.	*c* (600 K) / *c* (580 K) - 1	*c* (560 K) / *c* (580 K) - 1	Nucl.	*c* (600 K) / *c* (580 K) - 1	*c* (560 K) / *c* (580 K) - 1
^{90}Sr	-0.73%	0.54%	^{238}Pu	3.21%	-2.51%
^{134}Cs	2.24%	-1.54%	^{239}Pu	**5.09%**	**-3.77%**
^{137}Cs	0.00%	0.00%	^{240}Pu	8.83%	-5.82%
^{148}Nd	-0.05%	0.04%	^{241}Pu	2.49%	-1.76%
^{149}Sm	8.33%	-5.28%	^{242}Pu	6.84%	-4.72%
^{235}U	6.53%	-4.80%	^{241}Am	7.18%	-4.94%

European Commission

sck cen

Physical approximations: DBRC (on/off)

DBRC: used for ^{238}U, ^{240,242}Pu and ^{241}Am
No DBRC: ref. case

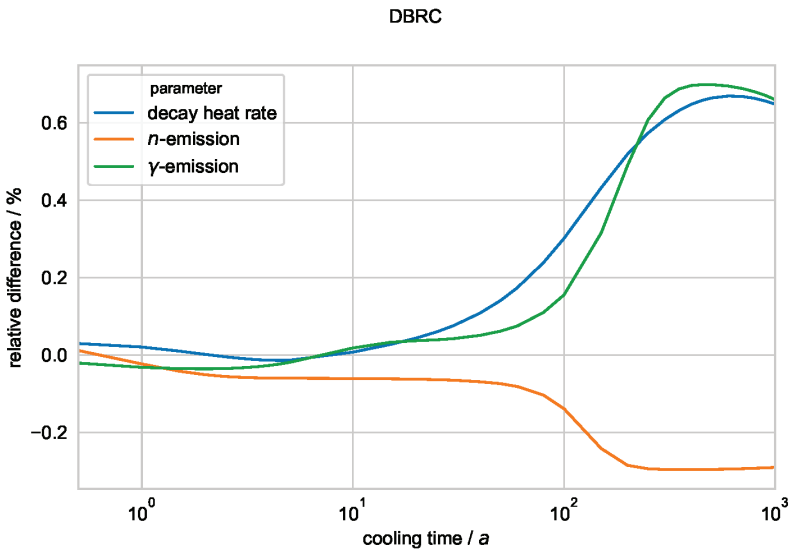

European Commission

sck cen

Summary and conclusions

Analysis of modelling uncertainties/biases – case study:

- Calculations: neutron transport (MC, det.) + depletion
- Case: simplified PWR assembly
- ND library: ENDF/B-VII.1
- Observed quantities: Nuclide vector, decay heat, neutron and γ-ray emission

Analysis of modelling uncertainties/biases – main results:

- Time discretization: optimal time step scheme is problem dependent.
- Spatial discretization of the depletion zones:
  - Optimal pin grouping depends on boundary conditions
  - For UO_2 fuel, 4 equi-volume radial depletion zones are sufficient (<0.1% bias for ^{244}Cm); 2 regions with optimized border are almost sufficient
- Operational conditions:
  - Axial moderator density important – non-linear effect (either 3D or 2D slices).
  - Radial fuel temperature: small differences, 1 radial zone almost sufficient.
- DBRC causes <1% difference in observables (has to be studied in more detail).

European Commission sck cen

Future work

⇒ Detailed sensitivity studies
- ⇒ Nuclear data
- ⇒ Operational history
- ⇒ Geometry & materials
- ⇒ Model parameters (depletion time steps, depletion zones, nuclide vector, etc.)

⇒ Experimental validation
- ⇒ Decay heat measurements from from SNF (e.g. SKB-50, „Blind Test“)
- ⇒ Neutron emission measurements from SNF (JRC/SCK)
- ⇒ SFCOMPO database
- ⇒ Nuclear data measurements (decay energies, actinide cross sections, etc.)

European Commission sck cen

6.2 Fuel properties characterisation and related uncertainty analysis: overview, status and planning; P. Schillebeeckx, JRC Geel; 1st research coordination meeting on the CRP on spent fuel characterisation; 06 - 10/12/2021

TASK 2
FUEL PROPERTIES CHARACTERISATION AND RELATED UNCERTAINTY ANALYSIS

Summary and status

P. Schillebeeckx, D. Rochman, M. Verwerft, R. Dagan, M. Seidl

The project leading to this application has received funding from the European Union's Horizon 2020 research and innovation programme under grant agreement n° 847593.

TASK 2: SNF CHARACTERISATION – SOURCE TERMS OF INTEREST

Main observables of SNF that are of interest for transport, handling, storage and disposal:

- Decay heat rate
- Neutron emission
- γ-ray emission
- Reactivity (burnup credit, nuclides with high neutron absorption cross section)
- Fissile material (Safeguards, non-proliferation), i.e. ^{235}U, ^{239}Pu
- Specific long-lived radionuclides (Long term safety), e.g. ^{14}C, ^{79}Se, ^{94}Nb, ^{99}Tc, ^{129}I, ^{226}Ra

⇒ requires knowledge of a **complex inventory of nuclides** with different characteristics

⇒ a full characterisation can only be obtained by **theoretical calculations**

THEORETICAL CALCULATIONS OF NUCLIDE INVENTORY

Burnup code: coupled neutron transport – nuclide depletion/creation calculations

Neutron transport

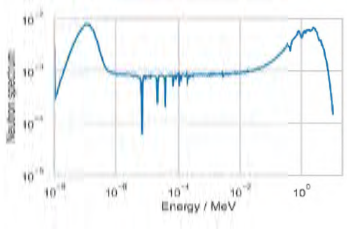

Bateman equation

$$\frac{dN_k}{dt} = Y\, N_f\, \sigma_f\, \varphi + \sum_i \lambda_i N_i + \sum_j \sigma_j N_j\, \varphi - (\lambda_k + \sigma_{k,a}\varphi) N_k$$

Update nuclide vector

TASK 2: IMPROVE PERFORMANCE OF BURNUP CALCULATIONS

Nuclear data
- Cross sections: (n,γ), (n,f), …
- Fission Yields
- Decay data
  - Half-lives
  - Emission probabilities
  - Recoverable energy

Burnup code

SNF input data
- Fuel properties
  - design
  - material data (IE)
- Operational history
  - burn-up (BU)
  - cooling time (CT)
  - …

Validate by experiment

Source terms
- Thermal power
- Neutron emission
- γ-ray
- ^{239}Pu
- …

Verify experimentally in industrial conditions

TASK 2: FUEL PROPERTIES CHARACTERISATION AND RELATED UNCERTAINTY ANALYSIS

- Subtask 2.1 "Theoretical study of SNF source terms" (Theory)
  co-ordinator PSI (D. Rochman)
  partners CIEMAT, JSI, JRC Geel, NAGRA, PSI, SCK CEN, VTT
- Subtask 2.2 "Develop, improve and demonstrate NDA methods/systems for SNF characterisation" (NDA)
  co-ordinator SCK CEN (M. Verwerft)
  partners CIEMAT, ENRESA (ENUSA), JRC Geel & Ispra, SCK CEN, SKB (UU)
- Subtask 2.3 "Calculate and determine experimentally the inventory of activation and FP in cladding" (Cladding)
  co-ordinator KIT (R. Dagan)
  partners CIEMAT, KIT, LEI, NAGRA, VTT, SURAO(CTU)
- Subtask 2.4 "Define and verify procedures to determine source terms of SNF with realistic confidence limits"
  co-ordinator PEL (KIT) (M. Seidl)
  partners CIEMAT, CPST, JRC Geel, ENRESA, JSI, PEL, SSTC NRS, KIT, SCK CEN, TUS, SKB (UU)

SUBTASK 2.1 THEORETICAL STUDY OF SNF SOURCE TERMS

- Cases to verify the performance of different codes and perform sensitivity and uncertainty analysis defined
  - BWR
    - Gundremmingen-7 sample (SFCOMPO)
      (UO_2, 25 MWd/kg, 4 cycles, 2.5 %)
    - ENRESA
      (UO_2, 41 MWd/kg, 3.95 %)
  - PWR
    - SF95-5 from the Takahama-3 reactor (SFCOMPO)
      (UO_2, 30 MWd/kg, 2 cycles, 4.1 %)
    - GU1 from ARIANE (public report)
      (UO_2, 60 MWd/kg, 4 cycles, 3.5 %)
    - GU3 from ARIANE (public report)
      (UO_2, 52 MWd/kg, 4 cycles, 3.5 %)
    - BM1 from ARIANE (public report)
      (MOX, 45-47 MWd/kg, 5 cycles, 4.2 % fissile)
    - NPP KršKo
      (UO_2, 40 MWd/kg, 4.95 %)
  - Calculated case:
    (sensitivity and uncertainty analysis)
    - S1.PWR (UO_2, 51 MWD/kg, 4.0 %)
  - Decay heat: PWR and BWR fuel assemblies
    - SKB-2006
    - GE-Morris

SUBTASK 2.1 THEORETICAL STUDY OF SNF SOURCE TERMS

- Cases to verify the performance of different codes and perform sensitivity and uncertainty analysis defined
- All results of calculations reported

Partner	Code(s)	Cases studied
CIEMAT	MCNP/EVOLCODE, MCNP/CINDER	SF95-5
ENRESA/ENUSA	POLARIS	BWR(ENRESA)
JSI (JRC)	SCALE (TRITON/NEWT, POLARIS), SERPENT2	S1.PWR, NPP Krško, SF95-5, SKB-2006
SCK CEN	MCNP/ALEPH2, SERPENT2	S1.PWR, SF95-5, SKB-2006
KIT	MCNP/CINDER, Nucleonica	SF95-5
NAGRA	SCALE(TRITON, POLARIS)	SF95-5, BM1, BWR(ENRESA), Gundremmingen-7 (B23), GE-Morris, SKB-2006
PSI	CASMO, CASMO/SIMULATE/SNF	GU1, GU3, BM1, BWR(ENRESA), GE-Morris, SKB-2006
VTT	SERPENT2	Gundremmingen-7 (B23)

+ in kind contribution from IRSN (FR) and Studsvik in the analysis of the data and preparation of final paper

SUBTASK 2.1: NUCLIDE INVENTORY

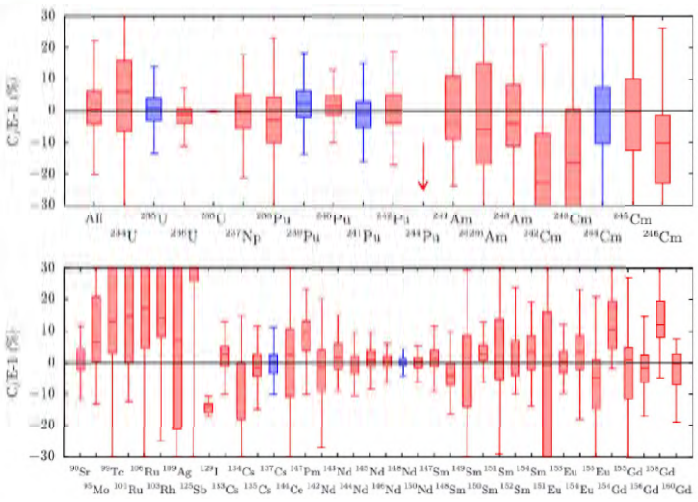

- C: calculated concentration
- E: experimentally determined

SUBTASK 2.1: DECAY HEAT RATE

CLAB calorimeter

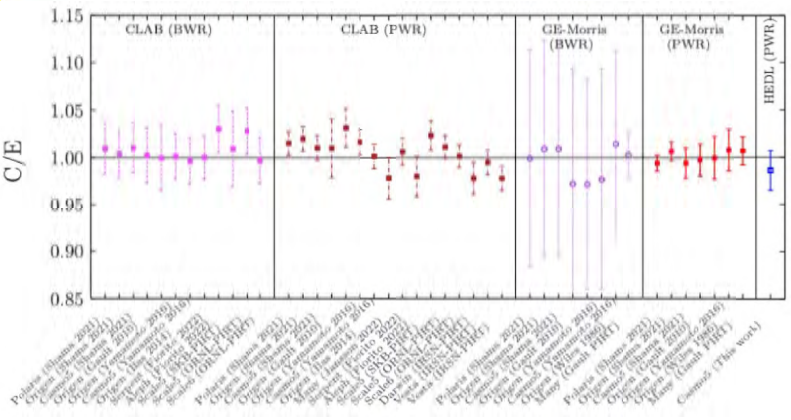

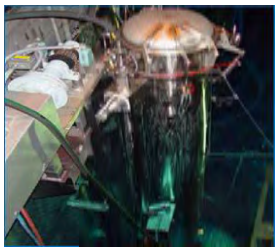

⇒ More detailed study: Romojaro et al.,"*On the use of decay heat measurements for code validation*" in Frontiers in Energy Research

SUBTASK 2.1 RECOMMENDATIONS

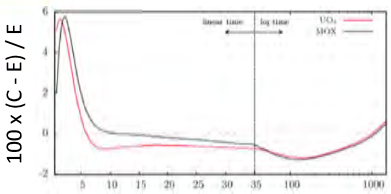

EPRI PIRT report +Ilas et al., Nucl. Eng. Des. 319 (2017) 176

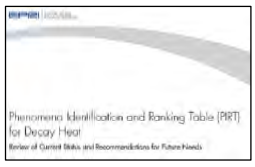

	^{148}Nd	^{137}Cs	^{235}U	^{239}Pu	BU	Decay heat rate
Relative uncertainty	4 %	5 %	4 %	4 %	5 %	> 4%
Relative difference	- 0.1%	- 0.4%	0.2%	2.5%	-	See fig.

Data set	Data set	Uncertainty (1 σ) (%)
Modeling data	Fuel design	0.20
	Operating data	0.85
	Total	0.87
Nuclear data	Cross sections	0.88
	Fission yields	0.26
	Total	0.92
Overall effect	Total	1.27

BWR, BU = 37 MWd/kg and CT = 15.6 a

UNCERTAINTY ANALYSIS (PHD AHMED SHAMA)

Data set	Decay heat rate, C/E	
	Average	St. Deviation
CLAB, BWR (81)	1.010	0.051
CLAB, PWR (71)	1.015	0.023
CLAB (152)	1.012	0.041

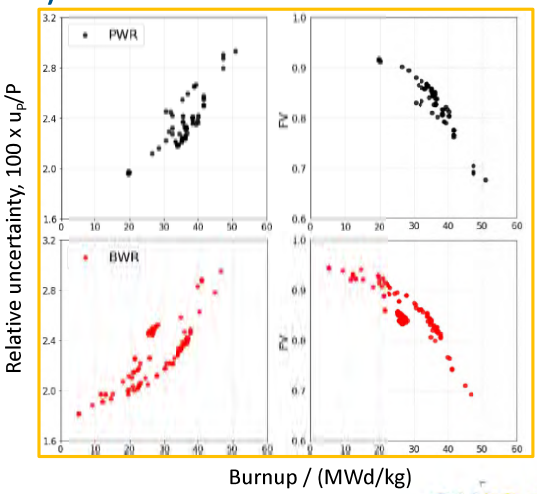

BLIND TEST (NOT INCLUDED IN EURAD): PAPER PUBLISHED

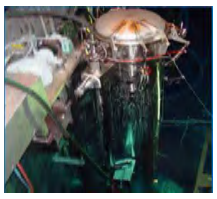

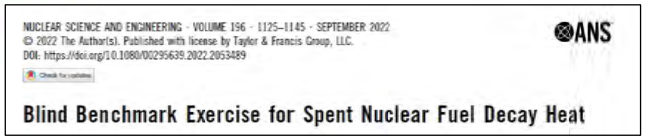
NUCLEAR SCIENCE AND ENGINEERING · VOLUME 196 · 1125–1145 · SEPTEMBER 2022
© 2022 The Author(s). Published with license by Taylor & Francis Group, LLC.
DOI: https://doi.org/10.1080/00295639.2022.2053489
ANS
Blind Benchmark Exercise for Spent Nuclear Fuel Decay Heat

- PWR assemblies
- Decay heat rate determined at CLAB

Assembly ID	BU	CT	IE	Decay heat rate	Gamma-escape
BT01	53 MWd/kg	4.5 a	3.95 wt%	1662 W	58 W
BT02	55 MWd/kg	8.6 a	3.95 wt%	1068 W	30 W
BT03	50 MWd/kg	9.8 a	3.95 wt%	895 W	21 W
BT04	51 MWd/kg	13.5 a	3.70 wt%	768 W	15 W
BT05	50 MWd/kg	21.4 a	3.60 wt%	663 W	12 W

BLIND TEST: CODES + LIBRARIES

Code	Library	Appendix Section
ALEPH 2.7.2	ENDF/B-VII.1	A.I.A
APOLLO2.8/DARWIN2.3	JEFF-3.1.1	A.I.B
CASMO-4E + ORIGEN-S	JEF-2.2	A.I.C
CASMO-5 (2.03)	ENDF/B-VII.1	A.I.D
CASMO-5 (2.12.00) + SNF (1.07.02)	ENDF/B-VII.1	A.I.E
DRAGON 4.0.5	ENDF/B-VII.1	A.I.F
EVOLCODE (MCNP + ACAB)	JEFF-3.3	A.I.G
MCNP-CINDER + Nukleonika (2D)	ENDF/B-VII.1	A.I.H
Monteburns v3 + CINDER	ENDF/B-VII.1	A.I.I
MOTIVE (KENO-VI + VENTINA)	ENDF/B-VII.1	A.I.J
MOTIVE (OpenMC + VENTINA)	ENDF/B-VIII	A.I.K
MVP 3	ENDF/B-VII.1	A.I.L
MVP 3	JEFF-3.2	A.I.M
MVP 3	JENDL-4.0	A.I.N
OREST	JEF-2.2 + ENDF/B-VI	A.I.O
SCALE 6.0: ORIGEN-ARP	ENDF/B-V	A.I.P
SCALE 6.1.3: ORIGEN-ARP	ENDF/B-V	A.I.Q
SCALE 6.2.3: ORIGAMI	ENDF/B-VII.1	A.I.P
SCALE 6.2.3: Polaris	ENDF/B-VII.1	A.I.R
SCALE 6.2.3: ORIGEN	ENDF/B-VII.1	A.I.R
SCALE 6.2.3: TRITON/KENO	ENDF/B-VII.1	A.I.S
SCALE 6.2.3: TRITON/NEWT	ENDF/B-VII.1	A.I.T
SEADEP	JEFF-3.1.1	A.I.U
Serpent 2.1.29	ENDF/B-VII.1	A.I.V
Serpent 2.1.29	JEFF-3.1.1	A.I.W
Serpent 2.1.31	JEFF-3.2 + JEFF-3.1.1	A.I.X

BLIND TEST: RESULTS

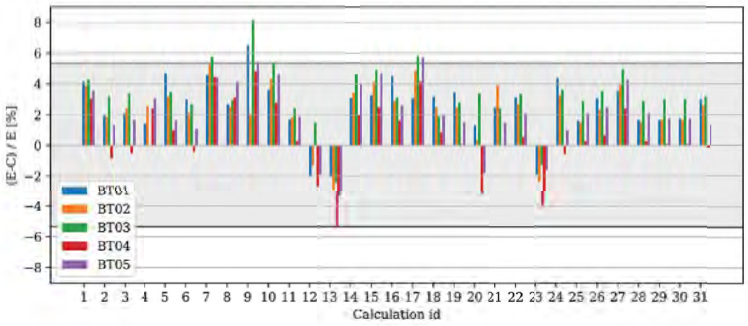

Assembly ID	CT	100 x (C-E)/E	St. dev.
BT01	4.5 a	2.5	1.9
BT02	8.6 a	2.3	1.8
BT03 (+ Gd)	9.8 a	3.3	1.9
BT04	13.5 a	0.6	2.3
BT05	21.4 a	2.1	2.1

EPRI report +llas et al., Nucl. Eng. Des. 319 (2017) 176

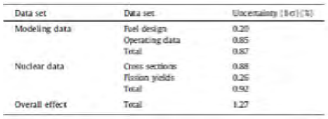

⇒ Uncertainty of 1.3 % realistic?

SUBTASK 2.2: DEVELOP AND IMPROVE NDA METHODS/SYSTEM

- Provide data to validate burnup codes
  - Neutron emission rate of a SNF by NDA at SCK CEN
  - Radiochemical analysis of BWR samples
  - Performance assessment and uncertainty evaluation of CLAB calorimeter (MSc Thesis of J. Ekman, A. Mehic)
- Improve NDA methods to characterise SNF assemblies (PhD Thesis V. Solans)
  - Gamma-ray scanning device at CLAB
  - Differential Die-away Self-Interrogation (DDSI)

SUBTASK 2.2: DEVELOP AND IMPROVE NDA METHODS/SYSTEMS

- Neutron emission rate of a SNF by NDA at SCK CEN
  - Experiments of REGAL sample at SCK CEN (finalised)
    - Publication data book in progress
    - Experiments finalised and reported (EUR30379 EN) (Journal paper in progress)
  - Experiments with improved detection system (delayed: summer 2023)
    - Design of improved transfer container finalised
    - Construction: delayed due to administrative procedures

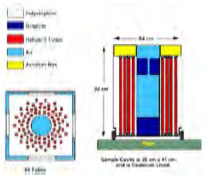

- Radiochemical analysis of a set of BWR samples (November 2022)
  - Data book finalised and distributed (21/03/2022)
  - Radiochemical analysis in progress (complications with radiochemical analysis: very instructive)
    - problems with nuclide inventory determined by Laser ablation ↔ radiochemical analysis
    - problems revealed by comparison with calculated data

SUBTASK 2.2: CALORIMETER AT CLAB

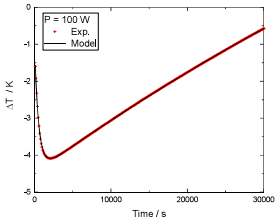

- Improve analysis procedure for calorimeter at CLAB (MSc Thesis of J. Ekman, A. Mehic)
  (ollaboration Vattenfall (SKB), JRC, JSI, SCK CEN)
  - Analytical model to describe heat transfer (finalised)
  - Study of the γ-ray escape from the calorimeter (ongoing)
    - MCNP (γ-ray transport) + SNF (fuel depletion)
    - SERPENT (γ-ray transport) + ALEPH2 (fuel depletion)

    ⇒ Compare results with present approach

    (γ-ray dosimeters combined with analytical expressions for the γ-ray transport)
  - Uncertainty assessment (December 2022, journal paper in progress)
    - Calibration electrical heater
    - Gamma-ray correction + correction for difference electrical heater – fuel assembly
    - Least squares fit procedures

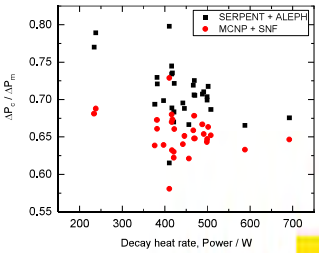

SUBTASK 2.2: DEVELOP AND IMPROVE NDA METHODS/SYSTEMS

- Improve analysis procedure for neutron and γ-ray based NDA measurements at CLAB
  (PhD Thesis of V. Solans, presentation at this meeting)

  Details: presentation of V. Solans
  - γ-ray measurements: finalised (presentation at IAEA symposium, journal paper in preparation)
    (intrinsic calibration for gamma-ray attenuation in assembly based
    on well-known principle applied for enrichment determination)
  - Differential Die away Self-Interrogation (DDSI): in progress

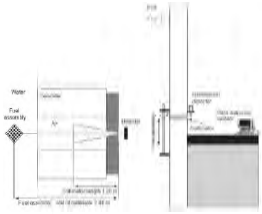

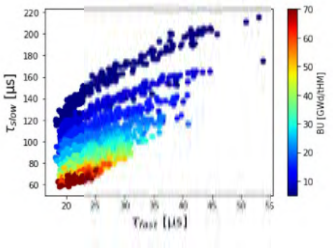

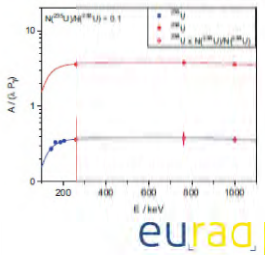

SUBTASK 2.3: CALCULATE AND DETERMINE THE INVENTORY IN CLADDIN

Cladding composition: important to study fuel integrity (PhD Tobias Köning, August 2022)

- Selection of Zircaloy samples irradiated in a PWR Gösgen (CH) (done)
  (UO2, 50.4 GWd/t, 4 cycles, 3.8%, 32 years cooling time)
  - Zircaloy-4 of UO_x fuel rod segment
  - Zircaloy-4 plenum of UO_X fuel rod segment
  - UO_x fuel fragment
- Experiments using various techniques at KIT
  - Scanning Electron Microscopy (SEM)
  - Wave Length X-ray spectroscopy (WDX)
  - Energy Dispersive X-ray spectroscopy (EDX)
  - X-ray Photo-electron spectroscopy (XPS)
  - Radiochemical analysis (α-spec,γ-spec, LSC, HR-ICP-MS)

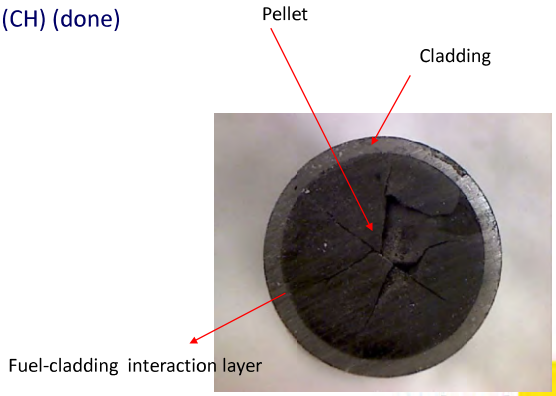

SUBTASK 2.3: CALCULATE AND DETERMINE THE INVENTORY IN CLADDING

Code validation

- Calculations (done)
  - MCNP/EVOLCODE CIEMAT,
  - MCNP/CINDER KIT
  - SCALE (TRITON) LEI
  - SCALE (KENO) NAGRA
  - SCALE (POLARIS 2D) NAGRA
  - VTT SERPENT2

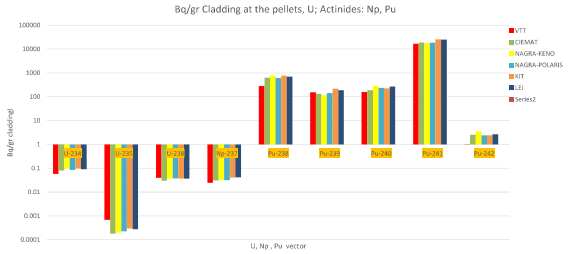

- Interpretation of data (in progress)
  - Good agreement for the cladding of the plenum and the cladding around the pellets
  - Singular deviations are being checked for their origin (input issues, code deficiencies, source of uncertainties, …)
  - Comparison with experimental data used to assess how much fuel is adherent to the inner surface of the cladding during manufacturing: important to estimate the risk of radiation damage during interim storage

INVENTORY OF ^{36}Cl AND ^{129}I

(PhD Tobias Köning, August 2022)

^{36}Cl activity in Zry-UOx, Zry – MOX
Experimental and calculated (MCNP/CINDER)

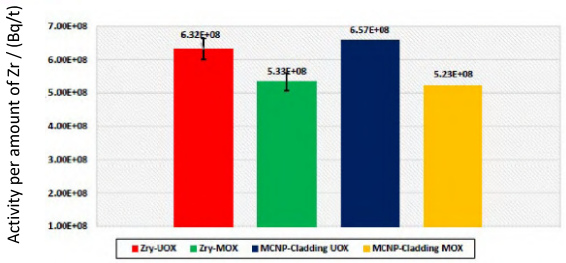

^{129}I activity (inventory)
Experimental and calculated (MCNP/CINDER)

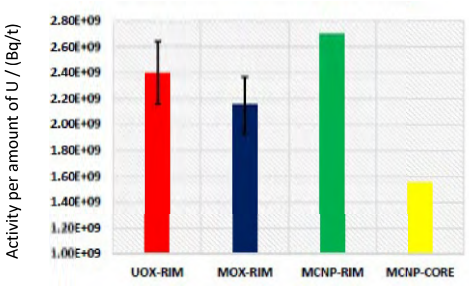

- First ever analysis of ^{36}Cl in PWR fuel rod components
- Calculations: 15 ppm ^{35}Cl in fuel and zircaloy
  (Häkkinen, Impurities in LWR fuel and structural materials, Finland 2019)

[HÄK19] S. Häkkinen, Impurities in LWR fuel and structural materials, VTT, Finland (2019).

SUBTASK 2.4: DEFINE AND VERIFY PROCEDURES TO DETERMINE SOURCE TERMS OF SNF WITH REALISTIC CONFIDENCE LIMITS

Planning was reviewed to account for delays due to COVID and signing of agreements

1. REGAL Sample from Task 2.2 (SCK CEN, JSI, JRC) (December 2022)
   - Data book/report in preparation
   - Neutron output: calculations with ALEPH2, SCALE, SERPENT2 (journal paper in preparation)
   - Report: February 2023
2. BWR SNF sample from task 2.2 (ENRESA/ENUSA) (in progress)
   - Data book/report produced and distributed (March 2022)
   - Calculations with MCNP/EVOLOCDE (CIEMAT), SCALE (PEL)
   - Report: December 2022
3. SKB-50 (in progress, December 2023) (details: presentation M. Seidl)
   - Non-Disclosure agreements signed by all partners
   - Analysis procedure defined
   - Interaction with different partners to improve the data book (dedicated VC meetings)
   - Report: December 2023

Code	Library	(α,n) Method	(α,n) Library	S_{sf} / (g^{-1}s^{-1})	$S_{\alpha,n}$ / (g^{-1}s^{-1})	Calculation/Experiment S_{sf}	Calculation/Experiment $S_{\alpha,n}$
SCALE	ENDF/B-VII.1	Y(α,n)		653	11.0	0.96	0.45
SERPENT(1)	ENDF/B-VII.1	Y(α,n)		689	14.3	1.01	0.58
SERPENT(2)	ENDF/B-VII.1	Y(α,n)		694	14.2	1.02	0.58
	ENDF/B-VIII.0	Y(α,n)		691	14.1	1.01	0.57
	JEFF-3.1.2	Y(α,n)		629	13.2	0.92	0.54
	JEFF-3.3	Y(α,n)		654	13.7	0.96	0.56
	JEFF-4T0	Y(α,n)		695	13.7	1.02	0.56
	JENDL-4.0			719	14.5	1.05	0.59
ALEPH28	ENDF/B-VIII.0	Y(α,n)		662	13.1	0.97	0.53
		σ(α,n)	TENDL2015		12.6		0.51
		σ(α,n)	JENDL_AN/500		10.6		0.43
	JEFF-3.3	Y(α,n		641	12.9	0.94	0.53
		σ(α,n)	TENDL2015		12.7		0.52
		σ(α,n)	JENDL_AN/500		10.5		0.43

TASK 2.4 SKB-50

- SKB50 data was received in Q2/22
- SKB50 data book is limited
- SKB50 pin data has been guessed by PEL's knowledge and/or published data
- SKB50 has been converted into standardized xml format to facilitate automation.
- SKB50 data has been distributed without measurement data to facilitate blind test (with participants from PEL, CIEMAT, (JSI, NAGRA, KIT, PSI, SCK CEN)

TASK 2.4 SKB-50

- SKB50: 2 main PWR types and 4 main BWR types:
  - 15x15 AFA/KWU, 17x17 F/HTP/AA/W
  - SVEA96, SVEA100, AA 8*8-1, Atrium 10B
- Not all assemblies have :
  decay heat rate & neutron & gamma-ray data
- First step: automatic SCALE runs by PEL and CIEMAT

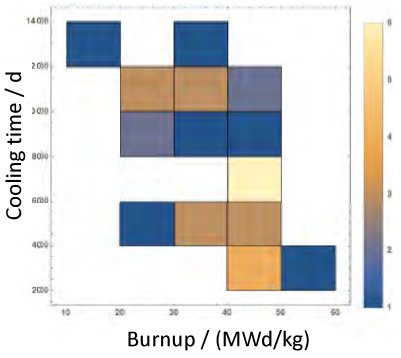

- PWR1: 8 cases were created to study robustness of simulations
  - CASMO5
  - SCALE6.2, v7-238, addnux=4, 1 average fuel region, NEWT deterministic transport
  - SCALE6.2, v7-252, addnux=4, 1 average fuel region, NEWT deterministic transport
  - SCALE6.2, v7-56, addnux=4, 1 average fuel region, NEWT deterministic transport
  - SCALE6.2, v7-238, addnux=0, 1 average fuel region, NEWT deterministic transport
  - SCALE6.2, v7-238, addnux=1, 1 average fuel region, NEWT deterministic transport
  - SCALE6.2, v7-238, addnux=1, 8 different fuel region, NEWT deterministic transport
  - SCALE6.2, v7-238, addnux=4, 1 average fuel region, KENOVI Monte Carlo transport

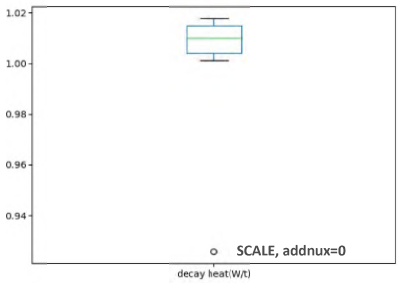

SCALE6 addnux parameter: for depletion calculations trace quantities of certain nuclides are added to the inventories of depletion materials in order to accurately track the nuclides' impact on cross section processing and transport calculations

CONTRIBUTION TO CRP TECDOC (JRC GEEL)

Overview NDA techniques for the characterisation of SNF

Missing:
- Active neutron interrogation
  - Differential Die Away
  - Detection delayed gamma (and neutron)
- References

Keep in touch

EU Science Hub: ec.europa.eu/jrc

@EU_ScienceHub

EU Science Hub – Joint Research Centre

EU Science, Research and Innovation

EU Science Hub

EU science

Thank you

6.3 Neutron resonance analysis and applications to material characterisation; P. Schillebeeckx, JRC Geel; LANL P/T Colloquium, April 2022; 28/04/2022

Neutron resonance analysis and applications to material characterisation

P. Schillebeeckx, H. Postma†, S. Kopecky and C. Paradela

European Commission

Joint Research Centre, Geel (BE)

LANL P/T Colloquium, April 2022

Contents

- Neutron facilities at JRC Geel
- Basic principles of Neutron Resonance Analysis (NRA)
- Applications
  - Cultural heritage and archaeology
  - Nuclear waste
  - Validation of nuclear data (resonance parameters)
- Analysis of complex samples
- Characterisation of SNF

Joint Research Centre

Headquarters in Brussels
and research facilities located
in 5 Member States:

- **Belgium (Geel)**
- Germany (Karlsruhe)
- Italy (Ispra)
- The Netherlands (Petten)
- Spain (Seville)

European Commission

JRC-Geel site

40 ha

14
major buildings

Around **230** staff
from **4** JRC Directorates

JRC.G.2 about 30%

European Commission

Nuclear facilities at JRC - Geel

GELINA
neutron time-of-flight facility for high-resolution neutron measurements

MONNET
tandem accelerator based fast neutron source

TARGET
nuclear target preparation laboratories

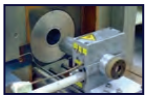

RADMET
laboratories for standardisation of radionuclide activity

HADES
low-level gamma-spectrometry laboratory

METRO
nuclear reference material and measurement facility

Operated by JRC.G.2 Unit

- Nuclear data
- Radionuclide measurements
- Nuclear safeguards metrology

European Commission

Nuclear data group: neutron induced interactions

GELINA
neutron time-of-flight facility for high-resolution neutron measurements

MONNET
tandem accelerator based fast neutron source

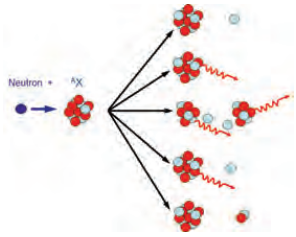

Neutron induced interaction cross sections

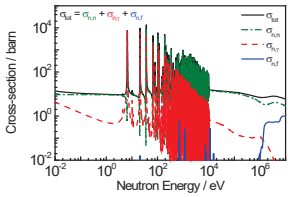

Fission process

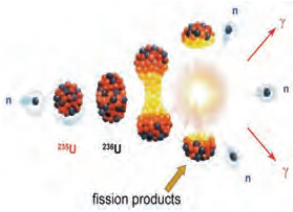

European Commission

Neutron facilities: GELINA and MONNET

GELINA

VdG,Tandem

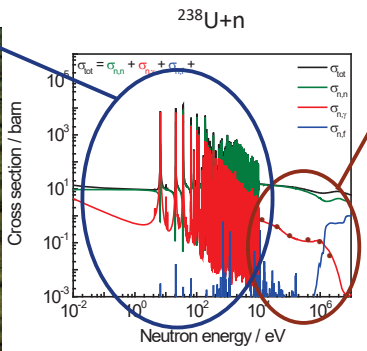

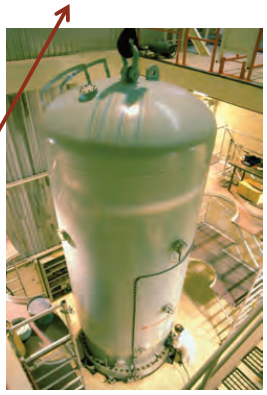

White neutron source
+
Time-of-flight (TOF)

Mono-energetic neutrons
(cp,n) reactions

GELINA - Experimental set-ups (see presentation C. Paradela)

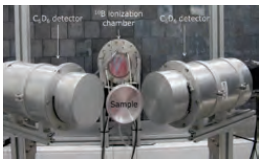

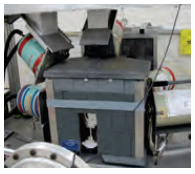

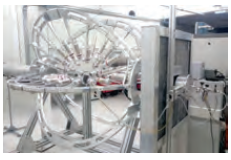

- Transmission
  - 10 m, 30 m, 50 m
- Capture
  - 10 m, 30m, 60 m
- Elastic, in-elastic scattering
  - 30 m
- In-elastic scattering (n,n'γ)
  - 30 m, 100 m
- Fission, (n,p), (n,α),
  - 10 m

Nuclear data libraries for nuclear applications

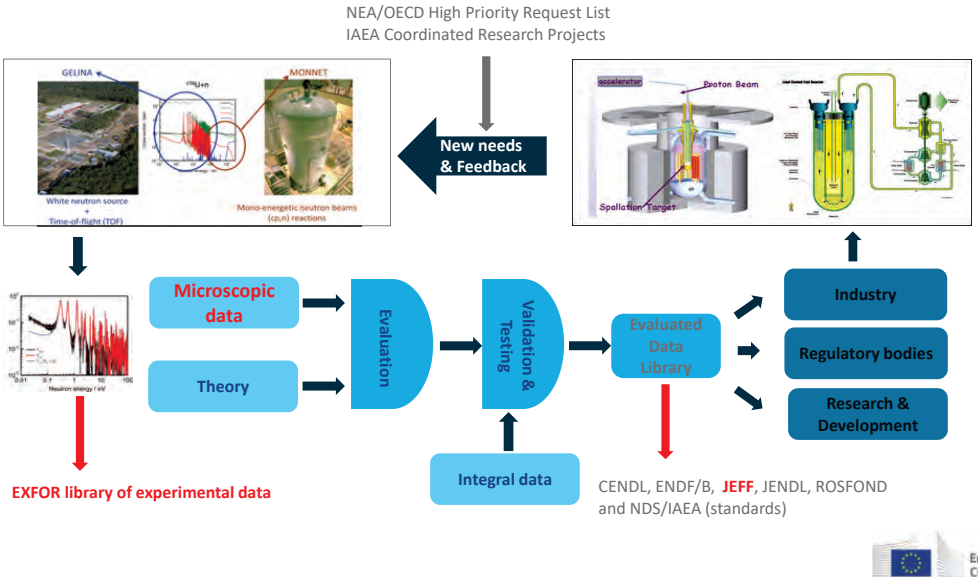

European Commission

Applications

- **Nuclear data for energy technology**
  - Safety of current systems
  - Development of innovative systems (e.g. MYRRHA)
  - Back-end: Spent Nuclear Fuel (Burn Up Credit, Decay heat, …)
    - *Intermediate storage*
    - *Transport of SNF*
    - *Reprocessing facilities*
    - *Final Disposal of SNF*

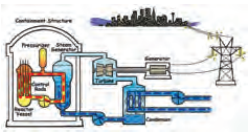

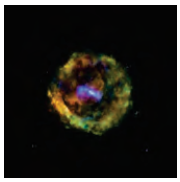

- Nuclear physics
- Nuclear medicine: diagnostics and therapy
- Nucleosynthesis and nuclear astrophysics
- Detector development
- Materials research (NAA, PGAA, **N**eutron **R**esonance **A**nalysis, …)
- ….

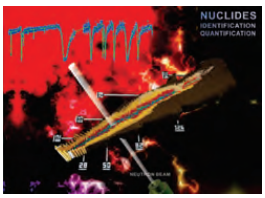

European Commission

Neutron Resonance Analysis (NRCA & NRTA)

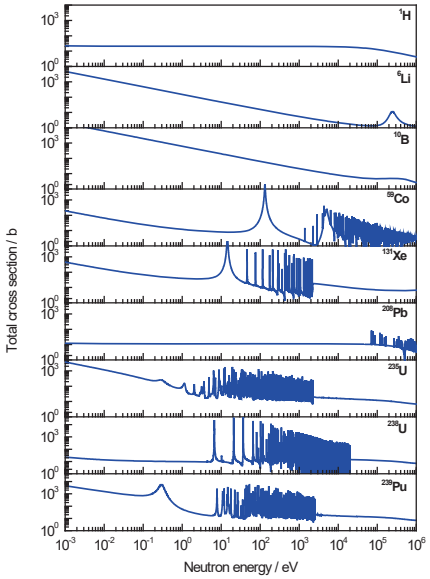

- Resonances appear at energies that are specific for each nuclide
- Position and amplitude of resonances can be used as fingerprints to
  - identify and quantify nuclides
  - elemental & isotopic composition
- Neutron Resonance Capture and Transmission Analysis (NRCA & NRTA)
  - Non-Destructive Analysis (NDA)
  - no sample preparation required
  - sensitive to almost all nuclides (except light)
  - **requirements:**
    TOF-measurements at a white neutron source
    (e.g. GELINA, LANSCE, J-PARC, ISIS)

European Commission

Cross section measurements

Total cross section

$$T \cong e^{-n\sigma_{tot}}$$

Capture cross section

$$Y_\gamma \approx (1-e^{-n\,\sigma_{tot}})\frac{\sigma_\gamma}{\sigma_{tot}}$$

Well-characterised (reference) samples
n: total number of atoms per unit area is well-known
⇓
accurate cross-sections can be determined

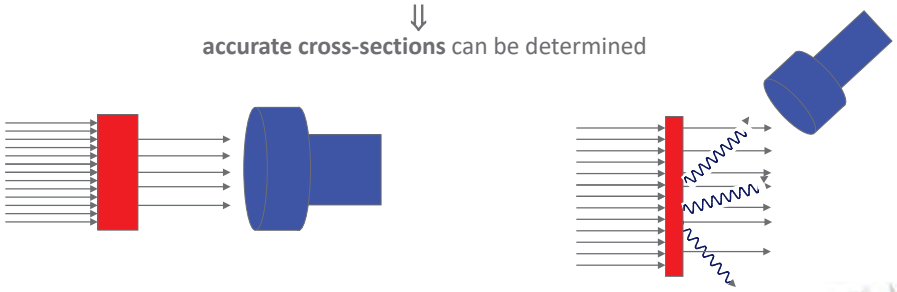

Schillebeeckx et al., Nuclear Data Sheets 113 (2012) 3054

European Commission

Neutron resonance analysis

NRTA

$$T \cong e^{-n\sigma_{tot}}$$

NRCA

$$Y_\gamma \approx (1 - e^{-n\sigma_{tot}}) \frac{\sigma_\gamma}{\sigma_{tot}}$$

Well-known cross sections

⇓

areal density can be determined

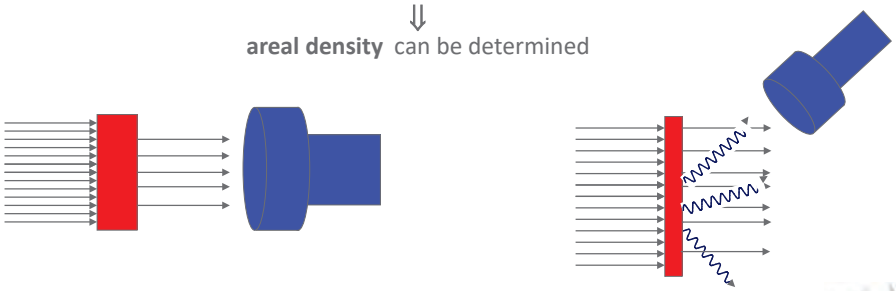

Schillebeeckx et al., Report EUR 26848-EN (2014)

Neutron Resonance Analysis

NRTA

$$T_{exp} = \frac{C_{in}}{C_{out}}$$

Resonance Shape Analysis: REFIT

$$\chi^2(n) = (T_{exp} - T_M(t,n))^T V_{T_{exp}}^{-1} (T_{exp} - T_M(t,n))$$

$$T_M(t) = \int R(t, E)\, T(E)\, dE$$

$$T(E) = e^{-n\bar{\sigma}_{tot}(E)}$$

n : areal density

total number of nuclei per unit area

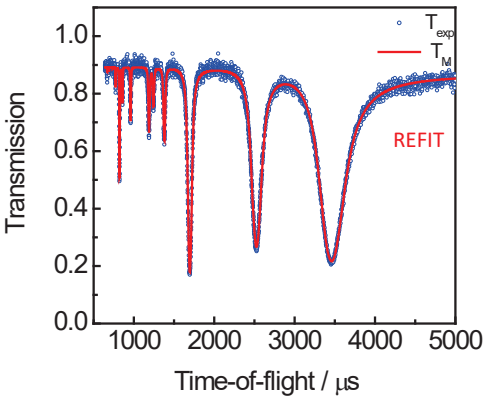

Schillebeeckx et al., Report EUR 26848-EN (2014)

NRTA and NRCA

Transmission: areal density Cu: 0.55 (2) g/cm^2

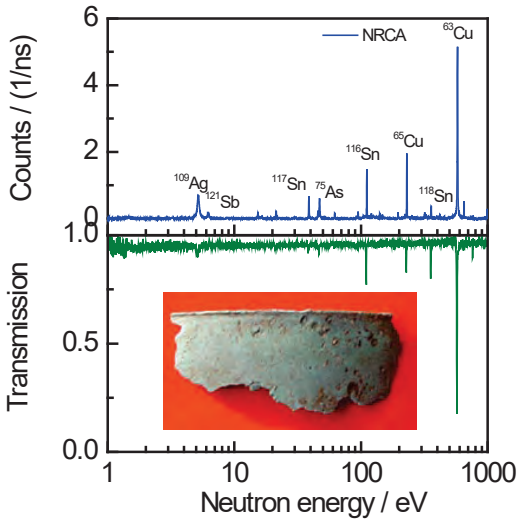

Element	Isotope	E_r/ eV	wt%
Cu	^{63}Cu	579.0	77.76 (11)
	^{65}Cu	230.0	
Sn	^{112}Sn	94.8	20.85 (10)
	^{116}Sn	111.2	
	^{117}Sn	38.8	
	^{118}Sn	45.7	
	^{119}Sn	222.6	
	^{120}Sn	427.5	
	^{124}Sn	62.0	
Fe	^{56}Fe	1147.4	0.77 (1)
As	^{75}As	47.0	0.34 (1)
Sb	^{121}Sb	6.2	0.20 (2)
	^{123}Sb	21.4	
Ag	^{107}Ag	16.3	0.09 (1)
	^{109}Ag	5.2	
In	^{115}In	1.46	0.0061 (3)

Uncertainties: only counting statistics

H. Postma and P. Schillebeeckx, in Neutron Methods for Archaeology and Cultural Heritage (Springer)

NRTA and NRCA

Transmission: areal density Cu: 0.55 (2) g/cm^2

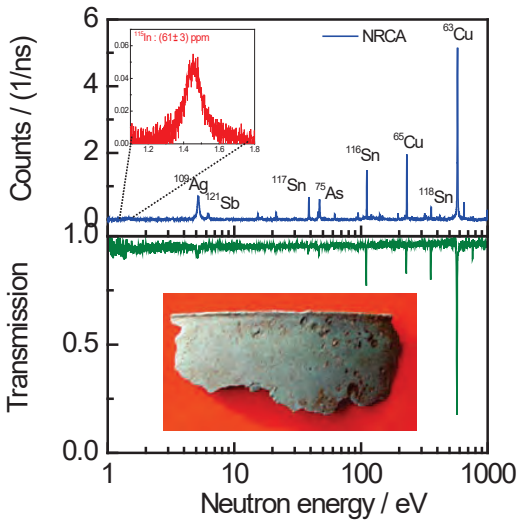

Element	Isotope	E_r/ eV	wt%
Cu	^{63}Cu	579.0	77.76 (11)
	^{65}Cu	230.0	
Sn	^{112}Sn	94.8	20.85 (10)
	^{116}Sn	111.2	
	^{117}Sn	38.8	
	^{118}Sn	45.7	
	^{119}Sn	222.6	
	^{120}Sn	427.5	
	^{124}Sn	62.0	
Fe	^{56}Fe	1147.4	0.77 (1)
As	^{75}As	47.0	0.34 (1)
Sb	^{121}Sb	6.2	0.20 (2)
	^{123}Sb	21.4	
Ag	^{107}Ag	16.3	0.09 (1)
	^{109}Ag	5.2	
In	^{115}In	1.46	0.0061 (3)

Uncertainties: only counting statistics

H. Postma and P. Schillebeeckx, in Neutron Methods for Archaeology and Cultural Heritage (Springer)

NRCA ⇔ PGAA at continuous incident beam

⇒ detection of **In** is **not hindered by** strong resonances of **other elements** (e.g. Cu)

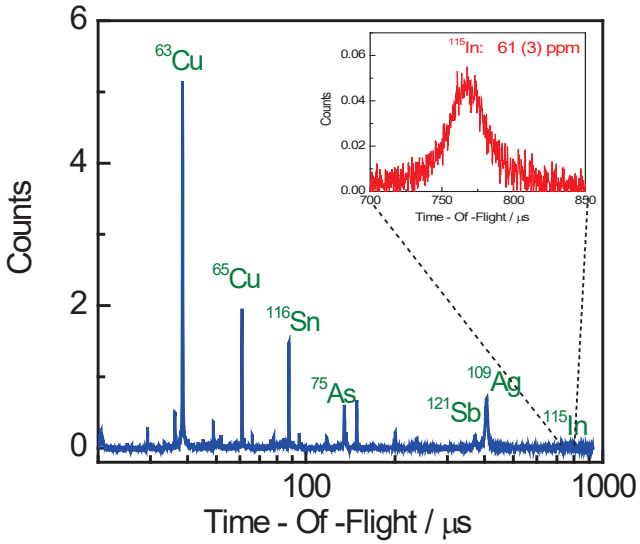

Postma et al., Czech. J. Phys. 53 (2003) A233

NRA: which elements can be detected?

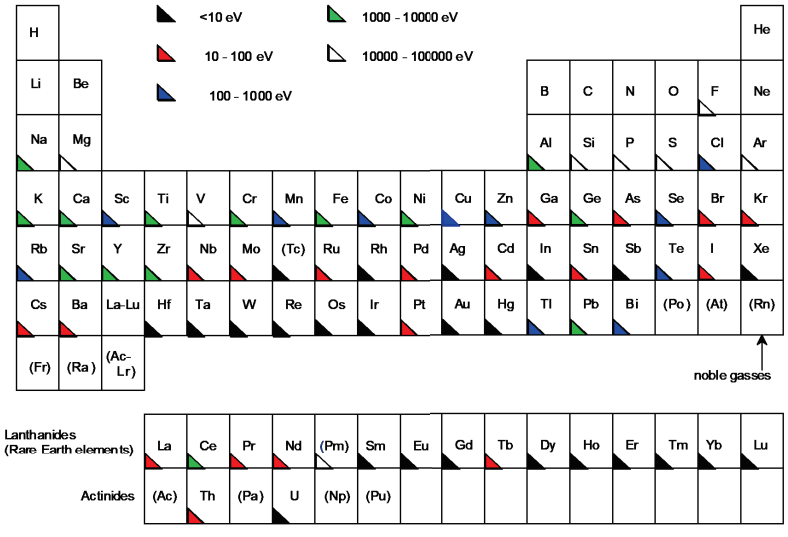

Energy region	detection limit
1 eV < E_μ < 10 eV	~ 10^{-6} (ppm)
10 eV < E_μ < 1000 eV	~ 10^{-5} - 10^{-3}
1 keV < E_μ	> 10^{-2} (%)

H. Postma and P. Schillebeeckx, in Neutron Methods for Archaeology and Cultural Heritage (Springer)

NRA for cultural heritage and archaeology

Started in 2000 by a collaboration between Univ. Delft and JRC Geel initiated by **Prof. H. Postma**

† April 2021

Journal papers

Postma et al., J. Radioanal. Nucl. Chem. 248 (2001) 115
Postma et al., Czech. J. Phys. 53 (2003) A233 – A240
Postma et al., Archaeometry, 46 (2004) 635
Postma and Schillebeeckx, J. Radioanal. Nucl. Chem. 265 (2005) 297
Postma et al., Il Nuovo Cimento, 30C (2007) 105
Perego et al., J. Radioanal. Nucl. Chem. 271 (2007) 89
Postma et al., J. Radioanal. Nucl. Chem. 271 (2007) 95
Schut et al., J. Radioanal. Nucl. Chem. 278 (2008) 151
Postma et al., J. Radioanal. Nucl. Chem. 283 (2010) 641
Perelli et al., Nucl. Instr. Meth. Phys. Res. A 623 (2010) 693
Perelli et al;, J. Anal. At. Spectrom. 26 (2011) 992
Postma et al., J. Archaeol. Sci. 38 (2011) 1810
Schillebeeckx et al., J. Instrumentation, 7 (2012) C03009
Postma et al., Analecta Praehistorica Leidensia, 47 (2017) 37








European Commission

NRA for cultural heritage and archaeology

Started in 2000 by a collaboration between Univ. Delft and JRC Geel initiated by **Prof. H. Postma**

† April 2021

Chapters in books

H. Postma and P. Schillebeeckx, “Neutron resonance capture and transmission analysis”
In: Encyclopedia of analytical chemistry (chapter a9070) ,
R.A. Meyers (Ed.), John Wiley & Sons Ltd. (2009)

H. Postma and P. Schillebeeckx, “Neutron Resonance Analysis”
In: Neutron Methods for Archaeology and Cultural Heritage (chapter 12),
N. Kardjilovand G. Festa (Eds.), Springer International Publishing Switzerland (2017)

P. Schillebeeckx and H. Postma, “Neutron resonance analysis (NRA)”
In: The SAS Encyclopedia of Archaeological Sciences,
S.L. Lopez Varela (Ed.), Wiley –Blackwell (2018)

P. Schillebeeckx and H. Postma, “Neutron Resonance Analysis methods for archaeological and cultural heritage applications”
In: Handbook of Cultural Heritage Analysis (pp. 145 – 187)
S. D’Amico and V. Venuti (Eds.), Springer International Publishing Switzerland (2022)

European Commission

NRCA: Authenticity of Etruscan artefacts

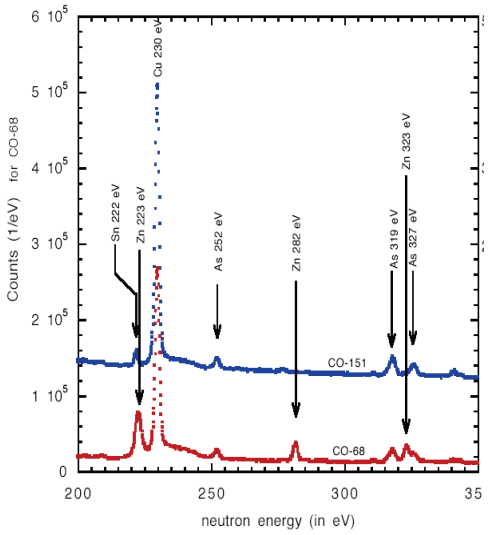

Statuettes from a collection assembled in the 18th century by count Corazzi of Cortona (It).

Now at the National Museum of Antiquities in Leiden (NL).

Postma et al., Archaeometry, 46 (2004) 635

European Commission

NRCA: Authenticity of artefacts

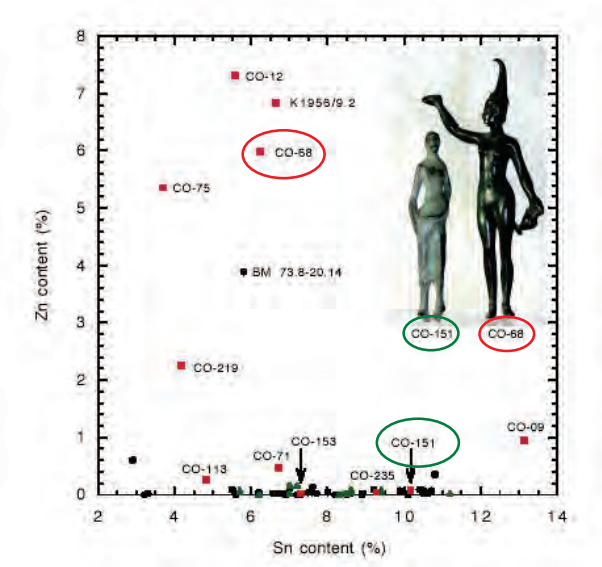

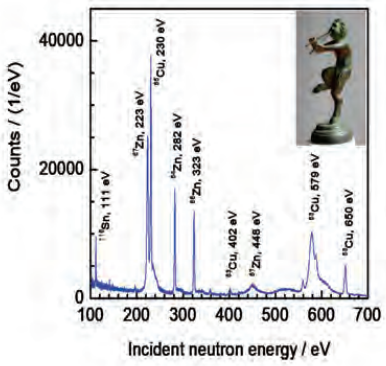

NRCA measurements at a 12.5 m station of GELINA of a figurine that is supposed to present the Greek god Pan.
Zn/Cu ratio: replica

European Commission

Roman water taps: NRCA combined with Neutron Diffraction (ND)

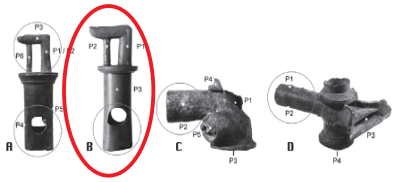

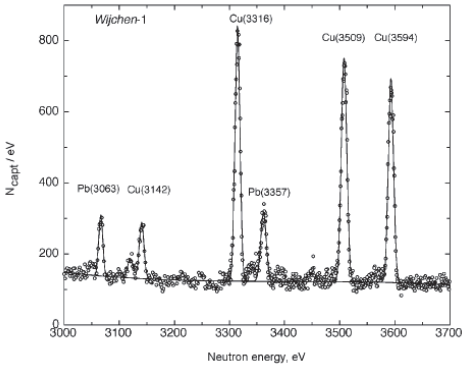

NRCA : material composition

ND : fabrication process

NRCA: 4.8 (5) g/cm^2 Cu

Element weight ratio	NRCA (GELINA)		Neutron diffraction (ISIS)		
			P1	P2	P3
Pb/Cu	0.335	(34)	0.415	0.337	0.402
Sn/Cu	0.0868	(25)	0.094	0.098	0.094
Zn/Cu	0.0036	(3)			
Sb/Cu	0.00167	(3)			
Fe/Cu	0.0012	(3)			
As/Cu	0.00098	(3)			
Ag/Cu	0.00096	(3)			

Schut et al., J. Radioanal. Nucl. Chem. 278 (2008) 151

Characterisation of PbI_2 by NRTA at GELINA

- JRC Geel target preparation group extracted:
  - 150 g Iodine (powder) from 210 liter from **reprocessed waste** (Le Hague)
  - (1.3 g/l Iodine and 40 MBq/l)
- Sample characterisation: by mass spectrometry , NAA and **NRTA**

Fig. 3. Addition of $Pb(NO_3)_2$ to the iodide solution to precipitate lead iodide.

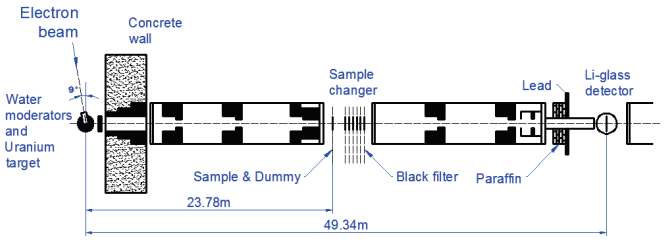

Noguere et al., Nucl. Instr. Meth. Phys. Res. A 575 (2007) 476

Characterisation of PbI_2 by NRTA at GELINA

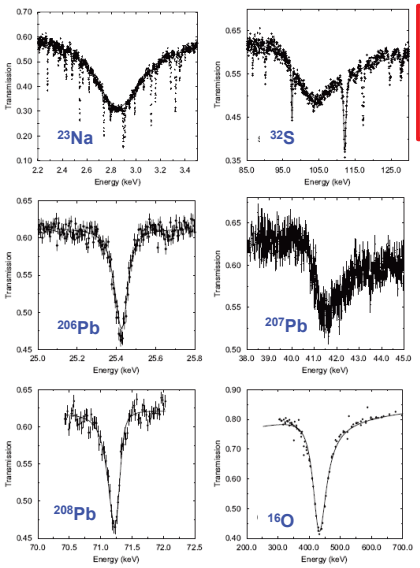

$$T_M(t_m, n) = \int R(t_m, E)\, e^{-n\,\sigma_{tot}(E)} dE$$

$$\chi^2(n) = \left(T_{exp} - T_M(t_m, n)\right)^T V_{T_{exp}}^{-1} \left(T_{exp} - T_M(t_m, n)\right)$$

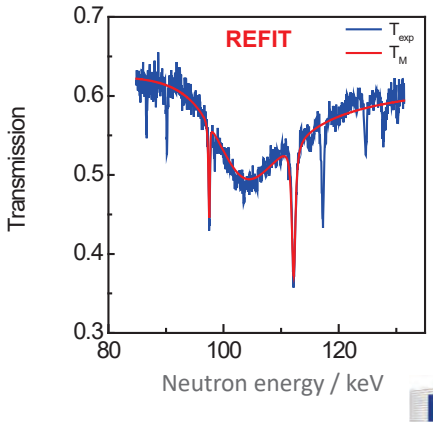

NRTA compared with NAA and ICP-MS

Element		NRTA	NAA	Mass spectrometry (PSI)
Iodine	total	20.24 (41)	19.75 (61)	19.86 (41)
	^{127}I	3.44 (5)	3.35 (10)	3.36 (8)
	^{129}I	16.80 (40)	16.40 (60)	16.50 (40)
Lead	Total	52.3 (17)	51.1 (1.8)	
	^{206}Pb	12.8 (5)		
	^{207}Pb	11.5 (1)		
	^{208}Pb	27.1 (17)		
Sulfur		5.44 (3)		
Sodium		0.72 (2)		1.0 (2)
Oxygen		13.92 (5)		14.5 (15)
Hydrogen		<0.13		0.020 (2)
Nitrogen				1.2 (4)

NRTA ↔ NAA, ICPMS :
- more elements analysed
- isotopic composition of Pb

NRTA of W sample: validation of resonance parameters

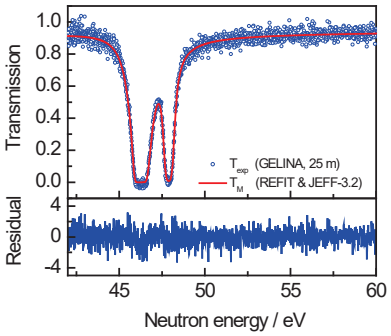

- Sample: metallic disc of ^{nat}W (1 mm thick)
  - homogeneous sample
  - areal density n : from weight and area
    ⇒ $u_n/n < 0.2\%$
- Transmission : absolute measurement
  - absolute measurement
  - methodology well understood (background, dead time correction,…)
    Nuclear Data Sheets 113 (2012) 3054 – 3100
    ⇒ $u_{T_{exp}}/T_{exp} < 0.3\ \%$

⇒ NRTA: one of the most accurate benchmark experiments to validate resonance parameters

NRTA of W sample: validation of resonance parameters

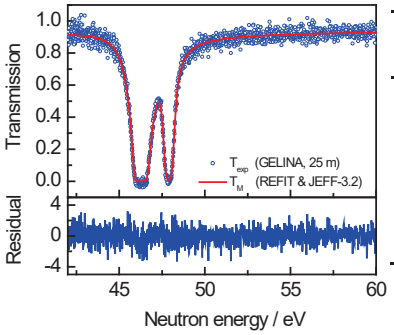

Reference		E_r = 46.26 eV Γ_n / meV	E_r = 46.26 eV Γ_γ / meV	E_r = 47.80 eV Γ_n / meV	E_r = 47.80 eV Γ_γ / meV	n_{NRTA}/n_{REF}
Lynn et al.	2002	162 (1)	72	126 (2)	72	0.983 (10)
Mughabghab	1984	140 (4)	77 (8)	108 (10)	78 (10)	1.198 (34)
Mughabghab	2006	162 (2)	77 (8)	122 (2)	78 (10)	0.992 (14)
JEFF-3.2		163.4	75.3	120.8	61.5	1.002 *(5)*
JENDL-3.3		154.0	46.0	119.0	81.0	1.113 *(5)*
ENDF/B-VII.1		154.0 (8)	46.0 (21)	119.0 (12)	81.0 (51)	1.113 (11)

⇒ Parameters in ENDF/B-VII.1 (JENDL-3.3) strongly biased and covariance data not reliable

NRTA of PuO_2 sample: validation of resonance parameters

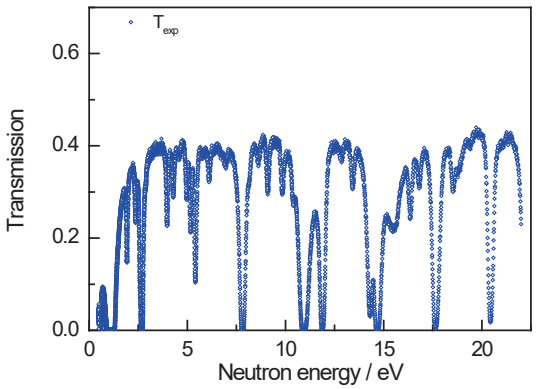

CBNM - 271

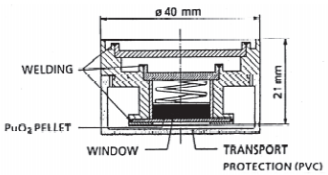

European Commission

NRTA of PuO_2 sample (pressed pellet) at GELINA (CBNM – 271)

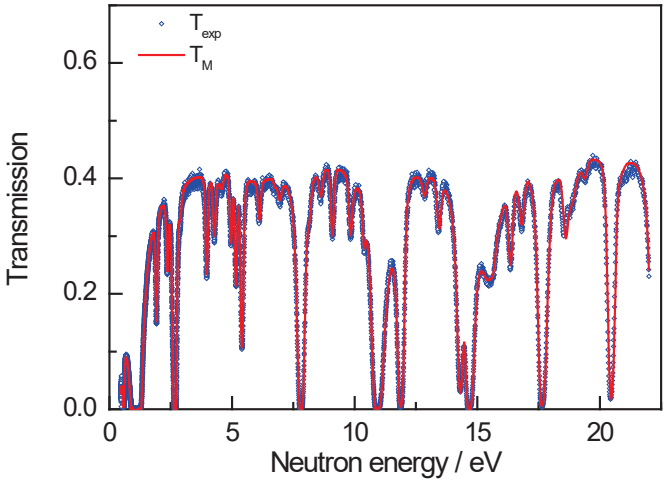

$$T_M(t_m, n) = \int R(t_m, E)\, e^{-n\,\sigma_{tot}(E)} dE$$

$$\chi^2(n) = (T_{exp} - T_M(t_m, n))^T\, V_{T_{exp}}^{-1}\, (T_{exp} - T_M(t_m, n))$$

REFIT

European Commission

NRTA of PuO_2 sample (pressed pellet) at GELINA (CBNM – 271)

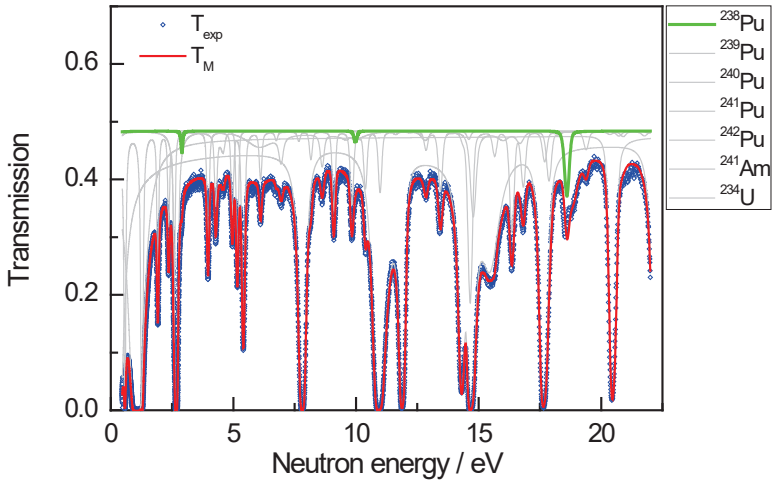

NRTA of PuO_2 sample (pressed pellet) at GELINA (CBNM – 271)

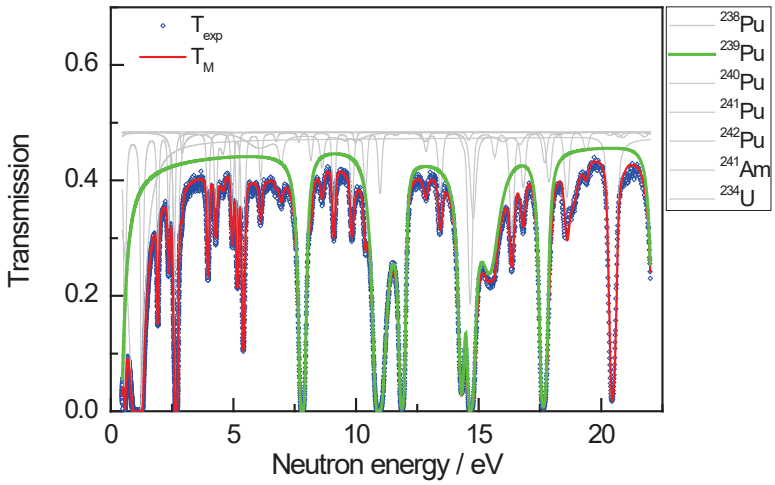

NRTA of PuO_2 sample (pressed pellet) at GELINA (CBNM – 271)

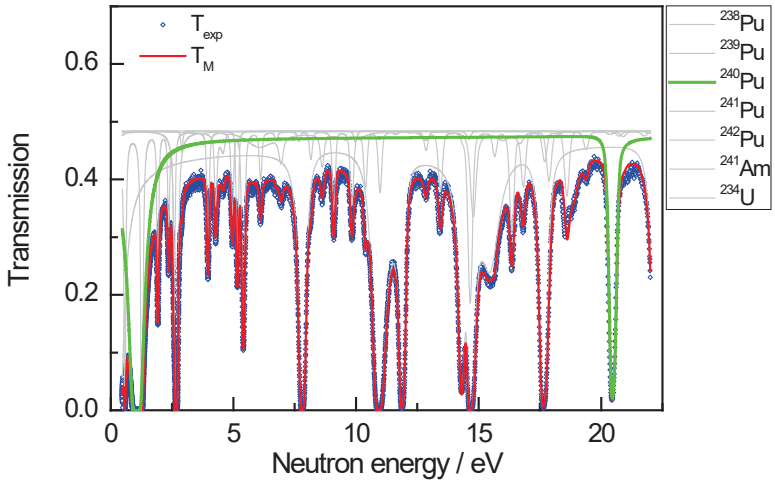

NRTA of PuO_2 sample (pressed pellet) at GELINA (CBNM – 271)

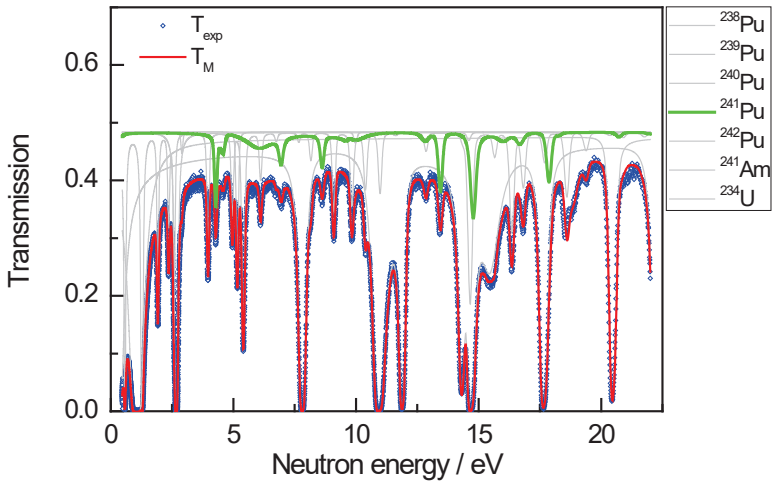

NRTA of PuO_2 sample (pressed pellet) at GELINA (CBNM – 271)

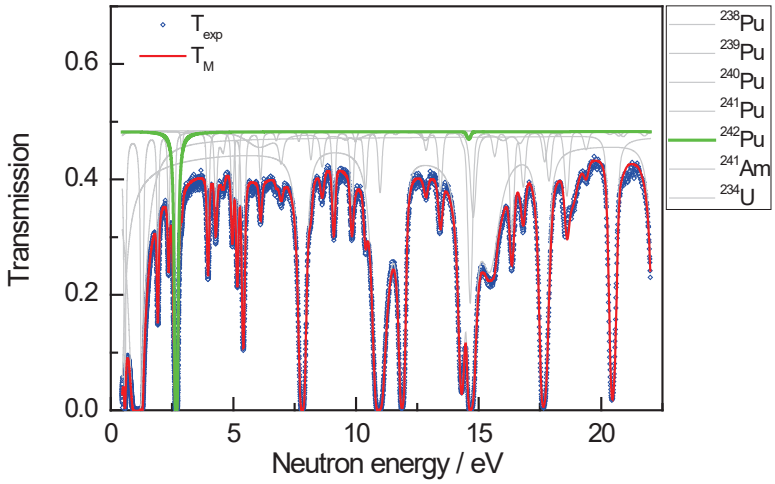

NRTA of PuO_2 sample (pressed pellet) at GELINA (CBNM – 271)

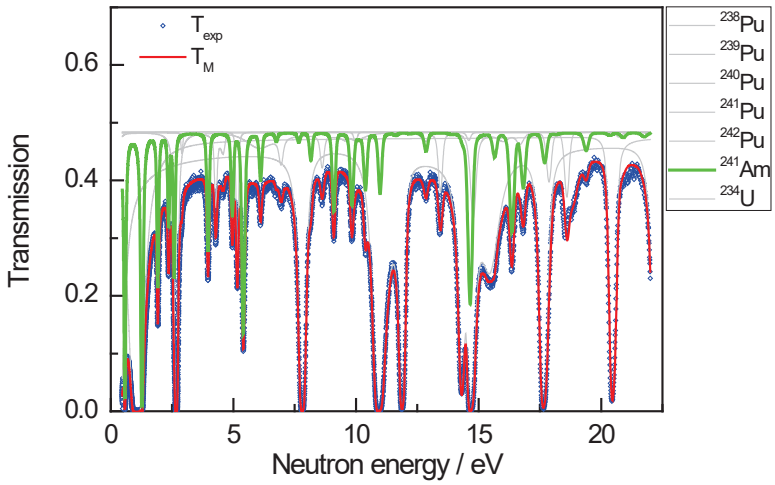

NRTA of PuO_2 sample (pressed pellet) at GELINA (CBNM – 271)

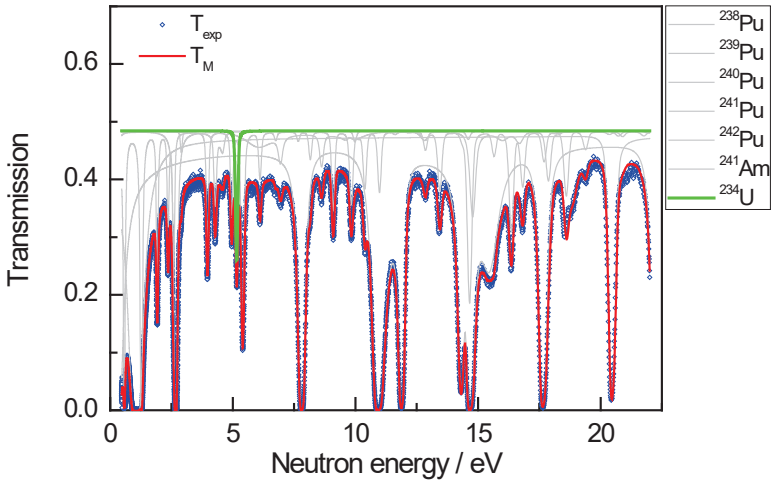

NRTA of PuO_2 sample: validation of resonance parameters

n_X/n_{Pu}

Nuclide	n_{REF}		n_{NRTA}				n_{NRTA} / n_{REF}			
			ENDF/B-VIII.0		JEFF-3.2		ENDF/B-VIII.0		JEFF-3.2	
^{238}Pu	0.009514	(20)	0.00783	(70)	0.00898	(70)	0.823	(74)	0.944	(74)
^{239}Pu	0.62603	(28)	0.62154	(90)	0.61530	(95)	0.9928	(14)	0.9829	(15)
^{240}Pu	0.25273	(24)	0.25699	(36)	0.26240	(32)	1.0169	(14)	1.0383	(13)
^{241}Pu	0.015697	(20)	0.01574	(10)	0.01577	(10)	1.0028	(64)	1.0045	(65)
^{242}Pu	0.041489	(60)	0.04334	(10)	0.04300	(10)	1.0447	(25)	1.0365	(24)
^{241}Am	0.06290	(63)	0.07236	(21)	0.06059	(20)	1.1503	(33)	0.9633	(32)
^{234}U	0.002918	(10)	0.00289	(10)	0.00287	(10)	0.989	(34)	0.982	(35)

RP in ENDF/B-VIII.0 for ^{241}Am are strongly biased: $\sigma(n,\gamma)$ underestimated

n: atomic abundance relative to total Pu
NRTA uncertainties only due to counting statistics

NRTA: characterisation of melted fuel

For **particle**- and **rock**- like debris of melted fuel the Lambert – Beer law is not directly applicable

Transmission is a non-linear function of n

- Homogeneous sample : $T = e^{-\,n\,\sigma_{tot}}$
- Heterogeneous sample : $< T > = < e^{-\,n\,\sigma_{tot}} > \neq e^{-<n>\,\sigma_{tot}}$

Levermore-Pomraning model (J. Math. Phys. 27, 2526, (1986))

- widely used for other problems dealing with radiation transport through stochastic media, e.g. scattering of sunlight in clouds
- starts from microscopic properties of the sample such as grain size
- in particular applicable for powder samples

implemented in **REFIT** and **validated** by experiments at **GELINA**

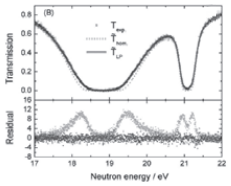

Becker et al., Eur. Phys. J. Plus 129 (2014) 58

PuO_2 mixed with carbon powder: NRTA at GELINA

^{242}Pu areal density : 2.51 10^{-5} at/b

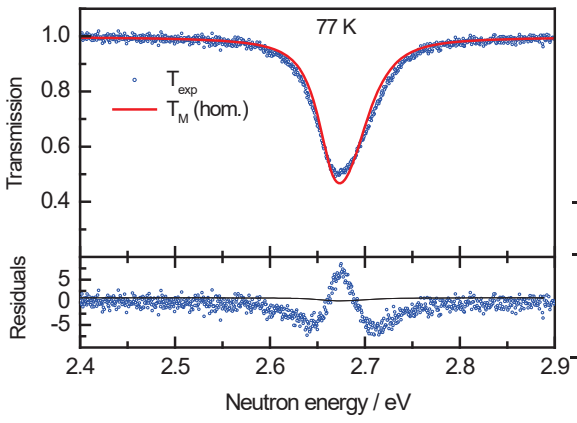

$$T_M(t_m, n) = \int R(t_m, E)\, T(E,n)\, dE$$

$$T(E, n_{1,\ldots,k}) = e^{-\sum_{j=1}^{k} n_j\, \sigma_{tot,j}(E)}$$

Suppose homogeneous without holes

Model	Areal density ^{242}Pu
Homogeneous	1.65 10^{-5} at/b

Underestimated by 35 %

Kopecky et al., ND2007, Nice, 2007

PuO_2 mixed with carbon powder: NRTA at GELINA

^{242}Pu areal density : 2.51 10^{-5} at/b

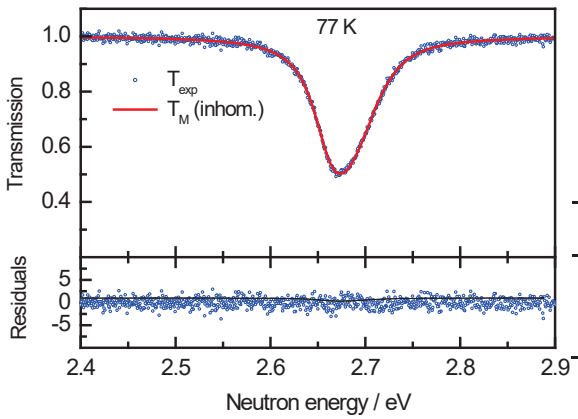

$$T_M(t_m, n) = \int R(t_m, E)\, T(E,n)\, dE$$

$$T(E, n) = \left[\int e^{-\sum_{j=1}^{k} n_k' \sigma_{tot,k}(E)} p(x)dx \right] (1 - f_h) + f_h$$

$$n_j' = \frac{n_j}{1 - f_h} \qquad p(x) = \frac{1}{x\sqrt{2\pi s^2}} \exp\left(-\frac{(\ln x + s^2/2)^2}{2s^2} \right)$$

Model	Areal density ^{242}Pu
Homogeneous	*1.65 10^{-5} at/b*
Inhomogeneous	2.50 10^{-5} at/b

⇒ bias < 1%

Model developed, implemented and validated at JRC Geel (S. Kopecky)

NRTA model for pellet samples

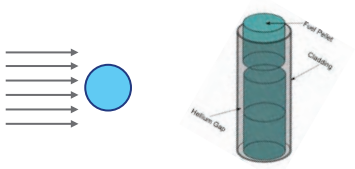

$$T(E) = f_h + (1 - f_h) \int_0^1 \frac{x}{\sqrt{1 - x^2}} e^{-\rho\, \sigma_{tot}(E)\, x}\, dx$$

REFIT

- x : track length (divided by 2R)
- f_h : holes fraction
- ρ : volume number density
- R : radius

Transmission through a pure Ag pellet sample

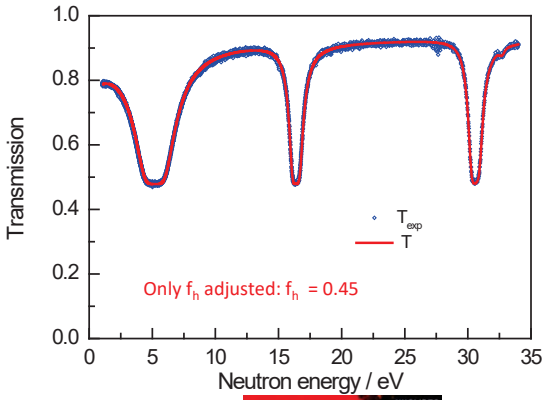

Model developed, implemented and validated at JRC Geel (S. Kopecky)

Fei Ma et al., J. Anal. At. Spectrom. 35 (2020) 478

NRTA: MINERVE samples

Collaboration with CEA Cadarche

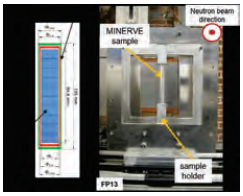

- NRTA of irradiated MINERVE pellet samples at GELINA (part of MAESRTRO)
  - Identification and quantification of impurities
  - Validation of resonance parameters of fission products
- Important for criticality safety studies based on Burn Up Credit (BUC)
- New transmission station (L = 10 m) constructed at GELINA

^{103}Rh
^{107,109}Ag
^{133}Cs
^{143,145}Nd
^{147,149,152}Sm,
^{151,153}Eu
^{161,162,163,164}Dy
^{168,170}Er
^{180}Hf

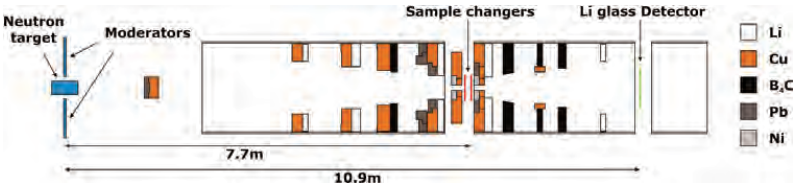

European Commission

NRTA: MINERVE samples

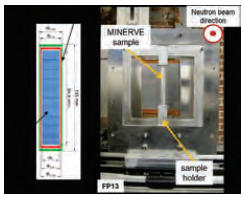

- NRTA of irradiated MINERVE pellet samples at GELINA (part of MAESRTRO)
  - Identification and quantification of impurities
  - Validation of resonance parameters of fission products
- Important for criticality safety studies based on Burn Up Credit (BUC)

^{109}Ag

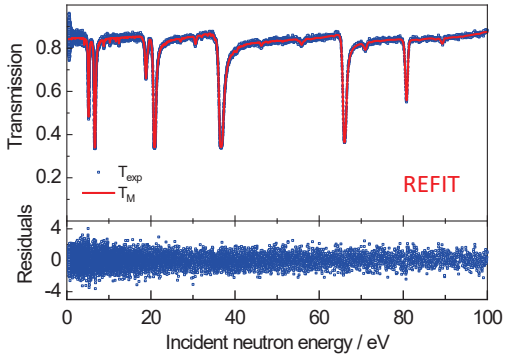

Note:

RP used result from a new evaluation for ^{107,109}Ag based on capture and transmission experiments at GELINA

Šalamon et al., Nucl. Instr. Meth. B 446 (2019) 19

European Commission

NRTA: MINERVE samples

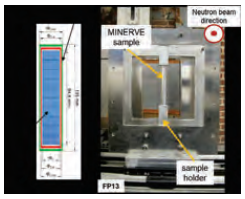

- NRTA of irradiated MINERVE pellet samples at GELINA (part of MAESRTRO)
  - Identification and quantification of impurities
  - Validation of resonance parameters of fission products
- Important for criticality safety studies based on Burn Up Credit (BUC)

^{109}Ag

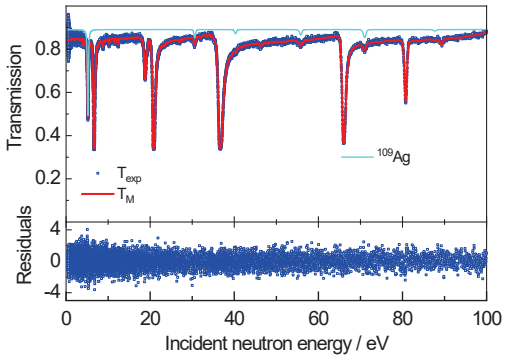

European Commission

NRTA: MINERVE samples

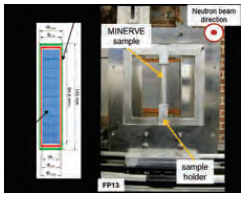

- NRTA of irradiated MINERVE pellet samples at GELINA (part of MAESRTRO)
  - Identification and quantification of impurities
  - Validation of resonance parameters of fission products
- Important for criticality safety studies based on Burn Up Credit (BUC)

^{109}Ag

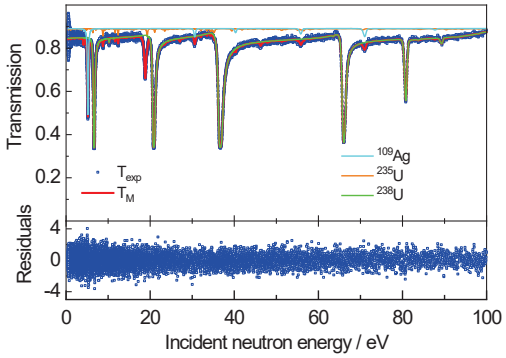

European Commission

NRTA: MINERVE samples

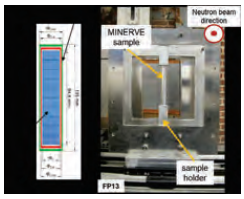

- NRTA of irradiated MINERVE pellet samples at GELINA (part of MAESRTRO)
  - Identification and quantification of impurities
  - Validation of resonance parameters of fission products
- Important for criticality safety studies based on Burn Up Credit (BUC)

^{109}Ag

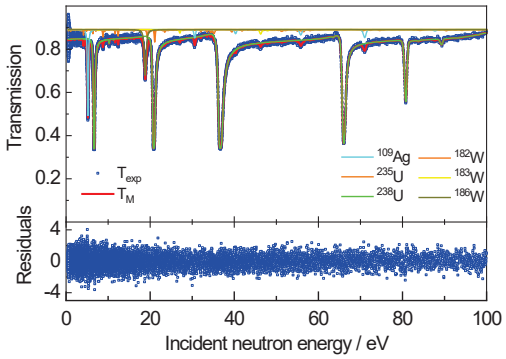

European Commission

NRTA: MINERVE samples

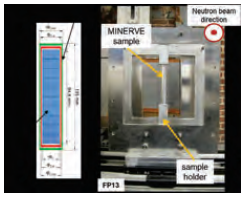

- NRTA of irradiated MINERVE pellet samples at GELINA (part of MAESRTRO)
  - Identification and quantification of impurities
  - Validation of resonance parameters of fission products
- Important for criticality safety studies based on Burn Up Credit (BUC)

^{109}Ag

	AG9C1		AG9C2	
	ICPMS	This work	ICPMS	This work
^{109}Ag	6.30 (8) x 10^{-4}	6.03 (2) x 10^{-4}	6.82 (8) x 10^{-5}	6.54 (2) x 10^{-5}
^{235}U	8.31 (10) x 10^{-5}	8.35 (20) x 10^{-5}	8.39 (10) x 10^{-5}	8.45 (20) x 10^{-6}
^{238}U	1.119 (14) x 10^{-2}	1.126 (5) x 10^{-2}	1.129 (14) x 10^{-2}	1.136 (5) x 10^{-2}
^{182}W		1.30 (4) x 10^{-5}		6.1 (3) x 10^{-6}
^{183}W		6.6 (2) x 10^{-6}		3.1 (2) x 10^{-6}
^{186}W		1.36 (1) x 10^{-5}		6.11 (3) x 10^{-6}

10^{24} at/cm^3

Šalamon et al., J. Radioanal. Nucl. Chem. 321 (2019) 519

European Commission

Back-end of the fuel cycle: spent fuel characterisation (SFC)

A **safe**, **secure**, **ecological** and **economic** handling, transport**,** intermediate storage and final disposal requires that **Spent Nuclear Fuel (SNF)** is **characterised** for the main observables or source terms of interest:

- Decay heat
- Neutron emission
- γ-ray emission
- Reactivity (BurnUp Credit) (i.e. Fission Product (FP), actinides)
- Fissile material (Nuclear Safeguards, i.e. ^{235}U, ^{239}Pu)
- Specific nuclides (Long term safety) i.e. ^{14}C, ^{36}Cl, ^{79}Se, ^{94}Nb, ^{99}Tc, ^{129}I, ^{226}Ra, ^{237}Np

⇒ requires knowledge of a **complex nuclide inventory**

⇒ can only be determined by **theoretical calculations**

Burnup calculations: e.g. SCALE, MCNP/CINDER, MCNP/ALEPH2, …

Coupled neutron transport – nuclide depletion/production

Neutron transport

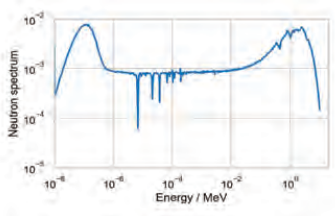

Bateman equation

$$\frac{dN_k}{dt} = Y\,N_f\,\sigma_f\,\varphi + \sum_{i\to k}\lambda_i N_i + \sum_{j\to k}\sigma_j N_j\,\varphi - (\lambda_k + \sigma_{k,a}\varphi)N_k$$

Update nuclide vector

Training material

Burnup calculations need to be validated

Nuclear data
- Cross sections: (n,γ), (n,f), …
- Fission Yields
- Decay data
  - Half-lives
  - Emission probabilities
  - Recoverable energy

Burnup code

SNF input data
- Fuel properties
  - design
  - material data (IE)
- Operational history
  - burn-up (BU)
  - cooling time (CT)
  - …

Source terms
- thermal power
- neutron emission
- γ-ray emission
- inventory specific nuclides
- …

One of the objectives of SFC
Validate by NDA experiment
- NRTA: nuclide inventory
- Neutron emission

Validation of depletion codes: neutron emission rate of SNF

NDA method to determine the neutron output of a **SNF** sample under **standard controlled area** conditions

Collaboration SCK CEN

Hot cell facility at SCK CEN

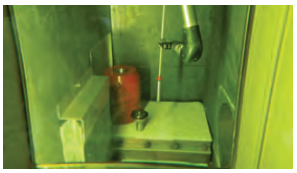

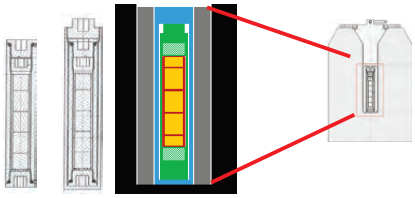

Standard controlled area

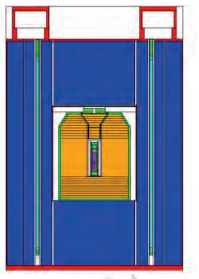

EURAD: Validation of depletion codes

- **Irradiation history** of the SNF
  - Segment (~ 50 mm) from rod D05 of FT1X57 (PWR)
  - PWR Assembly (15 x 15):
    188 UO_2 rod (4.5 wt% $^{235}U/U$) and 16 $(U,Gd)O_2$ rods
  - Irradiated at Tihange 1
  - Rod used for other international project
    (First-Nuclides, REGAL, WETFUEL & AGAF, SF-ALE)
- **SNF** segment **sample** by **NDA**

  Part of a set of 4 samples (**REGAL project**)
  - **Radiochemical analysis (BU)**
  - Microstructural analysis
  - Leach tests (low O_2)
  - Leach tests (high O_2)

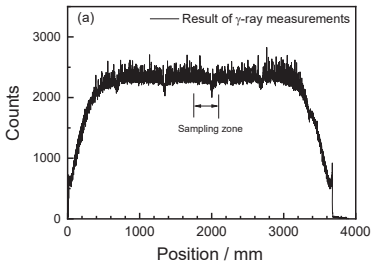

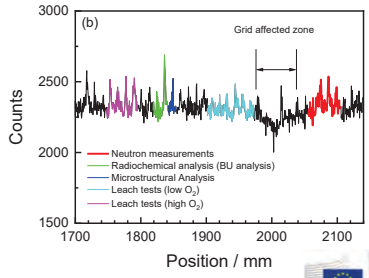

Results of radiochemical analysis

BU indicator	Date of analysis	Nuclide inventory mg/g	Cumulative fission yield (x 100)	Burnup GWd/t
^{137}Cs	10/21/2013	1.288 (28)	6.334	52.6 (11)
^{143}Nd + ^{144}Nd	02/05/2014	3.029 (32)	10.158	53.95 (56)
^{145}Nd + ^{146}Nd	02/05/2014	1.962 (21)	6.479	53.05 (56)
^{148}Nd	02/05/2014	0.534 (12)	1.724	53.3 (12)
^{150}Nd	02/05/2014	0.257 (11)	0.836	52.2 (23)
			Average:	52.78 (37)

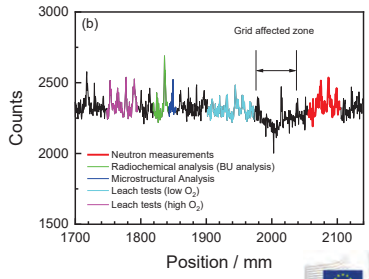

Schillebeeckx et al., JRC Technical Reports, EUR 30379 EN (2020)

Absolute neutron output of SNF segment sample: results

- SNF segment sample: characteristics

Parameter	Value
Length	52.01 (4) mm
Segment weight	42.616 (1) g
Cladding weight	6.71 (4) g
Net fuel weight	35.91 (4) g

- Neutron emission rate (exp) CT 18 a

S_{sf} = **24505 (375) s^{-1}**

$S_{\alpha n} / S_{sf}$ = 0.036 (15)

$\rho(S_{sf}, \alpha)$ = - 0.972

Neutron correlation analysis: Hage's point model
Hage and Cifarelli, Nucl. Instr. Meth. A236 (1985) 165

Detector calibrated with certified ^{252}Cf(sf) sources (Mn bath)

Note: neutron emission rate reflects ^{244}Cm inventory
radiochemical analysis uncertainty > 3%

Schillebeeckx et al., JRC Technical Reports, EUR 30379 EN (2020)

Absolute neutron output of SNF segment sample: code validation

Code	Library	(α,n) Method	(α,n) Library	S_{sf} / ($g^{-1}s^{-1}$)	S_{α} / ($g^{-1}s^{-1}$)	Calculation/Experiment S_{sf}	Calculation/Experiment $S_{\alpha n}$
SCALE	ENDF/B-VII.1	Y(α,n)		653	11.0	0.96	0.45
SERPENT(1)	ENDF/B-VII.1	Y(α,n)		689	14.3	1.01	0.58
SERPENT(2)	ENDF/B-VII.1	Y(α,n)		694	14.2	1.02	0.58
	ENDF/B-VIII.0	Y(α,n)		691	14.1	1.01	0.57
	JEFF-3.1.2	Y(α,n)		629	13.2	0.92	0.54
	JEFF-3.3	Y(α,n)		654	13.7	0.96	0.56
	JEFF-4T0	Y(α,n)		695	13.7	1.02	0.56
	JENDL-4.0			719	14.5	1.05	0.59
ALEPH28	ENDF/B-VIII.0	Y(α,n)		662	13.1	0.97	0.53
		σ(α,n)	TENDL2015		12.6		0.51
		σ(α,n)	JENDL_AN/500		10.6		0.43
	JEFF-3.3	Y(α,n		641	12.9	0.94	0.53
		σ(α,n)	TENDL2015		12.7		0.52
		σ(α,n)	JENDL_AN/500		10.5		0.43

All data normalised to ^{148}Nd inventory

Neutron emission rate:
- ^{244}Cm inventory
- Nuclear data: ^{241}Pu(n,γ) & ^{243}Am(n, γ)
- Very sensitive to BU

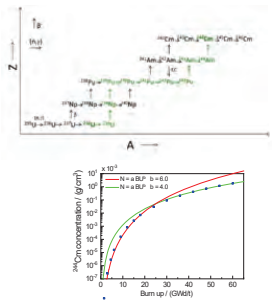

S_{sf} = 682 (10) g^{-1} s^{-1}

$S_{\alpha n} / S_{sf}$ = 0.036 (15)

⇒ influence
- nuclear data
- burnup code

NRTA on irradiated pellet ⇒ nuclide vector

- NRTA on spent fuel pellet at GELINA
  ⇒ **Nuclide vector by NDA** avoiding chemical analysis
- Analytical models already implemented in REFIT and validated at GELINA
- *Construct a transfer container fulfilling NRTA measurement requirements at GELINA*

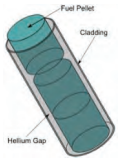

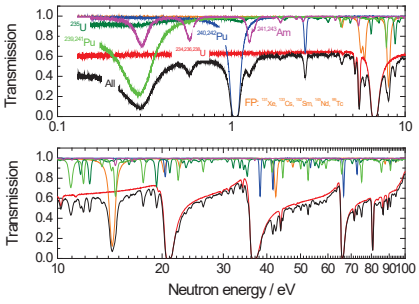

SNF: complex transmission spectrum, Priesmeyer et al.

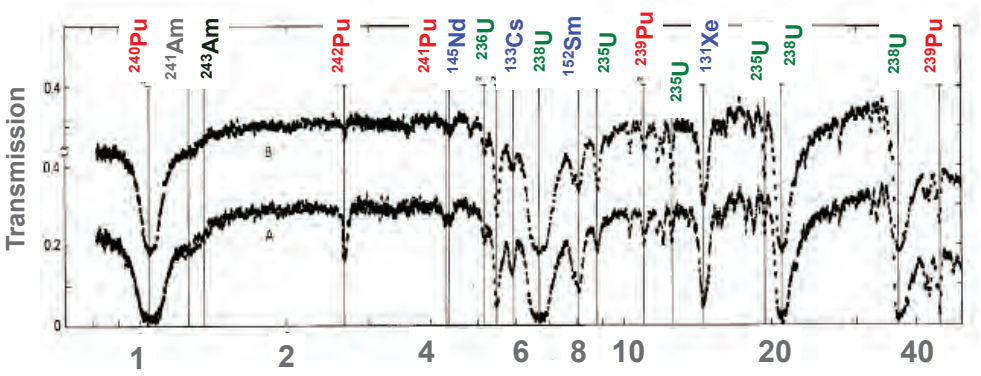

A : centre of fuel pin
B : end of fuel pin

H.G. Priesmeyer and U. Harz, Atomenergy 25 (1975) 109

Summary

- The use of NRCA & NRTA as NDA techniques for the characterisation of material and objects was presented
- Can be applied for a wide range of applications
  - Archaeology and cultural heritage
  - Validation of nuclear data
  - Nuclear waste
  - Imaging in case of high intense pulsed neutron beams (**LANSCE**, J-PARC)
  - …
- Use of NDA techniques important for SNF characterisation
  - Absolute determination of the neutron emission rate important to validate burnup codes: estimation of the ^{244}Cm inventory
  - NRTA: determine nuclide inventory (scheduled 2024…)

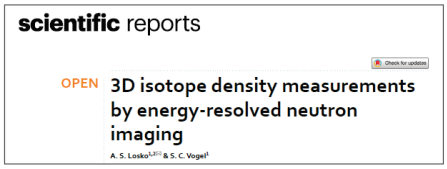
scientific reports

OPEN 3D isotope density measurements by energy-resolved neutron imaging

A. S. Losko[1,2*] & S. C. Vogel[1]

European Commission

Keep in touch

EU Science Hub: ec.europa.eu/jrc

@EU_ScienceHub

EU Science Hub – Joint Research Centre

EU Science, Research and Innovation

EU Science Hub

EU science

European Commission

Thank you

6.4 Untersuchung des Radionuklidinventars und chemischer Wechselwirkungsprozesse an der Grenzfläche zwischen Kernbrennstoff und Zircaloy-Hüllrohr von bestrahlten LWR-Brennstoffproben; R. Dagan, T. König et al., KIT; BGZ Studierendentag; 05 – 06/05/2022

Karlsruher Institut für Technologie

INE Institut für Nukleare Entsorgung

Untersuchung des Radionuklidinventars und chemischer Wechselwirkungsprozesse an der Grenzfläche zwischen Kernbrennstoff und Zircaloy-Hüllrohr von bestrahlten Leichtwasserreaktor-Brennstoffproben

T. König, R. Dagan, K. Dardenne, M. Herm, V. Metz, T. Prüßmann, J. Rothe, D. Schild, A. Walschburger und H. Geckeis

Karlsruher Institut für Technologie (KIT) - Institut für Nukleare Entsorgung (INE), 76344 Eggenstein-Leopoldshafen, Deutschland

KIT – Die Forschungsuniversität in der Helmholtz-Gemeinschaft

www.kit.edu

Vorstellung: Das Institut für Nukleare Entsorgung

Karlsruher Institut für Technologie

Wer sind wir?

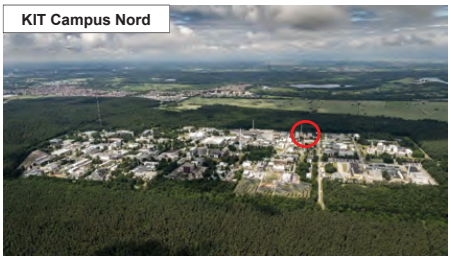

~90 Mitarbeiter und viele Studenten, Praktikanten, ausländische Gäste etc.

Gliederung

- **Einleitung:**
  - Kernbrennstoff – Vom Reaktor ins Endlager
- **Experimentelles:**
  - Untersuchte Kernbrennstoffe – *UO_X und MOX Brennstoff*
  - Radionuklidanalyse – *Inventarbestimmung von abgebrannten Kernbrennstoffen*
  - Spektroskopische Analysen – *Wechselwirkungsschicht zwischen Brennstoff und Hüllrohr*
  - Modellsysteme – *Experimente zur Bildung von Agglomeraten und Korrosion an der Reaktionsschicht*
- **Zusammenfassung**
- **Ein- & Ausblicke** – *Weitere Forschungsfelder am KIT-INE zu Zwischen- und Endlagerung*

Kernspaltung in Leichtwasserreaktoren

- **Neutroneninduzierte Fission** von spaltbarem Material (^{235}U, ^{239}Pu, etc.):
  - Freisetzung von Neutronen ➡ **Aufrechterhaltung der Kettenreaktion**.
  - Generierung von Spaltprodukten ➡ **2 – 3 Spaltfragmente pro Kernspaltung**.
  - Neutroneneinfangsreaktionen ➡ **Aufbau von Transuranen (Np, Pu, Am, etc.) & Aktivierungsprodukten (^{14}C, ^{36}Cl).**
- Brennstoffnutzung wird als **Abbrand** beschrieben:

➡ **Produzierte Energie pro Masse initialem Schwermetall [GWd/t_{SM}].**

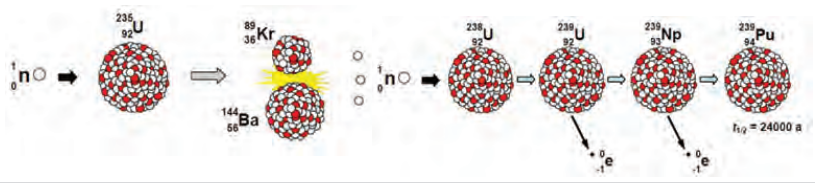

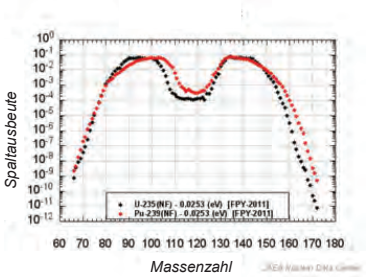

Abgebrannter Kernbrennstoff (KBS)

- Zusammensetzung von abgebranntem KBS (4,0% ^{235}U, 52 GWd/t_{SM}) in einem Leichtwasserreaktor:
  - **93,4% UO_2 Matrix:**
    92% ^{238}U, < 1% ^{235}U, < 0,5% ^{236}U
  - **1,2% Transurane / Actinide:**
    1% ^{239}Pu, ^{240}Pu, ^{241}Pu, ^{237}Np > ^{244}Cm > ^{241}Am,
  - **5,4% Spaltprodukte:**
    1,7% ^{90}Sr, $^{135, 137}Cs$, ^{129}I, etc.
    1,6% Lanthaniden
    1,3% ε-Phasen (^{99}Tc, ^{109}Pd, etc.)
    0,8% Spaltgase (Krypton, Xenon)
  - **Aktivierungsprodukte:**
    z. B. ^{14}C, ^{93}Zr, ^{36}Cl → **^{35}Cl (n,γ) ^{36}Cl**

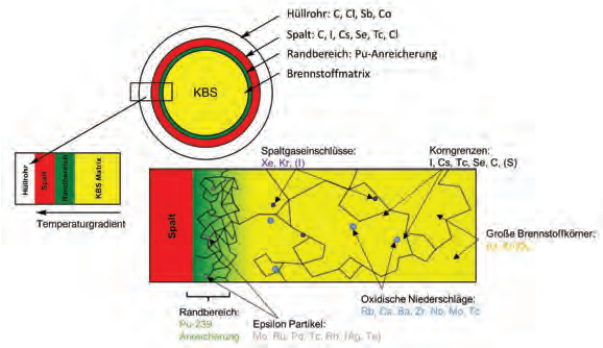

→ **Heterogene Verteilung der Radionuklide.**

Quelle: Hippler, Reaktorchemie, Leibniz Universität Hannover

Wechselwirkungsschicht zwischen KBS und Hüllrohr

- **Querschnitt einer Kernbrennstofftablette:**

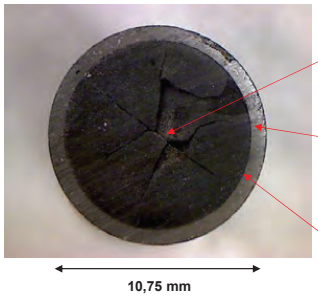

Pellet: Radiale Rissbildung durch Temperaturgradienten während der Bestrahlung; Migrationspfade für Radionuklide in der KBS Tablette.

Hüllrohr: Aufbau einer äußeren ZrO_2 Schicht durch Korrosion auf Grund des Primärkreislaufwassers; dünne ZrO_2 Schicht auf der Innenseite durch Zr / UO_2 Reaktionen.

Ringspalt: Schließt sich bei Abbränden > 40 GWd/t_{SM}; Ausbildung einer **Wechselwirkungsschicht.**

→ **Möglichkeit des Transports volatiler Spalt- und Aktivierungsprodukten zum Hüllrohr während der Bestrahlung und nachfolgende chemische Reaktionen zwischen KBS und Hüllrohr!**

Zwischenlagerung in Deutschland

- **Trockene Zwischenlagerung** ausgedienter Brennelemente in Transport-Lagerbehältern (TLB).
  - TLB garantiert **Abschirmung der Strahlung**, sowie einen temporären, **sicheren Einschluss der Radionuklide**.
  - Zwischenlagerung bestrahlter Brennelemente ist lediglich **für 40 Jahre genehmigt.**
  - Endlager voraussichtlich **erst 2050 verfügbar und Einlagerung der letzten Brennelemente erst einige Jahrzehnte später möglich!**

➡ **Notwendigkeit einer verlängerten Zwischenlagerung von 65 – 100 Jahren sowie Umlagerung (Konditionierung) von TLB in Endlagerbehälter!**

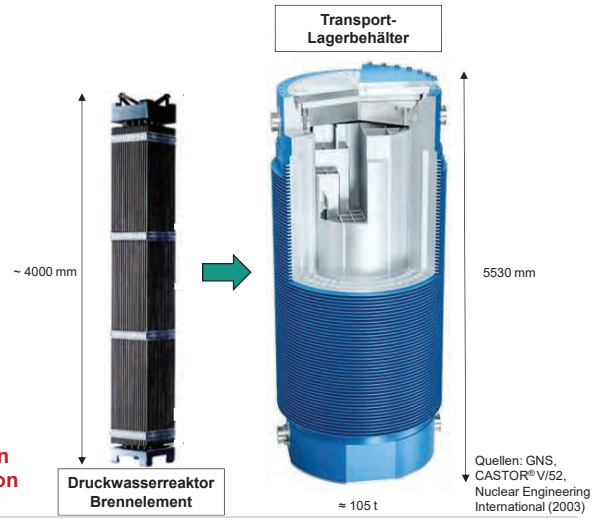

Vom Reaktor ins Endlager | Materialien und Methoden | Radionuklidanalyse | Spektroskopische Analysen | Zusammenfassung

Zwischenlagerung in Deutschland

- **Trockene Zwischenlagerung** ausgedienter Brennelemente in Transport-Lagerbehältern (TLB).
  - TLB garantiert **Abschirmung der Strahlung**, sowie einen temporären, **sicheren Einschluss der Radionuklide**.
  - Zwischenlagerung bestrahlter Brennelemente ist lediglich **für 40 Jahre genehmigt.**
  - Endlager voraussichtlich **erst 2050 verfügbar und Einlagerung der letzten Brennelemente erst einige Jahrzehnte später möglich!**

- Verschiedene Effekte beeinflussen die Integrität des Hüllrohrs während der Zwischenlagerung:
  - **Erhöhung des Hüllrohrinnendrucks** durch Schwellen der Pellets und α-Zerfälle.
  - **α-Strahlungsinduzierte Schädigung** des Hüllrohrs.
  - Rissbildung durch **Hydrid Re-Orientierung**.

$$Zr + 2\,H_2O \rightarrow ZrO_2 + 2\,H_2$$

  - **Korrosion des Hüllrohrs durch Spalt- und Aktivierungsprodukte**.

➡ **Bildung von Agglomeraten an Hüllrohrinnenseite durch thermischen Gradienten im KBS und somit Möglichkeit einer halogeninduzierten Spannungsrisskorrosion**.

Endlagerung in Deutschland

- Tiefengeologische Endlagerung:
  - **3 unterschiedliche Gesteinsarten** (Ton-, Salz- und Kristallingestein) werden in Betracht gezogen.
  - **Sicherer Einschluss über langen Zeitraum** muss gewährt werden (1 Million Jahre).

Sicherheitsbewertung erfordert grundlegende Kenntnisse über das Vorkommen und chemisches Verhalten von langlebigen und dosisrelevanten Radionukliden (z. B.^{36}Cl, ^{129}I, ^{135}Cs)

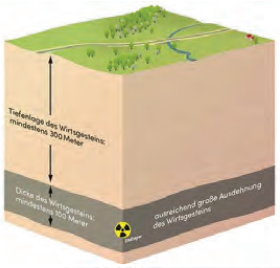

Quelle: https://www.einblicke.de/fileadmin/images/magazin/Einblicke_6/Kriterien_zur_Endlagersuche.jpg (aufgerufen am 04.04.2022)

[FLA18]: D. Flamikova, V. Necas, *Creation of Reference Biosphere Model for Safety Assessment of Deep Geological Repository*, AIP Conference Proceedings 1996, 020009 (2018).

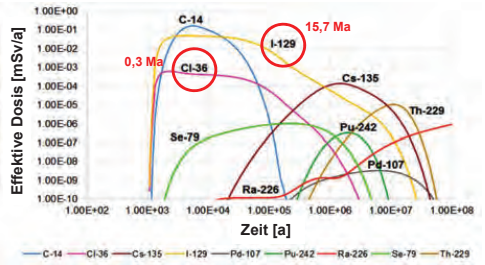

Fragestellung

- Wenn nach längerer Zeit (geo-) technische Barrieren den Zutritt von Wasser nicht mehr vollständig verhindern, werden ^{36}Cl und ^{129}I in Kernbrennstoff relativ wenig zurückgehalten! In welcher Konzentration und in welcher Form liegen ^{36}Cl und ^{129}I in Brennstäben vor?
  - **Quantifizierung und Lokalisierung von den unter Endlagerbedingungen relativ mobilen Radionukliden ^{36}Cl und ^{129}I in Kernbrennstoff und Hüllrohr.**
  - **Vergleich experimentell bestimmter Radionuklidkonzentrationen mit berechneten Inventardaten aus (neutronen-) physikalischen Modellierungen.**
- In welchem Zustand ist die Brennstoff-Hüllrohr-Grenzfläche während der Zwischenlagerung?
  - **In welcher Form liegen eventuell hüllrohrschädigende Elemente wie Chlor oder Iod in KBS und Hüllrohr vor?**
  - **Ist eine halogeninduzierte Lochfraßkorrosion auch bei Zwischenlagerungstemperaturen möglich?**

Kernbrennstoffproben

Brennstabsegment N0204, bestrahlt im Druckwasserreaktor, DWR Gösgen:

- Brennstofftyp: **UO_X** mit 3,8% ^{235}U Anreicherung.
- Hüllrohr: Zircaloy-4.
- Volllasttage: 1226 Tage in 4 Zyklen.
- Durchschnittliche lineare Leistung: 260 W/cm.
- Durchschnittlicher Abbrand: **50,4 GWd/t_{SM}**.
- Abklingzeit: ~ 32 Jahre.

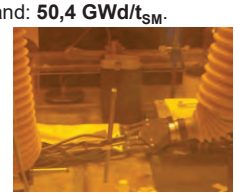

Brennstab 5810, bestrahlt im Druckwasserreaktor, DWR Obrigheim:

- Brennstofftyp: **MOX** mit 3,2% Pu_{fiss} Anreicherung.
- Hüllrohr: Zircaloy-4.
- Volllasttage: 1157 Tage in 4 Zyklen.
- Durchschnittliche lineare Leistung: 200 W/cm.
- Durchschnittlicher Abbrand: **38,0 GWd/t_{SM}**.
- Abklingzeit: ~ 35 Jahre.

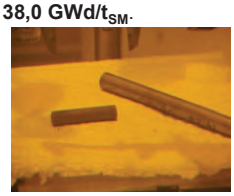

Präparation der Brennstoffproben

- Zuschneiden der Brennstoffproben in speziell ausgestatteten Laboren (**Heiße Zellen)** auf Grund der enormen Dosisleistung!
- Selektive Probennahme zur **Analyse lokaler Radionuklidanreicherungen**:
  - Fragmente aus **zentraler Position („CORE“)**.
  - Fragmente aus **peripherer Position („RIM“)**.
  - **Zircaloy-Hüllrohrsegmente**.

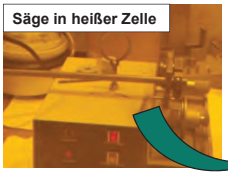

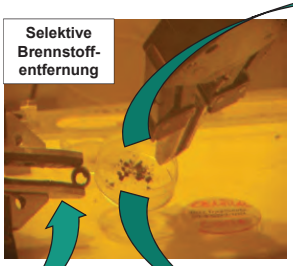

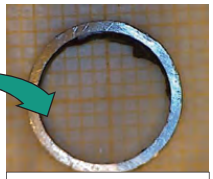

Vom Reaktor ins Endlager | Materialien und Methoden | Radionuklidanalyse | Spektroskopische Analysen | Zusammenfassung

Radiochemische Analytik & numerische Berechnungen

- **Saurer und alkalischer Aufschluss** von Zircaloy- und Brennstoffproben in HF / H_2SO_4, HNO_3 / HCl oder $(NH_4)_2CO_3$ / H_2O_2:
  - **γ-Spektrometrie:** ^{241}Am, $^{134, 137}$Cs, ^{125}Sb, $^{154, 155}$Eu, ^{60}Co, **^{129}I**.
  - **Flüssigszintillationsmessung: ^{129}I, ^{36}Cl**, ^{90}Sr. ➡ **Sehr hohe Reinheit der Proben erforderlich!**
  - **ICP-MS:** $^{235, 238}$U, ^{237}Np, $^{239, 240}$Pu, ^{241}Am, ^{244}Cm.
  - **Gas-MS:** Kr- und Xe-Isotope.
- **Berechnungen des Radionuklidinventars** mittels **MCNP Code** für Neutronenfluss und **CINDER Modul** für Abbrand-Berechnungen:
  - Numerische Berechnungen für die jeweiligen Brennstoffanordnungen, Reaktortypen und Bestrahlungsbedingungen.
  - Radionuklidkonzentrationen im zentralen und Randbereich des Pellets.


Aufschluss in Autoklaven für Spaltgasbestimmungen

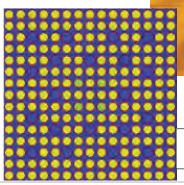
Simulationen der Brennstoffanordnungen

Vom Reaktor ins Endlager | Materialien und Methoden | Radionuklidanalyse | Spektroskopische Analysen | Zusammenfassung

Spektroskopische Messungen

- Präparation von Brennstofffragmenten und Zircaloy-Segmenten für Analysen mittels **SEM-EDX/-WDX**, **XPS** und **XAS an der KIT Light Source**. ➡ **Enorme Strahlenschutzmaßnahmen erforderlich!**
  - Proben für **Bestimmung der chemischen Zusammensetzung**.
  - Proben für **Speziationsmessungen**.

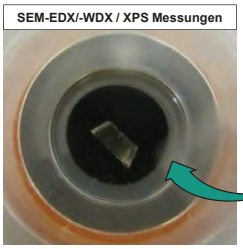
SEM-EDX/-WDX / XPS Messungen

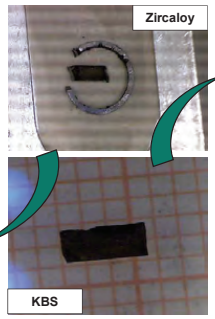


XAS Messungen für Cl und I Speziation


Karlsruhe Research Accelerator (KARA)

Vom Reaktor ins Endlager | Materialien und Methoden | Radionuklidanalyse | Spektroskopische Analysen | Zusammenfassung

Radionuklidanalyse – Trennungsgang ^{36}Cl / ^{129}I

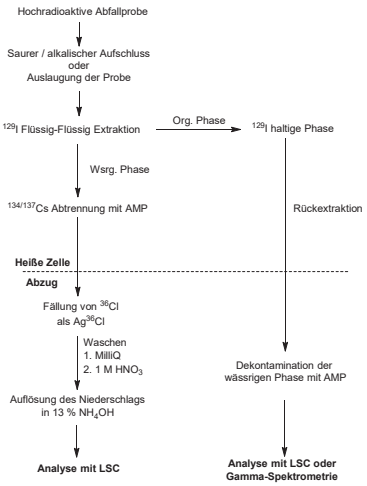


Cäsiumabtrennung mit AMP

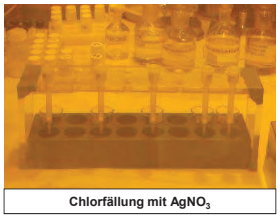
Chlorfällung mit $AgNO_3$

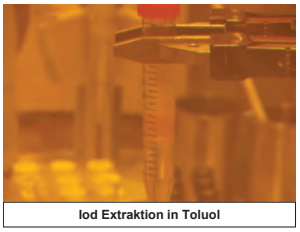
Iod Extraktion in Toluol

Chemische Ausbeute Chlor = 94±2%

Chemische Ausbeute Iod = 93±3%

Gute Ausbeuten trotz komplizierten Matrices und Arbeiten in hochkontaminierten Bereichen!

Vom Reaktor ins Endlager | Materialien und Methoden | Radionuklidanalyse | Spektroskopische Analysen | Zusammenfassung

Radionuklidanalyse – ^{36}Cl in KBS und Zircaloy

^{36}Cl Inventare	KBS		Zircaloy-Hüllrohr	
Probe	UO_X 50,4 GWd/t_{SM} [Bq/t_{SM}]	MOX 38,0 GWd/t_{SM} [Bq/t_{SM}]	UO_X 50,4 GWd/t_{SM} [Bq/t_{SM}]	MOX 38,0 GWd/t_{SM} [Bq/t_{SM}]
Experimentell	$3{,}62(\pm0{,}54)\times10^8$	$5{,}80(\pm0{,}87)\times10^8$	$6{,}32(\pm0{,}28)\times10^8$	$5{,}33(\pm0{,}24)\times10^8$
Berechnet	$4{,}73\times10^8$	$3{,}68\times10^8$	$6{,}57\times10^8$	$5{,}23\times10^8$
Verhältnis (exp/ber)	0,77 ± 0,12	1,58 ± 0,24	0,96 ± 0,04	1,02 ± 0,05

^{35}Cl (n,γ) ^{36}Cl

Numerische Berechnungen auf Grundlage „expert judgement“ 15 ppm ^{35}Cl Precursor in KBS und Hüllrohr [HÄK19].

Experimentelle Aktivitätsinventare sind in Einklang mit Berechnungen.

[HÄK19] S. Häkkinen, *Impurities in LWR fuel and structural materials*, VTT, Finnland (2019).

Erstmalige Analyse von ^{36}Cl in DWR Brennstoffkomponenten!

Radionuklidanalyse – Spaltprodukte

- Bestimmung des Spaltproduktinventars von **KBS Fragmenten aus der Wechselwirkungsschicht** und Vergleich mit MCNP Berechnungen.
- Keine signifikanten Unterschiede zwischen **UO_X (50,4 GWd/t_{SM})** und **MOX (38,0 GWd/t_{SM})** Brennstoff.

Vergleich des ^{129}I Inventars [Bq/t_{SM}]

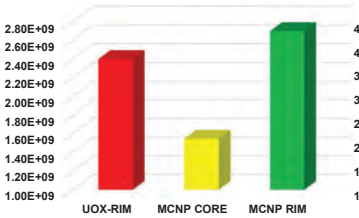

Vergleich des ^{137}Cs Inventars [Bq/t_{SM}]

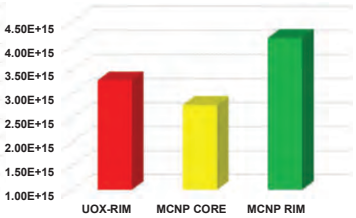

Vergleich MOX und UO_X KBS [Bq/t_{SM}]

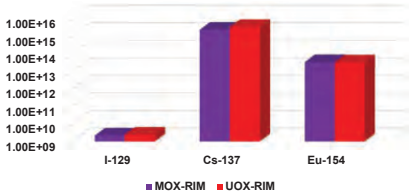

Erhöhte ^{129}I und ^{137}Cs Aktivität durch einen Anreicherungseffekt an der Hüllrohrgrenzfläche auf Grund des höheren lokalen Abbrands und dem Transport von Iod entlang eines thermischen Gradienten im Pellet.

Radionuklidanalyse – Actiniden

- Experimentelle und berechnete Inventardaten der Actiniden für verschiedene Regionen im Pellet in UO_X KBS.
- MOX Brennstoff zeigt im Vergleich zu UO_X Brennstoff eine **erhöhte Aktivität von minoren Actiniden** auf Grund des **erhöhten initialen Pu Gehalts**.

Vergleich MOX und UO_X [Bq/t_{SM}]

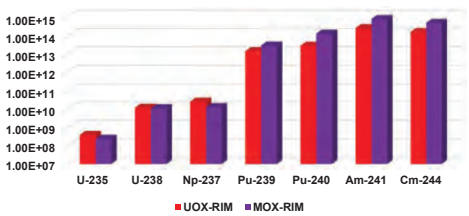

Vergleich des Actinideninventars [Bq/t_{SM}]

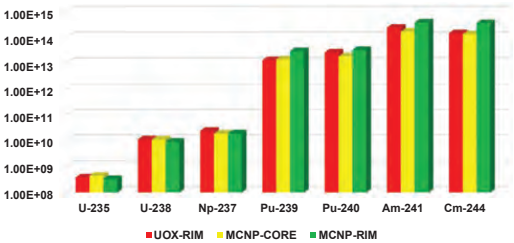

Inventarkenntnisse der Transurane sind wichtig für Berechnungen zu α-Strahlungsinduzierter Schädigung des Hüllrohrs während der Zwischenlagerung.

Vom Reaktor ins Endlager | Materialien und Methoden | Radionuklidanalyse | Spektroskopische Analysen | Zusammenfassung

Spektroskopische Analysen – SEM-EDX

- **Zircaloy in Kontakt mit abgebranntem UO_x / MOX KBS:**
  - **SEM-EDX:** Cl, Te, I, Cs, Fe, Zr, Ba, U.
  - **XPS:** Cl, Te, Cs, Fe, Zr, Ba, U.

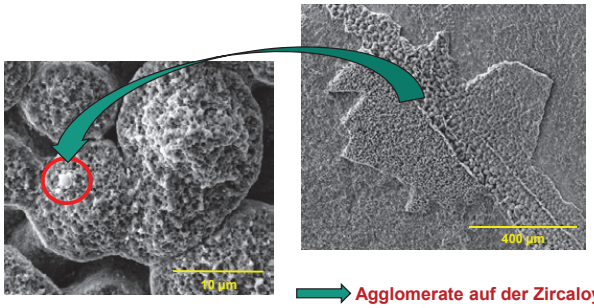

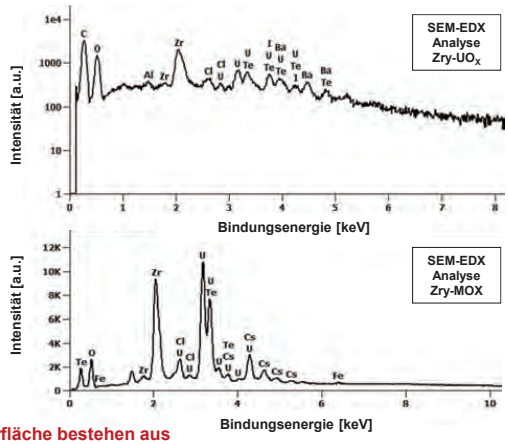

➡ **Agglomerate auf der Zircaloy Oberfläche bestehen aus U-O-Zr-Cs-Cl-I haltigen Phasen.**

Vom Reaktor ins Endlager | Materialien und Methoden | Radionuklidanalyse | Spektroskopische Analysen | Zusammenfassung

Spektroskopische Analysen – XAS

- Kenntnisse zur Konzentration und zur Speziation von Chlor (und Iod) in KBS und Zircaloy sind mit großen Unsicherheiten verbunden.
- Annahmen zur maximalen Chlor-Verunreinigung beziehen sich auf bis zu 25 ppm Cl im KBS und 20 ppm Cl in Zircaloy-Hüllrohren.
- **Erstmalige XAS Messungen für Iod und Chlor Speziation** in KBS und Zircaloy. ➡ **Komplexe Mischphasen!**

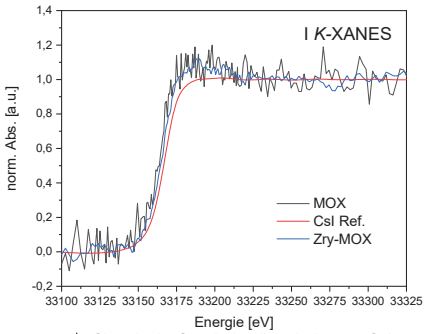

➡ **Chemische Speziation ähnelt der von CsI.**

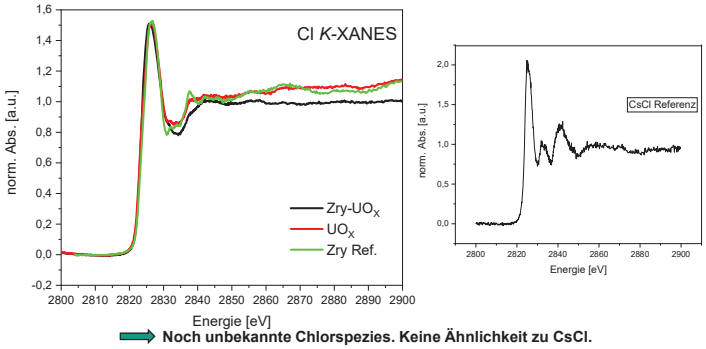

➡ **Noch unbekannte Chlorspezies. Keine Ähnlichkeit zu CsCl.**

Spektroskopische Analysen – Modellsystem

- Laborexperimente zur Ausbildung von Agglomeraten und Lochfraßkorrosion unter simulierten Zwischenlagerbedingungen:
  - **Cäsiumhalogenide in Kontakt mit Zircaloy und UO_2 Pellet** unter Ar Atmosphäre.
  - **Temperaturreduktion über 3 Monate** von 400°C auf Raumtemperatur.
  - Anschließende Analyse mit SEM-EDX und XPS.

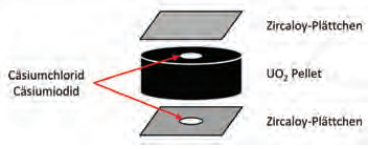

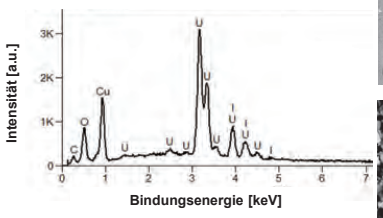

Halogeninduzierte Lochfraßkorrosion

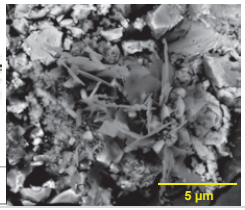

Ausbildung halogenreicher Agglomerate

Bestätigung der Mischphasenbildung und Lochfraßkorrosion bei T < 400°C!

Zusammenfassung

- **Radionuklidanalyse:**
  - Abtrennungsmethode für **^{36}Cl und ^{129}I aus hochradioaktiven Proben** entwickelt.
  - **Erstmalige Analyse des ^{36}Cl Inventars** in Druckwasserreaktor-Brennstoffkomponenten.
  - **Nachweis** von Iod-reichen Anreicherungen in der Wechselwirkungsschicht zwischen KBS und Zircaloy-Hüllrohr.
  - Gute Übereinstimmung zwischen Berechnungen und experimentell bestimmten Radionuklid-Inventardaten.
- **Spektroskopische Analysen:**
  - **Erstmalige Cl *K*- und I *K*-Kanten Messungen** an hochradioaktivem Material (KBS und Zircaloy).
  - Agglomerate in der Wechselwirkungsschicht bestehen unter anderem aus **halogenreichen Mischphasen (Cl und I)**, sowie Cs, Te, Ba, U und Pu.
  - **Bestätigung der ausgebildeten Agglomerate und Lochfraßkorrosion bei T < 400°C unter Laborbedingungen**.

Ein- & Ausblicke – (Nano-)mechanische Prüfverfahren

- Experimente zur Untersuchung der strukturellen Integrität von Hüllrohren nach Bestrahlung.
  ➡ **Anschwellen der KBS-Tablette.**
- Bestimmung des **Hüllrohrdurchmessers** und **Berechnung von Umfangsspannungen vor und nach Entfernen des Brennstoffs.**

➡ **INE-Beitrag zu BMWK SPIZWURZ.**

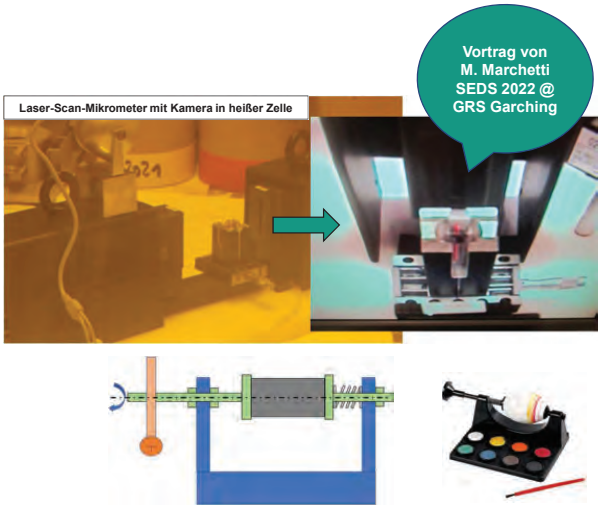

Ein- & Ausblicke – Strahlungsschäden

- **Untersuchungen von Strahlungsschäden** verursacht durch Actiniden an der Hüllrohr-KBS-Grenzfläche.
- Akkumulierte Schädigung während der Zwischenlagerung kann mittels **Monte Carlo basierten Codes** (z.B. FLUKA) und / oder **Messungen der Defekte mittels XRD / TEM** bestimmt werden.
- Untersuchung der **Korrelation zwischen mechanischen Eigenschaften** des Hüllrohrs bei Raumtemperatur und **Strahlungsschäden, zusammen mit Hydridgehalt und Hydrid-Morphologie**.

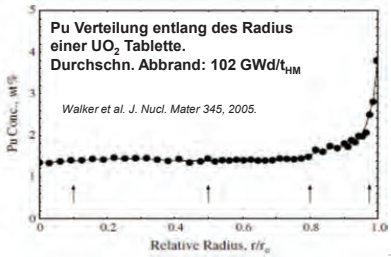

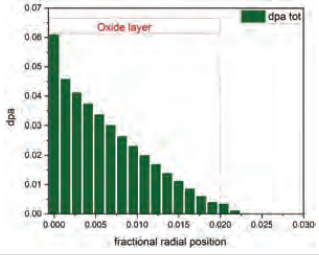

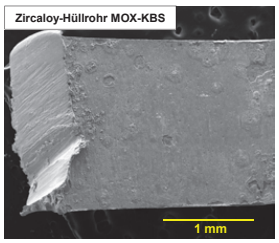

Ein- & Ausblicke – „Neues" Equipment am INE

- Raman-Sonden (**532 und 633 nm**) in heißen Zellen.
- Kalt-Einbettpresse (**VACUMET 52**).
- Schleif- und Poliermaschinen (**Bühler MiniMet 1000** und **VibroMet 2**).
- Nano-Indenter (**Femto-Indenter FT-104**).

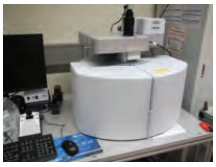

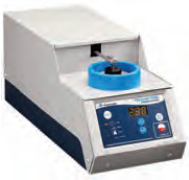

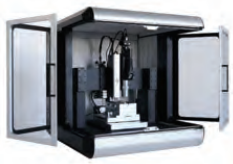

In heißer Zelle! **In Handschuhboxen**

BMWK KEK geförderte Doktorandenstelle

- **Untersuchung von Hüllrohr-Degradationsprozessen, insbesondere den kombinierten Einfluss von Hydriden, lokalen Spannungen und der Rolle von Strahlungsschäden während der trockenen Zwischenlagerung von abgebranntem KBS.**
- **Doktorarbeit ist in drei Arbeitspakete (AP) unterteilt:**
  - **AP1:** Probenpräparation und Charakterisierung; Hydridgehalt und Hydrid-Morphologie, Dicke der Oxidschicht und Material-Mikrostrukturanalysen mittels **SEM, EBSD und Synchrotron XRD**.
  - **AP2:** Evolution von mechanischen Eigenschaften des Hüllrohrs: **Lokale Elastizitätsmodule**, Härte wird mit **Nano-Indentierung** untersucht.
  - **AP3:** Untersuchung des **Einflusses von Strahlungsschäden** auf das Hüllrohr mit Modellen (z.B. FLUKA, PHITS).

Bei Interesse: Einfach anfragen, anschreiben oder anrufen!

Ein- & Ausblicke – KBS Korrosionsexperimente

- **Langzeituntersuchungen (~ 4 Jahre) zum Freisetzungsverhalten von Radionukliden** aus abgebranntem KBS in z.B. simulierten Grundwasserlösungen.
- **Korrosionsexperimente in Autoklaven unter Endlagerbedingungen (pH, red. Bedingungen, etc.)** und Analyse der Gasphase / Lösung.

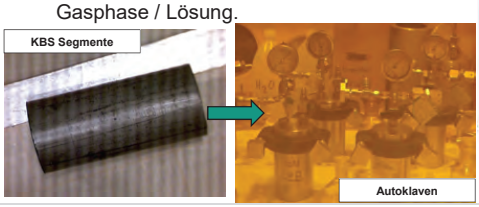

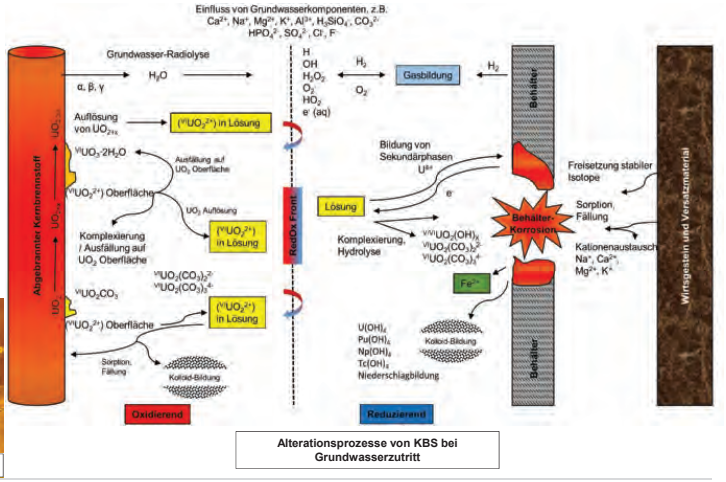

1980 - 2020
INE - 40
Institut für Nukleare Entsorgung

This project has received funding from the European Union's Horizon 2020 research and innovation programme under grant agreement N°847593

Danke für Ihre Aufmerksamkeit.

6.5 SFC Task 2: Fuel properties characterisation and related uncertainty analysis (summary and status); P. Schillebeeckx, JRC Geel; IAEA CRP spent fuel characterization ; 22 – 23/09/2022

European Joint Programme on Radioactive Waste Management

Spent Fuel Characterization and evolution until disposal

Task 2: Fuel properties characterisation and related uncertainty analysis

Ron Dagan	KIT
Dimitri Rochman	PSI
Peter Schillebeeckx	**JRC Geel (co-ordinator)**
Marcus Seidl	PEL
Marc Verwerft	SCK•CEN

Partners:

CIEMAT, CPST, CTU (SURAO), ENRESA, ENUSA, JRC, JSI, KIT, LEI, NAGRA, PEL, PSI, SCK•CEN, SKB, SSTC NRS, TUS, VTT, UU

ESARDA, 6 - 7 february 2020, SCK CEN Mol (BE)

European Commission

Spent Nuclear Fuel (SNF) intermediate storage or final disposal

A **safe**, **secure**, **economic** and **ecological** transport**,** storage and final disposal requires that **SNF** is **characterised** for the main source terms of interest:

- Decay heat
- Neutron emission
- γ-ray emission
- Reactivity (burnup credit)
  nuclides with high neutron absorption cross section)
- Fissile material (Safeguards)
  i.e. ^{235}U, ^{239}Pu
- Specific long-lived radionuclides (Long term safety)
  e.g. ^{14}C, ^{79}Se, ^{94}Nb, ^{99}Tc, ^{129}I, ^{226}Ra

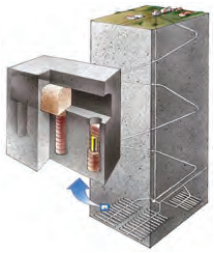

ESARDA, 6 - 7 february 2020, SCK CEN Mol (BE)

European Commission

Neutron emission by SNF

$$S_n(t) = \sum_k S_{n,k}(t)$$

- $S_{n,k}(t)$: contribution of radionuclide k
- $S_{n,k}(t) = (s_{sf,k} + s_{\alpha n,k})\, N_k(t)$
  - $N_k(t)$: number of nuclei of nuclide k at time t
  - $s_{sf,k}$: specific neutron emission rate of nuclide k due to sf
  - $s_{\alpha,k}$: specific neutron emission rate of nuclide k due to (α,n) reactions

PWR UO_2 pellet (5 g)
$^{235}U/U$ = 4.8 %
burnup = 44 GWd/t

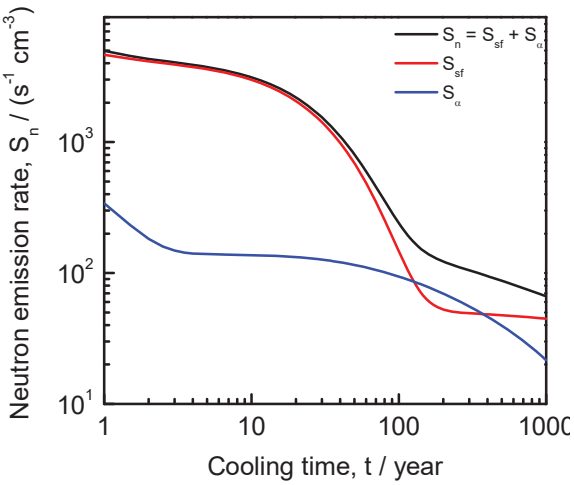

European Commission

Neutron emission by SNF

$$S_n(t) = \sum_k (s_{sf,k} + s_{\alpha n,k}) N_k(t)$$

PWR UO_2 pellet (5 g)
$^{235}U/U$ = 4.8 %
burnup = 44 GWd/t

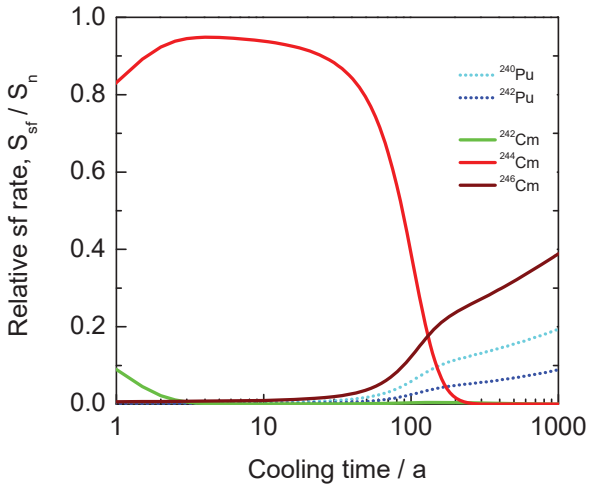

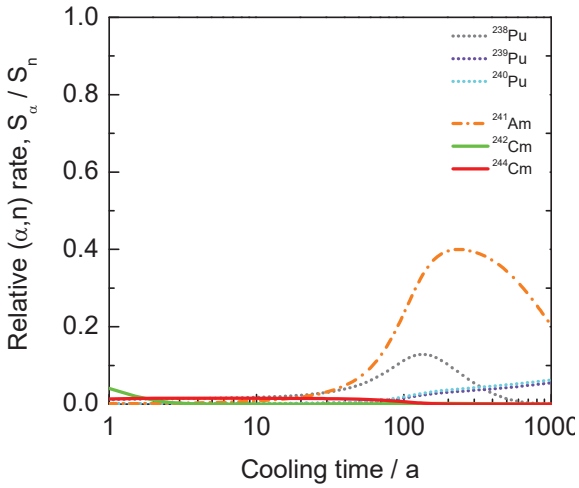

European Commission

Gamma-ray emission by SNF

$$S_\gamma(t) = \sum_k S_{\gamma,k}(E_\gamma, t)$$

PWR UO_2 pellet (5 g)
$^{235}U/U$ = 4.8 %
burnup = 44 GWd/t

^{95}Nb	35.0 d
^{95}Zr	64.0 d
$^{144}Ce/^{144}Pr$	284.9 d
$^{106}Ru/^{106}Rh$	1.02 a
^{134}Cs	2.06 a
^{154}Eu	8.8 a
$^{137}Cs/^{137m}Ba$	30.0 a

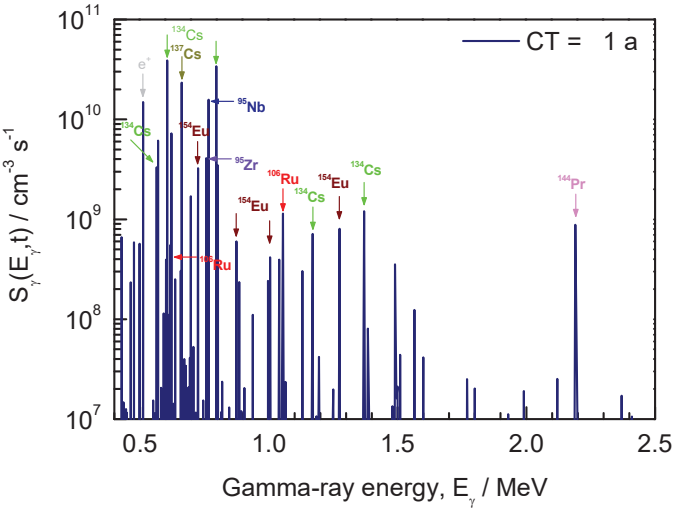

Gamma-ray emission by SNF

$$S_\gamma(t) = \sum_k S_{\gamma,k}(E_\gamma, t)$$

PWR UO_2 pellet (5 g)
$^{235}U/U$ = 4.8 %
burnup = 44 GWd/t

^{95}Nb	35.0 d
^{95}Zr	64.0 d
$^{144}Ce/^{144}Pr$	284.9 d
$^{106}Ru/^{106}Rh$	1.02 a
^{134}Cs	2.06 a
^{154}Eu	8.8 a
$^{137}Cs/^{137m}Ba$	30.0 a

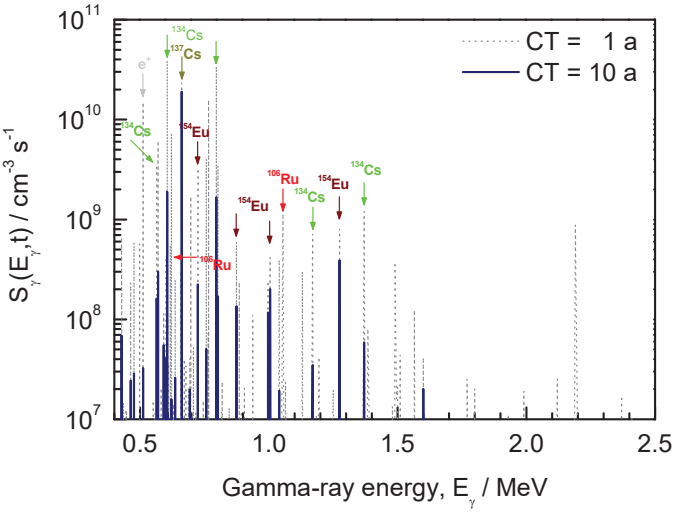

ESARDA, 6 - 7 february 2020, SCK CEN Mol (BE)

Gamma-ray emission by SNF

$$S_\gamma(t) = \sum_k S_{\gamma,k}(E_\gamma, t)$$

PWR UO_2 pellet (5 g)
$^{235}U/U$ = 4.8 %
burnup = 44 GWd/t

^{95}Nb	35.0 d
^{95}Zr	64.0 d
$^{144}Ce/^{144}Pr$	284.9 d
$^{106}Ru/^{106}Rh$	1.02 a
^{134}Cs	2.06 a
^{154}Eu	**8.8 a**
$^{137}Cs/^{137m}Ba$	**30.0 a**

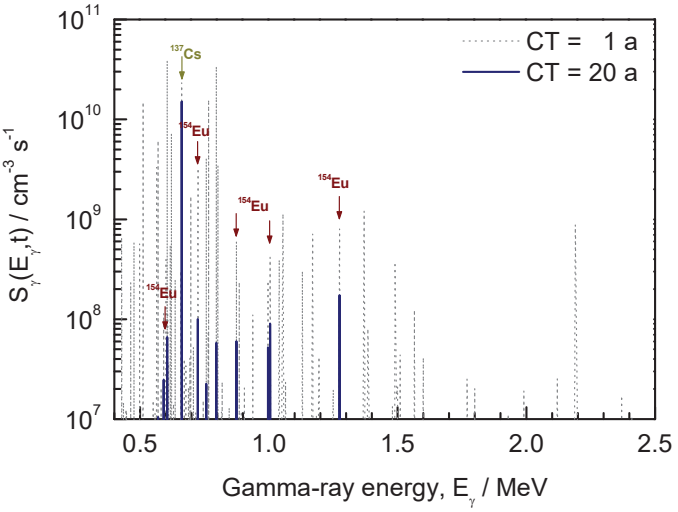

Gamma-ray emission by SNF

$$S_\gamma(t) = \sum_k S_{\gamma,k}(E_\gamma, t)$$

PWR UO_2 pellet (5 g)
$^{235}U/U$ = 4.8 %
burnup = 44 GWd/t

^{95}Nb	35.0 d
^{95}Zr	64.0 d
$^{144}Ce/^{144}Pr$	284.9 d
$^{106}Ru/^{106}Rh$	1.02 a
^{134}Cs	2.06 a
^{154}Eu	**8.8 a**
$^{137}Cs/^{137m}Ba$	**30.0 a**

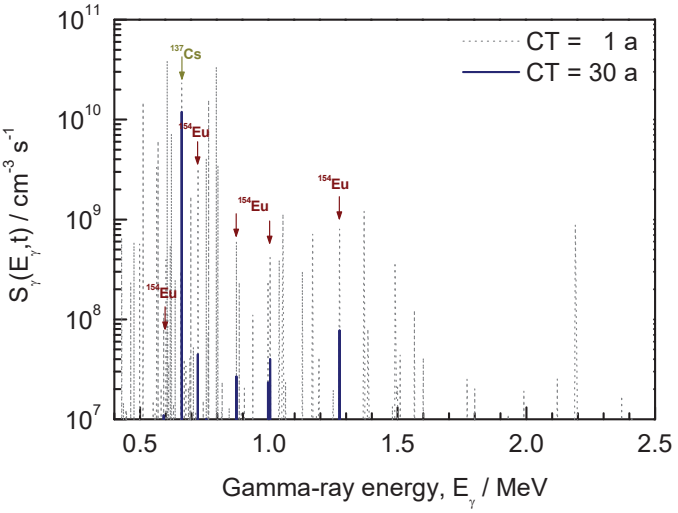

ESARDA, 6 - 7 february 2020, SCK CEN Mol (BE)

Characterisation of SNF

Main **source terms** of interest:

- Decay heat : H
- Neutron emission : S_n
- γ-ray emission : S_γ
- Reactivity : ^{235}U, ^{239}Pu, ^{241}Am, Fission Products (BUC)
- Fissile material : ^{235}U, ^{239}Pu
- Long-term safety : e.g. ^{14}C, ^{79}Se, ^{94}Nb, ^{99}Tc, ^{129}I, ^{226}Ra

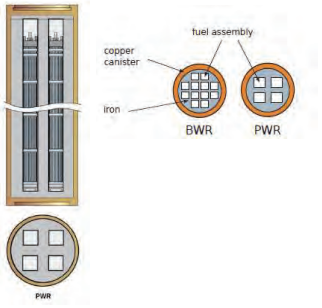

Contributions of nuclides with different characteristics

Difficult to be measured directly, in particular during industrial operation

e.g. decay heat by calorimetry at CLAB: accurate but long measurement times

⇒ Estimated by **theoretical calculations** using a burnup code

European Commission

$(N_k(t_0), k = 1, \ldots, n)$: by theoretical calculations

Coupled neutron transport – nuclide depletion/creation calculation

Neutron transport

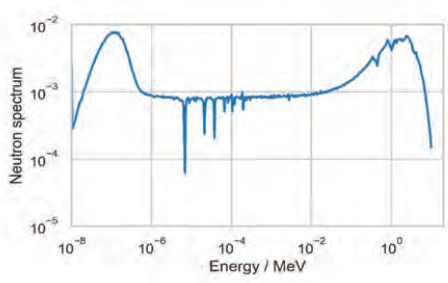

Bateman equation

$$\frac{dN_k}{dt} = Y\, N_f\, \sigma_f\, \varphi + \sum_i \lambda_i N_i + \sum_j \sigma_j N_j\, \varphi - (\lambda_k + \sigma_{k,a}\varphi) N_k$$

Update nuclide vector

ESARDA, 6 - 7 february 2020, SCK CEN Mol (BE)

European Commission

SFC – Task 2 (structure)

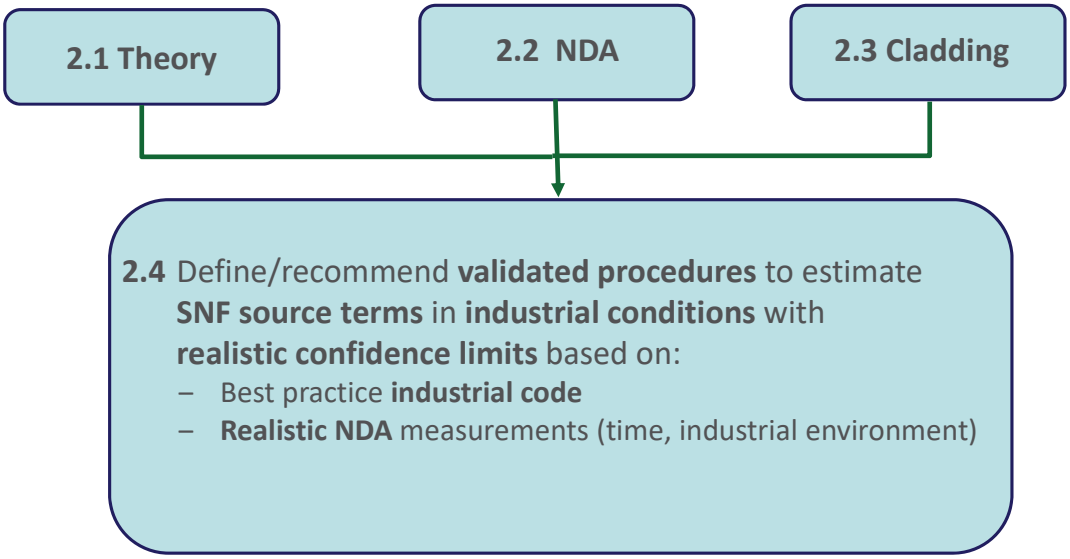

European Commission

SFC- Task 2: Code comparison

- CIEMAT : EVOLCODE (MCNP)
- JRC Geel : SERPENT, SCALE
- JSI : SCALE, DRAGON
- KIT : MCNP-CINDER
- NAGRA : SCALE
- PSI : CASMO
- SCK CEN : ALEPH-2 (MCNP)
- VTT : SERPENT

ESARDA, 6 - 7 february 2020, SCK CEN Mol (BE)

European Commission

Sensitivity and Uncertainty (S/U) analysis

- Input data:
  - **Nuclear Data (ND)**
    - Cross sections (neutron interactions)
    - Fission yields
    - Neutron emission probabilities
    - Decay data
  - **Fuel History (FH)**
    - Fuel properties (design, composition) e.g. Initial enrichment (IE)
    - Reactor operation and irradiation conditions e.g. Burnup (BU)
    - Cooling time (CT)

BurnUp (BU):
time integrated power per mass of initial fuel (MWd/kg)
$\propto$ *total number of fission x energy per fission event*

- Computational
  - Method: stochastic/deterministic
  - Model (2D/3D, boundary conditions, …)
  - Numerical approximations (depletion time steps, depletion zones, …)

European Commission

S/U analysis: ^{244}Cm production

$$\frac{dN_k}{dt} = Y\, N_f\, \sigma_f\, \varphi + \sum_i \lambda_i N_i + \sum_j \sigma_j N_j\, \varphi - (\lambda_k + \sigma_{k,a}\varphi) N_k$$

N = aBU^b

b = 6 for BU < 20 GWd/t

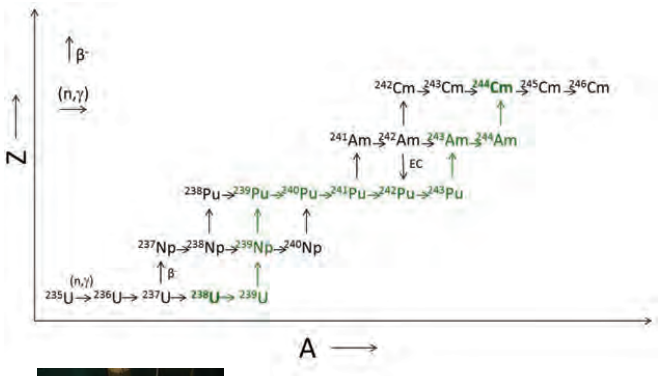

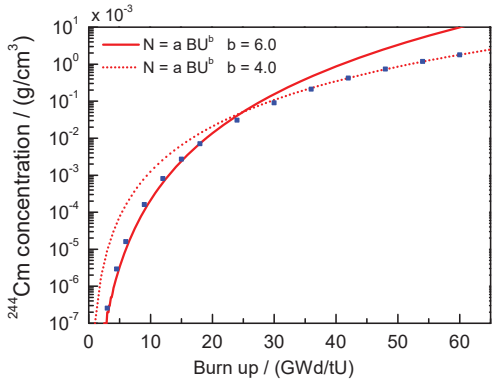

⇒ ^{244}Cm : burnup indicator

⇒ Neutron emission rate : burnup indicator

European Commission

S/U analysis: estimation of ^{244}Cm inventory

$$\frac{dN_k}{dt} = Y\, N_f\, \sigma_f\, \varphi + \sum_i \lambda_i N_i + \sum_j \sigma_j N_j\, \varphi - (\lambda_k + \sigma_{k,a}\varphi) N_k$$

Ref.	Library	Reactor	Fuel	BU GWd/t	IE wt%	^{244}Cm
Rochman	ENDF/B-VII.0	PWR	UO_2	10	4.1	18.7 %
	ENDF/B-VII.0	PWR	UO_2	20	4.1	16.9 %
	ENDF/B-VII.0	PWR	UO_2	30	4.1	15.5 %
	ENDF/B-VII.0	PWR	UO_2	40	4.1	14.1 %
Zwermann	SCALE-6.1	PWR	UO_2	40	4.1	8.5 %
Leary	ENDF/B-VII.1	PWR	UO_2	54	3.4	9.6 %
Rochman	ENDF/B-VII.1	PWR	UO_2	54	3.4	9.1 %
Rochman	ENDF/B-VII.1	PWR	UO_2	40	4.1	9.7 %

^{244}Cm inventory prediction production
- uncertainty due to nuclear data : ~10%
- due to ^{242}Pu(n,γ), ^{243}Am(n,γ)

⇒ Systematic study for key nuclides

⇒ Improve nuclear data
- Input HPRL NEA/OECD
- Input to SANDA (DG-RTD)
  https://cordis.europa.eu/project/id/847552
  Supplying Accurate Nuclear Data for energy and non-energy Applications

European Commission

Innovative NDA methods/systems for SNF characterisation

- **Innovative NDA** methods to characterise **pin segments**
  - **Validate codes** (alternative to radiochemical analysis)
  - Production of a reference pellet
- **NDA** methods to characterise **fuel assemblies** (SKB-50)
  - Improve theoretical source term predictions during industrial routine operation
    Improve fuel history data: e.g. BU
  - Validate codes
- Study **new detectors**
  - CLYC, *CVD*

ESARDA, 6 - 7 february 2020, SCK CEN Mol (BE)

European Commission

NDA methods to characterise pin segments

- **Neutron emission rate** of a SNF pin segment
  (collaboration SCK CEN – JRC Geel, Ispra)
  - Non-destructive method to determine ^{244}Cm content
  - Measurements in conventional controlled area conditions
    Hage's point model, JRC Ispra (B. Pedersen)

- **Nuclide vector** of SNF pin segment by **NRTA**
  (collaboration SCK CEN – JRC Geel)
  - **Non-destructive**; no chemical analysis
  - **Absolute** measurement (no calibration)
  - Measurements at **GELINA** facility of JRC Geel

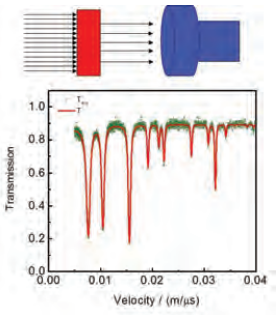

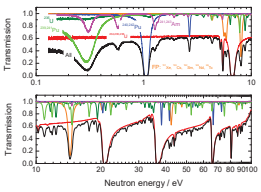

European Commission

Experiments at CLAB: SKB-50

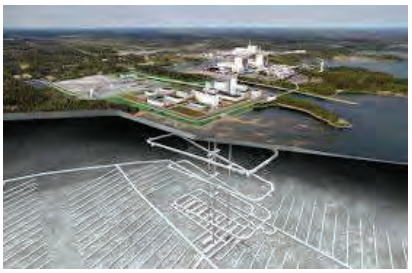

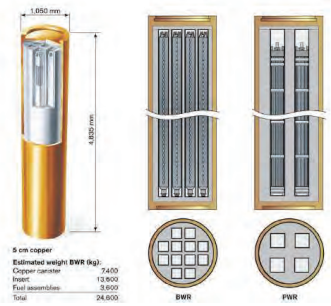

Installed systems

- Calorimeter
- Gamma-ray spectroscopic scanner

Testing of advanced systems (LANL)

- Differential Die-Away Self-Interrogation (DDSI)
- Differential Die-Away (DDA)

European Commission

Calorimeter at CLAB

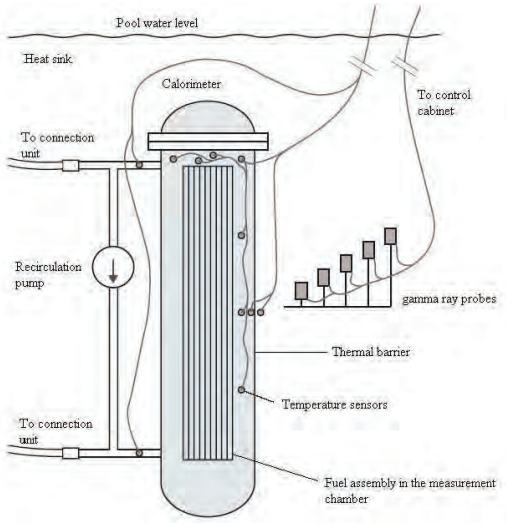

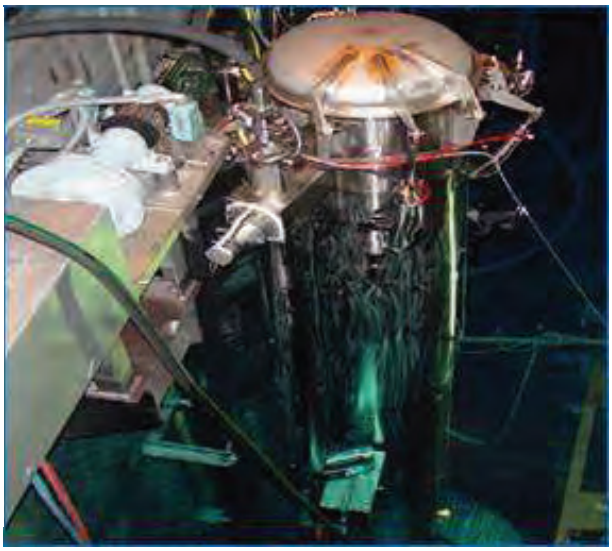

⇒ Target value uncertainty ≤ 2%

⇒ Reference instrument for decay heat of SNF

European Commission

Gamma-ray spectroscopic scanning system at CLAB

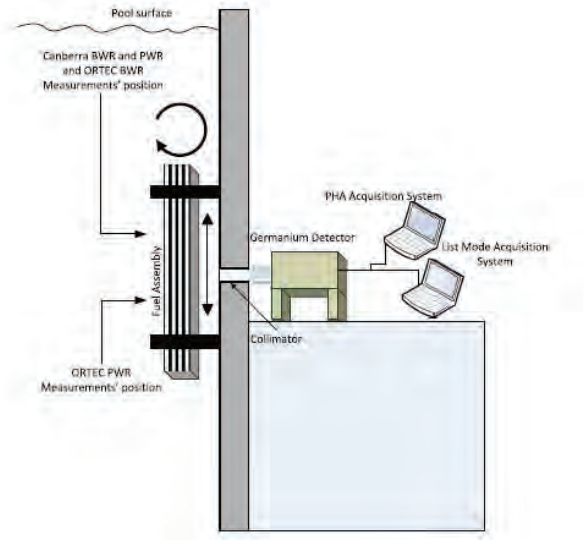

Vaccaro et al. NIMA 830 (2016) 325

^{134}Cs, ^{137}Cs, ^{154}Eu

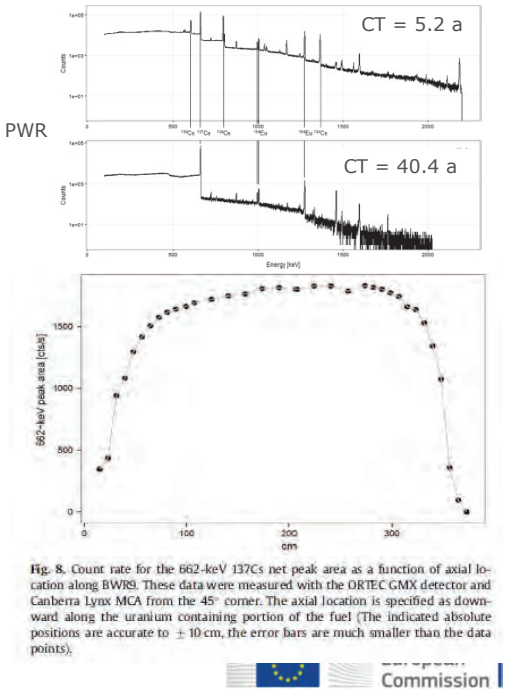

Fig. 8. Count rate for the 662-keV 137Cs net peak area as a function of axial location along BWR8. These data were measured with the ORTEC GMX detector and Canberra Lynx MCA from the 45° corner. The axial location is specified as downward along the uranium containing portion of the fuel (The indicated absolute positions are accurate to ± 10 cm, the error bars are much smaller than the data points).

European Commission

Fuel assemblies: DDSI and DDA at CLAB (LANL development, NGSI)

- Differential Die Away Self-Interrogation (DDSI, passive)

A.C. Trahan, LA-UR_16_20026 Kaplan et al., NIMA 764 (2014) 347 - 351

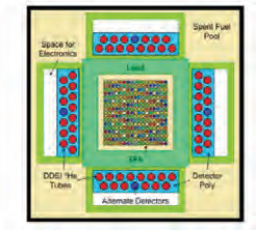

⇒ Optimise data analysis procedures for source term determination (not only safeguards)

- Differential Die Away (DDA, active)

V. Henzl, LANL-UR-123025

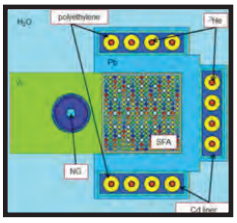

European Commission

Fuel assemblies: Finland

- Passive Neutron Albedo Reactivity (PNAR, NGSI)

LANL development, Tobin et al., NIMA 897 (2018) 32 - 37

Tobin et al., ESARDA bulletin 56 (2018) 12 - 18

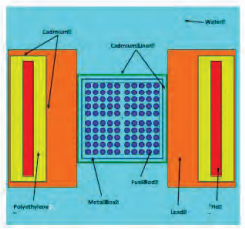

- Passive Gamma Ray Emission Tomography (PGET)

IAEA development, Honkamaa et al., Symp. Int. Safeguards, IAEA Vienna 2014

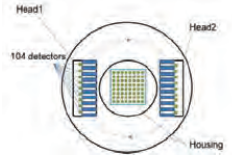

European Commission

EURAD-SFC (4 years project)

Define/recommend **validated procedures** to estimate **SNF source terms** (including fissile material) in **industrial conditions** with **realistic confidence limits** based on:

- Best practice **industrial code**
- **Realistic NDA** measurements (time, industrial environment)

European Commission

- EURAD project (SNF characterisation)
  - https://www.ejp-eurad.eu/about-eurad
  - NUGENIA, http://nugenia.org/call-for-mobility-grants-open/
- ARIEL
  support for open access, scientific visits, training early researchers, …
  - www.ariel-h2020.eu
- JRC Geel open access
  - https://ec.europa.eu/jrc/en/research-facility/open-access

ESARDA, 6 - 7 february 2020, SCK CEN Mol (BE)

European Commission

6.6 Performance assessment and uncertainty evaluation of the clab calorimeter; P. Schillebeeckx, JRC Geel; WPNCS Subgroup 12 meeting; 01/12/2022

PERFORMANCE ASSESSMENT AND UNCERTAINTY EVALUATION OF THE CLAB CALORIMETER

Work part of EURAD/SFC/Task2

P. Schillebeeckx,

European Commission, Joint Research Centre (JRC), Geel, Belgium

Contributors:

JRC Geel, SKB (Vattenfall), SCK CEN and JSI

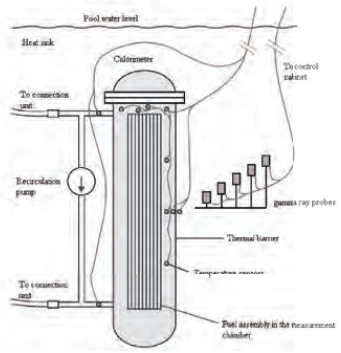

OVERVIEW OF DATA AT CLAB: PWR

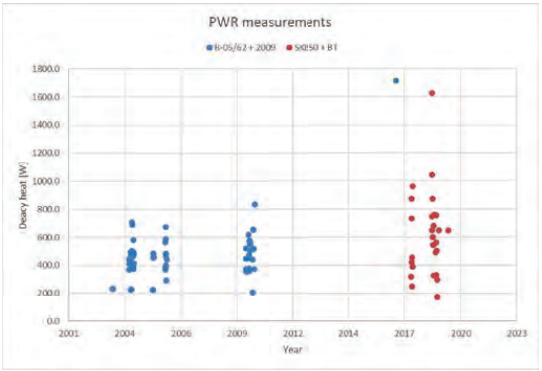

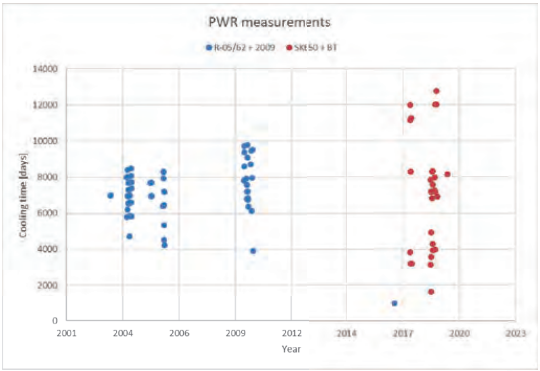

OVERVIEW OF DATA AT CLAB: BWR

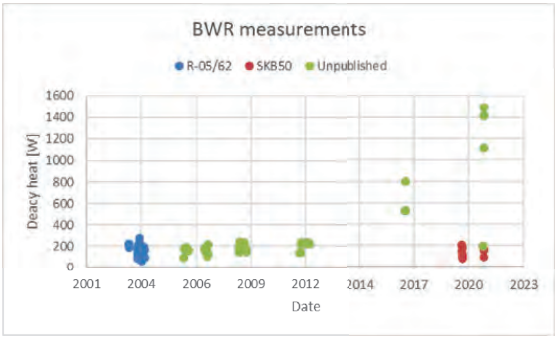

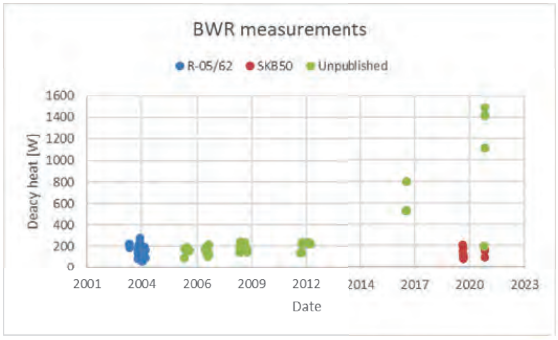

PERFORMANCE ASSESSMENT AND UNCERTAINTY EVALUATION OF THE CLAB CALORIMETER

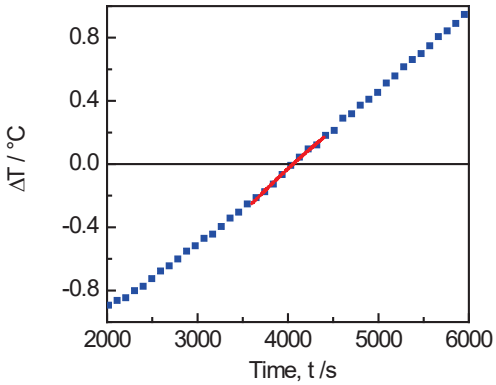

- Determine $\Delta T = T_c - T_p$ vs time
- Determine $d\Delta T/dt$ for $\Delta T = 0$

PERFORMANCE ASSESSMENT AND UNCERTAINTY EVALUATION OF THE CLAB CALORIMETER

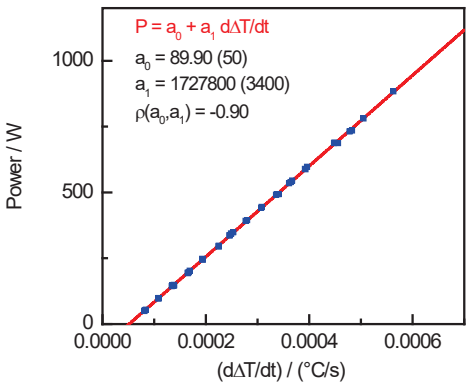

Calibration with an electrical heater

- Determine $\Delta T = T_c - T_p$ vs time
- Determine $d\Delta T/dt$ for $\Delta T = 0$
- Fit to data: $P = a_0 + a_1\, d\Delta T/dt$

PERFORMANCE ASSESSMENT AND UNCERTAINTY EVALUATION OF THE CLAB CALORIMETER

Spent nuclear fuel assembly

- Determine $\Delta T = T_c - T_p$ vs time
- Determine $d\Delta T/dt$ when $\Delta T = 0$
- $Q = a_0 + a_1\, K\, d\Delta T/dt$
- $P = Q + P_e$
  - K : correction factor due to thermal capacity difference between electrical heater and fuel assembly
  - P_e : heat loss due to γ-rays escaping from the calorimeter

Calibration with an electrical heater

- Determine $\Delta T = T_c - T_p$ vs time
- Determine $d\Delta T/dt$ for $\Delta T = 0$
- Fit to data: $P = a_0 + a_1\, d\Delta T/dt$

DATA ANALYSIS AND UNCERTAINTY EVALUATION

Define metrological parameters of the full measurement process and identify/quantify related uncertainty components

- Calibration of the heater
- Impact cables: loss due to cable length outside the calorimeter
- Define optimum fit procedure to determine the temperature gradient
- Uncertainty of temperature gradient
- Quality of calibration curve
- Verify repeatability over a long time period
- Correction factor: difference electrical heater – assembly
- Correction factor: loss of gamma-ray energy emitted by assembly

CALIBRATION ELECTRICAL HEATER

Electrical heater (ION 7600) was calibrated for its power output by a reference instrument

- 06/10/2008 ZERA TPZ 303
- 10/06/2020 ZERA MT3000

⇒ data show that the output of the electrical heater has to be corrected to avoid bias effects.

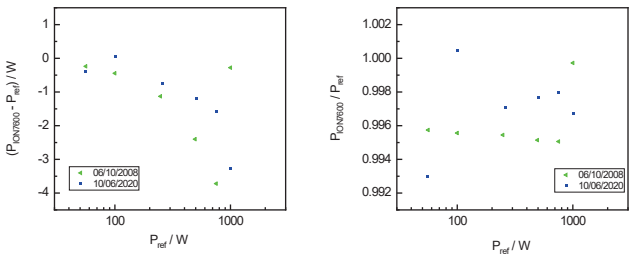

Average ratio & st.dev. of ratio

- 06/10/2008 0.9961 0.0018
- 10/06/2020 0.9972 0.0025

- Data taken between 2008 and 2020 have to be increased by 0.37% and an uncertainty of 0.2% has to be added due to the calibration
- Future: regular (yearly) calibration!

ENERGY LOSS DUE TO CABLES

- There is a power loss of the power provided by the calibration unit due to cables outside the calorimeter
- The heat loss is estimated from the length and electrical resistance per unit length
  - Outside
    - Length: 2 x 20 m
    - Resistance per unit length: 0.012 Ω/m
  - Inside (heating cable in calorimeter)
    - Length: 261 m
    - Resistance per unit length: 0.1 Ω/m

  ⇒ Power loss fraction: 26.1/(26.1 + 0.48) = 0.982

- Difficult to evaluate an uncertainty since the data are given with without uncertainty, in addition with a limited significant digits!

- Future: provide traceable data!

DEFINE OPTIMUM PROCEDURE TO DETERMINE TEMPERATURE GRADIENT

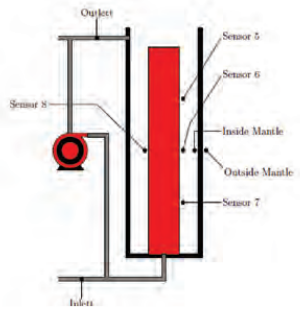

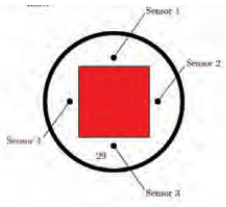

To be done :
- Define best temperature sensors
- Define optimum time region to fit!

$$\rho C_p \frac{\partial T}{\partial t} - k \frac{\partial^2 T}{\partial x^2} = S$$

Should be 0

DEFINE OPTIMUM PROCEDURE TO DETERMINE TEMPERATURE GRADIENT

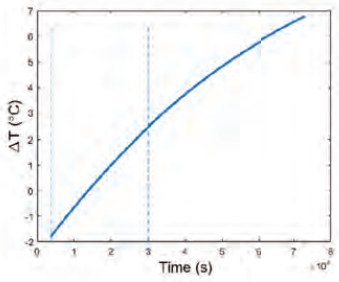

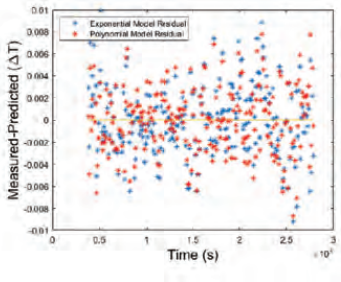

$$\Delta T_{poly} = c_1 + c_2 t + c_3 t^2.$$

$$\Delta T_{nl} = a_1 + a_2(1 - e^{-a_3 t})$$

$\Rightarrow$ no clear difference

To be done :

- Define best temperature sensors
- Define optimum time region to fit!

$$\rho C_p \frac{\partial T}{\partial t} - k\frac{\partial^2 T}{\partial x^2} = S$$

Should be 0

DEFINE OPTIMUM PROCEDURE: WHICH SENSOR, FUNCTION AND FIT REGION

Sensor 1

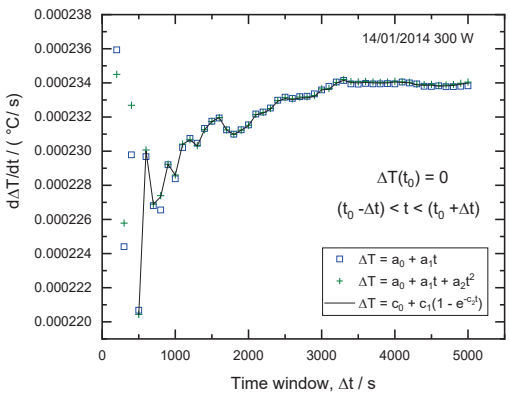

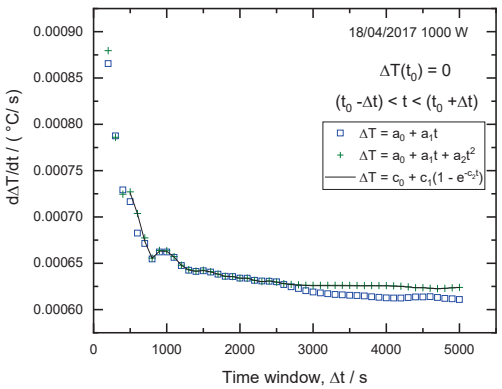

EVALUATE THE UNCERTAINTY OF THE GRADIENT (VARIANCE ANALYSIS)

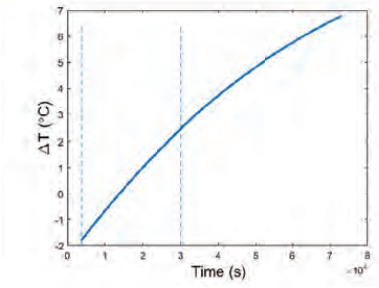

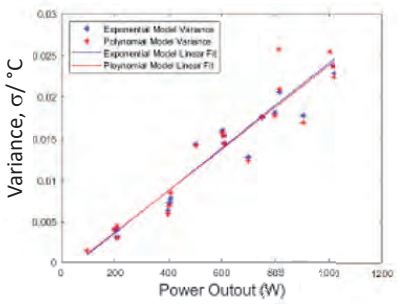

$$\sigma = \frac{\sum_i (\Delta T_i - \Delta T_{ai})^2}{N-1}$$

To be done

- Compare uncertainty with uncertainty of temperature output (assumed uncertainty is 0.01 °C)
- Propagate the uncertainty to the uncertainty of the slope value!

FIT DATA + REPEATIBILITY

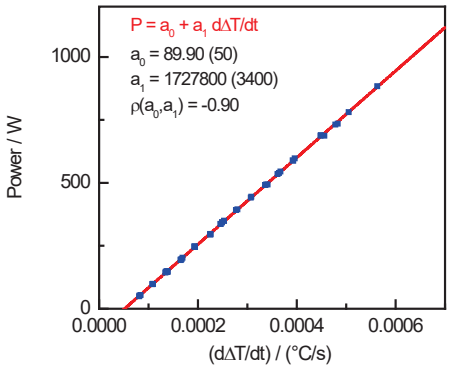

Electrical heater
Uncertainty evaluation based on variance analysis: green line

SNF assemblies
Repeated measurements

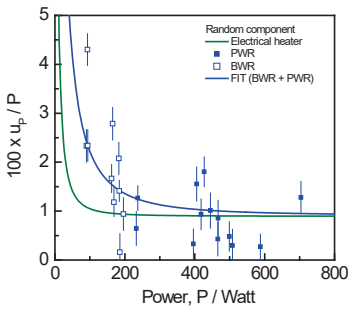

ENERGY LOSS DUE TO GAMMA-RAYS

$P_m = a_0 + a_1 K \, d\Delta T/dt$

$P = P_m + P_e$

Correction P_e: heat loss due to γ-rays escaping from calorimeter

- Present correction factor: based on dose rate measurements
- γ-ray transport calculations using SERPENT (JSI) and MCNP(SKB)
- To be done: impact of density change with BU

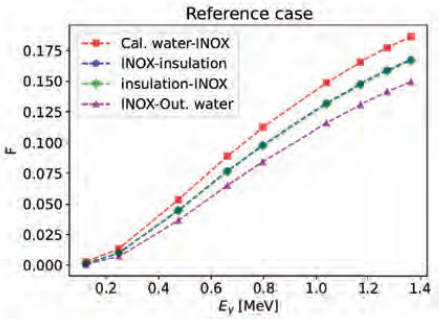

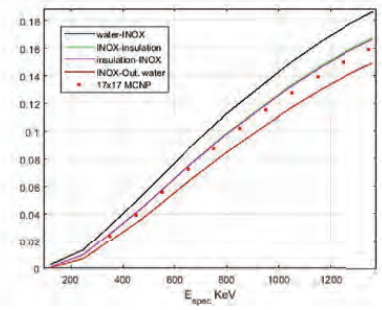

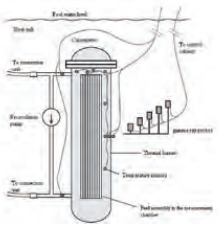

CORRECTION: HEATER - ASSEMBLY

Define correction factor K

$P_m = a_0 + a_1 \mathbf{K} \, d\Delta T/dt$

- Develop heat transfer model (done) MSc Thesis: J. Ekman (10/12/2021)

$$C_m \frac{dT_m}{dt} = -a_1(T_m - T_W) + Q_m$$

$$C_W \frac{dT_W}{dt} = a_1(T_m - T_W) - a_2(T_W - T_S) - a_3(T_W - T_P) + Q_W + a_c(T_W - T_c)$$

$$C_S \frac{dT_S}{dt} = a_2(T_W - T_S) - a_4(T_S - T_P)$$

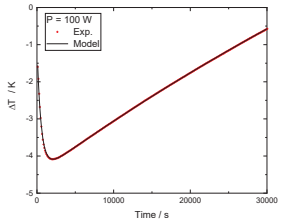

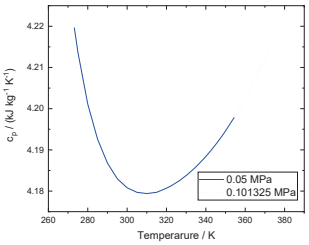

CALORIMETER AT CLAB – DATA ANALYSIS AND UNCERTAINTY EVALUATION

MSc Thesis: J. Ekman (10/12/2021)

Correction factor K: difference between electrical heater and assembly

$P_m = a_0 + a_1 \mathbf{K}\, d\Delta T/dt$

$P = P_m + P_e$

- Present correction factor based on total heat capacity:
  ratio of total heat capacity of calorimeter with fuel assembly and with electrical heater
- Use analytical model: ratio of the slope $d\Delta T/dt$ with fuel assembly and with electrical heater

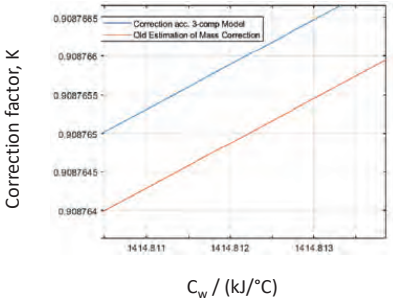

⇒ negligible difference
⇒ uncertainty evaluation in progress
⇒ Requires specifics of the materials

Keep in touch

EU Science Hub: ec.europa.eu/jrc

@EU_ScienceHub

EU Science Hub – Joint Research Centre

EU Science, Research and Innovation

EU Science Hub

EU science